
Stratigraphy, geochemistry and origin of products of complex volcanic centres, Newer Volcanics basaltic field, Victoria

by

Julie Ann Boyce, MGeosci (Hons)

Thesis submitted for the degree of

Doctor of Philosophy

at

Monash University

School of Earth, Atmosphere & Environment

Clayton Campus

Melbourne, Australia

May 2015



MONASH University



© Julie Boyce (2015). Except as provided in the Copyright Act 1968, this thesis may not be reproduced in any form without the written permission of the author.

I certify that I have made all reasonable efforts to secure copyright permissions for third-party content included in this thesis and have not knowingly added copyright content to my work without the owner's permission.

For my Grandfather, Eddy. This is for you. I miss you always. x



For the Djab Wurrung, Gunditj Mirring, Martang and Eastern Maar, who are the traditional custodians of this beautiful land.

“We are all visitors to this time, this place. We are just passing through. Our purpose here is to observe, to learn, to grow, to love... and then we return home.” Aboriginal proverb.



View of the Grampians and Victoria Ranges from Mount Rouse, West Victoria.
Eugene von Guérard, 1861, oil on canvas.

Declaration for thesis based or partially based on conjointly published or unpublished work
General Declaration

In accordance with Monash University Doctorate Regulation 17.2 Doctor of Philosophy and Research Master's regulations the following declarations are made:

I hereby declare that this thesis contains no material which has been accepted for the award of any other degree or diploma at any university or equivalent institution and that, to the best of my knowledge and belief, this thesis contains no material previously published or written by another person, except where due reference is made in the text of the thesis.

This thesis includes 3 original papers published in peer reviewed journals and 1 unpublished publication. The core theme of the thesis is Geochemistry and Physical Volcanology. The ideas, development and writing up of all the papers in the thesis were the principal responsibility of myself, the candidate, working within the School of Geoscience, Faculty of Science under the supervision of Prof. Reid Keays, Dr Ian Nicholls and Dr Patrick Hayman.

The inclusion of co-authors reflects the fact that the work came from active collaboration between researchers and acknowledges input into team-based research.

In the case of chapters 2, 3, 4 and 5 my contribution to the work involved the following:

| Thesis Chapter | Publication Title | Publication Status | Nature and extent of candidate's contribution |
|----------------|--|--------------------|---|
| 2 | The Newer Volcanics Province of southeastern Australia: a new classification scheme and distribution map for eruption centres | Published | 90% |
| 3 | Eruption centres of the Hamilton area of the Newer Volcanics Province, Victoria, Australia: pinpointing volcanoes from a multifaceted approach to landform mapping | Published | 80% |
| 4 | Stratigraphic architecture of Victoria's largest Cainozoic eruption centre: Mt Rouse, a complex polymagmatic monogenetic volcano, Newer Volcanics Province, south-east Australia | Submitted | 80% |
| 5 | Variation in parental magmas of Mt Rouse, a complex polymagmatic monogenetic volcano in the basaltic intraplate Newer Volcanics Province, southeast Australia | Published | 80% |

I have renumbered sections of submitted or published papers in order to generate a consistent presentation within the thesis.

Signed:

Date:



Table of contents

Please note that Chapters without section numbers represent published papers.

| | |
|----------------------------|------|
| Dedication | i |
| General Declaration | iii |
| Table of contents | v |
| List of figures | ix |
| List of tables | xiii |
| Acknowledgements | xv |
| Abstract | xvii |

| | | |
|----------|--|----|
| 1 | Introduction | |
| 1.1 | Introductory Statement | 1 |
| 1.1.1 | The Mt Rouse magmatic volcanic complex | 3 |
| 1.2 | Thesis aims | 4 |
| 1.3 | Tectonic setting of southeast Australia | 5 |
| 1.4 | Eastern Australian intraplate volcanism | 12 |
| 1.4.1 | Cainozoic volcanism in southeast Australia | 13 |
| 1.5 | Origin of eastern Australian volcanism | 15 |
| 1.6 | The Newer Volcanics Province of southeastern Australia | 18 |
| 1.6.1 | Volcano statistics of the Newer Volcanics Province | 20 |
| 1.6.2 | Age range of the Newer Volcanics Province | 23 |
| 1.6.3 | Geochemistry of the Newer Volcanics Province | 27 |
| 1.6.3.1 | Major and trace elements | 27 |
| 1.6.3.2 | $^{87}\text{Sr}/^{86}\text{Sr}$ isotopes | 35 |
| 1.6.3.3 | Metasomatism beneath the Newer Volcanics Province | 38 |
| 1.7 | Thesis structure | 40 |
| 1.8 | References | 41 |
| | Bridging text for Chapter 2 | 67 |
| 2 | The Newer Volcanics Province of southeastern Australia: a new classification scheme and distribution map for eruption centres | |
| | Boyce J. A. | |
| | Abstract | 69 |
| | Introduction | 69 |
| | Geological setting of the Newer Volcanics Province | 69 |
| | Origin of volcanism in the Newer Volcanics Province | 70 |
| | Methods | 71 |
| | Classification of eruption points of the Newer Volcanics Province | 72 |
| | Results and discussion | 75 |

| | | |
|----------|---|-----|
| | Central Highlands subprovince | 76 |
| | Western Plains subprovince | 77 |
| | Mt Gambier subprovince | 79 |
| | Conclusions | 79 |
| | Acknowledgements | 80 |
| | References | 80 |
| | Bridging text for Chapter 3 | 83 |
| 3 | Eruption Centres of the Hamilton area of the Newer Volcanics Province, Victoria, Australia: pinpointing volcanoes from a multifaceted approach to landform mapping | |
| | Boyce J. A., Keays R. R., Nicholls I. A. & Hayman P. C | |
| | Abstract | 85 |
| | Introduction | 85 |
| | Geological setting of the Newer Volcanics Province | 86 |
| | Methods | 87 |
| | Observations and results | 87 |
| | Eruption centres | 87 |
| | Confirmed eruption centres | 87 |
| | Questioned eruption centres | 93 |
| | Relative ages | 94 |
| | Geochemistry of the volcanics | 96 |
| | Discussion | 99 |
| | Conclusions | 101 |
| | Acknowledgements | 102 |
| | References | 102 |
| | Bridging text for Chapters 4 and 5 | 105 |
| 4 | Stratigraphic architecture of Victoria's largest Cainozoic eruption centre: Mt Rouse, a complex polymagmatic volcano, Newer Volcanics Province, Australia | |
| | Boyce J. A., Hayman P. C., Nicholls I. A. & Keays R. R. | |
| | Abstract | 107 |
| 4.1 | Introduction | 107 |
| 4.2 | Geological setting | 108 |
| 4.3 | Overview of the Mt Rouse volcanic complex | 109 |
| 4.4 | Methods | 111 |
| 4.5 | Facies description | 111 |
| 4.5.1 | Coherent Facies | 115 |
| 4.5.1.1 | Facies C1: Lavas | 115 |
| 4.5.1.2 | Facies C2: Discordant coherent basalt | 116 |
| 4.5.2 | Fragmental facies | 119 |
| 4.5.2.1 | Facies P1: Coarse grained, moderately to well sorted | |

| | | |
|-------|---|-----|
| | bedded ash–lapilli–bombs | 119 |
| | 4.5.2.2 Facies P2: Well sorted fine ash–fine lapilli | 121 |
| | 4.5.2.3 Facies P3: Moderately to well sorted fine ash–coarse lapilli/small blocks | 122 |
| | 4.5.2.4 Facies P4: Cross-bedded fine ash–fine lapilli | 123 |
| | 4.5.2.5 Facies P5: Palagonite altered, armoured fine lapilli-rich, ash | 125 |
| | 4.5.2.6 Facies P6: Spatter agglomerate | 127 |
| 4.6 | Discussion | 129 |
| 4.6.1 | Stratigraphic architecture and evolution of the Mt Rouse complex | 129 |
| | 4.6.1.1 Phase 1: Long lava flow extrusion | 130 |
| | 4.6.1.2 Phase 2: Low south–north cone-building phase | 130 |
| | 4.6.1.3 Phase 3: Main northern cone-building phase | 130 |
| | 4.6.1.4 Phase 4: Southern cone-building coupled with extrusion of the lava shield | 132 |
| 4.6.2 | Factors causing alternating eruption styles | 133 |
| 4.7 | Conclusions | 135 |
| 4.8 | Acknowledgements | 135 |
| 4.9 | References | 136 |

5 Variation in parental magmas of Mt Rouse, a complex polymagmatic monogenetic volcano in the basaltic intraplate Newer Volcanics Province, southeast Australia

Boyce J. A., Nicholls I. A., Keays R. R., & Hayman P. C

| | | |
|--|---|-----|
| | Abstract | 147 |
| | Introduction | 147 |
| | Geological setting | 148 |
| | Mt Rouse magmatic volcanic complex | 149 |
| | Methods | 149 |
| | Results | 149 |
| | Whole rock chemical composition | 149 |
| | Petrography | 152 |
| | Sr–Nd–Pb isotopes | 154 |
| | Discussion | 154 |
| | Fractionation | 156 |
| | Contamination | 159 |
| | Degree of partial melting and depth of origin | 159 |
| | The link between eruptive style and melt composition | 161 |
| | Structural influences during the eruption of Mt Rouse | 162 |
| | The origin of the magma batches of Mt Rouse | 163 |
| | Conclusions | 164 |
| | Acknowledgements | 164 |
| | References | 164 |

| | | |
|----------|--|-----|
| 6 | Conclusions and discussion | |
| 6.1 | Introduction | 169 |
| 6.2 | Distribution of volcanoes in the Newer Volcanics Province | 169 |
| 6.3 | Geochronology of the Newer Volcanics Province | 170 |
| 6.4 | Geochemistry of the Newer Volcanics Province | 171 |
| 6.5 | The complexity of the Mt Rouse magmatic volcanic complex | 172 |
| 6.6 | Hazard implications of renewed volcanism in the Newer Volcanics Province | 173 |
| 6.7 | Suggestions for further research | 175 |
| 6.8 | References | 175 |
| | Appendix 1. Outreach | 183 |
| | Appendix 2. NVP Project data | 205 |
| | Appendix 3. Hamilton geochemical data | 215 |
| | Appendix 4. Stratigraphic logs | 217 |
| | Appendix 5. X-Ray Diffraction results | 243 |
| | Appendix 6. Mt Rouse geochemical data | 245 |



List of figures

Chapter 1 Introduction

| | | |
|------|--|----|
| 1.1 | Tectonic setting of Australia | 5 |
| 1.2 | Geological map of western Victoria and southeast South Australia, showing main terranes and lithospheric structures | 6 |
| 1.3 | Eastern Australian fold belts and Victorian structural zones | 7 |
| 1.4 | Stratigraphic and basin event chart of the Otway Basin | 9 |
| 1.5 | Pre-Permian geology of Victoria | 11 |
| 1.6 | Map of eastern Australia, showing the distribution of volcano types | 12 |
| 1.7 | Distribution of Cainozoic volcanic rocks in Victoria | 14 |
| 1.8 | Age vs latitude of eastern Australian intraplate activity | 15 |
| 1.9 | Hotspot tracks in eastern Australia | 16 |
| 1.10 | Steps in lithospheric thickness across southeast Australia showing edge-driven convection in cross section and its relation to the Newer Volcanics Province | 18 |
| 1.11 | Distribution of volcano types in eastern Australia with relation to steps in lithospheric thickness | 19 |
| 1.12 | Distribution of volcanic centres in the Newer Volcanics Province | 20 |
| 1.13 | Age distribution of volcanic centres and basalt point samples in the Newer Volcanics Province | 24 |
| 1.14 | Scatter diagrams of volcano ages with latitude and longitude, and histogram of the number of volcanoes in 0.5 Ma intervals east and west of the Mortlake Discontinuity | 26 |
| 1.15 | TAS diagram of basalt compositions for the Newer Volcanics Province | 28 |
| 1.16 | Major elements vs MgO for the rock suites of the Newer Volcanics | 29 |
| 1.17 | Maximum recorded Mg-numbers of volcanic centres and basalt point samples in the Newer Volcanics Province | 30 |
| 1.18 | Trace elements vs MgO for the rock suites of the Newer Volcanics | 33 |
| 1.19 | Chondrite-normalised rare earth element diagram showing the range of Newer Volcanics Province values | 34 |
| 1.20 | Gd/Yb vs MgO for selected Newer Volcanics basalts | 34 |
| 1.21 | Maximum recorded $^{87}\text{Sr}/^{86}\text{Sr}$ isotope values of basalts traceable to volcanoes in the Newer Volcanics Province | 35 |
| 1.22 | $^{87}\text{Sr}/^{86}\text{Sr}$ isotopic composition of Newer Volcanics basalts along an E–W profile to the west of Melbourne | 37 |
| 1.23 | Southeast Australian geotherm | 40 |

Chapter 2 The Newer Volcanics Province of southeastern Australia: a new classification scheme and distribution map for eruption centres

| | | |
|-----|--|----|
| 2.1 | Distribution of volcanic centres by type in the Newer Volcanics Province of southeastern Australia | 70 |
| 2.2 | Locations of example volcanoes in the NVP | 72 |
| 2.3 | Simple volcanic centres of the NVP | 73 |
| 2.4 | Complex volcanic centres of the NVP | 74 |
| 2.5 | Central Highlands subprovince of the NVP | 77 |
| 2.6 | Volcanic distribution of the Western Plains subprovince in the Avoca and Moyston Fault areas | 78 |
| 2.7 | Mt Gambier subprovince of the NVP | 79 |

Chapter 3 Eruption Centres of the Hamilton area of the Newer Volcanics Province, Victoria, Australia: pinpointing volcanoes from a multifaceted approach to landform mapping

| | | |
|------|--|-----|
| 3.1 | Distribution of volcanic centres in the Newer Volcanics Province of southeastern Australia | 86 |
| 3.2 | Basic maps of the Hamilton area, showing basalt cover, roads and volcanoes, before and after ground truthing | 88 |
| 3.3 | Photographs of the magmatic volcanic complexes Mt Rouse and Mt Napier, and the lava shields of Sheepwash Hill, Green Hills and Mt Baimbridge | 90 |
| 3.4 | Photographs of the lava shields Mt Pierrepoint, Bunnugal Hill, Picaninny Hill and Jays Hill | 91 |
| 3.5 | Jays Hill lava shield, showing satellite imagery and magnetics | 92 |
| 3.6 | The Cas Maar, a maar–cone volcanic complex | 93 |
| 3.7 | Relative ages of the eruption centres in the Hamilton area | 95 |
| 3.8 | TAS diagram for the eruption products of the Hamilton area, compared to those of the Newer Volcanics Province | 98 |
| 3.9 | Chondrite normalised rare earth element diagrams for the Hamilton area, compared to Ocean Island Basalts and the Newer Volcanics Province | 99 |
| 3.10 | Variations in major and trace element compositions in the Hamilton area | 100 |

Chapter 4 Stratigraphic architecture of Victoria's largest Cainozoic eruption centre: Mt Rouse, a complex polymagmatic volcano, Newer Volcanics Province, Australia

| | | |
|-----|---|-----|
| 4.1 | The Newer Volcanics Province of southeastern Australia | 109 |
| 4.2 | Overview of the Mt Rouse complex | 110 |
| 4.3 | Combined stratigraphic log of Mt Rouse, correlating exposed deposits of the northern and southern scoria cones, and the main lava flows | 114 |
| 4.4 | Main lava flow features of Mt Rouse | 116 |
| 4.5 | Discordant coherent basalt | 118 |
| 4.6 | Facies P1 features | 120 |
| 4.7 | Facies P2 features | 121 |
| 4.8 | Facies P3 features | 123 |

| | | |
|------|---|-----|
| 4.9 | Facies P4 features | 124 |
| 4.10 | Facies P5 features | 126 |
| 4.11 | Facies P6 features | 128 |
| 4.12 | Evolution of the Mt Rouse complex showing facies distribution | 131 |

Chapter 5 Variation in parental magmas of Mt Rouse, a complex polymagmatic monogenetic volcano in the basaltic intraplate Newer Volcanics Province, southeast Australia

| | | |
|------|--|-----|
| 5.1 | The Newer Volcanics Province of southeastern Australia | 148 |
| 5.2 | Overview of the scoria cone complex of Mt Rouse | 150 |
| 5.3 | Lava flows of Mt Rouse, showing sample locations | 151 |
| 5.4 | Rare earth element profiles, TAS diagram and CIPW normative classification of the products of Mt Rouse | 152 |
| 5.5 | Selected major and trace elements vs MgO for Mt Rouse products | 155 |
| 5.6 | Typical photomicrographs of the products of Mt Rouse | 157 |
| 5.7 | Sr–Nd–Pb isotope compositions of the products of Mt Rouse | 158 |
| 5.8 | Vector diagram of Nd vs Sr showing fractional crystallisation vectors for the three magma batches of Mt. Rouse | 159 |
| 5.9 | Th/Yb vs Nb/Yb and Gd/Yb vs La/Lu diagrams showing increasing partial melting and no crustal contamination of the products of Mt Rouse | 161 |
| 5.10 | Southeast Australian geotherm, showing estimated temperatures and depths of origin of Mt Rouse products, compared to those of Mt Gambier | 162 |

Chapter 6 Conclusions and discussion

| | | |
|-----|---|-----|
| 6.1 | Newer Volcanics Province eruption centres in the Greater Melbourne area | 174 |
|-----|---|-----|



List of tables

Chapter 1 Introduction

| | | |
|-----|---|----|
| 1.1 | Volcanic centres of the Newer Volcanics Province, classified by subprovince and volcano type | 22 |
| 1.2 | Vents of the Newer Volcanics Province | 22 |
| 1.3 | Numbers of dated Newer Volcanics Province samples | 24 |
| 1.4 | Range of Mg-numbers of samples traceable to volcanoes in the Newer Volcanics Province | 31 |
| 1.5 | Incompatible element ratios for the primordial mantle and continental crust compared to the range of values for Newer Volcanics Province products | 34 |
| 1.6 | Range of $^{87}\text{Sr}/^{86}\text{Sr}$ isotope values of samples traceable to volcanoes in the Newer Volcanics Province | 36 |

Chapter 2 The Newer Volcanics Province of southeastern Australia: a new classification scheme and distribution map for eruption centres

| | | |
|-----|--|----|
| 2.1 | Volcanic centres of the Newer Volcanics Province | 75 |
| 2.2 | Eruption points of the Newer Volcanics Province | 76 |

Chapter 3 Eruption Centres of the Hamilton area of the Newer Volcanics Province, Victoria, Australia: pinpointing volcanoes from a multifaceted approach to landform mapping

| | | |
|-----|--|----|
| 3.1 | Validated and questioned eruption centres of the Hamilton area | 89 |
| 3.2 | Whole rock major and trace element data | 97 |

Chapter 4 Stratigraphic architecture of Victoria's largest Cainozoic eruption centre: Mt Rouse, a complex polymagmatic volcano, Newer Volcanics Province, Australia

| | | |
|-----|---|-----|
| 4.1 | Key facies characteristics of the volcanic products of Mt Rouse | 112 |
| 4.2 | Eruption styles associated with the facies of Mt Rouse | 113 |

Chapter 5 Variation in parental magmas of Mt Rouse, a complex polymagmatic monogenetic volcano in the basaltic intraplate Newer Volcanics Province, southeast Australia

| | | |
|-----|---|-----|
| 5.1 | Representative major and trace element analyses of Mt Rouse products | 153 |
| 5.2 | Petrographic descriptions of Mt Rouse products | 156 |
| 5.3 | Sr–Nd–Pb compositions of the products of Mt Rouse | 157 |
| 5.4 | Sr–Nd–Pb compositions for Mt Rouse from previous studies | 158 |
| 5.5 | Kd values of Sr and Nd in plagioclase feldspar, clinopyroxene and olivine used to model the shallow level fractional crystallisation | 159 |
| 5.6 | Average values of incompatible elements Th, Nd and Zr in the magma batches of Mt Rouse and the percentage of fractional crystallisation | |

| | | |
|-----|--|-----|
| | required to derive one from another | 160 |
| 5.7 | Incompatible element ratios for the primordial mantle and continental crust compared to the range of values for Mt. Rouse products | 161 |
| 5.8 | Calculated primary magma compositions | 162 |
| 5.9 | Eruption styles associated with the magma batches of Mt Rouse and their role in the stratigraphic architecture of the complex | 163 |



Acknowledgements

My list of thanks is long, and if I have missed you out, I apologise.

First and foremost I thank my supervisors, **Ian Nicholls**, **Reid Keays** and **Patrick Hayman**. Thanks for always being available to read my mumbo jumbo at short notice, for keeping me inspired with fresh ideas and new perspectives and for all the support during my illnesses; and for the endless patience with my retarded questions, especially the ones involving maths. **Ray Cas**, my surrogate supervisor, thanks for all our chats and the advice you've given me. It has always been a great pleasure of mine to share my discoveries with you and you have taught me a lot.

Ralf Gertisser (Keele University, UK), thank you for inspiring me to do a PhD in the first place by making my Masters so enjoyable.

No research is possible without discussion. For that I would like to thank **Bill Birch**, **Fons VandenBerg** (Museum Victoria), **David Higgins** (Geoscience Victoria), **Bernie Joyce**, **Roland Maas**, **David Phillips**, **Erin Matchan** (Melbourne University), **John Webb**, **Neville Rosengren** (LaTrobe University), **Darren Bennetts** (Peter J. Ramsay and Associates Pty Ltd), **Ross Cayley** (Geological Survey of Victoria) and **Ken Grimes** (Regolith mapping, Hamilton). I would also like to thank fellow PhD students for discussions and ArcGIS help during my research: **David Moore**, **Jackson van den Hove**, **Teagan Blaikie**, **Simone Jordan**, **Madelaine Willcock**, **Chris Folkes**, **Chris Medlin**, **Islay Laird** and **Jozua van Otterloo**.

Special thanks go to **Janine Kavanagh**, I really enjoyed spending time with you in the field at Mt Eccles and the Hamilton area; you definitely inspired me and made me look at things from a different perspective.

I would like to thank **Tony Rowe** at Bamstone quarries, for collecting mantle xenoliths for me, posting me out packages of basalt and taking me on quarry tours. I really appreciate all of the help you gave me during my research.

Thanks go to the **Penshurst Volcanoes Discovery Centre**, at the foot of the most splendid volcano in the Newer Volcanics Province, for all your help and encouragement during the course of my PhD. Special thanks also go to the people of the Hamilton area for allowing me on to their land to steal and fondle their rocks, sharing their knowledge of the land and welcoming me to the area with friendly handshakes and cups of tea. In particular I would like to thank **Bob & Sheila Krummel**, **Val Rentsch** and **Gary Starr**, **Stella & Steven Boots** (Stella is the bravest spider exterminator in Australia), **Jenny & Alan Spooner**, **Dion Ross**, **Katrina Boyd-Walsh**, **Judy and Vanne Trompf**, **Andrew & Jennifer Lacey**, **Mal Brinkman**, **Peter Bourke** (Tarrone Quarry), **Craig Kenny** (LK Quarry), **Robin Jackson** and **Brian O'Brien**. I've had lots of people help me with fieldwork, which I really appreciated. I enjoyed spending time with you all, from the Fraggie Rock jamming sessions and Hamlet auditions in the quarries, to ground-truthing the Cas Maar and being screamed at by angry farmers. **Jozua van Otterloo**, **Jackson van den Hove**, **Matthew Edwards**, **Dan Uehara**, **Janine**

Kavanagh, Pat Hayman and Bob Krummel thank you!

Thanks go to the many technical and admin staff at the School of Geosciences, without whom a PhD is impossible, and who are often taken for granted: **Chris & Rachelle Pierson, Robert Douglass, Junnel Alegado, Massimo Raveggi, Florita Henricus, Petrina Soh, Robert Oakley, Draga Gelt, Tien Chen, Silvana Cifaratti, Nicolette Solomon, Ana Pinto, Angelica Romero, Silvana Cifaratti, Katie Tran and Christine Jones.**

I've been through a lot of medical hassles since a year into my PhD, which greatly hindered my research, and I would *never* have completed my PhD if it was not for the help of the following people. **Everyone at the School of Earth, Atmosphere and Environment** have been amazing, always with kind words and helping hands, even when I was grumpy and short-tempered. The support I received from the School was more than I could have hoped for, and for this I thank at least **Roberto Weinberg, Sandy Cruden, Pete Betts, my wonderful supervisors, Tien Chen and Rob Oakley.** I would especially like to thank the people who have helped me out with lifts here there and everywhere, with my hospitalisations and so forth—**Tanmay Vegad, Hammad Haider, Jim Driscoll, Jozua van Otterloo, Maddy Willcock, Mel Finch, Sahereh Aivazpourporgou, Steph Mills, Roland Seubert, Marion Anderson, Peter and Georgina Gradev, Maryellen “Mommacakes” Temple Mills, Dr Jim Giannakopoulos, Dr Elisabeth Nash, Dr Andrew McQueen, Dr Graham Lowe; and Shri Purusothaman.**

I've been lucky enough to have some great office mates over the past four years, to keep me (in)sane and laughing with internet shopping sprees, giggling in the corner, YouTube jamming sessions (not to mention all the crazy videos), cake scoffing, coffee drinking, liquorice munching and endless innuendo. **Mel Finch, David Elliot, Dean Bradley, Henning Reichardt, Andrew Langendam, Daniel Thompson, Sahereh (Dr. Shazmatron) Aivazpourporgou, Jozua van Otterloo, Riti Das, Martin Schwindinger, Connor Turvey and Jack Matthews.** On this note, I'd like to thank **all of the postgrad students at Monash**, we've shared some great moments, and I know I've made some *life-long friends*, but I won't mention you all by name for fear of running out of paper! The exceptions are **Maddy Willcock**, because you are the best, and **Jim Driscoll**, my big brother.

Thanks also go to the greatest housemates/habibis/brothers/BFF's — **Tanmay ‘Tanu’ Vegad and Malik Hammad ‘Hammy’ Haider.** Thanks for being my Aussie family, for the fun times we've shared, and for taking me away from the world of geology.

Finally, I'd like to thank my friends and family back home, for always being there with love, advice, encouragement and support though so far away—**my parents**, my bro **James** my wonderful **Nag Bag** (the best Grandmother in the whole world), **Auntie J** and **Uncle B** (my second set of parents), and my fabulous friends **Charlotte ‘Charlie Farley’ Winter, Steve Banham and Steve Rogers.**

Dif-tor heh smusma...



Abstract

Monogenetic volcanoes are the most common form of continental basaltic volcanism on Earth and hence present great risk upon eruption in heavily populated areas. Recent studies of individual monogenetic volcanic centres demonstrate that, far from being simple in nature as traditionally assumed, large variations exist between centres in terms of the types of magmas involved in their formation, the sources of those magmas, their stratigraphic architectures, and the timing of the eruption products.

The Pliocene–Recent Newer Volcanics Province (NVP) and in particular the Mt Rouse magmatic volcanic complex were studied in detail using desktop, fieldwork and laboratory based techniques in order to gain further insights into the processes and occurrences of monogenetic volcanism in southeast Australia, as well as the complexity of monogenetic volcanism in general. The techniques used in this study can be applied to other monogenetic volcanic fields.

A database of NVP volcanoes was produced, documenting >729 vents from >437 volcanoes. A new classification scheme was proposed for the volcanoes of the NVP, whereby volcanic centres are either simple or complex, with subtypes including scoria cones, maars, ash cones and domes, plus magmatic, phreatomagmatic and maar–cone volcanic complexes. An average eruption frequency for the province is estimated to be 1:10 800 yrs.

The volcanoes of the Hamilton area in the Western Plains subprovince were examined in more detail, using desk and field-based studies. Sixteen eruption centres were recognised, including three previously unrecorded volcanoes. Three phases of volcanism were confirmed, with ages of >4 Ma (Phase 1), ~2 Ma (Phase 2) and <0.5 Ma (Phase 3). Geochemically, compositions become increasingly alkaline from Phase 1 to 2, with Phase 3 eruptions covering the entire geochemical range and extending into increasingly incompatible element-enriched compositions.

The complex stratigraphic architecture of Mt Rouse was investigated in detail using field mapping and sampling for petrography. Eight main facies were documented, of which two are coherent and six fragmental. The eruption styles giving rise to the facies include Hawaiian, Strombolian, micro-Plinian, violent-Strombolian and phreatomagmatic.

Major and trace element geochemical data were generated together with Sr–Nd–Pb isotope data for samples selected on the basis of the stratigraphic framework of Mt Rouse. The data define three magma batches, Batches A, B and C all of which are geochemically similar to Ocean Island Basalts. Each batch features LREE-enrichment, increasing from batch A to C; there is no evidence of crustal contamination. The Sr–Nd–Pb isotope data define two groupings, one comprising magma batch A and a second for batches B and C. Estimates of the depths of mantle melting from primary magma compositions suggest that the magmas were sourced from a zone extending across the lithosphere–asthenosphere boundary. Batch A was sourced from the deep lithosphere at a pressure of 1.7 GPa, corresponding to 55.5 km depth, and batches B and C from the shallow asthenosphere at 1.88 GPa/61 km and 1.94 GPa/63 km, respectively. A complex eruption sequence outlined for Mt Rouse includes sequential eruption of magma batches A, C and B, then simultaneous eruption of batches A and B, over four stages with multiple sub-stages and no evidence of time-breaks in eruption.

This study has shown that monogenetic volcanoes may be far from simple, often showing great complexity in terms of their eruption styles and magma genesis. This will have significant implications for studies of monogenetic volcanism and the emergent field of study of complex monogenetic volcanoes both in the NVP and worldwide.





Chapter 1

Introduction

1.1 Introductory Statement

Monogenetic volcanic fields represent the most common form of continental volcanism on Earth (Valentine & Gregg 2008), as well as being found on other planetary bodies in the solar system such as Mars (Baloga *et al.* 2007; Bishop 2008; Broz & Hauber 2012). They consist of widely-varying numbers of individual volcanic centres (between tens and hundreds) that may erupt intermittently over time or in temporal clusters (Condit & Connor 1996; Németh 2010; Le Corvec *et al.* 2013), with many volcanic fields having lifetimes of millions of years (Németh 2010).

Monogenetic volcanoes, such as scoria cones, maar volcanoes and small lava shields (Ollier 1967; Wood 1980; Cas & Wright 1987) were conventionally thought to only erupt once, formed during one short-lived phase of eruption, which may last hours to years (Foshag & Gonzales 1956; Kienle *et al.* 1980; Camp *et al.* 1987). This activity was believed to involve the eruption of a single batch of magma, as the low magma supply rate was thought to lead to the cooling of magma conduits that would normally be used in the ascension of further batches of magma (Walker 2000). Polygenetic volcanoes (for example typical large arc stratovolcanoes) are considered much more complex in terms of multiple, episodic eruptions from the same general vent, including multiple magma batches with a large magma supply rate enabling magma to follow preceding batches along still-hot pathways (Wadge 1981; Takada 1994).

More recent studies of monogenetic volcanoes define them as typically erupting relatively small volumes of magma in the order of 0.001–0.1 km³ dense rock equivalent (DRE; Kereszturi *et al.* 2010; Németh 2010) and rarely exceeding 1 km³ (Smith *et al.* 2008). This is in contrast to polygenetic volcanoes, which repeatedly erupt substantial volumes of material over thousands of years. Generally the total erupted volume of a monogenetic volcanic field may rival that of a typical polygenetic volcano (Németh 2010).

Although monogenetic volcanoes have in the past been regarded as volcanologically simple, Ollier (1967) observed that maar volcanoes show evidence of complexity in terms of multiple episodes of eruption; further, Fisher & Schmincke (1984) showed that different eruptive phases separated by small time intervals can give rise to complexity regarding compositional variations and eruption styles. More recent research has focussed on the stratigraphic architecture and geochemistry of single volcanoes, leading to the observation that each monogenetic volcano is unique. Some feature multiple separate batches of magma, and are therefore polymagmatic (whereas volcanoes featuring a single batch of magma are monomagmatic; e.g., Brenna *et al.* 2010), or show compositional variations within their eruption sequences. Such volcanoes, when produced from a single series of eruption events, cannot be defined as polygenetic (e.g., Brenna *et al.* 2010). Other volcanoes feature time-breaks between eruption phases, making them polycyclic. Monogenetic volcanoes also show great complexity in their eruption styles, with a range of styles evident in the stratigraphic record of

individual volcanoes from effusive lava extrusion to violent explosive events involving interaction with groundwater (phreatomagmatism; e.g., van Otterloo *et al.* 2013).

Complexity within individual monogenetic volcanoes has been detailed at relatively few sites worldwide in this emerging field of volcanology. Sequential eruption of two magma batches occurred at Parícutin, in the Michoacán-Guanajuato Volcanic Field, Mexico (Luhr 2001; Erlund *et al.* 2010), Brush Mountain, Round Barn Cones and two cones on the Popcorn Cave mafic shield, in the southern Cascades (Strong & Wolff 2003) and Udo, Jeju Island, South Korea (Brenna *et al.* 2010, 2011). Also on Jeju Island, the Ichilbong tuff cone erupted 2 or 3 magma batches (Sohn *et al.* 2012). Simultaneous eruption of two magma batches occurred at the Mt Gambier maar–cone volcanic complex, Newer Volcanics Province (NVP), Australia (van Otterloo *et al.* 2014) and also at the Red Rock maar–cone volcanic complex, NVP (Piganis 2010; Blaikie *et al.* 2012). Two magma batches erupted at Xitle, central Mexico, during late-stage mixing or recharge (Cervantes & Wallace 2003). This conclusion was based on melt inclusion analysis.

Compositional variation within eruption sequences has been found on Jeju Island, Korea, where the Songaksan and Suwolbong volcanoes each erupted pulses of single, rapidly evolving magma batches (Brenna *et al.* 2011). Complex stratigraphic architectures with multiple vents and preserved facies have been documented at Tower Hill in the NVP (Prata 2012), and Crater Hill, Auckland (Smith *et al.* 2008).

Polycyclic volcanoes have been documented in the NVP at Lake Purrumbete, one of the largest maar volcanoes in the world, where a single batch of magma was erupted in a complex sequence of events that involved a <16 year hiatus in the eruption sequence (Jordan *et al.* 2013). Other examples are Lady Julia Percy Island, also in the NVP, that featured a hiatus of ~1.58 Myr (Edwards 1994; Edwards *et al.* 2004) and Rangitoto in the Auckland Volcanic Field, where two discrete batches of magma were erupted, separated by a hiatus of 60 years (Needham *et al.* 2010).

Many monogenetic volcanic fields are in highly populated areas (for example the Auckland Volcanic Field, New Zealand) or contain cities or towns within their limits (such as the Newer Volcanics Province, southeast Australia and Mexico City, Mexico). It is important to gain a fuller understanding of the nature of volcanism in such areas to assist with hazard and risk analysis (e.g. Joyce 2004; Bebbington & Cronin 2011; Auckland Council 2013). Since there have been few studies involving detailed and systematic stratigraphic analysis of individual monogenetic volcanoes the processes giving rise to changes in eruption styles both within a single volcano and across volcanic fields are not well understood (Houghton *et al.* 1999). Such changes may be influenced by the inherent properties of the magma, source melting processes and fractionation of ascending magmas within the magma plumbing system as well as the properties of the country rock with regards to aquifers and hence magma:water interaction during ascent.

The Pliocene–Recent NVP of southeast Australia is an excellent candidate for further studies of monogenetic volcanism. The NVP is an intraplate monogenetic volcanic field, covering >19 000 km² from Melbourne, Victoria to the Mt Burr range in southeast South Australia. Composed of the volcanic products of >400 short-lived basaltic volcanoes, the stratigraphic record shows that, while effusive and mildly explosive eruptions dominate (e.g., from lava shields and small scoria cones), the NVP has also given rise to violently explosive phreatomagmatic eruptions forming the base surge deposits of substantial maar volcanoes, and several pyroclastic flow events. With the last eruption occurring at Mt

Gambier at ~ 5000 BP (Blackburn 1966; Barbetti & Sheard 1981; Blackburn *et al.* 1982; Robertson *et al.* 1996; Gouramanis *et al.* 2010) and an eruption frequency of ~ 1: 11 500 yrs (Cas *et al.* 1993) the NVP is considered an active volcanic province. This is highlighted by geophysical studies indicating elevated surface heat flow in several areas as well as the occurrence of mantle-derived CO₂ across the province and the presence of partial melts in the mantle under the northeastern section of the NVP (Wopfner & Thornton 1971; Chivas *et al.* 1983, 1987; Cartwright *et al.* 2002; Graeber *et al.* 2002; Aivazpourporgou *et al.* 2012; Davies & Rawlinson 2014). Despite this, no volcanic contingency plans are in place in case of future eruption and very few individual volcanoes have been studied in great detail, with research instead focussing on analysis of the province as a whole, especially in terms of its geochemistry and geodynamics. Although the numbers of volcanoes are generally well constrained, there are discrepancies between different studies, meaning that volcanic distribution maps should be updated from that of Joyce (1975).

It is therefore important to gain a fuller understanding of the nature of volcanism in the NVP in order to more realistically assess the hazard and risk in southeast Australia in terms of future eruptive events. In addition, further studies will contribute to petrogenetic and geodynamic modelling of the NVP and the study of other monogenetic fields, especially the emergent field of complex monogenetic volcanoes, a concept that may be the norm rather than an exception as more monogenetic centres are studied in detail. The wide range of eruption styles present across the NVP, and the fact that many volcanoes are known to feature the products of multiple eruption styles erupted in complex sequences of events, indicates that monogenetic volcanoes cannot be defined as ‘simple’ as great complexity exists in such volcanoes and each volcano erupting in such a volcanic field should be considered unique.

1.1.1 The Mt Rouse magmatic volcanic complex

Mt Rouse, a magmatic volcanic complex situated in the Western Plains subprovince of the NVP has been the focus of several previous studies. The volcano is the largest eruption source within the NVP, triple the size of any of the numerous other NVP volcanoes, in terms of both area covered and volume erupted (Elias 1973), with lava flows extending >60 km to the coast at Port Fairy (Sutalo 1996). The centre rises 120 m above the surrounding lava plains, and is composed of a main scoria cone with two overlapping craters running E–W and breached to the west. The volcano shows great complexity in terms of its eruption styles and morphology and, while certainly a complex monogenetic volcano, previous research based on a few geochemical analyses of scoria suggest that it may also be polymagmatic (Elias 1973), leading to the geochemical study outlined in this thesis. The main scoria cone features an extensively weathered spatter rampart (Whitehead 1986), while to the south is a third crater containing a low scoria cone (Ollier 1985; Whitehead 1986, 1991; Sutalo 1996; Sutalo & Joyce 2004). Two small satellite cones have been reported west of the main cone (Elias 1973). The northern scoria cone is reported to be the oldest feature of the complex (Joyce & Sutalo 1996), while the southern cone is younger, being the source of the small lava shield. The consensus is that the main 60 km of lava flows were emplaced before the scoria cones built up (Ollier 1985; Sutalo 1996; Joyce & Sutalo 1996). Geochemically, the products of Mt Rouse have been described as silica undersaturated alkali olivine basalts (Elias 1973; Whitehead 1986, 1991; Sutalo 1996). Few scorias were analysed,

but results suggest a complete chemical gradation from the lava field basalts to the basanitic northern scoriae (Elias 1973). A single geochemical analysis of a weathered sample from the spatter rampart features low values of SiO_2 and total alkalis, plots apart from other data and may represent a distinct magma type. Whitehead (1986) suggests that the origin of this material was a fractionated source due to its high differentiation index and low Mg-value, associating the composition with waning volcanism. He also postulated the existence of 2–3 magma batches for the lava flows from the available scattered Sr-isotope data. In addition, a small basanite dome is found 5 km to the south of Mt Rouse amongst the lava flows. This feature differs petrographically, geochemically and isotopically to the products of Mt Rouse, and is thought to be an eruption point along a north–south fissure, older than the lava flows (Whitehead 1986, 1991). Sutalo & Joyce (2004) hypothesise that the feature is a separate, older volcano, and unrelated to the Mt Rouse complex.

This thesis explores the NVP with new volcanic distribution maps, updating both numbers of eruption centres (volcanoes) and individual eruption points (vents) across the province. The Hamilton area of the Western Plains sub-province (the location of Mt Rouse) is explored in more detail to identify volcanoes and define phases of eruption in the area. Mt Rouse is then examined in detail, utilising detailed stratigraphic and geochemical analysis in order to constrain the stratigraphic architecture of the volcano. The petrogenesis of the complex is explored, including modelling of the temperature and depth of magma formation, and a new eruption sequence is outlined. Finally, the results will be discussed in the context of monogenetic volcanism and the NVP.

1.2 Thesis aims

Below is a summary of the research questions addressed in this thesis, and the processes used to answer them:

1. What is the nature of volcanism in the Hamilton area of the NVP in terms of numbers of volcanoes, magma types and eruption ages?
 - To identify volcanoes in the area of Mt Rouse in order to place the volcano in a local context, including reconnaissance geochemical analysis to distinguish phases of eruption and compositional changes in the area over time.
 - To produce a new map of the volcanoes in the Hamilton area of the NVP (and the NVP as a whole).
2. Why is there a sequence of alternating eruption styles from effusive (lavas) to explosive (pyroclastic deposits) present at Mt Rouse?
3. What was the petrogenesis of Mt Rouse? Is Mt Rouse a mono- or polygenetic volcano?
 - Combined stratigraphic and geochemical analysis of the scoria cones and lava fields to outline a more detailed eruption sequence for the volcano and identify and geochemical trends that are associated with eruption styles.
 - Modelling based upon geochemical data to help constrain the depth of mantle source melting. A better understanding of how basaltic magmas form and evolve has important implications for crust forming processes, and will help constrain models for the formation of NVP volcanism.

1.3 Tectonic setting of southeast Australia

Australia is situated within the interior of the Indo–Australian plate, and is considered tectonically passive (Figure 1.1) (Twidale & Bourne 1975; Ollier 1978). Southeast Australia is bounded by the Antarctic plate (spreading ridge) and the Pacific plate (subduction zone and collisional boundary). Although the continent is considered passive, present-day stresses in southeastern Australia point to a maximum horizontal compressive stress oriented NW–SE, controlled by plate boundary forces (Hillis *et al.* 2008).

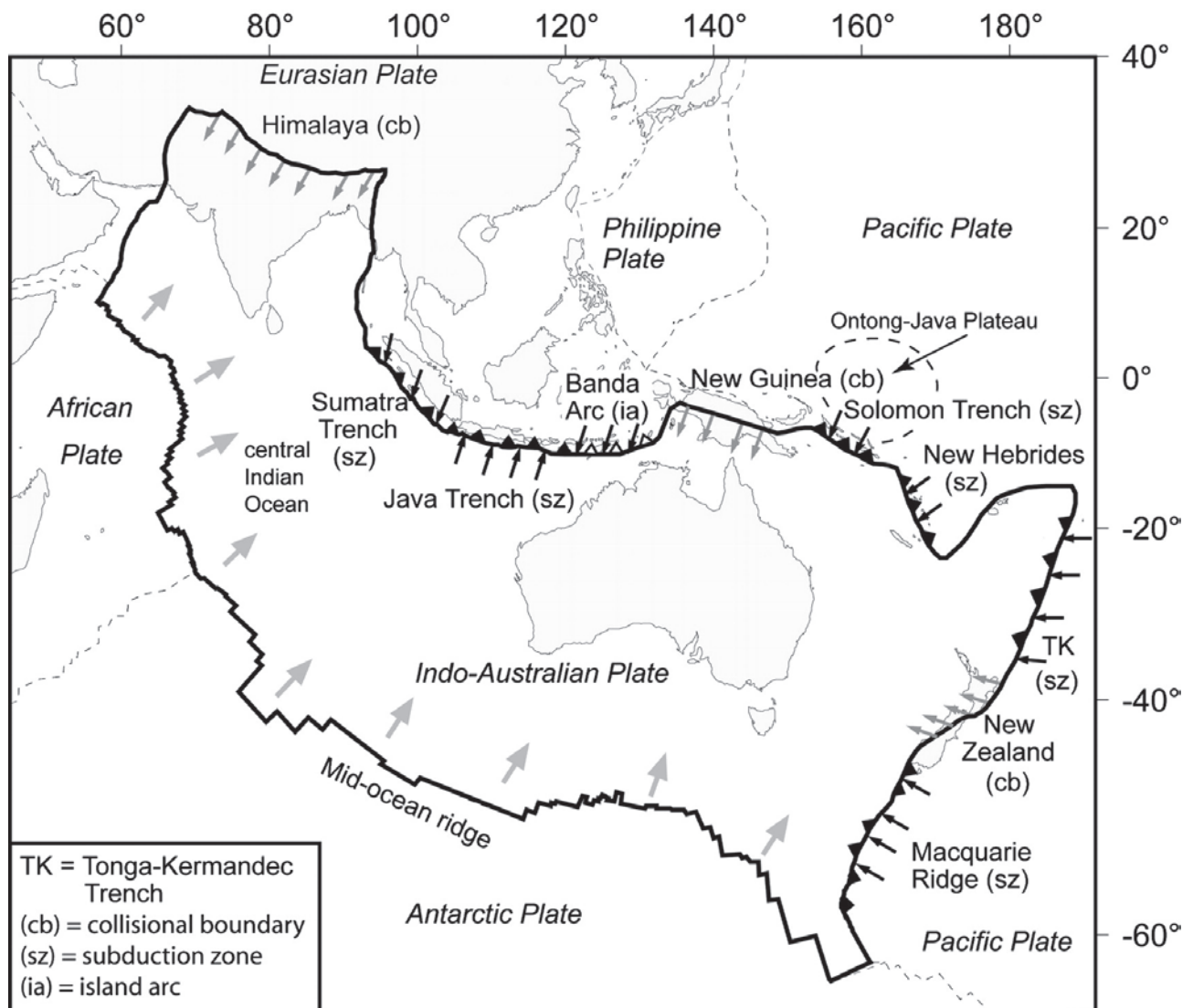


Figure 1.1 Tectonic setting of Australia, showing plate boundaries and present-day forces. Small black arrows show slab pull forces, large grey arrows show mid-ocean ridge push force and small grey arrows show resisting continent–continent collisional forces (Reynolds *et al.* 2003; Hillis *et al.* 2008).

The basement rocks of the NVP are composed of the Mesozoic–Cainozoic sedimentary rocks of the Otway Basin to the south, and parts of the Palaeozoic Delamerian and Lachlan fold belts to the north, within the Tasman Fold Belt System (VandenBerg *et al.* 2000; Gray *et al.* 2003; Lesti *et al.* 2008) (Figure 1.2). The Moyston Fault is an important lithospheric structure, as it forms the suture between the Delamerian and Lachlan orogens (Korsch *et al.* 2002; Cayley *et al.* 2011).

The Delamerian Orogeny occurred in the Late Cambrian (515–495 Ma), causing regional metamorphism, folding and faulting of Neoproterozoic–Cambrian rocks. The fold belt extends ~400 km west of the Moyston Fault into southeast South Australia (the edge of the Gawler Craton; Figure 1.3). A small portion of Delamerian rocks are exposed in Victoria, as Murray Basin sediments overlie

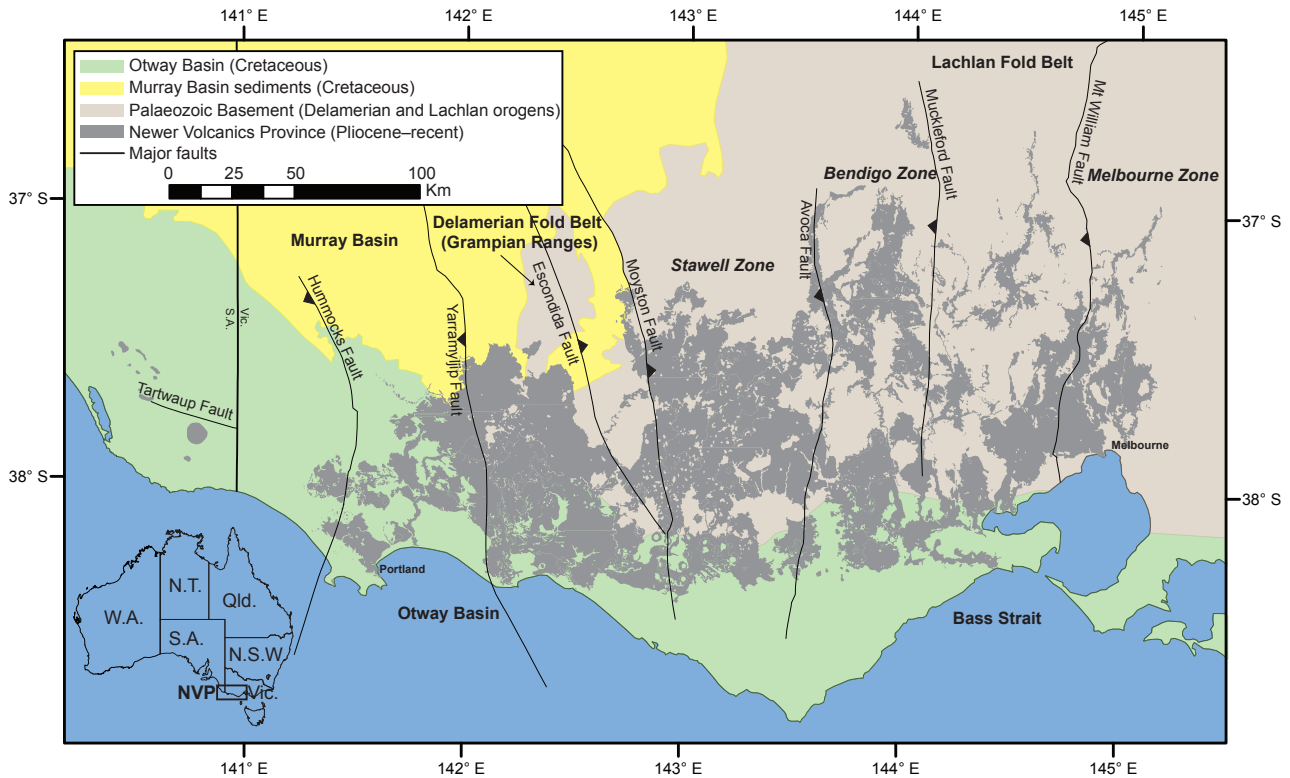


Figure 1.2 Geological map of western Victoria and southeast South Australia, showing main terranes and lithospheric structures. Faults taken from Simons & Moore (1999), terranes from Duddy (2003) and Lesti *et al.* (2008).

the majority. The Glenelg and Grampians–Stavely Zones (Harrington *et al.* 1974; VandenBerg 1978) are separated by the Yarramyllup Fault (Figure 1.3). The Glenelg Zone is composed of the Moralana Supergroup of carbonates and sandstone, plus intraplate and MORB basalts. The Grampians–Stavely Zone is made up of the Mount Stavely Volcanic Complex, Glenthompson Sandstone and the Dimboola Igneous Complex, unconformably overlain by the Grampians Group and Rocklands Volcanics (Figure 1.2). The Mount Stavely Volcanic Complex was deposited in a post-collisional continental rift setting (VandenBerg *et al.* 1995; Crawford *et al.* 1996), while the Dimboola Igneous Complex is from an unknown setting, thought to be an arc-forearc (Berry & Crawford 1988; Crawford & Berry 1992; VandenBerg *et al.* 2000). The Glenelg Zone was much more strongly deformed during the Delamerian Orogeny, characterised by northeast–southwest shortening which produced north/north-westerly structures. The Grampians–Stavely Zone shares the structural trends of the Glenelg Zone, but was less strongly deformed, and features lower metamorphic grades (VandenBerg *et al.* 2000).

The Lachlan Fold Belt is composed of deformed Cambrian–Devonian volcanic and granitic rocks, turbidites and cherts (Cas 1983; Gray & Foster 1997; Foster & Grey 2000). The fold belt is split into the Whitelaw and Benambran Terranes, west and east of the Governor Fault. The Whitelaw Terrane forms the basement to the NVP, and is further subdivided into the Stawell, Bendigo and Melbourne Zones accordingly (Figure 1.3; VandenBerg *et al.* 2000). The Whitelaw Terrane was affected by the Benambran and Tabberabberan Orogenies. The Benambran Orogeny (Late Ordovician–Early Silurian, 455–425 Ma) (Browne 1947; Foster *et al.* 1966a, b; Gray *et al.* 1997; VandenBerg 1999) was the main deformation event in the Bendigo and Stawell Zones, with minor deformation occurring at the margins of the Melbourne Zone; there was east–west contraction with 50–70% shortening (Cox *et al.* 1991; Gray & Willman 1991; Cayley & Taylor 2001). This major event caused the western margin of the Stawell Zone to be thrust over the Delamerian Fold Belt (Figure 1.3; Graeber *et al.* 2002; Cayley *et al.* 2011). The Benambran Orogeny was followed by a period of uplift and erosion and

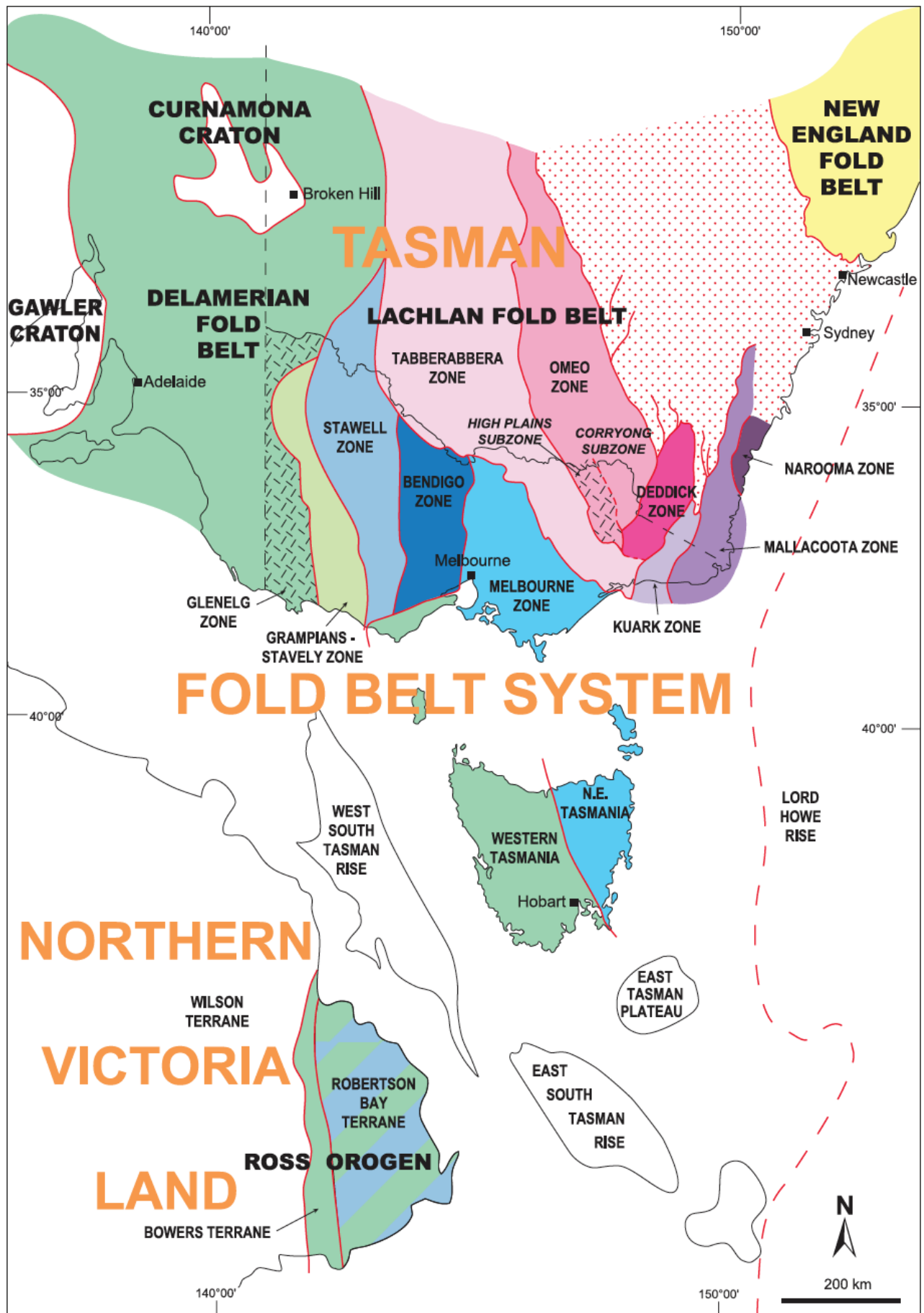


Figure 1.3 Eastern Australian fold belts and Victorian structural zones. Green colours indicate Delamerian/Tyennan fold belts, blue colours cover the Whitelaw Terrane. Reds and purples indicate the Benambra Terrane with only the zones extending into Victoria fully covered (VandenBerg *et al.* 2000).

the emplacement of post-tectonic granites (410–400 Ma, VandenBerg 1978; Rossiter 2003), before the Tabberabberan Orogeny caused a second period of east–west shortening in the Melbourne Zone during the Mid-Devonian (385–380 Ma). There was a short period of weak north–south shortening, and the orogeny caused fault reactivation in the Bendigo and Stawell Zones, with minor faulting. The Tabberabberan Orogeny was succeeded by a second period of uplift and erosion, and additional post-tectonic granite intrusions in the Bendigo and Melbourne Zones ~370 Ma (VandenBerg *et al.* 2000).

During the Early Carboniferous, the Kanimblan Orogeny (350–325 Ma) stabilised the southeast Australian crust, and cratonisation was complete (Gray 1997; VandenBerg *et al.* 2000). The southern continental margin of Australia, including Victoria's Otway, Bass and Gippsland Basins, were subsequently formed as a consequence of rifting associated with the breakup of Gondwana (Figure 1.2). Rifting, which resulted in the separation of Australia and Antarctica, began in the Late Jurassic–Early Cretaceous (Weissel & Hayes 1977; Mutter *et al.* 1985; Veevers 1986; Stagg *et al.* 1990; Drexel *et al.* 1993; Gaina *et al.* 2003). Breakup was complete by 90 Ma (Cande & Mutter 1982) and seafloor spreading began to form the Tasman Sea.

The coeval Bass and Gippsland Basins represent failed rift basins, and are separated from the Otway Basin by the Mornington Peninsula. The Otway Basin represents a passive margin and underlies the southern half of the NVP. It is an east–west trending graben west of Melbourne, extending 500 km to South Australia (Figure 1.3). The Otway Basin is filled by the five major successions that make up the Otway Supergroup, as well as the Sherbrook, Wangerrip, Nirranda and Heytesbury Groups. Sequence stratigraphy of the Otway Basin recognises several major phases (Jensen–Schmidt *et al.* 2002; Krassay *et al.* 2004), as shown in Figure 1.4 and summarised below:

- Rifting during the Tithonian–Barremian (Late Jurassic–Early Cretaceous) relating to the breakup of Gondwana resulted in the deposition of the Crayfish group of continental and fluvio-lacustrine sediments in a series of E–W trending half-grabens.
- Deposition of the Eumeralla Supersequence of volcanoclastic, fluvio-lacustrine and marine sediments occurred during the Aptian–Albian post-rift phase of continental sag when the Otway Basin subsided and widened. This ended deposition of the Otway Supergroup.
- Compression and inversion during the Mid-Cretaceous.
- Marginal sag during the Cenomanian (Upper-Cretaceous) to Eocene. New oceanic crust was formed and the Sherbrook group of deltaic and marine sediments were deposited in a continental shelf-type setting.
- The sub-basins of the Otway Basin were formed in the Late Maastrichtian–Mid Eocene, including the Gambier, Tyrrendarra and Port Campbell Embayments during several periods of uplift and erosion. The Wangerrip group mudstones including deposition of the Dilwyn Formation were deposited during this time.
- Mid Eocene–Early Oligocene clastic and carbonate deposition of the Nirranda group; inversion and thermal subsidence; Late Miocene uplift and erosion.
- Basin inversion due to NW–SE compression from the Miocene to the present resulted in deposition and uplift of the Bridgewater Formation sands and muds.
- Heytesbury group deposition during the Plio-Pleistocene, including the Gellibrand Marl and Port Campbell Limestone.
- Pliocene–recent volcanism, as described in section 1.6.

The subsurface structures beneath southeast Australia in the region of the Otway Basin comprise a series of major N–S inverse faults and minor E–W and NW–SE trending normal faults and (Figure 1.5; e.g., Simons & Moore 1999).

The major N–S faults in central and western Victoria are (E–W) the Hummocks, Yarramyljup, Escondida, Moyston, Avoca, Muckleford and Mt William Faults (Figures 1.2, 1.3). The structural zones associated with these faults are the Glenelg Zone (South Australia border to Yarramyljup Fault), Grampians–Stavely Zone (Yarramyljup to Moyston Faults), Stawell Zone (Moyston to Avoca Faults) and Bendigo Zone (Avoca to Mt William Faults) (see above). Throws of the major faults are in the order of 1–2 km (Gray *et al.* 2003)

The Glenelg Zone runs between South Australia and the Yarramyljup Fault, after which the Grampians–Stavely Zone runs to the Moyston Fault. Together they represent a poorly understood series of northwest-trending fault-bounded strips (VandenBerg *et al.* 2000). The Hummocks Fault (Glenelg Zone) and Yarramyljup Fault both dip to the west (Morand *et al.* 2003; R. Cayley pers. comm. 2014). The Yarramyljup Fault dips to the west just east of Mt Rouse (R. Cayley pers. comm. 2014) and was previously interpreted as 20 km west of Mt Rouse (e.g., Figure 1.2; Gray *et al.* 2003; Cayley *et al.* 2011).

The Escondida Fault in the Grampians–Stavely Zone dips to the east (Gray *et al.* 2003) and joins the Moyston Fault in the Shadwell area, which is an easterly-dipping deep-crustal structure, extending to the Moho (Cayley *et al.* 2011) and forms the suture between the Delamerian and Lachlan fold belts (Cayley & Taylor 2001; Korsch *et al.* 2002).

The Bendigo and Stawell zones that represent the Delamerian Orogen are part of a thick-skinned, easterly-vergent, crustal-scale fault system bound by the Moyston Fault to the west and the Mt William Fault to the east (Figures 1.2, 1.3). Low-angle faulting predominates at mid–lower crustal levels in the Cambrian mafic rocks and intercalated metasediments, and tight folding at upper crustal levels in metasediments (Cayley *et al.* 2011). The Avoca, Muckleford and Mt William Faults are all westerly-dipping, with the Avoca and Muckleford Faults being reverse in nature (Gray *et al.* 1988; Joyce 2007; Cayley *et al.* 2011). The Avoca Fault terminates mid-crust against the Moyston Fault (Cayley *et al.* 2011).

The minor E–W and NW–SE trending faults in Victoria show <50 m of displacement and are generally reverse in nature. They are accommodation structures associated with the axial traces of the regional folds (Gray *et al.* 2000).

Some of these faults may have acted as preferred pathways for magma ascent during the eruption of the recent episodes of volcanism in southeast Australia (see Chapters 2 and 3). Examples include the volcanoes of the Mt Burr Range, South Australia (Sheard 1990), the Lake Purrumbete maar volcano near Camperdown (Jordan *et al.* 2013) and the Mt Gambier maar–cone complex (van Otterloo *et al.* 2014). The Avoca Fault may have influenced the eruption of the volcanoes in the Lexton–Ballarat area (Mt Mitchell to Weatherboard Hill; Boyce 2013), where W/NW and N/NE jointing is thought to control the distribution of volcanic centres (Joyce 2007). The Mt William Fault may have influenced the eruption of volcanoes in the Goldie region, as several volcanoes lie close by (Boyce 2013). The Moyston Fault coincides with several maar volcanoes in the Noorat–Terang–Ecklin area (Boyce 2013). For further examples see Boyce 2013/Chapter 2.

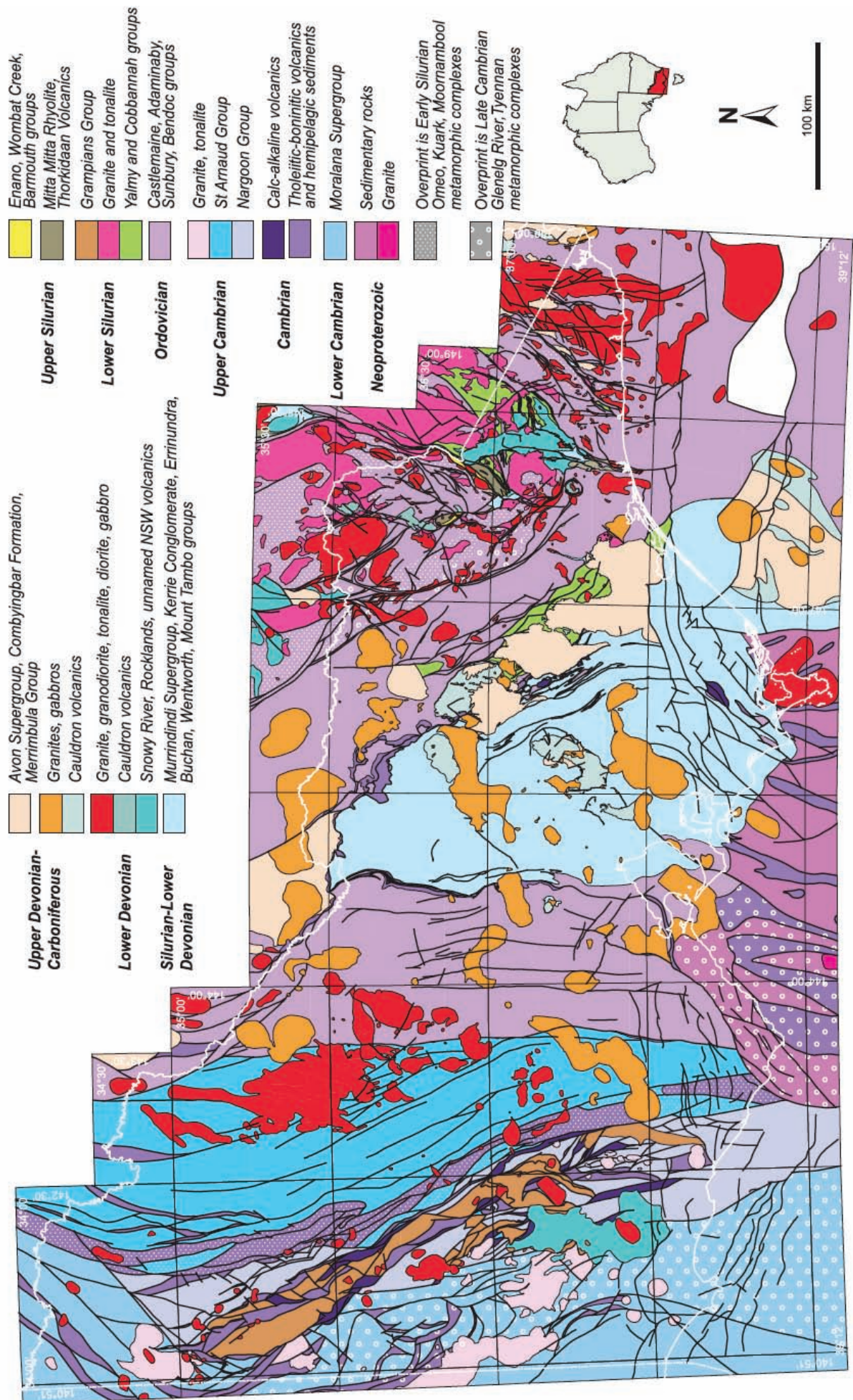
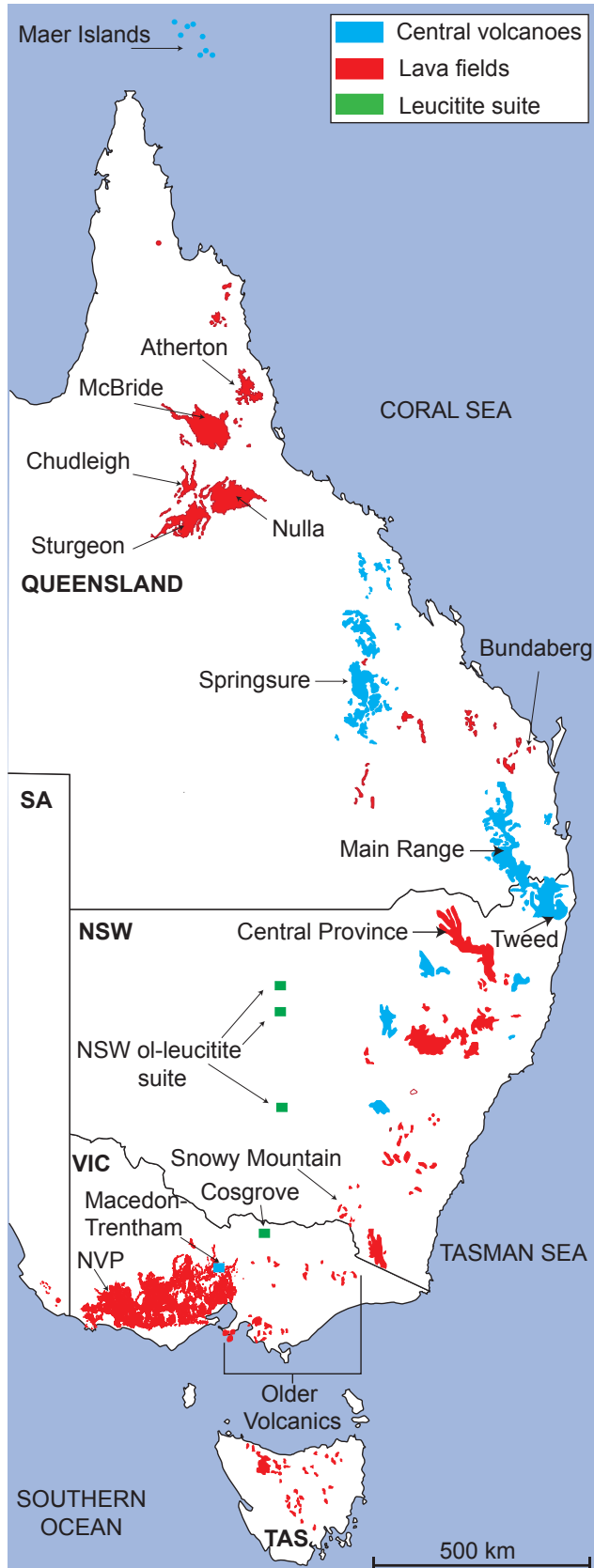


Figure 1.5 Pre-Permian geology of Victoria showing main structures as solid lines (VandenBerg *et al.* 2000).

1.4 Eastern Australian intraplate volcanism

Intraplate volcanism is that which has occurred away from the edges of tectonic plates. Eastern Australia has experienced intraplate basaltic volcanic activity since Jurassic times, with volcanic provinces stretching 4400 km down the eastern seaboard of Australia from the Maer Islands situated in the Torres Strait to the north, and down the Great Dividing Range to Tasmania and Victoria (Figure 1.6; Johnson & Wellman 1989).



The youngest expressions of volcanism are found in northern and southern Queensland, and southeast Australia to South Australia. In northern Queensland, the Atherton Province covers 2500 km², comprising 65 basaltic volcanoes (De Keyser & Lucas 1968; Stephenson 1989; Whitehead *et al.* 2007) dated to 7.06 Ma to <10 ka (Kershaw 1971, 1975; Atkinson 1986; Head *et al.* 1994; Whitehead *et al.* 2007). The McBride Province southwest of Atherton covers 5500 km² and contains 164 volcanoes (Griffin 1977; Stephenson 1989; Whitehead 2010) that have ages ranging from 8 My to 50, 000 BP (Griffin & McDougall 1975; Stephenson 1989; Gibson 2007). The Chudleigh, Sturgeon and Nulla Provinces (containing a total of ~144 volcanoes) form an almost continuous area of basaltic volcanism. The Chudleigh Province, which covers 2000 km², has ages ranging from 7 Ma to 0.25 Ma (Stephenson 1989); the Sturgeon Province covers 75 km² and has been dated to 5.5–0.92 Ma (Stephenson 1989; Stephenson & Griffin 1976); and the Nulla Province covers 7500 km², dated at 5.2 Ma to 13, 000 BP (Stephenson *et al.* 1978). Small-volume basaltic volcanic provinces in the Bundaberg area of southern Queensland, include the 1.1–0.9 Ma Hummock Basalt (Wellman 1978; Robertson *et al.* 1989), the late-Pleistocene Berrembea Basalt (Robertson 1985) and the 0.6 Ma Barambah Basalt (Wellman 1978). Finally, the Newer Volcanics Province of southeastern Australia contains >437 volcanoes

Figure 1.6 Map of eastern Australia showing the distribution of volcano types (modified after Wellman & McDougall 1974 and Johnson & Wellman 1989).

and extends from Melbourne, Victoria to southeast South Australia and has been dated from 8 Ma to 5000 BP (Blackburn 1966; McDougall *et al.* 1966; Barbetti & Sheard 1981; Blackburn *et al.* 1982; Cayley *et al.* 1995; Robertson *et al.* 1996; Edwards *et al.* 2004; Gouramanis *et al.* 2010; Boyce 2013).

Wellman & McDougall (1974) recognised three types of volcanic occurrences in eastern Australia—central volcano provinces, lava fields and leucitite suites (Figure 1.6). These volcano types are based on petrology; volcanological distinction is less clear, as many volcanoes of the central volcanoes type are not classic shield volcanoes, but rather plugs and residual lavas (Johnson & Wellman 1989). A description of the three types follows:

1. Central volcano provinces. Large volcanoes (30–100 km across) of predominantly basaltic eruptions from central vents. Felsic flows and both mafic and felsic intrusions are also found. Smaller provinces with felsic (rhyolite, trachyte, phonolite) flows, for example the Macedon–Trentham province of Victoria are also included in this classification (Wellman & McDougall 1974; Johnson & Wellman 1989). Examples of central volcanoes include the Springsure volcano (Veevers *et al.* 1964), the Tweed volcano (Wilkinson 1969), Nandewar volcano (Abbott 1969) and Main Range (Johnson & Wellman 1989).
2. Lava fields. Basaltic volcanism resulting in extensive lava fields of thin extensive flows (e.g., the NVP or north Queensland), or lava piles up to 1000 m thick. Lava fields may contain numerous small scoria cones, lava shields and maars. Other examples include the Snowy Mountain lavas (Mackenzie & White 1970), the Older Volcanics, Victoria (Edwards 1939) and the Central Province of New South Wales (Vallance *et al.* 1969).
3. Leucitite suite volcanoes. Minor intrusions and rare lavas which are mafic and highly potassic, petrologically and geochemically distinct from lava fields and central volcanoes. Examples include central New South Wales olivine leucitite (Joplin 1963) and Cosgrove, Victoria (Knutson 1989).

Estimates of volume are limited due to the extent of denudation and the difficulties of thickness estimation of the lavas; the total volume of eastern Australian volcanics is 20 000 km³ (Wellman & McDougall 1974), subdivided into 9000 km³ of central volcano products and 11 000 km³ of lava fields, with negligible volumes of leucitite volcanics (Johnson & Wellman 1989).

1.4.1 Cainozoic volcanism in southeast Australia

Volcanism of Late Cretaceous to Quaternary age in southeastern Australia can be divided into three groups (Figure 1.7): the 95–19 Ma Older Volcanics (Day 1983; Price *et al.* 2014), the 7.0–4.6 Ma Macedon–Trentham group (Wellman 1974; Dasch & Millar 1997; Ewart *et al.* 1985) and the 4.5 Ma to *ca* 5000 BP Newer Volcanics Province (Blackburn 1966; McDougall *et al.* 1966; Blackburn *et al.* 1982; Gray & McDougall 2009; Gouramanis *et al.* 2010).

The Older Volcanics outcrop in the eastern half of Victoria as relatively small, eroded lava fields 10–130 km across and some small dykes and plugs; compositions range from nephelinite to tholeiite. The Older Volcanics have been subdivided into fifteen provinces based on age and composition, and then four groups by age and distribution (Singleton & Joyce 1969; Day 1983, 1989; Knutson 1989;

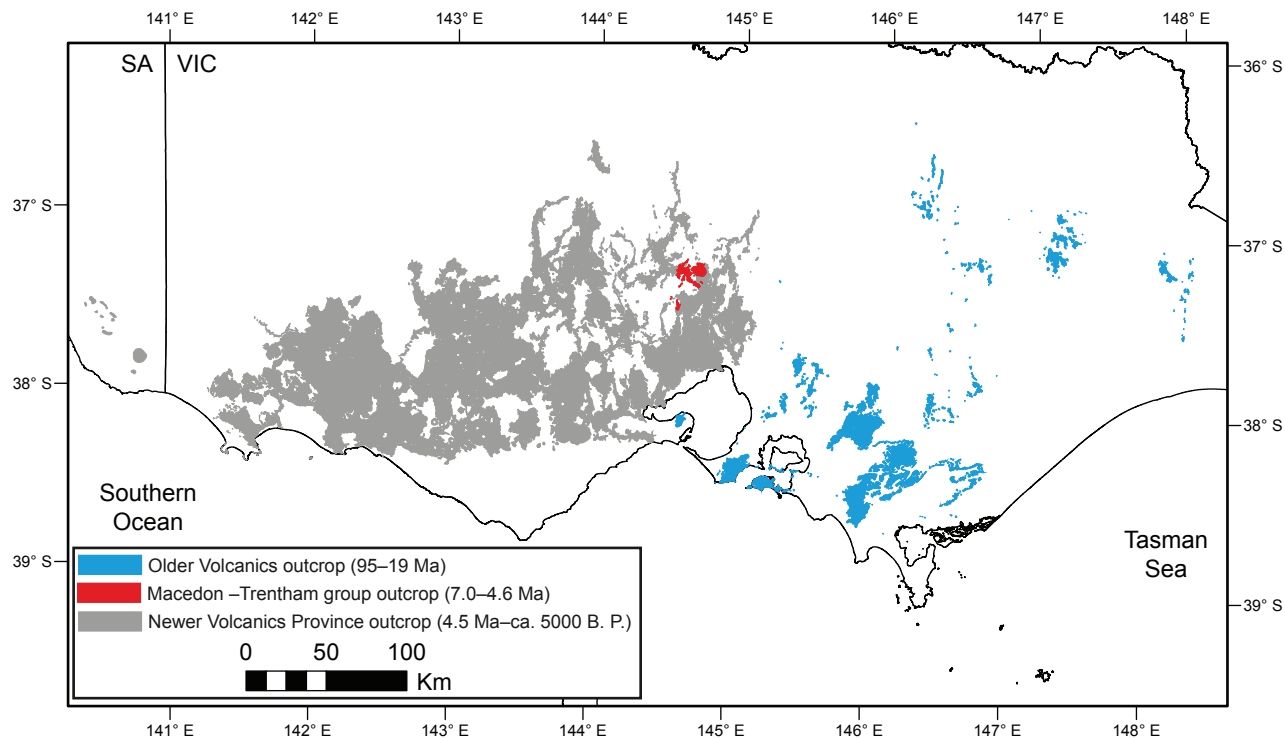


Figure 1.7 Distribution of Cainozoic volcanic rocks in Victoria.

Cas *et al.* 1993). Many of the products are subsurface, and erosion has been extensive; however, minimum volumes are estimated at 1500 km³ (Wellman 1971). Price *et al.* (2003) and VandenBerg (2007) discard the term Older Volcanics and instead refer to the eruption products as the Eastern Province, South Coast Province and Latrobe Province, however the terms Older and Newer Volcanics are still in use, as is the case in this study.

The Macedon–Trentham group outcrop northwest of Melbourne within the districts of Woodend, Trentham and Mt Macedon-Lancefield, and were previously referred to as the Woodend province (Ewart *et al.* 1985). The group contains the only Cainozoic rocks of felsic composition in Victoria (Edwards 1938; Edwards & Crawford 1940). The volcanics consist of lava domes, small flows, plugs and spines. More than 33 individual eruption centres have been identified (e.g., Singleton & Joyce 1970; Boyce 2013), such as Blue Mountain, Camels Hump and Hanging Rock. The Macedon–Trentham group forms a central volcano province under the classification of Wellman & McDougall (1974). The oldest age of NVP volcanoes in this area is 4.06 ± 0.01 Ma at Mt Gisborne (D. Phillips, pers. comm. 2012). The group is further distinguished from the NVP by their slightly higher strontium-isotopic ratios of $^{87}\text{Sr}/^{86}\text{Sr}$ 0.7042–0.7127 (Dasch & Miller 1977; Ewart *et al.* 1985), compared to the NVP $^{87}\text{Sr}/^{86}\text{Sr}$ 0.7034–0.7058 (Price *et al.* 1997). A wide range of rock types is represented, including basanites, basalts, hawaiites, mugearites, benmoreites and trachytes (e.g., O’Hanlon 1975; Ewart *et al.* 1985; Knutson & Nicholls 1989).

The NVP is the most recent phase of volcanic activity in Australia, extending 410 km from Melbourne in Victoria to the Mt Burr range in southeastern South Australia. The distribution and classification of eruptions is discussed in more detail in section 1.6, and geochemistry in section 1.6.3.

1.5 Origin of eastern Australian volcanism

A single model cannot explain intraplate volcanism in eastern Australia, as it is difficult to correlate timing of volcanism with changes in plate tectonics.

Central volcano provinces and leucitite suite volcanoes show a systematic younging to the south down the eastern seaboard of Australia (Figure 1.8; Wellman & McDougall 1974; Sutherland 1985, 2003; Sutherland *et al.* 2012). Although there is a clear southward progression in the volcanism of the central volcanoes and leucitite suite eruptives, there is much scatter evident for basalts of lava field origins (Figure 1.8; Sutherland 2003).

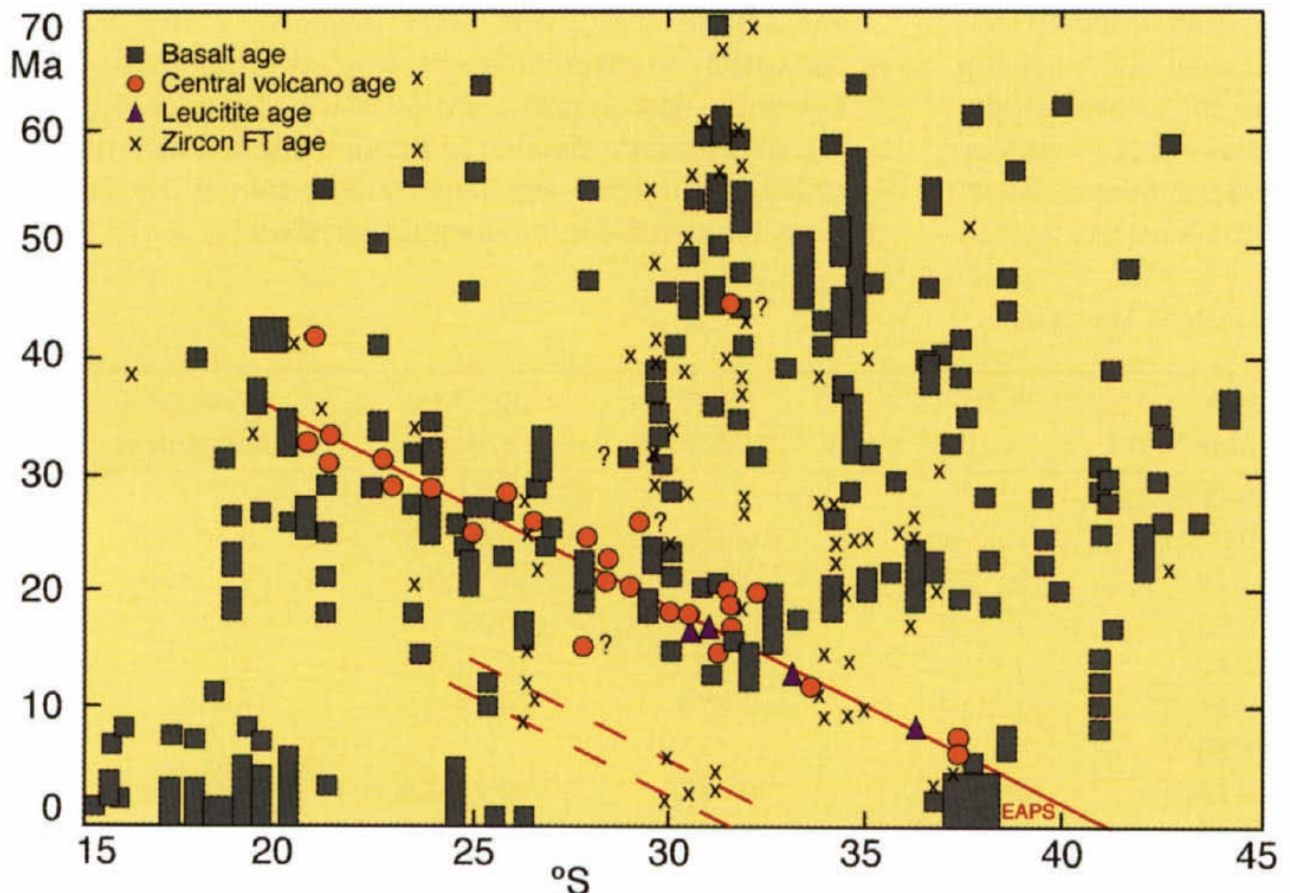


Figure 1.8 Age vs latitude of eastern Australian intraplate activity. Central volcanoes are orange filled circles, basaltic lava fields black filled squares, leucitite lava fields black filled triangles and zircon-bearing eruptives black crosses. The East Australian Plume System volcanic migratory trend (red line) comes from Duncan & McDougall (1989) and the zircon-bearing eruptive trends (red dashed lines) from Sutherland (1993). Data are plotted from Johnson (1989), Ashley *et al.* (1995), Exon *et al.* (1997), Everard *et al.* (1997), Cooper (1999) and other sources given in Sutherland (1991, 1993, 1999, 2003), Sutherland & Fanning (2001), Sutherland *et al.* (2002) and F. L. Sutherland and others unpublished data. From Sutherland (2003).

This southward younging was attributed to the passing of the Australian continent over a number of hot spots, termed the East Australian Plume System (Figure 1.9; Wellman & McDougall 1974; Wellman 1983; Duncan & McDougall 1989; Sutherland 1991; Matsumoto *et al.* 1997; Sutherland 2003). At least three hotspot tracks were invoked. One of these is through continental Australia (whose present-day position is suggested to be beneath Bass Strait (Wellman & McDougall 1974; Sutherland 2003; Kennett & Abdullah 2011; Sutherland *et al.* 2012). A second was through the Tasmanid Guyots and the third through the Lord Howe seamounts (Figure 1.9) (Vogt & Connolly 1971; Shaw 1978; Duncan & Clague 1985; McDougall & Duncan 1988; Duncan & McDougall 1989). The rate of migration of the volcanism has been calculated to be 6.6 mm/yr (Wellman & McDougall

1974), which correlates well with the average rate of separation of Australia and Antarctica, which has been estimated at 50–74 mm/yr (Le Pichon & Heirtzler 1968; McKenzie & Sclater 1971; Wellman & McDougall 1974; Weissel & Hayes 1977). The present position of the hotspot in Bass Strait (Figure 1.9) correlates with a high heat flow anomaly beneath the region and slow seismic velocities (O'Neill *et al.* 2003; Montelli *et al.* 2006).

There have been many variations in the hotspot models of volcanism for eastern Australia. For example, Sutherland (1991) delineated seven hotspots, Pilger (1982) postulated a migrating hotspot line that also included lava fields and Wellman (1983) proposed a single magma source triggering all central volcanoes and leucite suite volcanoes over an area of 800 km by 1900 km (Figure 1.9). Hotspot paths have been debated by Sutherland (1994) and Gaina *et al.* (1999) while experimental plume models have been outlined by Tychkov *et al.* (1998). Recent research suggests that although the Tasmanid Guyots and Lord Howe Seamount chains show well-defined hotspot traces, the central

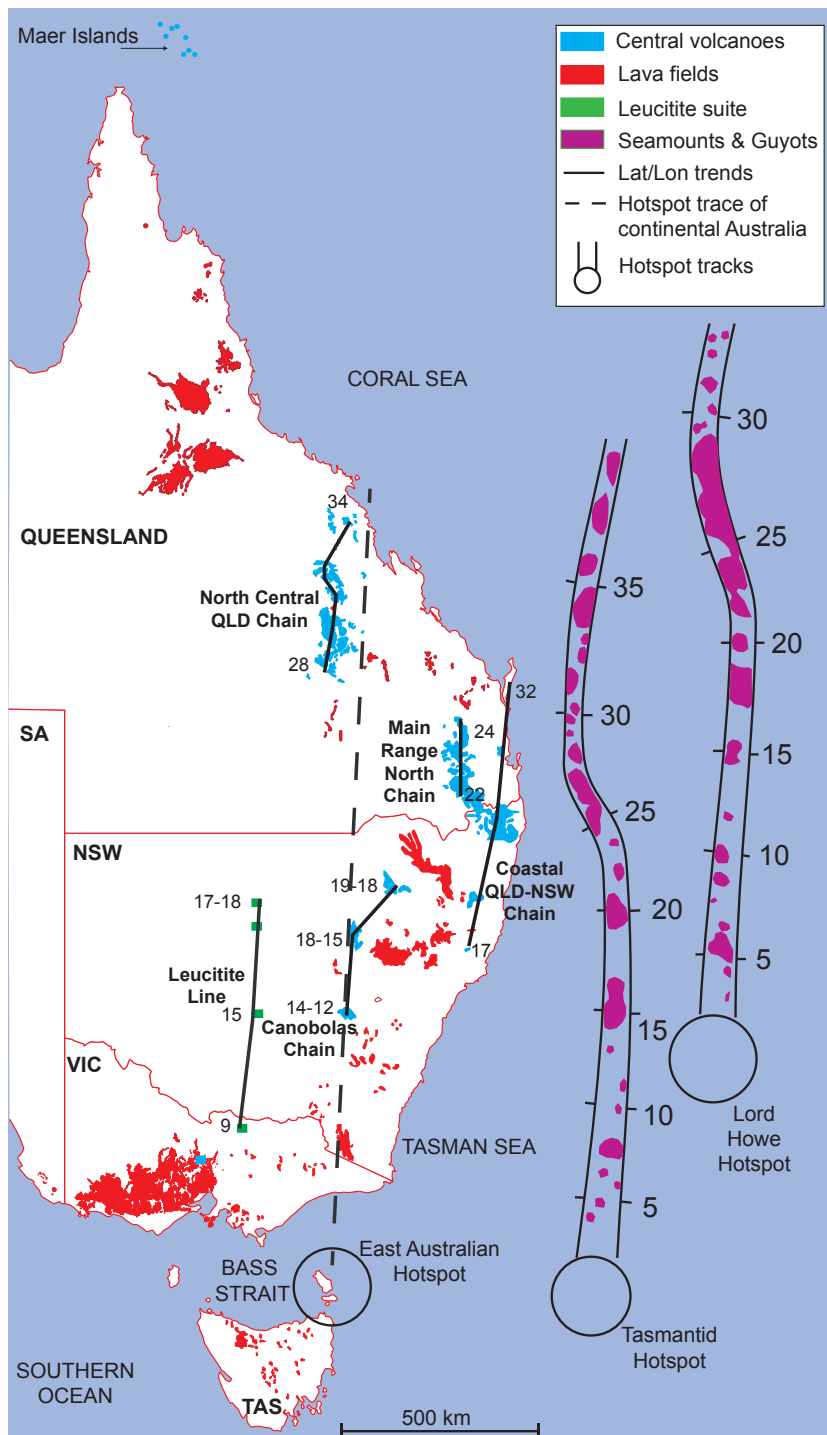


Figure 1.9 Map of eastern Australia showing the distribution of volcano types (modified after Wellman & McDougall 1974 and Johnson & Wellman 1989). Hotspot tracks of the Tasmanid Guyots and Lord Howe Seamounts shown with calculated ages at 5-Myr intervals and the current locations of the hotspots as circles (Knesel *et al.* 2008). Felsic younging trends in continental Australia are shown as solid lines with ages in Ma (Sutherland *et al.* 2012). Dashed line represents inferred hotspot trace for mainland Australia (Wellman 1983; Duncan & McDougall 1989).

volcanoes and leucitite suites of continental Australia instead show several younging trends (shown as black lines on Figure 1.9; Sutherland *et al.* 2012, 2014), making it difficult to relate definitive hotspot tracks to the volcanism (Figure 1.9).

Finn *et al.* (2005) suggested that all Cainozoic alkaline igneous rocks outcropping across the fragments of east Gondwana and adjacent oceanic lithosphere are parts of the “diffuse alkaline magmatic province (DAMP)”. The lateral and vertical flow of warm Pacific mantle generates magma and induces long-lived low-volume magmatism. The flow is triggered by instabilities induced by detached and sunken subducted slabs along the old Gondwana margins in the late Cretaceous.

Hotspot traces were used to explain the origin of the lava fields of the NVP (e.g., Wellman & McDougall 1974; Wellman 1983; Duncan & McDougall 1989; Sutherland 1991; Matsumoto *et al.* 1997). ‘Boomerang’ volcanism has been used to explain the western location of the NVP, whereby hotspot-related activity follows a stepping motion and diverges to the west in order to create large-volume volcanic fields and then back to the east to create small-volume fields. However, a hotspot must be ruled out as the NVP lies to the west of a projected line of volcanism (Price *et al.* 1997) and has an east–west orientation (Cas *et al.* 1993) that differs from the orientation of the theorised continental hotspot trace (Figure 1.6). Dating of volcanic rocks in the NVP has failed to find any age progressions (Gray & McDougall 2009; see section 1.6.2). In addition, despite Australia having drifted >300 km north over the past *ca* 5 Myr (the main timespan of eruption for the NVP), the province extends only ~100 km N–S.

Continental extension is another process used to explain NVP volcanism (Lister & Etheridge 1989; O’Reilly & Zhang 1995; Price *et al.* 1997). This is related to the breakup of Gondwana and the opening of the Tasman sea, whereby extension-induced lithospheric thinning and uplift at the base of the lithosphere is thought to have led to the release of mantle diapirs by thermal instabilities at depths of 200–400 km. These diapirs would take 20–100 Myr to reach the mantle solidus, explaining the presence of volcanism so long after rifting. In addition, extensional faults reactivated by the Tasman Fracture Zone have been argued to influence the activity of the NVP, whereby shear stresses are transferred from the oceanic crust to the continent, deforming along zones of weakness and providing pathways for magma ascent (Lesti *et al.* 2008). However, studies show that southeast Australia has been in a NW–SE compressive stress regime since the Pliocene, which places doubt on this theory (Hillis *et al.* 1995; Sandiford 2003; Sandiford *et al.* 2004).

Edge-driven convection is the most recent theory to explain intraplate volcanism, especially in lava fields such as the NVP (King & Anderson 1988; Demidjuk *et al.* 2007; Farrington *et al.* 2010; Davies & Rawlinson 2014). Steps in lithospheric thickness beneath the Australian continent (Fishwick *et al.* 2008; Fishwick & Rawlinson 2012) set up thermal contrasts due to differential motion between the fast-moving Australian lithosphere and the underlying asthenosphere. This acts to produce convection cells in the upper mantle at the steps in lithospheric thickness which travel with the overlying lithosphere and create upwelling of fertile mantle material downstream of the step (King & Anderson 1988; Demidjuk *et al.* 2007; Farrington *et al.* 2010). These upwellings are thought to be limited to the shallow asthenosphere (Davies & Rawlinson 2014). The upwelling asthenosphere would produce a convection cell 150% of the step-size in lithospheric thickness (Figure 1.10), which means that low seismic velocities would be absent at >200 km depth. It is noteworthy that while low seismic velocities associated with elevated temperatures are present at depth beneath the NVP, they

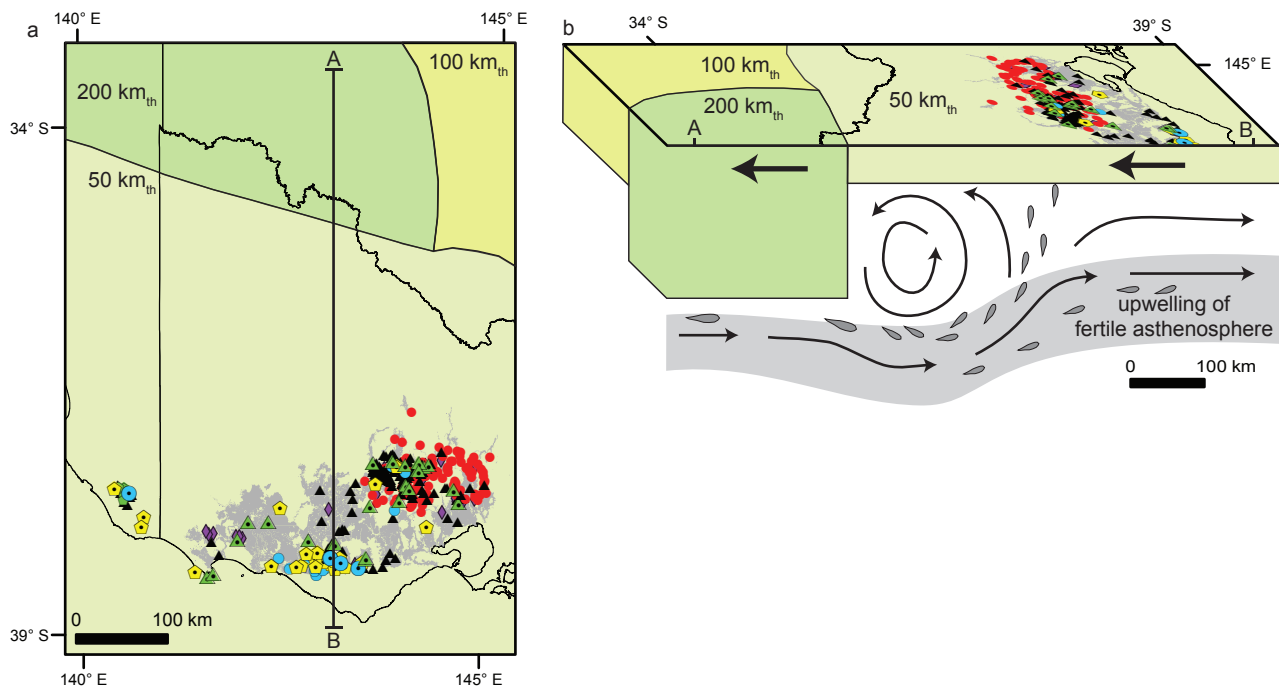


Figure 1.10 a) Southeast Australia, showing NVP outcrop and volcanoes (Boyce 2013) in relation to approximate steps in lithospheric thickness (th) (Fishwick *et al.* 2008); b) Scaled N-S cross section of southeast Australia, showing edge-driven convection, whereby the fast northward motion of the Australian plate relative to the underlying asthenosphere, coupled with steps in lithospheric thickness southwards act to set up convection cells 150% larger than the step size, which permit the upwelling of fertile asthenosphere which is subsequently expressed as volcanism on the surface of the thin lithosphere. Convection cell from Demidjuk *et al.* (2007).

disappear by 200 km depth (King & Anderson 1998; Rawlinson & Fishwick 2012). Recent research indicates that although the main lithospheric step in the region of the NVP is to the north, directly beneath the NVP there is a significant localisation and amplification of mantle upwelling (Rawlinson & Davies 2014). Edge-driven convection may also account for the presence of other young lava field provinces in eastern Australia, which also lie near steps in lithospheric thickness (Figure 1.11).

1.6 The Newer Volcanics Province of southeastern Australia

Classification of the products of the NVP in terms of the numbers and nature of eruption centres in the province are explored in Chapter 2, which was published in the Australian Journal of Earth Sciences in 2013. A summary is provided here in order to place the geochemical data of section 1.6.3 into context. Chapter 2 presents a new classification scheme and new distribution maps of the eruption centres of the NVP alongside a catalogue of these eruption points and centres. This section (1.6) will provide a 2015 update of the material, including updated volcano statistics and volcano distribution maps. It is therefore recommended that the reader familiarise themselves with the content of Chapter 2 before reading further.

The NVP covers an area of more than 19 000 km² in southeast Australia, from Melbourne Victoria to the Mt Burr Range in South Australia and its products range in age from 8 Ma to 5000 BP (Blackburn 1966; McDougall *et al.* 1966; Cayley *et al.* 1995; Price *et al.* 2003; Gray & McDougall 2009; Gouramanis *et al.* 2010). The NVP is subdivided into three subprovinces—the Central Highlands (a.k.a. Central Uplands), Western Plains and Mt Gambier subprovinces (Joyce 1975; Nicholls & Joyce 1989; Price *et al.* 2003). The province contains >400 volcanoes ranging from simple lava shields, scoria cones and maar volcanoes to magmatic, maar and maar–cone volcanic complexes (Figure

1.12; Joyce 1975; Boyce 2013/Chapter 2). The NVP contains the youngest expression of volcanism in Australia and is currently considered active. Evidence for this activity includes the occurrence of mantle-derived CO₂ in several areas of the province (Wopfner & Thornton 1971; Chivas *et al.* 1983, 1987; Cartwright *et al.* 2002) and elevated temperatures, low seismic velocities and hence possible partial melt beneath a large area of the Central Highlands subprovince (Rawlinson & Fishwick 2012; Aivazpourporgou 2013; Davies & Rawlinson 2014; Aivazpourporgou *et al.* 2014).

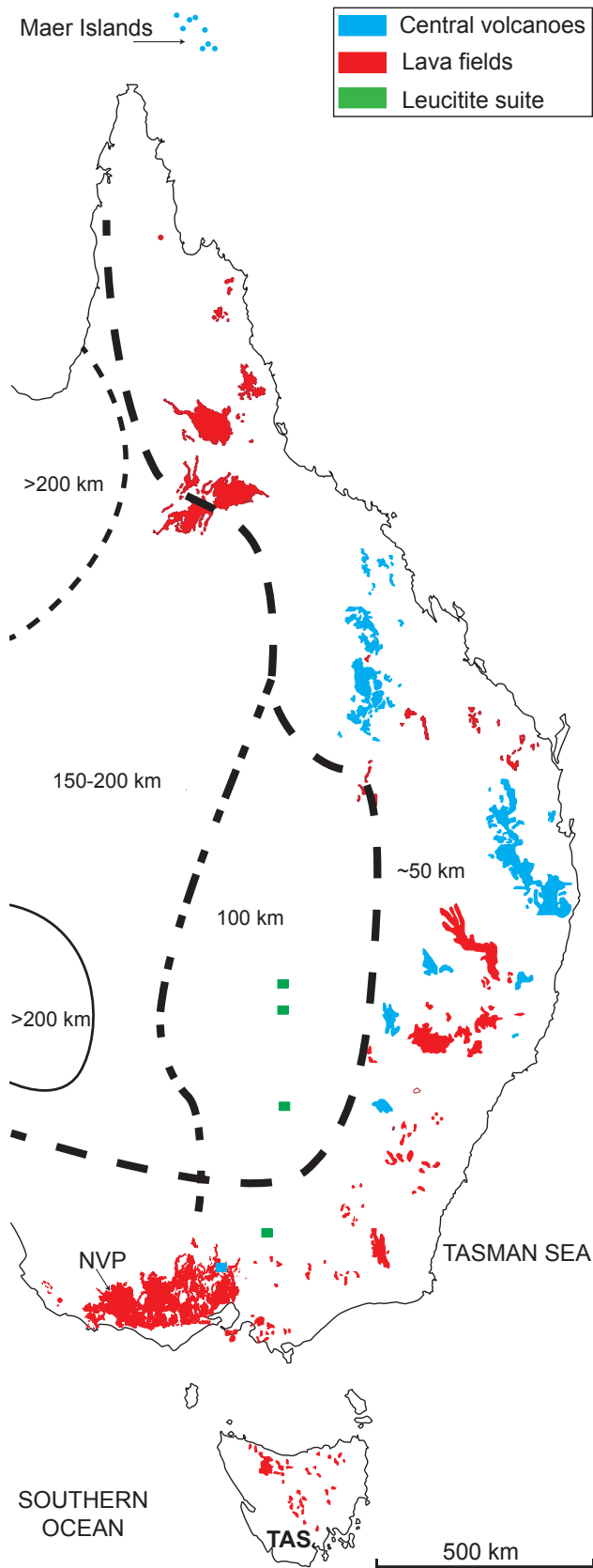


Figure 1.11 Map of eastern Australia showing the distribution of volcano types (modified after Wellman & McDougall 1974 and Johnson & Wellman 1989) overlain by steps in lithospheric thickness beneath eastern Australia (dashed lines), with estimated lithospheric thicknesses (Fishwick *et al.* 2008).

1.6.1 Volcano statistics of the Newer Volcanics Province

Statistics for numbers of volcanoes in the NVP have remained essentially the same since the volcano distribution map of Joyce (1975), which recognised >400 individual eruption centres. Despite this, data on volcanoes has been collated in several studies especially the unpublished Singleton & Joyce (1970) catalogue of post-Miocene volcanoes of Victoria, which was incorporated into a report on the eruption centres of the NVP by Rosengren (1994). There is also a list of volcanic vents in Victoria on the Seamless Geology DVD of Geoscience Victoria (D. Higgins, pers. comm. 2011). Because differing numbers of volcanoes were reported in each study, and following the recent discovery of unrecorded volcanoes in the NVP (Boyce *et al.* 2014/Chapter 3), the need has again arisen to create a readily accessible catalogue of eruption locations for the NVP. The material presented in Chapter 2 collated the available information from the studies listed above with additional information supplied by researchers at Monash University, and from various published (Ollier & Joyce 1964; Gill & Elmore 1974; Sheard 1990; Graham *et al.* 2003) and unpublished (Csaky 2002; Shaw–Stuart 2002; Cas *et al.* 2011; Prata 2012; Uehara 2012; Jordan 2013) articles and theses. Numerous unpublished Honours, Masters and PhD theses at Monash, Melbourne and LaTrobe universities may yet provide evidence for further volcanic vents and centres, but it was beyond the scope of this study to include them. Data were compiled using Google Earth and the 2010 Seamless Geology 1:250,000 k Google Earth Overlay (Geoscience Victoria) before a new volcano distribution map was created using ArcGIS (Boyce 2013/Chapter 2). A total of 416 volcanoes were documented, that had erupted from >704 vents (eruption points). The volcanoes of the Hamilton area were studied in greater detail through the analysis of ArcGIS Total Magnetism Intensity data, RGB ternary radiometrics, seamless geology and NASA ASTER digital elevation models. This allowed several of the older volcanoes to be placed into question and three previously unidentified volcanoes to be described (Boyce *et al.* 2014/Chapter

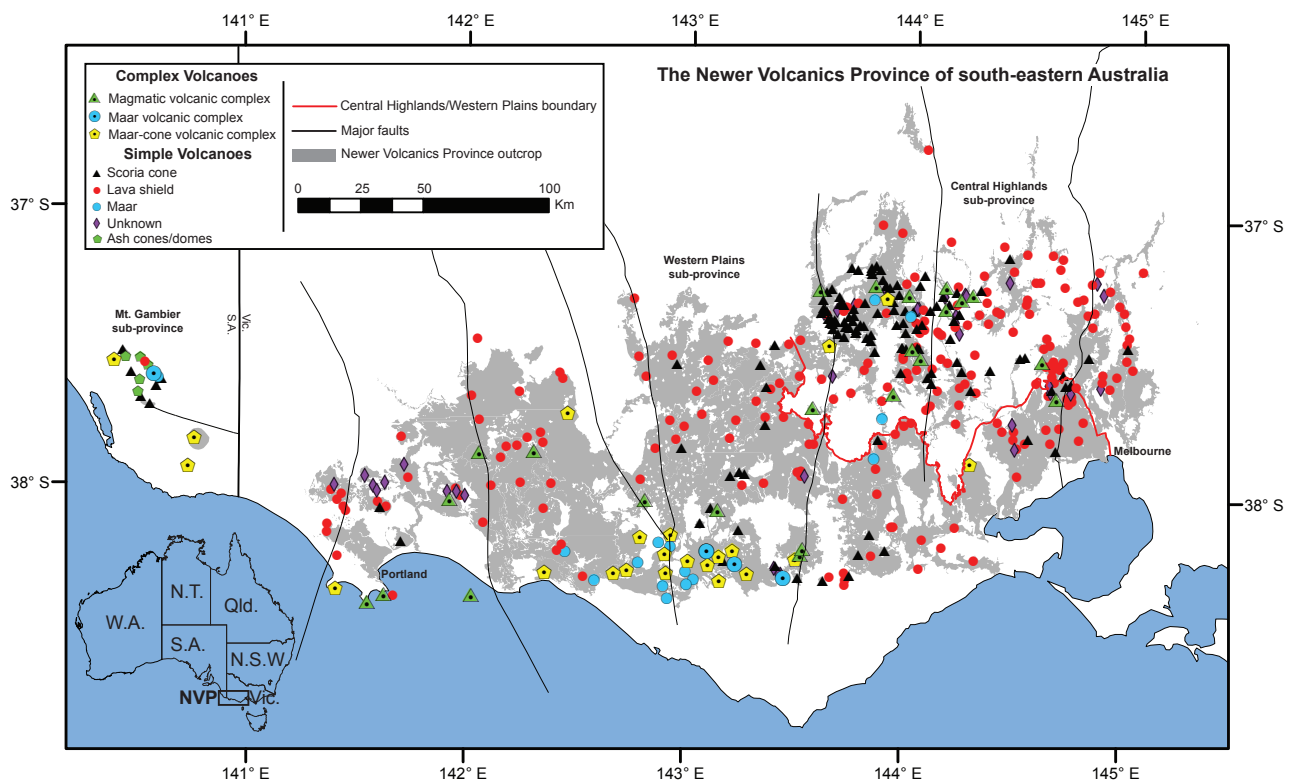


Figure 1.12 Distribution of volcanic centres by type in the Newer Volcanics Province, southeastern Australia, showing major faults and Newer Volcanics outcrop. Modified after Boyce (2013).

3). This information had already been incorporated into the Boyce (2013) study. After publication, the more rigorous process of using geophysical data and digital elevation models was applied to the remainder of the NVP and additional eruption centres were discovered, the nature of which will be outlined below.

The NVP catalogue outlined in this thesis represents a significant update of the locations of volcanism within southeastern Australia, and its uses are diverse. They include the drafting of new volcano distribution maps, which may be updated as new information becomes available. These can be used to examine changes with latitude and longitude in the NVP in terms of ages, numbers of vents, eruption types, major and trace element geochemistry and isotope geochemistry. The catalogue, which is now freely available online through the personal page of the author on Academia.edu and ResearchGate.net (and will be published as supplementary material in the Australian Journal of Earth Sciences in a future publication) has already been used in studies of volcanism in the province, and in studies of soil, water and geothermal activity. Accurate volcano distribution maps can be used in spatial statistical studies, such as the point pattern analysis performed on the Mt Gambier subprovince in order to recognise patterns of volcano distribution (Bishop 2007). In addition, the database is currently being used by researchers, including myself, at Monash University and the University of Melbourne to help draft a hazard and risk analysis for southeast Australia with possible future eruptions in mind.

It is important to note that volcanoes identified in the study of Lesti *et al.* 2008 were not used in the construction of the catalogue. Lesti *et al.* (2008) analysed the spatial distribution of vents in the NVP based on the identification of volcanic centres from Landsat images, to produce a density map and used this information to discuss the tectonic controls on volcanism. Volcanoes identified by these authors were not used in the present study for several reasons. Their analysis was based on the identification of circular features producing negative or positive relief, and excluded circular features characterised by shapes <100 m in diameter. However, there are many small edifices in the NVP, such as Picaninny and Sheepwash Hills in the Hamilton areas, with edifices less than 100 m in diameter. Lesti and co-authors identified a large number of vents between Portland and Mt Gambier, and also a group to the west of the Grampians. During the studies outlined in this thesis, both of these areas were examined in detail using the methods outlined above. In general, volcanoes of the NVP have a distinctive morphology with respect to the surrounding terrain, although considerable variability exists in terms of degree of symmetry and relief. No eruption centres were identified, and no NVP basalts have been reported in either area. The area to the west of Portland is mainly composed of Early Pleistocene Padthaway Formation lacustrine sediments, underlain by the Bridgewater Formation dune sands and calcrete—it is therefore possible that products of earlier volcanism may be buried, but there are certainly no visible volcanic rocks. As volcanoes of the Mt Burr Range in the Mt Gambier subprovince are partially overlain by Bridgewater Formation sands, any very low shield volcanoes in the area older than ~2.59 Ma could also have been buried. However, no NVP basalts have been reported from drill hole data, and there is a marked absence of eruption centres younger than this age. To the west of the Grampians, country rocks are composed mainly of sandstones of the Miocene–Pliocene age Loxton Sands, with no visible NVP eruption centres. In addition, the vent density map of Lesti *et al.* (2008) could not be accurately overlain onto that of the present study in ArcGIS, and no coordinates were given, so that detailed comparisons could not be performed.

An updated volcano distribution map is shown in Figure 1.11 and an updated catalogue is included on the enclosed CD. The NVP catalogue records >437 volcanic centres formed from >729 vents. These are minimum estimates owing to the methodology of the survey. The statistics are revised from those of Boyce (2013) (>416 volcanic centres from >709 vents) due to on-going studies in the province. For example, Lady Julia Percy Island was omitted from the original study, but restored here (see below), and an additional vent was added for The Sugarloaf (Springfield). From the analysis of digital elevation models, magnetics and radiometrics data, three previously deleted eruption centres were also restored to the spreadsheet. These are GeoVIC 194, 529 and 534 (a centre not related to an known eruption type and two lava shields). In addition, 12 lava shields, 1 maar and 5 centres of unknown character were added to the archive.

Updated statistics of eruption centres based on subprovince and volcano type are shown in Table 1.1, and vents are compared by subprovince in Table 1.2. The current data indicate that the NVP is composed of 50 complex and 387 simple volcanoes, yet almost half of the vents in the province are associated with complex centres. Ash cones/domes are found exclusively in the Mt Gambier subprovince. Although scoria-producing eruption centres are predominantly found in the Central Highlands, lava and scoria vent numbers are approximately equal in the Central Highlands and Western Plains subprovinces. The Western Plains features the greatest number of maars, due to their association with the aquifers of the underlying Otway Basin sediments. The distinction between simple and complex volcanoes is likely to change as more volcanoes are studied in greater detail, as monogenetic volcanoes have been shown to display great complexity with regards to the style and products of their eruptions (e.g., Brenna *et al.* 2010; van Otterloo *et al.* 2014; Boyce *et al.* 2015) and these distinctions may no longer hold true. Nevertheless, the number of eruption centres would

Table 1.1 Volcanic centres of the Newer Volcanics Province, Victoria, Australia; classified by subprovince and type of volcanic centre, with totals indicated in italics. Modified after Boyce (2013).

| | Simple volcanoes | | | | | Complex volcanoes | | | <i>Total</i> |
|--------------------------|------------------|--------------|-----------|---------------------|-----------|-------------------|----------|-----------|--------------|
| | Scoria cones | Lava shields | Maars | Ash cones/ domes | Unknown | Magmatic | Maar | Maar-cone | |
| Central Highlands | 89 | 103 | 3 | 0 | 17 | 12 | 0 | 2 | <i>226</i> |
| Western Plains | 28 | 105 | 11 | 0 | 18 | 11 | 4 | 17 | <i>194</i> |
| Mt Gambier | 6 | 1 | 1 | 5 | 0 | 0 | 1 | 3 | <i>17</i> |
| Total | <i>123</i> | <i>209</i> | <i>15</i> | <i>5</i> | <i>35</i> | <i>23</i> | <i>5</i> | <i>22</i> | <i>437</i> |

Table 1.2 Vents of the Newer Volcanics Province, Victoria, Australia; classified by subprovince and type of eruption, with totals indicated in italics. Modified after Boyce (2013).

| | Mainly scoria | | | Ash cones/ domes | | Spatter cone | | <i>Total</i> |
|--------------------------|---------------|-------------|-----------|---------------------|-----------|-----------------|--|--------------|
| | Mainly scoria | Mainly lava | Maar | domes | Unknown | | | |
| Central Highlands | 130 | 142 | 6 | 0 | 21 | 0 | | <i>299</i> |
| Western Plains | 140 | 136 | 70 | 0 | 22 | 16 | | <i>384</i> |
| Mt Gambier | 13 | 1 | 16 | 5 | 0 | 9 | | <i>44</i> |
| Total | <i>283</i> | <i>279</i> | <i>92</i> | <i>5</i> | <i>43</i> | <i>25</i> | | <i>727</i> |

remain the same. Unknown volcanoes relate to eruption centres that need to be ground truthed as there is no literature describing them and they could equally be scoria cones or lava shields from their morphology (Boyce 2013).

1.6.2 Age range of the Newer Volcanics Province

Although the NVP has a widely accepted nominal age range of 4.5 Ma to *ca* 5000 BP (Blackburn 1966; McDougall *et al.* 1966; Blackburn *et al.* 1982; Price *et al.* 2003; Gray & McDougall 2009; Gouramanis *et al.* 2010), this time span is generally not well constrained. Many eruption centres remain undated due to sampling bias towards younger, fresher material, and there are older buried flows and presumably therefore eruption centres. Dating of buried flows at Beaufort, northwestern Victoria, has yielded ages of 6.07 ± 0.11 Ma and 4.65 ± 0.07 Ma (Cayley *et al.* 1995), and the two eruption phases of Lady Julia Percy Island have been dated at 7.80 ± 0.08 Ma and 6.22 ± 0.06 Ma (Edwards *et al.* 2004). This implies that the onset of NVP volcanism was earlier than 7.8 Ma, thus almost doubling the timespan of volcanic activity. It also suggests that the NVP was active at the same time as the 7.0–4.6 Ma Macedon–Trentham group of basaltic to trachytic centres northwest of Melbourne, which is compositionally distinct from the dominantly basaltic NVP, and more closely resembles the central volcanic complexes of New South Wales and Queensland (Knutson & Nicholls 1989).

A distribution map of ages for the NVP (Figure 1.13) was drafted by adding published ages of NVP samples to the volcano catalogue. Because lavas can flow many kilometres, to recognise age progressions or clusters within the province requires the sampled basalts to be traced back to their point of origin (volcanic centre). However, many dated NVP samples could not be unambiguously traced back to an eruption centre as erosion has been severe in many areas, obscuring the relationships between lava flows. For this reason, in the distribution map eruption centre ages were plotted as circles and point samples of unclear origin as squares. The youngest phase of volcanism (<1 Ma) was subdivided into 0.5 Ma segments and from 1–4 Ma intervals of 1 Ma were used. Data were taken from Gill 1957; Turnbull *et al.* 1965; Blackburn 1966; Harding 1969; Bowler & Hamada 1971; Aziz–Ur–Rahman & McDougall 1972; Wellman 1974; Bennett *et al.* 1975; Dodson 1975; McDougall & Gill 1975; Singleton *et al.* 1976; Dasch & Millar 1977; Gill 1978, 1979; Barbetti & Sheard 1981; Gill 1981; Blackburn *et al.* 1982; McKenzie *et al.* 1984; Ollier 1985; Gill & Sherwood 1986; Smith & Prescott 1987; Webb 1989; Edwards 1990; Henley & Webb 1990; Wallace 1990; Wallace & Ollier 1990; Tickell 1991; Nicholls *et al.* 1993; Cayley *et al.* 1995; Edwards *et al.* 1996; Robertson *et al.* 1996; Taylor *et al.* 1996; Stone *et al.* 1997; Webb *et al.* 1998; Taylor *et al.* 2000; Edwards *et al.* 2001; Graham *et al.* 2003; Kotsonis & Joyce 2003; Edwards *et al.* 2004; Gibson 2007 and Gray & McDougall 2009.

It is very clear from Figure 1.13 and Table 1.3 that there are no dates available for the vast majority of eruption centres, with only 61 dated samples being traceable to no more than 39 of 437 known eruption centres. There are in some cases multiple dates for a single centre (e.g., 9 for Mt Rouse) and the number of dated centres constitutes $<9\%$ of the total number. There are almost twice as many map points for basalt point samples (Figure 1.13), with 66 sample locations for 97 samples (Table 1.3). Since these samples are not traceable to eruption centres, they are only useful in adding to

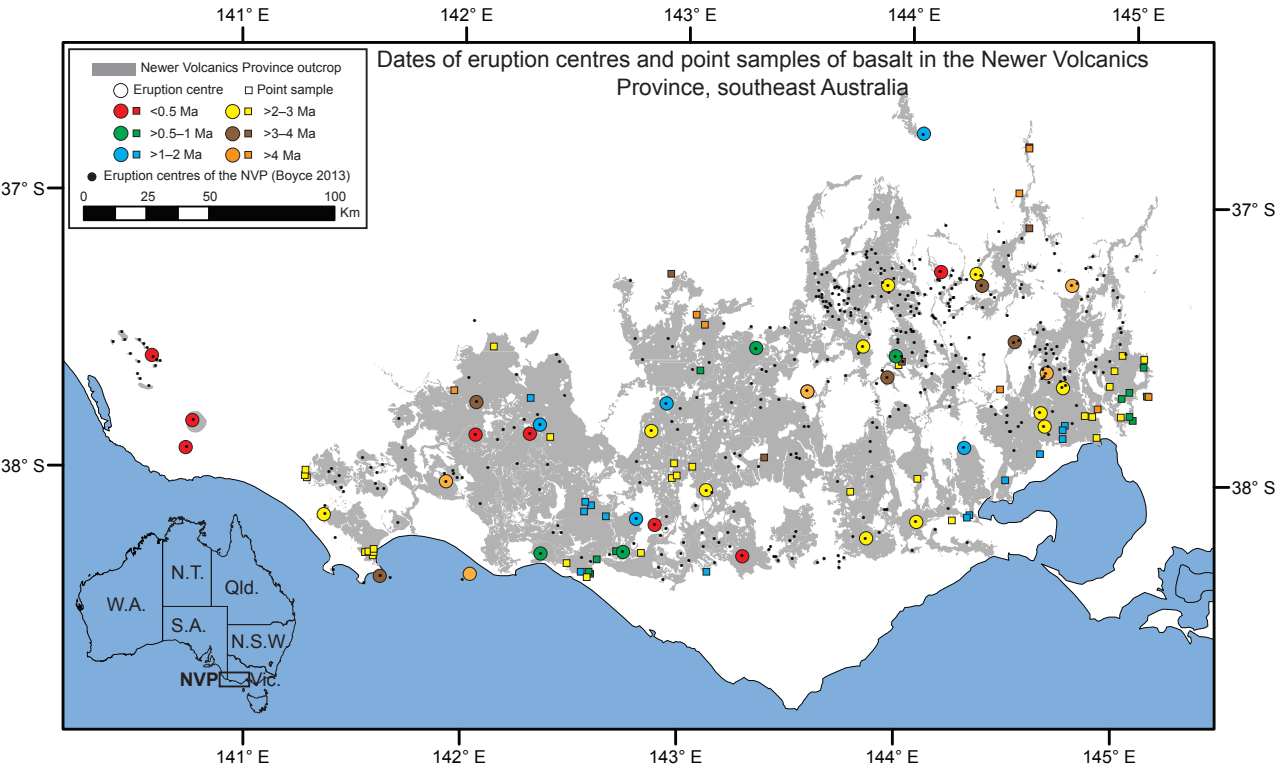


Figure 1.13 Ages of eruption centres (filled circles) and point samples of basalts (filled squares) in the Newer Volcanics Province, compared to the number of eruption centres in the province (small black filled circles).

| Centres | | | Point samples | | Table 1.3 Numbers of dated Newer Volcanics Province samples (both samples from known eruption centres and point samples) within defined age ranges (data summarised in Fig. 2). |
|--------------|-----------|-----------|---------------|-----------|---|
| Age (Ma) | Points on | Samples | Points on | Samples | |
| | map | | map | | |
| <0.5 | 9 | 18 | 0 | 0 | |
| 0.5-1 | 4 | 7 | 10 | 18 | |
| 1-2 | 5 | 5 | 14 | 14 | |
| 2-3 | 11 | 17 | 29 | 42 | |
| 3-4 | 5 | 7 | 5 | 9 | |
| >4 | 4 | 7 | 8 | 14 | |
| <i>Total</i> | <i>38</i> | <i>61</i> | <i>66</i> | <i>97</i> | |

the knowledge of the timespan of eruptions in the NVP. Only those samples traceable to an eruption centre can be used to place progressions or clusters of volcanic activity into a time frame, both locally and within the province as a whole. These major limitations highlight the fact that little is known about the timespan of eruptions in the NVP, and any inferences drawn from the available data must be considered as preliminary. Volcanism in the NVP began at approximately 7.8 Ma, with Lady Julia Percy Island being one of the oldest known volcanoes. Basalts older than 4 Ma have been found at Hamilton (4.46 Ma; McDougall *et al.* 1966; Gill 1957; Turnbull *et al.* 1965; Harding 1969; Ollier 1985; Gibson 2007), southeast of Ararat (6.07 Ma and 4.65 Ma; Cayley *et al.* 1995), Axedale (5.57 Ma and 4.82 Ma; Henley & Webb 1990; Edwards *et al.* 2001; Gibson 2007), NE Redesdale (4.49 Ma; Henley & Webb 1990; Graham *et al.* 2003; Gibson 2007), and Keilor (4.64 Ma; McDougall *et al.* 1966; Bennett *et al.* 1975; Gibson 2007). Eruptions older than 7.8 Ma may be buried beneath younger basalts.

In many studies, the NVP has been thought to be due to hot spot volcanism, as outlined in section 1.5 (Wellman & McDougall 1974; Wellman 1983; Duncan & McDougall 1989; Sutherland

1991; Matsumoto *et al.* 1997). However, as discussed in Section 1.5 and as obvious from Figure 1.13, there is no clear age progression of volcanic activity within the NVP. This is further supported by Figure 1.14, which shows sample ages in relation to latitude (Figure 1.14a) and longitude (Figure 1.14b). The latitude and longitude shown on the graph axes of Figures 1.14a and b were based on the volcanoes at the far edges of the province. These were: North, Bald Hill composite Lava Shield at Woodstock (-36.7673 144.0503); East, Round Hill Lava Shield at Broadford (-37.1830 145.0335); South, Lady Julia Percy Island Magmatic Volcanic Complex (-38.4159 142.003); and West, Mt Muirhead Maar–Cone Volcanic Complex (-37.5587 140.4044).

The Palaeozoic Moyston Fault, which is believed to represent the suture between the Delamerian and Lachlan orogens (Korsch *et al.* 2002; Cayley *et al.* 2011), is taken to be coincident with the Mortlake Discontinuity, which is based upon distinct ranges of Sr-isotope ratios of NVP basalts, and which subdivides the Western Plains subprovince into eastern and western sections, (Price *et al.* 1997; see below). Gray & McDougall (2009) presented a histogram of K–Ar ages for NVP basalts that distinguished ages to the east and west of the Mortlake Discontinuity and found a pronounced peak in volcanism between 3.0–1.8 Ma. They argue that this constitutes the period of maximum activity in the field, with the most widespread activity and most frequent eruptions; they further argue and volcanism began to wane after this age peak. In light of the fact that there are currently ages for <9% of the known volcanoes, such arguments may be inherently flawed. A similar histogram using age intervals of 0.5 Ma and distinguishing samples to the west and east of the Mortlake Discontinuity, using samples from all published studies traceable to eruption centres and highlighting basalts of the Central Highlands subprovince is shown in Figure 1.14c. The lack of data for eruption centres >4.5 Ma most likely reflects sampling bias, but volcanism has been continuous since at least 4.5 Ma. The same peak in volcanism was identified at *ca* 2–3 Ma but mainly in eruption centres to the east of the Mortlake Discontinuity. Contrary to the Gray & McDougall (2009) study, there is a pronounced peak in volcanism from <0.5 Ma, particularly to the west of the Mortlake Discontinuity. This peak is best illustrated by Mounts Gambier and Schank, and Lake Leake within the Mt Gambier subprovince; Mounts Rouse, Napier, Eccles and Porndon, and Lake Keilambete in the Western Plains subprovince; and Mt Franklin in the Central Highlands subprovince. This suggests that NVP volcanism is in fact not waning with time, but this conclusion may change as more dates are obtained for samples traceable to their parent volcanic centre. If suitable dating is undertaken on more of the remaining 91% of known eruption centres (e.g., from 4.5 Ma onwards at least), a better understanding of how volcanism has changed over time in the NVP will be gained, any age-clustering of volcanoes can be identified, and peaks in volcanism will be more meaningful and provide better predictive tools for any future volcanism.

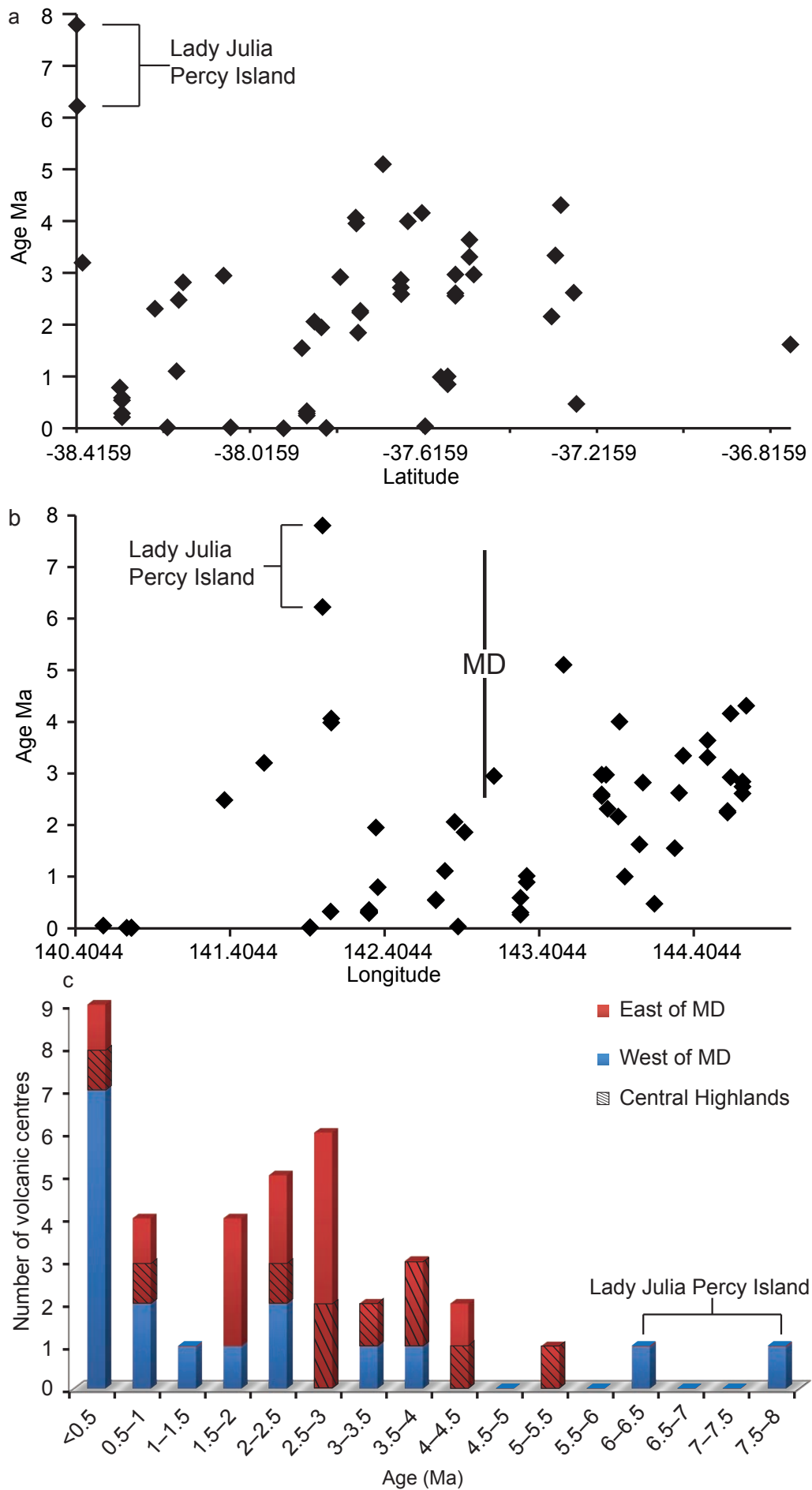


Figure 1.14 a, b) Available dates for samples traceable to eruption centres based on latitude and longitude; c) Histogram of the number of centres in 0.5 Ma intervals east and west of the Mortlake Discontinuity (MD), with centres in the Central Highlands subprovince shown by bars with diagonal shading.

1.6.3 Geochemistry of the Newer Volcanics Province

The NVP has been extensively studied in terms of the petrology and geochemistry of its products, which have been shown to cover a wide range of compositions. Early studies focussed on petrographic descriptions, such as those by Skeats & Summers (1912) and Edwards & Crawford (1940), and petrology (Edwards 1938). Chemical analyses of NVP rocks were first presented by Stanley (1909) and Grayson & Mahoney (1910); later work has focussed on the normative and modal classification of the rocks (e.g., Frey & Green 1974; Irving & Green 1976; Frey *et al.* 1978). During the 1980's, the basalts of the NVP were subdivided into two series—the Plains basalts and the Cones basalts (Price *et al.* 1988, Vogel & Keays 1997)—terms that are still in use. In recent years modern geochemical analyses have been used to try to understand the source regions of the parental magmas, using both major and trace elements as well as isotopic analysis (e.g., McDonough *et al.* 1985; Price *et al.* 1997, Vogel & Keays 1997; McBride *et al.* 2001; Demidjuk *et al.* 2007) and studies of mantle xenoliths hosted by NVP volcanic products (e.g., O'Reilly & Griffin 1988; McBride *et al.* 1996; Matsumoto *et al.* 2000).

1.6.3.1 Major and trace elements

A total of 218 major element analyses available in the literature were renormalised to 100% on a volatile-free basis after calculating $\text{Fe}_2\text{O}_3/\text{FeO}_{\text{total}}$ ratios (see enclosed CD). CIPW norms were then recalculated assuming a $\text{Fe}_2\text{O}_3/\text{FeO}_{\text{total}}$ ratio of 0.15 and used to classify the rocks as either Cones series alkaline (normative nepheline) or Plains series transitional (normative hypersthene + normative quartz <10%) or tholeiitic (normative hypersthene + normative quartz >10%) as outlined in Price *et al.* (1997). Data are provided on the enclosed CD. Most of the published analyses are alkaline (156), while relatively few are transitional (16) or tholeiitic (23). The majority of the published analyses were from studies focussing on the cones of the NVP, for example in studies by Irving & Green (1976), Ellis (1976) and McDonough *et al.* (1985). Many of the Plains series data are published in Price *et al.* (1997), who provide data tables for only 23 of >400 samples. This is the most comprehensive study of the Plains series and the full data set (including coordinates of sample locations) is currently being digitised alongside the other studies of NVP geochemistry in a joint effort between researchers and Geoscience Victoria (David Taylor pers. comm. 2014). All data used in this study have been made available and the database should be complete in 2015 and available online through Geoscience Victoria. The data may then be used to provide a significant update to the geochemical distribution maps presented below. Many additional geochemical data on NVP rocks remain unpublished in numerous Honours, Masters and PhD theses, and are not used in this study.

The renormalised literature values, when plotted on a Total Alkalis vs Silica (TAS) diagram (Le Bas *et al.* 1986; Le Maitre *et al.* 2002), show compositions ranging from basalts (alkaline and subalkaline), trachybasalts and basanites to basaltic andesites, trachyandesites and phonotephrites (Figure 1.15a). Price *et al.* (1997) results were also superimposed onto an expanded TAS diagram to show the more complete range of Plains suite basalts (Figure 1.15b). Plains basalts make up the extensive valley-forming lava fields and consist of dominantly tholeiitic and transitional compositions, with more strongly alkaline lavas comprising <2% of erupted products. Alkaline Cones basalts constitute

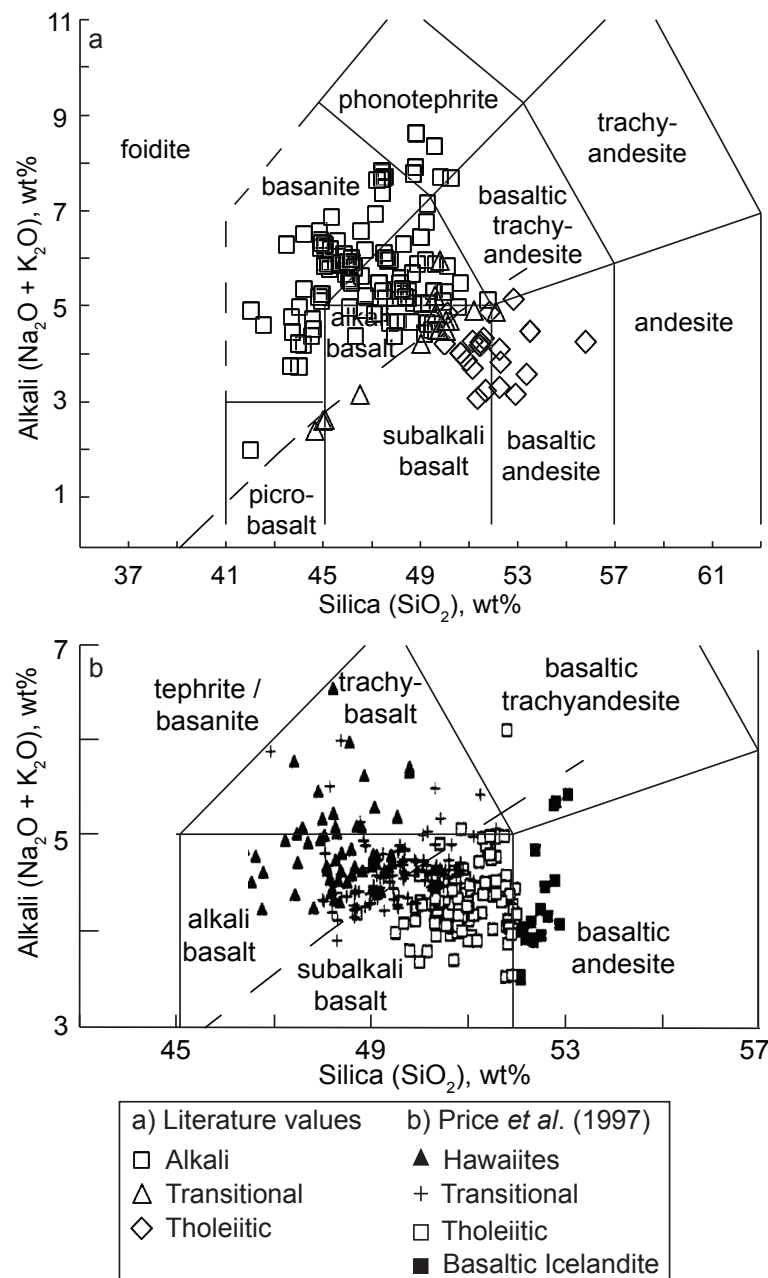


Figure 1.15 a) TAS diagram (Le Bas *et al.* 1986; Le Maitre *et al.* 2002) of basalt compositions for the Newer Volcanics Province. Data from Frey & Green 1974; Ellis 1976; Irving & Green 1976; Frey *et al.* 1978; Stone *et al.* 1997; Vogel & Keays 1997; McBride *et al.* 2001; Foden *et al.* 2002; Demidjuk *et al.* 2007. b) Price *et al.* 1997 data superimposed into a zoomed-in TAS diagram, showing a more comprehensive dataset of basalts.

those erupted at the smaller scoria cones, maars and tuff rings and are typically small-volume flows; they are dominantly basanites, nephelinites, nepheline hawaiites and nepheline mugearites (>60% of analysed samples) (Price *et al.* 1988; Ewart 1989; Vogel & Keays 1997). It is important to note that some of the larger volcanic cones are also associated with Plains basalt eruptions.

MgO contents range from 3.76–17.5 wt% (based on 218 published NVP samples; Figure 1.16). With decreasing MgO content, there is a general increase in the amount of Al₂O₃ and K₂O and a decrease in TiO₂, FeO and CaO, with the other oxides showing scattered data. These trends indicate that fractionation of olivine and pyroxene has played a key role in the evolution of NVP basalts (e.g., Irving & Green 1976; Price *et al.* 1997; Vogel & Keays 1997). The highest concentrations of TiO₂ and Al₂O₃ are found in both alkali and transitional samples, while higher MnO, Na₂O, K₂O and P₂O₅ are found in the more alkali rocks. K₂O and P₂O₅ are therefore thought to be reflective of lithology (Price *et al.* 1997).

Mg-numbers of basalts are used to estimate the primary nature of a basaltic liquid, as it may serve as an index of crystal fractionation (Oskarsson *et al.* 1982; Wilkinson 1982). Minimally modified mantle melts have a Mg-number of >70. Mg-numbers were calculated for available geochemical

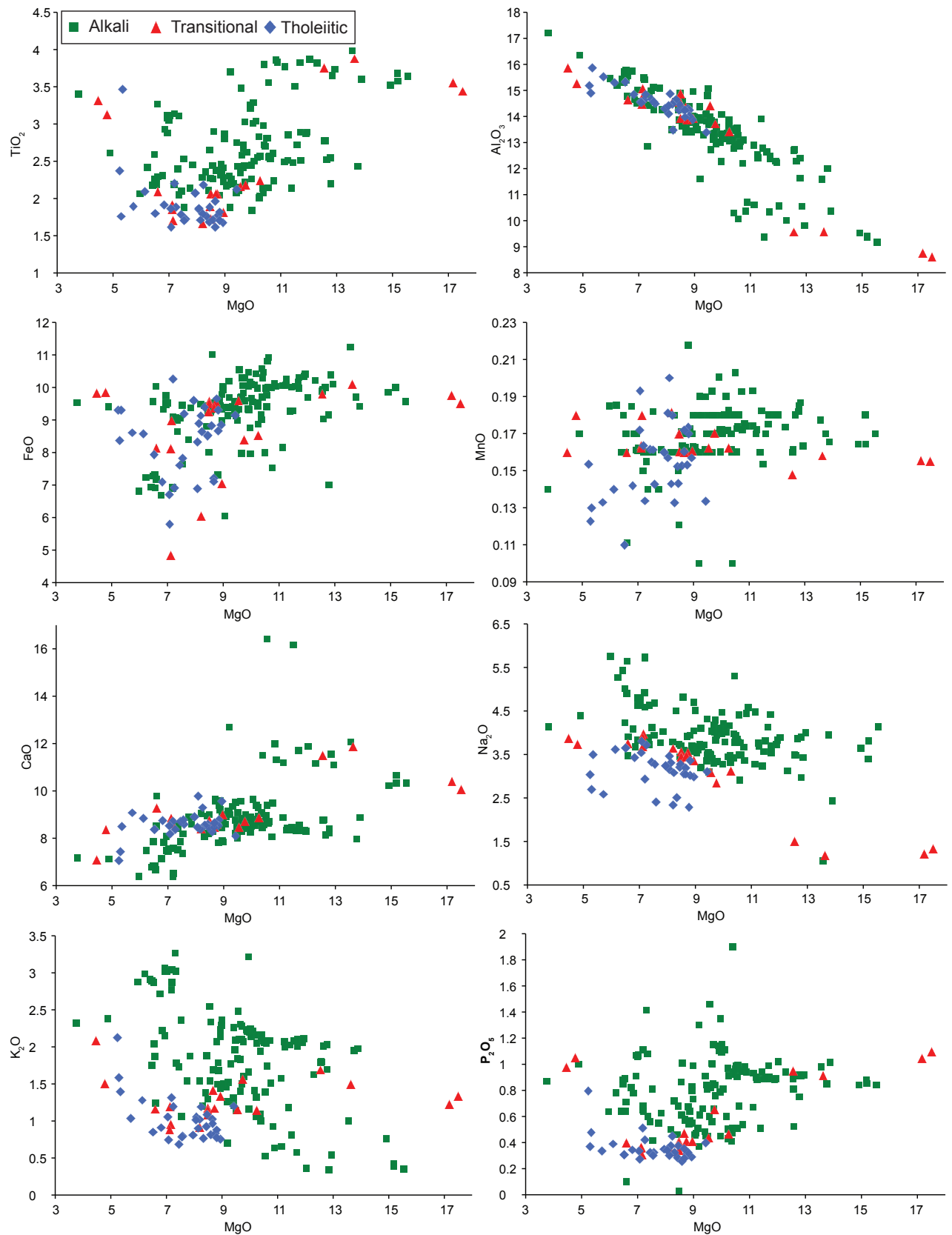


Figure 1.16 Major elements versus MgO for the rock suites of the NVP (n = 218). Data from Frey & Green (1974); Ellis (1976); Irving & Green (1976); Frey *et al.* (1978); McDonough *et al.* (1985); Stone *et al.* (1997); Price *et al.* (1997); Vogel & Keays (1997); McBride *et al.* (2001); Foden *et al.* (2002); Demidjuk *et al.* (2007).

data that were traceable to individual eruption centres in the NVP and the maximum values for each centre were plotted onto a volcano distribution map (Figure 1.17). This map is based on 287 analyses traceable to 49 eruption centres (Frey & Green 1974; Ellis 1976; Irving & Green 1976; Frey *et al.* 1978; McDonough *et al.* 1985; Stone *et al.* 1997; Foden *et al.* 2002; Demidjuk *et al.* 2007; Prata 2012; Uehara 2012; van Otterloo 2012; Boyce 2014). Data from Price *et al.* (1997) were excluded from the maps, but should be included in future publications when the data become available.

Green (1970) and Price *et al.* (1997) considered that the majority of basalts in the NVP could not represent primary magmas, with most having Mg-numbers lower than 68 and Ni lower than 400 ppm; however, other reported data suggest that some of the NVP alkaline and transitional series

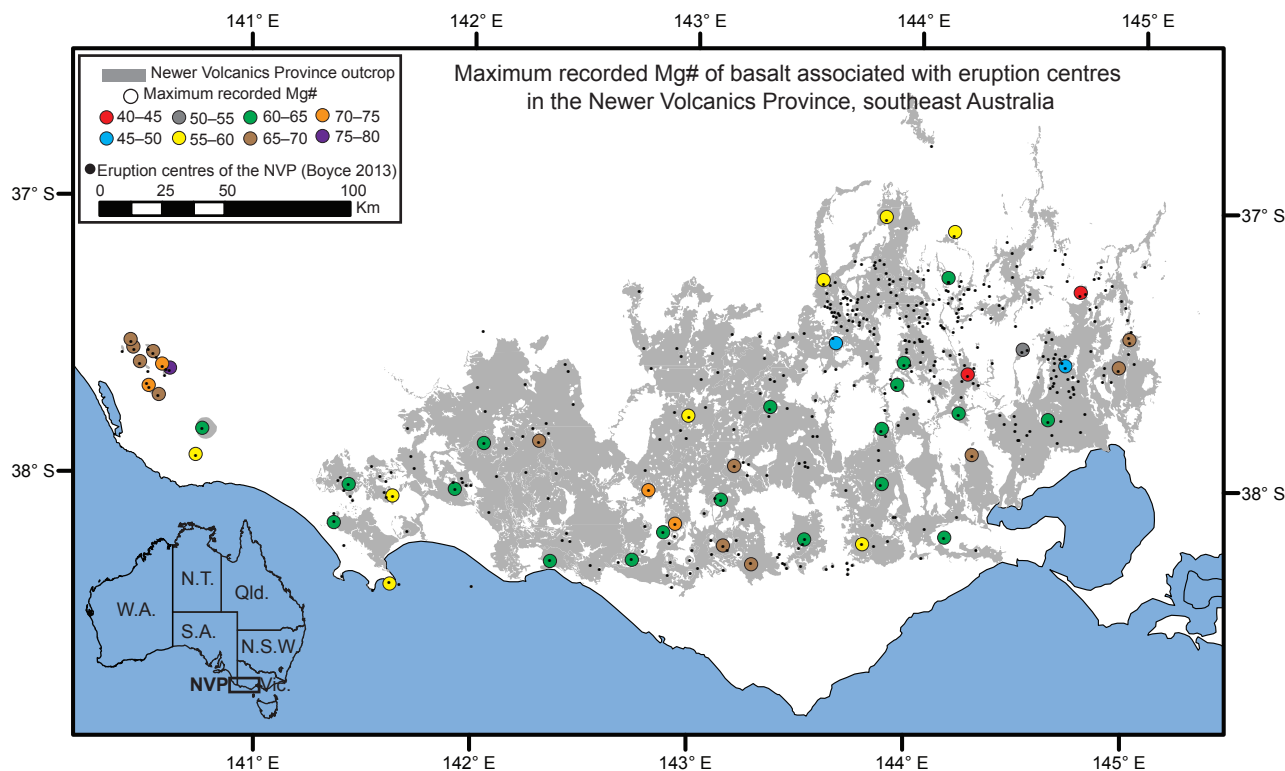


Figure 1.17 Maximum recorded Mg-numbers of basalts traceable to eruption centres in the Newer Volcanics Province (filled circles), compared to the number of eruption centres in the province (small black filled circles).

basalts could be considered primary (Figure 1.17). Primary magmas with Mg-numbers of >70 are shown on Figure 1.17 as orange (70–75) or blue circles (75–80). Many of the data shown in Figure 1.17 lie within the Mg-number range 60–70 (green and brown circles), and the corresponding products were therefore chemically modified to some degree en-route to the surface. The Mt Burr Range in South Australia contains a concentration of volcanic centres with high Mg-numbers that are between 58.53–68.24 for Mt Burr and 75.83–76.64 for Mt Edward (Table 1.4). High Mg-numbers are also found in centres located in the Western Plains sub-province such as Mt Noorat (62.59–71.65), Mt Shadwell (64.60–71.29), and Mt Frazer (68.75), all of which contain abundant mantle xenoliths, attesting to high rates of magma ascent. The lowest Mg-numbers are found in the Central Highlands at Melbourne Hill (44.71) and Mt Gorong (41.28; Table 1.4). An important consideration is the fact that, with the exception of centres such as Mounts Rouse, Gambier and Leura, the vast majority of eruption centres are classified on the basis of very few geochemical analyses, (Table 1.4). Maps such as those in Figure 1.17 will become more meaningful as more analyses become available for individual centres.

Table 1.4. Range of Mg-numbers of samples traceable to eruption centres in the Newer Volcanics Province, showing eruption centre, subprovince, latitude and longitude, Mg-number range and the number of samples.

| Volcanic Centre | Subprovince | Latitude | Longitude | Mg# Range | Number of samples |
|-----------------|-------------|----------|-----------|--------------|-------------------|
| Cape Grant | WP | -38.404 | 141.625 | 59.1 | 1 |
| Gow Hill | WP | -38.013 | 143.869 | 61.95 | 1 |
| Lake Keilambete | WP | -38.206 | 142.880 | 60.53 | 1 |
| Lake Leak | MG | -37.613 | 140.585 | 69.52–70.62 | 2 |
| Melbourne Hill | WP | -37.300 | 144.745 | 44.71 | 1 |
| Mt Bullengarook | CH | -37.510 | 144.493 | 53.93 | 1 |
| Mt Bunninyong | CH | -37.653 | 143.924 | 64 | 1 |
| Mt Burr | MG | -37.603 | 140.482 | 58.53–68.24 | 2 |
| Mt Callender | CH | -37.507 | 143.646 | 48.08 | 1 |
| Mt Consultation | CH | -37.098 | 144.169 | 56.68 | 1 |
| Mt Cottrill | WP | -37.763 | 144.623 | 62.18 | 1 |
| Mt Eccles | WP | -38.061 | 141.922 | 63.78 | 1 |
| Mt Eckersley | WP | -38.089 | 141.638 | 59.4 | 2 |
| Mt Edward | MG | -37.628 | 140.618 | 75.83–76.64 | 2 |
| Mt Elephant | WP | -37.961 | 143.198 | 64.31–68.34 | 3 |
| Mt Franklin | CH | -37.265 | 144.150 | 61.33–64.33 | 5 |
| Mt Fraser | CH | -37.462 | 144.978 | 68.65 | 2 |
| Mt Gambier | MG | -37.841 | 140.766 | 59.84–63.29 | 41 |
| Mt Gellibrand | WP | -38.234 | 143.791 | 59.6 | 2 |
| Mt Gorong | CH | -37.608 | 144.249 | 41.28 | 2 |
| Mt Graham | MG | -37.523 | 140.444 | 65.9–68.79 | 3 |
| Mt Hamilton | WP | -37.785 | 142.986 | 56.01 | 1 |
| Mt Holden | CH | -37.565 | 144.693 | 46.37 | 1 |
| Mt Kincaid | WP | -38.182 | 141.369 | 63.61 | 2 |
| Mt Kurweeton | WP | -38.086 | 143.140 | 63.96 | 1 |
| Mt Leura | WP | -38.251 | 143.155 | 61.81–65.48 | 21 |
| Mt McIntyre | MG | -37.568 | 140.544 | 65.58–68.87 | 4 |
| Mt Mercer | WP | -37.817 | 143.863 | 62.13 | 1 |
| Mt Mitchell | CH | -37.285 | 143.584 | 55.95 | 1 |
| Mt Moolort | CH | -37.047 | 143.860 | 58.68 | 1 |
| Mt Moriac | WP | -38.199 | 144.167 | 64.61 | 1 |
| Mt Muir | MG | -37.549 | 140.457 | 66.68–68.84 | 2 |
| Mt Napier | WP | -37.891 | 142.054 | 62.11–64.00 | 3 |
| Mt Noorat | WP | -38.176 | 142.934 | 62.59–71.65 | 10 |
| Mt Porndon | WP | -38.313 | 143.284 | 63.43–67.65 | 11 |
| Mt Ridley | CH | -37.566 | 144.933 | 62.93–65.64 | 2 |
| Mt Rouse | WP | -37.885 | 142.303 | 63.66–71.61 | 83 |
| Mt Schank | MG | -37.940 | 140.736 | 56.45–59.247 | 9 |
| Mt Shadwell | WP | -38.055 | 142.809 | 64.60–71.29 | 7 |

| | | | | | |
|----------------|----|---------|---------|-------------|----|
| Mt Wallace | CH | -37.751 | 144.213 | 60.26 | 1 |
| Mt Warrenheip | CH | -37.575 | 143.958 | 64.49–64.86 | 3 |
| Mt Warrnambool | WP | -38.307 | 142.737 | 63.49 | 1 |
| Mt Watch | MG | -37.692 | 140.525 | 72.97–74.32 | 6 |
| Mt Widderin | WP | -37.747 | 143.353 | 61.4 | 2 |
| Red Hill | WP | -38.045 | 141.435 | 63.83 | 1 |
| The Anakies | WP | -37.898 | 144.282 | 59.44–65.03 | 10 |
| The Bluff | MG | -37.72 | 140.565 | 68.21–69.52 | 2 |
| Tower Hill | WP | -38.317 | 142.360 | 61.96 | 23 |
| Warrion Hill | WP | -38.218 | 143.530 | 63.04 | 1 |

Fewer comprehensive trace element analyses than majors are available for the NVP. With decreasing MgO, there is a strong linear decrease in both Cr and Ni, which has been attributed to Cr-spinel, olivine and pyroxene fractionation (Figure 1.18) (e.g., Irving & Green 1976; Price *et al.* 1997; Vogel & Keays 1997). There is considerable scatter in the Large Ion Lithophiles (LILE), High Field Strength Elements (HFSE) and Rare Earth Elements (REE). Overall, the alkali Cones series contains the higher concentrations of trace elements and the Plains series the least, a feature that is also evident on chondrite-normalised REE plots (Figure 1.19; Ewart & Chappell 1989; Price *et al.* 1997; Vogel & Keays 1997). The REE patterns of NVP rocks (separated into Plains, Cones and Transitional basalts) are similar to those of Ocean Island Basalts (OIB) in showing enrichment in Light Rare Earth Elements (LREE) and depletion in Heavy Rare Earth Elements (HREE), indicating predominantly garnet-bearing source regions (Figure 1.19). There is a progressive steepening of slope from the tholeiitic to the alkaline suites, which indicates progressively smaller degrees of mantle source partial melting (Price *et al.* 1997; Vogel & Keays 1997).

As the degree of partial melting is typically inversely proportional to the melting depth (Langmuir *et al.* 1992), the depth of magma generation can be assumed to be shallower for the tholeiitic suite, deepening through the transitional to the alkaline suite (Irving & Green 1976; Price *et al.* 1997; Vogel & Keays 1997). The ratio Gd/Yb increase with increasing depths of melt generation; the reason for this is that Yb and the other HREE are retained in garnet during small degrees of partial melting (Irving & Frey 1987). The alkaline suite (Cones) have higher Gd/Yb ratios than the transitional or tholeiitic (Plains) suites (Figure 1.20). This indicates that the Cones suite basalts are from deeper mantle reservoirs than the Plains suite basalts. Variations in Gd/Yb have also been noted by Vogel & Keays (1997), who attribute the variations to declining degrees of partial melting. Based on their PGE analyses of the NVP, Vogel & Keays (1997) suggested that the transitional basalt suite (and by inference, the alkali suite) was probably derived from a refractory mantle source material, whereas the tholeiitic basalt suite evolved from a non-melt-depleted mantle reservoir.

Elemental ratios of La/Nb, Ba/Nb, Rb/Nb, Th/Nb, Th/La and Nb/U can be used to assess crustal contamination, as they generate constant ratios during partial melting and fractionation (Sun *et al.* 1989). Incompatible element ratios for the NVP samples show that on average, there has been little or no contamination of magmas en-route to the surface (Table 1.5). Ratios show average values similar to primordial mantle values, but some samples show contamination as being closer to continental crust values. However, there is not always consistent evidence for contamination across

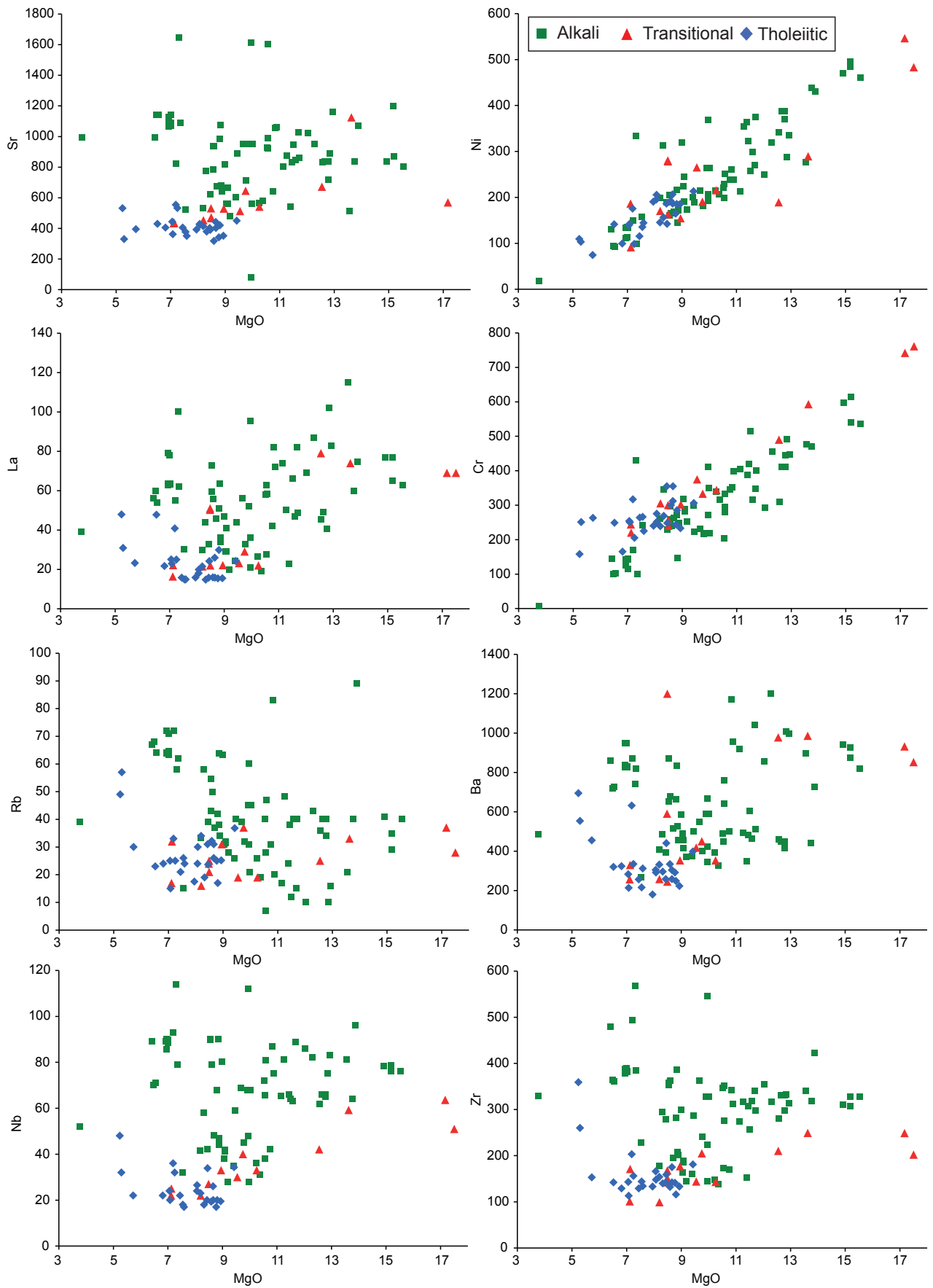


Figure 1.18 Trace element variation diagrams against MgO for the rock suites of the NVP (n = 105). Data from Frey & Green (1974); Ellis (1976); Irving & Green (1976); Frey *et al.* (1978); McDonough *et al.* (1985); Stone *et al.* (1997); Price *et al.* (1997); Vogel & Keays (1997); McBride *et al.* (2001); Foden *et al.* (2002); Demidjuk *et al.* (2007).

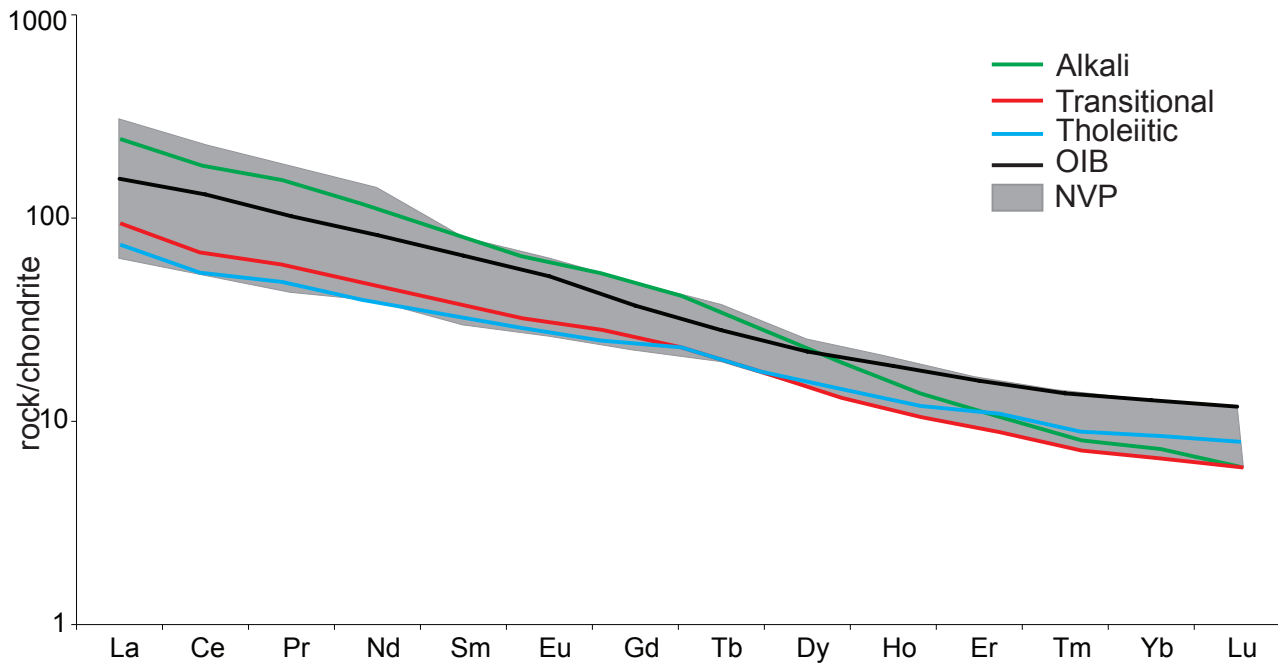


Figure 1.19 Chondrite-normalised rare earth element diagram showing the range of NVP values (grey shaded area) compared to the OIB average (Sun and McDonough 1989) and average values for the Tholeiitic Plains (blue line), Transitional Plains (red line) and Alkali Cones (green line) rock suites of the NVP (Price *et al.* 1997; Vogel and Keays 1997; McBride *et al.* 2001; Demidjuk *et al.* 2007).

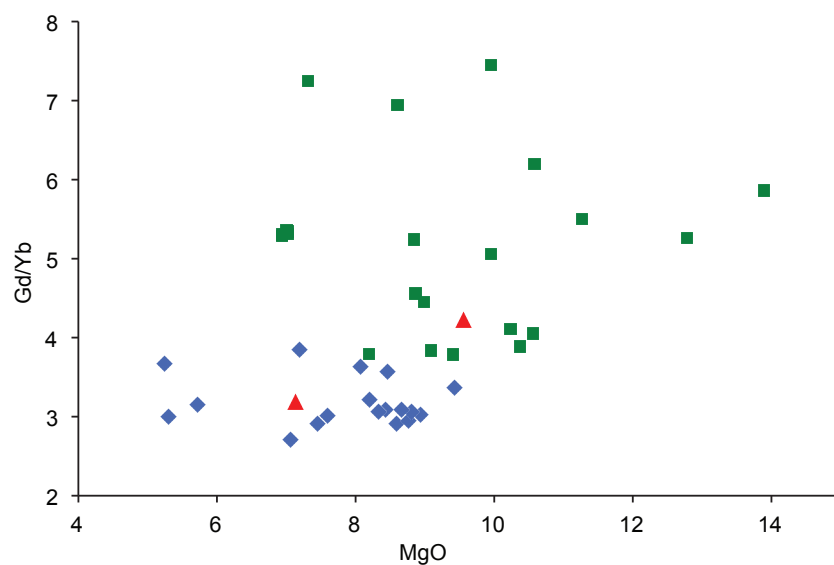


Figure 1.20 Gd/Yb vs MgO for selected NVP basalts, showing Cones series (alkali, green squares) and Plains series transitional basalts (red triangles) and tholeiitic basalts (blue diamonds). Data from McBride *et al.* (2001); Price *et al.* (1997); Vogel & Keays (1997) and Demidjuk *et al.* (2007).

Table 1.5 Incompatible element ratios for the primordial mantle and continental crust (values from Weaver 1991 with the exception of Nb/U of Hofmann *et al.* 1986) compared to the range of values for NVP products (average in brackets), showing mantle values for the volcano and no crustal contamination.

| | La/Nb | Ba/Nb | Rb/Nb | Th/Nb | Th/La | Nb/U |
|--------------------------|------------------|---------------------|------------------|------------------|------------------|------------------------|
| Primordial Mantle | 0.94 | 9 | 0.91 | 0.11 | 0.13 | 30 |
| Continental Crust | 2.2 | 54 | 4.7 0. | 44 | 0.2 | 10 |
| Alkali | 0.71–1.5 (0.91) | 10.46–20.68 (13.95) | 0.7–1.8 (1.18) | 0.1–0.25 (0.13) | 0.06–0.22 (0.15) | 11–40 (26.07) |
| Transitional | 0.7–1.87 (0.99) | 9.07–23.23 (13.62) | 0.55–1.28 (0.75) | 0.08–0.18 (0.12) | 0.05–0.2 (0.11) | 22–85 (46) (5 samples) |
| Tholeiitic | 0.58–1.42 (0.82) | 5.97–14.58 (9.77) | 0.11–1 (0.62) | 0.06–0.18 (0.1) | 0.07–0.24 (0.12) | 12.66–68.23 (42.61) |

all ratios—for instance, a sample may have slightly elevated Ba/Nb that would indicate slight crustal contamination, but high Nb/U ratios that would not.

1.6.3.2 $^{87}\text{Sr}/^{86}\text{Sr}$ isotopes

As there is often very little evidence for significant contamination of NVP magmas, isotopic ratios are used to provide information on the nature and location of the magma source regions. Strontium isotope analyses are available for >560 samples across the NVP (Cooper & Green 1969; Dasch & Green 1975; Stuckless & Irving 1976; McDonough *et al.* 1985; Whitehead 1986, 1991; Ewart *et al.* 1988; Price *et al.* 1997; McBride *et al.* 2001; Foden *et al.* 2002; Demidjuk *et al.* 2007). Isotopic ratios of NVP rocks have been found to correlate with rock composition, with alkaline rocks typically featuring lower ratios, through to tholeiitic basalts and basaltic trachyandesites, which have the highest ratios (Ewart & Menzies 1989). Early studies of Sr isotopes in NVP basalts gave a $^{87}\text{Sr}/^{86}\text{Sr}$ range of 0.7034–0.7045 (Dasch & Green 1975; Stuckless & Irving 1976; McDonough *et al.* 1985), similar to OIB (Demidjuk *et al.* 2007). This relatively large range was attributed to heterogeneous mantle source regions (Stuckless & Irving 1976). The Sr-isotopic values of NVP rocks are often attributable to sources with characteristics between those of HIMU (*ca* 0.7029) and EM1 (*ca* 0.705; Zindler & Hart 1986), both of which have trace element signatures that indicate some degree of mantle metasomatism in the source region.

Maximum recorded $^{87}\text{Sr}/^{86}\text{Sr}$ isotope values for 116 analyses traceable to 26 eruption centres are shown in Figure 1.21 and Table 1.6 (Cooper & Green 1969; Dasch & Green 1975; Stuckless & Irving 1976; McDonough *et al.* 1985; Whitehead 1986, 1991; Ewart *et al.* 1988; Price *et al.* 1997; McBride *et al.* 2001; Foden *et al.* 2002; Demidjuk *et al.* 2007; van Otterloo 2012; Boyce 2014). They do not include the analyses of Price *et al.* (1997) as they were not available to the author. Similar to

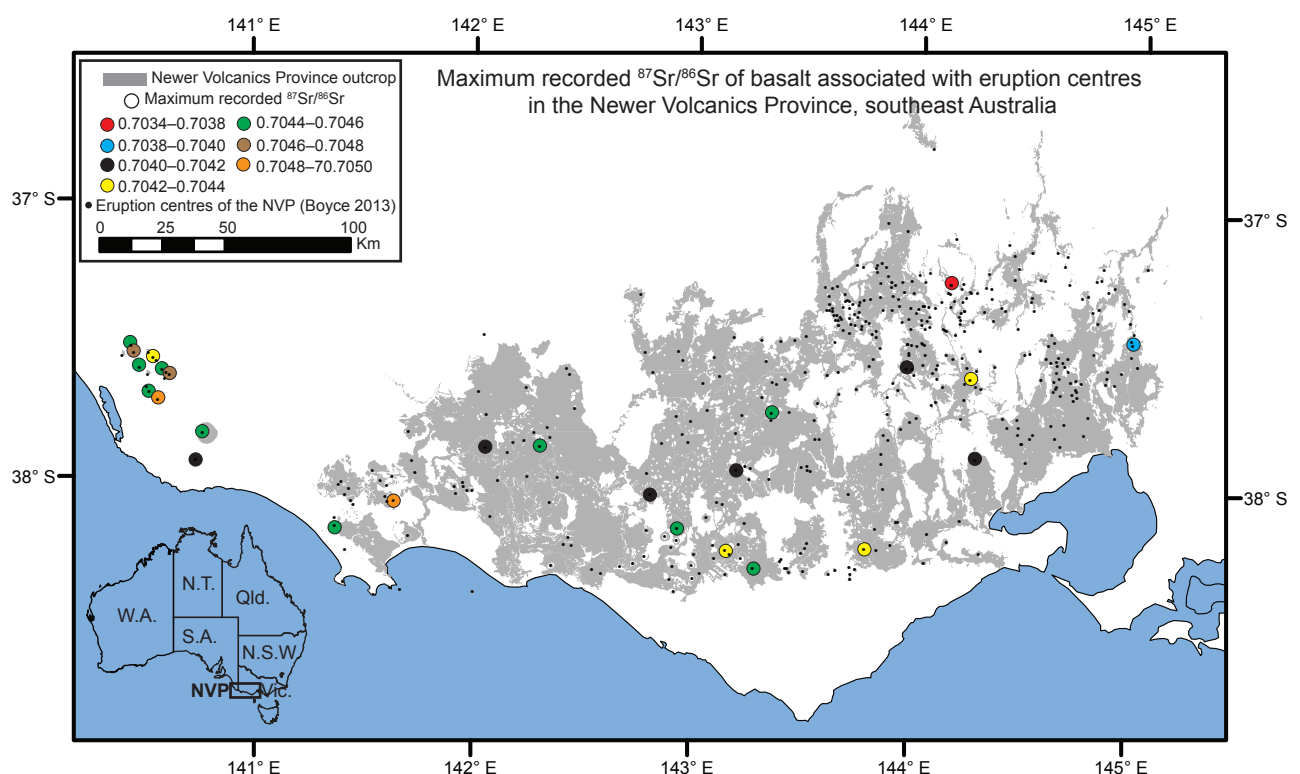


Figure 1.21 Maximum recorded $^{87}\text{Sr}/^{86}\text{Sr}$ isotope values of basalts traceable to eruption centres in the Newer Volcanics Province (filled circles), compared to the number of eruption centres in the province (small black filled circles).

Table 1.6 Range of $^{87}\text{Sr}/^{86}\text{Sr}$ isotope values of samples traceable to eruption centres in the Newer Volcanics Province, showing eruption centre, subprovince, latitude and longitude, Mg-number range and the number of samples.

| Volcanic Centre | Subprovince | Latitude | Longitude | $^{87}\text{Sr}/^{86}\text{Sr}$ range | No. of samples |
|-----------------|-------------|----------|-----------|---------------------------------------|----------------|
| Lake Leak | MG | -37.613 | 140.585 | 0.704 | 2 |
| Mt Burr | MG | -37.603 | 140.482 | 0.7044–0.7045 | 2 |
| Mt Eckersley | WP | -38.089 | 141.638 | 0.705 | 1 |
| Mt Edward | MG | -37.628 | 140.618 | 0.705 | 1 |
| Mt Elephant | WP | -37.961 | 143.198 | 0.704 | 1 |
| Mt Franklin | CH | -37.265 | 144.150 | 0.7036–0.7037 | 2 |
| Mt Fraser | CH | -37.462 | 144.978 | 0.704 | 1 |
| Mt Gambier | MG | -37.841 | 140.766 | 0.7036–0.7044 | 22 |
| Mt Gellibrand | WP | -38.234 | 143.791 | 0.7041–0.7043 | 2 |
| Mt Gorong | CH | -37.608 | 144.249 | 0.704 | 1 |
| Mt Graham | MG | -37.523 | 140.444 | 0.7042–0.7045 | 3 |
| Mt Kincaid | WP | -38.182 | 141.369 | 0.705 | 1 |
| Mt Leura | WP | -38.251 | 143.155 | 0.7038–0.7043 | 2 |
| Mt McIntyre | MG | -37.568 | 140.544 | 0.7041–0.7043 | 3 |
| Mt Muir | MG | -37.549 | 140.457 | 0.7044–0.7046 | 2 |
| Mt Napier | WP | -37.891 | 142.054 | 0.7039–0.7041 | 8 |
| Mt Noorat | WP | -38.176 | 142.934 | 0.7038–0.7045 | 4 |
| Mt Porndon | WP | -38.313 | 143.284 | 0.7039–0.7045 | 5 |
| Mt Rouse | WP | -37.885 | 142.303 | 0.7037–0.7045 | 27 |
| Mt Schank | MG | -37.940 | 140.736 | 0.7040–0.7041 | 7 |
| Mt Shadwell | WP | -38.055 | 142.809 | 0.7039–0.7041 | 3 |
| Mt Warrenheip | CH | -37.575 | 143.958 | 0.704 | 1 |
| Mt Watch | MG | -37.692 | 140.525 | 0.7042–0.7045 | 4 |
| Mt Widderin | WP | -37.747 | 143.353 | 0.704 | 1 |
| The Anakies | WP | -37.898 | 144.282 | 0.7035–0.7041 | 8 |
| The Bluff | MG | -37.72 | 140.565 | 0.7043–0.7050 | 2 |

age data, Sr-isotope ratios are available for only 6% of NVP eruption centres. If the 456 analyses of Price *et al.* (2007) were traced to eruption centres and added to the map, a more complete picture would be obtained of the variations within the NVP and could be used to direct further studies. Such maps could be correlated with geodynamical models and help us to better constrain the nature of the underlying mantle.

Price *et al.* (1997) recognised an isotopic discontinuity in basalts ~200 km west of Melbourne, coinciding with the Palaeozoic Moyston Fault—the suture between the Delamerian and Lachlan orogens. Basalts east and west of the Mortlake Discontinuity (MD) were found to feature a similar lower $^{87}\text{Sr}/^{86}\text{Sr}$ isotopic ratio limit of ~0.7037, but ratios were higher and more varied in the east (0.7037–0.7058) compared to the west (0.7037–0.7046) (Figure 1.22a). This indicates the influence of distinct sources within the eastern and western lithospheric mantle segments (Cooper & Green 1969; Dasch & Green 1975; Stuckless & Irving 1976; McDonough *et al.* 1985; Whitehead 1986; Ewart *et al.* 1988; Price *et al.* 1997, 2003; McBride *et al.* 2001; Foden *et al.* 2002; Demidjuk *et al.*

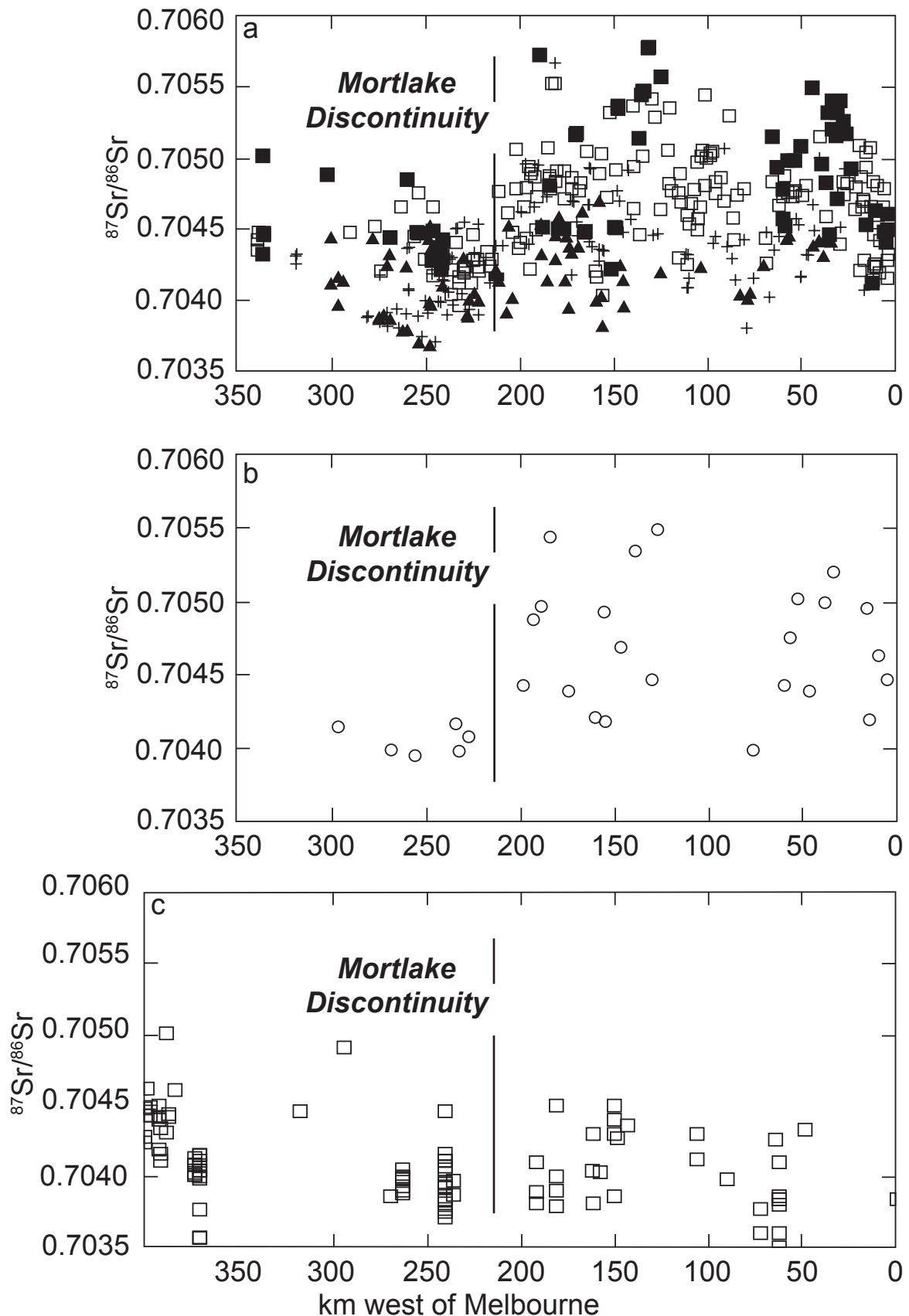


Figure 1.22 $^{87}\text{Sr}/^{86}\text{Sr}$ isotopic composition of Newer Volcanics Province basalts along an East to West profile to the West of Melbourne, showing the position of the Mortlake Discontinuity. a) 456 analyses based on composition, where filled squares are basaltic andesites, open squares tholeiites, crosses transitional basalts and filled triangles alkali rocks (modified after Price *et al.* 1997). b) A summary of figure (a), whereby the mean isotopic value of individual domains were calculated, and the average distance of the domain (modified after Price *et al.* 1997). c) Reported Sr isotope literature values from the remaining published literature to serve as a comparison with, and running further west than that of, Price *et al.* (1997) (Cooper & Green 1969; Dasch & Green 1975; Stuckless & Irving 1976; McDonough *et al.* 1985; Whitehead 1986; Ewart *et al.* 1988; McBride *et al.* 2001; Foden *et al.* 2002; Demidjuk *et al.* 2007).

2007). Price *et al.* (1997) used a combination of $^{87}\text{Sr}/^{86}\text{Sr}$ isotope data, petrography, major element geochemistry and age data to define 29 isotopic domains (groups with similar characteristics) across the Western Plains). These domains were interpreted as representing single large flows or groups of related flows. A plot of mean isotopic values for these domains makes the Mortlake Discontinuity more pronounced (Figure 1.22b). Data from other published studies were traced back to their volcano of origin and plotted on a similar diagram, with distances representing kilometres west of Melbourne to the point of origin (Figure 1.22c). The graph plots further west than that of the original study, as it includes the volcanoes of the Mt Burr Range and the 107 samples plotted only cover 26 of 437 volcanoes in the NVP. These data lowers the base $^{87}\text{Sr}/^{86}\text{Sr}$ isotopic ratio to ~ 0.7035 on both sides of the Mortlake Discontinuity, and it is clear that some volcanoes have been more extensively studied than others (e.g., Mts Rouse and Gambier; Table 1.6). It is suggested that when a full dataset becomes available for the Price *et al.* (1997) study, a comprehensive analysis of the 457 Sr-isotope sample locations should be undertaken in order to trace the flows back to their source and the results then plotted onto Figure 1.22c. This will enable the upper limit and variability of isotope compositions across the MD to be better assessed. Although the Western Plains sub-province is subdivided by the Mortlake Discontinuity, it behaves as a single geological entity, as it has the same time-span of eruptions, the same age range of peak activity (3.0–1.8 Ma) and the same progression from tholeiitic to alkaline compositions. The causes of activity therefore appear to be independent of crustal geology or the nature of the two mantle lithosphere segments involved (Gray & McDougall 2009).

Price *et al.* (1988) found that the Cones series basalts are isotopically distinct from the Plains series, with a $^{87}\text{Sr}/^{86}\text{Sr}$ range of 0.70379–0.70489 (24 samples) for the Cones basalts (McDonough *et al.* 1985) compared to 0.7036–0.7058 (400 samples) for the Plains basalts. On the basis of these differences, and also Os-isotope data, McBride *et al.* (2001) argued that the two series cannot be related to a single uniform mantle source by contrasted melting processes. Instead, they suggested that the Plains series basalts reflect either several mantle sources and/or show the effects of crustal contamination, due to their isotopic heterogeneity, whereas the Cones magmas ascended rapidly without significant crustal interaction.

1.6.3.3 Metasomatism beneath the Newer Volcanics Province

Observations on the mantle beneath western Victoria are possible through the study of mantle xenoliths, which are common to the east of the Mortlake Discontinuity, but are virtually unknown to the west (Price *et al.* 2003). Most mantle xenoliths occur within Cone series scoria cones and maars, predominantly associated with more strongly alkaline basalts. Therefore many localities are found in the Camperdown area (Price *et al.* 2003), which contains most of the maars. However, composition is not thought to be the sole control on xenolith occurrence (Nicholls *et al.* 1993). Peridotite xenoliths are the most common type, mainly spinel lherzolites, but harzburgites, dunites, pyroxenites and websterites are also present (Price *et al.* 2003). These nodules have been used to infer the nature of the lithosphere beneath the NVP (O'Reilly & Griffin 1985, 1988; Griffin *et al.* 1988). Granulitic and eclogitic xenoliths are also found at some localities (Griffin *et al.* 1988; O'Reilly & Griffin 1988).

Early studies suggested that the source regions of the host magmas differed from those of the xenoliths due to observed isotopic differences. Therefore the xenoliths are accidental in nature

and attest to the high ascent rates of the magmas, since dense xenoliths would sink in slowly rising magma. An origin in the lithospheric mantle is widely accepted for the peridotite xenoliths (Green *et al.* 1968; Kleeman *et al.* 1968; Frey & Green 1974; Dasch & Green 1975).

Both LREE-depleted and LREE-enriched types of xenoliths are present in NVP volcanic products. These are thought to reflect past melt depletion and enrichment events in the mantle (Frey & Green 1974; McDonough & McCulloch 1987). The lithospheric mantle underwent partial melting during stabilisation, leading to LREE-depletion, and eventually LREE-enrichment events occurred (McDonough & McCulloch 1987) due to metasomatism (McDonough & McCulloch 1987; O'Reilly & Griffin 1985; Griffin *et al.* 1988) during the late Proterozoic (McBride *et al.* 1996; Handler *et al.* 1997). These events resulted in contrasting degrees of depletion and enrichment over small areas, leading to a heterogeneous mantle (McDonough & McCulloch 1987). The mantle beneath western Victoria has undergone at least three metasomatic events (O'Reilly & Griffin 1988; Griffin *et al.* 1988) and metasomatism has been reported to increase with depth (Frey *et al.* 1978; McDonough *et al.* 1985, 1987; Boyce *et al.* 2014). The first episode involved recycled crust and is associated with garnet pyroxenites with high $^{87}\text{Sr}/^{86}\text{Sr}$ (500–300 Ma). The second event is associated with wehrlitic pyroxenites and mantle array Sr–Nd values (60 Ma–present); and more recently, local metasomatic overprinting has taken place via carbonatitic fluids and silicate melts (Stolz & Davies 1988; Yaxley *et al.* 1991, 1996; Yaxley & Kamenetsky 1999; Powell *et al.* 2004; O'Reilly & Griffin 2013). Metasomatism has led to the enrichment of incompatible trace elements such as REE, Sr, U and Th (apatite) and K, Ba, Nb and Ta (mica/amphibole) (O'Reilly & Griffin 2013). Mica and apatite, which are normally not present in mantle peridotites, are found in NVP xenoliths (O'Reilly *et al.* 1989). In addition, the mantle beneath western Victoria is thought to be heterogeneous on scales from centimetres to around 1 km (McDonough & McCulloch 1987; O'Reilly & Griffin 1988; O'Reilly *et al.* 1989).

A geotherm was defined for southeastern Australia based on mineral assemblages of garnet pyroxenite xenoliths from Lakes Bullen Merri and Gnotuk in the NVP (Figure 1.23; O'Reilly & Griffin 1985). Microprobe analyses were carried out on geochemically homogeneous minerals in order to calculate pressure-temperature values by several different methods, then used to derive the geotherm (Figure 1.23). The geotherm is useful, as it also shows univariant curves for the garnet lherzolite/spinel lherzolite (Herzberg 1978) and garnet pyroxenite/spinel pyroxenite transition zones (Kornprobst 1970; Irving 1974; Herzberg 1978), and the amphibole stability curve for ultramafic rocks (Milhollen *et al.* 1974). The amphibole-in curve intersects the geotherm at high temperatures (>1000°C), and is consistent with studies of mantle xenoliths in the NVP, many of which contain primary amphiboles (O'Reilly & Griffin 1985). In southeast Australia the crust–mantle boundary (which is believed to be gradational) lies at a depth of ~40 km (Aivazpourporgou 2013; Fontaine *et al.* 2013) and the lithosphere–asthenosphere boundary has been estimated at $\sim 61 \pm 11$ km (Ford *et al.* 2010). Estimates of temperature and depth of magma formation have been calculated for Mts. Rouse and Gambier, and the volcanoes of the Mt Burr range (Boyce *et al.* 2012, 2014, 2015; van Otterloo 2014; Holt *et al.* 2014). These suggest that the primary magmas were sourced from the lithosphere–asthenosphere boundary or shallow asthenosphere. If such models were developed for multiple volcanoes across the NVP using similar calculations, the volcano distribution maps could be used to constrain both the spatial extent of magma types and depths of melting across the province.

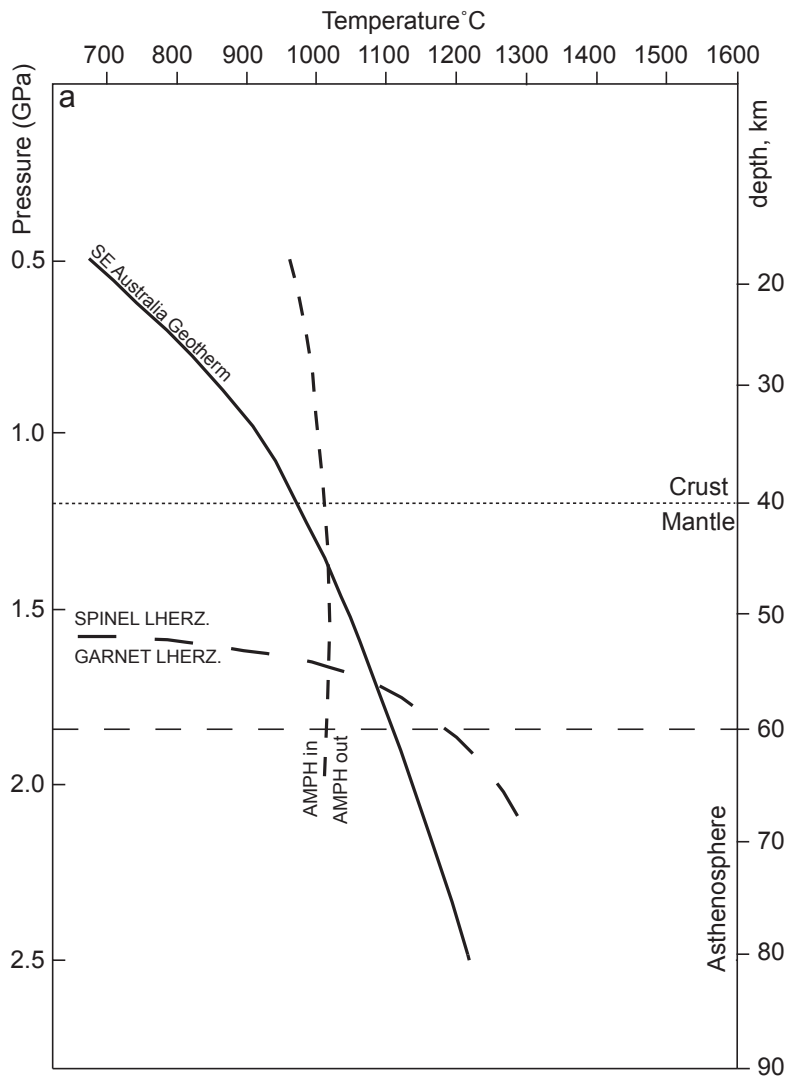


Figure 1.23 Southeast Australian Geotherm (heavy black line), showing garnet lherzolite/spinel lherzolite transition zone and amphibole stability curve. Modified after O'Reilly & Griffin (1985), with crust-mantle boundary from Aivazpourporgou (2013) and Fontaine *et al.* (2013) and lithosphere–asthenosphere boundary from Ford *et al.* (2010).

1.7 Thesis structure

This thesis is structured as an introduction chapter, four research chapters and a conclusions and discussion chapter. Research chapters have been structured as scientific journal articles; although this leads to the repetition of the introductory background of material in each chapter, this is an accepted format at Monash University.

Chapter 1 (this chapter) introduces the concept of monogenetic volcanism and outlines the aims of this project. It contains background information on the regional and tectonic setting of southeastern Australia, eastern Australian volcanism, the Newer Volcanics Province and major and trace element analysis and dating of Newer Volcanics rocks.

Chapter 2 is an overview of the NVP and presents a catalogue of eruption points (vents) and centres of the province, from a detailed desktop survey. This leads to the presentation of new volcanic distribution maps for eruption centres in the NVP. This article was published in the Australian Journal of Earth Sciences in July 2013 and is currently in the top 10 most-read articles of the journal.

Chapter 3 focuses on the eruption centres of the Hamilton area in order to place Mt Rouse within a local context. The relative ages of the volcanic centres are studied using radiometric data, and geochemical analyses of the volcanic products are presented, which define distinct phases of eruption in the area. Three new volcanoes are proposed, and the existence of several previously described centres are brought into question. This article was published in the Australian Journal of

Earth Sciences in June 2014 and is currently in the top 10 most-read articles of the journal.

Chapter 4 describes the complex stratigraphic architecture of Mt Rouse, detailing the various facies and eruption styles involved in the genesis of the volcano before outlining a new eruption sequence. This chapter is being prepared for submission to the *Journal of Volcanology and Geothermal Research*.

Chapter 5 explores the geochemical nature of the products of Mt Rouse, based on systematic sampling through a well-constrained stratigraphic framework. Results are discussed in terms of the petrogenesis of the volcanic centre. This article was published in *Contributions to Mineralogy and Petrology* in January 2015.

Chapter 6 summarises the results of the thesis, which are then discussed together with the results of other studies in terms of implications for monogenetic volcanism both in the NVP and worldwide.

Additional data for each research chapter, including geochemical analyses, stratigraphic logs and the database of eruption centres and associated files are contained in the relevant appendices at the end of the thesis and on an enclosed CD-ROM. Appendix 1 contains outreach relating to this PhD, including the Mt Rouse section of the IUGG 2011 field trip guide for trip VF01: 'Factors that influence varying eruption styles (from magmatic to phreatomagmatic) in intraplate continental basaltic volcanic provinces: The Newer Volcanics Province of southeastern Australia'; an article published in *Geology Today* in May 2014 for the general reader on volcanism in the NVP; and a web page and volcano tour written for the Penshurst Volcanoes Discovery Centre.

1.8 References

AIVAZPOURPORGOU S., THIEL S., HAYMAN P., MORESI L. & HEINSON G. 2012. The upper mantle thermal structure of the Newer Volcanic Province, Western Victoria, Australia from long period Magnetotelluric (MT) array. Extended Abstract, 21st EM Induction Workshop, Darwin, Australia, 25–31 July 2012.

AIVAZPOURPORGOU S. 2013. Lithospheric structures of the Newer Volcanics Province, western Victoria, Australia from a long-period magnetotelluric array. Unpublished PhD thesis, Monash University.

AIVAZPOURPORGOU S., THIEL S., HAYMAN P. C., MORESI L. N. & HEINSON G. 2014. Decompression melting driving intraplate volcanism in Australia: Evidence from magnetotelluric sounding. *Geophysical Research Letters* **42**: doi GL060088

ABBOT M. J. 1969. Petrology of the Nandewar volcano, N.S.W., Australia. *Contributions to Mineralogy and Petrology* **20**, 115–134.

ASHLEY P. M., DUNCAN R. A. & FEEBRAY C. A. 1995. Ebor volcano and Crescent complex, northeastern New South Wales: age and geological development. *Australian Journal of Earth Sciences* **42**, 471–480.

- ATKINSON F. A. 1986. Cainozoic basaltic rocks and their relationships to stanniferous deposits in the watershed of the upper Herbert River, north Queensland. MSc thesis, James Cook University, Townsville (Unpublished).
- AUCKLAND COUNCIL. 2013. Auckland Volcanic Field Contingency Plan. Civil Defence and Emergency Management, Auckland. <http://www.aucklandcivildefence.org.nz/About-Us/Document-Library/Supporting-Plans/>
- AZIZ-UR-RAHMAN & MCDUGALL I. 1972. Potassium–argon ages on the Newer Volcanics of Victoria. *Proceedings of the Royal Society of Victoria* **85**, 61–69.
- BALOGA S. M., GLAZE L. S. & BRUNO B. C. 2007. Nearest-neighbor analysis of small features on Mars: Applications to tumuli and rootless cones. *Journal of Geophysical Research* **112**, E03002.
- BARBETTI M. & SHEARD M. J. 1981. Palaeomagnetic results from Mounts Gambier and Schank, South Australia. *Journal of the Geological Society of Australia* **28**, 385–394.
- BEBBINGTON M. S. & CRONIN S. J. 2011. Spatio-temporal hazard estimation in the Auckland Volcanic Field, New Zealand, with a new event-order model. *Bulletin of Volcanology* **73**, 55–72.
- BENNETT R., PAGE R. W. & BLADON G. M. 1975. Catalogue of isotopic age determinations on Australian rocks, 1966–70. *Bureau of Mineral Resources Australia Report* **162**.
- BERRY R. F. & CRAWFORD A. R. 1988. The tectonic significance of Cambrian allochthonous mafic-ultramafic complexes in Tasmania. *Australian Journal of Earth Sciences* **35**, 523–533.
- BISHOP M. A. 2007. Point pattern analysis of eruption points for the Mount Gambier volcanic sub-province: a quantitative geographical approach to the understanding of volcano distribution. *Area* **39.2**, 230–241.
- BISHOP M. A. 2008. Higher-order neighbor analysis of the Tartarus Colles cone groups, Mars: The application of geographical indices to the understanding of cone pattern evolution. *Icarus* **197**, 73–83.
- BLACKBURN G. 1966. Radiocarbon dates relating to soil development and volcanic ash deposition in south-east South Australia. *Australian Journal of Earth Sciences* **29**, 50–52.
- BLACKBURN G., ALLISON G. B. & LEANEY F. W. J. 1982. Further evidence on the age of the tuff at Mount Gambier, South Australia. *Transactions of the Royal Society of South Australia* **106**, 163–167.
- BLAIKIE T. N., AILLERES, L., CAS R. A. F. & BETTS P. G. 2012. Three-dimensional potential field modelling of a multi-vent maar-diatreme — The Lake Coragulac maar, Newer Volcanics Province,

south-eastern Australia. *Journal of Volcanology and Geothermal Research* **235**, 70–83.

BOWLER J. M. & HAMADA T. 1971. Late Quaternary stratigraphy and radiocarbon chronology of water level fluctuations in Lake Keilambete, Victoria. *Nature* **232**, 330–332.

BOYCE J., NICHOLLS I., KEAYS R. & HAYMAN P. 2012. The multiple magma batches of Mt Rouse, Newer Volcanics Province, Victoria, Australia. Abstract, IAVCEI 4IMC conference, Auckland, New Zealand, 20 February 2012.

BOYCE J. A. 2013. The Newer Volcanics Province of southeastern Australia: a new classification scheme and distribution map for eruption centres. *Australian Journal of Earth Sciences* **60**, 449–462.

BOYCE J. A., KEAYS R. R., NICHOLLS I. A. & HAYMAN P. C. 2014. Eruption centres of the Hamilton area of the Newer Volcanics Province, Victoria, Australia: pinpointing volcanoes from a multifaceted approach to landform mapping. *Australian Journal of Earth Sciences* **61**, 735–754.

BOYCE J. A., NICHOLLS I. A., KEAYS R. R. & HAYMAN P. C. 2015. Variation in parental magmas of Mt Rouse, a complex polymagmatic monogenetic volcano in the basaltic intraplate Newer Volcanics Province, southeast Australia. *Contributions to Mineralogy and Petrology* **169**, doi 10.1007/s00140-015-1106-y

BRENNAN M., CRONIN S. J., SMITH I. E. M., SOHN S. Y. & NÉMETH K. 2010. Mechanisms driving polymagmatic activity at a monogenetic volcano, Udo, Jeju Island, South Korea. *Contributions to Mineralogy and Petrology* **160**, 1–20.

BRENNAN M., CRONIN S. J., NÉMETH K., SMITH I. E. M., & SOHN Y. 2011. The influence of magma plumbing complexity on monogenetic eruptions, Jeju Island, Korea. *Terra Nova* **23**, 70–75.

BROWNE W. M. 1947. Leucogranites and the related rhyolite-basalt dyke swarm near Corryong, northeast Victoria. B.Sc. (Hons) thesis, La Trobe University, Melbourne (unpublished).

BROZ P. & HAUBER E. 2012. A unique volcanic field in Tharsis, Mars: Pyroclastic cones as evidence for explosive eruptions. *Icarus* **218**, 88–99.

CAMP V. E., HOOPER P. R., ROOBOL M. J. & WHITE D. L. 1987. The Madinah eruption, Saudi Arabia: Magma mixing and simultaneous extrusion of three basaltic chemical types. *Bulletin of Volcanology* **49**, 489–508.

CANDE S. C. & MUTTER J. C. 1982. A revised identification of the oldest sea-floor spreading anomalies between Australia and Antarctica. *Earth and Planetary Science Letters* **58**, 151–160.

CARTWRIGHT I., WEAVER T., TWEED S., AHEARNE D., COOPER M., CZAPNIK K.

& TRANTER J. 2002. Stable isotope geochemistry of cold CO₂- bearing mineral spring waters, Daylesford, Victoria: sources of gas and water and links with waning volcanism. *Chemical Geology* **185**, 71–91.

CAS R. A. F. 1983. Palaeogeographic and tectonic development of the Lachlan Fold Belt of southeastern Australia. *Geological Society of Australia Special Publication* **10**, 104.

CAS R. & Wright J. V. 1987. *Volcanic Successions: Modern and Ancient*. Chapman & Hall.

CAS R., SIMPSON C. & SATO H. 1993. Newer Volcanics Province—Processes and products of phreatomagmatic activity. IAVCEI Canberra 1993—Excursion guide. Australian Geological Survey Organisation, Canberra.

CAS R., BLAIKIE T., BOYCE J., HAYMAN P., JORDAN S., PIGANIS F., PRATA G. & VAN OTTERLOO J. 2011. Factors that influence varying eruption styles (from magmatic to phreatomagmatic) in intraplate continental basaltic volcanic provinces: The Newer Volcanics Province of southeastern Australia. Field trip guide VF01, pp. 7–31. IUGG 2011 General Assembly. *Earth on the Edge: Science for a Sustainable Planet*.

CAYLEY R. A., WEBB A. W. & HENLEY K. J. 1995. Radiometric dating (K/Ar) on two samples of Newer Volcanic olivine basalt from the southwestern part of the Beaufort 1:100 000 map sheet area. Geological Survey of Victoria Unpublished Report 1995/15.

CAYLEY R. A., KORSCH R. J., MOORE D. H., COSTELLOE R. D., AKAMURA A., WILLMAN C. E., RAWLING J., MORAND V. J., SKLADZIEN P. B. & 'SHEA P. J. 2011. Crustal architecture of central Victoria: results from the 2006 deep crustal reflection seismic survey. *Australian Journal of Earth Sciences* **58**, 113–156.

CAYLEY R. A. & TAYLOR D. H. 2001. Ararat 1:100 000 geological map report. *Geological Survey of Victoria Report* **115**.

CERVANTES P. & WALLACE P. 2003. Magma degassing and basaltic eruption styles: a case study of ~2000 year BP Xitle volcano in central Mexico. *Journal of Volcanology and Geothermal Research* **120**, 249–270.

CHIVAS A. R., BARNES I. E., LUPTON J. E. & COLLERSON K. 1983. Isotopic studies of south-east Australian CO₂ discharges. *Geological Society of Australia Abstract* **12**, 94–95.

CHIVAS A. R., BARNES I., EVANS W. C., LUPTON J. E. & STONE J. O. 1987. Liquid carbon dioxide of magmatic origin and its role in volcanic eruptions. *Nature* **326**, 587–589.

CONDIT C. D. & CONNOR C. B. 1996. Recurrence rates of volcanism in basaltic volcanic fields:

An example from the Springerville volcanic centre, Arizona. *Geological Society of America Bulletin* **108**, 1225–1241.

COOPER S. 1999. Bingara diamond field. *Minfo, New South Wales Mining and Exploration Quarterly* **63**, 13–15.

COOPER J. A. & GREEN D. H. 1969. Lead isotope measurements on lherzolite inclusions and host basanites from western Victoria, Australia. *Earth and Planetary Science Letters* **6**, 69–76.

COX S. F., ETHERIDGE M.A., CAS R. A. F. & CLIFFORD B. A. 1991. Deformational style of the Castlemaine area, Bendigo-Ballarat zone: Implications for evolution of crustal structure in central Victoria. *Australian Journal of Earth Sciences* **38**, 151–170.

CRAWFORD A. J. & BERRY R. F. 1992. Tectonic implications of Late Proterozoic–Early Palaeozoic igneous rock associations in western Tasmania. In: Fergusson C. L. & Glen R. A. eds. *The Palaeozoic eastern margin of Gondwanaland: Tectonics of the Lachlan Fold Belt, southeastern Australia and related orogens*. *Tectonophysics* **214**, 37–56.

CRAWFORD A. J., DONAGHY A. G., BLACK L. P. & STUART–SMITH P.G. 1996. Mount Read Volcanics correlatives in western Victoria: a new exploration opportunity. *Australian Institute of Geoscience Bulletin* **20**.

CSAKY D. 2002. The varied eruptive history of the Mount Porndon volcanic complex in the Newer Volcanics Province of Victoria. Honours thesis, School of Geosciences, Monash University, 207 pp.

DASCH E. J. & GREEN D. H. 1975. Strontium isotope geochemistry of lherzolite inclusions and host basaltic rocks, Victoria, Australia. *American Journal of Science* **275**, 461–469.

DASCH E. J. & MILLAR D. J. 1977. Age and strontium-isotope geochemistry of differentiated rocks from the Newer Volcanics, Mt Macedon area, Victoria, Australia. *Journal of the Geological Society of Australia* **24**, 195–201.

DAVIES D. R. & RAWLINSON N. 2014. On the origin of recent intraplate volcanism in Australia. *Geology* doi 10.1130/G363093.1

DAY R. A. 1983. Petrology and geochemistry of the Older Volcanics of Victoria. PhD thesis, Monash University.

DAY R. A. 1989. Older Volcanics. In: Johnson R. W. ed. *Intraplate volcanism in Eastern Australia and New Zealand*, pp. 133–136. Cambridge University Press, Cambridge.

DE KEYSER F. & LUCAS K. G. 1968. Geology of the Hodgkinson and Laura Basins, north

Queensland. *Bureau of Mineral Resources, Australia Bulletin* **84**.

DEMIDJUK Z., TURNER S., SANDIFORD M., GEORGE R., FODEN J. & ETHERIDGE M. 2007. U-series isotope and geodynamic constraints on mantle melting processes beneath the Newer Volcanic Province in South Australia. *Earth and Planetary Science Letters* **261**, 517–533.

DODSON J. R. 1975. Vegetation history and water fluctuations at Lake Leake, south-eastern Australia. II. 50,000 B. P. to 10,000 B. P. *Australian Journal of Botany* **23**, 815–831.

DREXEL J. F., PREISS W. V. & PARKER A. J. 1993. The geology of South Australia. Volume 1: The Precambrian. *South Australian Geological Survey Bulletin* **54**.

DUDDY I. R. 2003. Mesozoic. A time of change in tectonic regime. In: Birch W. D. ed. *Geology of Victoria*, pp. 239–286. *Geological Society of Australia Special Publication* **23**.

DUNCAN R. A. & CLAGUE D. A. 1985. Pacific plate motion recorded by linear volcanic chains. In: Nairn A. E. M. ed. *The Ocean Basins and Margins, volume 7A, The Pacific Ocean*. Plenum, New York.

DUNCAN R. A. & MCDOUGALL I. 1989. Framework for volcanism. Volcanic Time-Space Relationships. In: Johnson R. W. ed. *Intraplate volcanism in Eastern Australia and New Zealand*, pp. 43–54. Cambridge University Press, Cambridge.

EDWARDS A. B. E. 1938. The Tertiary volcanic rocks of central Victoria. *Quarterly Journal of the Geological Society* **94**, 243–320.

EDWARDS A. B. 1939. Petrology of the Tertiary Older Volcanic rocks of Victoria. *Proceedings of the Royal Society of Victoria* **51**, 73–98.

EDWARDS J. 1994. The Geology, Petrography and Geochemistry of Lady Julia Percy Island. MSc thesis, University of Melbourne.

EDWARDS J. 1990. Radiometric age determinations Colac 1: 250 000 map sheet of the Geological Survey of Victoria. *Geological Survey of Victoria Unpublished Report* **1990/44**.

EDWARDS A. B. & CRAWFORD W. 1940. The Cainozoic volcanic rocks of the Gisbourne district, Victoria. *Proceedings of the Royal Society of Victoria* **52**, 281–311.

EDWARDS J., LEONARD J. G., PETTIFER G. R. & MCDONALD P. A. 1996. Colac, 1:250 000 map geological report. *Geological Survey of Victoria Report* **98**.

EDWARDS J., SLATER K. R. & MCHAFFIE I. W. 2001. Bendigo 1: 250 000 map area geological

report. *Victorian Initiative for Minerals and Petroleum Report* **72**.

EDWARDS J., CAYLEY R. A. & JOYCE E. B. 2004. Geology and geomorphology of the Lady Julia Percy Island volcano, a late Miocene submarine and subaerial volcano off the coast of Victoria, Australia. *Proceedings of the Royal Society of Victoria* **116**, 15–35.

ELIAS M. 1973. The Geology and Petrology of Mount Rouse, A Volcano in the Western District of Victoria. BSc thesis (unpublished), University of Melbourne.

ELLIS D. J. 1976. High pressure cognate inclusions in the Newer Volcanics of Victoria. *Contributions to Mineralogy and Petrology* **58**, 149–180.

ERLUND E. J., CASHMAN K. V., WALLACE P. J., PIOLIL., ROSI M., JOHNSON E. & DELGADO GRANADOS H. 2010. Compositional evolution of magma from Paricutin Volcano, Mexico: The tephra record. *Journal of Volcanology and Geothermal Research* **197**, 167–187.

EVERARD J. L., CALVER C. R., PEMBERTON J., TAHERI J. & DIXON G. 1997. Geology of the islands of southwestern Bass Strait. *Tasmanian Geological Survey Record* **1977/03**.

EVERNDEN J. F. & RICHARDS J. R. 1962. Potassium–Argon ages in eastern Australia. *Journal of the Geological Society of Australia* **9**, 1–50.

EWART A., CHAPPELL B. W. & Le MAITRE R. W. 1985. Aspects of the mineralogy and chemistry of the intermediate-silicic Cainozoic volcanic rocks of eastern Australia. Part 1: Introduction and geochemistry. *Australian Journal of Earth Sciences* **32**, 359–382.

EWART A., CHAPPELL B. W. & MENZIES M. A. 1988. An overview of the geochemical and isotopic characteristics of the eastern Australian Cainozoic volcanic provinces. *Journal of Petrology. Special Lithosphere Issue*, 225–273.

EWART A. & CHAPPELL B. W. 1989. Chapter 5.4 Trace element Geochemistry. In: Johnson R. W. ed. *Intraplate volcanism in Eastern Australia and New Zealand*, pp. 219–235. Cambridge University Press, Cambridge.

EWART A. & MENZIES M. A. 1989. Chapter 5.5 Isotope Geochemistry. In: Johnson R. W. ed. *Intraplate volcanism in Eastern Australia and New Zealand*, pp. 235–246. Cambridge University Press, Cambridge.

EXON N. F., BERRY R. F., CRAWFORD A. J. & HILL P. J. 1997. Geological evolution of the East Tasman Plateau, a continental fragment south east of Tasmania. *Australian Journal of Earth Sciences* **44**, 597–608.

- FARRINGTON R. J., STEGMAN D. R., MORESI L. N., SANDIFORD M. & MAY D. A. 2010. Interactions of 3D mantle flow and continental lithosphere near passive margins. *Tectonophysics* **483**, 20–28.
- FINN C. A., MEULLER R. D. & PANTER K. S. 2005. A Cainozoic diffuse alkaline magmatic province (DAMP) in the southwest Pacific without rift or plume origin. *Geochemistry, Geophysics, Geosystems* **6**, Q02005.
- FISHWICK S., HEINTZ M., KENNETT B. L. N., READING A. M. & YOSHIZAWA K. 2008. Steps in lithospheric thickness within eastern Australia, evidence from surface wave tomography. *Tectonics* **27**, TC4009.
- FISHWICK S. & RAWLINSON N. 2012. 3-D structure of the Australian lithosphere from evolving seismic data sets. *Australian Journal of Earth Sciences* **59**, 809–826.
- FISHER R. V. & SCHMINCKE H. U. 1984. Pyroclastic rocks. Springer Verlag, Berlin.
- FODEN J., SONG S. H. S., TURNER S., ELBURG M., SMITH P. B., VAN DER STELDT B. & VAN PENGLIS D. 2002. Geochemical evolution of lithospheric mantle beneath S.E. South Australia. *Chemical Geology* **182**, 663–695.
- FONTAINE F. F., TKALCIC H. & KENNETT L. N. 2013. Imagining crustal structure variation across southeastern Australia. *Tectonophysics* **582**, 112–125.
- FORD H. A., FISCHER K. M., ABT D. L., RYCHERT C. A. & ELKINS–TANTON L. T. 2010. The lithosphere–asthenosphere boundary and cratonic lithospheric layering beneath Australia from Sp wave imaging. *Earth and Planetary Science Letters* **300**: 299–310.
- FOSHAG W. F. & GONZÁLEZ R. 1956. Birth and development of Parícutin Volcano, Mexico. *Geological Survey Bulletin* **965-D**, 355–489.
- FOSTER D. A., KWAK T. A. P. & GRAY D. R. 1996a. Timing of gold mineralisation and relationship to metamorphism, thrusting, and plutonism in Victoria. In: Hughes M. J., Ho S. E. & Hughes C. E. eds. *Recent Developments in Victorian Geology and Mineralisation. Australian Institute of Geoscientists Bulletin* **20**, 49–53.
- FOSTER D. A., GRAY D. R. & OFFLER R. 1966b. The western sub-province of the Lachlan Fold Belt: structural style, geochronology, metamorphism, and tectonics. *Specialist Group in Geochemistry, Mineralogy and Petrology Field Guide* **1**.
- FOSTER D. R. & GRAY D. A. 2000. Evolution and structure of the Lachlan Fold Belt (orogen) of Eastern Australia. *Annual Review of Earth and Planetary Sciences* **28**, 47–80.

- FREY F. A. & GREEN D. H. 1974. The mineralogy, geochemistry and origin of lherzolite inclusions in Victorian basanites. *Geochimica et Cosmochimica Acta* **38**, 1023–1059.
- FREY F. A., GREEN D. H. & ROY D. 1978. Integrated models of basalt petrogenesis: a study of quartz tholeiites to olivine melilitites from South Eastern Australia utilising geochemical and experimental petrological data. *Journal of Petrology* **19**, 463–513.
- GAINA C., MÜLLER R. D., ROYER J-Y. & SYMONDS P. 1999. The evolution of the Lousiade triple junction. *Journal of Geophysical Research* **104**, 12927–12939.
- GAINA C., MÜLLER R. D., BROWN B. & ISHIHARA T. 2003. Chapter 26—Microcontinent formation around Australia. *Geological Society of Australia Special Publication* **22**, 399–410.
- GIBSON D. L. 2007. Potassium–Argon ages of Late–Mesozoic and Cainozoic igneous rocks of eastern Australia. *CRC LEME Open File Report* **193**, pp.53.
- GILL E. D. 1957. The stratigraphical occurrence and palaeoecology of some Australian Tertiary marsupials. *Memoirs of the National Museum of Victoria* **21**, 135–199.
- GILL E. D. 1978. Radiocarbon dating of the volcanoes of western Victoria, Australia. *Australian Naturalist* **95**, 152–158.
- GILL E. D. 1979. The Tyrendarra lava flow, western Victoria, Australia. *Victorian Naturalist* **96**, 227–229.
- GILL E. D. 1981. Potassium/argon age of basalt in the floor of Hopkins River, Allansford, SW Victoria, Australia. *Victorian Naturalist* **98**, 188–190.
- GILL E. D. & SHERWOOD J. 1986. Hopkins estuary and Point Ritchie sites, Warrnambool. Unpublished excursion guide.
- GILL E. D. & ELMORE L. K. M. 1974. Importance of the Mount Napier Volcanic Complex near Hamilton, Victoria, Australia. *Victorian Naturalist* **91**, 167–174.
- GOURAMANIS C., WILKINS D. & DEDECKKER P. 2010. 6000 years of environmental changes recorded in Blue Lake, South Australia, based on ostracod ecology and valve chemistry. *Palaeogeography, Palaeoclimatology, Palaeoecology* **297**, 223–237.
- GRAEBER F. M., HOUSEMAN G. A. & GREENHALGH S. A. 2002. Regional teleseismic tomography of the western Lachlan Orogen and the Newer Volcanic Province, southeast Australia. *Geophysical Journal International* **149**, 249–266.

GRAHAM I., HOLLIS J., SUTHERLAND L. & JOYCE B. 2003. Insights into the Newer Volcanic Province of Victoria. *Specialist Group in Geochemistry, Mineralogy and Petrology, Field Guide, Geological Society of Australia*.

GRAY D. R. 1997. Tectonics of the southeastern Australian Lachlan Fold Belt: structural and thermal aspects. *Geological Society of London Special Publication* **121**.

GRAY D. R., ALLEN R. L., ETHERIDGE M. A., FERGUSON C. L., GIBSON G. M., MORAND V. J., VANDENBERG A. H. M., WATCHORN R. B. & WILSON C. J. L. 1988. Structure & Tectonics. In: Douglas J. G. & Ferguson J. A. eds. *Geology of Victoria. Geological Society of Australia Special Publication* **5**.

GRAY D. R. & WILLMAN C. E. 1991. Deformation in the Ballarat Slate Belt, central Victoria, and implications for the crustal structure across southeast Australia. *Australian Journal of Earth Science* **38**: 171–201.

GRAY D. A. & FOSTER D. R. 1997. Orogenic concepts—application and definition: Lachlan fold belt, eastern Australia. *American Journal of Science* **297**: 859–891.

GRAY D. R., FOSTER D. A., MORAND V. J., WILLMAN C. E., CAYLEY R. A., SPAGGIARI C. V., TAYLOR D. H., GRAY C. M., VANDENBERG A. H. M., HENDRICKS M. A. & WILSON C. J. L. 2003. Chapter 2. Structure, metamorphism, geochronology and tectonics of Palaeozoic rocks. In: Birch W. D. ed. *Geology of Victoria. Geological Society of Australia Special Publication* **23**.

GRAY C. M. & MCDUGALL I. 2009. K–Ar geochronology of basalt petrogenesis, Newer Volcanics Province, Victoria. *Australian Journal of Earth Sciences* **56**, 245–258.

GRAYSON H. J. & MAHONEY D. J. 1910. The geology of the Camperdown and Mount Elephant districts. *Memoirs of the Geological Survey of Victoria* **9**.

GREEN D. H., MORGAN J. W. & HEIER K. S. 1968. Thorium, uranium and potassium abundances in Peridotite inclusions and their host basalts. *Earth and Planetary Science Letters* **4**, 155–166.

GREEN D. H. 1970. The origin of basaltic and nephelinitic magmas. *Transactions of the Leicester Literary & Philosophical Society* **64**, 28–54.

GRIFFIN T. J. 1977. The geology, mineralogy and geochemistry of the McBride basaltic province, northern Queensland. James Cook University of North Queensland PhD thesis unpublished.

GRIFFIN T. J. & MCDUGALL I. 1975. Geochronology of the Cainozoic McBride volcanic province, northern Queensland. *Journal of the Geological Society of Australia* **22**, 387–397.

- GRIFFIN W. L., O'REILLY S. Y. & STABEL A. 1988. Mantle metasomatism beneath western Victoria, Australia: II. Isotopic geochemistry of Cr-diposide lherzolites and Al-augite pyroxenites. *Geochimica et Cosmochimica Acta* **52**, 449–459.
- GOURAMANIS C., WILKINS D. & DEDECKKER P. 2010. 6000 years of environmental changes recorded in Blue Lake, South Australia, based on ostracod ecology and valve chemistry. *Palaeogeography, Palaeoclimatology, Palaeoecology* **297**, 223–237.
- GRAY C. M. & MCDOUGALL I. 2009. K–Ar geochronology of basalt petrogenesis, Newer Volcanic Province, Victoria. *Australian Journal of Earth Sciences* **56**, 245–258.
- GRAY D. R. & WILLMAN C. E. 1991. Deformation in the Ballarat Slate Belt, central Victoria and implications for the crustal structure across southeast Australia. *Australian Journal of Earth Sciences* **38**, 171–201.
- GRAY D. R., FOSTER D. A. & BUCHER M. 1997. Recognition and definition of orogenic events in the Lachlan Fold Belt. *Australian Journal of Earth Sciences* **44**, 489–581.
- HANDLER M.R., BENNETT V.C. & ESAT T. M. 1997. The persistence of off-cratonic lithospheric mantle: Os isotopic systematics of variably metasomatised southeast Australian xenoliths. *Earth and Planetary Science Letters* **151**, 61–75.
- HARDING R. R. 1969. Catalogue of age determinations on Australian rocks, 1962–1965. *Bureau of Mineral Resources Australia Report* **117**, pp. 105.
- HARRINGTON H. J., BURNS K. L., THOMPSON B.R. & OZOLINS A. P. 1974. Regional geology of Victoria in relation to satellite imagery. A preparatory study. CSIRO Minerals Research Laboratories Division of Mineral Physics Investigation Report **106** and *Geological Survey of Victoria*.
- HEAD M. J., TAYLOR L. J. & WALKER D. 1994. ANU radiocarbon date list XI: radiocarbon dates from Lakes Barrine and Eacham, Atherton Tableland, north Queensland. *Radiocarbon* **36**, 73–94.
- HENLEY K. J. & WEBB A. 1990. Radiometric dating on various granites and Newer Volcanics basalts. *Geological Survey of Victoria Unpublished Report* **1990/27**.
- HERZBERG C. 1978. Pyroxene geothermometry and geobarometry: experimental and thermodynamic evaluation of some subsolidus phase relations involving clinopyroxenes in the system CaO–MgO–Al₂O₃–SiO₂. *Geochimica et Cosmochimica Acta* **42**, 945–957.
- HILLIS R. R., MONTE S. A., TAN C. P. & WILLOUGHBY D. R. 1995. The contemporary stress field of the Otway Basin, South Australia: implications for hydrocarbon exploration and production. *Australian Petroleum Exploration Association Journal* **35**, 494–506.

HILLIS R. R., SANDIFORD M., REYNOLDS S. D. & QUIGLEY M. C. 2008. Present-day stresses, seismicity and Neogene-to-recent tectonics of Australia's 'passive' margins: intraplate deformation controlled by plate boundary forces. *Geological Society of London Special Publication* **306**, 71–90.

HOFMANN A. W., JOCHUMK P., SEUFERT M. & WHITE W. M. 1986 Nb and Pb in oceanic basalts: new constraints on mantle evolution. *Earth and Planetary Science Letters* **79**, 33–45.

HOLT S. J., HOLFORD S. P. & FODEN J. 2014. New insights into the magmatic plumbing system of the South Australian Quaternary Basalt province from 3D seismic and geochemical data. *Australian Journal of Earth Sciences* **60**, 797–817.

HOUGHTON B. F., WILSON C. J. N. & SMITH I. E. M. 1999. Shallow-seated controls on styles of explosive basaltic volcanism: a case study from New Zealand. *Journal of Volcanology and Geothermal Research* **91**, 97–120.

IRVING A. J. 1974. Geochemical and high-pressure experimental studies of garnet pyroxenites and pyroxene granulite xenoliths from the Delegate basaltic pipes, Australia. *Journal of Petrology* **15**, 1–40.

IRVING A. J. & FREY F. A. 1987. Distribution of trace elements between garnet megacrysts and host volcanic liquids of kimberlitic to rhyolitic composition. *Geochimica et Cosmochimica Acta* **42**, 771–787.

IRVING A. J. & GREEN D. H. 1976. Geochemistry and petrogenesis of the Newer basalts of Victoria and South Australia. *Journal of the Geological Society of Australia* **23**, 46–66.

JENSEN-SCHMIDT B., COCKSHELL C. D. & BOULT P. J. 2002. Chapter 5. Structural and Tectonic Setting. In: Boulton P. J. & Hibbert J. E. Eds. *The Petroleum Geology of South Australia*. Department of Primary Industries and Resources, Adelaide.

JOHNSON R. W. 1989. Intraplate volcanism in Eastern Australia and New Zealand. Cambridge University Press, Cambridge.

JOHNSON R. W. & WELLMAN S. R. 1989. Framework for volcanism. Introduction to Intraplate Volcanism. In: Johnson R. W. ed. *Intraplate volcanism in Eastern Australia and New Zealand*, pp. 1–12. Cambridge University Press, Cambridge.

JOPLIN, G. A. 1963. Chemical analysis of Australian rocks. I, Igneous and Metamorphic. *Bureau of Mineral Resources, Geology and Geophysics, Australia* **65**, 1–446.

JORDAN S. C. 2013. Factors controlling the formation of a very large maar volcano and the fragmentation process in phreatomagmatic eruptions: Lake Purrumbete Maar, southeastern Australia.

PhD thesis, Monash University.

JORDAN S. C., CAS R. A. F. & HAYMAN P. C. 2013. The origin of a large (>3 km) maar volcano by coalescence of multiple shallow craters: Lake Purrumbete maar, southeastern Australia. *Journal of Volcanology and Geothermal Research* **254**, 5–22.

JOYCE E. B. 1975. Quaternary volcanism and tectonics in southeastern Australia. In: Suggate R. P. & Cresswell M. M. eds. *Quaternary studies*, pp. 169–178. The Royal Society of New Zealand, Wellington.

JOYCE E. B. 2004. The young volcanic regions of southeastern Australia: early studies, physical volcanology and eruption risk. *Proceedings of the Royal Society of Victoria* **116**, 1–13.

JOYCE E. B. 2007. Volcanoes of the Creswick Deep Leads region in the Western Uplands of Victoria. Creswick deep leads goldfields tour ‘Buried rivers of gold’. Saturday 1st December, 2007; Earth Sciences History Group Field Guide Series No. 1., Earth Sciences History Group, GSA Inc., Melbourne, Victoria.

JOYCE E. B. & SUTALO F. 1996. Long basaltic flows in southeastern Australia: Mt Rouse and other late-Cenozoic flows of the Newer Volcanic Province. In: Whitehead P. W. ed. *Conference on long lava flows*. Townsville, Queensland, pp. 30–31.

KENNETT B. L. N. & ABDULLAH A. 2011. Seismic wave attenuation beneath the Australasian region, Australia. *Australian Journal of Earth Sciences* **58**, 285–295.

KERESZTURI G., CSILLAG G., NÉMETH K., SEBE K., BALOGH K. & JÁGER V. 2010. Volcanic architecture, eruption mechanism and landform evolution of a Plio/Pleistocene intracontinental basaltic polycyclic monogenetic volcano from Bakony–Balaton Highland Volcanic Field, Hungary. *European Journal of Geosciences* **2**, 362–384.

KERSHAW A. P. 1971. A pollen diagram from Quincan crater, north-east Queensland, Australia. *New Phytologist* **70**, 669–681.

KERSHAW A. P. 1975. Stratigraphy and pollen analysis of Bromfield Swamp, northeast Queensland, Australia. *New Phytologist* **75**, 173–191.

KIENLE J., KYLE P. R., SELF S., MOTYKA R. J. & LORENZ V. 1980. Ukinrek Maars, Alaska, I. April 1977 eruption sequence, petrology and tectonic setting. *Journal of Volcanology and Geothermal Research* **7**, 11–37.

KING S. D. & ANDERSON D. L. 1998. Edge-driven convection. *Earth and Planetary Science Letters* **160**, 289–296.

- KLEEMAN J. D., GREEN D. H. & LOVERING J. F. 1968. Uranium distribution in ultramafic inclusions from Victorian basalts. *Earth and Planetary Science Letters* **5**, 449–458.
- KNESEL K. M., COHEN B. E., VASCONCELOS P. M. & THIEDE D.S. 2008. Rapid change in drift of the Australian plate records collision with Ontong Java plateau. *Nature* **454**, 754–758.
- KNUTSON, J. 1989. East Australian Volcanic Geology. In: Johnson R. W. ed. *Intraplate volcanism in Eastern Australia and New Zealand*, pp. 89–155. Cambridge University Press, Cambridge.
- KNUTSON J. & NICHOLLS I. A. 1989. Macedon–Trentham. In: Johnson R. W. ed. *Intraplate volcanism in Eastern Australia and New Zealand*, pp. 136–137. Cambridge University Press, Cambridge.
- KORNPORST J. 1970. Les péridotites et les pyroxenolites du massif ultrabasique des Beni Bouchera: une étude expérimentale entre 1100 et 1550°C, sous 15 à 30 kilobars de pression sèche. *Contributions to Mineralogy and Petrology* **29**, 290–309.
- KORSCH R. J., BARTON T. J., GRAY D. R., OWEN A. J. & FOSTER D. A. 2002. Geological interpretation of a deep seismic reflection transect across the boundary between the Delamerian and Lachlan Orogens, in the vicinity of the Grampians, western Victoria. *Australian Journal of Earth Sciences* **49**, 1057–1075.
- KOTSONIS A. & JOYCE E. B. 2003. The regolith of the Bendigo 1:100 000 map. *Victorian Initiative for Minerals and Petroleum Report 77*. Department of Primary Industries, Victoria.
- KRASSAY A. A., CATHRO, D. L. & RYAN, D. J. 2004. A regional tectonostratigraphic framework for the Otway Basin. In: Bould P. J., Johns D. R. & Lang S. C. eds. *Eastern Australasian Basins Symposium II, Petroleum Exploration Society of Australia, Special Publication*, 97–116.
- LE BAS M. J., LE MAITRE R. W., STRECKEISEN A. L. & ZANETTIN B. 1986. A chemical classification of volcanic rocks based on the total alkali-silica diagram. *Journal of Petrology* **27**, 745–750.
- LE CORVEC N., SPÖRLI K. B., ROWLAND J. & LINDSAY J. 2013. Spatial distribution and alignments of volcanic centers: Clues to the formation of monogenetic volcanic fields. *Earth-Science Reviews* **124**, 96–114.
- LE MAITRE R. W., STRECKEISEN A. L., ZANETTIN B., LE BAS M. J., BONIN B., BATEMAN P., BELLINI G., DUDEK A., EFREMOVA S., KELLER J., LAMEYRE J., SABINE P. A., SCHMID R., SØRENSEN H. & WOOLEY A. R. 2002. Igneous rocks: A classification and glossary of terms. Cambridge University Press, Cambridge, UK.

- LE PICHON X. & HEIRTZLER J. R. 1968. Magnetic anomalies in the Indian Ocean and sea-floor spreading. *Journal of Geophysical Research* **73**, 2101–2107.
- LESTI C., GIORDANO G., SALVINI F. & CAS R. 2008. Volcano tectonic setting of the intraplate, Pliocene-Holocene Newer Volcanics Province (southeast Australia): Role of crustal fracture zones. *Journal of Geophysical Research* **113**, B07407.
- LANGMUIR C. H., KLEIN E. M., & PLANK T. 1992. Petrological systematics of mid-ocean ridge basalts: constraints on melt generation beneath ocean ridges. In: Phipps M. J, Blackman D. K. & Sinton J. M. eds. *Mantle Flow and Melt Generation at Mid-Ocean Ridges. American Geophysical Union Monograph* **71**, 183-280.
- LISTER G. S. & ETHERIDGE M. A. 1989. Detachment modes for uplift and volcanism in the eastern highlands, and their application to the origin of passive margin mountains. In: Johnson R. W. ed. *Intraplate volcanism in Eastern Australia and New Zealand*, pp. 297–313. Cambridge University Press, Cambridge.
- LUHR J. F. 2001. Glass inclusions and melt volatile contents at Parícutin Volcano, Mexico. *Contributions to Mineralogy and Petrology* **142**, 261-283.
- MACKENZIE D. E. & WHITE A. J. R. 1970. Phonolite globules in basanites from Kiandra, Australia. *Lithos* **3**, 309–317.
- MATSUMOTO T., HONDA M., MCDOUGALL I., YATSEVICH I. & O'REILLY S. Y. 1997. Plume-like neon in a metasomatic apatite from the Australian lithospheric mantle. *Nature* **388**, 162–164.
- MATSUMOTO T., HONDA M., MCDOUGALL I., O'REILLY S. Y., NORMAN M. & YAXLEY G. 2000. Noble gases in pyroxenites and metasomatised peridotites from the Newer Volcanics, southeastern Australia: implications for mantle metasomatism. *Chemical Geology* **168**, 49–73.
- MCBRIDE J. S., LAMBERT D. D., GREIG A. & NICHOLLS I. A. 1996. Multistage evolution of Australian subcontinental mantle: Re-Os isotopic constraints from Victorian mantle xenoliths. *Geology* **24**, 631–634.
- MCBRIDE J. S., LAMBERT D. D., NICHOLLS I. A. & PRICE R. C. 2001. Osmium isotopic evidence for crust-mantle interaction in the genesis of continental intraplate basalts from the Newer Volcanics Province, southeastern Australia. *Journal of Petrology* **6**, 1197–1218.
- MCDONOUGH W. F., MCCULLOCH M. T. & SUN S. S. 1985. Isotopic and geochemical systematics in Tertiary-Recent basalts from southeastern Australia and implications for the evolution of the subcontinental lithosphere. *Geochimica et Cosmochimica Acta* **49**, 2051–2067.

MCDONOUGH W. F. & MCCULLOCH M. T. 1987. The southeast Australian lithospheric mantle: isotopic and geochemical constraints on its growth and evolution. *Earth and Planetary Science Letters* **86**, 327–340.

MCDUGALL I., ALLSOP H. L. & CHAMALAUN F. H. 1966. Isotopic dating of the Newer Volcanics of Victoria, Australia and geomagnetic polarity epochs. *Journal of Geophysical Research* **71**, 6107–6118.

MCDUGALL I. & GILL E. D. 1975. Potassium-Argon ages from the Quaternary succession in the Warrnambool – Port Fairy area, Victoria, Australia. *Proceedings of the Royal Society of Victoria* **12**, 295–332.

MCKENZIE D. A., NOTT R. J. & BOLGER P. F. 1984. Radiometric age determinations. *Geological Survey of Victoria Report* **74**.

MCDUGALL I. & DUNCAN R. A. 1988. Age progressive volcanism in the Tasmanid seamounts. *Earth and Planetary Science Letters* **89**, 207–220.

MCKENZIE D. P. & SCLATER J. G. 1971. The evolution of the Indian Ocean since the Late Cretaceous. *Geophysical Journal of the Royal Astronomical Society* **24**, 437–528.

MILHOLLEN G. L., IRVING A. J. & WYLLIE P. J. 1974. Melting interval of Peridotite with 5.7 per cent water to 30 kilobars. *Journal of Geology* **82**, 575–587.

MONTELLI R., NOLET G., DAHLEN F. A. & MASTERS G. 2006. A catalogue of deep mantle plumes: New results from finite-frequency tomography. *Geochemistry, Geophysics, Geosystems* **7**, Q111010.111029/112006GC001248.

MORAND V. J., WOHLT K. E., CAYLEY R. A., TAYLOR D. H., KEMP A. I. S., SIMONS B. A. & MAGART A. P. M. 2003. Glenelg special map area Geological Report. *Geological Survey of Victoria Report* **123**.

MUTTER J. C., HEGARTY K. A., CANDE S. C. & WEISSEL J. K. 1985. Breakup between Australia and Antarctica: A Brief Review in the light of new data. *Tectonophysics* **114**, 255–279.

NEEDHAM A., LINDSAY J. M., SMITH I. E. M., AUGUSTINUS P. & SHANE P. A. 2010. Sequential eruption of alkaline and sub-alkaline magmas from a small monogenetic volcano in the Auckland Volcanic Field, New Zealand. *Journal of Volcanology and Geothermal Research* **1-4**, 126–142.

NÉMETH K. 2010. Monogenetic volcanic fields: Origin, sedimentary record, and relationship with polygenetic volcanism. *The Geological Society of America Special Paper* **470**.

NICHOLLS I. A. & JOYCE E. B. 1989. East Australian volcanic geology—Victoria and South

Australia—Newer Volcanics. In: Johnson R.W. ed. *Intraplate volcanism in Eastern Australia and New Zealand*, pp. 137–142. Cambridge University Press, Cambridge.

NICHOLLS I. A., GREIG A. G., GRAY C. M. & PRICE R. C. 1993. IAVCEI General Assembly Canberra, September 1993. Pre-Conference field trip A-4 excursion guide: Newer Volcanics Province – basalts, xenoliths and megacrysts. *Record of the Australian Geological Survey Organisation* **1993/58**.

O'HANLON E. M. 1975. A petrographic and geochemical study of the Devonian and Tertiary volcanics of the Macedon district, central Victoria. LaTrobe University, unpublished BSc honours thesis.

O'NEILL C. O., MORESI L., LENARDIC A. & COOPER C. M. 2003. Influences on Australia's heat flow and thermal structure from mantle correction modelling results. In: Hillis R. & Müller R. D. Eds. *Evolution and Dynamics of the Australian Plate*, pp. 169–184. *Geological Society of Australia Special Publication* **22** and *Geological Society of America Special Paper* **372**.

O'REILLY S. Y. & GRIFFIN W. L. 1985. A xenolith-derived geotherm for southeastern Australia and its geophysical implications. *Tectonophysics* **111**, 41–63.

O'REILLY S. Y. & GRIFFIN W. L. 1988. Mantle metasomatism beneath western Victoria, Australia: I. Metasomatic processes in Cr-diopside lherzolites. *Geochimica et Cosmochimica Acta* **52**, 433–447.

O'REILLY S. Y., NICHOLLS I. A. & GRIFFIN S. Y. 1989. Xenoliths and megacrysts of eastern Australia. In: Johnson R.W. ed. *Intraplate volcanism in Eastern Australia and New Zealand*, pp. 249–274. Cambridge University Press, Cambridge.

O'REILLY Y. O. & ZHANG M. 1995. Geochemical characteristics of lava field basalts from eastern Australia and inferred sources: connections with the subcontinental lithospheric mantle? *Contributions to Mineralogy and Petrology* **121**, 148–170.

O'REILLY S. Y. & GRIFFIN W. L. 2013. Chapter 12. Mantle Metasomatism, In: Harlov D. E. & Austrheim H. eds. *Metasomatism and the Chemical Transformation of Rock. Lecture Notes in Earth System Sciences*, pp. 471–533. Springer Berlin Heidelberg.

OLLIER C. D. 1967. Landforms of the Newer Volcanic Province of Victoria. In: Jennings J. N. & Mabbutt J. A. eds. *Landform studies from Australia and New Guinea*, pp. 315–339. Australian National University Press, Canberra.

OLLIER C. D. 1978. Tectonics and geomorphology of the Eastern Highlands. In: Davies J. L. & Williams M. A. eds. *Landform Evolution in Australia*. ANU Press, 5–47.

- OLLIER C. D. 1985. Lava flows of Mt Rouse, western Victoria. *Proceedings of the Royal Society of Victoria* **97**, 167–174.
- OLLIER C. D. & JOYCE E. B. 1964. Volcanic physiography of the Western Plains of Victoria. *Proceedings of the Royal Society of Victoria* **77**, 357–376.
- OSKARSSON N., SIGVALDSON G. E. & STEINTHORSSON S. 1982. A dynamic model of rift zone petrogenesis and the regional petrology of Iceland. *Journal of Petrology* **23**, 28–74.
- PIGANIS F. 2011. A volcanological investigation of the polymagmatic Red Rock Volcanic Complex and a 3D geophysical interpretation of the subsurface structure and geology of the poly-lobate Lake Purdigulac maar, Newer Volcanics Province, southeastern Australia. MSc thesis (unpublished), Monash University.
- PILGER R. H. JR. 1982. The origin of hotspot traces: Evidence from eastern Australia. *Journal of Geophysical Research* **87**, 1825–1834.
- POWELL W., ZHANG M., O'REILLY S. Y. & TIEPOLO M. 2004. Mantle amphibole trace-element and isotopic signatures trace multiple metasomatic episodes in lithospheric mantle, western Victoria, Australia. *Lithos* **75**, 141–171.
- PRATA G. 2012. Complex eruption style and deposit changes during the evolution of the late Pleistocene Tower Hill maar–scoria cone Volcanic Complex, Newer Volcanics Province, Victoria, Australia. MSc thesis, Monash University.
- PRICE R. C., GRAY C. M. & FREY F. A. 1997. Strontium isotopic and trace element heterogeneity in the plains basalts of the Newer Volcanic Province, Victoria, Australia. *Geochimica et Cosmochimica Acta* **61**, 171–192.
- PRICE R. C., GRAY C. M., NICHOLLS I. A. & DAY A. 1988. Cainozoic volcanic rocks. In: Douglas J. G. & Ferguson J. A. eds. *Geology of Victoria* pp. 439–451. Geological Society of Australia, Victoria Division, Melbourne.
- PRICE R. C., NICHOLLS I. A. & GRAY C. M. 2003. Cainozoic igneous activity. In: Douglas J. G. & Ferguson J. A. eds. *Geology of Victoria*, pp. 361–375. Geological Society of Victoria, Victorian Division, Melbourne.
- PRICE R. C., NICHOLLS I. A. & DAY A. 2014. Lithospheric influences on magma compositions of late Mesozoic and Cenozoic intraplate basalts (the Older Volcanics) of Victoria, south-eastern Australia. *Lithos* **206**: 179–200.
- RAWLINSON N. & FISHWICK S. 2012. Seismic structure of the southeast Australian lithosphere

from surface and body wave tomography. *Tectonophysics* **572–573**, 111–122.

RAWLINSON N. & DAVIES R. 2014. Localisation of edge driven convection beneath the Australian continent. *EGU General Assembly 2014, Vienna, Austria Abstract* **3520**.

REYNOLDS S. D., COBLENTZ D. & HILLIS R. R. 2003. Influences of plate-boundary forces on the regional intraplate stress field of continental Australia. *In*: Hillis R. R. & Müller R. D. eds. *Evolution and Dynamics of the Australian Plate. Geological Society of Australia, Special Publication* **22**, 59–70.

ROBERTSON A. D. 1985. Cainozoic volcanic rocks in the Bundaberg–Gin Gin–Pialba area, Queensland. *University of Queensland Department of Geology Papers* **11**, 72–92.

ROBERTSON A. D., SUTHERLAND F. L. & HOLLIS J. D. 1989. Bundaberg and Boyne. *In*: Johnson R. W. ed. *Intraplate volcanism in Eastern Australia and New Zealand*, pp. 107–109. Cambridge University Press, Cambridge.

ROBERTSON G. B., PRESCOTT J. R. & HUTTON J. T. 1996. Thermoluminescence dating of volcanic activity at Mount Gambier, South Australia. *Transactions of the Royal Society of South Australia* **120**, 7–12.

ROSENGREN N. 1994. Eruption points of the Newer Volcanics Province of Victoria—an inventory and evaluation of scientific significance. National Trust of Australia (Victoria) and the Geological Society of Australia (Victoria Division), Melbourne.

ROSSITER A. G. 2003. Chapter 8. Granitic rocks of the Lachlan Fold Belt in Victoria. *In*: Birch W. D. Ed. *Geology of Victoria. Geological Society of Australia Special Publication* **23**.

SANDIFORD M. 2003. Neotectonics of southeastern Australia: linking the Quaternary faulting record with seismicity and in situ stress. *Geological Society of Australia Special Publication* **22** and *Geological Society of America Special Paper* **372**, 107–119.

SANDIFORD M., WALLACE M. & COBLENTZ D. 2004. Origin of the in situ stress field in southeastern Australia. *Basin Research* **16**, 325–338.

SHAW R. D. 1978. Sea floor spreading in the Tasman Sea: a Lord Howe Rise-eastern Australian reconstruction. *Bulletin of the Australian Society of Exploration Geophysics* **9**, 75–81.

SHAW–STUART A. 2002. Varied basaltic eruption style at the Mount Leura volcanic complex in the Newer Volcanics Province of southeastern Australia. M.Sc thesis, School of Geosciences, Monash University, 207 pp.

- SHEARD M. J. 1990. A guide to Quaternary Volcanoes in the Lower South-East of South Australia. *Mines and Energy Review, South Australia* **157**, 40–50.
- SIMONS B. A. & MOORE D. H. 1999. Victoria 1:1 000 000 Pre-Permian Geology. Geological Survey of Victoria.
- SINGLETON O. P. & JOYCE E. B. 1969. Cainozoic volcanicity in Victoria. *Geological Society of Australia Special Publication* **2**, 145–154.
- SINGLETON O. P. & JOYCE E. B. 1970. Catalogue of post-Miocene volcanoes of Victoria, Australia. Prepared for IAVCEI Catalogue of post-Miocene Volcanoes of the World (unpublished). Incorporated with permission into: Rosengren N. 1994. Eruption Points of the Newer Volcanics Province of Victoria. National Trust of Australia (Victoria) & Geological Society of Australia (Victorian Division), Melbourne.
- SINGLETON O. P., MCDUGALL I. & MALLET C. W. 1976. The Pliocene–Pleistocene boundary in southeastern Australia. *Journal of the Geological Society of Australia* **23**, 299–311.
- SKEATS E. W. & SUMMERS H. S. 1912. The geology and petrology of the Macedon district. *Geological Survey of Victoria bulletin* **24**.
- SMITH B. W. & PRESCOTT J. R. 1987. Thermoluminescence dating of the eruption of Mt Schank, South Australia. *Australian Journal of Earth Sciences* **34**, 335–342.
- SMITH I. E., BLAKE S., WILSON C. J. N. & HOUGHTON B. F. 2008. Deep-seated fractionation during the rise of a small-volume basalt magma batch: Crater Hill, Auckland, New Zealand. *Contributions to Mineralogy and Petrology* **155**, 511–527.
- SOHN Y. K., CRONIN S. J., BRENNAN M., SMITH I. E. M., NEMETH K., WHITE J. D. L., MURTAGH R. M., JEON Y. M. & KWON C. W. 2012. Ilchulbong tuff cone, Jeju Island, Korea, revisited: A compound monogenetic volcano involving multiple magma pulses, shifting vents, and discrete eruptive phases. *Geological Society of America Bulletin* **3-4**, 259–274.
- STAGG H. M. J., COCKSHELL C. D., WILCOX J. B., HILL A. J., NEEDHAM D. J. L., THOMAS B., O'BRIEN G. W. & HOUGH L. P. 1990. Basins of the Great Australian Bight region: geology and petroleum potential. Bureau of Mineral Resources, Geology and Geophysics, Australia. *Continental Margins Program Folio* **5**.
- STANLEY E. R. 1909. Complete analysis of the Mount Gambier basalt with petrographic descriptions. *Transactions of the Royal Society of South Australia* **33**, 82–100.
- STEPHENSON P. J. 1989. Northern Queensland. In: Johnson R. W. ed. *Intraplate volcanism in*

Eastern Australia and New Zealand, pp. 89–97. Cambridge University Press, Cambridge.

STEPHENSON P. J. & GRIFFIN T. J. 1796. Some long basaltic lava flows in north Queensland. *In*: Johnson R. W. ed. *Volcanism in Australasia*. Elsevier, Amsterdam, pp. 41–51.

STEPHENSON P. J., POLACH H. & WYATT D. H. 1978. The age of the Toomba basalt, north Queensland. *Third Australian Geological Convention, Townsville, Abstract 62*.

STOLZ A. J. & DAVIES G. R. 1988. Chemical and isotopic evidence from spinel lherzolite xenoliths for episodic metasomatism of the upper mantle beneath southeastern Australia. *Journal of Petrology Special Lithosphere Issue* 303–330.

STONE J. O., PETERSON J. A., FIFIELD L. K. & CRESSWELL R. G. 1997. Cosmogenic chlorine-36 exposure ages for two basalt flows in Newer Volcanics Province, Western Victoria. *Proceedings of the Royal Society of Victoria* **109**, 121–131.

STRONG M. & WOLFF J. 2003. Compositional variations within scoria cones. *Geology* **31**, 143–146.

STUCKLESS J. S. & IRVING A. J. 1976. Strontium isotope geochemistry of megacrysts and host basalts from southeastern Australia. *Geochimica et Cosmochimica Acta* **40**, 209–213.

SUN S. S. & MCDONOUGH W. F. 1989. Chemical and isotopic systematics of oceanic basalts: implications for mantle composition and processes. *In*: Saunders A. D. & Norry M. J. eds. *Magmatism in Ocean Basins. Geological Society of London Special Publication* **42**, 313–345.

SUN S. S., MCDONOUGH W. F. & EWART A. 1989. Four component model for east Australian basalts. *In*: Johnson R. W. ed. *Intraplate volcanism in Eastern Australia and New Zealand*, pp. 333–347. Cambridge University Press, Cambridge.

SUTALO F. 1996. The Geology and Regolith Terrane Evaluation of the Mount Rouse Lava Flows, Western Victoria. BSc thesis (unpublished), University of Melbourne.

SUTALO F. & JOYCE E. B. 2004. Long basaltic lava flows of the Mt Rouse volcano in the Newer Volcanic Province of Southeastern Australia. *Proceedings of the Royal Society of Victoria* **116**, 37–49.

SUTHERLAND F. L. 1985. Regional controls in eastern Australian volcanism. *In*: Sutherland F. L., Franklin B. J. & Waltho A. E. eds. *Volcanism in Eastern Australia with Case Histories from New South Wales*, pp. 13–31. Geological Society of Australia, New South Wales Division, Sydney.

SUTHERLAND F. L. 1991. Cainozoic volcanism, Eastern Australia: a predictive model on migration over multiple ‘hotspot’ mantle sources. *In*: Williams M. A. J., DeDeckker P. & Kershaw A. P. eds. *The*

Cainozoic in Australia: a re-appraisal of the evidence, pp. 15–43. *Geological Society of Australia Special Publication* **18**.

SUTHERLAND F. L. 1993. Late thermal events based on zircon fission track ages in northeastern New South Wales and southeastern Queensland: links to Sydney Basin seismicity? *Australian Journal of Earth Sciences* **40**, 461–470.

SUTHERLAND F. L. 1994. Tasman Sea evolution and hotspot trails. In: Van der Lingen G. J., Swanson K. M. & Muir R. J. eds. *Evolution of the Tasman Sea Basin*, pp. 35–51. A. A. Balkema, Rotterdam, Netherlands.

SUTHERLAND F. L. 1999. Volcanism, geotherms, gemstones and lithosphere, since orogenesis, N.E. New South Wales. In: Flood P. G. ed. *New England Orogen. Regional Geology Tectonics and Metallogensis*, pp. 355–364. Earth Sciences, University of New England, Armidale.

SUTHERLAND F. L. 2003. ‘Boomerang’ migratory intraplate Cenozoic volcanism, eastern Australian rift margins and the Indian– Pacific mantle boundary. *Geological Society of America Special Paper* **372**, 203–221.

SUTHERLAND F. L. & FANNING C. M. 2001. Gem-bearing basaltic volcanism, Barrington, New South Wales: Cenozoic evolution, based on basalt K–Ar ages and zircon fission track and U–Pb isotope dating. *Australian Journal of Earth Sciences* **48**, 221–237.

SUTHERLAND F. L., GRAHAM I. T., POGSON R. E., SCHWARZ D., WESS G. B., COENRAADS R. R., FANNING C. M., HOLLIS J. D. & ALLEN T. C. 2002. The Tumbarumba basaltic gem field, New South Wales: In relation to sapphire–ruby deposits of eastern Australia. *Records of the Australian Museum* **54**, 215–248.

SUTHERLAND F. L., GRAHAM I. T., MEFFRE S., ZWINGMANN H. & POGSON R. E. 2012. Passive-margin prolonged volcanism, East Australian Plate: outbursts, progressions, plate controls and suggested causes. *Australian Journal of Earth Sciences* **59**, 983–1005.

SUTHERLAND F. L., GRAHAM I. T., HOLLIS J. D., MEFFRE S., ZWINGMANN H., JOURDAN F. & POGSON R. E. 2014. Multiple felsic events within post-10 Ma volcanism, Southeast Australia: inputs in appraising proposed magmatic models. *Australian Journal of Earth Sciences* **61**, 241–267.

TAKADA A. 1994. The influence of regional stress and magmatic input on styles of monogenetic and polygenetic volcanism. *Journal of Geophysical Research* **99**, 13563–13573.

TAYLOR D. H., WHITEHEAD M. L., OLSHINA A. & LEONARD J. G. 1996. Ballarat 1: 100 000 map geological report. *Geological Survey of Victoria Report* **101**.

TAYLOR D. H., WOHLT K. E., SIMONS B.A., MAHER S., MORAND V. J. & SAPURMAS P. 2000. Creswick 1:100 000 map area geological report. *Geological Survey of Victoria Report* **117**.

TICKELL S. T. 1991. Radiometric dating of the Tower Hill volcano and Colac quarry. *Geological Survey of Victoria Unpublished Report* **1991/38**.

TURNBULL W. D., LUNDELIUS E. L. & MCDOUGALL I. 1965. A Potassium/Argon dated Pliocene marsupial fauna from Victoria, Australia. *Nature* **206**, 186.

TWIDALE C. R. & BOURNE J. A. 2008. Geomorphological evolution of part of the eastern Mount Loft Ranges, South Australia. *Transactions of the Royal Society of South Australia* **99**, 197–210.

TYCHKOV S. A., RYCHKOVA E. V. & VASILEVSKII A. N. 1998. Interaction between a plume and thermal convection in the continental upper mantle. *Russian Geology and Geophysics* **39**, 423–434.

UEHARA D. 2012. Geophysical and volcanological study on the Mount Leura volcanic complex of the Newer Volcanics Province, south western Victoria. Honours thesis, School of Geosciences, Monash University, 207 pp.

VALENTINE G. A. & GREGG T. K. P. 2008. Continental basaltic volcanoes – processes and problems. *Journal of Volcanology and Geothermal Research* **177**, 857–873.

VALLANCE T. G., WILKINSON J. F. G., ABBOT M. J., FAULKS I. G., STEWART J. R. & BEAN J. M. 1969. Mesozoic and Cainozoic rocks. In: Packham G. H. ed. *The Geology of New South Wales*. *Journal of the Geological Society of Australia* **16**, 513–541.

VAN OTTERLOO J. 2012. Complexity in monogenetic volcanic systems: factors influencing alternating magmatic and phreatomagmatic eruption styles at the 5 ka Mt Gambier Volcanic Complex, South Australia. Monash University PhD thesis.

VAN OTTERLOO, J., CAS R. A. F. & SHEARD M. J. 2013 Eruption processes and deposit characteristics at the monogenetic Mt Gambier volcanic complex, SE Australia: implications for alternating magmatic and phreatomagmatic activity. *Bulletin of Volcanology* **75**, 1–21.

VAN OTTERLOO J., RAVEGGI M., CAS R. A. F. & MAAS R. 2014. Polymagmatic activity at the monogenetic Mt Gambier volcanic complex in the Newer Volcanics Province, SE Australia: New Insights into the occurrence of intraplate volcanic activity in Australia. *Journal of Petrology* **55**, 1317–1351.

VANDENBERG A. H. M., WILLMAN C. E., MAHER S., SIMONS B. A., CAYLEY R., TAYLOR D. H., MORAND V. J., MOORE D. H & RADOJKVIC, A. 2000. The Tasman Fold Belt System in Victoria. Geological Survey of Victoria Special Publication, Melbourne.

VANDENBERG A. H. M. 1978. The Tasman Fold Belt System in Victoria. In: Scheibner E. ed. The Phanerozoic Structure of Australia and variations in tectonic style. *Tectonophysics* **48**, 267–297.

VANDENBERG A. H. M., WILLMAN C. E., HENDRICKX M. A., BUSH M. A. & SANDS B. 1995. The geology and prospectivity of the 1993 Mount Wellington Airborne Survey area. *Victorian Initiative for Minerals and Petroleum Report* **2**.

VANDENBERG A. H. M. 1999. Discussion. Llandovery–Ludlow graptolites from central Victoria: new correlation perspectives of the major formations. *Australian Journal of Earth Sciences* **46**, 659–661.

VANDENBERG A. H. M. 2007. Saying goodbye to old friends – vale the Newer and Older Volcanics of Victoria. *The Australian Geologist* **143**, 25–26.

VEEVERS J. J. 1986. Break-up of Australia and Antarctica estimated as mid-Cretaceous (95 ± 5 Ma) from magnetic and seismic data at the continental margin. *Earth and Planetary Science Letters* **77**, 91–99.

VEEVERS J. J., MOLLAN R. G., OLGERS F. & KIRKEGAARD A. G. 1964. The geology of the Emerald 1:250 000 sheet area, Queensland. *Bureau of Mineral Resources, Australia Report* **68**.

VOGEL D. C. & KEAYS R. R. 1997. The petrogenesis and platinum-group element geochemistry of the Newer Volcanic Province, Victoria, Australia. *Chemical Geology* **136**, 181–204.

VOGT P. R. & CONNOLLY J. R. 1971. Tasmanid guyots, the age of the Tasman Basin, and motion between the Australian plate and the mantle. *Geological Society of America Bulletin* **82**, 2577–2584.

WADGE G. 1981. The variation of magma discharge during basaltic eruptions. *Journal of Volcanology and Geothermal Research* **11**, 139–168.

WALKER G. P. L. 2000. Basaltic volcanoes and volcanic systems. In: Sigurdsson H. ed. *Encyclopaedia of Volcanoes*. Academic Press, New York, pp. 283.

WALLACE D. A. 1990. Petrology and geochemistry of the Newer Volcanics of the Western Highlands of Victoria, Australia. M.Sc thesis, School of Geology, La Trobe University, 121 pp.

WALLACE D. A. & OLLIER C. D. 1990. The Cainozoic lava flows of Barfold Gorge. *Victorian Naturalist* **103**, 175–177.

WEBB A. W. 1989. K–Ar chronology of VAD101–116. AMDEL report for the Geological Survey of Victoria.

WEBB A. W. & MCDOUGALL I. 1967. A comparison of mineral and whole rock potassium–argon ages of Tertiary volcanics from central Queensland, Australia. *Earth and Planetary Science Letters* **3**, 41–47.

WEBB A. W., OSBORNE C. R., TAYLOR D. H. & CAYLEY R. A. 1998. K–Ar geochronology of Newer Volcanics on the Ballarat 1:250 000 map sheet. *Geological Survey of Victoria Unpublished Report* **1998/10**.

WEISSEL J. K. & HAYES D. E. 1977. Evolution of the Tasman Sea Reappraised. *Earth and Planetary Science Letters* **36**, 77–84.

WELLMAN P. 1974. Potassium–argon ages of the Cainozoic volcanic rocks of eastern Victoria, Australia. *Journal of the Geological Society of Australia* **21**, 359–376.

WELLMAN P. 1971. The age and Palaeomagnetism of the Australian Cenozoic Volcanic Rocks. Thesis, Australian National University, Canberra.

WELLMAN P. 1978. Potassium–argon ages of Cainozoic volcanic rocks from the Bundaberg, Rockhampton and Clermont areas of eastern Queensland. *Proceedings of the Royal Society of Queensland* **89**, 59–64.

WELLMAN P. 1983. Hotspot volcanism in Australia and New Zealand: Cainozoic and mid-Mesozoic. *Tectonophysics* **96**, 225–243.

WELLMAN P. & MCDOUGALL I. 1974. Cainozoic igneous activity in eastern Australia. *Tectonophysics* **23**, 49–65.

WHITEHEAD P. W. 1986. The geology and geochemistry of the Mt Rouse and Mt Napier volcanic centres, western Victoria. BSc thesis (unpublished), LaTrobe University, Melbourne.

WHITEHEAD P. W. 1991. The geology and geochemistry of Mt Napier and Mt Rouse, western Victoria. In: Williams M. A. J., DeDeckker P. & Kershaw A. P. eds. *The Cainozoic in Australia: a re-appraisal of the evidence*. *Geological Society of Australia Special Publication* **18**, 309–320.

WHITEHEAD P. W. 2010. The regional context of the McBride Basalt Province and the formation of the Undara Lava flows, tubes, rises and depressions. In: *Proceedings of the 14th International Symposium on Vulcanospeleology, Undara Volcanic National Park, Queensland*, pp. 9–18.

WHITEHEAD P.W., STEPHENSON P. J., MCDOUGALL I., HOPKINS M. S., GRAHAM A. W., COLLERSON K. D. & JOHNSON D. P. 2007. Temporal development of the Atherton Basalt Province, north Queensland. *Australian Journal of Earth Sciences* **54**, 691–709.

- WILKINSON J. F. G. 1969. Mesozoic and Cainozoic igneous rocks. B. Northeastern New South Wales. In: Packham G. H. ed. *The Geology of New South Wales. Journal of the Geological Society of Australia* **16**, 530–541.
- WILKINSON J. F. G. 1982. The genesis of mid-ocean ridge basalt. *Earth Science Reviews* **18**, 1–57.
- WOOD C. A. 1980. Morphometric evolution of cinder cones. *Journal of Volcanology and Geothermal Research* **7**, 387–413.
- WOPFNER H. & THORNTON R. C. N. 1971. The occurrence of carbon dioxide in the Gambier Embayment. In: Wopfner H. & Douglas J. G. eds. *The Otway Basin of Southeastern Australia*, pp. 377–384. *Geological Surveys of South Australia and Victoria Special Bulletin*.
- YAXLEY G. M., CRAWFORD A. J. & GREEN D. H. 1991. Evidence for carbonatite metasomatism in spinel peridotite xenoliths from western Victoria, Australia. *Earth and Planetary Science Letters* **107**, 305–317.
- YAXLEY G. M., GREEN D. H. & KAMENETSKY V. 1996. Carbonatite metasomatism in the southeastern Australian Lithosphere. *Journal of Petrology* **39**, 1917–1930.
- YAXLEY G. M. & KAMENETSKY V. 1999. In situ origin for glass in mantle xenoliths from southeastern Australia: insights from trace element compositions of glasses and metasomatic phases. *Earth and Planetary Science Letters* **172**, 97–109.
- ZINDLER A. & HART S. R. 1986 Chemical geodynamics. *Annual Review of Earth and Planetary Sciences* **14**, 493–571.



Chapter 2 is a paper which was published in The Australian Journal of Earth Sciences in July 2013.

At the beginning of this PhD project, an initial literature review revealed a disparity between the ~400 volcanoes of the Newer Volcanics Province (NVP) recognised in the standard map of the province (Joyce 1975 based on Singleton & Joyce 1970; incorporated into Rosengren 1994) and the 609 volcanoes listed on the Geoscience Victoria Seamless Geology DVD (October 2011 edition; 32 volcanoes listed were of the Macedon–Trentham Province, rather than the NVP). In addition, a review of satellite imagery in the vicinity of Mt Rouse coupled with fieldwork revealed three previously unrecorded volcanoes. Because of the importance of local and regional contexts for any new studies, and the fact that in order to create satisfactory maps in ArcGIS geospatial data should be as accurate as possible, a new study was initiated to log the locations of volcanoes and vents of the NVP.

A detailed desktop study followed, which correlated historical data with the detailed satellite images provided on Google Earth alongside the Seamless Geology 250k Google Earth Overlay (Geoscience Victoria) and resulted in a spreadsheet catalogue of geospatial data for volcanoes and vents. The spreadsheet was imported into ArcGIS in order to create new volcano distribution maps for the NVP and for subsequent studies and reviews of the geochronological (Chapter 1.6.2), geochemical (Chapter 1.6.3; Chapter 3) and isotopic (Chapter 1.6.3.2) characteristics of NVP volcanoes.

Subsequently, the NVP was studied in greater detail by analysing geospatial data on ArcGIS, such as NASA ASTER digital elevation models, Total Magnetism Intensity data and RGB ternary radiometrics (outlined for the Hamilton area in Chapter 3). An update to Chapter 2 is outlined in Chapter 1.6.1, and it is recommended that the reader should become familiar with the content of Chapter 2 before reading the update.

The full catalogue of geospatial data for NVP volcanoes, a kml file for Google Earth, layer files for ArcGIS and explanatory notes can be found in Appendix 2.

JOYCE E. B. 1975. Quaternary volcanism and tectonics in southeastern Australia. *In*: Suggate R. P. & Cresswell M. M. eds. *Quaternary studies*, pp. 169–178. The Royal Society of New Zealand, Wellington.

ROSENGREN N. 1994. Eruption points of the Newer Volcanics Province of Victoria—an inventory and evaluation of scientific significance. National Trust of Australia (Victoria) and the Geological Society of Australia (Victoria Division), Melbourne.

SINGLETON O. P. & JOYCE E. B. 1970. Catalogue of post-Miocene volcanoes of Victoria, Australia. Prepared for IAVCEI Catalogue of post-Miocene Volcanoes of the World (unpublished). Incorporated with permission into: Rosengren N. 1994. Eruption Points of the Newer Volcanics Province of Victoria. National Trust of Australia (Victoria) & Geological Society of Australia (Victorian Division), Melbourne.

Declaration for Thesis Chapter 2

Declaration by candidate

In the case of Chapter 2, the nature and extent of my contribution to the work was the following:

| Nature of contribution | Extent of contribution (%) |
|--|----------------------------|
| Data collection, analysis and interpretation, preparation of the manuscript. | 90% |

The following people contributed to this work:

| Name | Nature of contribution | Extent of contribution (%) |
|------------------|------------------------|----------------------------|
| Dr Ian Nicholls | Supervisory role | 5% |
| Prof. Reid Keays | Supervisory role | 5% |

The undersigned hereby certify that the above declaration correctly reflects the nature and extent of the candidate's and co-authors' contributions to this work*.

Julie Boyce

Date

Prof. Reid Keays (main supervisor)

Date

Dr Ian Nicholls

Date



The Newer Volcanics Province of southeastern Australia: a new classification scheme and distribution map for eruption centres

J. BOYCE

School of Geosciences, Building 28, Monash University, Clayton, VIC 3800, Australia.

A new volcanic distribution map of the 4.5 Ma–5000 B.P. continental intraplate Newer Volcanics Province in southeastern Australia has been produced in order to document >704 eruption points from >416 volcanic centres. Volcanic centres were classified as either simple or complex, with simple centres featuring few eruption points and simple morphologies, while complex centres have multiple eruption points and complex morphologies. Centres were further characterised according to the nature of their deposits. Simple volcanoes take the form of lava shields, scoria cones, maars, ash cones and domes, and unknown eruption types. Complex centres may feature exclusively magmatic eruption products such as lava and scoria, and are therefore classified as magmatic volcanic complexes; maar volcanic complexes feature exclusively phreatomagmatic eruption products and have erupted under the influence of external water, while maar–cone volcanic complexes feature both magmatic and phreatomagmatic eruption products. Approximately half of the eruption points in the Newer Volcanics Province are associated with complex volcanic centres. The minimum area of the Newer Volcanic Province was calculated to be >19 000 km², which may be a great underestimation, and it is estimated that the province has an eruption frequency of 1:10 800 yrs. This research has highlighted a need for further research into the Newer Volcanics Province, as many of the apparently ‘simple’ volcanic centres are likely to be more complex in nature. A spreadsheet database has been made freely available to download for research purposes, along with shapefiles for ArcGIS and kml files for Google Earth.

KEY WORDS: Newer Volcanics Province, monogenetic eruption centres, intraplate basaltic volcanism

INTRODUCTION

The continental intraplate Newer Volcanics Province (NVP) constitutes the most recent phase of volcanic activity in Australia, with eruptions spanning from 4.5 Ma to *ca* 5000 BP (Blackburn 1966; McDougall *et al.* 1966; Blackburn *et al.* 1982; Gray & McDougall 2009; Gouramanis *et al.* 2010). The NVP is also known as the Western District Province in Victoria alone. Since this term does not cover the most recent occurrences of volcanism in South Australia, which are geochemically similar to Victorian volcanoes erupted since *ca* 4.5 Ma, the term NVP is used throughout this paper.

The standard map of the NVP shows nearly 400 eruption points in Victoria and South Australia, including those of the Macedon–Trentham group (an older group of volcanics) (Joyce 1975). This map came about from a series of publications during the previous decade, for example the Victorian maps showing basalt cover and dot distributions of eruption points (Ollier & Joyce 1964, 1968; Ollier 1967, 1969; Singleton & Joyce 1969) and the unpublished Singleton & Joyce (1970) catalogue of post-Miocene volcanoes of Victoria, which was subsequently incorporated into a report prepared for the National

Trust of Australia and the Geological Society of Australia on the eruption points of the Newer Volcanics Province (Rosengren 1994). These maps gradually became more detailed (Joyce 1975) leading to a map of eruption points in Victoria (Joyce 1988a).

Subsequently, Geoscience Victoria listed 609 eruption points in Victoria (DPI Seamless Geology DVD October 2011; David Higgins, pers. comm. 2011), many of which do not correlate closely with the Joyce (1975) map. These discrepancies, alongside results of the author’s research in the Hamilton area, identified a need to amalgamate eruption-point information into a single repository and create an updated map. This article introduces updated volcanic distribution maps of the NVP alongside a spreadsheet of eruption points, shapefiles for ArcGIS and kml files for Google Earth, available to download from VHUB, a site dedicated to collaborative volcano research.

Geological setting of the Newer Volcanics Province

The NVP extends approximately 410 km from Melbourne in Victoria to the Mt Burr Range in southeastern South Australia (Figure 1), covering an area of

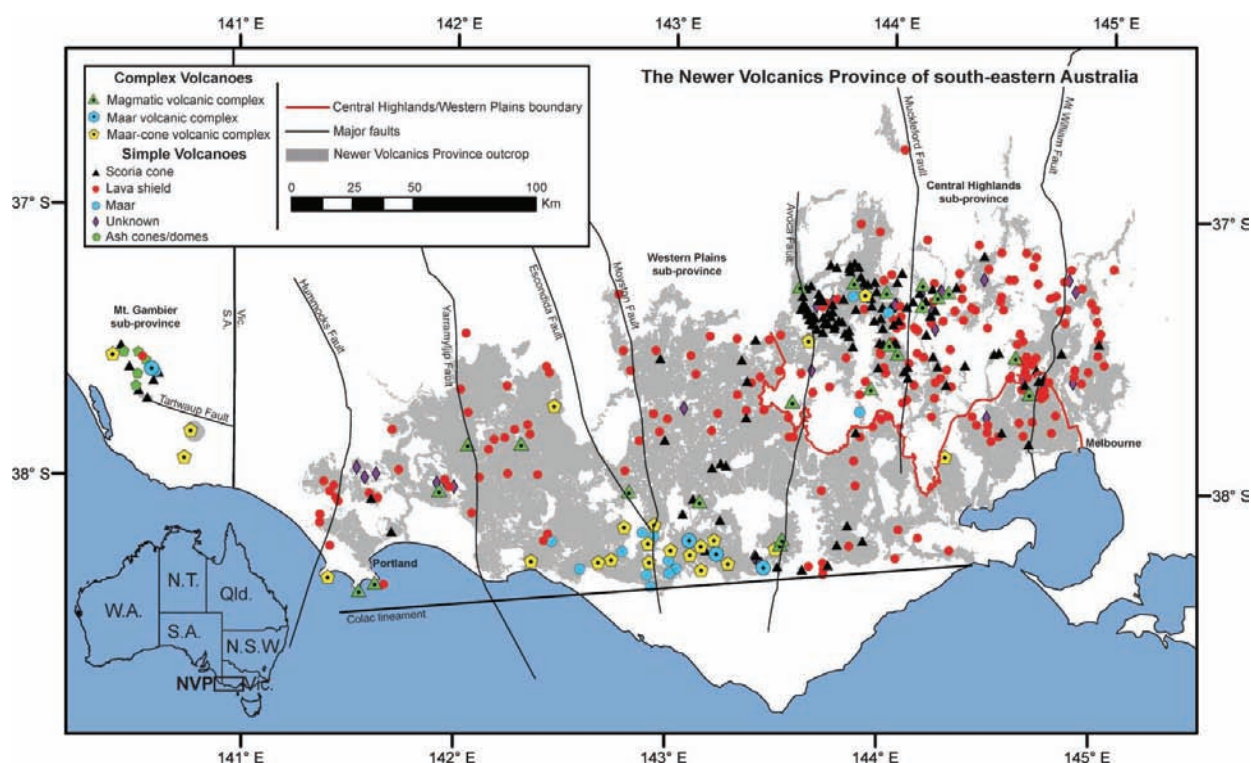


Figure 1 Distribution of volcanic centres by type in the Newer Volcanics Province, south-eastern Australia, showing major faults and Newer Volcanics outcrop.

>19 000 km² (calculated in ArcGIS during this study from DPI seamless geology October 2011 edition), which is significantly larger than the traditionally used estimate of 15 000 km² (Ollier 1967), but lower than estimates of 25 000 km² (McDougall *et al.* 1966; van Otterloo 2012) and 27 000 km² (Cas & van Otterloo 2011). The NVP is the youngest of three voluminous groups of Cenozoic volcanic activity (Joyce & Day 1989), which also include the 95–19 Ma Older Volcanics (Day 1983) outcropping in the eastern half of Victoria and the Otway Ranges to the west, and the 7.0–4.6 Ma Macedon–Trentham group northwest of Melbourne (Wellman 1974; Dasch & Millar 1977; Ewart *et al.* 1985). The Macedon–Trentham group is not considered part of the NVP, as it is compositionally distinct, resembling and possibly related to the central volcanic complexes of New South Wales and Queensland (Knutson & Nicholls 1989). This paper focuses on the Newer Volcanics group.

The NVP is a monogenetic volcanic field (Ollier & Joyce 1964; Joyce 1975) composed of the products of short-lived basaltic volcanoes in the form of scoria cones, lava shields, maars and composite centres. It has been subdivided into the Central Highlands, Western Plains and Mt Gambier subprovinces from east to west based on geomorphology (Joyce 1975; Nicholls & Joyce 1989). The Central Highlands cover the dissected uplands of Paleozoic metasediments and granites northwest of Melbourne (Nicholls & Joyce 1989; Price *et al.* 2003), the Western Plains fill the pre-existing subdued topography of the Otway Basin, and the Mt Gambier subprovince lies over the Gambier Embayment sediments, metasediments of the Delamerian Orogeny and Otway Basin sediments (van Otterloo & Cas 2011). The southern edge

of the NVP is marked by the Colac Lineament and is controlled by faulting (Joyce 1975; Carey 1986).

Although volcanism in the NVP has been referred to as simple and short-lived, recent research indicates that some centres are complex in nature, and can be classified as polymagmatic, featuring two or more magma batches with complex evolutions, such as Mt Gambier, Mt Rouse and the Red Rock (Alvie) volcanic complex (Piganis 2011; Blaikie *et al.* 2011; van Otterloo 2012; Boyce *et al.* 2013). Furthermore, Lake Purrumbete shows evidence of polygenetic behaviour, having a volcanic hiatus in the form of epiclastic volcanogenic deposits between eruption products (Jordan *et al.* 2013). Quarrying and drilling in The Bluff and Mt McIntyre areas of the Mt Burr Range has revealed interbedded paleosols, which also indicate a polygenetic character (Sheard 1990).

Origin of volcanism in the Newer Volcanics Province

The source of volcanic activity in the NVP has been, and continues to be, widely debated, with theories relating to hotspot and mantle-plume activity, continental extension and post-rift diapirism, reactivation of extensional faults, lateral and vertical flow of warm mantle and edge-driven convection.

Mantle plumes have been used to explain the origins of volcanism in the NVP. There are theories that the province is the most recent manifestation of the hotspot trace of eastern Australia, which created the volcanic provinces of the Great Dividing Range from Queensland to Victoria as the Australian plate moved north over one or more mantle plumes (e.g. Wellman & McDougall 1974;

Wellman 1983; Duncan & McDougall 1989; Sutherland 1991; Matsumoto *et al.* 1997). However, the NVP lies to the west of a projected line of volcanism (Price *et al.* 1997), and has an east–west orientation (Cas *et al.* 1993) that differs from the NNE–SSW orientation of the Great Dividing Range hotspot trace, the present-day position of which is suggested to be beneath Bass Strait (e.g. Wellman & McDougall 1974; Sutherland 2003; Kennett & Abdullah 2011; Sutherland *et al.* 2012). Age dating in the NVP has failed to identify any age progression (Gray & McDougall 2009), coupled with the fact that it is the latest appearance of volcanic activity in Victoria (Johnson *et al.* 1989), with basaltic volcanism being almost continuous throughout the Cenozoic (Price *et al.* 1997, 2003). Sutherland (2003) used the concept of ‘boomerang’ volcanism to explain the western location of the NVP, whereby plume activity follows a stepping motion and diverges to the west, away from the trend of plate-motion vectors, in order to create a large-volume volcanic field, before swinging back to the east to create ‘pinches’ of small-volume fields; the resultant fields together forming a boomerang shape. Other plume-related models involve the mixing of melts derived from the lithosphere and a mantle plume (McDonough *et al.* 1985) or generation either by plume-related activity or within the subcontinental lithosphere, with varying degrees of crustal contamination en route to the surface (McBride *et al.* 2001).

Continental extension related to the breakup of Gondwana and the opening of the Tasman Sea (the separation of Australia and Antarctica was complete by 90 Ma) has been cited as a possible mechanism for NVP volcanism (Lister & Etheridge 1989; O'Reilly & Zhang 1995; Price *et al.* 1997). Extension-induced lithospheric thinning and uplift at the base of the lithosphere are thought to have created a thermal instability, which was followed by the release of mantle diapirs leading to lithospheric melting. As the diapirs originate from depths of 200–400 km, they will take 20–100 Ma to reach the mantle solidus, and this is why volcanism is present so long after rifting has ceased. However, southeast Australia is currently in a NW–SE compressive stress regime (Hillis *et al.* 1995; Sandiford *et al.* 2004). Lesti *et al.* (2008) argued that active tectonics influenced eruption of the NVP, with extensional faults reactivated by the Tasman Fracture Zone (TVZ), which transferred shear stresses from oceanic crust to the continent, in turn deforming along zones of weakness and provided pathways for magma ascent.

Finn *et al.* (2005) proposed that all Cenozoic alkaline igneous rocks outcropping across the fragments of East Gondwana and the adjacent oceanic lithosphere form a diffuse alkaline magmatic province (DAMP) of low-volume but long-lived magmatism. Magma is generated by the lateral and vertical flow of warm Pacific mantle, triggered by instabilities induced by detached and sunken subducted slabs along the old Gondwana margins in the late Cretaceous. The warm mantle interacted with metasomatised subcontinental lithosphere and induced magmatism along zones of weakness.

The NVP measures ~100 km N–S, despite Australia having drifted north >300 km over the past *ca* 5 Ma (the timespan of eruption for the NVP). There is also a lack of extension and no spatial patterning in the province.

Edge-driven convection (Demidjuk *et al.* 2007; Farrington *et al.* 2010) may help to explain these observations and rule out plume activity. In this model, steps in lithospheric thickness are associated with thermal contrasts (e.g. King & Anderson 1998), which, alongside shear forces generated by motion of the Indo-Australian plate, produce secondary convection cells. Asthenospheric upwelling results in basaltic magmatism downstream, with a periodicity of in the order of 10 Ma. Metasomatism is required for melting to occur, and therefore the NVP reflects the distribution of fertile mantle. Fishwick *et al.* (2008) confirm the presence of lithospheric steps beneath Australia, thinning towards the east. Rawlinson & Fishwick (2012) favour the edge-driven convection model, but do not rule out narrow plume activity. So, the great debate as to the source of NVP volcanism continues.

METHODS

Geoscience Victoria supplied a list and Google Earth kml file of 609 eruption points in Victoria (David Higgins, pers. comm. 2011). These were correlated with eruption points from Rosengren (1994), which incorporates 354 Victorian eruption centres from Singleton & Joyce (1970). Google Earth was used to accurately plot the eruption points, utilising the zoom, pan, tilt and vertical exaggeration functions, alongside the Seamless Geology 250k 2010 Google Earth Overlay (Geoscience Victoria). Data for each eruption point were then entered into a spreadsheet, including information such as co-ordinates, descriptors (see below), interpretations or comments, the subprovince each eruption point belongs to, alternative names, appropriate Geoscience Victoria eruption point numbers and references.

Thirty-two volcanoes of the Macedon–Trentham group were listed on a separate spreadsheet tab and not used in the production of any maps, as they are not part of the NVP. Additional and more accurately located individual eruption points for some of the larger centres, such as Mt Gambier, Mt Rouse, Mt Eccles, Red Rock volcanic complex, Mt Noorat and Lake Purrumbete, were provided by Monash University PhD students and researchers (see acknowledgements), and some centres from relevant honours, masters and PhD theses. These, however, do not affect the overall location of the eruption centres. Numerous Honours and other theses at Monash, Melbourne and LaTrobe universities may yet provide further eruption points.

The spreadsheet was imported into ArcGIS and volcanic centres were overlain onto seamless geology (DPI Seamless Geology DVD October 2011) to form a map. The geomorphological boundary between the Central Highlands and Western Plains subprovinces was redefined in ArcGIS using older classifications and georeferenced images (Joyce 1975; Wallace 1990) as a guide, alongside NASA ASTER digital elevation models, seamless geology and Google Earth terrain. Where possible, the boundary was placed along edges of NVP basalt outcrop (as per Wallace 1990). The finished shapefile was then exported to kml for visualisation in Google Earth. Structures were added to the map using georeferenced images as a

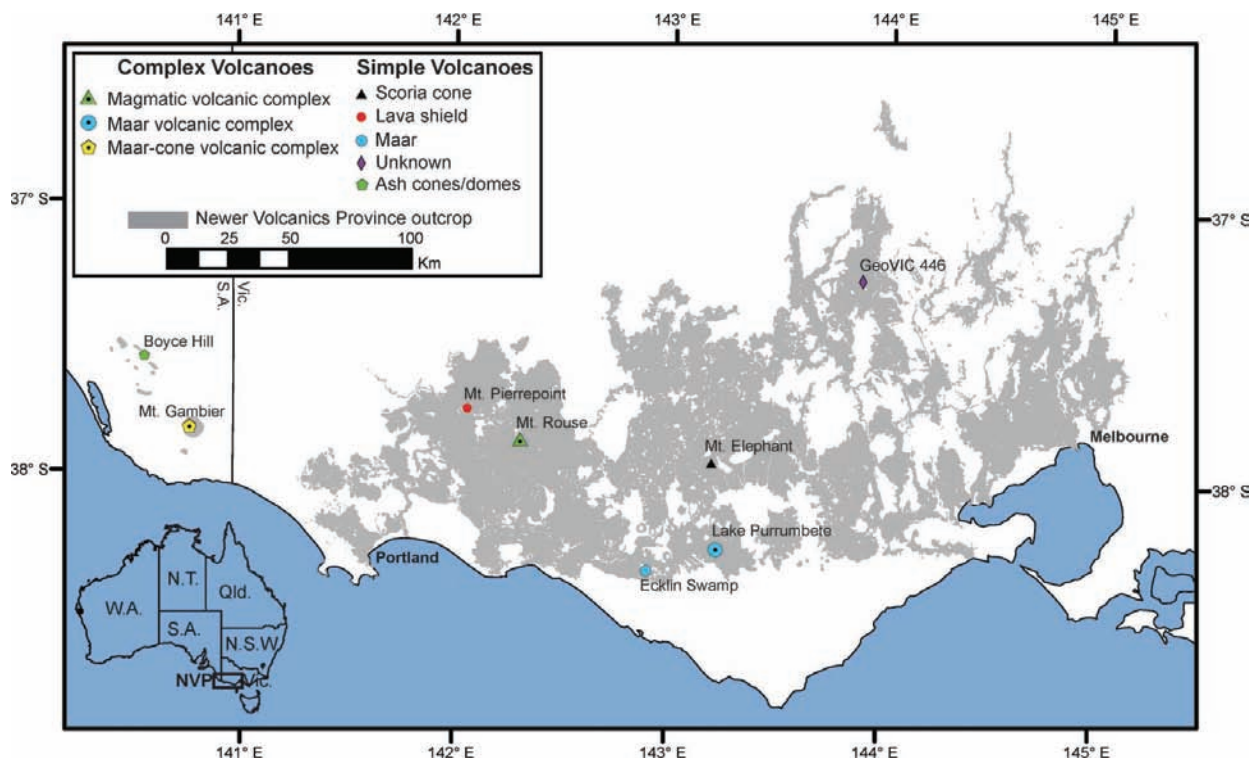


Figure 2 Locations of example volcanoes in the Newer Volcanics Province.

guide for Victoria (Simons & Moore 1999; VandenBerg *et al.* 2000), and the South Australia GIS Dataset (October 2007).

The area of the NVP and its subprovinces was calculated in ArcGIS by splitting the polygons associated with NVP outcrop along the boundary between the Central Highlands and Western Plains subprovinces, using seamless geology (DPI Seamless Geology DVD October 2011). The area of the Mt Gambier subprovince was calculated using the South Australia State GIS Dataset (October 2007).

All eruption points were saved in Google Earth as a kml file, in which they were placed in folders according to subprovince, and subfolders according to deposit type. Additional folders for central co-ordinates of complex eruption points were added. Kml files allow features like coordinates and their associated place marks to be displayed on geospatial software such as Google Earth, Google Maps and ArcGIS.

The spreadsheet, kml file and ArcGIS layers are available to download from the VHUB NVP Group (<<https://vhub.org/groups/nvp>>). Additionally, the general public is able to access the kml file from the Penshurst Volcanoes Discovery Centre website (<<http://www.penshurst-volcano.org.au>>).

Classification of eruption points of the Newer Volcanics Province

Eruption centres of the NVP have previously been classified from their geomorphological variations, using dominant eruption type and products (e.g. Edwards 1938; Coulson 1954; Ollier & Joyce 1964; Ollier 1967; Singleton & Joyce 1970; Rosengren 1994). Rosengren (1994)

recognised three categories further subdivided into type—effusive (lavas), explosive (scoria, maars) and miscellaneous (composite lava/scoria eruptions, tuff mounds, mamelons). A new approach was used in this study, whereby eruption centres were described as either simple or complex, using further subdivision under these categories. One eruption centre may have varying numbers of eruption points of different character. Central co-ordinates were assigned to each volcanic centre in the spreadsheet, to which individual eruption points were then assigned numbers in ascending order and a main deposit descriptor (mainly scoria, mainly lava, maar, ash cone/dome, spatter or unknown). The volcanic centre was then assigned an overall descriptor based on the amalgamation of its eruption point data. Simple volcanoes feature very few known eruption points and these are dominantly of one form, with simple morphologies. They are described as scoria cones, lava shields, maars, ash cones/domes and unknown eruption types. Complex volcanoes feature multiple eruption points, with intricate morphologies. They are described as magmatic, maar or maar-cone volcanic complexes. These definitions will now be explored in more detail, with relevant examples of NVP volcanoes, the locations of which may be found in Figure 2.

SIMPLE VOLCANIC CENTRES

Lava shields form from the gradual buildup of fluidal lava flows and welded spatter around a central vent. Lava can flow many kilometres, evidenced by the extensive Western Plains lava fields. Many of the lava shields in the NVP are very low in nature and difficult to see in aerial photographs. They can therefore be easily



Figure 3 Simple volcanic centres of the Newer Volcanics Province. (a) Mt Pierrepont lava shield. (b) Mt Elephant scoria cone. (c) Ecklin Swamp maar. (d) Boyce Hill ash cone. (e) GeoVIC 446 unknown eruption type.

mistaken for parts of lava flows, but are very broad and may be associated with substantial lava flows, e.g. Mt Hydewell. A good example of a lava shield is Mt Pierrepont, Hamilton (Figure 2, 3a). The volcano features at least two individual flows (Bennetts *et al.* 2003), with an ill-defined crater featuring a rim of basalt along the western half, and lava flows of >1 km in length. Mt Pierrepont is among the oldest volcanoes of the NVP, dated by K–Ar to 3.9 ± 0.1 Ma (McDougall *et al.* 1966), and is severely weathered.

Scoria cones form by the gradual, near-vent accumulation of pyroclastic material in the form of lapilli, bombs and minor ash. Many scoria cones in the NVP are composite in nature, associated with late-stage lava flows as the magma became gas-poor. Mt Elephant, at Derrinalum, is a good example of a scoria cone (Figure 2, 3b). The cone rises 215 m above the surrounding lava plains, and comprises a 90 m-deep crater, breached to the northeast (Birch 1994). Deposits are purely magmatic in the form of scoria, blocks and bombs, deposited during fire-fountaining eruptions (Rosengren 1994). Some of the NVP scoria cones feature two or three eruption points, for example Saddleback Hill in the Learmonth region of the Central Highlands subprovince. These are not classified as complex eruptions as they are not

morphologically complex. However, future detailed examination may reveal some of these centres to be more complex than previously assumed.

Maars are the product of phreatomagmatic eruptions, as opposed to lava shields and scoria cones, which are the products of magmatic eruptions. Phreatomagmatic eruptions are a result of the interaction between rising magma and ground/surface waters. The result is a bowl-shaped crater with a low rim of fine-grained ejecta, rich in country rock fragments. There are relatively few simple maars in the NVP, as most phreatomagmatic volcanism tends to occur either in combination with magmatic eruptions, resulting in maar-cone volcanic complexes, or as multiple coalescing phreatomagmatic eruptions resulting in maar volcanic complexes. Fourteen simple maars are documented in the NVP, of which Ecklin Swamp is a fine example (Figures 2, 3c). Located 14 km south of Terang in the Western Plains subprovince, the maar features an elongate tuff ring approximately $1 \text{ km} \times 0.75 \text{ km}$ composed of finely fragmented tuff and ejected country rock from the underlying Gellibrand Marl (Rosengren 1994).

Several ash cones and domes were reported in the Mt Burr volcanic group (Sheard 1990). These are also phreatomagmatic in origin, but feature steeper dipping ejecta

and craters that are above the ground surface. Boyce Hill (Figures 2, 3d) is an ash cone located at the southeastern edge of Mt McIntyre in the Mount Burr Range. Rising 69 m above the surrounding plains and composed of lapilli and agglomerate, the eruption centre is associated with a basement-high fault, which also runs through several other volcanic centres (Sheard 1990).

The NVP features many eruption points of an unknown character. No associated literature could be found describing them, and all need to be ground-truthed. In most cases, seamless geology associates these eruption points with lava, but some are located near clusters of scoria cones, and could be scoria cones themselves. It was therefore deemed more suitable to plot them as unknown eruption types rather than as lava eruptions.

The majority of these unknown eruption points are unnamed volcanic centres defined either in the Rosengren (1994) report, by Geoscience Victoria or by the MONVOLC research group (Monash University Volcanology, either by the author or Jackson van den Hove). These centres should all be ground-truthed before assigning descriptors, as the vast majority were assigned by Geoscience Victoria, based on the assumption that every high point in the DEM was an eruption point (VandenBerg, pers. comm. 2012). This assumption is not necessarily true, as ground-truthing in the Hamilton area by the author has recently suggested.

A few unknown eruption points are associated with complex volcanic centres, namely four points at Madden

Hill (which has been deemed a magmatic volcanic complex, as none of the unknown eruption points are likely to be phreatomagmatic in origin) and two points at Mt Napier, both of which form craters that are magmatic in origin, but are not defined as either scoriaceous or lava eruptions (Gill & Elmore 1974).

An example of an unknown eruption point is GeoVIC 446 (Figures 2, 3e). Located near Ullina in the Central Highlands subprovince, this obvious eruption point is situated between several scoria cones such as Kelly Hill (Glengower) and Stewart Hill to the north and northeast, Clover Hill maar–cone volcanic complex to the south, and the Leishman Hill magmatic volcanic complex to the west. Low in profile and approximately 40 m high with a gently sloping base of almost 0.8 km, this eruption point could either be a small lava shield or a scoria dome.

COMPLEX VOLCANIC CENTRES

Magmatic volcanic complexes feature a combination of lava shields, scoria cones and/or spatter cones, all of which are magmatic in origin. These are found scattered across the Western Plains and Central Highlands. Mt Rouse at Penshurst in the Western Plains is an excellent example of a magmatic volcanic complex (Figure 2, 4a). Mt Rouse is the largest eruption centre in the NVP, featuring eight magmatic eruption points of scoria, lava and spatter. Dated to $0.3 \text{ Ma} \pm 0.01$ (Matchan & Phillips 2011), the lava flows cover an area of $>511 \text{ km}^2$ (Boyce



Figure 4 Complex volcanic centres of the Newer Volcanics Province. (a) Mt Rouse magmatic volcanic complex. (b) Lake Purrumbete maar volcanic complex. (c) Mt Gambier maar–cone volcanic complex, Valley Lake.

et al. 2012), extending 60 km to the coast at Port Fairy (Sutalo 1996) and are composed of one magma batch (Elias 1973; Whitehead 1986, 1991; Sutalo 1996; Sutalo & Joyce 2004; Boyce 2011; Boyce *et al.* 2013). Detailed stratigraphic analysis of the scoria cones revealed a further two magma batches (Boyce *et al.* 2013). The nature of the stratigraphy points to a complex system of propagating dykes beneath the Mt Rouse complex, leading to the sequential eruption of three magma batches, then simultaneous eruption of two more (Boyce *et al.* 2013).

Maar volcanic complexes feature dominantly phreatomagmatic eruption products. At present, there are only four such complexes in the NVP, as many phreatomagmatic eruptions are also associated with cone-forming magmatic activity. Lake Purrumbete, near Camperdown in the Western Plains subprovince, is the best example of such a complex (Figures 2, 4b) and is one of the largest maar volcanoes both in the NVP and worldwide. Recent research (Jordan *et al.* 2013) shows that magma propagation was influenced by a NW–SE Mesozoic fault intersecting with a N–S Paleozoic structure. Jordan *et al.* (2013) suggest that the 3 km-diameter lake formed over three main stages, by the coalescence of at least three shallow maar craters, and including multiple vent migration events, re-opening of former vents and simultaneous activity of two vents. The eruption was dominantly phreatomagmatic, but featured a significant magmatic influence during the opening stages of eruption to produce surge-modified fallout deposits. Towards the end of the eruption, there was a small-volume pyroclastic flow, possibly the result of vent clearing. Lake Purrumbete again challenges the accepted view that NVP volcanoes are all monogenetic, as there was a significant volcanic hiatus between the second and third eruption stages, during which a crater lake formed.

Maar–cone volcanic complexes feature a combination of magmatic and phreatomagmatic eruption products, in the form of maars, scoria cones and/or lava flows and spatter cones. There are 20 such complexes in the NVP, outcropping in all subprovinces, but mainly in the Camperdown region of the Western Plains, owing to the interaction of the magma with the underlying aquifers of the Otway Basin (see Discussion). Mt Gambier is one such example (Figures 2, 4c). Located in southeast South Australia in the Mt Gambier subprovince, the complex is the youngest volcano in the NVP, dated to *ca* 5000 BP (Blackburn 1966; Barbetti & Sheard 1981; Blackburn *et al.* 1982; Robertson *et al.* 1996). Mt Gambier is extremely complex and erupted over 13 stages to produce >14 eruption points aligned parallel to the Tartwaup Fault System (van Otterloo & Cas 2011; van Otterloo

2012) along WNW–ESE-trending lineaments (Wopfner & Thornton 1971; van Otterloo & Cas 2011; van Otterloo 2012). Eruption styles at the complex randomly alternated between magmatic and phreatomagmatic to create maars, scoria and spatter cones, tuff cones, lavas and pyroclastic flows. The products of Mt Gambier were the result of two simultaneously erupting, mantle-derived magma batches, giving the complex a polymagmatic character (van Otterloo & Cas 2011; van Otterloo 2012).

RESULTS AND DISCUSSION

Based on these new data, the Newer Volcanics Province is composed of >704 known eruption points from >416 volcanic centres, the products of which cover an area of >19 000 km² (Figure 1; Tables 1, 2). These are minimum estimates, owing to the nature of the survey. It is likely that additional eruption points will be added to these totals, as more in-depth research is undertaken at the more complex volcanic centres. NVP area was calculated from the latest seamless geology and does not take into account overlying deposits such as alluvium, duricrust, lake and swamp deposits, sands (especially in the Mt Gambier subprovince), or areas where lavas flowed beyond the present-day coastline, which is beyond the scope of this project. The area covered is therefore an underestimation and is likely to be closer to earlier estimates of 25 000–27 000 km² (McDougall *et al.* 1966, Cas & van Otterloo 2011; van Otterloo 2012).

Table 1 gives statistics for NVP eruption centres based on subprovince and volcano type. There are a total of 49 complex volcanoes and 367 simple volcanoes across the NVP. It is clear from these data that almost half of the eruption points of the NVP are associated with complex volcanism.

In addition to the 704 eruption points defined, 81 points were plotted in a separate spreadsheet. These are made up of 54 single Geoscience Victoria points and 27 of the Singleton & Joyce (1970)/Rosengren (1994) points (of which 13 are also associated with additional Geoscience Victoria points to those aforementioned). Reasons for separation include positioning of some points in granite, sandstone or ignimbrite outcrops according to seamless geology (and with features looking dissimilar to general NVP landmarks); erosional features being mistaken for eruption points, for example adjacent to rivers; and some points being located in flat terrain with no evidence of eruption on aerial imagery, DEM, magnetics or radiometrics. For example, three eruption points occur in the Willimigongong Ignimbrite of Devonian age at

Table 1 Volcanic centres of the Newer Volcanics Province, Victoria, classified by subprovince and type of volcanic centre, with totals indicated in *italics*.

| | Simple volcanoes | | | | Complex volcanoes | | | | Total |
|-------------------|------------------|--------------|-------|-----------------|-------------------|----------|------|-----------|-------|
| | Scoria cones | Lava shields | Maars | Ash cones/domes | Unknown | Magmatic | Maar | Maar–cone | |
| Central Highlands | 89 | 101 | 3 | 0 | 17 | 12 | 0 | 2 | 224 |
| Western Plains | 28 | 92 | 10 | 0 | 14 | 10 | 4 | 17 | 175 |
| Mt Gambier | 6 | 1 | 1 | 5 | 0 | 0 | 1 | 3 | 17 |
| Total | 123 | 194 | 14 | 5 | 31 | 22 | 7 | 20 | 416 |

Table 2 Eruption points of the Newer Volcanics Province, Australia, classified by subprovince and type of eruption, with totals indicated in *italics*.

| | Mainly scoria | Mainly lava | Maar | Ash cones/domes | Unknown | Spatter cone | <i>Total</i> |
|-------------------|---------------|-------------|-----------|-----------------|-----------|--------------|--------------|
| Central Highlands | 129 | 137 | 6 | 0 | 21 | 0 | <i>293</i> |
| Western Plains | 140 | 121 | 69 | 0 | 21 | 16 | <i>367</i> |
| Mt Gambier | 14 | 1 | 16 | 4 | 0 | 9 | <i>44</i> |
| Total | <i>283</i> | <i>259</i> | <i>91</i> | <i>4</i> | <i>42</i> | <i>25</i> | <i>704</i> |

Mt Macedon, none of which can be found in other NVP literature, and the areas the points are located in are dissimilar to NVP eruption centres. These points would represent an additional 75 eruption centres if ground-truthed to be part of the NVP (and can easily be added to the database and map), and would bring the total number of eruption points to 785 over 491 eruption centres.

Volcanic centres of the 7.0–4.6 Ma Macedon–Trentham Group were also plotted in a separate spreadsheet, comprising 32 eruption points from 24 centres. Although they are not needed for the NVP map, it was deemed useful to document them.

Lack of detailed work on eruption centres, coupled with poor preservation and lack of outcrop, mean that many potentially complex volcanoes have been classified as simple. Future research may bring to light additional eruption points for these volcanic centres, which can easily be redefined.

Calculations from this study estimate that the NVP has an eruption frequency of 1:10 800 yrs. (4.5 Ma/416). If, however, the additional 75 eruption centres proved to be genuine NVP volcanoes, this would change to 1:9200 yrs. (4.5 Ma/491). This is similar to estimates of 1:11 500 yrs (Cas *et al.* 1993) and 1: 12 500 yrs (Joyce 1988a, b, 2003, 2004, 2005).

The NVP is considered an active volcanic province, with the occurrence of mantle-derived CO₂ emissions at Mt Gambier, Garvoc, Wangoom (Wopfner & Thornton 1971; Chivas *et al.* 1987) and the Daylesford region of the Central Highlands (Chivas *et al.* 1983; Cartwright *et al.* 2002), plus the presence of a heat anomaly beneath the Central Highlands subprovince (Graeber *et al.* 2002; Aivazpourporgou *et al.* 2012). Researchers agree that further eruptions are possible, and the hazards associated would be from lava flows, scoria-cone and maar formation, and the production of ash plumes (e.g. Blong 1984, Joyce 2003, 2004; Cas & van Otterloo 2011). This new repository of eruption-point data will help to update available risk and hazard analysis evaluations for Victoria and South Australia, for example that of Joyce (2003).

Central Highlands subprovince

The Central Highlands subprovince covers the dissected uplands of Paleozoic metasediments and granites north-west of Melbourne (Nicholls & Joyce 1989) and is 140 km across (Figure 5). The subprovince contains 54% of NVP volcanic centres, contrasting with a previously estimated 75% (Joyce 1975). Dominant eruption points are 72% of the simple scoria cones and 52% of simple lava shields in the NVP, with only 14 complex volcanic centres and three simple maars (Table 1). Products from these centres cover an area of > 4277 km², which is 71%

smaller than that covered by eruption products of the Western Plains subprovince.

Table 2 shows numbers of individual eruption points in the subprovinces (eruption centres feature varying numbers of eruption points). The Central Highlands is made up of approximately half the lava and scoria eruptions of the NVP, as it contains 42% of the total number of NVP eruption points. This is due to the fact that there are a slightly higher proportion of simple volcanoes in the Central Highlands when compared with the Western Plains.

The west of the subprovince is dominated by scoria-cone eruptions in two notable concentrations (Figure 5) trending NW–SE. The first runs 33 km from Lexton to Ballarat in a 10-km swathe consisting of 34 scoria cones, four lava shields, three unknown eruption types and one magmatic volcanic complex (Mt Mitchell) (see also Figure 6a). The second concentration runs approximately 52 km from Mount Cameron–Newlyn–Gordon in a 7-km swathe consisting of >27 scoria cones, four magmatic volcanic complexes and numerous lava shields towards the Gordon area. These trends may correspond to the general basement structural trends of the Lachlan Orogen, which are NNW–SSE to N–S, coinciding with the orientation of the present-day compressive stress regime (Hillis *et al.* 1995; Jones *et al.* 2000).

It is difficult to associate faults with volcanism (Joyce 1975), and the heterogeneous nature of the subsurface (e.g. Cayley *et al.* 2011) brings into question to what extent faults have influenced volcanic activity in the NVP. With this in mind, there are several outcroppings of volcanic centres across the NVP, which seemingly coincide with major crustal structures. Some of the Lexton to Ballarat centres (Mt Mitchell to Weatherboard Hill) align with the Avoca Fault (Figure 6a), which is reverse in nature, steeply dipping to the west (Gray *et al.* 1988), and does not reach the Moho but terminates mid-crust against the Moyston Fault (Cayley *et al.* 2011). Magma from the eruption centres in this region has been emplaced through granite, and both local faults and W/NW and N/NE jointing have controlled the distribution patterns (Joyce 2007). The westerly dipping Mt William Fault (Cayley *et al.* 2011) lies close to centres in the Goldie region, such as The Sugarloaf, Woodlands and several unnamed eruption centres. The Paleozoic Muckleford Fault (Figure 5), which is a west-dipping reverse fault, splits the Central Highlands into east and west and indicates a major tectonic difference at depth (Joyce 2007). The area to the west forms an uplifted bedrock plateau, on which scoria cones are dominant, compared with lava shields to the east (Joyce 2007), although both volcano types are found across the Central Highlands.

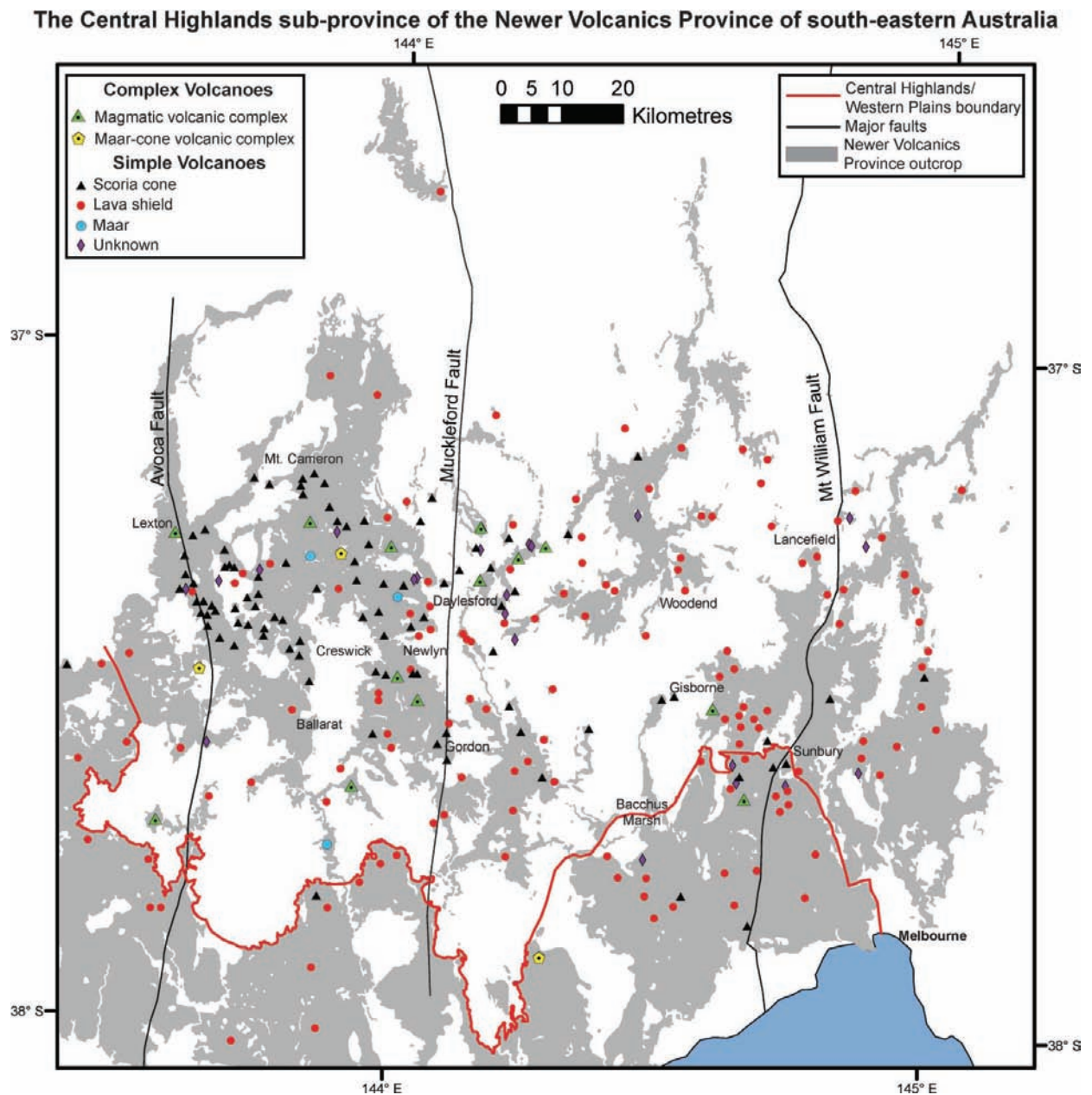


Figure 5 Central Highlands subprovince of the Newer Volcanics Province.

Notable concentrations of lava shields found in the Gisborne–Sunbury area straddle the border between the Central Highlands and the Western Plains, and consist mainly of lava shields forming extensive lava fields (Clarke 1984; O'Neill 1984), and a line of lava shields running from Kilmore to Craigieburn, both trending NW–SE. Late-Pliocene movement along the Rowsley Fault near Bacchus Marsh caused lava flows in the area to be monoclinaly folded across the fault (Joyce 1975, 2009). These lavas were dated to 4 Ma (Azis-ur-Rahman & McDougall 1972).

Complex volcanic centres take the form of magmatic complexes such as Mt Franklin and Mt Kooroocheang, while there are two maar–cone volcanic complexes at Lake Burrumbete and Clover Hill.

Western Plains subprovince

The Western Plains subprovince extends 320 km from Melbourne west to Portland and is characterised by extensive plains forming lava fields, filling the pre-existing subdued topography of the Otway Basin (Figure 1). The subprovince contains 42% of NVP volcanic centres in the form of 23% of the NVP's simple scoria cones, 47% of lava shields, 71% of simple maars and 63% of the complex centres (Table 1). The products of these eruptions cover an area of >14 600 km², making this the largest subprovince in the NVP.

The Western Plains contains 52% of the total number of eruption points in the NVP (Table 2), similar to the Central Highlands in that it contains almost half of the

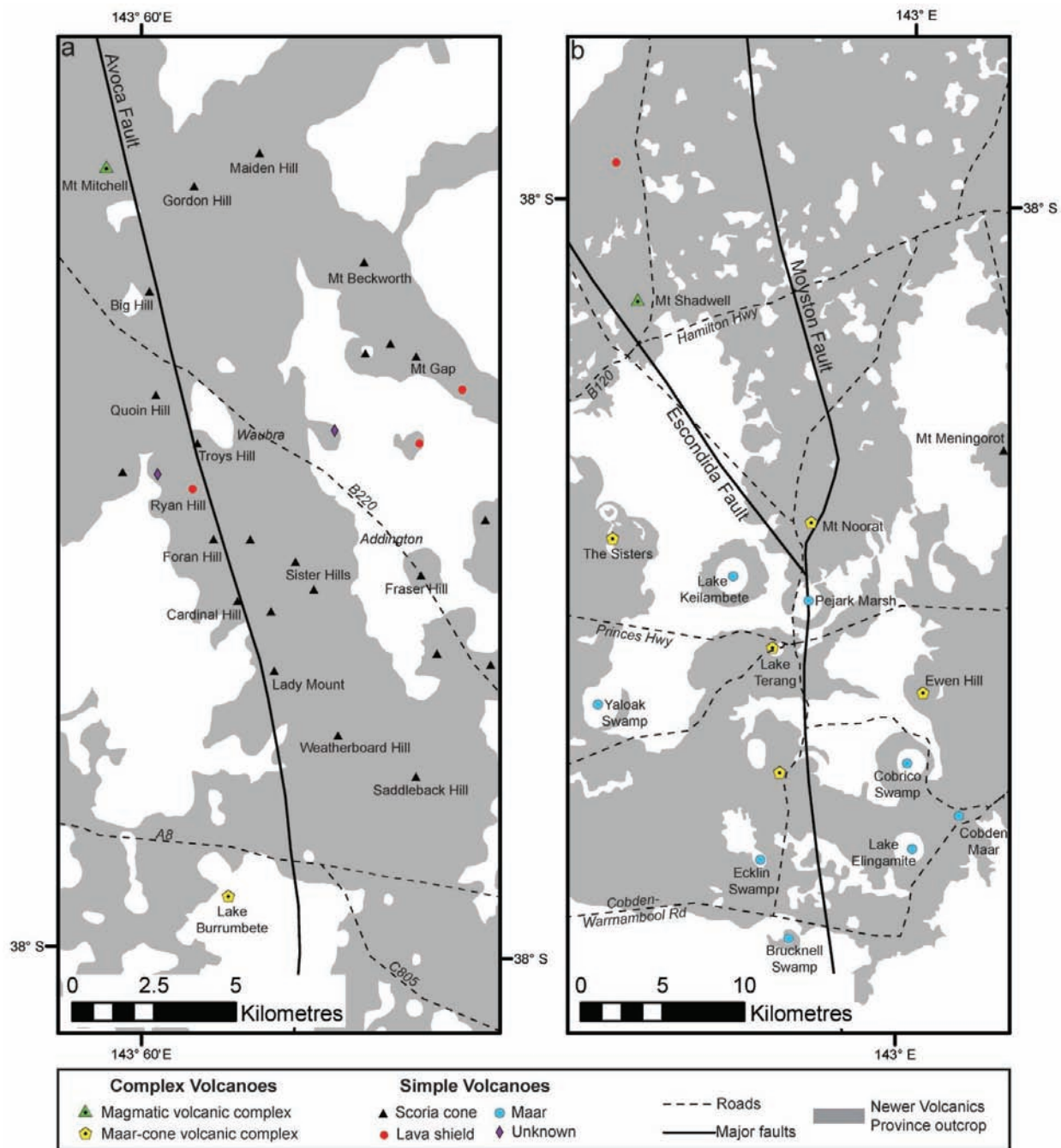


Figure 6 Volcanic distribution of the Western Plains subprovince in (a) the Avoca Fault area, and (b) the Moyston and Escondida Fault area.

lava and scoria eruptions. However, the subprovince features most of the maar volcanoes in the NVP; these are concentrated in the Warrnambool-Colac region, where they are associated with the aquifers of the underlying Cenozoic Otway Basin sediments (Joyce 1975) and Mesozoic structures. They range from simple volcanoes such as the Cobden Maar, to maar volcanic complexes like Lakes Purrumbete and Bullen Merri. Maar-cone volcanic complexes such as Tower Hill and Red Rock can have substantial numbers of eruption points (19 and 40, respectively). Lake Purrumbete and Tower Hill are among the largest maars in the world. One large maar-cone volcanic

complex recently discovered near Woodhouse, Hamilton, by the author constitutes the most northern maar in the western half of the Western Plains, and was formed away from the influence of the Otway Basin aquifers. The vast majority of simple scoria cones of the Western Plains (93%) outcrop in the east of the subprovince.

The Mortlake Discontinuity (Price *et al.* 1997) splits the Western Plains into East and West, and corresponds to the Paleozoic Moyston Fault, the suture between the Delamerian and Lachlan orogens (Korsch *et al.* 2002; Cayley *et al.* 2011). The volcanics to the east have higher Sr-isotopic ratios (0.7037–0.7058) than those in the west,

indicating distinct mantle sources (0.7037–0.7046; Price *et al.* 1997). The Moyston Fault dips to the east, probably extending to the Moho (Cayley *et al.* 2011), and coincides with the outcropping of several maar volcanoes in the Noorat–Terang–Ecklin area (Figure 6b), such as the simple maars of Lake Keilambete, Pejark Marsh and Ecklin and Brucknell swamps, and the maar–cone volcanic complexes of Mt Noorat, Lake Terang and Staughton Hill. Mt Shadwell coincides with the Escondida Fault, which dips to the east (Gray *et al.* 2003).

The Dartmoor Ridge contains a concentration of eight lava shields, such as Mt Deception and Mt Vandyke, with ages of 3–2 Ma (Nicholls & Joyce 1989); and the Portland area features three large coastal complexes, Capes Bridgewater, Nelson and Sir William Grant. The Hummocks Fault dips steeply west (Morand *et al.* 2003) through the Mt Deception area and an unnamed but possibly related Geoscience Victoria eruption point.

Other major faults in the Western Plains (Figure 1) include the easterly dipping Yarramyllup Fault (Gray *et al.* 2003), which runs between Hamilton-area volcanoes such as Mt Baimbridge, Mt Pierrepont and Mt Napier, and Mt Ripponhurst and Vine Bank; the Avoca Fault, close to Robertson Hill, Red Rock maar–cone complex and Warrion Hill; and the westerly dipping Mt William Fault (Cayley *et al.* 2011) in the Sunbury area near Cowies Hill, Mt Atkinson, Ryans Hill and Bald Hill.

Mt Gambier subprovince

The Mt Gambier subprovince is located in southeast South Australia, 60 km west of the Western Plains subprovince (Figures 1, 7), and contains only 4% of NVP volcanic centres concentrated in two clusters, the Mt Burr Volcanic Group and the Mt Gambier Volcanic Group (Sprigg 1952; Sheard 1990, 1995). The Mt Gambier subprovince contains only 6% of total eruption points in the NVP (Table 2), with its products covering an area of >99 km². Mt Gambier is therefore the smallest subprovince, amounting to approximately 1% of total NVP area. Sheard (1990) estimated the aerial extent of the volcanics to be 110 km², while Demidjuk (2005) used drill-hole data to estimate a subaerial extent of 217 km².

The Mt Burr Volcanic Group, east of Millicent, consists of 14 confirmed volcanic centres, concentrated along a basement high and related to three northwest-trending lineaments (Sheard 1978, 1990; Nicholls & Joyce 1989). Pollen and radiocarbon studies on lake sediments overlying volcanic ash deposits at Lake Leake suggest that the maar is older than 50 000 B.P. (which was the limit of radiocarbon dating) (Dodson 1975). The deposits have suffered erosional modification by high sea-levels during the Pleistocene and are overlain by the Bridgewater Formation sands (Sheard 1978, 1990). A range of volcanic centres are preserved, such as composite centres of lava and scoria (Mt Graham and Mt Burr), a maar–cone complex (Mt Muirhead), simple and complex maars (Lakes Edward and Leake) and several phreatomagmatic tuff cones (e.g. Mt Lyon, Boyce Hill).

The Mt Gambier Volcanic Group is made up of two maar–cone volcanic complexes, Mt Gambier and Mt Schank. Eruption points at Mt Schank are aligned

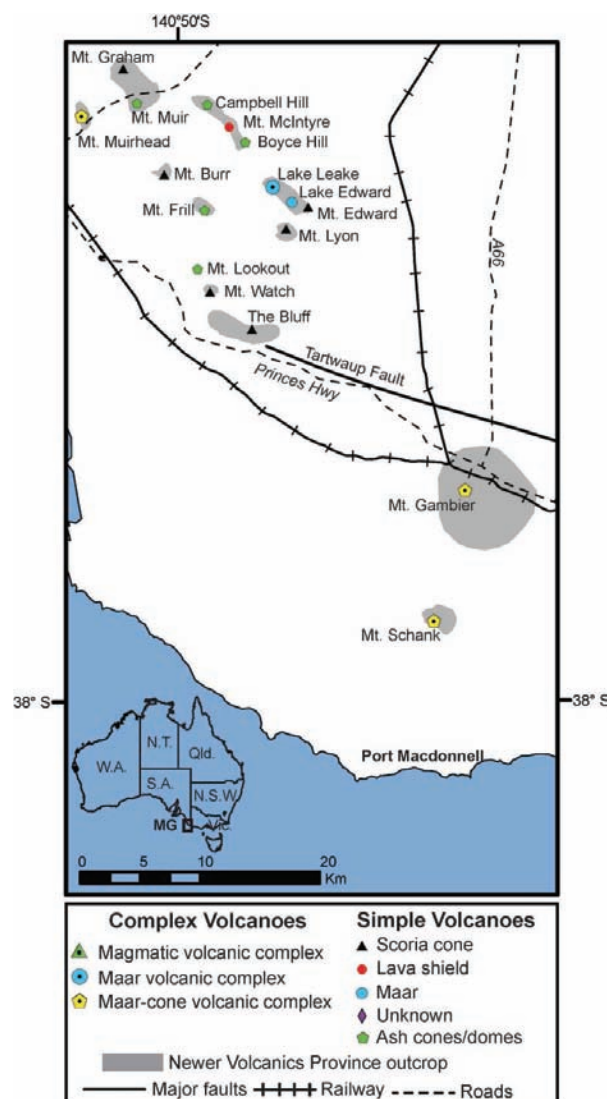


Figure 7 Mt Gambier subprovince of the Newer Volcanics Province, southeastern South Australia.

NNW–SSE, and at Mt Gambier NW–SE along the Tartwaup Fault (van Otterloo 2012).

CONCLUSIONS

Analysis of eruption points in the Newer Volcanics Province has allowed the drafting of a new map based on eruption type, and gives a minimum estimate of >704 eruption points from >416 volcanic centres. The Newer Volcanics Province covers an area of >19 000 km² and may be significantly larger. This project highlights the need for additional research to be undertaken in the NVP. Recent and ongoing research indicates that many apparently simple volcanoes are complex, with multiple eruption points and varieties of eruption products. This is illustrated by the composite nature of many of the scoria cones in the province. Recent discoveries of three volcanoes (including one large complex) in the Hamilton area by the author, and several more unknown eruption

points during the course of this study, show that there are probably many more volcanoes to be discovered in the province. Numerous Honours and other theses at Monash, Melbourne and LaTrobe universities may yet provide evidence for further eruption points. Also, because of the extremely low profile of many of the lava shields, it is more than likely older edifices have been completely buried by younger volcanism, for example by the Mt Rouse lava flows, which extend >60 km from Mt Rouse to the sea at Port Fairy, and flow around one such volcano (Fox Hill). Poor preservation and outcrop also hinder efforts to define eruption points. Because the NVP is considered an active province, it is important to gain a fuller understanding of the nature of eruption products and their frequency. It is estimated that the NVP has an eruption frequency ranging from 1:10 800 years (this study) to 1:11 500 years (Cas *et al.* 1993) and 1:12 500 years (Joyce 1988a, b, 2003, 2004, 2005).

ACKNOWLEDGEMENTS

This paper represents part of the PhD research undertaken by JB under the supervision of Prof. Reid Keays, Dr Ian Nicholls and Dr Patrick Hayman. JB acknowledges a Monash University School of Geosciences research scholarship and Dean's International Postgraduate Research Scholarship. Thanks go to David Higgins for supplying Geoscience Victoria eruption points and Bill Birch (Museum Victoria) for supplying a copy of the Rosengren (1994) report. Jozua van Otterloo (Monash University) is thanked for supplying ArcGIS layer files for the geology of the Mt Gambier subprovince, as is David Moore for helpful discussions relating to geological structures in the NVP. The following Monash University students are thanked for supplying eruption point data for their areas of research, and for the scientific discussions about the NVP during the course of our PhDs: Jozua van Otterloo (Mt Gambier subprovince), Teagan Blakie (Red Rock), Jackson van den Hove (Mt Noorat, The Basins and surrounds, Lake Purrumbete) and Simone Jordan (Lake Purrumbete). Dr Janine Kavanagh (University of Liverpool) supplied eruption point data for Mt Eccles. Thanks go to Teagan Blakie, Jozua van Otterloo and Jackson van den Hove for supplying images of Ecklin Maar, Boyce Hill, Mt Gambier and Lake Purrumbete. Fons VandenBerg is thanked for scientific discussions relating to Geoscience Victoria classifications. Thanks go to Bill Birch, Bernie Joyce, Ian Nicholls, Reid Keays and Ray Cas for in-depth reviewing of this paper and their helpful comments.

REFERENCES

- AIKAZPOURPOURGOU S., THIEL S., HAYMAN P., MORESI L. & HEINSON G. 2012. The upper mantle thermal structure of the Newer Volcanic Province, Western Victoria, Australia from long period Magnetotelluric (MT) array. *Extended Abstract, 21st EM Induction Workshop, Darwin, Australia, 25–31 July 2012*.
- AZIZ-UR-RAHMAN & McDUGALL I. 1972. Potassium-argon ages on the Newer Volcanics of Victoria. *Royal Society of Victoria Proceedings* **85**, 61–69.
- BARBETTI M. & SHEARD M. J. 1981. Palaeomagnetic results from Mounts Gambier and Schank, South Australia. *Journal of the Geological Society of Australia* **28**, 385–394.
- BENNETTS D. A., WEBB J. A. & GRAY C. M. 2003. Distribution of Plio-Pleistocene basalts and regolith around Hamilton, Western Victoria, and their relationship to groundwater recharge and discharge. *Advances in regolith: proceedings of the CRC LEME Regional Regolith Symposia 2003*, 11–15.
- BIRCH B. 1994. Volcanoes in Victoria. Royal Society of Victoria, Melbourne, VIC.
- BLACKBURN G. 1966. Radiocarbon dates relating to soil development and volcanic ash deposition in south-east South Australia. *Australian Journal of Earth Sciences* **29**, 50–52.
- BLACKBURN G., ALLISON G. B. & LEANEY F. W. J. 1982. Further evidence on the age of the tuff at Mount Gambier, South Australia. *Transactions of the Royal Society of South Australia* **106**, 163–167.
- BLAKIE T., PIGANIS F., CAS R., AILLERES L. & BETTS P. 2011. Red Rock Volcanic Complex. In: Cas R., Blakie T., Boyce J., Hayman P., Jordan S., Piganis F., Prata G. & van Otterloo J. eds. *Factors that influence varying eruption styles (from magmatic to phreatomagmatic) in intraplate continental basaltic volcanic provinces: The Newer Volcanics Province of southeastern Australia*. Field trip guide VF01, pp. 32–45. IUGG 2011 General Assembly. Earth on the Edge: Science for a Sustainable Planet.
- BLONG R. J. 1984. *Volcanic hazards—a sourcebook on the effects of eruptions*. Academic Press, Sydney.
- BOYCE J. 2011. Mount Rouse Volcano. In: Cas R., Blakie T., Boyce J., Hayman P., Jordan S., Piganis F., Prata G. & van Otterloo J. eds. *Factors that influence varying eruption styles (from magmatic to phreatomagmatic) in intraplate continental basaltic volcanic provinces: The Newer Volcanics Province of southeastern Australia*. Field trip guide VF01, pp. 46–54. IUGG 2011 General Assembly. Earth on the Edge: Science for a Sustainable Planet.
- BOYCE J., NICHOLLS I., KEAYS R. & HAYMAN P. 2012. The multiple magma batches of Mt. Rouse, Newer Volcanics Province, Victoria, Australia. *Abstract, IAVCEI 4IMC conference, Auckland, New Zealand, 20 February 2012*.
- BOYCE J. A., NICHOLLS I., KEAYS R. & HAYMAN P. 2013. Triple magma batches and a complex eruption history of a monogenetic volcano: geochemical analysis of Mt. Rouse, Newer Volcanics Province, Australia. *Abstract, Volcanic and Magmatic Studies Group Annual Meeting, 7–9 January 2013, Bristol, UK*.
- CAREY S. W. 1986. Geotectonic setting of Australasia. In: Glenie R. C. ed. *PESA Symposium, 14–15 November 1985, Melbourne. Petroleum Exploration Society of Australia, Victorian and Tasmanian Branch*, pp. 3–25.
- CARTWRIGHT I., WEAVER T., TWEED S., AHEARNE D., COOPER M., CZAPNIK K. & TRANTER J. 2002. Stable isotope geochemistry of cold CO₂-bearing mineral spring waters, Daylesford, Victoria: sources of gas and water and links with waning volcanism. *Chemical Geology* **185**, 71–91.
- CAS R. & VAN OTTERLOO J. 2011. Introduction to the IUGG Excursion Guide. In: Cas R., Blakie T., Boyce J., Hayman P., Jordan S., Piganis F., Prata G. & van Otterloo J. eds. *Factors that influence varying eruption styles (from magmatic to phreatomagmatic) in intraplate continental basaltic volcanic provinces: The Newer Volcanics Province of southeastern Australia*. Field trip guide VF01, pp. 7–31. IUGG 2011 General Assembly. Earth on the Edge: Science for a Sustainable Planet.
- CAS R., SIMPSON C. & SATO H. 1993. Newer Volcanics Province—Processes and products of phreatomagmatic activity. *IAVCEI Canberra 1993—Excursion guide*. Australian Geological Survey Organisation, Canberra.
- CAYLEY R. A., KORSCH R. J., MOORE D. H., COSTELLOE R. D., NAKAMURA A., WILLMAN C. E., RAWLING J., MORAND V. J., SKLADZIEN P. B. & O'SHEA P. J. 2011. Crustal architecture of central Victoria: results from the 2006 deep crustal reflection seismic survey. *Australian Journal of Earth Sciences* **58**, 113–156.
- CHIVAS A. R., BARNES I. E., LUPTON J. E. & COLLERSON K. 1983. Isotopic studies of south-east Australian CO₂ discharges. *Geological Society of Australia Abstract* **12**, 94–95.
- CHIVAS A. R., BARNES I., EVANS W. C., LUPTON J. E. & STONE J. O. 1987. Liquid carbon dioxide of magmatic origin and its role in volcanic eruptions. *Nature* **326**, 587–589.
- CLARKE W. 1984. The geology and hydrogeology of the Lancefield area. BSc Honours report, University of Melbourne.

- COULSON A. 1954. The volcanic rocks of the Daylesford district. *Proceedings of the Royal Society of Australia* **65**, 113–124.
- DASCH E. J. & MILLAR D. J. 1977. Age and strontium-isotope geochemistry of differentiated rocks from the Newer Volcanics, Mt. Macedon area, Victoria, Australia. *Journal of the Geological Society of Australia* **24**, 195–201.
- DAY R. A. 1983. Petrology and geochemistry of the Older Volcanics of Victoria. PhD thesis, Monash University.
- DEMIDJUK Z. 2005. U-series insights into melting processes and magma evolution beneath the New Volcanic Province in South Australia. Macquarie University Honours thesis.
- DEMIDJUK Z., TURNER S., SANDIFORD M., GEORGE R., FODEN J. & ETHERIDGE M. 2007. U-series isotope and geodynamic constraints on mantle melting processes beneath the Newer Volcanic Province in South Australia. *Earth and Planetary Science Letters* **261**, 517–533.
- DODSON J. R. 1975. Vegetation history and water fluctuations at Lake Leake, south-eastern Australia. II. 50,000 B. P. to 10,000 B. P. *Australian Journal of Botany* **23**, 815–831.
- DUNCAN R. A. & McDUGALL I. 1989. Volcanic time–space relationships. In: Johnson R. W. ed. *Intraplate volcanism in Eastern Australia and New Zealand*, pp. 43–53. Cambridge University Press, Cambridge.
- EDWARDS A. B. E. 1938. The Tertiary volcanic rocks of central Victoria. *Quarterly Journal of the Geological Society* **94**, 243–320.
- ELIAS M. 1973. The geology and petrology of Mount Rouse, a volcano in the Western District of Victoria. Honours research report, University of Melbourne.
- EWART A., CHAPPELL B. W. & LE MAITRE R. W. 1985. Aspects of the mineralogy and chemistry of the intermediate-silicic Cainozoic volcanic rocks of eastern Australia. Part 1: Introduction and geochemistry. *Australian Journal of Earth Sciences* **32**, 359–382.
- FARRINGTON R. J., STEGMAN D. R., MORESI L. N., SANDIFORD M. & MAY D. A. 2010. Interactions of 3D mantle flow and continental lithosphere near passive margins. *Tectonophysics* **483**, 20–28.
- FINN C. A., MÜLLER R. D. & PANTER K. S. 2005. A Cenozoic diffuse alkaline magmatic province (DAMP) in the southwest Pacific without rift or plume origin. *Geochemistry, Geophysics, Geosystems* **6**, Q02005.
- FISHWICK S., HEINTZ M., KENNETT B. L. N., READING A. M. & YOSHIZAWA K. 2008. Steps in lithospheric thickness within eastern Australia, evidence from surface wave tomography. *Tectonics* **27**, TC4009.
- GILL E. D. & ELMORE L. K. M. 1974. Importance of the Mount Napier Volcanic Complex near Hamilton, Victoria, Australia. *Victorian Naturalist* **91**, 167–174.
- GOURAMANIS C., WILKINS D. & DEDECKER P. 2010. 6000 years of environmental changes recorded in Blue Lake, South Australia, based on ostracod ecology and valve chemistry. *Palaeogeography, Palaeoclimatology, Palaeoecology* **297**, 223–237.
- GRAEBER F. M., HOUSEMAN G. A. & GREENHALGH S. A. 2002. Regional teleseismic tomography of the western Lachlan Orogen and the Newer Volcanic Province, southeast Australia. *Geophysical Journal International* **149**, 249–266.
- GRAY D. R., ALLEN R. L., ETHERIDGE M. A., FERGUSON C. L., GIBSON G. M., MORAND V. J., VANDENBERG A. H. M., WATCHORN R. B. & WILSON C. J. L. 1988. Structure and tectonics. In: Douglas J. G. & Ferguson J. A. eds. *Geology of Victoria*, pp. 1–36. Geological Society of Victoria, Victorian Division, Melbourne.
- GRAY D. R., FOSTER D. A., MORAND V. J., WILLMAN C. E., CAYLEY R. A., SPAGGIARI C. V., TAYLOR D. H., GRAY C. M., VANDENBERG A. H. M., HENDRICKX M. A. & WILSON C. J. L. 2003. Structure, metamorphism, geochronology and tectonics of Palaeozoic rocks. In: Birch W. D. ed. *Geology of Victoria*, pp. 15–71. Geological Society of Australia Special Publication 23.
- GRAY C. M. & McDUGALL I. 2009. K–Ar geochronology of basalt petrogenesis, Newer Volcanic Province, Victoria. *Australian Journal of Earth Sciences* **56**, 245–258.
- HILLIS R. R., MONTE S. A., TAN C. P. & WILLOUGHBY D. R. 1995. The contemporary stress field of the Otway Basin, South Australia: implications for hydrocarbon exploration and production. *Australian Petroleum Exploration Association Journal* **35**, 494–506.
- JOHNSON R. W., SUN S.-S. & WELLMAN P. 1989. Problems, uncertainties and issues. In: Johnson R. W. ed. *Intraplate volcanism in Eastern Australia and New Zealand*, pp. 347–354. Cambridge University Press, Cambridge.
- JONES R. M., BOULT P. J., HILLIS R. R., MILDREN S. D. & KALDI J. 2000. Integrated hydrocarbon seal evaluation in the Penola Trough, Otway Basin. *Australian Petroleum Exploration Association Journal* **40**, 194–211.
- JORDAN S. C., CAS R. A. F. & HAYMAN P. C. 2013. The origin of a large (>3 km) maar volcano by coalescence of multiple shallow craters: Lake Purrumbete maar, southeastern Australia. *Journal of Volcanology and Geothermal Research* **254**, 5–22.
- JOYCE E. B. 1975. Quaternary volcanism and tectonics in southeastern Australia. In: Suggate R. P. & Cresswell M. M. eds. *Quaternary studies*, pp. 169–178. The Royal Society of New Zealand, Wellington.
- JOYCE E. B. 1988a. Newer volcanic landforms. In: Douglas J. G. & Ferguson J. A. eds. *Geology of Victoria*, pp. 419–426. Geological Society of Australia, Victorian Division.
- JOYCE E. B. 1988b. Cainozoic volcanism in Victoria. In: Clark I. & Cook B. eds. *Victorian geology excursion guide*, pp. 71–80. Australian Academy of Science, Canberra.
- JOYCE E. B. 2003. The young volcanic province of southeastern Australia: physical volcanology and eruption risk. In: Graham I. ed. *Geological Society of Australia Abstracts 71, Insights into volcanic processes, mantle sampling and gems*, pp. 20–26. SGGMP, Central Victoria, 30 September–4 October 2003.
- JOYCE E. B. 2004. The young volcanic regions of southeastern Australia: early studies, physical volcanology and eruption risk. *Proceedings of the Royal Society of Victoria* **116**, 1–13.
- JOYCE E. B. 2005. How can eruption risk be assessed in young monogenetic areal basalt fields? An example from southeastern Australia. *Zeitschrift für Geomorphologie NF, Supplementary Volume* **140**, 195–207.
- JOYCE E. B. 2007. Volcanoes of the Creswick Deep Leads region in the western uplands of Victoria. In: Holdgate G. R. ed. *Creswick deep leads goldfields tour 'Buried rivers of gold'*, pp. 17–29. Saturday 1 December, 2007; Earth Sciences History Group, Geological Society of Australia, Melbourne.
- JOYCE E. B. 2009. The origin and development of the western uplands of Victoria: a different story to the rest of the Australian Highlands. In: Norvick M. S. & Gallagher S. J. eds. *Origin of the Australian Highlands, Selwyn Symposium of the GSA Victoria Division, September 2009, Geological Society of Australia Extended Abstracts* **94**, 63–79.
- JOYCE E. B. & DAY R. A. 1989. Victoria and South Australia. In: Johnson R. W. ed. *Intraplate volcanism in Eastern Australia and New Zealand*, pp. 132–133. Cambridge University Press, Cambridge.
- KENNETT B. L. N. & ABDULLAH A. 2011. Seismic wave attenuation beneath the Australasian region, Australia. *Australian Journal of Earth Sciences* **58**, 285–295.
- KING S. D. & ANDERSON D. L. 1998. Edge-driven convection. *Earth and Planetary Science Letters* **160**, 289–296.
- KNUTSON J. & NICHOLLS I. A. 1989. Macedon–Trentham. In: Johnson R. W. ed. *Intraplate volcanism in Eastern Australia and New Zealand*, pp. 136–137. Cambridge University Press, Cambridge.
- KORSCH R. J., BARTON T. J., GRAY D. R., OWEN A. J. & FOSTER D. A. 2002. Geological interpretation of a deep seismic reflection transect across the boundary between the Delamerian and Lachlan Orogens, in the vicinity of the Grampians, western Victoria. *Australian Journal of Earth Sciences* **49**, 1057–1075.
- LESTI C., GIORDANO G., SALVINI F. & CAS R. 2008. Volcano tectonic setting of the intraplate, Pliocene–Holocene, Newer Volcanic Province (southeast Australia): Role of crustal fracture zones. *Journal of Geophysical Research* **113**, B07407.
- LISTER G. S. & ETHERIDGE M. A. 1989. Detachment modes for uplift and volcanism in the eastern highlands, and their application to the origin of passive margin mountains. In: Johnson R. W. ed. *Intraplate volcanism in Eastern Australia and New Zealand*, pp. 297–313. Cambridge University Press, Cambridge.
- MATCHAN E. & PHILLIPS D. 2011. New $^{40}\text{Ar}/^{39}\text{Ar}$ ages for selected young (<1 Ma) basalt flows of the Newer Volcanic Province, southeastern Australia. *Quaternary Geochronology* **6** (3–4), 356–368.
- MATSUMOTO T., HONDA M., McDUGALL I., YATSEVICH I. & O'REILLY S. Y. 1997. Plume-like neon in a metasomatic apatite from the Australian lithospheric mantle. *Nature* **388**, 162–164.
- MCBRIDE J. S., LAMBERT D. D., NICHOLLS I. A. & PRICE R. C. 2001. Osmium isotopic evidence for crust–mantle interaction in the genesis of continental intraplate basalts from the Newer Volcanics Province, southeastern Australia. *Journal of Petrology* **42**, 1197–1218.
- MCDONOUGH W. F., MCCULLOCH M. T. & SUN S.-S. 1985. Isotopic and geochemical systematics in Tertiary–Recent basalts from

- southeastern Australia and implications for the evolution of the sub-continental lithosphere. *Geochimica et Cosmochimica Acta* **49**, 2051–2067.
- MCDUGALL I., ALLSOP H. L. & CHAMALAUN F. H. 1966. Isotopic dating of the Newer Volcanics of Victoria, Australia and geomagnetic polarity epochs. *Journal of Geophysical Research* **71**, 6107–6118.
- MORAND V. J., WOHLT K. E., CAYLEY R. A., TAYLOR D. H., KEMP A. I. S., SIMONS B. A. & MAGART A. P. M. 2003. Glenelg special map area Geological Report. *Geological Survey of Victoria Report* **123**.
- NICHOLLS I. A. & JOYCE E. B. 1989. East Australian volcanic geology—Victoria and South Australia—Newer Volcanics. In: Johnson R. W. ed. *Intraplate volcanism in Eastern Australia and New Zealand*, pp. 137–142. Cambridge University Press, Cambridge.
- O'REILLY Y. O. & ZHANG M. 1995. Geochemical characteristics of lava-field basalts from eastern Australia and inferred sources: connections with the subcontinental lithospheric mantle? *Contributions to Mineralogy and Petrology* **121**, 148–170.
- OLLIER C. D. 1967. Landforms of the Newer Volcanic Province of Victoria. In: Jennings J. N. & Mabbutt J. A. eds. *Landform studies from Australia and New Guinea*, pp. 315–339. Australian National University Press, Canberra.
- OLLIER C. D. 1969. *Volcanoes (an introduction to systematic geomorphology)*, pp. 136–179. Australian National University Press, Canberra.
- OLLIER C. D. & JOYCE E. B. 1964. Volcanic physiography of the Western Plains of Victoria. *Proceedings of the Royal Society of Victoria* **77**, 357–376.
- OLLIER C. D. & JOYCE E. B. 1968. Geomorphology of the Western District volcanic plains, lakes and coastline. In: McAndrew J. & Marsden M. A. H. eds. *A Regional Guide to Victorian Geology*, pp. 55–68. University of Melbourne, Department of Geology, Melbourne.
- O'NEILL G. F. L. 1984. Geology of the Sunbury area—geochemistry of silcrete in the Sunbury area. University of Melbourne, Department of Geology, BSc Honours report.
- PIGANIS F. 2011. A volcanological investigation of the polymagmatic Red Rock Volcanic Complex and a 3D geophysical interpretation of the subsurface structure and geology of the poly-lobate Lake Purdigulac maar, Newer Volcanics Province, southeastern Australia. Monash University, MSc thesis.
- PRICE R. C., GRAY C. M. & FREY F. A. 1997. Strontium isotopic and trace element heterogeneity in the plains basalts of the Newer Volcanic Province, Victoria, Australia. *Geochimica et Cosmochimica Acta* **61**, 171–192.
- PRICE R. C., NICHOLLS I. A. & GRAY C. M. 2003. Cainozoic igneous activity. In: Douglas J. G. & Ferguson J. A. eds. *Geology of Victoria*, pp. 361–375. Geological Society of Victoria, Victorian Division, Melbourne.
- RAWLINSON N. & FISHWICK S. 2012. Seismic structure of the southeast Australian lithosphere from surface and body wave tomography. *Tectonophysics* **572–573**, 111–122.
- ROBERTSON G. B., PRESCOTT J. R. & HUTTON J. T. 1996. Thermoluminescence dating of volcanic activity at Mount Gambier, South Australia. *Transactions of the Royal Society of South Australia* **120**, 7–12.
- ROSENGREN N. 1994. *Eruption points of the Newer Volcanics Province of Victoria—an inventory and evaluation of scientific significance*. National Trust of Australia (Victoria) and the Geological Society of Australia (Victoria Division), Melbourne.
- SANDIFORD M., WALLACE M. & COBLENTZ D. 2004. Origin of the *in situ* stress field in south-eastern Australia. *Basin Research* **16**, 325–338.
- SHEARD M. J. 1978. Geological history of the Mount Gambier volcanic complex, southeast South Australia. *Transactions of the Royal Society of South Australia* **102**, 125–139.
- SHEARD M. J. 1990. A guide to Quaternary Volcanoes in the Lower South-East of South Australia. *Mines and Energy Review, South Australia* **157**, 40–50.
- SHEARD M. J. 1995. Quaternary volcanic activity and volcanic hazards. In: Drexel J. F. & Preiss W. V. eds. *The geology of South Australia. Vol. 2, The Phanerozoic*, pp. 264–268. Geological Survey of South Australia, Adelaide.
- SIMONS B. A. & MOORE D. H. 1999. Victoria 1:1 000 000 Pre-Permian Geology. *Geological Survey of Victoria*.
- SINGLETON O. P. & JOYCE E. B. 1969. Cainozoic volcanicity in Victoria. *Geological Society of Australia Special Publication* **2**, 145–154.
- SINGLETON O. P. & JOYCE E. B. 1970. Catalogue of the post-Miocene volcanoes of Victoria, Australia. Prepared for the IAVCEI Catalogue of post-Miocene Volcanoes of the World (unpublished). Incorporated with permission into: Rosengren N. 1994. *Eruption Points of the Newer Volcanics Province of Victoria*. National Trust of Australia (Victoria) & Geological Society of Australia (Victorian Division), Melbourne.
- SPRIGG R. C. 1952. The geology of the South-East Province, South Australia, with special reference to Quaternary coast-line migrations and modern beach developments. *Geological Survey of South Australia Bulletin* **29**.
- SUTALO F. 1996. The geology and regolith terrain evaluation of the Mount Rouse lava flows, Western Victoria. Honours research report, University of Melbourne.
- SUTALO F. & JOYCE B. 2004. Long basaltic lava flows of the Mt. Rouse volcano in the Newer Volcanic Province of southeastern Australia. *Proceedings of the Royal Society of Victoria* **116**, 37–47.
- SUTHERLAND F. L. 1991. Cainozoic volcanism, Eastern Australia: a predictive model on migration over multiple 'hotspot' mantle sources. In: Williams M. A. J., DeDeckker P. & Kershaw A. P. eds. *The Cainozoic in Australia: a re-appraisal of the evidence*, pp. 15–43. Geological Society of Australia Special Publication **18**.
- SUTHERLAND F. L. 2003. 'Boomerang' migratory intraplate Cenozoic volcanism, eastern Australian rift margins and the Indian-Pacific mantle boundary. *Geological Society of America Special Paper* **372**, 203–221.
- SUTHERLAND F. L., GRAHAM I. T., MEFFRE S., ZWINGMANN H. & POGSON R. E. 2012. Passive-margin prolonged volcanism, East Australian Plate: outbursts, progressions, plate controls and suggested causes. *Australian Journal of Earth Sciences* **59**, 983–1005.
- VANDENBERG A. H. M., WILLMAN C. E., MAHER S., SIMONS B. A., CAYLEY R. A., TAYLOR D. H., MORAND V. J., MOORE D. H. & RADOJKOVIC A. 2000. *The Tasman Fold Belt System in Victoria*. Geological Survey of Victoria Special Publication, Melbourne.
- VAN OTTERLOO J. 2012. Complexity in monogenetic volcanic systems: factors influencing alternating magmatic and phreatomagmatic eruption styles at the 5 ka Mt. Gambier Volcanic Complex, South Australia. Monash University PhD thesis.
- VAN OTTERLOO J. & CAS R. 2011. Mount Gambier Volcanic Complex. In: Cas R., Blakie T., Boyce J., Hayman P., Jordan S., Piganis F., Prata G. & van Otterloo J. eds. *Factors that influence varying eruption styles (from magmatic to phreatomagmatic) in intraplate continental basaltic volcanic provinces: The Newer Volcanics Province of southeastern Australia*. Field trip guide VF01, pp. 65–81. IUGG 2011 General Assembly. Earth on the Edge: Science for a Sustainable Planet.
- WALLACE D. A. 1990. Petrology and geochemistry of the Newer Volcanics of the Western Highlands of Victoria, Australia. M.Sc thesis, School of Geology, La Trobe University, 121 pp.
- WELLMAN P. 1974. Potassium–argon ages of the Cainozoic volcanic rocks of eastern Victoria, Australia. *Journal of the Geological Society of Australia* **21**, 359–376.
- WELLMAN P. 1983. Hotspot volcanism in Australia and New Zealand: Cainozoic and mid-Mesozoic. *Tectonophysics* **96**, 225–243.
- WELLMAN P. & MCDUGALL I. 1974. Cainozoic igneous activity in eastern Australia. *Tectonophysics* **23**, 49–65.
- WHITEHEAD P. W. 1986. The geology and geochemistry of the Mt. Rouse and Mt. Napier volcanic centres, western Victoria. Honours research report, La Trobe University, Melbourne.
- WHITEHEAD P. W. 1991. The geology and geochemistry of Mt. Napier and Mt. Rouse, western Victoria. In: Williams M. A. J., DeDeckker P. & Kershaw A. P. eds. *The Cainozoic in Australia: a re-appraisal of the evidence*, pp. 309–320. Geological Society of Australia Special Publication **18**.
- WOPFNER H. & THORNTON R. C. N. 1971. The occurrence of carbon dioxide in the Gambier Embayment. In: Wopfner H. & Douglas J. G. eds. *The Otway Basin of Southeastern Australia*, pp. 377–384. Geological Surveys of South Australia and Victoria Special Bulletin.

Received 24 August 2012; accepted 11 May 2013



Chapter 3 is a paper which was published in The Australian Journal of Earth Sciences in June 2014.

This study was initiated in order to place Mt Rouse, the largest volcano in the Newer Volcanics Province (NVP) into a local context in terms of the volcano distribution and geochemistry of eruption products. Following on from the material presented in Chapter 2, this chapter focuses on the Hamilton area of the NVP surrounding Mt Rouse, and forms a companion paper to Chapter 2. The study correlates geospatial data on the locations of volcanoes with ground truthing and desktop based analyses such as ArcGIS Total Magnetic Intensity, seamless geology data, NASA ASTER digital elevation models.

Three new volcanoes were proposed in the Hamilton area, and several previously defined volcanoes were brought into question based on field and desk-based observations.

Radiometrics and published geochronological data were correlated and used to confirm three phases of volcanic eruption, with information on the state of weathering of outcrops being used to further subdivide the phases into older and younger groupings. These were also found to correlate with geochemical analysis of samples from each volcano, with the dominantly basaltic products becoming increasingly alkaline and enriched in incompatible elements with time.

Geochemical analyses of the products of volcanism in the Hamilton area can be found in Appendix 3.

Declaration for Thesis Chapter 3

Declaration by candidate

In the case of Chapter 3, the nature and extent of my contribution to the work was the following:

| Nature of contribution | Extent of contribution (%) |
|---|----------------------------|
| Fieldwork, data collection, sample preparation, interpretation of major and trace element data, preparation of the manuscript | 80% |

The following co-authors contributed to this work:

| Name | Nature of contribution | Extent of contribution (%) |
|-------------------|---|----------------------------|
| Prof. Reid Keays | Supervisory role. Advice on data interpretation of major and trace element data. Preparation of the manuscript. | 8% |
| Dr Ian Nicholls | Supervisory role. Advice on data interpretation of major and trace element data. Preparation of the manuscript. | 7% |
| Dr Patrick Hayman | Supervisory role | 5% |

The undersigned hereby certify that the above declaration correctly reflects the nature and extent of the candidate's and co-authors' contributions to this work*.

Julie Boyce

Date

Prof. Reid Keays (main supervisor)

Date

Dr Ian Nicholls

Date

Dr Patrick Hayman

Date



Eruption centres of the Hamilton area of the Newer Volcanics Province, Victoria, Australia: pinpointing volcanoes from a multifaceted approach to landform mapping

J. A. BOYCE*, R. R. KEAYS, I. A. NICHOLLS AND P. HAYMAN

School of Geosciences, Building 28, Monash University, Clayton, VIC 3800, Australia.

Volcanic eruption centres of the mostly 4.5 Ma–5000 BP Newer Volcanics Province in the Hamilton area of southeastern Australia were examined in detail using a multifaceted approach, including ground truthing and analysis of ArcGIS Total Magnetic Intensity and seamless geology data, NASA Advanced Spaceborne Thermal Emission and Reflection Radiometer (ASTER) digital elevation models and Google Earth satellite image interpretation. Sixteen eruption centres were recognised in the Hamilton area, including three previously unrecorded volcanoes—one of which, the Cas Maar, constitutes the northernmost maar–cone volcanic complex in the Western Plains subprovince. Seven previously allocated eruption centres were placed into question based on field and laboratory observations. Three phases of volcanic activity have been suggested by other authors and are interpreted to correlate with ages of >4 Ma, ca 2 Ma and <0.5 Ma, which may be further subdivided based on preservation of outcrop. Geochemical compositions of the dominantly basaltic products become increasingly alkaline and enriched in incompatible elements from Phases 1 to 2, with Phase 3 eruptions both covering the entire geochemical range and extending into increasingly enriched compositions. This research highlights the importance of a multifaceted approach to landform mapping and demonstrates that additional volcanic centres may yet be discovered in the Newer Volcanics Province.

KEY WORDS: Newer Volcanics Province, relative ages, geochemistry, monogenetic volcanism, radiometrics, intraplate basaltic volcanism, Google Earth.

INTRODUCTION

The Newer Volcanics Province (NVP) of southeastern Australia constitutes the most recent phase of volcanic activity in Australia, with eruptions spanning from largely 4.5 Ma to ca 5000 BP (Blackburn 1966; McDougall *et al.* 1966; Blackburn *et al.* 1982; Price *et al.* 2003; Gray & McDougall 2009; Gouramanis *et al.* 2010), and is currently considered active.

Mapping of volcanic centres in the NVP has mainly focused on the analysis of topographic, geomorphic and geometrical data, with little physical ground truthing of the smaller eruption centres, owing to a lack of resources. Boyce (2013) amalgamated eruption point data for the NVP into a single repository to create a new volcanic distribution map of the NVP, containing >704 eruption points (vents) from >416 volcanic centres. A significant number of previously identified eruption points (81) were removed from the database in order to arrive at these figures, owing to the possible misplacement of points in erosional features, obvious non-NVP outcrop

or flat terrain with no hills on digital elevation models, and no significant responses on Total Magnetism Intensity (TMI) imagery or red green blue (RGB) radiometrics ternary images.

The research outlined herein is complementary to the distribution maps of Boyce (2013), and explains the positioning of eruption centres in the Hamilton area of the Western Plains subprovince.

We performed a detailed desktop study of the eruption centres of the Hamilton (7322) 1:100 000 map sheet area, carried out during a study of the Mt Rouse magmatic volcanic complex in order to place the volcano in a local context with respect to other eruption centres. Subsequent ground truthing involved fieldwork during site visits that enabled the identification of three new eruption centres and placed into question some that were previously proposed. Desktop studies before and after ground truthing involved the interpretation of satellite imagery, magnetism and radiometrics data and digital elevation models, and reconnaissance geochemical analysis to define phases of volcanic activity in the Hamilton area.

*Corresponding author: [REDACTED]

GEOLOGICAL SETTING OF THE NVP

Volcanic activity in Victoria has been almost continuous during the Cenozoic, with three peaks in volcanism (Price *et al.* 2003). The NVP (the focus of this study) is considered the youngest of these volcanic groups, which also includes the Older Volcanics in eastern Victoria and the Otway Ranges to the west (95–19 Ma; Day 1983) as well as the Macedon–Trentham group northwest of Melbourne (7.0–4.6 Ma; Wellman 1974; Dasch & Millar 1977; Ewart *et al.* 1985; Sutherland *et al.* 2014). The latter resembles the central volcanoes of New South Wales and Queensland (Knutson & Nicholls 1989).

Although the age range of the NVP is given as a time-span of the last *ca* 4.5 Ma, the ages of NVP products are generally not well constrained, with many eruption centres and older buried lava flows undated. This is due to sampling bias towards younger products that are fresher and easier to sample (Cayley *et al.* 1995; Edwards *et al.* 2004). It is highly probable that products of NVP composition began to erupt at *ca* 8 Ma or earlier. The NVP basalts in Beaufort, northern Victoria were dated to 6.07 ± 0.11 Ma and 4.65 ± 0.07 Ma (Cayley *et al.* 1995); approximately 70 m of older NVP flows underlie these basalts. In addition, Lady Julia Percy Island is considered part of the NVP—this polycyclic volcano erupted in two phases, at 7.80 ± 0.08 Ma and 6.22 ± 0.06 Ma (Edwards *et al.* 2004). The centre was removed from the volcanic distribution map of Boyce (2013), owing to its older age, and should be re-entered.

The NVP is a continental intraplate basaltic volcanic field, containing the products of >416 late Neogene–Recent eruption centres stretching 410 km from Melbourne, Victoria to the Mt Burr range, southeast South Australia (Figure 1; Ollier & Joyce 1964, 1968; Ollier 1967; Joyce 1975; Nicholls & Joyce 1989; Lesti *et al.* 2008; Boyce 2013). Covering an area of >19 000 km² (Boyce 2013), the NVP has an estimated volume of 1300 km³ (Wellman 1971). The NVP is composed of the products of short-lived apparently monogenetic basaltic volcanoes (Ollier & Joyce 1964; Joyce 1975), which are defined as either simple or complex. One eruption centre (e.g. Mt Rouse) may have more than one eruption point (vent). The simple eruption centres are scoria cones, lava shields, maars, ash cones/domes and some centres of unknown character, which are morphologically simple with few eruption points. The complex volcanoes are more diverse in nature, with intricate morphologies and multiple eruption points forming dominantly magmatic, maar or maar–cone volcanic complexes (Boyce 2013). The products of phreatomagmatic eruptions (e.g. tuff cones) arise owing to magma–water interaction, which is not the case for magmatic products such as lava shields, scoria cones and/or spatter cones.

The NVP is subdivided into three subprovinces on the basis of geomorphology, viz: the Central Highlands (a.k.a. Central Uplands), Western Plains and Mt Gambier subprovinces (Joyce 1975; Nicholls & Joyce 1989; Price *et al.* 2003) (Figure 1). The Western Plains subprovince (the focus of this study) extends 320 km from Melbourne

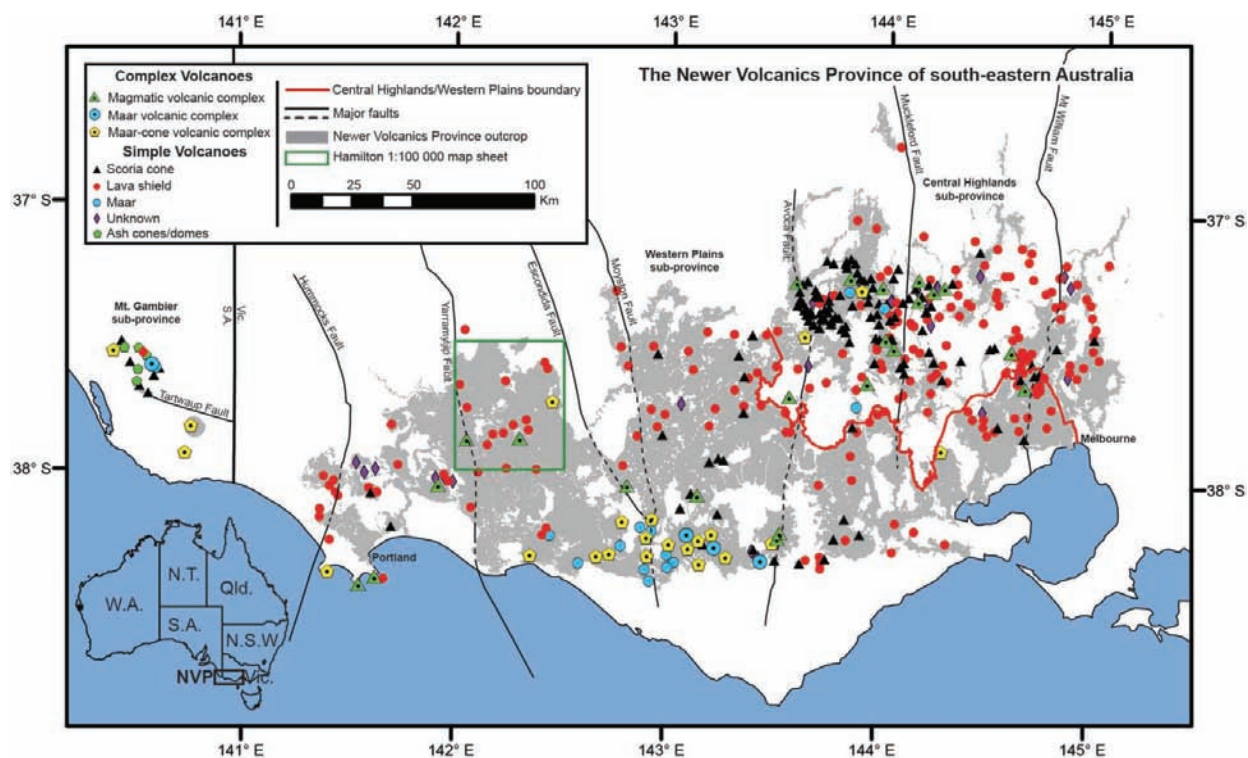


Figure 1 Western Newer Volcanics Province of southeastern Australia, showing major faults (inferred by dashed lines through basalts), Newer Volcanics outcrop and distribution of eruption centres, with the Hamilton area outlined by green square. Modified after Boyce (2013).

to Portland and covers an area of $>14\,600\text{ km}^2$. The Western Plains basalts are characterised by extensive plains-forming lava fields filling the subdued topography of the Otway Basin, and the subprovince contains 42% of NVP volcanic centres (Boyce 2013). A concentration of phreatomagmatic eruption centres is found in the Colac–Warrnambool area, attributed to magma–water interaction with the Cenozoic sedimentary aquifers of the Otway Basin (Joyce 1975). The Paleozoic Moyston Fault splits the Western Plains into eastern and western sectors, as it is the boundary between the Delamerian and Lachlan Fold belts, which have different ages and geological histories (Figure 1; Korsch *et al.* 2002; Cayley *et al.* 2011). The Moyston Fault corresponds to the Mortlake Discontinuity of the NVP (Price *et al.* 1997). East of the discontinuity, volcanic products consist of maars, tuff rings and large scoria cones, with abundant mantle xenoliths and megacrysts, and higher reported Sr-isotopic values of 0.7035–0.7058. Volcanic products to the west of the Mortlake Discontinuity contain few mantle xenoliths or megacrysts, and have a narrower range of Sr-isotope values of 0.7035–0.7047, which are believed to indicate distinct mantle sources within the eastern and western lithospheric mantle segments (Cooper & Green 1969; Dasch & Green 1975; Stuckless & Irving 1976; McDonough *et al.* 1985; Whitehead 1986; Ewart *et al.* 1988; Price *et al.* 1997, 2003; McBride *et al.* 2001; Foden *et al.* 2002; Demidjuk *et al.* 2007).

The Hamilton area (the focus of this study) lies to the west of the Mortlake Discontinuity. This area contains approximately seven eruption centres according to the volcanic distribution maps of Joyce (1975); however, six appear in Rosengren (1994), and 16 on the Victoria Seamless Geology DVD (October 2011). These consist of mainly lava shields, but also two large volcanic complexes (Mt Rouse and Mt Napier). There is therefore a need for amalgamation of eruption centre data.

METHODS

A detailed desktop study of the Hamilton (7322) 1:100 000 map sheet area was performed utilising previously identified eruption points, ArcGIS TMI, RGB ternary radiometrics diagrams and seamless geology data, NASA ASTER digital elevation models and Google Earth satellite image interpretation.

Eruption points from Rosengren (1994) (based on an unpublished manuscript by Singleton & Joyce 1969) were correlated with and plotted alongside those contained within the Victoria Seamless Geology DVD (D. Higgins, pers. comm. 2011) onto ArcGIS and Google Earth. The Hamilton map sheet area was examined on Google Earth, with the options to zoom, pan, tilt and vertically exaggerate the data, for both recorded and unrecorded eruption centres. Data were then viewed in ArcGIS, utilising seamless geology, TMI images, RGB radiometrics ternary images and NASA ASTER digital elevation models, where eruption centres were correlated with magnetic anomalies (high values appear grey and red, whereas low values appear blue and purple) or areas of mapped scorias/tuffs where possible.

NASA ASTER digital elevation models were used in this study, obtained through the online Data Pool at the NASA Land Processes Distributed Active Archive Center (LP DAAC), USGS/Earth Resources Observation and Science (EROS) Center, Sioux Falls, South Dakota (https://lpdaac.usgs.gov/get_data). ASTER is an imaging instrument on the Earth Observing System (EOS) satellite and is used to create detailed elevation maps of the Earth's surface. Volcanoes generally form elevated topography, owing to the formation of scoria cones, and the gradual buildup of lava shields. However, many lava shields, maars, tuff cones and older weathered centres are low in nature, so digital elevation models were used alongside magnetics data and satellite imagery, with ground truthing to identify eruption centres.

Ground truthing was undertaken in early March 2012 by visiting the proposed eruption centres to confirm their validity based on field evidence—for example the preservation of craters, spatter ramparts and shield or cone edifices. Samples were collected from each proven eruption centre where practical and sent for geochemical analysis.

Absolute age estimates from literature values were plotted alongside RGB ternary radiometric imagery (Victoria Geoscientific Databases DVD July 2010) in order to assess relative ages. Radiometrics works on the principle that all rocks and soils contain naturally occurring isotopes of ^{40}K , ^{232}Th and ^{238}U that emit characteristic gamma rays from the top 0.3–0.4 m of soil. These gamma rays are measured by instruments onboard light aircraft, and subsequently combined and presented as ternary ratio element maps, whereby the elements are represented as different colours (K red, Th green and U blue), which become brighter with concentration. Intense weathering causes K and U depletion, and so fresh basalts will offer a higher response than older weathered basalts where soil formation has been prevalent, and thus appear Th-enriched (green). These techniques were used to confirm three phases of eruption (Bennetts *et al.* 2003), and field observations such as weathering of outcrops were used to further subdivide the phases into older and younger groupings.

OBSERVATIONS AND RESULTS

Eruption centres

Twenty eruption centres were previously suggested in the Hamilton area (Figure 2a; Table 1; Joyce 1975; Rosengren 1994; Victoria Seamless Geology DVD October 2011). The desktop survey showed a need for ground truthing of the centres, as some were uncertain identifications. Ground truthing then showed that 13 eruption centres were valid, and seven were questionable. Three undescribed eruption centres were identified in the area, giving 16 confirmations (Figure 2b).

CONFIRMED ERUPTION CENTRES

The Hamilton area revealed two significant magmatic volcanic complexes, one maar–cone volcanic complex and 11 simple and two composite lava shields (Table 1 [1–16], Figure 2b).

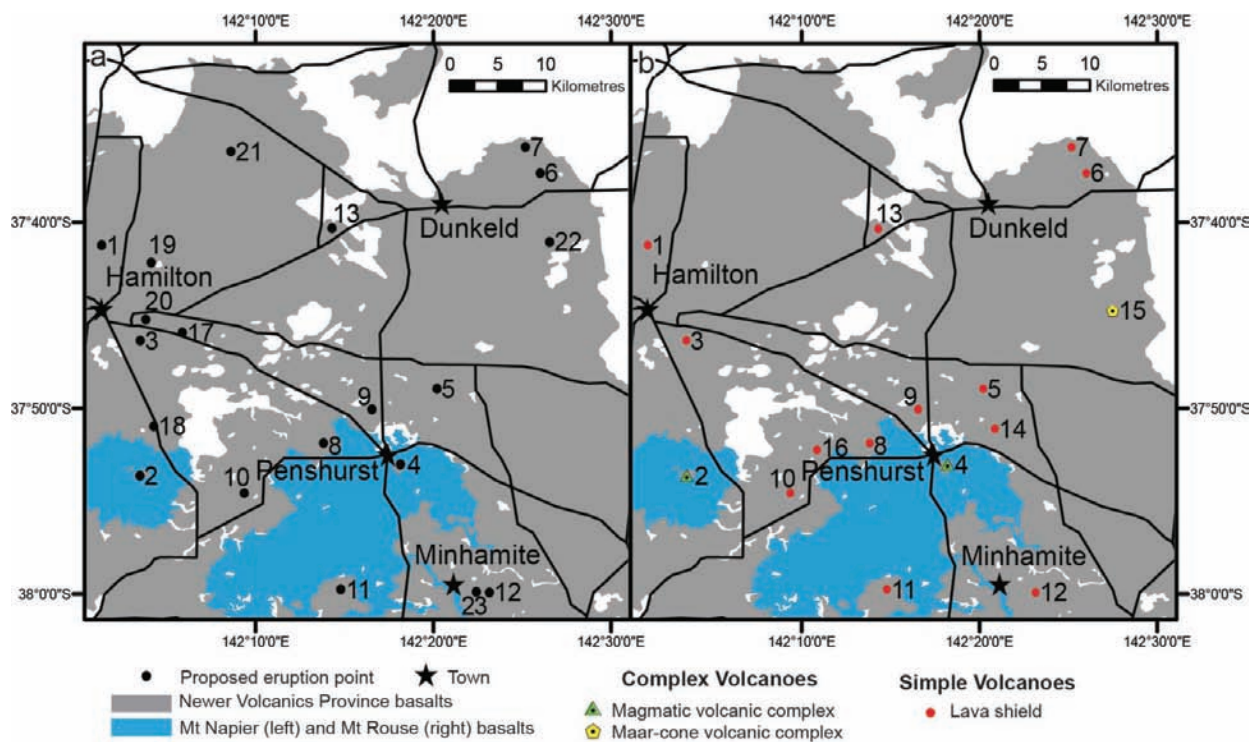


Figure 2 Basic maps of the Hamilton area, showing basalt cover, roads and eruption points. (a) Proposed eruption centres of the Hamilton area. (b) Confirmed eruption centres of the Hamilton area after desktop survey and ground truthing. Volcano numbering [1] Mt Baimbridge, [2] Mt Napier, [3] Mt Pierrepont, [4] Mt Rouse, [5] Blackwood Hill, [6] Sheepwash Hill, [7] Bunnugal Hill, [8] Acacia Hill, [9] Picaninny Hill, [10] Gazette Hill, [11] Fox Hill, [12] Green Hills, [13] Moutajup Hill, [14] Jays Hill, [15] Cas Maar and [16] Burgers Hill. Questioned eruption locations [17] GV 277, [18] GV 280 Buckley Swamp, [19] GV 285, [20] GV 286, [21] GV 479, [22] GV 481 and [23] GV 483.

Mt Rouse and Mt Napier (Figures 2b, 3a,b) are magmatic volcanic complexes. Mt Rouse rises 120 m above the surrounding lava plains, and includes at least eight eruption points in the form of a northern double scoria cone, an early eruption centre, and a low southern cone featuring two satellite cones (Boyce *et al.* 2013). Mt Rouse is the largest eruption source in the NVP, with flows triple the size of other volcanoes in area covered and volume erupted; the flows extend >60 km to the coast at Port Fairy (Sutalo 1996) and cover >511 km² (Boyce *et al.* 2012). Mt Rouse is the product of three magma batches sourced from increasing mantle depths (Boyce *et al.* 2013). Lava flows, including the interbedded lava shield, represent a single magma batch (Elias 1973; Whitehead 1986, 1991; Sutalo 1996; Sutalo & Joyce 2004; Boyce *et al.* 2013), while the scorias formed from two further magma batches (Boyce *et al.* 2013). Mt Napier, whose summit forms the highest point in the Western Plains, contains 23 eruption points of scoria, lava and spatter cones, with lava flows extending for 15 km westward down the Harman Valley (Gill & Elmore 1974; Whitehead 1991).

The 11 simple lava shields in the Hamilton area are Mounts Baimbridge and Pierrepont, and Blackwood, Bunnugal, Acacia, Picaninny, Gazette, Fox, Moutajup, Burgers and Jays Hills (Table 1; Figure 2b). Sheepwash Hill and Green Hills (Figures 2b, 3c, d) are lava shields, which feature minor scoria deposits, making them composite in nature.

Sheepwash Hill, 8.3 km ENE of Dunkeld, is 19 m higher than the surrounding lava plains, approximately 0.5 km wide E–W but at least 0.8 km N–S, with a lava escarpment on the western flank and lava flows to the north and south. Thought to be a low lava cone (Cayley & Taylor 1997), a recent quarry in the southeastern flank now shows that scoria was initially produced. Green Hills lies 14 km southeast of Mt Rouse. The size for this eruption centres is uncertain, as a broad, low lava shield over 1 km in diameter and 30 m overlaps the surrounding lava plains. The basalts are weathered, and largely obscured by soils. However, the highest point in the area (at a trigonometrical station) is probably the point of eruption, with weathered lava boulders, eroded spatter clasts and columnar jointing, along with lobes of lava along the surrounding slopes from a late-stage flow.

Mt Baimbridge (Figure 3e), a deeply weathered lava shield (Ollier 1967; Rosengren 1994) north of Hamilton, has two identifiable lava flows (Bennetts *et al.* 2003). These originate from the ill-defined breached crater (Ollier & Joyce 1964), which is about 300 m wide. The broad hill (at least 1 km across) includes gently sloping lava flows of more than 1.5 km to the south and east.

Mt Pierrepont (Figure 4a), another broad and low weathered lava shield, southeast of Hamilton, has ill-defined lava flows (Ollier & Joyce 1964; Ollier 1967). Ollier & Joyce (1964) suggest that the crater is breached and hard to define; however there is a clear basalt rim along the western half, while the crater itself is breached

Table 1 Validated and questioned eruption centres of the Hamilton region, showing the numbering system used throughout the research, names, coordinates and descriptions.

| Validated eruption centres (1–16) | No. | Name | Local name | Latitude | Longitude | Description |
|-------------------------------------|-----|------------------------|----------------|----------|-----------|--|
| | 1 | Mt Baimbridge | Mt Baimbridge | –37.6870 | 142.0222 | Lava shield |
| | 2 | Mt Napier, GV 268, 269 | Mt Napier | –37.8938 | 142.0582 | Magmatic volcanic complex |
| | 3 | Mt Pierrepont, GV 270 | Mt Pierrepont | –37.7727 | 142.0584 | Lava shield |
| | 4 | Mt Rouse | Mt Rouse | –37.8837 | 142.3025 | Magmatic volcanic complex |
| | 5 | Unnamed HN1 | Blackwood Hill | –37.8159 | 142.3368 | Lava shield |
| | 6 | GV 131 | Sheepwash Hill | –37.6224 | 142.4336 | Lava shield |
| | 7 | GV 132 | Bunnugal Hill | –37.5993 | 142.4198 | Lava shield |
| | 8 | GV 278 | Acacia Hill | –37.8646 | 142.2304 | Lava shield |
| | 9 | GV 279 | Picaninny Hill | –37.8346 | 142.2759 | Lava shield |
| | 10 | GV 281 | Gazette Hill | –37.9094 | 142.1559 | Lava shield |
| | 11 | GV 283 | Fox Hill | –37.9959 | 142.2466 | Lava shield |
| | 12 | GV 482 | Green Hills | –37.9986 | 142.3860 | Lava shield |
| | 13 | GV 480 | Moutajup Hill | –37.6721 | 142.2382 | Lava shield |
| | 14 | Jays Hill | | –37.8517 | 142.3479 | Lava shield |
| | 15 | Cas Maar, Bald Hill | Bald Hill | –37.7457 | 142.4583 | Maar-cone volcanic complex |
| Questioned eruption centres (17–23) | 16 | Burgers Hill | | –37.8710 | 142.1810 | Lava shield |
| | 17 | GV 277 | | –37.7657 | 142.0979 | Part of Mt Pierrepont lava flows |
| | 18 | GV 280 | Buckley Swamp | –37.8495 | 142.0711 | Buckley Swamp; part of lava plains |
| | 19 | GV 285 | | –37.7028 | 142.0687 | Part of Mt Baimbridge lavas; west of basalt ponded lake |
| | 20 | GV 286 | | –37.7538 | 142.0637 | Dissected by river to east, creating topography. Part of Mt Pierrepont lava flow |
| | 21 | GV 479 | | –37.6030 | 142.1435 | Part of lava plains |
| | 22 | GV 481 | Lake Repose | –37.6841 | 142.4425 | Ponded lakes in valley flows |
| | 23 | GV 483 | | –37.9982 | 142.3737 | Part of Green Hills lava flow |

to the northeast. Lavas extend radially for at least 1 km, but the flow outline is indistinguishable. Bennetts *et al.* (2003) suggest at least two individual flows.

Blackwood Hill (Figure 4b) is a small lava shield 7.6 km northeast of Penshurst. The eruption centre features a base 0.75 km across, a shallow crater breached to the west and is 40 m high. Lava flows are hard to define, but extend at least 2 km to the west and 1 km to the north.

Bunnugal Hill (Figure 4c) lies 2.7 km northeast of Sheepwash Hill, 8.7 km NE of Dunkeld (Cayley & Taylor 1997). The hill is 30 m higher than the surrounding plains, measuring approximately 1.4 km E–W and 0.9 km N–S from the buildup of lava flows. It features lava blocks on all sides and a spattery lava escarpment to the north. The surrounding low hummocky lava flows probably originated from this volcanic edifice.

Picaninny Hill (Figure 4d) is a small lava shield 4.7 km NNW of Penshurst. The 20 m high hill, about

0.5 km in diameter, features prominent lava escarpments at its edges. The lava flows are obscured in the hummocky terrain, but flowed at least 1.3 km south (there is an obvious ridge in satellite imagery), and also a short distance to the west, north and east.

Moutajup Hill is 9.5 km WSW of Dunkeld (Figure 2). An eruption point was not evident on the ground, but a 3 km wide hill (Figure 3a) over this broad region shows probable lava flows extending 6 km to the west and south. These resemble RGB radiometric signatures of lava flows from Mounts Baimbridge and Pierrepont, which yield high Th responses (green), and low K and U. This lava shield was interpreted using digital elevation models by A. H. M. VandenBerg (A.H.M. VandenBerg pers. comm. 2012). Bennetts *et al.* (2003) assigned this eruption centre to Phase 1 eruptions.

Gazette, Burgers and Acacia Hills form three hills between Mt Rouse and Mt Napier. They are deeply eroded remnants of broad, low lava shields, which also



Figure 3 Magmatic volcanic complexes of (a) Mt Rouse, looking SE from Acacia Hill (6.5 km) and (b) Mt Napier, looking W from the summit of Mt Rouse (20 km). Lava shields of (c) Sheepwash Hill (0.5 km from summit, looking W), (d) Green Hills (0.6 km from summit, looking W) and (e) Mt Baimbridge (1.2 km from summit, looking NE).

show high Th responses (green) similar to earlier eruptions in the area (e.g. Moutajup Hill). Lava flows of Mt Rouse about the eastern and southern edges of all three centres, partly obscuring the underlying lava flows. Acacia Hill is 5.5 km WNW of Penshurst. It is a broad, gently sloping but prominent hill, 30 m high, measuring roughly 1.3 km N–S, and 3 km E–W according to digital elevation models. No crater is evident within its weathered lava escarpments. Burgers Hill lies 4.5 km WSW of Acacia Hill. Mt Rouse lava flows fill the low topography

between the two eruption centres. No eruption points were visible because of land clearing. The eruption centre, 2 km across, suggests a broad shallow crater. Lavas appear to have flowed towards the northwest, as suggested by radiometrics and digital elevation models. Gazette Hill, the largest of the three centres, is >3 km across but with a low gradient. Suitable images of the three eruption centres were hindered by their low profiles and the abundance of trees, and lack of outcrop hindered sampling of Burgers Hill and Gazette Hill.

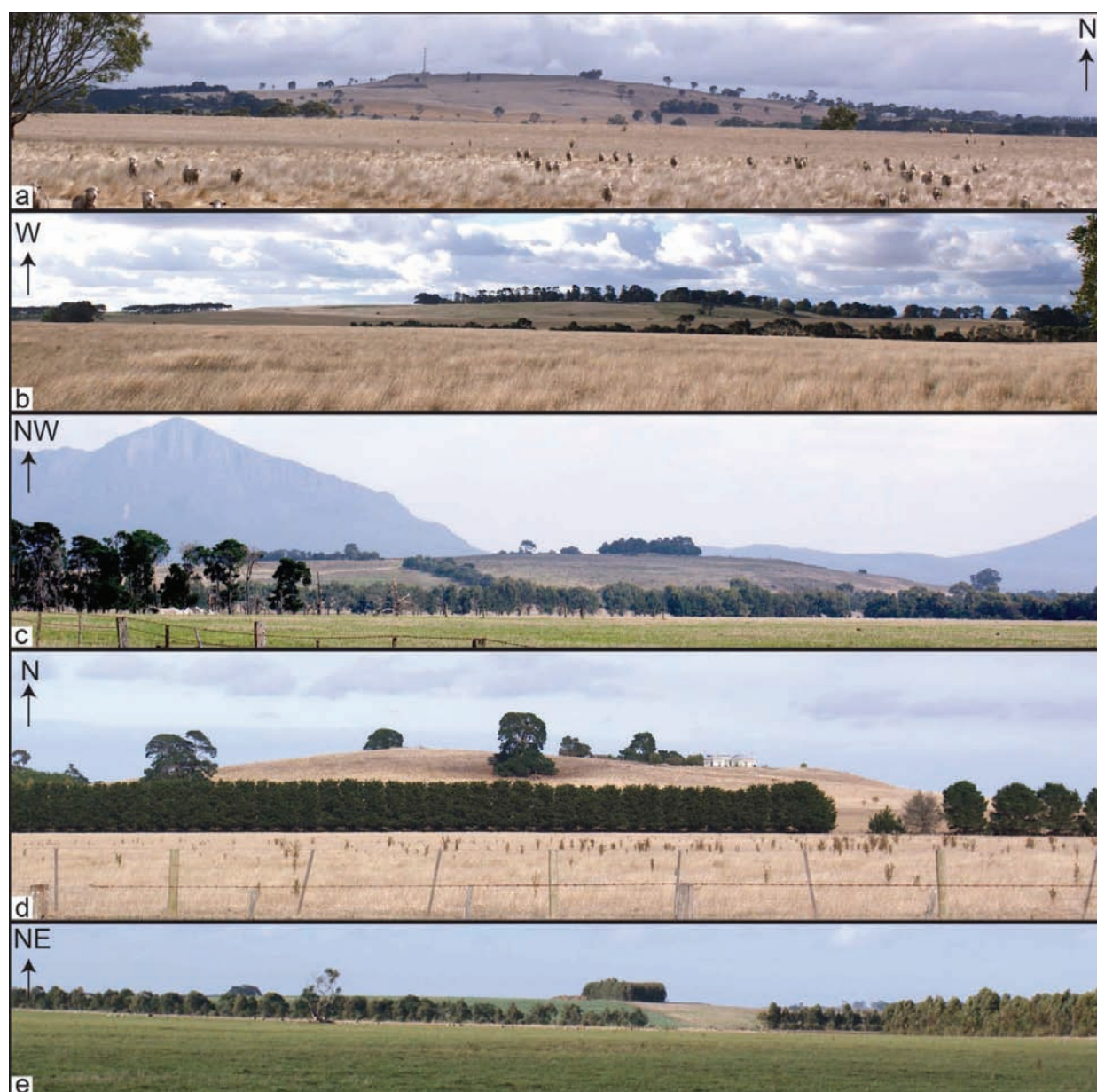


Figure 4 Lava shields of (a) Mt Pierrepoint (3.8 km from summit, looking N), (b) Blackwood Hill (3.4 km from summit, looking W), (c) Bunnugal Hill (1 km from summit, looking NW), (d) Picaninny Hill (1 km from summit, looking N), and (e) Jays Hill (0.8 km from summit, looking NE).

Fox Hill lies 13 km SE of Mt Rouse, whose flows completely surround this eruption centre (Figure 2). The exposed portion of Fox Hill is >4 km in diameter, associated with a hill, has a similar radiometrics response to Mt Pierrepoint (high Th, low K and U; green). This old eroded centre has been cleared for grazing and therefore lacks a definitive eruption point.

Jays Hill (Figure 4e), 5.7 km NE of Penshurst, was first defined as an eruption centre from satellite imagery on Google Earth, and is a very low hill with radiating lava flows (Figure 5a, b). Magnetism imagery shows a high (red) (Figure 5c) over the edifice, which is 0.5 km in diameter and only 9 m in height. Loose basalt blocks are scattered over the flanks, although most of the hill has been cleared, with large blocks up to 3 m in diameter

piled at the top. Lava flowed south for at least 1 km, but the flow is partly obscured by younger flows of Mt Rouse and is therefore older. A single K–Ar date of 1.95 ± 0.02 Ma (Gray & McDougall 2009) was obtained for outcrop beside the Hamilton Highway 1.8 km SE of the eruption point, which lies beyond the lava flows of Mt Rouse, and probably relates to material from Jays Hill.

A large maar–cone volcanic complex was discovered from satellite imagery south of the Glenelg Highway, 37 km east of Hamilton. The maar (unofficially named Cas Maar, after Ray Cas) features an asymmetrical crater up to 0.9 km wide with a rim 30 m above the surrounding plains and a probable scoria cone to the south (Bald Hill) (Figure 6a, b). An alternating sequence of scoriaceous tuffs and spattery lava flows dip away from the

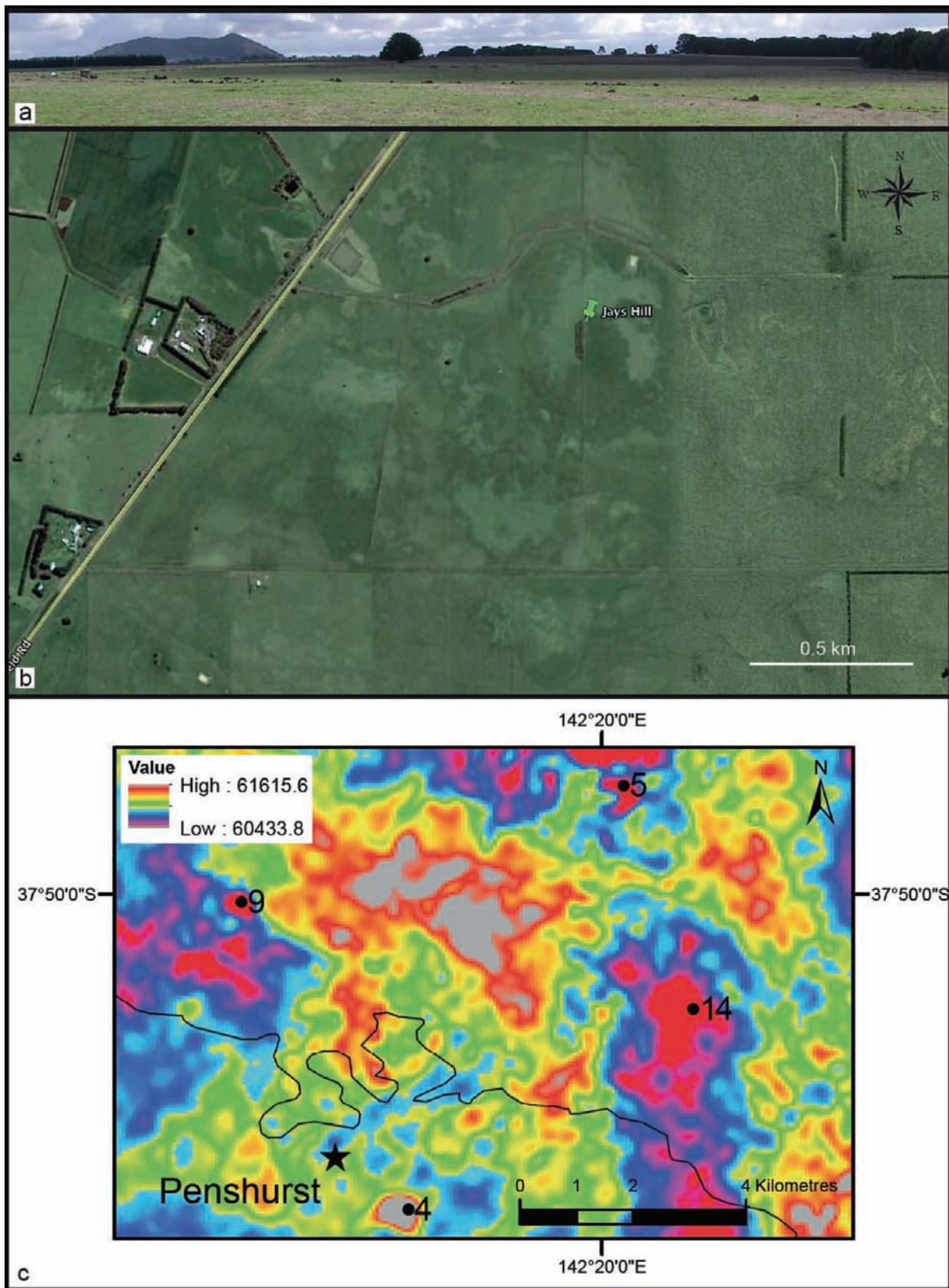


Figure 5 (a) Low profile of Jays Hill lava shield, with Mt Rouse in the background; (b) Google Earth satellite image of Jays Hill showing the circular nature of the lava shield and radial lava flows to the S; and (c) magnetic imagery around Mt Rouse showing magnetic anomalies associated with the lava shields of Jays Hill [14], Picaninny Hill [9] and Blackwood Hill [5], and the scoria cones of Mt Rouse [4]. Black line is the northern edge of the Mt Rouse lava flows



Figure 6 Cas Maar (maar–cone complex) showing: (a) the wide asymmetrical maar, approximately 0.9 km across; (b) the eastern maar-rim sequence showing two layers of spattery lava; (c) lower sequence of spattery lavas underlain by scoriaceous tuff (covered by vegetation); and (d) upper sequence of spattery lavas and scoriaceous tuff showing sharp contact between the two materials. Hammer is 40 cm long.

crater (Figure 6c, d), which is 10 m lower than the rim. Volcanic material is well preserved at the Cas Maar eruption centre, providing fresh samples. The maar includes at least two points of eruption owing to its scalloped shape. During the violent phreatomagmatic fragmentation event, xenoliths of country rock were incorporated into the magma and are ubiquitous throughout the lavas and scoriaceous tuffs down to millimetre-sized clasts. The xenoliths resemble fragments of the adjacent Paleozoic Bushy Creek Granodiorite (e.g. porphyritic phase G395b; Whelan *et al.* 2007), which must underlie the Cas Maar volcanic complex. This eruption centre constitutes the most northern maar in the Western Plains subprovince, lying 45 km north of the Campdown region maars, where magmas interacted with the aquifers in the Otway Basin sediments (Joyce 1975). The maar rim shows a prominent 300 m (a.s.l.) hill on the digital elevation models, with similar heights for just over 1 km north and northwest of the maar crater. The maar rim sequence was mapped as a tuff ring (e.g.

Victoria—Seamless Geology DVD October 2011) but lacks published detail or assignment as an eruption point by DPI.

QUESTIONED ERUPTION CENTRES

Seven previously suggested eruption centres are placed into question here based on both field and laboratory observations, with five forming part of adjacent centres.

Three points relate to Mt Pierrepont: GV277 [17], GV280 [18] and GV286 [20] (Figure 2a). The Victoria Seamless Geology DVD (October 2011) located an eruption point at Buckley Swamp (GV280; Table 1 [18]). Here, two circular depressions near the edge of the Mt Napier lava flows are not volcanic craters, but dried swamp, ponded in the low-lying parts of the lava plain. Digital elevation models show the area to be slightly raised, without a significant magnetic response. Owing to the undulating topography in this area, Buckley Swamp is considered only part of the underlying plains basalt.

Buckley Swamp may form the southerly expression of Mt Pierrepont's (8.23 km north) lava flows, which are difficult to distinguish. GV286 (Table 1 [20]) is also part of Mt Pierrepont's lava flows; at 2.15 km NNE of the crater, ground truthing revealed part of a lava flow. There is no hill at this point, or a TMI anomaly. Radiometrics shows low K and U, but high Th (green), and links to the Mt Pierrepont edifice. GV277 (Table 1 [13]) is in Tarrington, at the football oval, which is not a vent. According to the digital elevation models, the seamless geology eruption point is centred near a large roughly circular hill measuring approximately 5 km diameter. TMI shows high responses that are identical to Mt Pierrepont, while radiometrics are green, also identical to Mt Pierrepont. In the field no outcrop suggests an eruption point, but it could underlie the Tarrington township. Although within a general hill on the digital elevation models, a low area between this feature and Mt Pierrepont is also visible in satellite imagery and formed by paleostreams cutting around the edge of the Mt Pierrepont edifice in a wide arc. Three present-day streams also have their heads towards GV277. Erosion has obscured the region, with Muddy Creek river systems cutting a valley around the western slopes of Mt Pierrepont to form Muddy Creek, into which the present-day streams and paleostreams flow. Bennetts *et al.* (2003) mapped a basalt flow from Mt Pierrepont extending west to Lake Kennedy, so GV277 is part of the Mt Pierrepont eruption centre, which created a substantial stony rises type lava flow that has since been eroded by rivers and streams over *ca* 4 Ma.

One questioned point, GV285 (Table 1 [19]), 4.3 km southeast of Mt Baimbridge adjacent to Lake Doling Doling, lies among undulating lava plains with many similar-sized hills, and no field evidence of eruption either from the hill or the lake. The site is unremarkable on digital elevation models and similar to the peak of Mt Baimbridge on radiometrics imagery. Bennetts *et al.* (2003) trace the Mt Baimbridge flow across this point east to Strathkellar using radiometric mapping and isotopic domains.

GV 483 (Table 1 [22]), on the western flank of Green Hills 1.06 km from the summit, is not interpreted to be a secondary eruption point. Green Hill is a broad low lava shield, with a stream between the two points, which, on gravity and radiometrics, are seen as one feature. There is no field evidence for an eruption point, only that it forms part of the westerly lava flow of Green Hills.

GV481 [22] lies 10 km ESE of Dunkeld at Lake Repose. The area was considered an eruption point from geomorphic and radiometric data only (D. Bennetts, pers. comm. 2012). The lakes in the area are ponded in basalt flows; no evidence of an eruption exists in this area, and the lakes are not maars. Lake Repose lies on basalts most likely from Sheepwash Hill to the north and/or the Cas Maar to the south.

GV479 (21) lies southwest of Karabeal, a former swamp. Assigned on the basis of being a hill on digital elevation models (A.H.M. VandenBerg, pers. comm. 2012), no field evidence supports an eruption in this area. Although the area is elevated, there is a low gradient of 0.01 (40 m over 3.2 km), and there are no magnetic anomalies. In radiometrics, the area shows a similar

response to Phase 2 basalts (Bennetts *et al.* 2003; see below). Other volcanoes of this age are eroded but still display evidence of eruption.

RELATIVE AGES

Three phases of volcanic activity characterise the Hamilton area based on radiometric imagery, early landform mapping and isotopic domain mapping (Gibbons & Gill 1964; Ollier & Joyce 1986; Martin & Meyer 1987; Mann *et al.* 1992; Bennetts *et al.* 2003). The first-phase basalts have ages of >4 Ma, the second *ca* 2 Ma and the third <0.5 Ma (Bennetts *et al.* 2003). The three phases were confirmed in this study using a combination of absolute ages from literature values, RGB radiometric ternary images and field-based observations (Figure 7). All three phases can be split into older and younger groupings based on the preservation of outcrop.

The majority of Phase 1 basalts outcrop to the west of the Hamilton area, with isolated centres elsewhere. Radiometrics show high Th but low K and U, appearing green. The oldest volcanoes of Phase 1 are Fox, Moutajup, Burgers, Gazette and Acacia Hills; the latter three are all abutted by the lava flows of Mt Rouse, while Fox Hill is completely surrounded by Mt Rouse lavas. The centres are all severely eroded, and local soil cover obscures the location of vents, superposition relationships and collection of representative samples. Later Phase 1 eruption centres are Green Hills at Minhamite (also abutted by Mt Rouse flows), Bunnugal Hill and Mounts Baimbridge and Pierrepont. Although severely eroded, outcrops, such as spatter ramparts, are preserved at each centre; Mt Pierrepont has a K–Ar age of 4.0 ± 0.1 Ma (McDougall *et al.* 1966; Gibson 2007). Basalt at Grange Burn, just outside the Hamilton map area, was dated to 4.6 Ma (Turnbull *et al.* 1965; Gibson 2007), and is most likely related to Mt Baimbridge. This age also means that the eroded centres in the Hamilton area (e.g. Moutajup Hill) are likely to be older than 5 Ma.

Phase 2 basalts outcrop mainly north and east of Hamilton. Eruption centres include Picaninny and Jays Hill, whose flows are abutted or covered by those of Mt Rouse, as well as Sheepwash Hill. Jays Hill has a K–Ar age of 1.95 ± 0.02 Ma (Gray & McDougall 2009). Radiometrics appear blue–green, owing to their moderate Th and K responses and low U.

Phase 3 eruption centres include Mounts Rouse and Napier, which are both substantial edifices. Mt Rouse has been dated to 0.294–0.38 Ma in several studies using K–Ar and Ar–Ar (McDougall & Gill 1975; Ollier 1985; Gray & McDougall 2009; Matchan & Phillips 2011), while Mt Napier has been dated at 32 ± 3 Ka, dated by ^{36}Cl exposure dating (Stone *et al.* 1997). Radiometrics show high K signatures, thus appearing red, with Mt Napier more so owing to its younger age.

The Cas Maar has been placed in Phase 3, despite being radiometrically similar to Phase 2 eruption centres. The phreatomagmatic deposits at the Cas Maar, with their fragmented and fine-grained sizes, would weather faster than the lava flows, which dominate the Hamilton area. This would affect their response on radiometric imagery, making them appear older than they actually are.

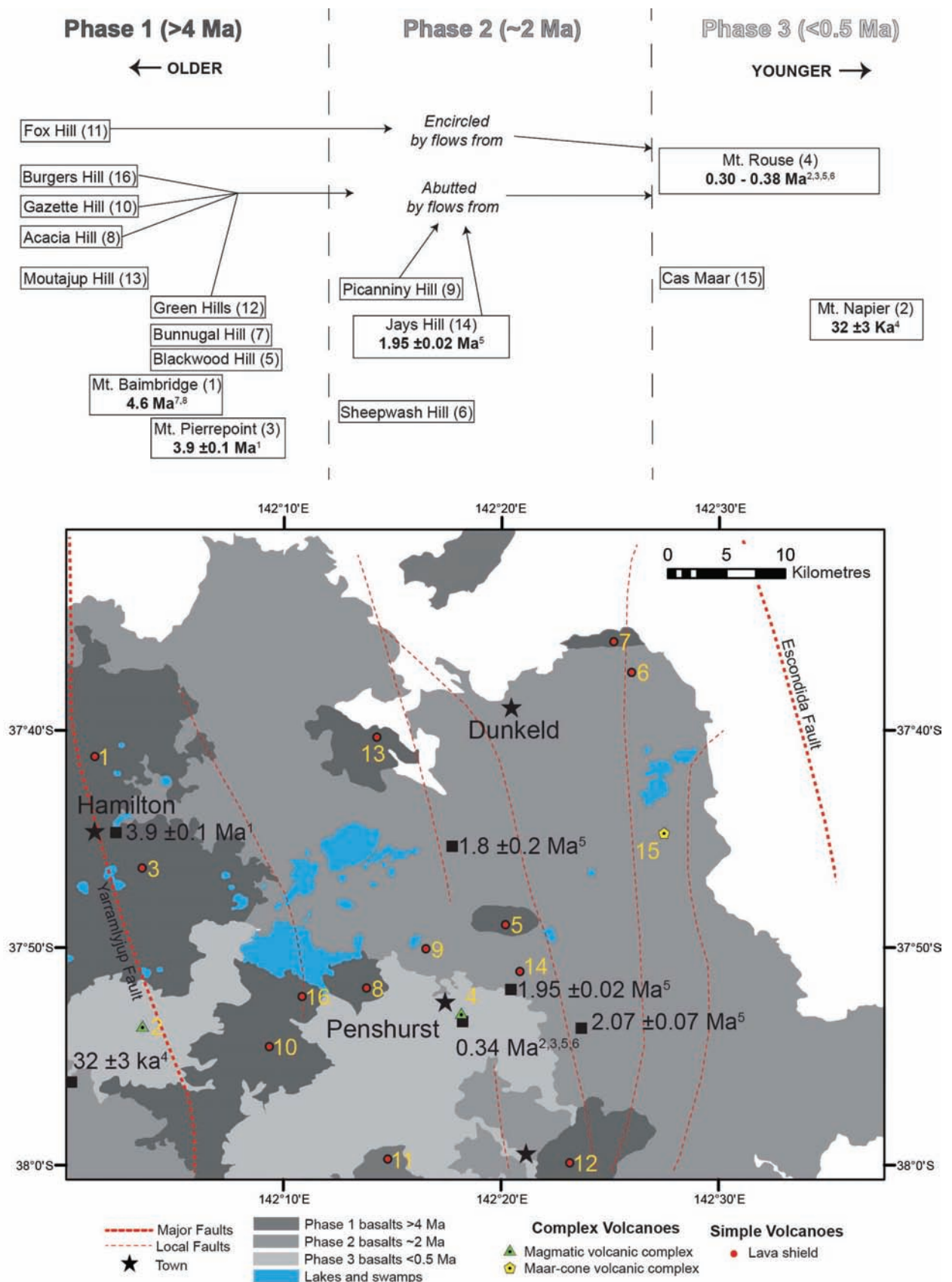


Figure 7 Relative ages of eruption centres in the Hamilton area, and the superposition of the volcanoes in relation to each other and the major and local faults in the pre-basaltic underlying rocks. Age dating in superscript: ¹McDougall *et al.* (1966) (K–Ar), ²McDougall & Gill (1975), ³Ollier (1985) (K–Ar), ⁴Stone *et al.* (1997) (³⁶Cl), ⁵Gray & McDougall (2009) (K–Ar), ⁶Matchan & Phillips (2011) (⁴⁰Ar–³⁹Ar), ⁷Turnbull *et al.* (1965) (K–Ar), and ⁸Gibson (2007). Volcano numbers as in Figure 2.

GEOCHEMISTRY OF THE VOLCANICS

Thirteen representative samples were selected from the eruption centres of the Hamilton area for reconnaissance geochemical analysis to complement existing large geochemical data sets for Mt Rouse and Mt Napier. Four samples were from the Cas Maar, where a diverse range of eruption products were found. Bulk cleaned samples were sent to the Geoscience Laboratories, Sudbury, Canada, where they were pulverised and analysed for major and trace elements by XRF and ICP-MS, respectively. Normalised major element data are shown in Table 2. Total iron was reported as Fe_2O_3 ; FeO and Fe_2O_3 contents were recalculated assuming $\text{Fe}_2\text{O}_3/\text{FeO}_{\text{total}} = 0.15$.

CIPW norms were used to classify the rocks as alkaline (normative nepheline in the range 0–5%), transitional (normative hypersthene \pm normative quartz <10%) or tholeiitic (normative hypersthene \pm normative quartz >10%) (Table 2; Price *et al.* 1997). The majority of tholeiites belonged to Phase 1. The larger eruption centres (Mt Rouse, Mt Napier and the Cas Maar) show variation from alkaline to transitional basalts.

The products of the Phase 1 and 2 lava shields classify as basalt (*sensu stricto*; both alkali and subalkali) when plotted on a TAS diagram (Figure 8). Phase 3 eruption centres cover a wider range of compositions, with Mt Napier ranging from subalkali basalt to trachybasalt, Mt Rouse subalkali basalt to basanite and the Cas Maar trachybasalt. The volcanic products have similar rare earth element (REE) patterns to those of an average Ocean Island Basalt (OIB) (Figure 9a, b). They are characteristically depleted in heavy rare earth element (HREE), which suggests magma sources in garnet-bearing mantle. In the region of the NVP, this corresponds to depths of >55 km (O'Reilly & Griffin 1985). Phase 1 basalts have lower REE contents than those of Phase 2 (Figure 9a). This suggests there was a change in chemistry from Phase 1 to 2 to more alkaline products with greater enrichment in incompatible elements. However, only single samples were available from most individual eruption centres. Phase 2 basalts and Moutajup Hill (Phase 1) have prominent negative Ce anomalies, which could be due to localised incipient weathering, a feature observed in other NVP basalts (Price *et al.* 1991). Phase 3 products (Figure 9b) cover a wider range of compositions, all depleted in HREE with respect to OIB. Mt Napier has compositions similar to the Phase 1 basalts, while Mt Rouse shows clear evidence for three magma batches, with pyroclastic products featuring the greatest light rare earth element (LREE) enrichment, while the lavas are similar to Phase 1 basalts (Boyce *et al.* 2013). The Cas Maar is similar to Mt Rouse in that its products feature high LREE contents, the La/Yb ratios of which lie between those of two of the Mt Rouse magma batches.

Primitive mantle normalised incompatible element plots for the Hamilton area are shown in Figure 9c, d. The Hamilton products are similar to OIB; Phases 1 and 2 are slightly depleted with respect to OIB, while the Cas Maar and the scoriaceous products of Mt Rouse (uppermost batches on incompatible element diagrams) are enriched in highly incompatible elements. The incompatibles therefore also show a trend of increasing

enrichment over time, but with decreasing K to produce negative anomalies. The increased trace element content of these products must reflect the metasomatised nature of the underlying mantle, which is thought to have undergone at least three metasomatic events (O'Reilly & Griffin 1988; Griffin *et al.* 1988). These were at 500–300 Ma (garnet pyroxenites associated with recycled crust, with high $^{87}\text{Sr}/^{86}\text{Sr}$); 60 Ma to present (wehrlitic pyroxenites associated with mantle array Sr–Nd values); and more recent local metasomatic overprinting from carbonatitic fluids and silicate melts (Yaxley *et al.* 1991, 1996; Powell *et al.* 2004; O'Reilly & Griffin 2013). The result of these metasomatic events was the enrichment of incompatible trace elements in the mantle during modal metasomatism, which is the addition of minerals normally uncommon in peridotite, deposited by metasomatic fluids. Examples include the addition of apatite, which leads to the enrichment of REE, Sr, U, and Th; and mica and/or amphibole, leading to K, Ba, Nb and Ta enrichment (O'Reilly & Griffin 2013). All of these enrichments are seen in the products of the Hamilton area and elsewhere in the NVP; and amphibole, mica and apatite are found in xenoliths of the NVP (O'Reilly *et al.* 1989). The K-anomalies of the basalts could reflect either increased stabilisation of residual phlogopite and/or amphibole in the source (owing to metasomatism), decreasing degrees of source melting (see below), or both. It is therefore implied that metasomatism increases with depth in the lithospheric mantle, as the products of Hamilton increase in trace element content over time. However, more detailed geochemical analysis should be performed on individual eruption centres. The mantle beneath the NVP has been inferred to be heterogeneous on scales from centimetres to around 1 km (McDonough & McCulloch 1987; O'Reilly & Griffin 1988; O'Reilly *et al.* 1989).

The volcanic products around Hamilton do not show geochemical evidence for crustal contamination as all plot along the mantle array on variation diagrams (e.g. Th/Yb vs Nb/Yb; Figure 10a) designed to highlight crustal influence (Pearce 2008). Ratios such as Nb/Yb and Gd/Yb may be used as proxies for degrees of mantle source partial melting, with lower ratios indicating increased percent partial melting (Pearce 2008). The Phase 1 and 2 eruption centres, plus Mt Napier and Mt Rouse lava flows, suggest relatively larger degrees of mantle partial melting from a source similar to those of OIB; the more alkaline products of the Cas Maar and the scoria cones of Mt Rouse were probably related to lower degrees of melting. The high Sr contents (up to 1100 ppm) of samples from the Cas Maar and Mt Rouse scoria cones indicate parental magmas probably formed by lower degrees of partial mantle melting than other Hamilton eruption products with lower Sr contents (up to 638 ppm Sr; Figure 10b). The degree of mantle partial melting involved in melt generation is usually inversely proportional to the melting depth (Langmuir *et al.* 1992). The depth of magma generation of the Hamilton volcanic products can be assessed by the ratio Gd/Yb. This ratio increases with deeper melt generation within the garnet stability zone when Yb and the other HREE are retained in garnet during low degree partial melting at depths beyond which Cr-spinel is the aluminous phase in the mantle (>50–60 km; Irving & Frey 1987). The Cas Maar

Table 2 Whole-rock major- and trace-element data for the eruption centres of the Hamilton region.

| Sample no. | Mt Bainbridge | Blackwood Hill | Mt Pierrepont | Acacia Hill | Green Hills | Bunnugal Hill | Picaninny Hill | Sheepwash Hill | Jays Hill | Cas Maar 1 | Cas Maar 2 | Cas Maar 3 | Cas Maar 4 |
|--------------------------------|---------------|----------------|---------------|-------------|-------------|---------------|----------------|----------------|-----------|------------|------------|------------|------------|
| Rock type | Alk | Th | Th | Tr | Th | Alk | Tr | Alk | Tr | Th | Th | Tr | Alk |
| Phase | 1 | 1 | 1 | 1 | 1 | 1 | 2 | 2 | 2 | 3 | 3 | 3 | 3 |
| SiO ₂ | 48.46 | 50.83 | 51.32 | 49.81 | 50.52 | 49.32 | 50.05 | 49.03 | 50.32 | 49.13 | 50.04 | 49.34 | 48.39 |
| TiO ₂ | 2.10 | 2.02 | 1.81 | 1.96 | 1.89 | 1.89 | 2.19 | 2.05 | 2.07 | 2.18 | 2.09 | 2.09 | 1.91 |
| Al ₂ O ₃ | 14.33 | 14.76 | 14.60 | 14.85 | 15.37 | 13.95 | 15.39 | 15.10 | 14.54 | 15.74 | 14.85 | 15.56 | 17.14 |
| Fe ₂ O ₃ | 1.85 | 1.89 | 1.71 | 1.79 | 1.84 | 1.75 | 1.89 | 1.85 | 1.82 | 1.73 | 1.87 | 1.79 | 1.62 |
| FeO | 9.42 | 9.64 | 8.74 | 9.11 | 9.37 | 8.94 | 9.63 | 9.44 | 9.26 | 8.84 | 9.56 | 9.10 | 8.28 |
| MnO | 0.17 | 0.16 | 0.14 | 0.22 | 0.15 | 0.16 | 0.15 | 0.18 | 0.17 | 0.21 | 0.16 | 0.16 | 0.14 |
| MgO | 8.50 | 5.71 | 7.58 | 7.30 | 6.58 | 9.08 | 5.57 | 7.71 | 7.17 | 7.79 | 8.41 | 7.79 | 8.34 |
| CaO | 8.99 | 8.57 | 8.36 | 8.66 | 8.58 | 8.91 | 8.44 | 8.01 | 8.35 | 6.29 | 7.07 | 6.86 | 6.73 |
| Na ₂ O | 3.41 | 3.60 | 3.45 | 3.57 | 3.44 | 3.34 | 3.59 | 3.59 | 3.54 | 2.97 | 2.94 | 3.39 | 3.83 |
| K ₂ O | 1.28 | 1.19 | 0.94 | 1.29 | 0.70 | 1.27 | 1.36 | 1.42 | 1.34 | 2.36 | 2.20 | 2.11 | 1.98 |
| P ₂ O ₅ | 0.43 | 0.39 | 0.36 | 0.43 | 0.35 | 0.44 | 0.47 | 0.47 | 0.46 | 0.70 | 0.81 | 0.63 | 0.63 |
| Mg# | 61.62 | 51.00 | 60.70 | 58.81 | 55.28 | 64.50 | 50.35 | 59.08 | 58.09 | 58.98 | 61.77 | 60.08 | 63.99 |
| (Q+Hy)-Ne | -1.58 | | | | | -0.14 | | -0.28 | | | | | -2.91 |
| Hy | | 10.73 | 15.82 | 1.76 | 15.62 | | 6.44 | | 6.59 | 10.26 | 12.06 | 2.93 | |
| Cs | 0.30 | 0.19 | 0.23 | 0.30 | 0.12 | 0.25 | 0.21 | 0.25 | 0.16 | 0.86 | 0.54 | 0.46 | 0.59 |
| Ba | 386 | 383 | 292 | 450 | 239 | 361 | >1740 | 456 | 374 | 824 | 665 | 758 | 555 |
| Rb | 26.8 | 25.0 | 18.1 | 27.5 | 8.1 | 26.2 | 27.6 | 28.5 | 26.5 | 45.9 | 39.5 | 40.0 | 27.1 |
| Sr | 557 | 535 | 443 | 542 | 447 | 550 | 638 | 598 | 511 | 1100 | 895 | 1009 | 920 |
| Pb | 2.30 | 1.60 | 1.80 | 2.20 | 1.90 | 2.30 | 2.60 | 2.30 | 1.80 | 2.80 | 2.74 | 3.40 | 3.20 |
| Th | 3.30 | 2.64 | 2.23 | 3.53 | 2.44 | 3.15 | 3.88 | 3.81 | 3.30 | 7.03 | 6.38 | 6.08 | 5.37 |
| U | 0.82 | 0.60 | 0.50 | 0.89 | 0.43 | 0.72 | 0.84 | 0.94 | 0.77 | 1.67 | 1.64 | 1.53 | 1.53 |
| Zr | 173 | 150 | 144 | 177 | 156 | 151 | 177 | 191 | 175 | 337 | 287 | 296 | 270 |
| Hf | 4.04 | 3.59 | 3.47 | 4.07 | 3.74 | 3.53 | 4.21 | 4.38 | 4.05 | 7.20 | 6.34 | 6.32 | 5.72 |
| Nb | 34.1 | 30.3 | 25.2 | 36.6 | 22.7 | 32.5 | 36.1 | 35.9 | 34.6 | 67.2 | 64.3 | 61.1 | 56.0 |
| Y | 22.2 | 20.0 | 21.5 | 26.2 | 25.3 | 20.0 | 33.8 | 28.1 | 31.2 | 29.8 | 27.3 | 21.3 | 20.5 |
| La | 25.6 | 21.9 | 21.3 | 30.8 | 26.9 | 23.5 | 45.9 | 37.1 | 44.5 | 68.3 | 53.8 | 47.7 | 45.6 |
| Ce | 50.9 | 43.4 | 39.2 | 55.2 | 50.0 | 46.3 | 65.3 | 57.3 | 58.2 | 109.2 | 95.3 | 91.5 | 85.9 |
| Pr | 6.53 | 5.47 | 5.37 | 6.89 | 6.71 | 5.81 | 10.2 | 8.43 | 9.08 | 13.9 | 11.2 | 10.9 | 10.3 |
| Nd | 27.0 | 23.0 | 22.9 | 28.1 | 27.9 | 24.1 | 41.9 | 34.4 | 36.9 | 54.5 | 43.2 | 42.7 | 39.8 |
| Sm | 6.11 | 5.47 | 5.63 | 6.31 | 6.65 | 5.63 | 8.71 | 7.51 | 8.10 | 10.5 | 8.93 | 8.66 | 8.08 |
| Eu | 2.09 | 1.91 | 1.93 | 2.12 | 2.26 | 1.88 | 2.90 | 2.57 | 2.55 | 3.44 | 2.79 | 2.81 | 2.59 |

(continued)

Table 2 (Continued)

| Sample no. | Mt Baimbridge | Blackwood Hill | Mt Pierrepont | Acacia Hill | Green Hills | Bunnugal Hill | Picaninny Hill | Sheepwash Hill | Jays Hill | Cas Maar 1 | Cas Maar 2 | Cas Maar 3 | Cas Maar 4 |
|------------|---------------|----------------|---------------|-------------|-------------|---------------|----------------|----------------|-----------|------------|------------|------------|------------|
| Gd | 5.92 | 5.37 | 5.60 | 6.26 | 6.52 | 5.36 | 8.75 | 7.41 | 8.10 | 9.37 | 7.76 | 7.24 | 6.84 |
| Tb | 0.85 | 0.77 | 0.81 | 0.92 | 0.97 | 0.77 | 1.25 | 1.06 | 1.15 | 1.23 | 1.10 | 0.97 | 0.90 |
| Dy | 4.73 | 4.38 | 4.62 | 5.12 | 5.45 | 4.32 | 6.99 | 6.05 | 6.42 | 6.32 | 5.51 | 5.00 | 4.71 |
| Ho | 0.87 | 0.78 | 0.84 | 0.94 | 0.99 | 0.78 | 1.27 | 1.09 | 1.17 | 1.05 | 0.98 | 0.83 | 0.77 |
| Er | 2.14 | 2.01 | 2.13 | 2.38 | 2.48 | 1.96 | 3.22 | 2.77 | 2.85 | 2.44 | 2.18 | 1.91 | 1.80 |
| Tm | 0.28 | 0.26 | 0.28 | 0.31 | 0.32 | 0.26 | 0.41 | 0.36 | 0.37 | 0.29 | 0.25 | 0.23 | 0.22 |
| Yb | 1.65 | 1.51 | 1.63 | 1.78 | 1.87 | 1.50 | 2.34 | 2.10 | 2.10 | 1.60 | 1.36 | 1.25 | 1.17 |
| Lu | 0.23 | 0.21 | 0.22 | 0.25 | 0.25 | 0.21 | 0.33 | 0.30 | 0.29 | 0.21 | 0.19 | 0.17 | 0.15 |
| V | 192 | 167 | 157 | 172 | 187 | 189 | 211 | 170 | 178 | 146 | 146 | 126 | 135 |
| Cr | 305 | 329 | 350 | 300 | 304 | 353 | 275 | 292 | 290 | 371 | 363 | 385 | 341 |
| Ni | 224 | 200 | 238 | 200 | 206 | 261 | 162 | 224 | 173 | 336 | 27 | 308 | 292 |
| Cu | 48.5 | 41.4 | 33.2 | 40.8 | 40.0 | 43.8 | 37.6 | 46.4 | 47.9 | 31.6 | 37.1 | 24.5 | 25.6 |
| Zn | 114 | 118 | 107 | 117 | 116 | 106 | 121 | 128 | 114 | 135 | 140 | 123 | 135 |

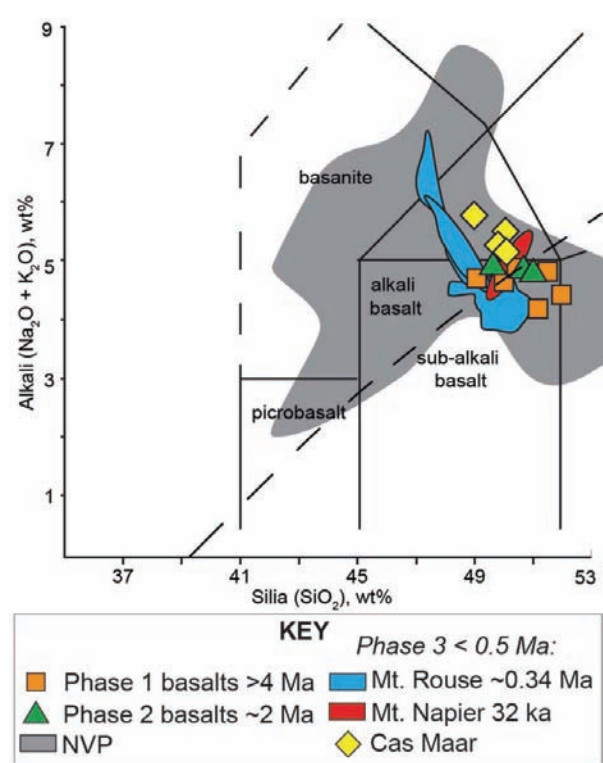


Figure 8 Total alkali *vs* silica diagram for the eruption products of the Hamilton area compared with the NVP as a whole. Phase 1 basalts orange filled squares, Phase 2 basalts green filled triangles, Mt Napier red oval field, Mt Rouse blue fields to left, Cas Maar yellow filled diamonds. NVP grey shaded field: >218 analyses (data from Frey & Green 1974; Ellis 1976; Irving & Green 1976; Frey *et al.* 1978; Price *et al.* 1997; Stone *et al.* 1997; Vogel & Keays 1997; McBride *et al.* 2001; Foden *et al.* 2002; Demidjuk *et al.* 2007). Subdivision of alkali and subalkali rocks from Irvine & Baragar (1971).

and the Mt Rouse scoria cone samples have markedly higher Gd/Yb ratios than the remaining samples, indicating their magmas formed at greater depths (Figure 10c).

The increase in Al₂O₃ contents relative to both CaO and TiO₂, shown by both the high and low Gd/Yb groups, suggests crystal fractionation of olivine and Ca-rich clinopyroxene, and reflects the fact that Al-rich plagioclase was not a major fractionating phase in these alkaline magmas. However, the systematic increase in TiO₂, especially in Mt Rouse, Mt Napier (Whitehead 1986, 1991) and Cas Maar products (Figure 10d), suggests that the proportion of Ti-rich clinopyroxene in fractionating mafic mineral assemblages was relatively low. Fractionation cannot be assessed for the Phase 1 and 2 basalts owing to insufficient samples.

The Cas Maar samples, with their conspicuously high Al₂O₃ (14.8–17.3 wt%), K₂O (2.0–2.4 wt%) and P₂O₅ (0.64–0.81 wt%) contents but very low CaO (6.4–7.1 wt%) are distinctive. As these rocks have relatively high Ni contents, the parent magmas are unlikely to have crystallised significant early olivine or Ca-rich clinopyroxene and so retain characteristics related to the composition of the magma source (e.g. a low-Ca

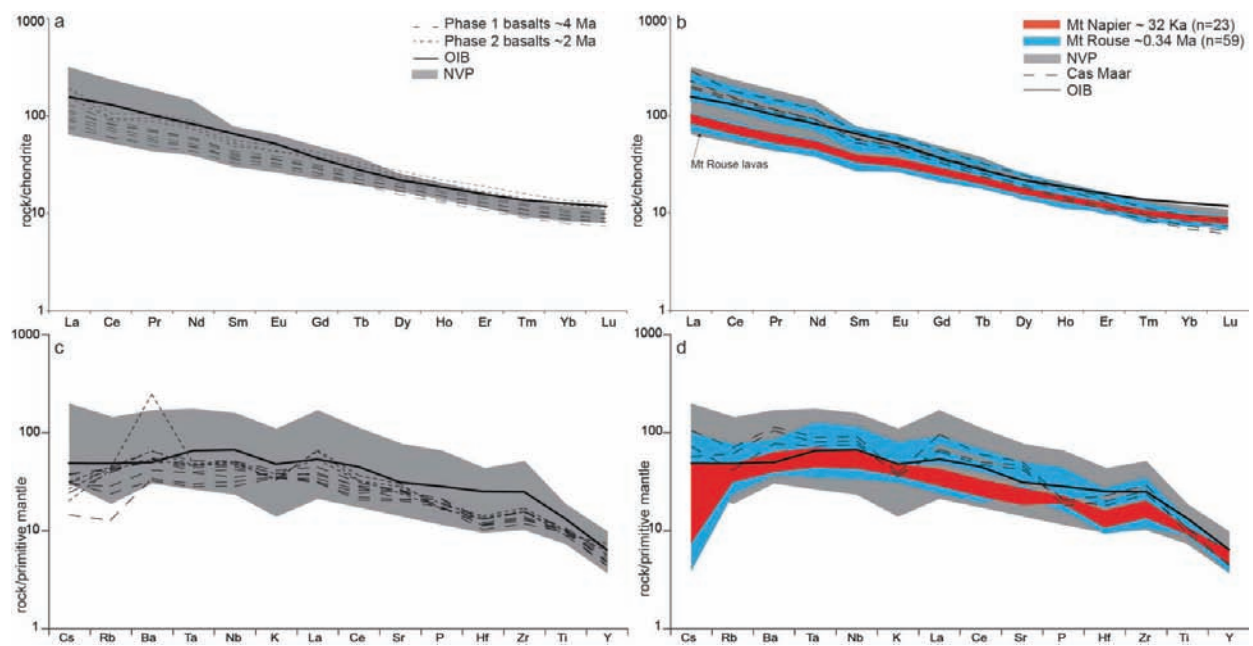


Figure 9 (a, b) Chondrite normalised rare earth element diagrams and (b, c) primitive mantle normalised incompatible element diagrams for the Hamilton area, compared with Ocean Island Basalts and the Newer Volcanics Province. (left) Phase 1 long dashed lines, Phase 2 short dashed lines. (right) Phase 3: Mt Napier red shaded area, Mt Rouse blue shaded area (upper two fields constitute scorias, lower field lavas), Cas Maar dashed lines. OIB represented by thick black line (Sun & McDonough 1989), and NVP shaded area (Frey *et al.* 1978; Price *et al.* 1997; Vogel & Keays 1997; McBride *et al.* 2001; Foden *et al.* 2002; Demidjuk *et al.* 2007).

harzburgite source) or the partial melting processes (especially a low degree of melting). Further geochemical samples are needed to constrain magma evolution more closely. Although the Cas Maar shows unusual geochemistry for the Hamilton area, such compositions are found throughout the NVP. Elevated P_2O_5 (>0.5 wt%) and K_2O (>1.44 wt%) is commonly recognised in NVP lavas (e.g. Frey & Green 1974; Ellis 1976; Irving & Green 1976; Frey *et al.* 1978; McDonough *et al.* 1985; Vogel & Keays 1997; Demidjuk *et al.* 2007). Similar geochemistry, including high Al_2O_3 and low CaO, is documented in nepheline normative alkalic basalts at The Anakies, Mt Franklin, Mt Callender, Mt Gorong, Melbourne Hill and Mt Moolort (Ellis 1976; Irving & Green 1976; McDonough *et al.* 1985).

DISCUSSION

The eroded nature of many older volcanoes in the Hamilton area commonly makes it difficult to define eruption centres on field evidence alone. Many of the older centres have undergone significant soil formation and recent landscape modifications owing to agriculture, destroying or obscuring many original features. The multifaceted approach outlined in this paper has helped to pinpoint eruption centres by either confirming their locations or finding lack of evidence for or absence of other eruption centres. Large areas of basalt in the Hamilton region cannot be clearly attributed to individual eruption centres, especially as eruption centres appear scarce in the central and northeastern parts of the Hamilton area. Several explanations may apply. It is difficult

to map lava flows in areas without relief and with deep weathering. Shield volcanoes in the NVP can be broad and low (e.g. Mt Hydewell), and lavas can flow for many kilometres (e.g. Mt Rouse). Basalt cover in the east could be attributable to Sheepwash Hill (6) and the Cas Maar (15), while central basalts may belong to Picaninny Hill (9) and Jays Hill (14). The northwest is harder to define. The Victoria–Seamless Geology DVD (October 2011) placed an eruption centre at -37.6030° , 142.1435° (GSV479) (Figure 2a), but this was discounted herein owing to lack of evidence; Badger Hill lava shield lies 3.5 km north of the northwestern edge of the Hamilton map sheet, and may account for the lavas to the north. Ollier & Joyce (1964) suggest that fissure eruptions may have contributed to the veneer of plains basalts, but that erosion has not yet revealed the feeder dykes.

Several eruption centres in the Hamilton area are positioned near faults, which represent weak points in the crust and therefore may act as preferred pathways for ascending magmas. Several near-linear trends of eruption points may reflect local faults, which were superimposed onto Figure 7 from the Victoria 1:100 000 Pre-Permian Geology map (Simons & Moore 1999). These are (a) Moutajup Hill (13), Acacia Hill (9) and Mt Rouse (4); (b) Blackwood Hill (5), Jays Hill (14) and Green Hills (12); and (c) Sheepwash Hill (6), Bunnugal Hill (7) and the Cas Maar (15). Burgers Hill (16) lies on a lineament, and eight volcanoes are aligned from Mt Napier to the Cas Maar, orthogonal to the NW–SE trend of the regional faults. The two major faults in the Hamilton area are the Escondida and Yarramylyup faults, which converge north of the Grampians (Cayley *et al.* 2011). The Escondida fault lies away from NVP eruption centres in the

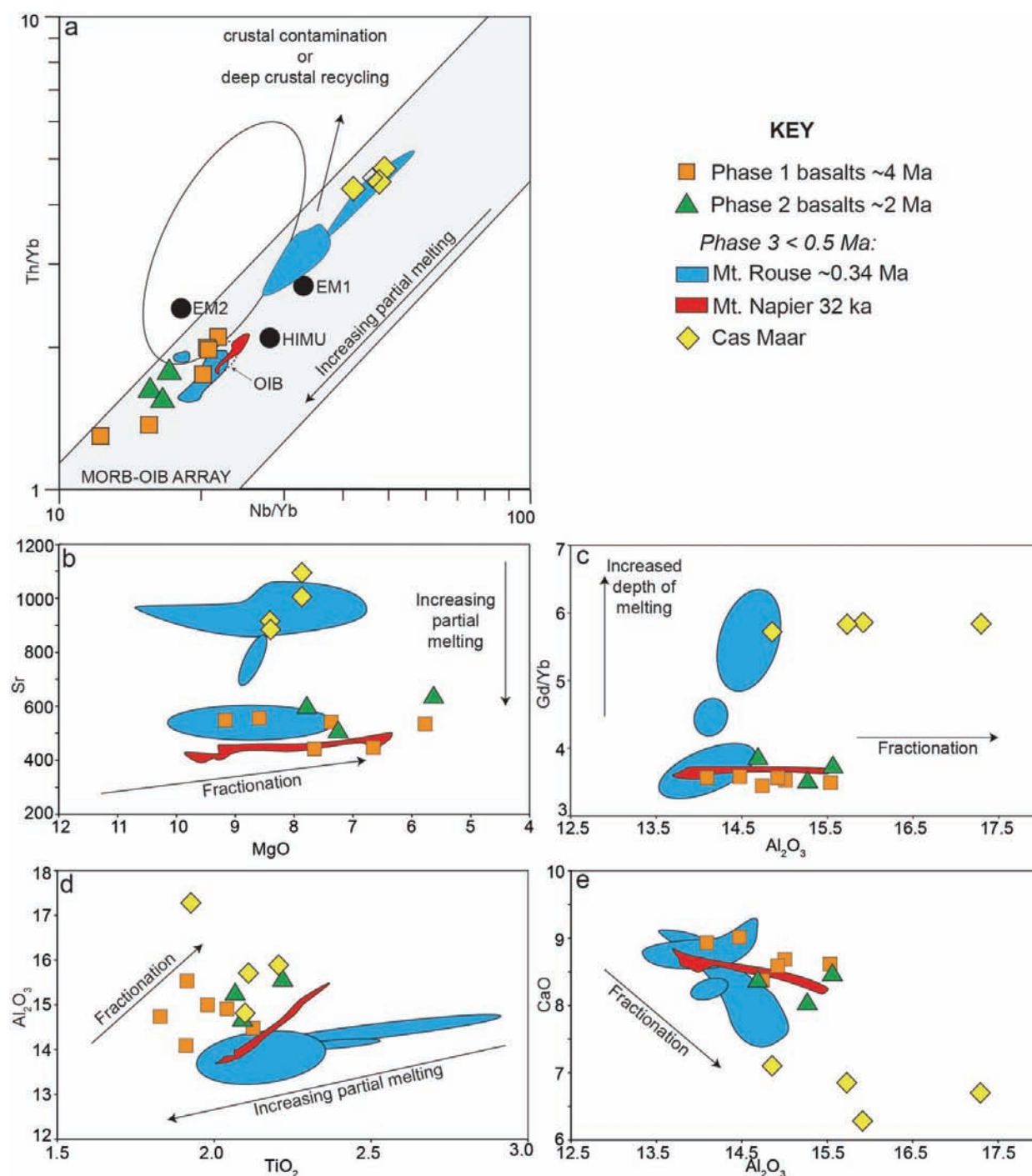


Figure 10 Variation in major and trace element compositions for the Hamilton area eruption centres. (a) Th/Yb vs Nb/Yb, compared with Enriched Mantle 1 (EM1), Enriched Mantle 2 (EM2), high $^{238}\text{U}/^{204}\text{Pb}$ mantle (HIMU) and Ocean Island Basalt (OIB). (b) Sr vs MgO, showing evidence for increased partial melting to produce magmas associated with the lava shields compared with Mt Rouse scoria cones and the Cas Maar. (c) Gd/Yb vs Al_2O_3 showing evidence for increased depth of melting for magmas of Mt Rouse scoria cones and the Cas Maar. (d) Al_2O_3 vs TiO_2 showing evidence for fractionation of olivine from the systematic increase of both oxides. (e) CaO vs Al_2O_3 illustrating the low CaO and high Al_2O_3 contents of the Cas Maar products.

Hamilton area, and has therefore not influenced eruptions here. The Yarramylyup Fault was originally interpreted as running 20 km west of Mt Rouse in a NNW–SSE direction (e.g. Cayley *et al.* 2011; Figure 7), with a possible near-vertical dip (Gibson & Nihill 1992). With that positioning, it runs through Mounts

Baimbridge, Pierrepoint and Napier. However, recent reinterpretation suggests that it is moderately westerly dipping, lying just east of Mt Rouse, extending north to Dunkeld (R. Cayley, pers. comm. 2014). The Yarramylyup Fault could not have influenced the eruptions of the western volcanoes in the Hamilton area, but may be

related to the eruption of Mt Rouse by acting as a preferred pathway for magma ascent.

Price *et al.* (2003) state that ultramafic xenoliths are virtually unknown west of the Mortlake Discontinuity, with centres such as Mt Rouse being barren. However, this study found small mantle xenoliths in lava samples at Mt Rouse, Mt Baimbridge and Blackwood Hill, while the Cas Maar features small amounts of disaggregated mantle xenoliths. Only limited material was examined at these centres (except at Mt Rouse), so that estimating size and abundance is not possible for all centres. Ultramafic xenoliths mostly range around ~4 mm and are relatively rare. The presence of mantle xenoliths in the basalts attests to a fairly rapid ascent rate of host magmas.

Modelling of the pressure and temperature of the primary magmas of Mt Rouse, based on a full geochemical dataset, indicates that the magmas were sourced from the lithosphere–asthenosphere boundary (Boyce *et al.* 2012). Similar results are obtained for Mt Napier (calculations based upon geochemical data of A. Needham) and Mt Gambier (van Otterloo 2012). Volcanoes of the Burr Range in South Australia have been ascribed shallow asthenospheric source regions (Holt *et al.* 2014). A relationship is suggested between the pressure of magma formation and the age of eruption centres in the Mt Gambier region, with pressures/depths decreasing with age (between the older Burr Range volcanoes and the younger Mounts Gambier and Schank) (Holt *et al.* 2014). It is plausible that such a relationship may exist within clustered volcanic centres, although the opposite seems to be the case for the Hamilton area. However, Mt Gambier and Mt Rouse, which are 135 km apart, feature multiple magma batches with different depths of origin that were erupted simultaneously (Boyce *et al.* 2012; van Otterloo 2012). This suggests that volcanism in the NVP is more complex than traditionally assumed, and a full stratigraphic and geochemical analysis needs to be performed on individual eruption centres to determine their petrogenetic history. Pressure–temperature observations, however, suggest that the lithosphere–asthenosphere boundary is of importance in the generation of NVP magmas. Consistent with the modelling is the suggestion that basaltic melts are neutrally buoyant at the lithosphere–asthenosphere boundary (O'Reilly & Griffin 2010; Niu *et al.* 2012; Crépeau *et al.* 2014). This would result in metasomatism of the surrounding rocks, and the crystallisation of eclogites at depth; subsequent ascending magmas would become enriched in incompatible elements (Niu 2008; Niu *et al.* 2012). What drives magmas from the lithosphere–asthenosphere boundary to erupt is still unknown, and has been related to mantle plumes (e.g. Wellman & McDougall 1974; Matsumoto *et al.* 1997) and continental extension relating to the breakup of Gondwana (e.g. Lister & Etheridge 1989; Price *et al.* 1997). The most recent theory of edge-driven convection (Demidjuk *et al.* 2007; Farrington *et al.* 2010) explains that steps in lithospheric thickness to the south beneath the Australian continent (Fishwick *et al.* 2008) are associated with thermal contrasts that produce convection cells that travel with the overlying lithosphere to produce upwelling of fertile asthenospheric material downstream.

The discovery and verification of eruption centres are important for ongoing research in the NVP. The last known eruption occurred at Mt Gambier at approximately 5000 years BP (Blackburn 1966; Barbetti & Sheard 1981; Blackburn *et al.* 1982; Gouramanis *et al.* 2010), and the province is considered active, with mantle-derived CO₂ emissions occurring at Garvoc, Wangoom and Mt Gambier (Wopfner & Thornton 1971; Chivas *et al.* 1987) and the Daylesford region (Chivas *et al.* 1983; Cartwright *et al.* 2002). With estimates of eruption frequencies ranging from 1:10 800 years (Boyce 2013) to 1:12 000 years (Joyce 1988a, b, 2003, 2004, 2005; Cas *et al.* 1993), a fuller understanding of the nature of eruptions and their frequency is needed. The discovery of a large maar volcano using Google Earth in such a well-documented volcanic province illustrates that other volcanic centres in the NVP may be discovered. Additionally, advances in technology (e.g., widespread radiometrics and LIDAR) make it easier to find new eruption centres and test the validity of proposed centres. This study shows that more proposed eruption centres in the province may be placed into question. Better controls on the numbers of eruption centres allow for more accurate calculations of eruption frequencies (which are calculated by dividing the timespan of eruption of the province by the number of eruption centres in the province) and hence volcanic hazard maps (e.g. Joyce 2004) for future eruptions.

CONCLUSIONS

- (1) Sixteen eruption centres in the Hamilton area include three newly recognised centres, one of which is a substantial maar volcanic complex (the northernmost maar in the Western Plains). This study shows the usefulness of a multifaceted approach to eruption point identification. Google Earth is an excellent tool for manipulation of satellite imagery, with the ability to zoom, tilt and vertically exaggerate. When Google Earth satellite imagery and tools are used alongside seamless geology data, which is increasingly available as Google Earth overlays that can be toggled on or off, this adds to the ways geologists can manipulate data.
- (2) Seven previously proposed eruption centres were placed into question based on field and laboratory observations.
- (3) Three phases of eruption previously recognised around Hamilton were confirmed by using RGB radiometric ternary imagery—Phases 1, 2 and 3 (>4 Ma, ca 2 Ma and <0.5 Ma respectively). Based on preservation of outcrop, eruption centres within each phase can be subdivided into older and younger groupings. Using radiometric ternary imagery for interpreting ages of volcanic centres is uncertain in areas containing unconsolidated maar deposits, which weather at a faster rate than lava flows, and can give misleading relative ages. Older volcanoes in Phase 1 may be substantially older than 4 Ma.
- (4) Reconnaissance geochemical studies of the Hamilton eruption centres further confirmed three phases of eruption, with compositions becoming increasingly more alkaline and enriched in incompatible elements

through Phases 1 and 2. Phase 3 eruption products cover the entire geochemical range of earlier erupted products and extend into more enriched compositions.

- (5) The compositions of lava shields of Phases 1 and 2 and the lava flows of Mt Napier and Mt Rouse suggest higher degrees of melting of shallower mantle source regions than for the more alkaline compositions of Cas Maar and the scoria cones of Mt Rouse.
- (6) Additional volcanic centres in the NVP may be discovered, while detailed research may lead to questioning of some loosely identified eruption points. Better volcanic distribution maps and consequent estimates of eruption frequently will allow more accurate eruption forecasting and hazard analyses of future eruptions.

ACKNOWLEDGEMENTS

This paper represents part of the PhD research undertaken by Julie Boyce under the supervision of Prof. Reid Keays, Dr Ian Nicholls and Dr Patrick Hayman. Julie Boyce acknowledges a Monash University School of Geosciences research scholarship and Dean's International Postgraduate Research Scholarship. We thank David Higgins for supplying Geoscience Victoria eruption points, and Fons VandenBerg, Bill Birch (Museum Victoria), Bernie Joyce (Melbourne University), John Webb, Neville Rosengren (La Trobe University), Darren Bennetts (Peter J Ramsay and Associates Pty Ltd), Ross Cayley (Geological Survey of Victoria) and Ken Grimes (Regolith mapping, RRN, Hamilton) for very helpful discussions relating to the positioning of eruption centres, structural influences in the Hamilton area, and age dating in the NVP. We thank Dion Ross, Katrina Boyd-Walsh, Judy and Vanne Trompf, Robin Jackson and Brian O'Brien for access to eruption centres, and the Volcanoes Discovery Centre at Penshurst. Thanks go to Jozua van Otterloo and Janine Kavanagh for help with fieldwork and ground truthing of the eruption points (Jays Hill is unofficially named for Julie, Janine and Jozua), and Jackson van den Hove for help with supplying radiometrics. Andrew Needham is thanked for geochemical data of Mt Napier, and Roland Maas (Melbourne University) for supplying literature on the Bushy Creek Pluton. We thank Fons VandenBerg (Museum Victoria), and Lin Sutherland (University of Western Sydney) for reviews.

REFERENCES

- BARBETTI M. & SHEARD M. J. 1981. Palaeomagnetic results from Mounts Gambier and Schank, South Australia. *Journal of the Geological Society of Australia* **28**, 385–394.
- BENNETTS D. A., WEBB J. A. & GRAY C. M. 2003. Distribution of Plio–Pleistocene basalts and regolith around Hamilton, Western Victoria, and their relationship to groundwater recharge and discharge. *Advances in regolith: proceedings of the CRC LEME Regional Regolith Symposia 2003*, 11–15.
- BLACKBURN G. 1966. Radiocarbon dates relating to soil development and volcanic ash deposition in south-east South Australia. *Australian Journal of Earth Sciences* **29**, 50–52.
- BLACKBURN G., ALLISON G. B. & LEANEY F. W. J. 1982. Further evidence on the age of the tuff at Mount Gambier, South Australia. *Transactions of the Royal Society of South Australia* **106**, 163–167.
- BOYCE J. 2013. The Newer Volcanics Province of southeastern Australia: a new classification scheme and distribution map for eruption centres. *Australian Journal of Earth Sciences* **60**, 449–462.
- BOYCE J., NICHOLLS I., KEAYS R. & HAYMAN P. 2012. The multiple magma batches of Mt Rouse, Newer Volcanics Province, Victoria, Australia. Abstract, IAVCEI 41MC conference, Auckland, New Zealand, 20 February 2012.
- BOYCE J. A., NICHOLLS I., KEAYS R. & HAYMAN P. 2013. Triple magma batches and a complex eruption history of a monogenetic volcano: geochemical analysis of Mt Rouse, Newer Volcanics Province, Australia. Abstract, Volcanic and Magmatic Studies Group Annual Meeting, 7–9 January 2013, Bristol, UK.
- CARTWRIGHT I., WEAVER T., TWEED S., AHEARNE D., COOPER M., CZAPNIK K. & TRANTER J. 2002. Stable isotope geochemistry of cold CO₂-bearing mineral spring waters, Daylesford, Victoria: sources of gas and water and links with waning volcanism. *Chemical Geology* **185**, 71–91.
- CAS R., SIMPSON C. & SATO H. 1993. Newer Volcanics Province—Processes and products of phreatomagmatic activity. *IAVCEI Canberra 1993—Excursion guide*, Australian Geological Survey Organisation, Canberra, ACT.
- CAYLEY R. A., KORSCH R. J., MOORE D. H., COSTELLOE R. D., NAKAMURA A., WILLMAN C. E., RAWLING T. J., MORAND V. J., SKLADZIEK P. B. & O'SHEA P. J. 2011. Crustal architecture of central Victoria: results from the 2006 deep crustal reflection seismic survey. *Australian Journal of Earth Sciences* **58**, 113–156.
- CAYLEY R. A. & TAYLOR D. H. 1997. Grampians. Special map area geological report. *Geological Survey of Victoria Report 107*. Melbourne Vic.
- CAYLEY R. A., WEBB A. W. & HENLEY K. J. 1995. Radiometric dating (K/Ar) on two samples of Newer Volcanic olivine basalt from the southwestern part of the Beaufort 1:100 000 map sheet area. *Geological Survey of Victoria Unpublished Report 1995/15*. Melbourne Vic.
- CHIVAS A. R., BARNES I., EVANS W. C., LUPTON J. E. & STONE J. O. 1987. Liquid carbon dioxide of magmatic origin and its role in volcanic eruptions. *Nature* **326**, 587–589.
- CHIVAS A. R., BARNES I. E., LUPTON J. E. & COLLIERSON K. 1983. Isotopic studies of south-east Australian CO₂ discharges. *Geological Society of Australia Abstract* **12**, 94–95.
- COOPER J. A. & GREEN D. H. 1969. Lead isotope measurements on lherzolite inclusions and host basanites from western Victoria, Australia. *Earth and Planetary Science Letters* **6**, 69–76.
- CRÉPISSON C., MORARD G., BUREAU H., PROUTEAU G., MORIZET Y., PETITGIRARD S. & SANLOUP C. 2014. Magmas trapped at the continental lithosphere–asthenosphere boundary. *Earth and Planetary Science Letters* **393**, 105–112.
- DASCH E. J. & GREEN D. H. 1975. Strontium isotope geochemistry of lherzolite inclusions and host basaltic rocks, Victoria, Australia. *American Journal of Science* **275**, 461–469.
- DASCH E. J. & MILLAR D. J. 1977. Age and strontium-isotope geochemistry of differentiated rocks from the Newer Volcanics, Mt. Macedon area, Victoria, Australia. *Journal of the Geological Society of Australia* **24**, 195–201.
- DAY R. A. 1983. Petrology and geochemistry of the Older Volcanics of Victoria. PhD thesis, Monash University.
- DEMIDJUK Z., TURNER S., SANDIFORD M., GEORGE R., FODEN J. & ETHERIDGE M. 2007. U-series isotope and geodynamic constraints on mantle melting processes beneath the Newer Volcanic Province in South Australia. *Earth and Planetary Science Letters* **261**, 517–533.
- EDWARDS J., CAYLEY R. A. & JOYCE E. B. 2004. Geology and geomorphology of the Lady Julia Percy Island volcano, a late Miocene submarine and subaerial volcano off the coast of Victoria, Australia. *Proceedings of the Royal Society of Victoria* **116**, 15–35.
- ELIAS M. 1973. *The geology and petrology of Mount Rouse, a volcano in the Western District of Victoria*. Honours research report, University of Melbourne.
- ELLIS D. J. 1976. High pressure cognate inclusions in the Newer Volcanics of Victoria. *Contributions to Mineralogy and Petrology* **58**, 149–180.
- EWART A., CHAPPELL B. W. & LE MAITRE R. W. 1985. Aspects of the mineralogy and chemistry of the intermediate–silicic Cainozoic volcanic rocks of eastern Australia. Part 1: Introduction and geochemistry. *Australian Journal of Earth Sciences* **32**, 359–382.
- EWART A., CHAPPELL B. W. & MENZIES M. A. 1988. An overview of the geochemical and isotopic characteristics of the eastern Australian

- Cainozoic volcanic provinces. In: Menzies M. A. & Cox K. G. eds. *Oceanic and Continental Lithosphere: Similarities and Differences*. *Journal of Petrology. Special Lithosphere Issue*, 225–273. Clarendon Press, Oxford.
- FARRINGTON R. J., STEGMAN D. R., MORESI L. N., SANDIFORD M. & MAY D. A. 2010. Interactions of 3D mantle flow and continental lithosphere near passive margins. *Tectonophysics* **483**, 20–28.
- FISHWICK S., HEINTZ M., KENNETT B. L. N., READING A. M. & YOSHIZAWA K. 2008. Steps in lithospheric thickness within eastern Australia, evidence from surface wave tomography. *Tectonics* **27**, TC4009.
- FODEN J., SONG S. H. S., TURNER S., ELBURG M., SMITH P. B., VAN DER STELT B. & VAN PENGELS D. 2002. Geochemical evolution of lithospheric mantle beneath S.E. South Australia. *Chemical Geology* **182**, 663–695.
- FREY F. A. & GREEN D. H. 1974. The mineralogy, geochemistry and origin of lherzolite inclusions in Victorian basanites. *Geochimica et Cosmochimica Acta* **38**, 1023–1059.
- FREY F. A., GREEN D. H. & ROY D. 1978. Integrated models of basalt petrogenesis: a study of quartz tholeiites to olivine melilitites from South Eastern Australia utilising geochemical and experimental petrological data. *Journal of Petrology* **19**, 463–513.
- GIBBONS F. & GILL E. D. 1964. Terrains and soils of the basaltic plains of far-western Victoria. *Proceedings of the Royal Society of Victoria* **77**, 387–395.
- GIBSON D. L. 2007. Potassium–argon ages of late Mesozoic and Cainozoic igneous rocks of Eastern Australia. *CRC LEME Open File Report* **193**. CSIRO, Kensington, Western Australia.
- GIBSON G. M. & NIHILL D. N. 1992. Glenelg River Complex: Western margin of the Lachlan Fold Belt or extension of the Delamerian Orogen into Western Victoria? *Tectonophysics* **214**, 69–91.
- GILL E. D. & ELMORE L. K. M. 1974. Importance of the Mount Napier Volcanic Complex near Hamilton, Victoria, Australia. *Victorian Naturalist* **91**, 167–174.
- GOURAMANIS C., WILKINS D. & DEDECKER P. 2010. 6000 years of environmental changes recorded in Blue Lake, South Australia, based on ostracod ecology and valve chemistry. *Palaeogeography, Palaeoclimatology, Palaeoecology* **297**, 223–237.
- GRAY C. M. & McDUGALL I. 2009. K–Ar geochronology of basalt petrogenesis, Newer Volcanic Province, Victoria. *Australian Journal of Earth Sciences* **56**, 245–258.
- GRIFFIN W. L., O'REILLY S. Y. & STABEL A. 1988. Mantle metasomatism beneath western Victoria, Australia: II. Isotopic geochemistry of Cr-diopside lherzolites and Al-augite pyroxenites. *Geochimica et Cosmochimica Acta* **52**, 449–459.
- HOLT S. J., HOLFORD S. P. & FODEN J. 2014. New insights into the magmatic plumbing system of the South Australian Quaternary Basalt province from 3D seismic and geochemical data. *Australian Journal of Earth Sciences* **60**, 797–817.
- IRVINE T. N. & BARAGER W. R. A. 1971. A guide to the chemical classification of the common volcanic rocks. *Canadian Journal of Earth Sciences* **8**, 523–548.
- IRVING A. J. & FREY F. A. 1987. Distribution of trace elements between garnet megacrysts and host volcanic liquids of kimberlitic to rhyolitic composition. *Geochimica et Cosmochimica Acta* **42**, 771–787.
- IRVING A. J. & GREEN D. H. 1976. Geochemistry and petrogenesis of the Newer basalts of Victoria and South Australia. *Journal of the Geological Society of Australia* **23**, 46–66.
- JOYCE E. B. 1975. Quaternary volcanism and tectonics in southeastern Australia. In: Suggate R. P. & Cresswell M. M. eds. *Quaternary studies*, pp. 169–178. The Royal Society of New Zealand, Wellington.
- JOYCE E. B. 1988a. Newer volcanic landforms. In: Douglas J. G. & Ferguson J. A. eds. *Geology of Victoria*, pp. 419–426. Geological Society of Australia, Victorian Division.
- JOYCE E. B. 1988b. Cainozoic volcanism in Victoria. In: Clark I. & Cook B. eds. *Victorian geology excursion guide*, pp. 71–80. Australian Academy of Science, Canberra.
- JOYCE E. B. 2003. The young volcanic province of southeastern Australia: physical volcanology and eruption risk. In: Graham I. ed. *Geological Society of Australia Abstracts 71, Insights into volcanic processes, mantle sampling and gems*, pp. 20–26. SGGMP, Central Victoria, 30 September–4 October 2003.
- JOYCE E. B. 2004. The young volcanic regions of southeastern Australia: early studies, physical volcanology and eruption risk. *Proceedings of the Royal Society of Victoria* **116**, 1–13.
- JOYCE E. B. 2005. How can eruption risk be assessed in young monogenetic areal basalt fields? An example from southeastern Australia. *Zeitschrift für Geomorphologie NF, Supplementary Volume* **140**, 195–207.
- KNUTSON J. & NICHOLLS I. A. 1989. Macedon–Trentham. In: Johnson R. W. ed. *Intraplate volcanism in Eastern Australia and New Zealand*, pp. 136–137. Cambridge University Press, Cambridge.
- KORSCH R. J., BARTON T. J., GRAY D. R., OWEN A. J. & FOSTER D. A. 2002. Geological interpretation of a deep seismic reflection transect across the boundary between the Delamerian and Lachlan Orogens, in the vicinity of the Grampians, western Victoria. *Australian Journal of Earth Sciences* **49**, 1057–1075.
- LANGMUIR C. H., KLEIN E. M. & PLANK T. 1992. Petrological systematics of mid-ocean ridge basalts: constraints on melt generation beneath ocean ridges. In: Phipps M. J., Blackman D. K. & Sinton J. M. eds. *Mantle Flow and Melt Generation at Mid-Ocean Ridges*. American Geophysical Union Monograph **71**, 183–280. Washington DC.
- LESTI C., GIORDANO G., SALVANI F. & CAS R. 2008. Volcano tectonic setting of the intraplate, Pliocene–Holocene Newer Volcanic Province (southeast Australia): Role of crustal fracture zones. *Journal of Geophysical Research* **113**, B07407.
- LISTER G. S. & ETHERIDGE M. A. 1989. Detachment modes for uplift and volcanism in the eastern highlands, and their application to the origin of passive margin mountains. In: Johnson R. W. ed. *Intraplate volcanism in Eastern Australia and New Zealand*, pp. 297–313. Cambridge University Press, Cambridge UK.
- MANN B. S., STANLEY D. R. & BOLGER P. F. 1992. Basalt plains hydrogeological and salinity investigation (Progress Report No. 2—Hamilton–Dunkeld Sub Region). *Rural Water Commission Unpublished Report* **1992/1**.
- MARTIN J. M. & MAYER J. J. 1987. Soil and landforms of south-western Victoria, part 1: Inventory of soils and their associated landscapes. *Department of Agricultural and Rural Affairs, Research Report Series* **40**.
- MATCHAN E. & PHILLIPS D. 2011. New $^{40}\text{Ar}/^{39}\text{Ar}$ ages for selected young (<1 Ma) basalt flows of the Newer Volcanic Province, southeastern Australia. *Quaternary Geochronology* **6** (3–4), 356–368.
- MATSUMOTO T., HONDA M., McDUGALL I., YATSEVICH I. & O'REILLY S. Y. 1997. Plume-like neon in a metasomatic apatite from the Australian lithospheric mantle. *Nature* **388**, 162–164.
- MCBRIDE J. S., LAMBERT D. D., NICHOLLS I. A. & PRICE R. C. 2001. Osmium isotopic evidence for crust–mantle interaction in the genesis of continental intraplate basalts from the Newer Volcanics Province, southeastern Australia. *Journal of Petrology* **6**, 1197–1218.
- MCDONOUGH W. F. & MCCULLOCH M. T. 1987. The southeast Australian lithospheric mantle: isotopic and geochemical constraints on its growth and evolution. *Earth and Planetary Science Letters* **86**, 327–340.
- MCDONOUGH W. F., MCCULLOCH M. T. & SUN S. S. 1985. Isotopic and geochemical systematics in Tertiary–Recent basalts from southeastern Australia and implications for the evolution of the subcontinental lithosphere. *Geochimica et Cosmochimica Acta* **49**, 2051–2067.
- MCDUGALL I., ALLSOP H. L. & CHAMALAUN F. H. 1966. Isotopic dating of the Newer Volcanics of Victoria, Australia and geomagnetic polarity epochs. *Journal of Geophysical Research* **71**, 6107–6118.
- MCDUGALL I. & GILL E. D. 1975. Potassium–Argon ages from the Quaternary succession in the Warrnambool–Port Fairy area, Victoria, Australia. *Proceedings of the Royal Society of Victoria* **12**, 295–332.
- NICHOLLS I. A. & JOYCE E. B. 1989. East Australian volcanic geology—Victoria and South Australia—Newer Volcanics. In: Johnson R. W. ed. *Intraplate volcanism in Eastern Australia and New Zealand*, pp. 137–142. Cambridge University Press, Cambridge UK.
- NIU Y. 2008. The origin of alkaline lavas. *Science* **320**, 883–884.
- NIU Y., WILSON M., HUMPHREYS E. R. & O'HARA M. J. 2012. A trace element perspective on the source of ocean island basalts (OIB) and fate of subducted ocean crust (SOC) and mantle lithosphere (SML). *Episodes* **35**, 310–317.
- O'REILLY S. Y. & GRIFFIN W. L. 1985. A xenolith-derived geotherm for southeastern Australia and its geophysical implications. *Tectonophysics* **111**, 41–63.
- O'REILLY S. Y. & GRIFFIN W. L. 1988. Mantle metasomatism beneath western Victoria, Australia: I. Metasomatic processes in Cr-diopside lherzolites. *Geochimica et Cosmochimica Acta* **52**, 433–447.

- O'REILLY S. Y. & GRIFFIN W. L. 2010. The continental lithosphere–asthenosphere boundary: Can we sample it? *Lithos* **120**, 1–13.
- O'REILLY S. Y. & GRIFFIN W. L. 2013. Chapter 12. Mantle Metasomatism. In: Metasomatism and the Chemical Transformation of Rock. In: Harlov D. E. & Austrheim H. eds. *Metasomatism and the chemical transformation of rock*, pp. 471–533. Lecture Notes in Earth System Sciences, Springer Berlin Heidelberg.
- O'REILLY S. Y., NICHOLLS I. A. & GRIFFIN W. L. 1989. Xenoliths and megacrysts of Eastern Australia. In: Johnson R. W. ed. *Intraplate volcanism in Eastern Australia and New Zealand*, pp. 249–287. Cambridge University Press, Cambridge UK.
- OLLIER C. D. 1967. Landforms of the Newer Volcanic Province of Victoria. In: Jennings J. N. & Mabbutt J. A. eds. *Landform studies from Australia and New Guinea*, pp. 315–339. Australian National University Press, Canberra ACT.
- OLLIER C. D. 1985. Lava flows of Mt Rouse, western Victoria. *Proceedings of the Royal Society of Victoria* **97**, 167–174.
- OLLIER C. D. & JOYCE E. B. 1964. Volcanic physiography of the Western Plains of Victoria. *Proceedings of the Royal Society of Victoria* **77**, 357–376.
- OLLIER C. D. & JOYCE E. B. 1968. Geomorphology of the Western District volcanic plains, lakes and coastline. In: McAndrew J. & Marsden M. A. H. eds. *A Regional Guide to Victorian Geology*, pp. 55–68. University of Melbourne, Department of Geology, Melbourne Vic.
- OLLIER C. D. & JOYCE E. B. 1986. Regolith terrain units of the Hamilton 1: 100 000 sheet area, western Victoria. *Bureau of Mineral Resources, Geology and Geophysics Record* 1986/33.
- PEARCE J. A. 2008. Geochemical fingerprinting of oceanic basalts with applications to ophiolite classification and the search for Archean oceanic crust. *Lithos* **100**, 14–48.
- POWELL W., ZHANG M., O'REILLY S. Y. & TIEPOLO M. 2004. Mantle amphibole trace-element and isotopic signatures trace multiple metasomatic episodes in lithospheric mantle, western Victoria, Australia. *Lithos* **75**, 141–171.
- PRICE R. C., GRAY C. M. & FREY F. A. 1997. Strontium isotopic and trace element heterogeneity in the plains basalts of the Newer Volcanic Province, Victoria, Australia. *Geochimica et Cosmochimica Acta* **61**, 171–192.
- PRICE R. C., GRAY C. M., WILSON R. E., FREY F. A. & TAYLOR S. R. 1991. The effects of weathering on rare-earth element, Y and Ba abundances in Tertiary basalts from southeastern Australia. *Chemical Geology* **93**, 245–265.
- PRICE R. C., NICHOLLS I. A. & GRAY C. M. 2003. Cainozoic igneous activity. In: Birch W. D. ed. *Geology of Victoria*, pp. 361–375. *Geological Society of Australia Special Publication*. Vol. **23**. Geological Society of Australia (Victorian Division).
- ROSENGREN N. 1994. *Eruption points of the Newer Volcanics Province of Victoria—an inventory and evaluation of scientific significance*, National Trust of Australia (Victoria) and the Geological Society of Australia (Victoria Division), Melbourne.
- SIMONS B. A. & MOORE D. H. 1999. Victoria 1:1 000 000 Pre-Permian Geology. Geological Survey of Victoria, Melbourne, Vic.
- SINGLETON O. P. & JOYCE E. B. 1970. Cainozoic volcanicity in Victoria. *Geological Society of Australia Special Publication* **2**, 145–154.
- SINGLETON O. P. & JOYCE E. B. 1970. Catalogue of the post-Miocene volcanoes of Victoria, Australia. Prepared for the IAVCEI Catalogue of post-Miocene Volcanoes of the World (unpublished). Incorporated with permission into: Rosengren N. 1994. *Eruption Points of the Newer Volcanics Province of Victoria*, National Trust of Australia (Victoria) & Geological Society of Australia (Victorian Division), Melbourne.
- STONE J., PETERSON J. A., FIFIELD L. K. & CRESSWELL R. G. 1997. Cosmogenic chlorine-36 exposure ages for two basalt flows in the Newer Volcanics Province, Western Victoria. *Proceedings of the Royal Society of Victoria* **109**, 121–131.
- STUCKLESS J. S. & IRVING A. J. 1976. Strontium isotope geochemistry of megacrysts and host basalts from southeastern Australia. *Geochimica et Cosmochimica Acta* **40**, 209–213.
- SUN S. S. & McDONOUGH W. F. 1989. Chemical and isotopic systematics of oceanic basalts: implications for mantle composition and processes. In: Saunders A. D. & Norry M. J. eds. *Magmatism in Ocean Basins. Geological Society of London Special Publication* Vol. **42**, pp. 313–345. London.
- SUTALO F. 1996. *The geology and regolith terrain evaluation of the Mount Rouse lava flows, Western Victoria*. Honours research report, University of Melbourne.
- SUTALO F. & JOYCE B. 2004. Long basaltic lava flows of the Mt Rouse volcano in the Newer Volcanic Province of southeastern Australia. *Proceedings of the Royal Society of Victoria* **116**, 37–47.
- SUTHERLAND F. L., GRAHAM I. T., MEFFRE S., ZWINGMANN H., JOURDAN F. & POGSON R. E. 2014. Multiple felsic events within post-10 Ma volcanism, Southeast Australia: inputs in appraising proposed magmatic models. *Australian Journal of Earth Sciences* **61**, 241–267.
- TURNBULL W. D., LUNDELIUS J. E. L. & McDUGALL I. 1965. A potassium/argon dated Pliocene marsupial fauna from Victoria, Australia. *Nature* **206**, 816.
- VAN OTTERLOO J. 2012. Complexity in monogenetic volcanic systems: factors influencing alternating magmatic and phreatomagmatic eruption styles at the 5 Ka Mt. Gambier Volcanic Complex, South Australia. PhD thesis (unpublished), Monash University.
- VICTORIA DEPARTMENT OF PRIMARY INDUSTRIES 2011. Victoria – Seamless Geology DVD October 2011. ISBN 978-1-74264-976-4(DVD), Melbourne vic.
- VOGEL D. C. & KEAYS R. R. 1997. The petrogenesis and platinum-group element geochemistry of the Newer Volcanic Province, Victoria, Australia. *Chemical Geology* **136**, 181–204.
- WELLMAN P. 1971. The age and palaeomagnetism of the Australian Cenozoic volcanic rocks. PhD thesis, The Australian National University, Canberra ACT.
- WELLMAN P. 1974. Potassium–argon ages of the Cainozoic volcanic rocks of eastern Victoria, Australia. *Journal of the Geological Society of Australia* **21**, 359–376.
- WELLMAN P. & McDUGALL I. 1974. Cainozoic igneous activity in eastern Australia. *Tectonophysics* **23**, 49–65.
- WHELAN J., HERGT J. & WOODHEAD J. 2007. Granite–greenstone connection in western Victoria: an example from the Bushy Creek Igneous Complex. *Australian Journal of Earth Sciences* **54**, 975–990.
- WHITEHEAD P. W. 1986. *The geology and geochemistry of the Mt Rouse and Mt Napier volcanic centres, western Victoria*. Honours research report, La Trobe University, Melbourne.
- WHITEHEAD P. W. 1991. The geology and geochemistry of Mt Napier and Mt Rouse, western Victoria. In: Williams M. A. J., DeDecker P. & Kershaw A. P. eds. *The Cainozoic in Australia: a re-appraisal of the evidence*, pp. 309–320. Geological Society of Australia Special Publication Vol. **18**. Sydney NSW.
- WOPFNER H. & THORNTON R. C. N. 1971. The occurrence of carbon dioxide in the Gambier Embayment. In: Wopfner H. & Douglas J. G. eds. *The Otway Basin of Southeastern Australia*, pp. 377–384. Geological Surveys of South Australia and Victoria Special Bulletin, Adelaide SA.
- YAXLEY G. M., CRAWFORD A. J. & GREEN D. H. 1991. Evidence for carbonate metasomatism in spinel peridotite xenoliths from western Victoria, Australia. *Earth and Planetary Science Letters* **107**, 305–317.
- YAXLEY G. M., GREEN D. H. & KAMENETSKY V. 1996. Carbonatite metasomatism in the southeastern Australian Lithosphere. *Journal of Petrology* **39**, 1917–1930.

Received 20 November 2013; accepted 5 May 2014



Chapters 4 and 5 respectively relate to the physical volcanology and geochemistry of Mt Rouse, the largest eruption source in the Newer Volcanics Province, and are designed to be companion papers. Chapter 4 will be submitted to *The Journal of Volcanology and Geothermal Research* while Chapter 5 was published in *Contributions to Mineralogy and Petrology* in January 2015.

Mt Rouse is shown in these studies to be a very complex volcano, having erupted eight facies from at least seven vents. Because at least three magma batches were involved in the genesis of the volcano (which is nevertheless monogenetic because it erupted during a single series of events), and some facies are shared across at least two of those magma batches, a detailed stratigraphy of the products is essential in establishing both the eruptive history of the complex and the geochemical variation of magmas during its life.

The stratigraphic architecture of Mt Rouse is explored in Chapter 4. Two coherent eruptive facies and six fragmental facies are described prior to discussion of the evolution of the complex in light of the geochemical data (which is presented in full in Chapter 5). As eruption styles varied widely at Mt Rouse, the factors leading to these variations are discussed, with magma composition, mass flux rate, the content of dissolved volatiles in the melt, the involvement of external water during the eruption and vent re-use being the main controls recognised.

Chapter 5 focuses on the geochemical and isotopic analysis of the volcanic products of Mt Rouse. Three batches of magma with major/trace element and isotopic characteristics similar to those of Ocean Island Basalts were identified, mainly on the basis of increasing Light Rare Earth Element enrichment from batch A through B and C. Both isotopic data and the use of geochemical data to estimate the depth and extent of mantle source melting indicate that parental magmas were sourced from a region extending across the lithosphere–asthenosphere boundary. This conclusion was also reached by the analysis of the surrounding volcanoes in the Hamilton area (Chapter 3). The depth of magma generation in the mantle is believed to exert a first-order control on whether the resultant volcano will erupt explosively (upper asthenosphere-derived) or effusively (lower lithosphere-derived), with deeper magmas derived from an increasingly metasomatised mantle. The results of the study will have important implications for petrogenetic modelling in the NVP, because detailed geochemical data can be used to further constrain geodynamic models of magma generation.

Stratigraphic logs for Mt Rouse are contained within Appendix 4, the results of an XRD analysis of a mineral found in the vesicles of basalts close to the coast are in Appendix 5 and the geochemical data for the products of Mt Rouse are in Appendix 6.

Declaration for Thesis Chapter 4

Declaration by candidate

In the case of Chapter 4, the nature and extent of my contribution to the work was the following:

| Nature of contribution | Extent of contribution (%) |
|---|----------------------------|
| Fieldwork, data collection, sample preparation, sieve analysis, SEM analysis, data interpretation and preparation of the manuscript | 80% |

The following co-authors contributed to this work:

| Name | Nature of contribution | Extent of contribution (%) |
|-------------------|---|----------------------------|
| Dr Patrick Hayman | Supervisory role, data interpretation and manuscript preparation. | 10% |
| Dr Ian Nicholls | Supervisory role, manuscript preparation. | 5% |
| Prof. Reid Keays | Supervisory role, manuscript preparation | 5% |

The undersigned hereby certify that the above declaration correctly reflects the nature and extent of the candidate's and co-authors' contributions to this work*.

Julie Boyce

Date

Prof. Reid Keays (main supervisor)

Date

Dr Ian Nicholls

Date

Dr Patrick Hayman

Date



Chapter 4

Stratigraphic architecture of Victoria's largest Cainozoic eruption centre: Mt Rouse, a complex polymagmatic monogenetic volcano, Newer Volcanics Province, Australia

Julie A. Boyce, Patrick C. Hayman, Ian A. Nicholls, Reid R. Keays

Abstract

Mt Rouse is a complex monogenetic volcano, located in the Newer Volcanics Province of southeastern Australia. Here, we present a detailed study of the stratigraphic architecture of Mt Rouse, based on stratigraphic mapping and systematic sampling for petrography. The volcanic products can be divided into eight main facies—two coherent and six fragmental. Coherent lithofacies are C1 lava and C2 discordant coherent basalt. Fragmental lithofacies are P1 coarse grained, moderately to well sorted bedded ash–lapilli–bombs; P2 well sorted fine ash–fine lapilli; P3 moderately to well sorted fine ash–coarse lapilli/small blocks; P4 cross bedded fine ash–fine lapilli; P5 palagonite altered, armoured fine lapilli-rich, ash and P6 spatter agglomerate. The eruption styles associated with these facies include Hawaiian (C1), Strombolian (P1, P6), micro-Plinian (P3, P4), violent-Strombolian (P2) and phreatomagmatic (P5). The products of Mt Rouse define three magma batches (A, B and C), which were erupted from at least seven vents in a complex sequence comprising four phases with no evidence of significant time-breaks. This included sequential eruption of batches A, C and B, then simultaneous eruption of batches A and B, and involved vent reuse, particularly from the southern crater. Controls on eruption style at Mt Rouse may include magma composition, mass flux rate, vent reuse, water influencing the eruption and probably the volatile content of the melt. Mt Rouse is one of the most complex volcanoes in the Newer Volcanics Province, and is unusual worldwide due to its tri-magmatic monogenetic character. This research has broader implications in the emerging field of complex monogenetic volcanism, adding to the observations that monogenetic volcanoes may show great complexity in terms of their stratigraphy, eruption products and timing of events.

4.1 Introduction

Monogenetic volcanoes are among the most common types of continental basaltic volcanism on Earth (Valentine & Gregg 2008), yet they remain poorly understood. Traditionally, monogenetic volcanoes were thought to be simple in nature, each representing a single batch of magma that erupts in a simple manner during one short-lived phase of eruption, which may last hours to years (e.g., Walker 2000). Recent detailed research into individual volcanic centres has shown that, although some monogenetic volcanoes may fit this description, others show extremely complex eruption sequences, and can contain multiple facies and magma batches, or short time-breaks between eruption (e.g., Luhr 2001; Strong & Wolff 2003; Brenna *et al.* 2010, 2011; Erlund *et al.* 2010; Needham *et al.* 2010;

Piganis 2011; Blaikie *et al.* 2012; Jordan *et al.* 2013; van Otterloo 2014; Boyce *et al.* 2015/Chapter 5). The complexity recognised in these volcanic centres rivals that of many large stratovolcanoes (cf. Kereszturi *et al.* 2010; Németh 2010), and can be influenced by the interplay of a wide range of factors such as magma composition, flux rates and extent of degassing, the properties of the country rock and external water availability (e.g., Lorenz 2003; Németh *et al.* 2012; Sohn *et al.* 2012). It is important to gain a fuller understanding of the range of eruption products and complexities of monogenetic volcanoes in order to understand how volcanic fields evolve over time. This will lead to better hazard management of future eruptions. The hazards associated with monogenetic volcanism include lava flows, scoria cone formation, ash plumes, base surges or pyroclastic flows. These may result in severe economic losses, damage to infrastructure and loss of lives.

Mt Rouse, a magmatic volcanic complex in the Newer Volcanics Province (NVP) of southeastern Australia, is an example of a complex polymagmatic monogenetic volcano. Here we present a detailed stratigraphic analysis of the products of Mt Rouse, and show that the volcano erupted three magma batches from at least seven vents to produce a complex stratigraphy via the interplay of eight facies (both coherent and fragmental). This study is a companion paper to Boyce *et al.* 2015/Chapter 5, which explores the geochemistry in more detail. Eruption styles giving rise to these facies are discussed along with the factors influencing eruption style, which varied at Mt Rouse from effusive Hawaiian to relatively low intensity Strombolian eruptions through micro-Plinian, violent-Strombolian and phreatomagmatic. An eruption sequence for the volcano is outlined, including the sequential eruption of the products of the three magma batches, and then the simultaneous eruption of two (e.g., Boyce *et al.* 2015/Chapter 5). Mt Rouse is one of the most complex monogenetic volcanoes known in the NVP, and unusual worldwide due to its tri-magmatic character.

4.2 Geological Setting

The NVP is a late Cainozoic intraplate monogenetic volcanic field, covering >19 000 km², and extending 410 km from Melbourne, Victoria to the Mt Burr range in southeastern South Australia (Figure 4.1). The NVP is composed of >437 short-lived monogenetic basaltic volcanoes (Ollier & Joyce 1964; Joyce 1975; Boyce 2013/Chapter 2; Boyce *et al.* 2014/Chapter 3) which erupted between 8 Ma and *ca* 5000 BP (Blackburn 1966; McDougall *et al.* 1966; Blackburn *et al.* 1982; Cayley *et al.* 1995; Edwards *et al.* 2004; Gray & McDougall 2009; Gouramanis *et al.* 2010). Volcanoes of the NVP range from relatively small scoria cones, lava shields, maars and ash cones/domes to complex volcanoes such as magmatic, phreatomagmatic or maar-cone volcanic complexes (Boyce 2013/Chapter 2). All of the hazards associated with monogenetic volcanism are observed in the stratigraphic record of the NVP, although lava flows and scoria cone formation are most common.

The NVP is subdivided into three subprovinces from east to west—the Central Highlands, Western Plains and Mt Gambier subprovinces (Joyce 1975; Nicholls & Joyce 1989; Sheard 1990; Demidjuk 2005). The Western Plains subprovince (the focus of this study) covers >14 600 km² (Boyce 2013) from Melbourne west to Portland (Figure 4.1), and is characterised by extensive plains-forming lava fields (Nicholls & Joyce 1989). The Western Plains features 42% of NVP volcanic centres (Boyce 2013) and is split by the Mortlake Discontinuity (Price *et al.* 1997), which corresponds to the Palaeozoic Moyston Fault—the boundary between the Delamerian and Lachlan orogens (Korsch *et*

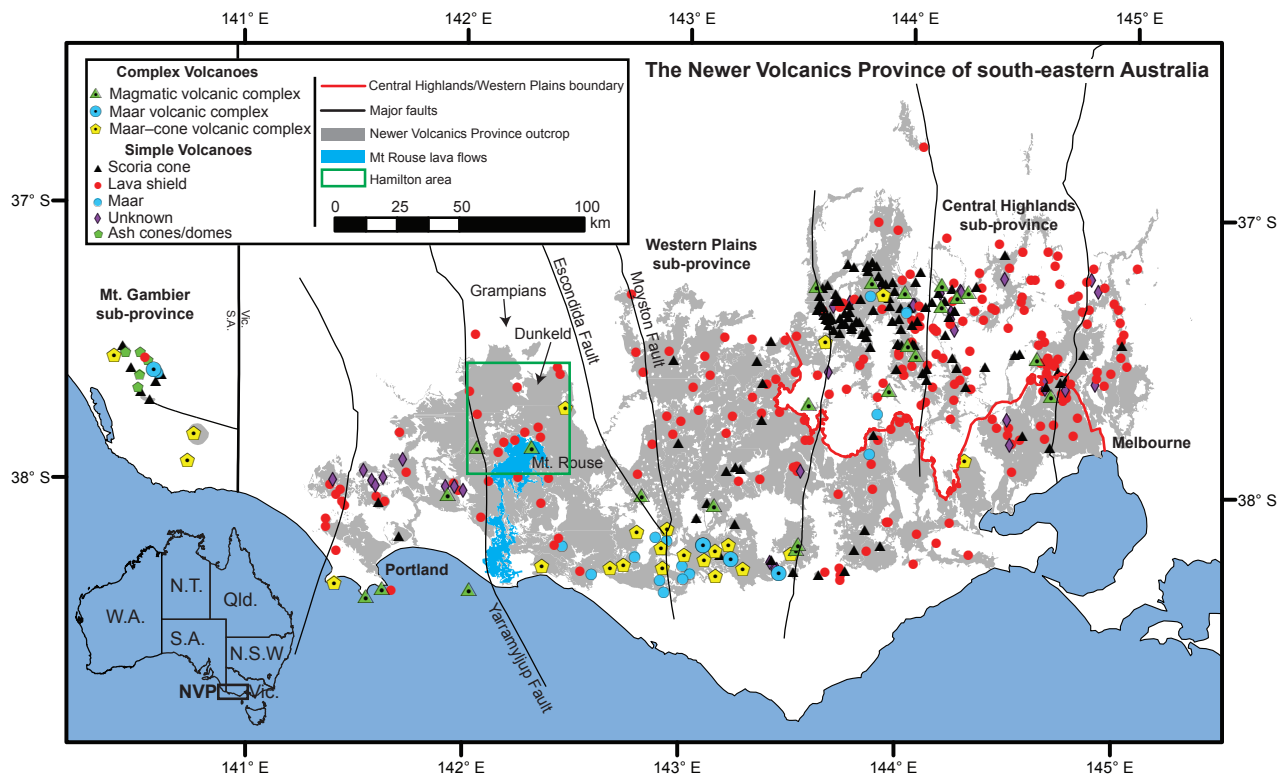


Figure 4.1 The Newer Volcanics Province of southeastern Australia, showing major faults, Newer Volcanics outcrop and distribution of eruption centres, with the Hamilton area outlined by a green square (after Boyce (2013) and Boyce *et al.* (2014)).

al. 2002; Cayley *et al.* 2011). The Mortlake Discontinuity separates higher ^{87}Sr – ^{86}Sr basalts in the east (0.7035–0.7058) from lower ^{87}Sr – ^{86}Sr basalts in the west (0.7035–0.7047) (Cooper & Green 1969; Dasch & Green 1975; Stuckless & Irving 1976; McDonough *et al.* 1985; Whitehead 1986; Ewart *et al.* 1988; Price *et al.* 1997; McBride *et al.* 2001; Foden *et al.* 2002; Demidjuk *et al.* 2007).

4.3 Overview of the Mt Rouse volcanic complex

Mt Rouse is one of the youngest of 16 volcanoes in the Hamilton area of the Western Plains subprovince (Figure 4.1; Boyce 2013/Chapter 2; Boyce *et al.* 2014/Chapter 3), and the largest eruption centre of the NVP by area and volume. Erupting from at least seven vents (this study), the volcano is composed of a 120 m high scoria cone complex and long lava flows up to 60 km in length (Elias 1973; Ollier 1985; Whitehead 1986, 1991; Sutalo 1996; this study) (Figure 4.2; section 4.6.1).

Previous studies of Mt Rouse have focussed mainly on the lava field (Elias 1973; Whitehead 1986, 1991; Sutalo 1996; Sutalo & Joyce 2004). Eruption sequences vary little between authors; with suggestions that the main lava flows were emplaced before the scoria cones and lava shield, and that the northern scoria cone was emplaced before the southern scoria cones (Elias 1973; Sutalo 1996).

K–Ar and ^{40}Ar – ^{39}Ar dating yields ages of 0.284–0.309 Ma for the lava flows of Mt Rouse (Figure 4.2; McDougall & Gill 1975; Ollier 1985; Gray & McDougall 2009; Matchan & Phillips 2011, 2014). Ollier (1985) dated an interbedded lava flow in the southern scoria cone to 1.82 Ma by K–Ar, but this date is considered erroneous (B. Joyce pers. comm. 2010; Matchan & Phillips 2011) because of the narrow spread of the ages of the other samples and the fact that the laws of superposition do not allow for later-erupted products to be 1.52 Myr older than earlier-erupted units. Two samples from the same location have been dated at ~0.45 Ma (Figure 4.2; McDougall & Gill 1975; Matchan

& Phillips 2011); however, both of these dates are considered inaccurate due to extraneous argon contamination in the basalts. Argon contamination results from the incorporation of xenolithic or xenocrystic material, or undegassed glass (Matchan & Phillips 2011). Some of the basalts of Mt Rouse do contain small amounts of xenolithic material (see section 4.5.1.2). An eruption age of 0.284 ± 0.18 Ma is suggested for Mt Rouse (Matchan & Phillips 2014).

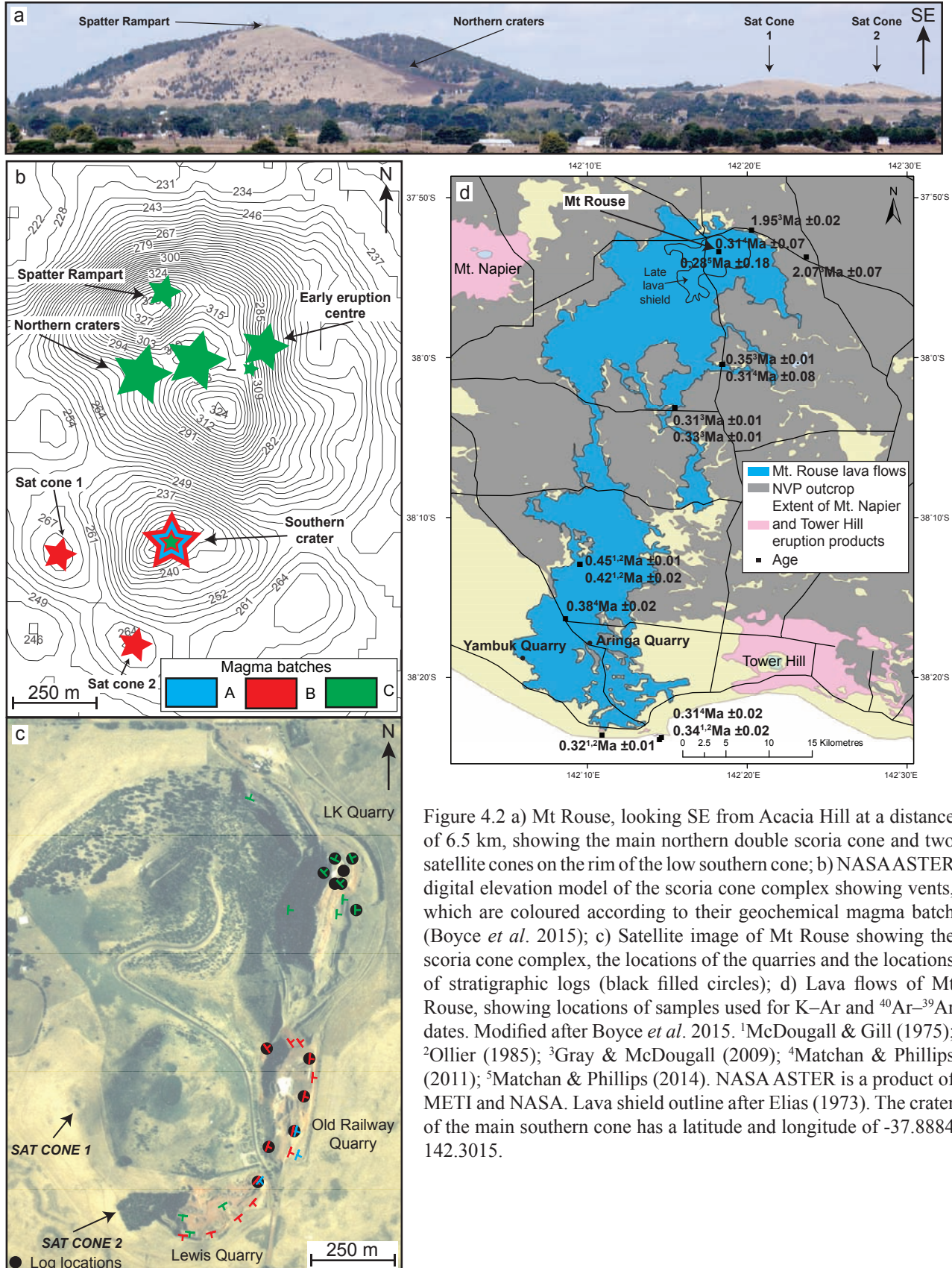


Figure 4.2 a) Mt Rouse, looking SE from Acacia Hill at a distance of 6.5 km, showing the main northern double scoria cone and two satellite cones on the rim of the low southern cone; b) NASA ASTER digital elevation model of the scoria cone complex showing vents, which are coloured according to their geochemical magma batch (Boyce *et al.* 2015); c) Satellite image of Mt Rouse showing the scoria cone complex, the locations of the quarries and the locations of stratigraphic logs (black filled circles); d) Lava flows of Mt Rouse, showing locations of samples used for K–Ar and ^{40}Ar – ^{39}Ar dates. Modified after Boyce *et al.* 2015. ¹McDougall & Gill (1975); ²Ollier (1985); ³Gray & McDougall (2009); ⁴Matchan & Phillips (2011); ⁵Matchan & Phillips (2014). NASA ASTER is a product of METI and NASA. Lava shield outline after Elias (1973). The crater of the main southern cone has a latitude and longitude of -37.8884 142.3015.

4.4 Methods

Detailed stratigraphic mapping was undertaken across the scoria cone complex, with representative samples collected for petrographic and geochemical analysis. Stratigraphic logging of scoria and lava deposits was carried out in the Lewis and Old Railway quarries to the southeast, and quarry faces were mapped on all four levels of the LK quarry to the northeast (Figure 4.2c). Stratigraphic logs could not be produced in the LK quarry due to the complex nature of the deposits and because of active quarrying. Many areas of the quarry were inaccessible as previous quarrying left dangerously unstable, high vertical faces, especially in the southern main LK quarry, and the northern entrance. Two samples were removed from the entrance quarry; the southern LK quarry was inaccessible. Stratigraphic logs may be found in Appendix 4.

Samples were also taken from the southern crater, satellite cones and spatter rampart, and the long lava flows and lava shield were sampled systematically using quarries and roadside cuttings where possible, or flow tops. Flows were not mapped, as they have been well described in previous studies (e.g., Elias 1973; Ollier 1985; Sutalo 1996; Sutalo & Joyce 2004).

Quarry logs and mapped faces were correlated across the scoria cones to determine an order of eruption and unravel the stratigraphic relationships.

4.5 Facies descriptions

The volcanic products of Mt Rouse can be divided into eight main facies, two of which are coherent and six fragmental. Descriptions of the lithofacies follow and are based on field observations, grain-size analysis, and petrographic and scanning electron microscope observations, and are summarised in Table 4.1. A combined stratigraphic log for the complex is shown in Figure 4.3.

Facies descriptions are followed by interpretations, which include the eruption styles responsible for each of them. Identification of eruption styles was based on comparison with those described by Valentine & Gregg (2008), with the addition of micro-Plinian eruptions, which form massive, mainly planar and continuous beds of lapilli and blocks with minor fine ash (Table 4.2; Francis *et al.* 1990; Behncke *et al.* 2006; Cas *et al.* 2011; Blaikie *et al.* 2012; van Otterloo *et al.* 2013; Jordan *et al.* 2013).

Table 4.1 Key facies characteristics of the volcanic products of Mt Rouse

| Facies | Internal Characteristics | Clast Population (group size and shape columns) | Clast shape | Other information | Interpretation |
|-----------|---|--|--|--|---|
| C1 | Massive coherent basalt >14 m thick; local dolerite pods in thick flows; locally hydrothermally altered. | N/A | N/A | Small (4 cm) mantle xenoliths; magma batch A | Pahoehoe lava flows (Hawaiian). |
| C2 | Discordant to bedding; coherent basalt | N/A | N/A | Disaggregated mantle xenoliths; magma batch C | Dyke; coalesced spatter. |
| P1 | Well bedded (0.5 m beds); laterally continuous for ~10 m; bombs define bedding in places; moderately to well sorted | Fine ash-coarse lapilli (~100 µm to 70 cm); most clasts coarse lapilli and bomb size; large spatter bombs up to 1 m long by 15–20 cm thick) | Fluidal, flattened bombs; angular scoria; moderately vesicular; jagged vesicles | Magma batch C | Near-vent pyroclastic airfall (Strombolian) |
| P2 | Well bedded (2 cm to 0.25 m beds); laterally continuous for >38 m; well sorted; reverse graded | Fine ash-fine lapilli (~100 µm to 20 mm); most clasts 0.5–8 mm; few bombs | Angular; vesicularity ranges from low to high and varies within individual clasts | Magma batches B and C | Near-vent pyroclastic airfall (violent-Strombolian) |
| P3 | Well bedded to massive (0.25 m to >1.5 m); moderately to well sorted | Variable; fine ash-fine lapilli (<1–3 mm) to coarse lapilli-small blocks (60–100 mm); mostly of material in 2–64 mm range; small blocks and bombs common | Angular; vesicularity ranges from low to high and varies within individual clasts | Magma batches B and C | Near-vent pyroclastic airfall (micro-Plinian) |
| P4 | Two beds found (30 cm and >1.5 m); cross bedded; well sorted | Fine ash-fine lapilli (~100 µm to 8 mm); most clasts coarse ash (52.43%) to fine lapilli (47.10%); Pele's tears <1 mm to 1 cm | Angular scoria; Pele's hairs and tears ranging from fusiform to spherical | Magma batch A (Pele's hairs and tears); Magma batch B (scorias) | Near-vent dry surge (micro-Plinian) |
| P5 | Massive; mainly structureless with possible relict cross beds; very poorly sorted | Fine ash-fine lapilli (0.03–6 mm); 53% ash; free crystals of olivine (<0.01–0.23 mm), pyroxene (<0.01–0.33 mm) and plagioclase microlites (<0.08 mm); all clasts and many free crystals form armoured lapilli coated in ash rinds 0.1–2.2 mm thick | Vary from angular and vesicular or rounded and vesicular to blocky, poorly-vesiculated and plagioclase-mirolite rich | Glass altered to palagonite; grades upwards into well-developed soil | Small-volume wet pyroclastic flow (Phreatomagmatic. Near-vent.) |
| P6 | Spatter agglomerate | Flattened spatter bombs varying in size with location (see text); ash-coarse lapilli agglutinated matrix (up to 20 mm) (absent in SW satellite cone) | Spatter bombs contain vesiculated interiors and breadcrusted rinds | Magma batches B and C; forms spatter ramparts; 4 mm mantle xenolith in magma batch C at top of northern cone | Near-vent pyroclastic airfall (Strombolian) |

Table 4.2 Eruption styles associated with the facies of Mt Rouse

| Eruption style | Bedding | Texture and grading | Clast size | Clast shape | Clast vesicularity | Welding | Column Height | Reference |
|---------------------------------|--|--|---|---|---|--|---------------|--|
| <i>Proximal (cone) deposits</i> | | | | | | | | |
| Hawaiian | Lenticular to continuous over >10 m | Massive to reverse graded | Coarse lapilli and bombs | Aerodynamic and fluidal (e.g., wrapping around underlying clasts), ragged margins | Moderate vesicularity with a wide range of sizes | Densely to partially welded over much of cone extent | | Valentine & Gregg (2008) |
| Strombolian | Mainly lenticular over several metres to ~10 m, Reverse graded to decimetres to ~1 m thick massive | | Coarse lapilli, blocks and bombs | Aerodynamic shapes (e.g., ribbon, spindle) of coarsest clasts, angular to slightly rounded smaller clasts | Moderate vesicularity with a wide range of sizes | Local moderate to dense welding very close to vent, non-welded elsewhere | | Valentine & Gregg (2008) |
| Micro-Plinian | Massive; mainly planar and continuous | Massive and well sorted. Diffuse stratification | Lapilli and blocks with minor fine ash | Mainly blocky and angular to slightly rounded. Sparse aerodynamic shapes | Highly vesiculated | Non-welded | 6 km | Francis <i>et al.</i> (1990); Behncke <i>et al.</i> (2006); Blaikie <i>et al.</i> (2012); van Otterloo <i>et al.</i> (2013); Jordan <i>et al.</i> (2014) |
| Violent-Strombolian | Mainly planar, continuous over >10 m, locally lenticular. Many thin, stratified beds. Localised, thin, ash-rich cross-bedded horizons. | Massive to graded, internal planar stratification, local reverse-graded lenses reflecting grain avalanches | Coarse ash to coarse lapilli, sparse blocks and bombs | Mainly blocky and angular to slightly rounded. Sparse aerodynamic shapes | Moderate to highly vesicular with abundant small vesicles | | | Macdonald (1972); Pioli <i>et al.</i> (2008); Valentine & Gregg (2008); Erlund <i>et al.</i> (2010); van Otterloo <i>et al.</i> (2013) |

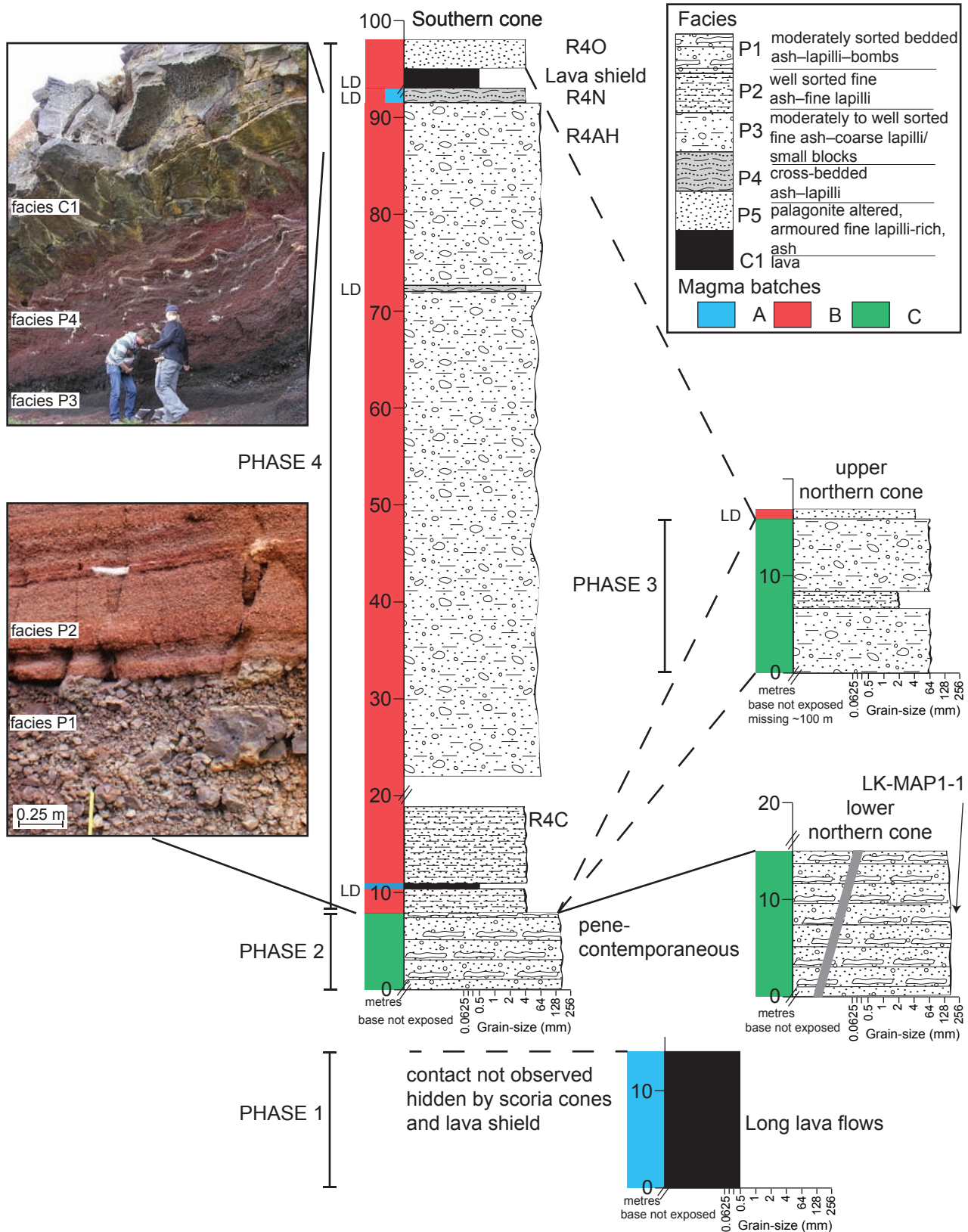


Figure 4.3 Combined stratigraphic log of Mt Rouse, correlating exposed deposits of the northern and southern scoria cones, and the main lava flows and showing samples referred to in the text, main phases of eruption and magma batches of Boyce *et al.* (2015/Chapter 5). The bulk of the northern scoria cone deposits are inaccessible. LD = laterally discontinuous.

4.5.1 Coherent Facies

4.5.1.1 Facies C1: Lavas

Description

The lava flows of Mt Rouse extend 60 km to the coast at Port Fairy and a short distance into present-day coastal waters (Sutalo 1996), covering an area of >511 km² (Figure 4.2). The aerial extent of the flows was calculated in ArcGIS from the Department of Primary Industries seamless geology October 2011 edition. The lava flows form stony rises; these consist of ridges and depressions 3–10 m in height, with 15–30 m between rises creating lobes of lava (Ollier 1985). Sampling and observations were restricted to roadside exposures and quarries. The succession is >14 m thick in quarries (Figure 4.2 4.4a,) and pods of coarse-grained dolerite are found within the interiors of thicker basal flows. The tops of the stony rises are vesicular and internally vesicles are arranged in sheet- and pipe-like formations throughout. The interior of the flows feature vertical cooling joints and horizontal jointing, and have a somewhat rubbly appearance, most likely a product of mining activities (blasting) at the quarry faces (Figure 4.4a).

The lava shield surrounds Mt Rouse for more than 3 km and is visible on satellite imagery as a break in slope (Figure 4.2; Elias 1973; Whitehead 1986; Sutalo 1996). Separate from the long lava flows, the lava shield is associated with a set of interbedded flows in the later deposits of the southern scoria cone (Figures 4.3, 4.4b). Close to the vent, they consist of ropy pahoehoe surfaces and minor lava stalagmites and stalactites, and the final eruption products of the southern crater feature crude columnar jointing (Figure 4.4c). The lava shield itself is distinguished by its stony rises terrain, which has higher ridges and depressions than the earlier lava flows (Sutalo 1996).

Closer to the coast, some basalts show a characteristic light green weathering colour, contain carbonate and clay minerals infilling vesicles and pore spaces, and also magnesite (MgCO₃ as determined by XRD—see appendix 5).

Fresher samples from within the lava flows are light blue-grey in hand specimen (hence their local name “Bluestone”) and fine grained, with a glomeroporphyritic texture composed of glomerocrysts and microphenocrysts of olivine and clinopyroxene in a groundmass of plagioclase, pyroxene and minor opaques (see Boyce *et al.* 2015/Chapter 5). Rare spinel lherzolite xenoliths up to 4 mm occur in the lava flows. They have a coarse equant structure, and are mainly composed of olivine with minor clinopyroxene and Cr-spinel, and common alteration veins of iddingsite.

Interpretation

The lava flows of Mt Rouse are interpreted to be typical products of effusive Hawaiian-style eruptions, representing the least violent activity. Stony rises form when the lava flows beneath semi-solidified crust to create a braided network of inflated lava tubes (Macdonald 1953; Ollier 1985; Hon *et al.* 1994; Self *et al.* 1998). Flow features such as the ropy surfaces found in the lava shield form by deformation of the semi-solidified crust by the motion of the lava (Macdonald 1972; Fink & Fletcher 1978), and lobes from the advancement of the lava flow (Hon *et al.* 1994; Self *et al.* 1998).

The dolerite pods feature the same mineralogy as the host basalts, and represent *in-situ* fractionation, formed due to the insulating effects of the surrounding lava flows (cf. Kuno 1965;

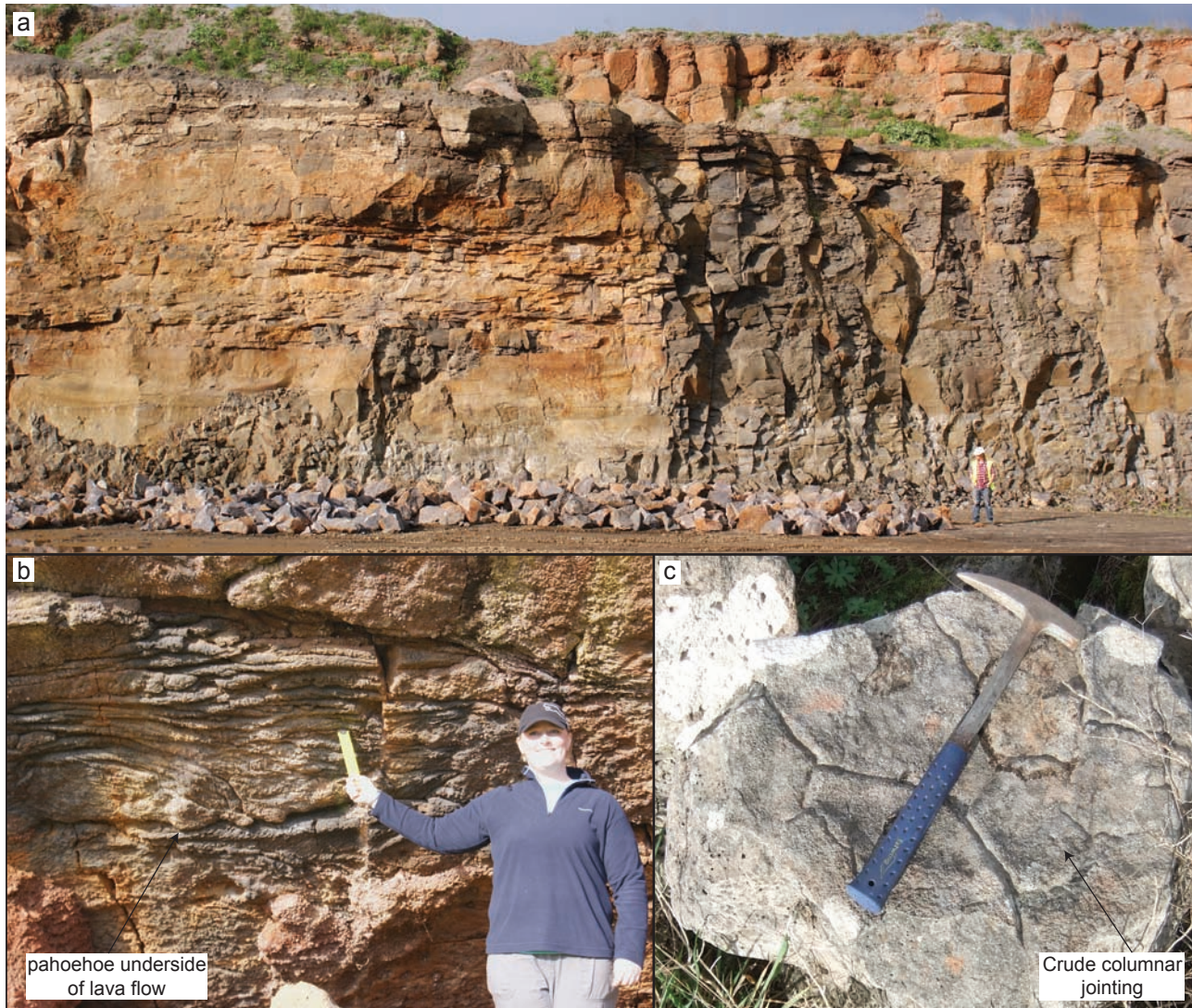


Figure 4.4 Main lava flow features of Mt Rouse. a) Stacked lava flows in Tarrone Quarry 40 km south of the vent (belonging to long lava flows of Figure 3); b) Well-preserved underside of a pahoehoe lava flow, Old Railway Quarry (belonging to lava shield phase of Figure 3); c) crude columnar jointing in basalt block from southern crater (belonging to lava shield phase of Figure 3). Hammer is 40 cm long.

Rogan *et al.* 1996). Rogan *et al.* (1996) analysed pegmatoid autoliths (derived from the flow in which they are contained) and their host basalt from the Auckland Volcanic Field, New Zealand (a similar monogenetic volcanic field to the NVP). They found the autoliths and host flows had sub-parallel Rare Earth Element (REE) profiles, with the autoliths being considerably REE-enriched. The dolerite pods of facies C1 are similar, as they also feature sub-parallel, enriched REE profiles to the host basalt. The hydrothermally altered basalts were produced when meteoric water interacted with the cooling lava, precipitating secondary phases.

4.5.1.2 Facies C2: Discordant coherent basalt

Description

Facies C2 is found in the LK Quarry to the northeast of the volcanic complex, deep within the stratigraphy of the early eruption centre in two separate locations.

Discordant coherent basalt appears in the scoria pile of facies P1. During active quarrying, the basalt feature was reported as ~0.5 m in thickness, planar and vertically oriented, trending NW–SE for ~30 m (C. Kenny, pers. comm. 2012). Only a small portion of the end of the structure remains to

the NW as fingers of branching coherent rock, discordant to the bedding of the facies P1 scoria and with sharp contacts (Figure 4.5a)

An irregularly-shaped mass of coherent basalt occurs in the scoria pile of facies P1, where a cross-section has been revealed by quarrying (Figure 4.5d). The centre of the mass is approximately 1.8 m wide (NNW–SSE) and 1.9 m high (but the base is not exposed) and consists of coherent basalt with no indication of bedding or any individual clasts. The feature appears to be entirely contained within facies P1, although the lower contact is missing due to quarrying. Contacts are either sharp or gradational with the surrounding P1 facies. Gradations occur over 0.5 m, grading from coherent basalt, to friable, discoloured scoria and into moderately-to-well sorted bedded scoria (P1 facies) (Figure 4.5b,c).

Petrographically, the two coherent bodies of the early eruption centre are similar, being blue-grey and fine-grained in hand specimen, with a microporphyritic texture, composed of a groundmass of glass, plagioclase microlites, pyroxene needles, abundant magnetite and material of cryptocrystalline nature. Microphenocrysts of olivine and clinopyroxenes up to 0.25 mm are evenly distributed throughout, and many of the larger crystals are skeletal or embayed, indicating disequilibrium and fast rates of cooling. The basalt has weakly vertically-oriented microlites, small kink-banded olivines and pyroxenes, and in one case a megacrystic kink-banded olivine, the latter presumably representing disaggregated mantle xenolith material. Both samples are petrographically and geochemically similar to the scorias of Mt Rouse and different to the lava flows in terms of phenocryst grain size as the lava flows feature a glomeroporphyritic texture while the coherent bodies are aphanitic (Boyce *et al.* 2015/Chapter 5).

Interpretation

The orientation of the planar coherent basalt pre-quarrying and its coherent and cross-cutting, vertical nature are a clear testament to an intrusive origin (dyke), injected into unconsolidated P1 facies. The branching nature of the coherent basalt represents one of the extremities of the dyke, at the forefront of propagation. As the vast majority of material has been quarried away, it is difficult to say whether the dyke represents a feeder-dyke or a late-stage intrusion.

The large coherent body in the early eruption centre is interpreted as clastogenic in origin, the result of *in-situ* coalescence of spatter bombs, as evidenced by the gradational contacts with the spatter facies. The basalt does not represent an intrusion of magma into the scoria pile, which would result in distorted bedding and sharp contacts. The main body of coherent basalt is indistinguishable from that of the dyke material and there are no visible clasts. However, at the gradational margins, small friable scoria clasts *are* discernable in thin-section and in outcrop. The best interpretation is therefore that this body represents coalescence of fluidal, molten spatter bombs, which are common in the formation of the surrounding P1 facies. This can occur in low-viscosity, high temperature eruptions, as molten pyroclasts rapidly accumulate and coalesce, forming a homogeneous liquid that is degassed (Brown *et al.* 2008). In such deposits, textures may be identical to those of coherent rocks that have not undergone fragmentation (Hayman & Cas 2011).

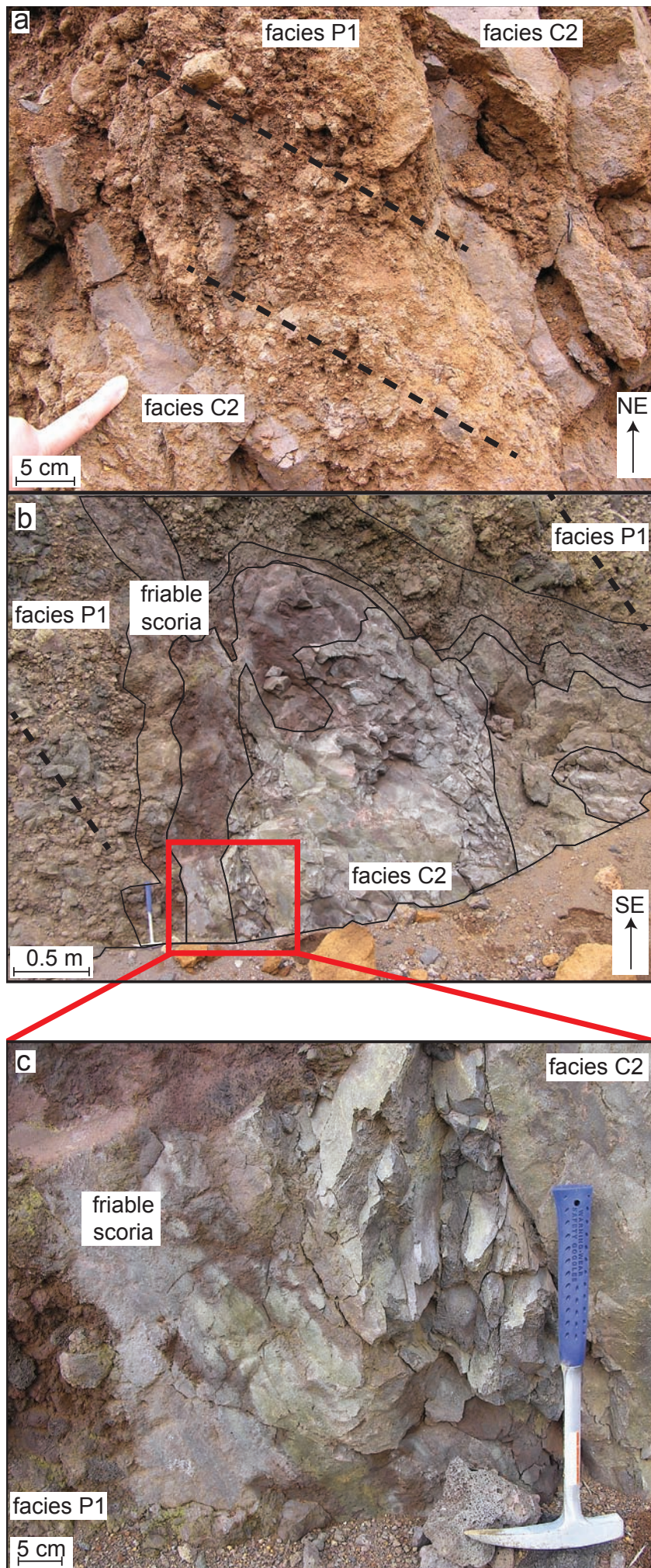


Figure 4.5 a) Close-up photograph of the end-portion of planar coherent basalt, showing branching, discordant intrusion through facies P1, with dashed lines indicating bedding of facies P1; b, c) Body of coherent basalt grading into facies P1.

4.5.2 Fragmental Lithofacies

Fragmental lithofacies can be divided into six types: (1) coarse grained, moderately to well sorted bedded ash–lapilli–bombs, (2) well sorted fine ash–fine lapilli, (3) moderately to well sorted fine ash–coarse lapilli/small blocks, (4) cross-bedded ash–fine lapilli, (5) palagonite altered, armoured fine lapilli-rich, ash and (6) spatter agglomerate.

4.5.2.1 Facies P1: Coarse grained, moderately to well sorted bedded ash–lapilli–bombs

Description

Facies P1 is found in the lower stratigraphy of both the northern and southern scoria cones of Mt Rouse (Figure 4.3). In the northern LK Quarry, beds dip steeply at 50° SW towards a buried vent (Figure 4.6a), while in the southern Lewis Quarry they dip 30° radially away from the southern crater (Figure 4.6b). The base is not exposed in either quarry, leaving approximately 8 m of visible vertical stratigraphy in the south and 15 m in the north. The northern LK quarry exposes beds across an area of 80 m N–S while outcrop is limited to several small sections in the Lewis Quarry due to excavations.

In the lower stratigraphy of the southeastern side of the southern scoria cone (Lewis Quarry; Figure 4.2c), facies P1 directly underlies facies P2 (well sorted fine ash–fine lapilli; Figure 4.3). The contact between the two units is sharp—there is no evidence of erosion or soil formation, but neither does the unit grade upwards from one facies to the next. Both units dip away from the southern crater of Mt Rouse, from which they erupted. In contrast, in the lower stratigraphy of the eastern side of the northern scoria cone (LK Quarry; Figure 4.2c), a gradational contact (several centimetres thick) is seen between facies P1 and P2 (Figure 4.6c).

Facies P1 is generally well bedded; with bed thickness on the order of 0.5 m. Beds are traceable for several metres before being obscured by quarrying because of their steep dip.

Facies P1 consists of fine ash to coarse lapilli (~100 µm to 70 cm), with large spatter bombs. The deposit is moderately to well sorted, with most of the clasts in the coarse lapilli and bomb size ranges. Bombs are ~15–20 cm in diameter (with lengths sometimes in excess of 1 m) with a fluidal appearance, having stretched vesicles in places. They define the bedding in the lower LK Quarry deposits. The remainder of the clast population consists of angular juvenile scoria coated in fine–coarse ash and free crystals of olivine and pyroxene (Figure 4.6d). The scoria clasts are moderately vesicular with vesicles defined by fine crystals rather than glass (Figure 4.6e).

Interpretation

Facies P1 is interpreted as a near-vent scoria airfall deposit formed by a Strombolian-style eruption. Fragmentation was by dry magmatic processes as evidenced by the cusped glass shards and vesicularity (e.g., Heiken 1972, 1974; Heiken & Wohletz 1985; Büttner *et al.* 1999; Dellino *et al.* 2001), and the zone of fragmentation was apparently above the level of the country rock (blocks of which are absent from the deposit) (Table 4.1). The high angle of the bedding and presence of large numbers of spatter bombs indicate that the material was deposited close to vent.

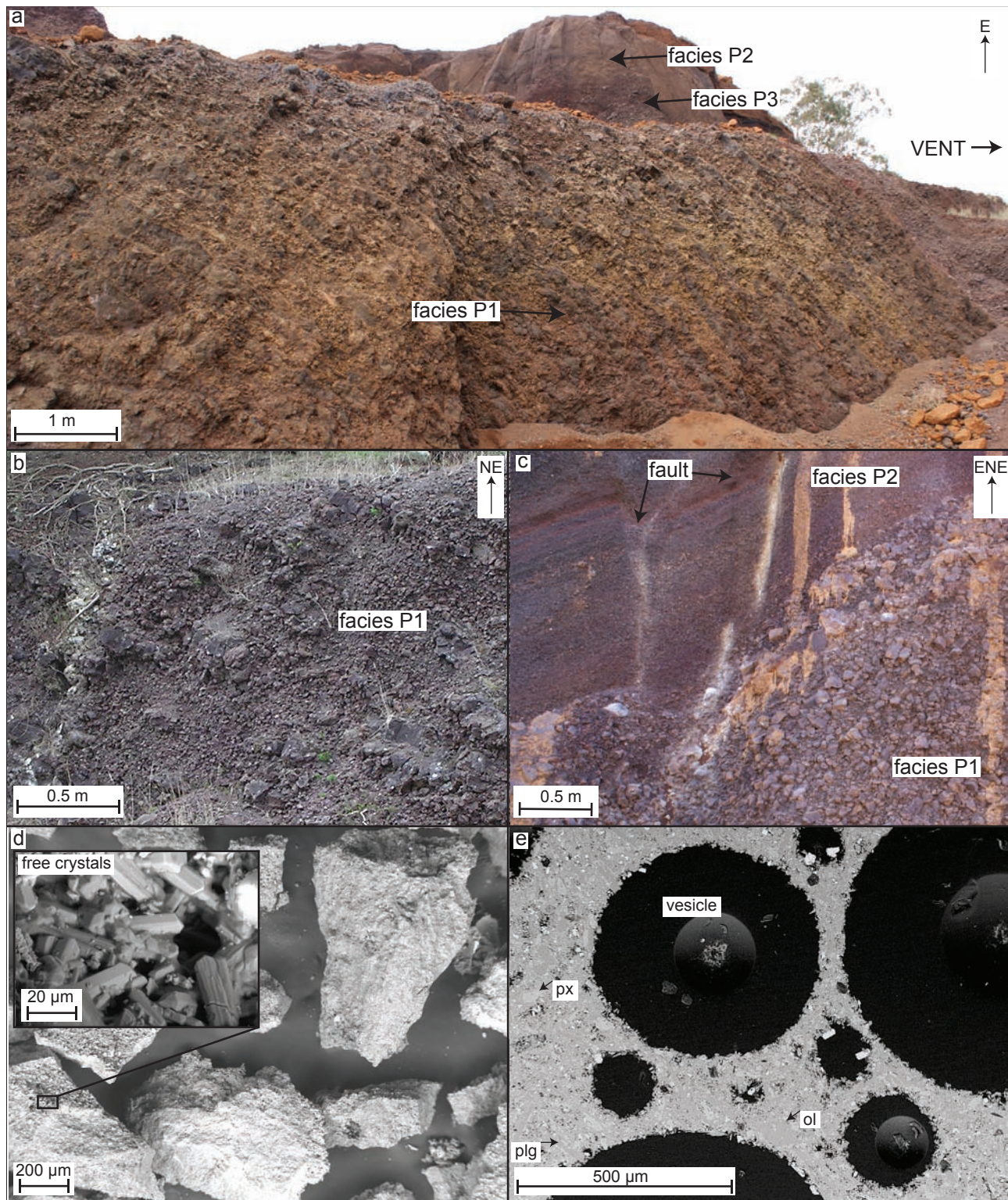


Figure 4.6 a) Moderately to well sorted scoria proximal to the vent, with large spatter bombs defining bedding in the LK Quarry on the northeastern flank of Mt Rouse; b) Poorly sorted scoria in the Lewis Quarry in the southeastern flank of Mt Rouse; c) Contact between facies P1 and P2 in the LK Quarry, showing P1 grading into P2 over a short distance; d, e) Typical backscattered electron images of facies P1 (sample LK-MAP1-1); d) Loose juvenile material of (a), showing ash coating clasts, composed of microcrystals of olivine and plagioclase (inset); e) Typical interior of scoria clasts of facies P1, showing glass (light grey), crystals of olivine and pyroxene with plagioclase microlites (darker greys) and abundant oxides (white).

4.5.2.2 Facies P2: Well sorted fine ash–fine lapilli

Description

Facies P2 is found in the stratigraphy of both the northern and southern cones. In the southern cone, approximately 10 m of the facies directly overlies the basal P1 facies (Figure 4.3). Facies P1 is traceable for >500 m. In the north, 1.8 m of facies P2 is interbedded with, and in gradational contact to, facies P3 in the upper stratigraphy of the northern cone (Figure 4.3). The unit is laterally continuous for approximately 38 m, but is bound by normal faults. Facies P2 is well bedded, with bed thickness ranging from 2 cm (very thin) to ~0.25 m and features reverse grading.

Facies P2 consists of angular juvenile clasts of scoria with cusped glass shards in the matrix (Figure 4.7a). Vesicularity ranges from low to high and varies within individual clasts (Figure 4.7b). Clast sizes range from fine ash (~100 μm) to fine lapilli (20 mm maximum), with the majority of clasts falling in the 0.5–8 mm size range (coarse ash–fine lapilli). Although there are very few bombs in the deposit, bombs do define a single layer towards the top of the southern cone deposits. No identifiable accessory lithics, accidental clasts or mantle xenolith material are present in the scoria and no welded material is present.

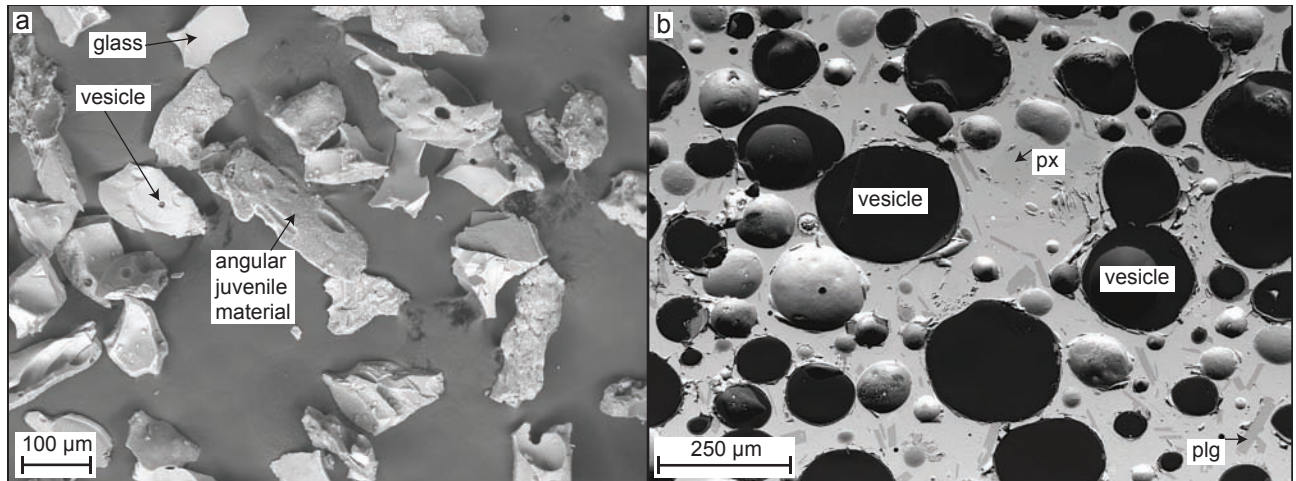


Figure 4.7 Typical backscattered electron images of facies P2 (sample R4C). a) Cusped glass shards of fine ash; b) Typical interior of scoria clasts, showing vesicles (black), glass (light grey) and crystals of olivine and pyroxene with plagioclase microlites (darker greys).

Interpretation

Facies P2 is pyroclastic in origin and was formed by dry magmatic eruptions with the zone of fragmentation above the level of the country rock, shown by the cusped glass shards and lack of country rock fragments respectively. Conformable, planar, continuous bedding mantling topography is indicative of pyroclastic fallout, and the thickness of the beds and degree of fragmentation (1–20 mm-sized clasts) are indicative of violent-Strombolian eruptions (Table 4.1). Such events are more explosive than micro-Plinian eruptions (Cas *et al.* 2011), with increasing magma flux rates, and feature a higher degree of fragmentation. Pulsatory eruptions produce higher eruption columns, which deposit fallout that mantles topography as multiple thin, stratified beds (Macdonald 1972; Pioli *et al.* 2008; Valentine & Gregg 2008; Erlund *et al.* 2010; Cas *et al.* 2011; van Otterloo *et al.* 2013).

The gradation from facies P1 into facies P2 in the northern cone is interpreted as reflecting a sudden increase in eruption intensity over a short period, from Strombolian to violent-Strombolian. The contact between facies P1 and P2 in the south is related to differences in the chemistry of the magmas involved (see section 4.6.1).

4.5.2.3 Facies P3: Moderately to well sorted fine ash–coarse lapilli/small blocks*Description*

Facies P3 forms the main deposits of both the northern and southern scoria cones (Figure 4.3). Approximately 70 m of facies P3 was logged in the deposits of the southern cone, and ~15 m in the upper northern cone. Upwards of 50 m of facies P3 is observable in unstable and inaccessible quarry faces through the northern cone, but the contact with the underlying P1 facies is not observed. Facies P2 and P3 are observed to grade into each other in the northern cone stratigraphy (Figure 4.3, 4.8a), but contacts between facies are not observed in the southern cone due to overburden in the Old Railway Quarry. In the north, beds dip away from the northern double crater, and in the south they dip away from the southern crater. Bedding thickness varies from 0.25 m to >1.5 m thick and is laterally continuous for >500 m.

Facies P3 consists of angular juvenile clasts of scoria with cusped glass shards in the matrix (Figure 4.8b). Vesicularity ranges from low to high and varies within individual clasts (Figure 4.8c). Clast sizes are quite variable within beds and range from fine ash–fine lapilli (~<1–3 mm) to coarse lapilli–small blocks (60–100 mm). However, on sieving, the majority of material falls within the 2–64 mm range (fine lapilli–small blocks), making ash a minor constituent. Small blocks/bombs are common in the deposit, but there are no identifiable accessory lithics, accidental clasts or mantle xenolith material. No welded material is present.

Interpretation

Facies P3 is pyroclastic in origin, from dry magmatic eruptions with the zone of fragmentation above the level of the country rock, evidenced by the cusped glass shards and lack of country rock. Bedding that mantles topography and well sorted deposits are indicative of pyroclastic fallout (Cas & Wright 1987). The thickness of the beds (0.5 m to >1.5 m) and degree of fragmentation (average 2–64 mm-sized clasts) are indicative of micro-Plinian eruptions (Table 4.1; Francis *et al.* 1990; Behncke *et al.* 2006; Blaikie *et al.* 2012; van Otterloo *et al.* 2013; Jordan *et al.* 2014), rather than Strombolian eruptions, because the material mantles the topography, indicating fallout from a sustained eruption column. The violent-Strombolian eruptions of facies P2 are clearly different both in terms of bed thickness (2 cm to 0.25 m) and grain size (average 0.5–8 mm).

The grading of facies P2 (violent-Strombolian) into P3 (micro-Plinian) indicates that the eruption style varied in intensity throughout a single series of eruptions.

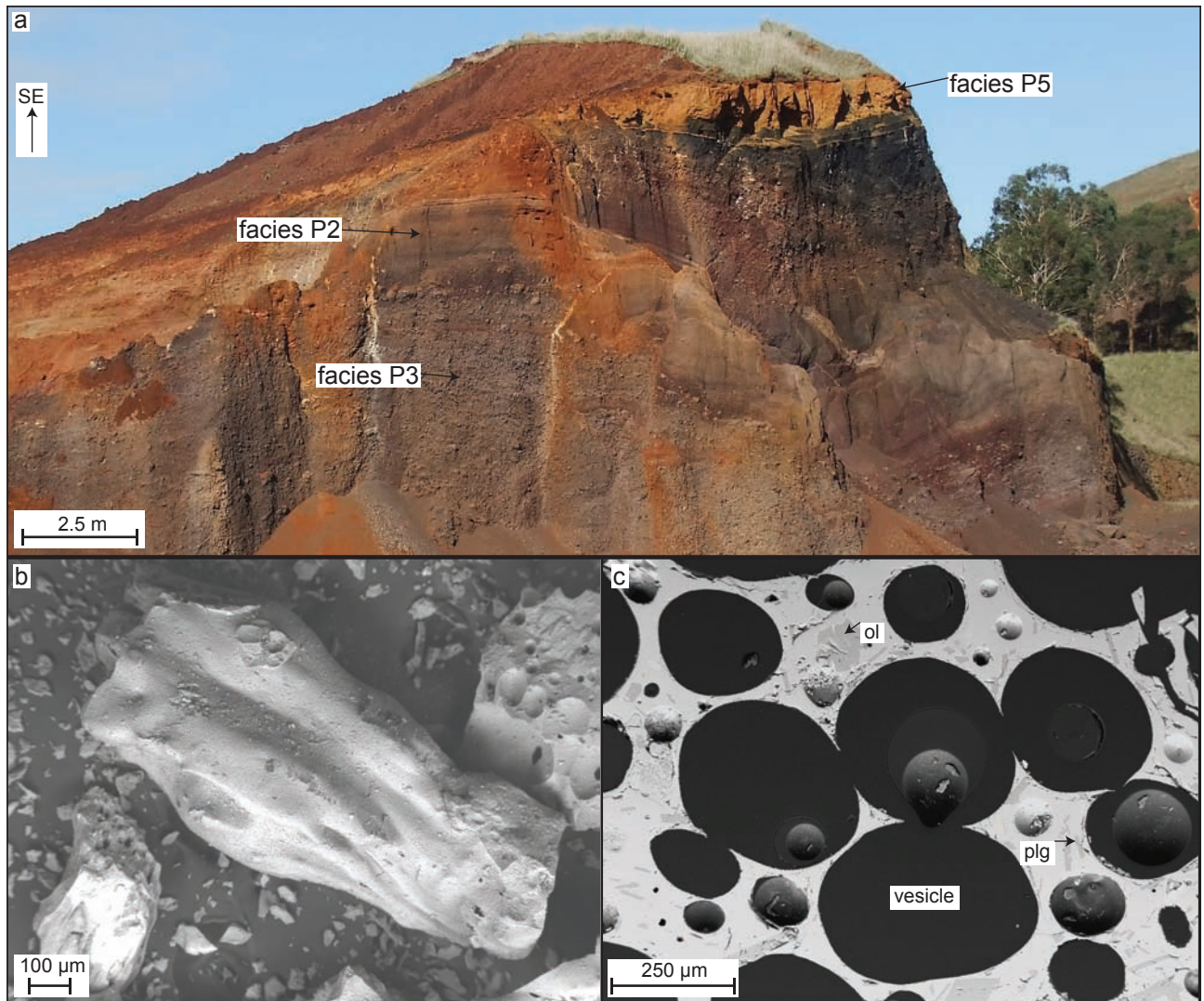


Figure 4.8 a) Facies P3 grading into facies P2 in the LK Quarry to the northeast of Mt Rouse; b, c) Typical backscattered electron images of facies P3 (sample R4AP); b) cusped glass shards of fine and coarse ash; c) typical interior of scoria clasts, showing vesicles (black), glass (light grey) and crystals of olivine with plagioclase microlites (darker greys) (sample R4AP).

4.5.2.4 Facies P4: Cross-bedded fine ash–fine lapilli

Description

Facies P4 is found exclusively in the deposits of the upper southern cone (Figure 4.3); it has a thickness of 1.8 m over two units that are stratigraphically approximately 20 m apart (lower unit = 30 cm and upper unit = >1.5 m thick; Figure 4.3). Cross bedding in the form of pinch-and-swell structures is ubiquitous (Figure 4.9a). Facies P4 is laterally discontinuous, but the uppermost unit can be traced for more than 300 m before it pinches out beneath facies C1 (lavas).

Facies P4 consists of well sorted angular juvenile clasts of scoria ranging from fine ash to fine lapilli (100 µm to 8 mm). However on sieving the majority of clasts fall in the coarse ash (52.43%) to fine lapilli (47.10%) size range and there are no accretionary lapilli (Figure 4.9b). The uppermost (and thicker) of the two units also contains both well preserved and broken up Pele's tears (achneliths) and fragments of broken Pele's hair (Figure 4.9c, d). The tears form a variety of shapes and sizes from <1 mm to 1 cm, perfectly spherical, classic teardrop shapes, fusiform or globular, while the hairs are broken into fragments up to 9 mm long and can be extremely fine and delicate (Figure 4.9c, d). Many tears are still attached to the hairs, and feature crystal clusters in the head and elongated stretched vesicles with their long axes running through the hair.



Figure 4.9 a) Cross-bedded fine ash–fine lapilli deposit showing pinch and swell structures; b) backscattered electron image of deposit R4N showing angular juvenile scoria clasts and a single Pele's tear in the field of view; c) Pele's tears ranging from perfectly spherical to classic teardrop shapes; d) Broken fragments of Pele's hair.

Interpretation

The lack of substantial amounts of fine ash (<1%) and the presence of clasts with sharp, cusped boundaries are indicative of dry magmatic pyroclastic eruptions, while the pinch and swell structures are evidence of transportation and deposition via a surge event. Phreatomagmatism creates clasts that are blocky in shape with stepped fracture from brittle fragmentation (Heiken 1972, 1974; Heiken & Wohletz 1985; Dellino & La Volpa 1995; Büttner *et al.* 1999, 2002; Dellino *et al.* 2001) and accretionary lapilli are a common occurrence (but are not found in facies P4). Dry surge events are common during micro-Plinian and violent-Strombolian events (Francis *et al.* 1990; Valentine & Gregg 2008), as gas builds up in the magma, or very small amounts of water entering the eruption column generate lateral explosions of gas, which sweep up loose pyroclasts and deposit them. Indeed, two individual surge events can be seen in the stratigraphy of the southern cone of Mt Rouse, both of which grade upwards from micro-Plinian fallout. However, Pele's hair and tears form during Hawaiian-style fire-fountaining events through the explosive eruption of low viscosity magmas (Walker & Croasdale 1971; Duffield *et al.* 1977; Heiken & Wohletz 1985; Moune *et al.* 2007; Porritt *et al.* 2012)—a direct contrast to the higher viscosity magmas leading to violent-Strombolian and micro-Plinian deposits. No literature could be found relating to Pele's tears and surge deposits, meaning that such deposits are unusual worldwide. It is most likely that the achneliths formed first and were entrained into the surge deposit as it travelled.

The upper surge deposit, which pinches out beneath lava flows, was either eroded before the lava was emplaced or by the lavas themselves.

4.5.2.5 Facies P5: Palagonite altered, armoured fine lapilli-rich, ash

Description

Facies P5 is the uppermost deposit across the eastern side of the southern scoria cone and the northeastern side of the northern scoria cone. It is a rich orange colour, varying in thickness from <0.25 m in the far north and south of the scoria cones, to 3 m in the southeast. Facies P5 occurs above facies P2, P3 and C1 and grades upwards into a well-developed soil approximately 1–1.5 m thick (Figure 4.10a). To the north, the contact with facies P3 is sharp, as there is a sudden increase in ash content and palagonitisation is ubiquitous in facies P5. The contact with facies C1 to the south is also sharp as C1 is a lava flow and P5 pyroclastic. In the southern cone P5 shows a sharp contact with facies P3 and is defined by a layer at the top of P3 rich in bombs (Figure 4.10a,b). The contact between facies P5 and facies P2 varies between planar and undulating. Where the contact is undulating it appears as a gradational discolouration downwards (orange) into the fresh black scoria of facies P2. Where the contact is sharp, black scoria is overlain by the orange ash and armoured lapilli-rich P5 facies. Facies P5 appears massive and structureless in all locations; however, on excavation in a few places it is possible to discern some relict bedding that appears haphazard and laterally discontinuous. It is unclear if these beds represent cross beds; no directional data could be obtained from them.

Facies P5 is unconsolidated and very poorly sorted, with clast sizes ranging from fine ash to fine lapilli (0.03–6 mm with 53% of the deposit comprised of ash). The matrix material is a mid-brown colour and is composed of abundant glass, which is mainly altered to palagonite (glass altered to an orange colour represents gel palagonite and dark brown areas are most likely smectite; Figure 4.10c). Facies P5 also contains abundant free crystals of olivine (<0.01–0.23 mm), pyroxene (<0.01–0.33 mm) and plagioclase microlites (up to 0.08 mm long) (Figure 4.10d). The matrix forms the rinds of armoured lapilli, which are lithic fragments or free crystals surrounded by a coating of ash and are similar to those described by other authors (e.g., Waters & Fisher 1971; Vespermann & Schmincke 2000; White & Houghton 2000; Thordarson 2004), where the microlites sometimes show preferred orientation around the internal clasts. All scoria clasts represent armoured lapilli, being coated in rinds (0.1–2.2 mm thick) of the unstructured ash. Three different populations of armoured lapilli are observed based on differences between core clast type as identified in thin section: (1) angular vesiculated juvenile clasts with variable palagonitisation (2) rounded vesicular clasts with palagonitised glass (Figure 4.10d) and (3) blocky, very poorly vesiculated, plagioclase-microlite rich clasts. Free crystals of olivine and pyroxene 0.1–0.2 mm are also abundant in Facies P5 as the smaller fraction of armoured lapilli; these have ash rinds 45 µm to 0.1 mm in width (Figure 4.10e). No country rock material is found in facies P5.

Interpretation

The massive and poorly sorted character of the P5 facies indicates deposition by mass flow, while the proximity to the southern crater of Mt Rouse and volcanic nature of components suggest either a pyroclastic or debris flow. Due to the presence of large amounts of armoured lapilli facies P5 is most likely a small-volume pyroclastic flow that entrained and abraded material during deposition. It is common for such flows to produce poorly sorted massive deposits (Brown & Andrews 2015). Ash has filtered down through the underlying deposits over time, partly obscuring the internal structure.

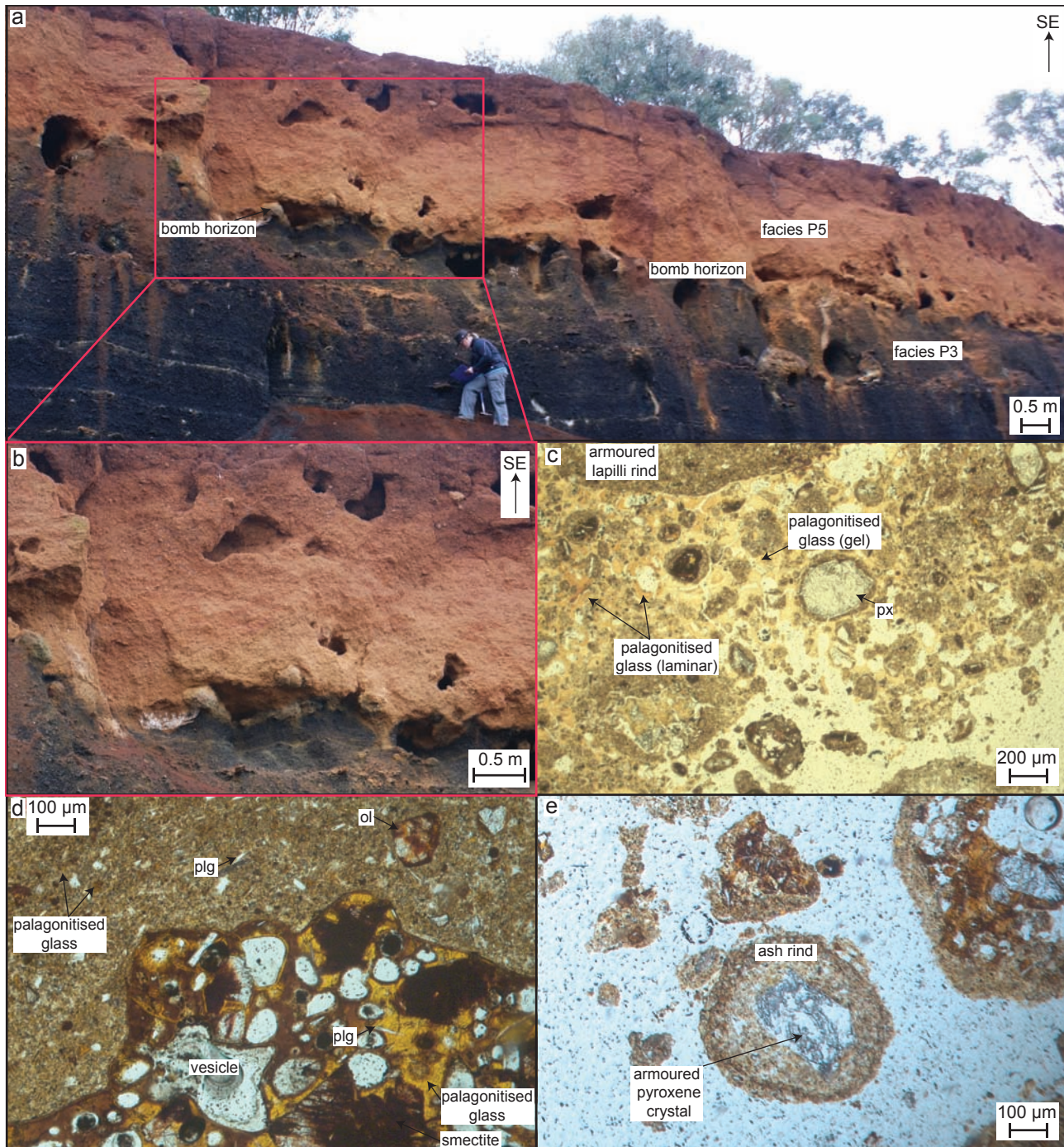


Figure 4.10 a) Facies P5 overlying facies P3 in the Old Railway Quarry, associated with a bomb-rich horizon; b) close-up of the contact between facies P5 and P3; c) ash matrix of facies P5 showing gel and laminar palagonite-altered glass and free crystal of pyroxene (sample R40); d) armoured lapilli with reworked, rounded, palagonite-altered core (right) and thick ash rind (left) with olivine microphenocrysts and rich in plagioclase microlites (sample R40); e) small armoured lapilli with free crystal of pyroxene making up the core (sample R40).

The abundance of ash in the deposit (>53%) coupled with the presence of armoured lapilli indicates phreatomagmatism. Ash tends to aggregate when there is >5% water available during an eruption (Houghton *et al.* 2015) and water forms the dominant control on armoured lapilli formation (Gilbert & Lane 1994; Sparks *et al.* 1997; Costa *et al.* 2010; Durant *et al.* 2010; Folch *et al.* 2010; Telling & Dufek 2012). The absence of country rock lithic clasts indicates surface waters drove magma fragmentation, rather than an aquifer. The intensity of alteration is further support for a phreatomagmatic origin, with the water incorporated into the fragmental debris driving alteration reactions.

The first population of armoured lapilli (1) are inferred as juvenile clasts due to their angularity.

Population (2) are reworked accidental clasts abraded during the eruptive event. Rounding of scoria clasts is indicative of abrasion, and either long transport histories or significant interaction in a turbulent flow (e.g., Dufek & Manga 2008; Kueppers *et al.* 2012). Since the material is close to the vent and the deposit is not found further from the vent than ~800 m, interaction in a turbulent flow is more likely. Such abrasion can also add substantial amounts of ash to a deposit (Dufek & Manga 2008). Population (3) are cognate lithics, which are typically non-vesiculated (Cas & Wright 1987). Due to their crystalline nature, they were most likely eroded from the conduit walls during eruption.

Basaltic glass can be altered to palagonite either during a hydrovolcanic eruption or post-deposition by either weathering or from hydrothermal activity (Vaniman *et al.* 1992; Stroncik & Schmincke 2002). Hydrothermal activity is ruled out in the case of Mt Rouse due to the restriction of palagonite only to facies P5, but weathering must have played some role (which is probably ongoing).

4.5.2.6 Facies P6: Spatter agglomerate

Description

Facies P6 is found in association with facies P1 in the lower stratigraphy of the northern cone and as isolated outcrops at the top of the northern cone and southern satellite cones.

In the lower stratigraphy, the spatter deposit is approximately 14 m thick, and although it seems discordant with the bedding of facies P1 and laterally discontinuous at approximately 12 m across (Figure 4.11a), relict bedding of facies P1 can be faintly seen. On top of the northern scoria cone facies P6 forms a linear NE–SW spatter rampart approximately 60 m in length formed of isolated boulders that is ~1.6 m high (Figure 4.11b). The facies below P6 is unknown due to the presence of vegetation, but is presumed to be fragmental in nature as the location is the summit of the northern scoria cone. The placement of a weather station at the summit may have led to the removal of part of the spatter rampart. To the south, facies P6 is found at the vents of the two satellite cones on the rim of the southern crater. At the southwestern satellite cone, a small spatter rampart 13 m long and 1.5 m high can be seen; while the southern satellite cone features low (<0.25 m) weathered boulders with the outlines of spatter clasts still visible.

In the lower stratigraphy, facies P6 forms a poorly sorted mixture of fluidal spatter bombs of variable sizes. The largest bombs are ~1.3 m in length and 0.5 m high, flattened on impact and the smallest 0.25 m long and 0.4 m high. In general the bombs have vesiculated interiors and breadcrusted rinds. The matrix consists of fine ash–coarse lapilli and is similar to that of facies P1 (but less abundant), with which it is associated.

On top of the northern cone, facies P6 consists of flattened spatter bombs up to 0.5 m long and 8 cm thick in a matrix of agglutinated coarse ash–medium oxidised lapilli (2–20 mm). A single mantle xenolith was found in the deposits; this was 4 mm in length and was composed mainly of kink-banded olivine. In contrast, the spatter rampart of the southwestern satellite cone is composed of large blocks and lapilli are absent.

Interpretation

The presence of spatter bombs and lapilli is indicative of dry magmatic, low intensity fragmentation above the level of country rock as airfall deposited close to the vent in order for

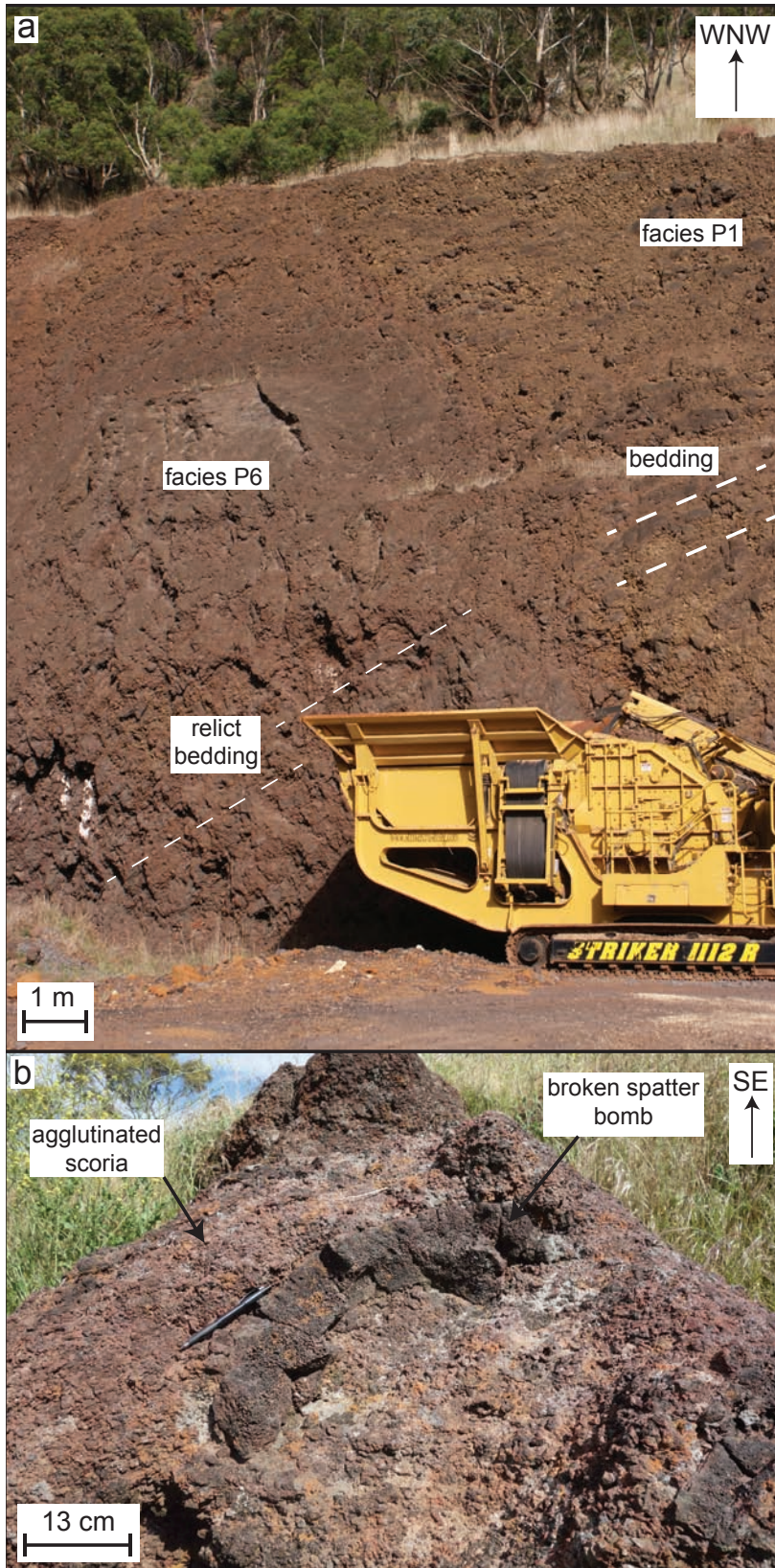


Figure 4.11 a) Facies P6 in association with facies P1 in the lower stratigraphy of the northern cone, showing an area dense with spatter bombs that show relict bedding consistent with the surrounding P1 deposits; b) Facies P6 deposits at the top of the northern scoria cone showing agglutinated scorias and large broken spatter bomb.

agglutination to occur. Spatter is characteristic of Strombolian eruptive styles (Table 4.1) as fragments of magma erupted near-vent are plastically deformed while hot and form agglutinate on contact (Blackburn *et al.* 1976; Batiza & White 2000; Vergnolle & Mangan 2000).

The deposits in the lower stratigraphy were erupted contemporaneously to facies P1 as relict bedding can be seen—they represent an increase in the proportion of spatter bombs during the eruption and most likely not a small vent forming a spatter cone as initially interpreted by Boyce *et al.* (2015; Chapter 5). Those of the northern scoria cone and southern satellite cones are the final eruption products and represent waning magmatism.

4.6 Discussion

4.6.1 Stratigraphic architecture and evolution of the Mt Rouse complex

Mt Rouse is a complex volcano, having erupted eight different facies from at least seven vents; many of these eruptions were discrete and some involved the reuse of already-open conduits. The geochemistry of the deposits provides further constraints on eruption sequence of Mt Rouse and highlights the complex nature of the stratigraphic architecture and eruption sequence of the volcano.

The products of Mt Rouse have been geochemically analysed throughout the stratigraphy detailed in this study (Boyce *et al.* 2015/Chapter 5). Geochemically the products are similar to Ocean Island Basalts, and three distinct magma batches were defined with increasing alkalinity (batches A, B and C; Boyce *et al.* 2015/Chapter 5). Batch A consists of alkali to subalkali basalts, batch B ranges from alkali basalt to hawaiite and batch C alkali basalt through hawaiite to basanite. The magmas are increasingly enriched in the Light Rare Earth Elements from batch A through to batch C (Boyce *et al.* 2015/Chapter 5).

Magma batch A constitutes the entirety of facies C1 (lavas), which encompasses the long lava flows and the interbedded lava shield (including the final eruption products of the southern crater), and the achneliths of the upper unit of facies P4 (cross bedded fine ash–fine lapilli) but not the scorias (Figure 4.3). This has important implications for the stratigraphic architecture of the complex. Magma batch A erupted over at least two phases—the long lava flows and the lava shield. The latter must have begun with Hawaiian fire fountaining that created the achneliths that were consequently swept up into the dry surge deposit of a different magma batch (see below). Because the surge grades upwards from fallout, and both the surge and the lava dip away from the southern crater, this implies that two batches of magma were erupting from the same or closely spaced vents at similar times. The eruption that created the achneliths went on to create the lava flow directly above the surge deposit that is associated with the lava shield.

Magma batch B constitutes the upper half of the pyroclastic deposits of the southern cone, which include facies P2 (well sorted fine ash –fine lapilli), P3 (moderately to well sorted fine ash–coarse lapilli/small blocks), the scorias of facies P4 (cross-bedded fine ash–fine lapilli), and the armoured lapilli of facies P5 (palagonite altered, armoured lapilli-rich, ash). That these facies are found both above and below the interbedded lava flow, all dipping away from the southern cone, provides further evidence of two magma batches erupting at similar times from the same or closely-spaced vents.

Magma batch C comprises the entirety of facies P1 (coarse grained, moderately to well sorted bedded ash–lapilli–bombs) in the lower northern and southern cones, and facies P2, P3, P6 and C2 in the northern cone. This implies that two small Strombolian cones were active before the main northern cone built up.

The architecture and evolution of the Mt Rouse complex can be split into four distinct phases using stratigraphic, geochemical and facies analysis together (Figure 4.3 and 4.12; Table 4.3), viz: (1) extrusion of the long lava flows, (2) low cone-building south–north (3) main northern cone-building and (4) southern cone-building coupled with extrusion of the lava shield. This is shown in Figure 4.12 alongside the facies distribution.

4.6.1.1 Phase 1: Long lava flow extrusion

The long lava flows of Mt Rouse were the first products to erupt because the scoria cones sit on top of them (e.g., Elias 1973; Whitehead 1991; Sutalo 1996). The lavas (facies C1; magma batch A) were erupted onto relatively flat topography with an average gradient of 1:200 (300 m in 60 km) from cone to sea (Ollier 1985). Geomorphic and regolith relationships suggest the flows are all from Mt Rouse (Ollier, 1985; Whitehead 1991; Sutalo & Joyce, 2004), and this study shows the lavas to be geochemically and petrographically similar. During eruption of pahoehoe, little lava usually accumulates near-vent because of the efficiency of transport of the fluidal lava through crusted-over lava tubes (Self *et al.* 1998).

Vents for the initial lava flows must have been buried by the construction of the scoria cones. Since they are not exposed through quarrying, the vent type is unknown; however, it is clear that any edifice that built up was of very low profile. These eruptions do not constitute a separate volcano because magmas of identical composition and petrology erupted during the building of the southern scoria cone to create the lava shield (Boyce *et al.* 2015/Chapter 5). Low profile lava shields are common in the NVP—for example the edifice of the nearby Jays Hill lava shield is only 9 m high (Boyce *et al.* 2014/Chapter 3).

4.6.1.2 Phase 2: Low south–north cone-building phase

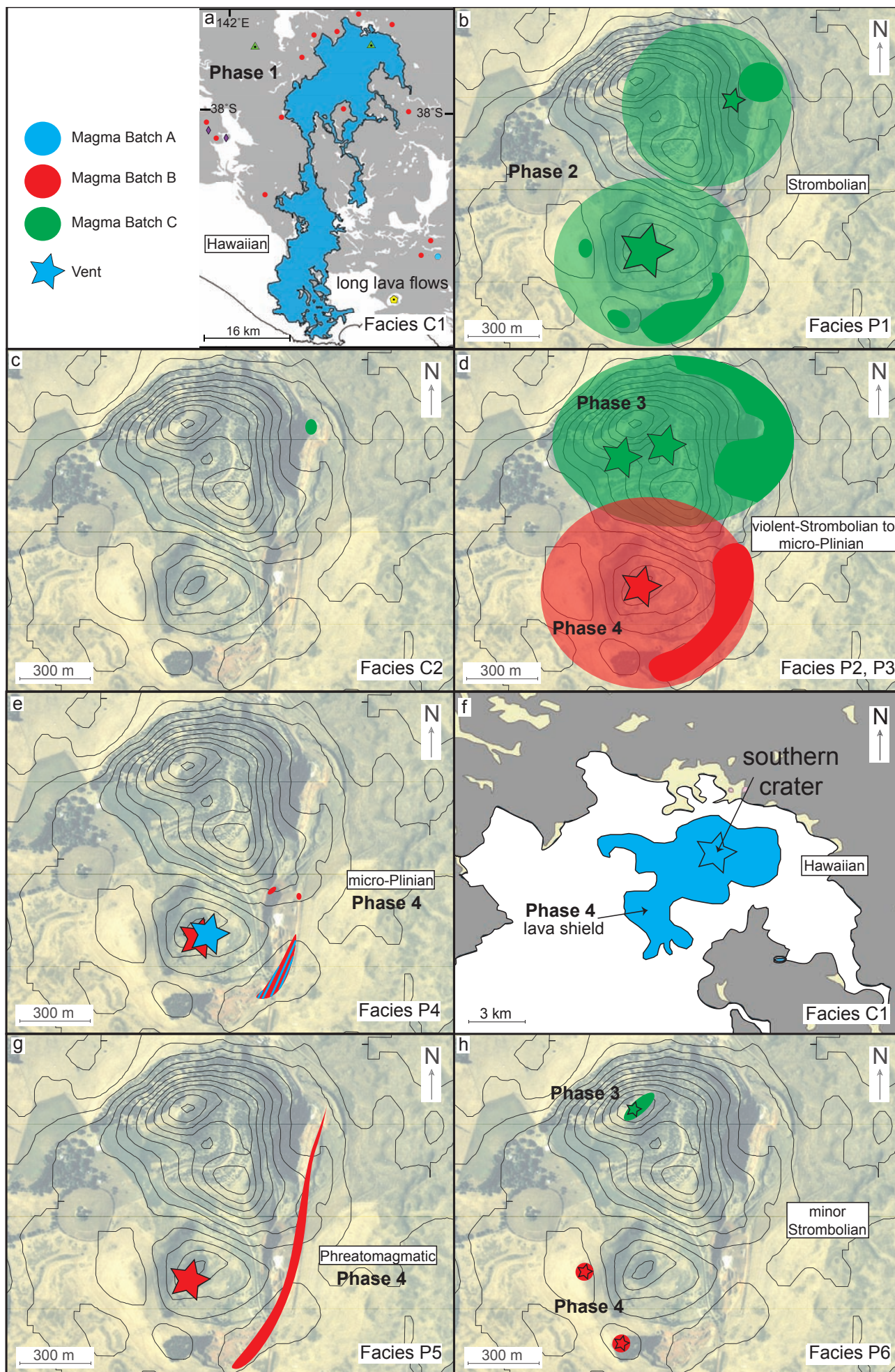
By examining the lower parts of the stratigraphy of both the northern LK Quarry (levels 3 and 4; Appendix 4) and southern Lewis Quarry, two vents can be identified (by strike/dip of beds e.g., Figure 4.2) which erupted facies P1 (coarse grained, moderately to well sorted bedded ash–lapilli–bombs) to form two low Strombolian scoria cones, both of magma batch C composition (Figure 4.3).

Although the contact between the two cones was not observed, it is likely that the eruptions began in the south with the construction of the southern Strombolian cone before shifting to the north, because the eruption of magma batch C then intensified (Phase 3) to create the main northern cone.

4.6.1.3 Phase 3: Main northern cone-building phase

The stratigraphy of the upper LK Quarry and the summit of the northern cone reveal the nature of the main cone-building phase of the northern scoria cone, which is composed of magma batch C. The two main vents for Phase 3 form a double crater with a horseshoe shape reaching ~95 m above the surrounding lava plains that is breached to the west. Because the quarries examined are on the outer flanks of the scoria cone they only reveal details of the later parts of the material produced by the eruption; these consist of facies P2 (well sorted fine ash–fine lapilli; violent-Strombolian) and P3 (moderately to well sorted fine ash–coarse lapilli/small blocks; micro-Plinian), with minor amounts

Figure 4.12 (right) Digital elevation models of Mt Rouse (NASA ASTER) for each facies, showing exposed (solid) and inferred (transparent) distribution. Colours refer to the magma batches of Boyce *et al.* (2015)/Chapter 5, according to increasing alkalinity: batch A, blue; batch B, red; batch C, green. Stars refer to vents for each eruption, coloured by magma batch. Facies: C1 lava; C2 discordant coherent basalt; P1 coarse grained, moderately to well sorted bedded ash–lapilli–bombs; P2 well sorted fine ash–fine lapilli; P3 moderately to well sorted fine ash–coarse lapilli/small blocks; P4 cross bedded fine ash–fine lapilli; P5 palagonite altered, armoured lapilli-rich, ash; P6 spatter agglomerate. NASA ASTER GDEM is a product of METI and NASA.



of facies P6 (spatter agglomerate) as the final eruption products. Syn-depositional faulting is evident throughout the stratigraphy, but more so in the distal areas of the upper scoria cone (levels 1 and 2 of the LK quarry), signifying partial collapse of the scoria cone during construction.

At the summit of the northern cone lies an additional vent in the form of a spatter rampart, which is approximately 60 m long and 1.5 m high made up of facies P6 (spatter agglomerate). Weak columnar jointing on nearby blocks indicates the vent position. This was erupted in a mild Strombolian eruption as the final eruption product of magma batch C.

4.6.1.4 Phase 4: Southern cone-building coupled with extrusion of the lava shield

The final phase of activity at Mt Rouse was deduced by examining the stratigraphy of both the Old Railway Quarry and the Lewis Quarry to the south and east of the southern scoria cone. The eruptions during this phase were varied and complex, involving two magma batches (A and B) and five facies (P2–P6).

The southern scoria cone of Mt Rouse is much lower than the northern cone. The crater itself is only 25 m higher than the surrounding lava plains, and the edges of the scoria cone range from 64 to 72 m above sea level at the satellite cones. Immediately overlying the low southern Strombolian cone of Phase 2 (facies P1) is facies P2 (well sorted fine ash–fine lapilli). These deposits represent the initial eruptions of magma batch B and the eruption varied between violent-Strombolian (facies P2) and micro-Plinian (facies P3—moderately to well sorted fine ash—coarse lapilli/small blocks).

The remainder of the stratigraphy of Mt Rouse involves the eruption products of magma batch B and the renewed eruption of magma batch A. There is evidence for both magmas erupting at the same or similar times from closely spaced vents (if not the same) in the southern crater. Facies P4 (cross bedded fine ash–fine lapilli) grades upwards from facies P3 and represents a gas build-up in magma batch B. However, in the upper parts of the stratigraphy the final surge contains scoria of magma batch B and achneliths of magma batch A. This implies that magma batch A had begun erupting again through Hawaiian-style fire fountaining *at the same time* that magma batch B was erupting during a micro-Plinian event. The vent must be inferred as at or close to the southern crater of Mt Rouse, as lava flows that overlie the facies P4 surge (facies C1; magma batch A; Figure 4.3) originate from this crater. Immediately overlying the thin lava flow is facies P5 (palagonite altered, armoured lapilli-rich, ash), which originates from a phreatomagmatic eruption of magma batch B. The vent for this eruption has been obliterated, but as the deposit is thickest in the southeast of Mt Rouse, thinning to the north and south, it must have originated from the southern crater, which was the source of magma batch B. The final eruption products of magma batch B were the two satellite cones on the rim of the southern crater. These are not covered with facies P5 and are composed of facies P6 (spatter agglomerate). The eruption of Mt Rouse ended with the emplacement of the lava shield (which may have been on-going since the initial re-eruption of magma batch A) through a breach in the western side of the southern crater.

4.6.2 Factors causing alternating eruption styles

Eruption styles at Mt Rouse were controlled by magma composition, mass flux rate, the amount of dissolved volatiles in the melt, external water becoming involved in the eruption and vent re-use.

Compositionally, all of the effusive Hawaiian-style facies of Mt Rouse (C1 and the Pele's hair and tears of P4) are magma batch A of Boyce *et al.* (2015/Chapter 5). The early Strombolian cones are magma batch C, while micro-Plinian and violent-Strombolian eruption styles are compositionally magma batches B and C. Minor Strombolian products are also found as the final eruption products of magma batches B and C.

The mass flux rate of the magma is an important control on eruption, and can be linked with the composition. Flux rate controls the movement of gas bubbles. In a low-flux magma with low bubble rise rates, a vesicular foam is erupted (Hawaiian-style) due to bubble overpressure (Wilson & Head 1981; Parfitt 2004; Houghton & Gonnermann 2008). When the magma flux rate is low, but the magma is actively degassing, bubbles coalesce to form slugs and drive Strombolian activity at the vent as they burst (Blackburn *et al.* 1976; Wilson 1980; Parfitt & Wilson 1995). At high flux rates, the bubbles remain in the melt and have less time for interaction. As the magma rises, the exsolved gases expand, and this results in greater acceleration and higher eruption velocities (Parfitt & Wilson 1995), leading to violent-Strombolian and micro-Plinian eruption styles. Therefore at Mt Rouse it can be inferred that both the initial (facies P1; Strombolian) and final (facies P6; minor Strombolian) eruptions of magma batch C and the final eruption of magma batch B (facies P6; minor Strombolian) were low flux. The initial eruption of magma batch C was Strombolian due to the low flux rate of the magma as it erupted at the surface via a previously unused conduit to the south, and as the eruption migrated to the north. As the magma flux increased and varied in intensity, eruption styles alternated between micro-Plinian and violent-Strombolian (Phases 3–4; Figure 4.12). The eruption of magma batch B in the south (Phase 4; facies P2) began as a violent-Strombolian event rather than Strombolian. This is most likely due to the batch of magma using the already open, and as-yet unsolidified conduit from which the southern early eruption centre of magma batch C erupted, promoting rapid flow (e.g., Carrigan & Eichelberger; see section 4.7). The spatter ramparts that represent the final eruption products of magma batches B and C formed as the magma flux significantly waned and ceased.

The amount of dissolved volatiles in the melt is important because it can affect the properties of the ascending magma, including the rheology (e.g., lead to increased buoyancy through exsolution via decompression; Sparks *et al.* 1978), and the eruptive behaviour, as reviewed in detail by Houghton & Gonnermann (2008). We can infer that magma batch A of Mt Rouse, which erupted effusively, featured a lower volatile content than magma batches B and C, which were explosive. This is linked to the chemistry of the magmas and the nature of the underlying lithosphere beneath western Victoria, for which there is evidence of increasing metasomatism with depth (e.g., Frey *et al.* 1978; McDonough *et al.* 1985; McDonough & McCulloch 1987; Boyce *et al.* 2014). On a broader scale, the two series of geochemically and isotopically distinct basalts in the NVP, the Plains series and the Cones series (McDonough *et al.* 1985; Price *et al.* 1988; Vogel & Keays 1997) were most likely derived from a deepening source region, with the Plains basalts (which include magma batch A) from a shallower area of the lithosphere than the Cones basalts (which include magma batches B and C) (Frey *et al.*

1978; McDonough *et al.* 1985; McDonough & McCulloch 1987; Boyce *et al.* 2014, 2015). Further studies should therefore focus on the volatile contents of the magmas, for example by the analysis of melt inclusions and groundmass glasses, to study the pre-eruptive volatile contents and degassing paths of the magmas (e.g., Atlas *et al.* 2006).

Water had an important control on the eruption style at Mt Rouse, but only during the later phases of eruption. Initial eruptions were not phreatomagmatic as there was presumably no aquifer in the granitic basement beneath Mt Rouse. The interaction of magma batch B with an unknown surface water source led to the generation of a small-volume, armoured lapilli-rich pyroclastic flow. The water must have been ponded in a low-lying area of the cone away from the main vent(s) for magma batch A, which was erupting at similar times.

Monogenetic volcanoes are traditionally thought to be the product of single batches of magma, after the passage of which pathways cool sufficiently to prevent the eruption of subsequent magma batches (e.g., Walker 2000). Recently, several monogenetic volcanoes have been described as being composed of two batches of magma (e.g., Luhr 2001; Strong & Wolff 2003; Brenna *et al.* 2010, 2011; van Otterloo 2014); however, few authors discuss conduit reuse due to stratigraphic relationships obscuring vent locations. Conduit reuse is described at Udo, Jeju Island, South Korea, which erupted two sequential magma batches, with some samples of intermediate composition (Brenna *et al.* 2010). Conduits were also reused during eruptions of Rangitoto in the Auckland Volcanic Field, New Zealand. Rangitoto is a polycyclic volcano that erupted two magma batches through separate vents with a time gap of ~60 years (Needham *et al.* 2010).

In the southern cone of Mt Rouse, there appears to have been conduit reuse by all three magma batches involved in the genesis of the volcano. The orientation of the bedding indicates that these magmas erupted from the southern crater (Figure 4.2; section 4.6.1.4). There is no evidence of time breaks between eruptions or of magma mixing in the geochemistry of the deposits. In addition, a surge deposit containing the products of two magma batches indicates that fire fountaining of magma batch A and micro-Plinian eruptions of magma batch B were occurring simultaneously from closely-spaced vents at the southern crater (section 4.5.2.5; this is the only deposit containing the products of two magma batches). For magma batches A and B to erupt simultaneously, there must have been particular properties of the magmas that prevented them from geochemically mixing. Temperature, density and viscosity contrasts can act to inhibit mixing, as can high flux rates. The magmas originated from the lithosphere–asthenosphere boundary and must have had relatively rapid ascent rates to entrain small mantle xenoliths (batches A and C at least; Boyce *et al.* 2015/Chapter 5); and they likely used the same pathways from depth. With batch A erupting effusively and batch B explosively, the viscosity of batch A must have been substantially lower than that of B. This could have led to core-annular flow in the conduit—the lower viscosity magma may have migrated to the conduit walls, acting as a lubricant for the higher viscosity magma, which would have formed the core of the flow and erupted separately (Carrigan & Eichelberger 1990). Slight differences in temperature between the magma batches could have acted to produce chilling at the boundaries between the magmas and prevent mixing (Brenna *et al.* 2010), while high flux rates are inferred for the violent-Strombolian and micro-Plinian eruption events of magma batch B (see above).

4.7 Conclusions

1. Mt Rouse consists of eight facies, which were sourced from three different magma batches that erupted from at least 7 vents (including vent reuse).
2. Facies identified at Mt Rouse include both coherent and fragmental types. These are C1 lavas; C2 discordant coherent basalt; P1 coarse grained, moderately to well sorted bedded ash–lapilli–bombs; P2 well sorted fine ash–fine lapilli; P3 moderately to well sorted fine ash–coarse lapilli/small blocks; P4 cross bedded fine ash–fine lapilli; P5 palagonite altered, armoured lapilli-rich, ash; P6 spatter agglomerate.
3. Eruption styles at Mt Rouse varied from Hawaiian and Strombolian to micro-Plinian through violent-Strombolian and phreatomagmatic.
4. Controls on eruption style at Mt Rouse include magma composition, mass flux rate, vent reuse, the possible involvement of external water in the eruption and presumably the juvenile volatile content of the melt.
5. Mt Rouse erupted over four phases. Magma batches A, C and B were erupted sequentially, followed by batches A and B simultaneously.
6. Mt Rouse is an extremely complex polymagmatic yet monogenetic volcano, which does not fit the traditional assumption that monogenetic volcanoes are simple in nature, produced from the short-lived eruption of a single magma batch.

4.8 Acknowledgements

This paper represents part of the PhD research undertaken by Julie Boyce under the supervision of Prof. Reid Keays, Dr Ian Nicholls and Dr Patrick Hayman. Julie Boyce acknowledges a Monash University School of Geosciences research scholarship, Dean's International Postgraduate Research Scholarship and Postgraduate Publication Award. Thanks go to Jackson van den Hove, Dan Uehara, Janine Kavanagh, Bob Krummel and Jozua van Otterloo for help with fieldwork and Tony Rowe (Bamstone Quarries) for collecting mantle xenoliths and organising quarry tours. Thanks also to Peter Bourke (Tarrone quarries) and Craig Kenny (LK Quarries) for quarry access, the Volcanoes Discovery Centre at Penshurst, and Prof. Ray Cas for scientific discussions relating to Mt Rouse and the NVP.

4.9 References

- ATLAS Z. D., DIXON J. E., SEN G., FINNY M., & MARTIN-DEL POZZO A. L. 2006. Melt inclusions from Volcán Popocatepetl and Volcán de Colima, Mexico: Melt evolution due to vapor-saturated crystallization during ascent. *Journal of Volcanology and Geothermal Research* **153**, 221–240.
- BATIZA R. & WHITE J. D. L. 2000. Submarine lavas and hyaloclastite. *In*: Sigurdsson H. ed. *Encyclopaedia of Volcanoes*, pp. 361–381. Academic Press, New York.
- BEHNCKE B., NERI M., PECORA E. & ZANON V. 2006. The exceptional activity and growth of the southeast crater, Mount Etna (Italy), between 1996 and 2001. *Bulletin of Volcanology* **69**, 149–173.
- BLACKBURN G. 1966. Radiocarbon dates relating to soil development and volcanic ash deposition in south-east South Australia. *Australian Journal of Science* **29**, 50–52.
- BLACKBURN E. A., WILSON L. & SPARKS R. S. J. 1976. Mechanisms and dynamics of Strombolian activity. *Journal of the Geological Society of London* **132**, 429–440.
- BLACKBURN G., ALLISON G. B. & LEANEY F. W. J. 1982. Further evidence on the age of the tuff at Mount Gambier, South Australia. *Transactions of the Royal Society of South Australia* **106**, 163–167.
- BLAIKIE T. N., AILLERES, L., CAS R. A. F. & BETTS P. G. 2012. Three-dimensional potential field modelling of a multi-vent maar-diatreme — The Lake Coragulac maar, Newer Volcanics Province, south-eastern Australia. *Journal of Volcanology and Geothermal Research* **235**, 70–83.
- BOYCE J. 2013. The Newer Volcanics Province of southeastern Australia: a new classification scheme and distribution map for eruption centres. *Australian Journal of Earth Sciences* **60**, 449–462.
- BOYCE J. A., KEAYS R. R., NICHOLLS I. A. & HAYMAN P. C. 2014. Eruption centres of the Hamilton area of the Newer Volcanics Province, Victoria, Australia: pinpointing volcanoes from a multifaceted approach to landform mapping. *Australian Journal of Earth Sciences* **61**, 735–754.
- BOYCE J. A., NICHOLLS I. A., KEAYS R. R. & HAYMAN P. C. 2015. Variation in parental magmas of Mt Rouse, a complex polymagmatic monogenetic volcano in the basaltic intraplate Newer Volcanics Province, southeast Australia. *Contributions to Mineralogy and Petrology* **169**: DOI 10.1007/s00410-015-1106-y
- BRENNAM., CRONIN S. J. SMITH I. E. M., SOHN S. Y. & NÉMETH K. 2010. Mechanisms driving polymagmatic activity at a monogenetic volcano, Udo, Jeju Island, South Korea. *Contributions to*

Mineralogy and Petrology **160**, 1–20.

BRENNA M., CRONIN S. J. NÉMETH K., SMITH I. E. M., & SOHN Y. 2011. The influence of magma plumbing complexity on monogenetic eruptions, Jeju Island, Korea. *Terra Nova* **23**, 70–75.

BROWN R. J., BUSE, B., SPARKS R. S. J. & FIELD M. 2008. On the welding of pyroclasts from very low-viscosity magmas: examples from kimberlite volcanoes. *The Journal of Geology* **116**, 354–374.

BROWN R. J. & ANDREWS G. D. M. 2015. Deposits of pyroclastic density currents. In: Sigurdsson H., Houghton B., McNutt S. R., Rymer H. & Stix J. eds. *The Encyclopedia of Volcanoes*, pp. 631–648. Academic Press, New York.

BÜTTNER, R., DELLINO P. & ZIMANOWSKI B. 1999. Identifying magma–water interaction from the surface features of ash particles. *Letters to Nature* **401**, 688–690.

BÜTTNER, R., DELLINO P., LA VOLPE L., LORENZ V. & ZIMANOWSKI B. 2002. Thermohydraulic explosions in phreatomagmatic eruptions as evidenced by the comparison between pyroclasts and products from Molten Fuel Coolant Interaction experiments. *Journal of Geophysical Research* **107**, B112277.

CARRIGAN C. & EICHELBERGER J. C. 1990. Zoning of magmas by viscosity in volcanic conduits. *Nature* **343**, 248–251.

CAS R., BLAIKIE T., BOYCE J., HAYMAN P., JORDAN S., PIGANIS F., PRATA G & VAN OTTERLOO J. 2011. Factors that influence varying eruption styles (from magmatic to phreatomagmatic) in intraplate continental basaltic volcanic provinces: The Newer Volcanics Province of southeastern Australia. Field trip guide VF01, pp. 7–31. IUGG 2011 General Assembly. Earth on the Edge: Science for a Sustainable Planet.

CAS R. & Wright J. V. 1987. *Volcanic Successions: Modern and Ancient*. Chapman & Hall.

CAYLEY R. A., WEBB A. W. & HENLEY K. J. 1995. Radiometric dating (K/Ar) on two samples of Newer Volcanic olivine basalt from the southwestern part of the Beaufort 1:100 000 map sheet area. *Geological Survey of Victoria Unpublished Report* **1995/15**.

CAYLEY R. A., KORSCH R. J., MOORE D. H., COSTELLOE R. D., NAKAMURAA., WILLMAN C. E., RAWLING J., MORAND V. J., SKLADZIEN P. B. & O'SHEA P. J. 2011. Crustal architecture of central Victoria: results from the 2006 deep crustal reflection seismic survey. *Australian Journal of Earth Sciences* **58**, 113–156.

COOPER J. A. & GREEN D. H. 1969. Lead isotope measurements on lherzolite inclusions and host

basanites from western Victoria, Australia. *Earth and Planetary Science Letters* **6**, 69-76.

COSTA A., FOLCH A. & MACEDONIO G. 2010. A model for wet aggregation of ash particles in volcanic plumes and clouds: 1. Theoretical formulation. *Journal of Geophysical Research* **115**, B09201.

DASCH E. J. & GREEN D. H. 1975. Strontium isotope geochemistry of lherzolite inclusions and host basaltic rocks, Victoria, Australia. *American Journal of Science* **275**, 461-469

DELLINO P., ISAIA R., LA VOLPE L. & ORSI G. 2001. Statistical Analysis of textural data from complex pyroclastic sequences: implications for fragmentation processes of the Agnano-Monte Spina Tephra (4.1 ka), Phlegraean Fields, southern Italy. *Bulletin of Volcanology* **63**, 443-461.

DELLINO P. & LA VOLPE L. 1995. Fragmentation versus transportation mechanisms in the pyroclastic sequence of Monte Pilato-Rocche Rosse (Lipari, Italy). *Journal of Volcanology and Geothermal Research* **64**, 211-231.

DEMIDJUK Z. 2005. U-series insights into melting processes and magma evolution beneath the New Volcanic Province in South Australia. Macquarie University Honours thesis.

DEMIDJUK Z., TURNER S., SANDIFORD M., GEORGE R., FODEN J. & ETHERIDGE M. 2007. U-series isotope and geodynamic constraints on mantle melting processes beneath the Newer Volcanic Province in South Australia. *Earth and Planetary Science Letters* **261**, 517-533.

DUFEK J. & MANGA M. 2008. In situ production of ash in pyroclastic flows. *Journal of Geophysical Research* **113**, B09207.

DUFFIELD W. A., GIBSON E. K. & HEIKEN G. H. 1977. Some characteristics of Pele's hair. *Journal of Research of the U.S. Geological Survey* **5**, 93-101.

DURANT A. J., BONADONNA C. & HORWELL C. J. 2010. Atmospheric and environmental impacts of volcanic particulates. *Elements* **6**, 235-240.

EDWARDS J., CAYLEY R. A. & JOYCE E. B. 2004. Geology and geomorphology of the Lady Julia Percy Island volcano, a late Miocene submarine and subaerial volcano off the coast of Victoria, Australia. *Proceedings of the Royal Society of Victoria* **116**, 15-35.

ELIAS M. 1973. The Geology and Petrology of Mt Rouse, A Volcano in the Western District of Victoria. BSc thesis (unpublished), University of Melbourne.

EWART A., CHAPPELL B. W. & MENZIES M. A. 1988. An overview of the geochemical and isotopic characteristics of the eastern Australian Cainozoic volcanic provinces. *Journal of Petrology*.

Special Lithosphere Issue, 225–273.

ERLUND E. J., CASHMAN K. V., WALLACE P. J., PIOLI L., ROSI M., ERLUND E. J., CASHMAN K. V., WALLACE P. J., PIOLI L., ROSI M., JOHNSON E. & DELGADO GRANADOS H. 2010. Compositional evolution of magma from Paricutin Volcano, Mexico: The tephra record. *Journal of Volcanology and Geothermal Research* **197**, 167–187.

FINK J. H. & FLETCHER R. C. 1978. Ropy pahoehoe: surface folding of a viscous fluid. *Journal of Volcanology and Geothermal Research* **4**, 151–170.

FODEN J., SONG S. H. S., TURNER S., ELBURG M., SMITH P. B., VAN DER STELDT B. & VAN PENGLIS D. 2002. Geochemical evolution of lithospheric mantle beneath S.E. South Australia. *Chemical Geology* **182**, 663–695.

FOLCH A., COSTA A., DURANT A. & MACEDONIO G. 2010. A model for wet aggregation of ash particles in volcanic plumes and clouds: 2. Model application. *Journal of Geophysical Research* **115**, B09202.

FRANCIS P. W., GLAZE L. S., PIERI D., OPPENHEIMER C. M. M. & ROTHERY D. A. 1990. Eruption terms. *Nature* **346**, 519–519.

FREY F. A., GREEN D. H. & ROY D. 1978. Integrated models of basalt petrogenesis: a study of quartz tholeiites to olivine melilitites from South Eastern Australia utilising geochemical and experimental petrological data. *Journal of Petrology* **19**, 463–513.

GILBERT J. S. & LANE S. J. 1994. The origin of accretionary lapilli. *Bulletin of Volcanology* **56**, 398–411.

GOURAMANIS C., WILKINS D. & DEDECKKER P. 2010. 6000 years of environmental changes recorded in Blue Lake, South Australia, based on ostracod ecology and valve chemistry. *Palaeogeography, Palaeoclimatology, Palaeoecology* **297**, 223–237.

GRAY C. M. & MCDOUGALL I. 2009. K–Ar geochronology of basalt petrogenesis, Newer Volcanics Province, Victoria. *Australian Journal of Earth Sciences* **56**, 245–258.

HAYMAN P. C. & CAS R. A. F. 2011. Criteria for interpreting kimberlite as coherent: insights from the Muskox and Jericho kimberlites (Nanavut, Canada). *Bulletin of Volcanology* **73**, 1005–1027.

HEIKEN G. 1972. Morphology and petrography of volcanic ashes. *Geological Society of America Bulletin* **83**, 1691–1988.

HEIKEN G. 1984. An atlas of volcanic ash. *Smithsonian Contributions to the Earth Sciences* **12**.

- HEIKEN G. & WOHLTZ K. 1985. Volcanic ash. University of California Press, Berkeley.
- HON K., KAUAHIKAUA J., DENLINGER R. & MACKAY K. 1994. Emplacement and inflation of pahoehoe sheet flows: Observations and measurements of active lava flows on Kilauea Volcano, Hawaii. *Geological Society of America Bulletin* **106**, 351–370.
- HOUGHTON B. F. & GONNERMANN H. M. 2008. Basaltic explosive volcanism: Constraints from deposits and models. *Chemie der Erde—Geochemistry* **68**, 117–140.
- HOUGHTON B., WHITE D. L. & VAN EATON A. R. 2015. Phreatomagmatic and related eruption styles. In: Sigurdsson H., Houghton B., McNutt S. R., Rymer H. & Stix J. eds. *The Encyclopedia of Volcanoes*, pp. 537–552. Academic Press, New York.
- JORDAN S. C., CAS R. A. F. & HAYMAN P. C. 2013. The origin of a large (>3 km) maar volcano by coalescence of multiple shallow craters: Lake Purrumbete maar, southeastern Australia. *Journal of Volcanology and Geothermal Research* **254**, 5–22.
- JOYCE E. B. 1975. Quaternary volcanism and tectonics in southeastern Australia. In: Suggate R. P. & Cresswell M. M. eds. *Quaternary studies*, pp. 169–178. The Royal Society of New Zealand, Wellington.
- KERESZTURI G., CSILLAG G., NÉMETH K., SEBE K., BALOGH K. & JÁGER V. 2010. Volcanic architecture, eruption mechanism and landform evolution of a Plio/Pleistocene intracontinental basaltic polycyclic monogenetic volcano from Bakony–Balaton Highland Volcanic Field, Hungary. *European Journal of Geosciences* **2**, 362–384.
- KORSCH R. J., BARTON T. J., GRAY D. R., OWEN A. J. & FOSTER D. A. 2002. Geological interpretation of a deep seismic reflection transect across the boundary between the Delamerian and Lachlan Orogens, in the vicinity of the Grampians, western Victoria. *Australian Journal of Earth Sciences* **49**, 1057–1075.
- KUEPPERS U., PUTZ C., SPIELER O. & DINGWELL D. B. 2012. Abrasion in pyroclastic density currents: Insights from tumbling experiments. *Physics and Chemistry of the Earth* **45**, 33–39.
- KUNO H. 1965. Fractionation trends of basalt magmas in lava flows. *Journal of Petrology* **6**, 302–321.
- LORENZ V. 2003. Maar-diatreme volcanoes, their formation, and their setting in hard-rock or soft-rock environments. *Geolines — Journal of the Geological Institute of AS Czech Republic* **15**, 72–83.
- LUHR J. F. 2001. Glass inclusions and melt volatile contents at Parícutin Volcano, Mexico. *Contributions to Mineralogy and Petrology* **142**, 261–283.

- MACDONALD G. A. 1953. Pahoehoe, aa, and block lava. *American Journal of Science* **251**, 169–191.
- MACDONALD G. A. 1972. *Volcanoes*. Prentice-Hall Inc., Eaglewood Cliffs, New Jersey, U.S.A.
- MATCHAN E. & PHILLIPS D. 2011. New $^{40}\text{Ar}/^{39}\text{Ar}$ ages for selected young (<1 Ma) basalt flows of the Newer Volcanic Province, southeastern Australia. *Quaternary Geochronology* **6**, 356–368.
- MATCHAN E. L. & PHILLIPS D. 2014. High precision multi-collector $^{40}\text{Ar}/^{39}\text{Ar}$ dating of young basalts: Mount Rouse volcano (SE Australia) revisited. *Quaternary Geochronology* **22**, 57–64.
- MCBRIDE J. S., LAMBERT D. D., NICHOLLS I. A. & PRICE R. C. 2001. Osmium isotopic evidence for crust-mantle interaction in the genesis of continental intraplate basalts from the Newer Volcanics Province, southeastern Australia. *Journal of Petrology* **6**, 1197–1218.
- MCDUGALL I., ALLSOP H. L. & CHAMALAUN F. H. 1966. Isotopic dating of the Newer Volcanics of Victoria, Australia and geomagnetic polarity epochs. *Journal of Geophysical Research* **71**, 6107–6118.
- MCDUGALL I. & GILL E. D. 1975. Potassium-Argon ages from the Quaternary succession in the Warrnambool – Port Fairy area, Victoria, Australia. *Proceedings of the Royal Society of Victoria* **12**, 295–332.
- MCDONOUGH W. F. & MCCULLOCH M. T. 1987. The southeast Australian lithospheric mantle: isotopic and geochemical constraints on its growth and evolution. *Earth and Planetary Science Letters* **86**, 327–340.
- MCDONOUGH W. F., MCCULLOCH M. T. & SUN S. S. 1985. Isotopic and geochemical systematics in Tertiary-Recent basalts from southeastern Australia and implications for the evolution of the sub-continental lithosphere. *Geochimica et Cosmochimica Acta* **49**, 2051–2067.
- MOUNE S., FAURE F., GAUTHIER P-J. & SIMS, K. W. W. 2007. Pele's hairs and tears: Natural probe of volcanic plume. *Journal of Volcanology and Geothermal Research* **164**, 244–253.
- NEEDHAM A.J., LINDSAY J.M., SMITH I.E.M., AUGUSTINUS P., SHANE P.A. 2010. Sequential eruption of alkaline and sub-alkaline magmas from a small monogenetic volcano in the Auckland Volcanic Field, New Zealand. *Journal of Volcanology and Geothermal Research* **201**, 126–142.
- NÉMETH K. 2010. Monogenetic volcanic fields: Origin, sedimentary record, and relationship with polygenetic volcanism. *The Geological Society of America Special Paper* **470**, 43–66.
- NÉMETH K., CRONIN S. J., SMITH I. E. M. & FLORES J. A. 2012. Amplified hazard of small-

volume monogenetic eruptions due to environmental controls, Orakei Basin, Auckland Volcanic Field, New Zealand. *Bulletin of Volcanology* **74**, 2121–2137.

NICHOLLS I. A. & JOYCE E. B. 1989. East Australian volcanic geology—Victoria and South Australia—Newer Volcanics. In: Johnson R. W. ed. *Intraplate volcanism in Eastern Australia and New Zealand*, pp. 137–142. Cambridge University Press, Cambridge.

OLLIER C. D. 1985. Lava flows of Mt Rouse, western Victoria. *Proceedings of the Royal Society of Victoria* **97**, 167–174.

OLLIER C. D. & JOYCE E. B. 1964. Volcanic physiography of the Western Plains of Victoria. *Proceedings of the Royal Society of Victoria* **77**, 357–376.

PARFITT E. A. 2004. A discussion of the mechanisms of explosive basaltic eruptions. *Journal of Volcanology and Geothermal Research* **134**, 77–107.

PARFITT E. A. & WILSON L. 1995. Explosive volcanic eruptions – IX. The transition between Hawaiian-style lava fountaining and Strombolian explosive activity. *Geophysical Journal International* **121**, 226–232.

PIGANIS F. 2011. A volcanological investigation of the polymagmatic Red Rock Volcanic Complex and a 3D geophysical interpretation of the subsurface structure and geology of the poly-lobate Lake Purdigulac maar, Newer Volcanics Province, southeastern Australia. MSc thesis (unpublished), Monash University.

PIOLI L., ERLUND E., JOHNSON E., CASHMAN K., WALLACE P., ROSI M. & DELGADO GRANADOS H. 2008. Explosive dynamics of violent Strombolian eruptions: The eruption of Parícutin Volcano, 1943–1952 (Mexico). *Earth and Planetary Science Letters* **271**, 359–368.

PORRITT L. A., RUSSELL J. K. & QUANE S. L. 2012. Pele's tears and spheres: Examples from Kilauea Iki. *Earth and Planetary Science Letters* **333**, 171–180.

PRICE R. C., GRAY C. M. & FREY F. A. 1997. Strontium isotopic and trace element heterogeneity in the plains basalts of the Newer Volcanic Province, Victoria, Australia. *Geochimica et Cosmochimica Acta* **61**, 171–192.

PRICE R. C., GRAY C. M., NICHOLLS I. A., DAY A. 1988. Cainozoic volcanic rocks. In: Douglas J. G. & Ferguson J. A. (eds). *Geology of Victoria*. Geological Society of Australia, Victoria Division, Melbourne, pp. 439–451.

ROGAN W., BLAKE S. & SMITH I. 1996. In situ chemical fractionation in thin basaltic lava flows: examples from the Auckland volcanic field, New Zealand, and a general physical model. *Journal of*

Volcanology and Geothermal Research **74**, 89–99.

SELF S., KESZTHELYI L. & THORDARSON T. 1998. The importance of pahoehoe. *Annual Review of Earth and Planetary Sciences* **26**, 81–110.

SHEARD M. J. 1990. A guide to Quaternary Volcanoes in the Lower South-East of South Australia. *Mines and Energy Review, South Australia* **157**, 40–50.

SOHN Y. K., CRONIN S. J., BRENNAN M., SMITH I. E. M., NEMETH K., WHITE J. D. L., MURTAGH R. M., JEON Y. M. & KWON C. W. 2012. Ilchulbong tuff cone, Jeju Island, Korea, revisited: A compound monogenetic volcano involving multiple magma pulses, shifting vents, and discrete eruptive phases. *Geological Society of America Bulletin* **3–4**, 259–274.

SPARKS R. S. J. 1978. The dynamics of bubble formation and growth in magmas: a review and analysis. *Journal of Volcanology and Geothermal Research* **3**, 1–37.

SPARKS R. S. J., BURSİK M. I., CAREY S. N., GILBERT J. S., GLAZE L. S., SIGURDSSON H. & WOODS A. W. 1997. Volcanic Plumes, pp. 574. John Wiley & Sons, Chichester.

STRONCIK N. A. & SCHMINCKE H-U. 2002. Palagonite—a review. *International Journal of Earth Sciences* **91**, 680–697.

STRONG M. & WOLFF J. 2003. Compositional variations within scoria cones. *Geology* **31**, 143–146.

STUCKLESS J. S. & IRVING A. J. 1976. Strontium isotope geochemistry of megacrysts and host basalts from southeastern Australia. *Geochimica et Cosmochimica Acta* **40**, 209–213.

SUTALO F. 1996. The geology and regolith terrain evaluation of the Mount Rouse lava flows, Western Victoria. Honours research report, University of Melbourne.

SUTALO F. & JOYCE B. 2004. Long basaltic lava flows of the Mt Rouse volcano in the Newer Volcanic Province of southeastern Australia. *Proceedings of the Royal Society of Victoria* **116**, 37–47.

TELLING J. & DUFEK J. 2012. An experimental evaluation of ash aggregation in explosive volcanic eruptions. *Journal of Volcanology and Geothermal Research* **209**, 1–8.

THORDARSON T. 2004. Accretionary-lapilli-bearing pyroclastic rocks at ODP Leg 192 Site 1184: a record of subaerial phreatomagmatic eruptions on the Ontong Java Plateau. In: Fitton J. G., Mahoney J. J., Wallace P. J. & Saunders A. D. eds. *Origin and Evolution of the Ontong Java Plateau*, pp. 275–306. *Geological Society of London Special Publication* **229**.

- VALENTINE G. A. & GREGG T. K. P. 2008. Continental basaltic volcanoes – processes and problems. *Journal of Volcanology and Geothermal Research* **177**, 857–873.
- VAN OTTERLOO J., CAS R. A. F. & SHEARD M. J. 2013. Eruption processes and deposit characteristics at the monogenetic Mt Gambier Volcanic Complex, SE Australia: implications for alternating magmatic and phreatomagmatic activity. *Bulletin of Volcanology* **75**, 737. DOI 10.1007/s00445-013-0737-y.
- VAN OTTERLOO J., RAVEGGI M., CAS R. A. F. & MAAS R. 2014. Polymagmatic activity at the monogenetic Mt Gambier volcanic complex in the Newer Volcanics Province, SE Australia: New Insights into the occurrence of intraplate volcanic activity in Australia. *Journal of Petrology* **55**, 1317–1351.
- VANIMAN D. T., HEIKEN G., WOHLLETZ K. & BLACIC J. 1992. Palagonites and Martian soil simulants. *Abstracts of the Lunar and Planetary Science Conference* **23**, 1463–1464.
- VERGNIOLLE S. & MANGAN M. 2000. Hawaiian and Strombolian eruptions. In: Sigurdsson H. ed. *Encyclopedia of Volcanoes*, pp. 447–461. Academic Press, New York.
- VESPERMANN D. & SCHMINCHE H. 2000. Scoria cones and tuff rings. In: Sigurdsson H. ed. *Encyclopaedia of Volcanoes*, pp. 683–694. Academic Press, New York.
- VOGEL D. C. & KEAYS R. R. 1997. The petrogenesis and platinum-group element geochemistry of the Newer Volcanic Province, Victoria, Australia. *Chemical Geology* **136**, 181–204.
- WALKER G. P. L. 2000. Basaltic volcanoes and volcanic systems. In: Sigurdsson H. ed. *Encyclopedia of Volcanoes*, pp. 283. Academic Press, New York.
- WALKER G. P. L. & CROASDALE R. 1971. Characteristics of some basaltic pyroclasts. *Bulletin of Volcanology* **35**, 303–317.
- WATERS A. & FISHER R. V. 1971. Base surges and their deposits: Capelinhos and Taal volcanoes. *Journal of Geophysical Research* **76**, 5596–5614.
- WHITE J. D. L. & HOUGHTON B. 2000. Surtseyan and related phreatomagmatic eruptions. In: Sigurdsson H. ed. *Encyclopedia of Volcanoes*, pp. 495–511. Academic Press, New York.
- WHITEHEAD P. W. 1986. The geology and geochemistry of the Mt Rouse and Mt Napier volcanic centres, western Victoria. Honours research report, La Trobe University, Melbourne.
- WHITEHEAD P. W. 1991. The geology and geochemistry of Mt Napier and Mt Rouse, western Victoria. In: Williams M. A. J., DeDeckker P. & Kershaw A. P. eds. *The Cainozoic in Australia: a*

re-appraisal of the evidence, pp. 309–320. Geological Society of Australia Special Publication 18.

WILSON L. 1980. Relationships between pressure, volatile content and ejecta velocity in 3 types of volcanic explosion. *Journal of Volcanology and Geothermal Research* **8**, 297–313.

WILSON L. & HEAD J. W. 2001. Lava fountains from the 1999 Tvashtar Catena fissure eruption on Io: implications for dike emplacement mechanisms, eruption rates, and crystal structure. *Journal of Geophysical Research* **106**, 32997–33004.



Declaration for Thesis Chapter 5

Declaration by candidate

In the case of Chapter 5, the nature and extent of my contribution to the work was the following:

| Nature of contribution | Extent of contribution (%) |
|--|----------------------------|
| Fieldwork, data collection, sample preparation, interpretation of major and trace element and Sr–Nd–Pb data, and manuscript preparation. | 80% |

The following co-authors contributed to this work:

| Name | Nature of contribution | Extent of contribution (%) |
|-------------------|---|----------------------------|
| Dr Ian Nicholls | Supervisory role, interpretation of major and trace element and Sr–Nd–Pb data, and manuscript preparation. | 8% |
| Prof. Reid Keays | Supervisory role, interpretation of major and trace element and Sr–Nd–Pb data, and manuscript preparation.. | 7% |
| Dr Patrick Hayman | Supervisory role, manuscript preparation | 5% |

The undersigned hereby certify that the above declaration correctly reflects the nature and extent of the candidate's and co-authors' contributions to this work*.

Julie Boyce

Date

Prof. Reid Keays (main supervisor)

Date

Dr Ian Nicholls

Date

Dr Patrick Hayman

Date

Variation in parental magmas of Mt Rouse, a complex polymagmatic monogenetic volcano in the basaltic intraplate Newer Volcanics Province, southeast Australia

Julie A. Boyce · Ian A. Nicholls · Reid R. Keays · Patrick C. Hayman

Received: 13 February 2014 / Accepted: 7 January 2015
© Springer-Verlag Berlin Heidelberg 2015

Abstract Monogenetic volcanoes have long been regarded as simple in nature, involving single magma batches and uncomplicated evolutions; however, recent detailed research into individual centres is challenging that assumption. Mt Rouse (Kolor) is the volumetrically largest volcano in the monogenetic Newer Volcanics Province of southeast Australia. This study presents new major, trace and Sr–Nd–Pb isotope data for samples selected on the basis of a detailed stratigraphic framework analysis of the volcanic products from Mt Rouse. The volcano is the product of three magma batches geochemically similar to Ocean–Island basalts, featuring increasing LREE enrichment with each magma batch (batches A, B and C) but no evidence of crustal contamination; the Sr–Nd–Pb isotopes define two groupings. Modelling suggests that the magmas were sourced from a zone of partial melting crossing the lithosphere–asthenosphere boundary, with batch A forming a large-volume partial melt in the deep lithosphere (1.7 GPa/55.5 km); and batches B and C from similar areas within the shallow asthenosphere (1.88 GPa/61 km and 1.94 GPa/63 km, respectively). The formation and extraction of these magmas may have been due to high deformation rates in the mantle caused by edge-driven convection and asthenospheric upwelling. The lithosphere–asthenosphere boundary is important with respect to NVP

volcanism. An eruption chronology involves sequential eruption of magma batches A, C and B, followed by simultaneous eruption of batches A and B. Mt Rouse is a complex polymagmatic monogenetic volcano that illustrates the complexity of monogenetic volcanism and demonstrates the importance of combining detailed stratigraphic analysis alongside systematic geochemical sampling.

Keywords Monogenetic volcanism · Newer Volcanics Province · Intraplate basaltic volcanism · Polymagmatic

Introduction

Monogenetic volcanoes are the most common form of continental basaltic volcanism on Earth, although poorly understood. Walker (2000) states “...a volcano is monogenetic if the magma supply is so small or episodic that any pathways have cooled down and are no longer favoured routes for the next magma batch”. Thus, individual monogenetic volcanic centres are thought to represent one short-lived phase of eruption, simple in nature and involving single magma batches.

Recent research on monogenetic volcanism (e.g. Luhr 2001; Brenna et al. 2010, 2011) has led to the emergent field of study into complex and/or polymagmatic monogenetic volcanic centres, whereby detailed research on individual centres in monogenetic volcanic fields has found that they may be complex in nature, involving more than one magma batch or magma pulse with complex evolutions, yet were produced from a single series of eruptive events and therefore cannot be defined as polygenetic. Examples of such volcanic centres include the sequential eruption of two magma batches at Parícutin, in the Michoacán–Guanajuato volcanic field, Mexico (Luhr 2001; Erlund et al. 2010) and four centres in the Southern Cascades—Brush Mountain,

Communicated by Timothy L. Grove.

Electronic supplementary material The online version of this article (doi:10.1007/s00410-015-1106-y) contains supplementary material, which is available to authorized users.

J. A. Boyce (✉) · I. A. Nicholls · R. R. Keays · P. C. Hayman
School of Earth, Atmosphere and Environment, Monash
University, Clayton, VIC 3168, Australia
e-mail: [REDACTED]

Published online: 30 January 2015

 Springer

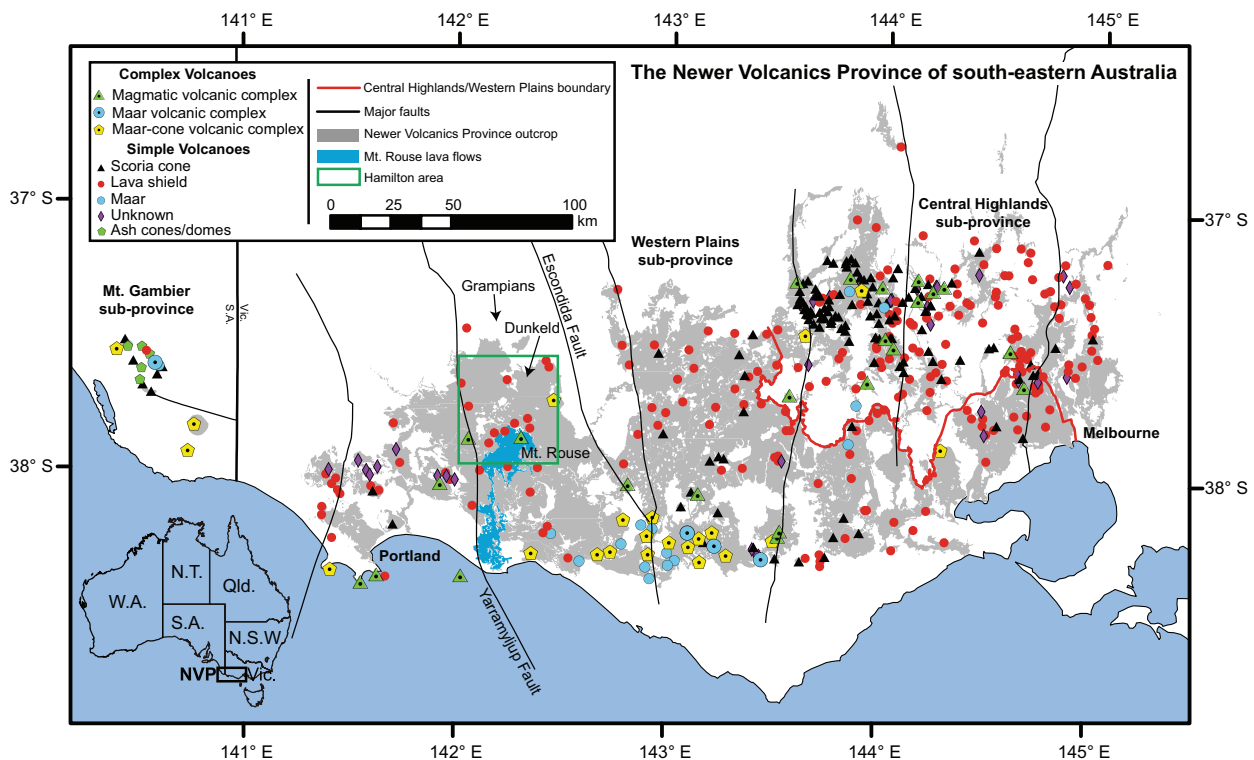


Fig. 1 The Newer Volcanics Province of southeastern Australia, showing eruption centres, lava flow cover and major faults. Mt Rouse lava flows outlined in blue, and the Hamilton area indicated by a green box. Modified after Boyce (2013) with additional eruption centres

Round Barn Cones and two cones on the Popcorn Cave mafic shield (Strong and Wolff 2003). Jeju Island, an intra-plate stratovolcano in South Korea containing >300 monogenetic scoria cones, has been of recent interest with the discovery of several complex cones—Udo erupted two magma batches in succession (Brenna et al. 2010, 2011), while Ichilbong erupted two or three magma batches in pulses (Sohn et al. 2012) and Songaksan and Suwulbong were each derived from pulses of a single, rapidly evolving magma batch (Brenna et al. 2011). Xitle, central Mexico may have erupted two magma batches, based on analysis of melt inclusions (Cervantes and Wallace 2003), and both Mt Gambier and the Red Rock Volcanic Complex in the Newer Volcanics Province (NVP), southeast Australia were derived from two simultaneously erupting magma batches resulting in complex deposits (Piganis 2011; van Otterloo et al. 2014). In addition, Rangitoto in the monogenetic Auckland Volcanic Field, New Zealand, featured sequential eruption of two magma batches, with a ~60-year time gap between eruption of the magmas (Needham et al. 2010).

This study focuses on Mt Rouse (which has the Aboriginal name of Kolor), the volumetrically largest eruption centre in the NVP. Through detailed and systematic stratigraphic and geochemical analysis, we show that Mt Rouse

is an unusual monogenetic volcano; it was formed from multiple magma batches that were emplaced during a complex eruption sequence involving the sequential eruption of three magma batches followed by the simultaneous eruption of two, in a single series of events.

Geological setting

The late Cainozoic NVP is a continental intraplate monogenetic volcanic field covering >19,000 km² from Melbourne, VIC to the Mt Burr range in southeast South Australia—a distance of 410 km (Fig. 1). The 8 Ma to ca 5,000 BP NVP (Blackburn 1966; McDougall et al. 1966; Blackburn et al. 1982; Cayley et al. 1995; Edwards et al. 2004; Gray and McDougall 2009; Gouramanis et al. 2010) is composed of >437 short-lived monogenetic basaltic volcanoes (Ollier and Joyce 1964; Joyce 1975; Boyce 2013; this study) with an estimated total volume of 1,300 km³ (Wellman 1971). The centres are defined as either simple or complex; scoria cones, lava shields, maars, ash cones/domes and some centres of unknown character are morphologically simple, with few vents, while magmatic, maar or maar-cone volcanic complexes are indeed complex, featuring intricate morphologies and multiple vents (Boyce 2013).

The NVP is subdivided into three subprovinces based on geomorphology; from east to west, they are the Central Highlands, Western Plains and Mt Gambier subprovinces (Joyce 1975; Nicholls and Joyce 1989). The Western Plains (the focus of this study) is the largest subprovince, extending 320 km from Melbourne to Portland, covering an area of >14,600 km² and is characterised by extensive plains-forming lava fields filling the subdued surface topography of the underlying Otway Basin. The subprovince contains 42 % of all NVP volcanic centres (Boyce 2013), with a concentration of phreatomagmatic eruption centres in the Colac–Warrnambool area to the south, attributed to magma/water interaction within the Cainozoic sedimentary aquifers of the Otway Basin (Joyce 1975). The Western Plains is split by the Mortlake Discontinuity (Price et al. 1997), whereby Sr-isotopic ratios of basalts are higher in the east, with values of 0.7035–0.7058 compared with the west with values of 0.7035–0.7047 (Cooper and Green 1969; Dasch and Green 1975; Stuckless and Irving 1976; McDonough et al. 1985; Whitehead 1986; Ewart et al. 1988; Price et al. 1997; McBride et al. 2001; Foden et al. 2002; Demidjuk et al. 2007). The Mortlake Discontinuity corresponds to the Palaeozoic Moyston Fault, which marks the boundary between the Delamerian and Lachlan fold belts (Korsch et al. 2002; Cayley et al. 2011).

Mt Rouse magmatic volcanic complex

Mt Rouse lies in the Hamilton area of the Western Plains subprovince (Figs. 1, 2) and is a composite volcano of lava and scoria. Mt Rouse is one of the youngest of 16 volcanic centres in the Hamilton area, and underlying local faults may have influenced its location. Dating of lavas by K–Ar and ⁴⁰Ar–³⁹Ar has yielded ages within the range of 0.31–0.45 Ma (McDougall and Gill 1975; Ollier 1985; Gray and McDougall 2009; Matchan and Phillips 2011), with a suggested eruption age of 0.303 Ma (Matchan and Phillips 2011).

The scoria cone complex is ~1.2 km in diameter, rising 120 m above the surrounding lava plains and consisting of at least eight vents (Fig. 2). The cones sit on top of the early lava flows of the complex, which extend 60 km to the coast, covering an area of >511 km² (Fig. 3). To the northeast is an early eruption centre of coarse spatter bombs and scoria, covering a small contemporaneous spatter cone. This was in turn covered by the main double scoria cone, which itself is composed of two overlapping craters running east–west. An additional vent is located at the top of the main cone in the form of a spatter rampart and columnar jointed blocks. A low scoria cone developed in the south by the interaction of three magma batches. The late lava shield was erupted from this crater, which also features two small satellite cones (Fig. 2).

Methods

Detailed stratigraphic mapping was undertaken across the scoria cone complex, with representative samples collected for later analysis along with samples from throughout the lava field and also the satellite cones (Figs. 2, 3). Quarry logs and mapped faces were correlated across the scoria cones to determine a sequence of eruption and unravel the stratigraphic relationships. Samples were then petrographically analysed for signs of alteration/weathering before being selected for geochemical analysis. Samples were cleaned, crushed using a rock splitter and jaw crusher and screened to remove weathered material, before being reduced to powder in an agate Tema mill and analysed for major (XRF) and trace (ICP–MS) elements at either Monash University (Australia; traces), James Cook University (Australia; majors), Geolabs or Acme (Sudbury, Canada). Ferric and ferrous iron were calculated from the Fe₂O₃(TOT) of the raw data, using a Fe₂O₃/Fe₂O₃(TOT) ratio of 0.15, and results were normalised to 100 % on a volatile-free basis. Based upon the results of the analyses, a subset of samples were sent for isotopic Sr–Nd–Pb analysis at Melbourne University (Australia), where analyses were performed on either powders or acid-leached chips and Sr, Nd and Pb were extracted using anion exchange and EICHRON RE, LN and SR resin chromatography. Isotope analysis was performed on a NU Plasma MC–ICPMS following methods by Maas et al. (2005).

The 59 analysed samples comprise 32 scoria samples, 20 lava samples, one spatter fragment, three crater blocks and two samples of coherent intrusions and one of Pele’s tears (Fig. 2). Geochemical and isotopic values were used to outline the petrogenetic evolution of Mt Rouse, and in the determination of a new eruption sequence for the volcanic centre.

Results

Whole rock chemical compositions

The eruption products of Mt Rouse define three compositionally distinct magma batches based on rare earth element patterns (REE) (Fig. 4a; Table 1; supplementary data table). Patterns are similar to those of the Ocean–Island basalts (OIB) range, characteristically depleted in the heavy REE (Tb–Lu), suggesting a garnet-bearing mantle source origin. Light rare earth elements (LREEs; La–Gd) are enriched, showing increasing levels of enrichment in magma batches A through C. The REE patterns are similar to those of other NVP rocks, encompassing virtually the entire observed range reported by Price et al. (1997), Vogel

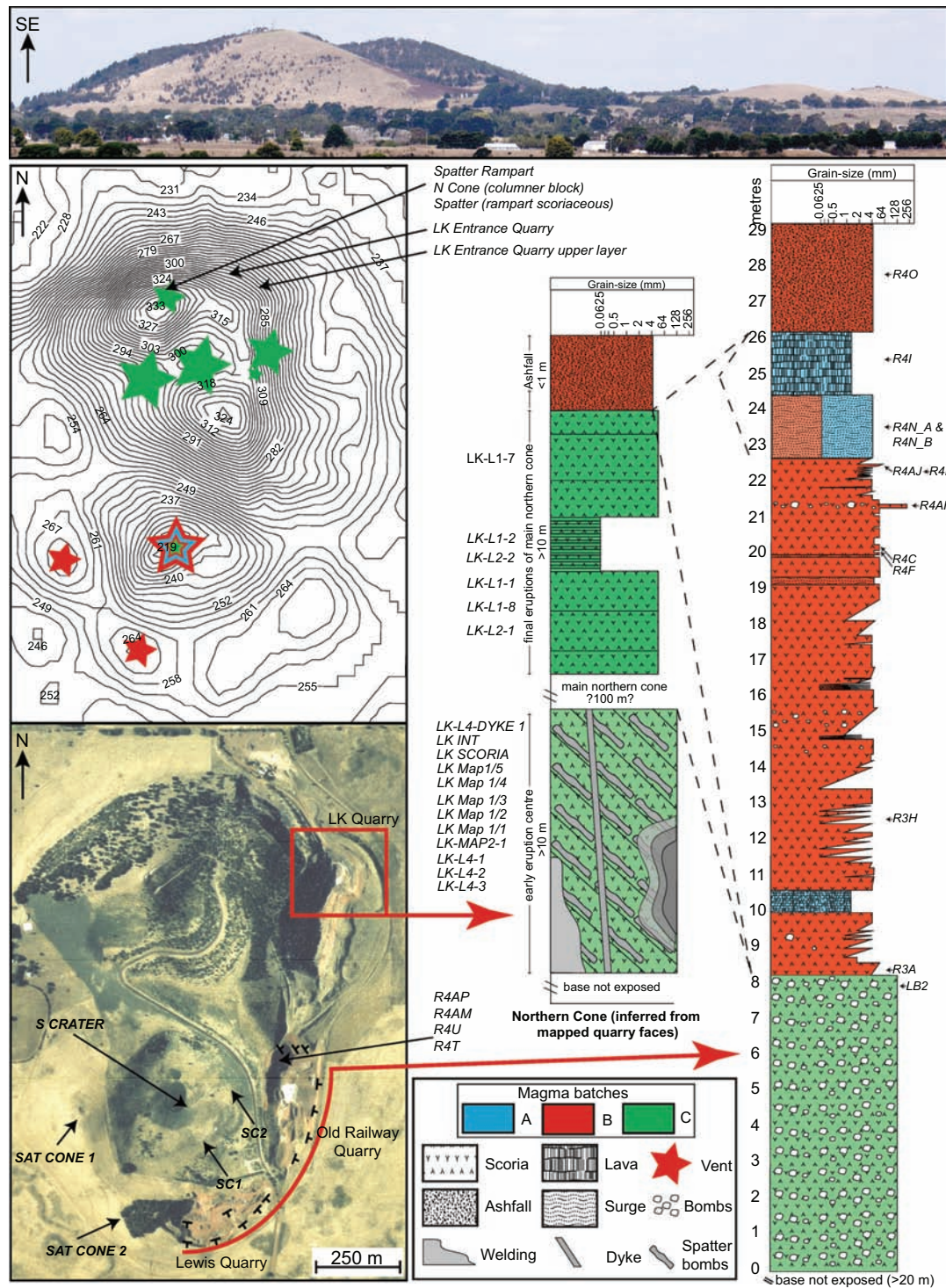
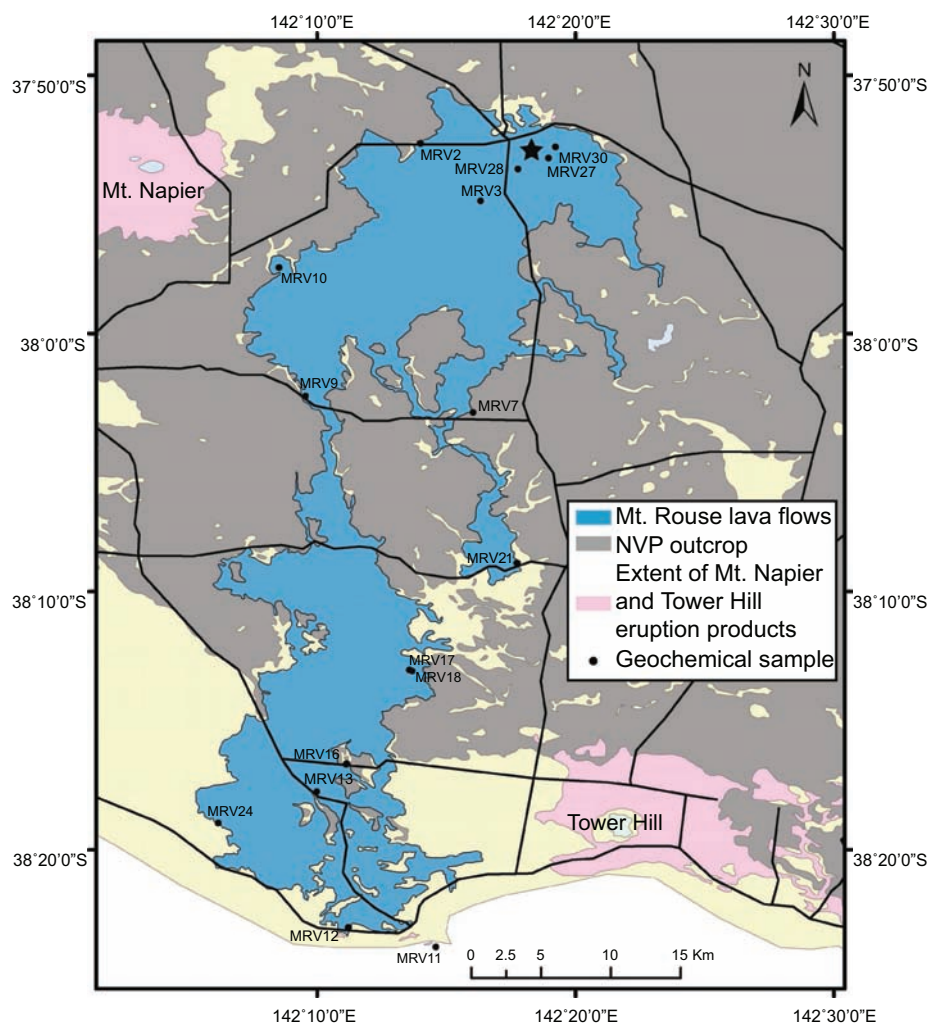


Fig. 2 *Top* Overview of the scoria cone complex of Mt Rouse, looking SE from Acacia Hill at a distance of 6.5 km, showing the main double scoria cone to the north and the two satellite cones to the southeast, with the southern crater lower than the surrounding plains. *Bottom* NASA ASTER digital elevation model of the scoria cone complex of Mt Rouse, showing composite stratigraphic log of the

southern cone and inferred log for the northern cone, with sample numbers in *italics*. Southern cone samples are placed where removed, northern cone samples are approximately placed due to the samples being removed from active quarries where faces were mapped. All log samples were erupted after the main lava field. NASA ASTER GDEM is a product of METI and NASA

Fig. 3 Lava flows of Mt Rouse, showing locations of geochemically analysed samples



and Keays (1997), McBride et al. (2001) and Demidjuk et al. (2007) (Fig. 4a).

On the basis of total alkalis versus silica (TAS) relationships, there is some overlap in composition between the three magma batches, which have typical NVP compositions (Fig. 4b). Batch A is composed of alkali basalts to subalkali basalts, constituting the 60 km of lava flows, interbedded lava in the southern cone, Pele's tears in an intermingled surge deposit directly below the interbedded lava, and the final eruption products in the southern crater (Figs. 2, 3, 4b). Batch B ranges from alkali basalt to trachybasalt (and may be further subdivided into hawaiites on the basis of $\text{Na}_2\text{O} - 2.0 \geq \text{K}_2\text{O}$). These products outcrop as the upper portion of scoria layers in the southern cone, including those of the surge deposit, and the two satellite cones, which have the lowest SiO_2 and highest total alkalis ($\text{Na}_2\text{O} + \text{K}_2\text{O}$) of the batch (Fig. 2, 4b). Batch C has similar compositions to batch B, again ranging from alkali basalts to trachybasalts to basanites, forming the early

eruption centre, northern cone and the lower scoria layers of the southern cone (Figs. 2, 4b).

Following the method of Price et al. (1997), rocks were classified using CIPW norms (see supplementary data) as alkaline (0–5 % normative nepheline), transitional (<10 % normative hypersthene \pm normative quartz) or tholeiitic (normative hypersthene \pm normative quartz >10 %). Plotting the proportions of olivine, diopside and nepheline or hypersthene in the basalt tetrahedron of Thompson (1984), the products of Mt Rouse are classified as nepheline-normative alkali-olivine basalts and basanites, hypersthene-normative olivine basalts and olivine tholeiites (Fig. 4c). The lavas (batch A) are slightly silica-undersaturated alkali-olivine basalts and silica-saturated olivine tholeiites (lava shield and some random flow samples). The pyroclastics (batches B and C) are mainly silica-undersaturated basanites, with few alkali-olivine basalts.

The three magma batches are also clearly apparent when plotting major and trace elements as a function of MgO

Fig. 4 **a** Rare earth element (REE) profiles, normalised to chondritic values, showing three distinct magma batches for the eruption products of Mt Rouse (this study; Batch A *blue*; Batch B *red*; Batch C *green*), plotted alongside the OIB average (Sun and McDonough 1989) and compared with the other published data for the Newer Volcanics Province (Price et al. 1997; Vogel and Keays 1997; McBride et al. 2001; Demidjuk et al. 2007). **b** TAS diagram (Le Bas et al. 1986; Le Maitre et al. 2002) of compositions for the eruption products of Mt Rouse compared with the NVP as a whole (>218 analyses). NVP data from Frey and Green (1974), Ellis (1976), Irving and Green (1976), Frey et al. (1978), Stone et al. (1997), Price et al. (1997), Vogel and Keays (1997), McBride et al. (2001), Foden et al. (2002) and Demidjuk et al. (2007). Subdivision of alkali and sub-alkali rocks from Irvine and Barager (1971). **c** CIPW normative classification (basalt tetrahedron) based on the proportions of olivine, diopside and nepheline or hypersthene, showing silica-undersaturated samples (*left*) and silica-saturated rocks (*right*) (after Thompson 1984). Batch A are *blue diamonds*; batch B southern cone scorias *red triangles*; batch B satellite cones *yellow triangles*; batch C *green squares*

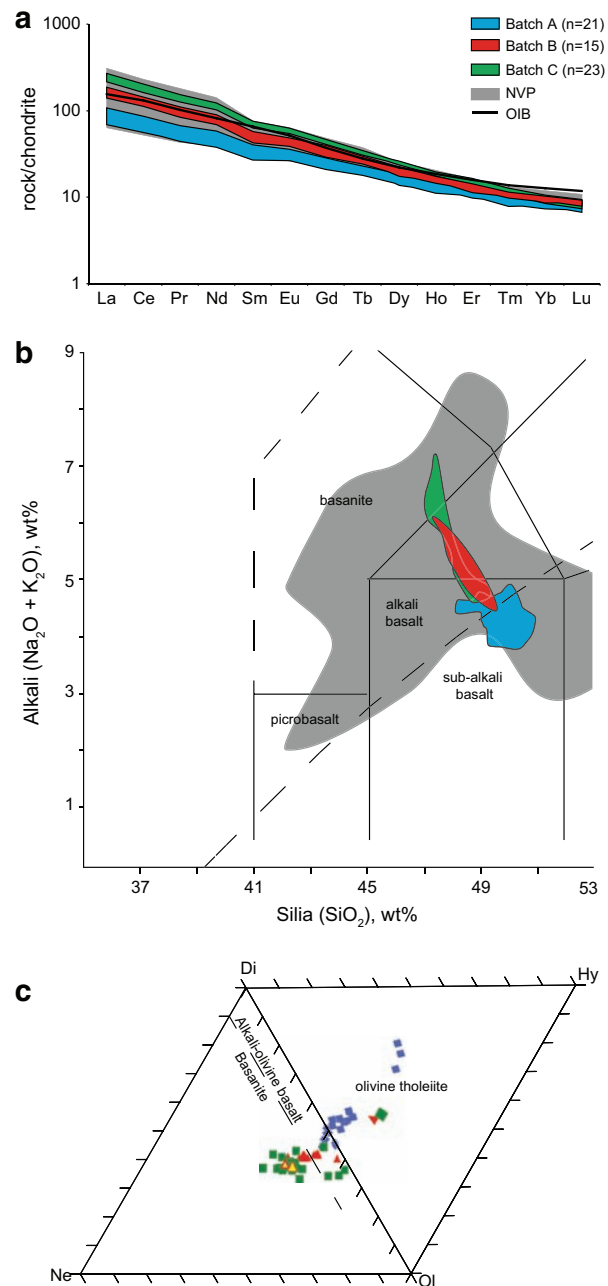
(Fig. 5). Batches A and C have similar ranges of MgO content (10.3–7.4 and 10.7–6.8 wt%, respectively). Although batch C contains two outliers, these are in fact the least differentiated samples, representing an intrusion into the lower levels of the early eruptive products (10.7 wt%) and jointed basalt at the top of the northern cone (9.3 wt%)—these both stratigraphically belong to magma batch C. Batch B has a narrower range of MgO content (9.1–8.6 wt%). The satellite cones belong to this magma batch in terms of trace element values and petrography; however, they are more differentiated.

Batch A (lava flows) exhibits a narrow range of major element concentrations with the exception of MgO. The data in this study correlate well with data published by Elias (1973), Whitehead (1991) and Sutalo (1996) (Fig. 5). Batches B and C show slight decreases of MgO and CaO with increasing TiO_2 , P_2O_5 and Th (Fig. 5).

The trace elements define the magma batches more clearly, with increased concentrations of high-field-strength elements (HFSEs), REE and large-ion-lithophile elements (LILEs) in each batch from A through C. This indicates progressively lower degrees of source partial melting as low degree partial melts contain higher concentrations of incompatible elements.

Petrography

The lavas (which all belong to magma batch A) are fine grained in hand specimen, with a glomeroporphyritic texture composed of glomerocrysts (<20 %) of olivine and clinopyroxene and rare plagioclase phenocrysts in a groundmass of slightly smaller plagioclase laths, granular to prismatic clinopyroxene and minor magnetite and ilmenite (Table 2; Fig. 6). Most analysed samples are vesicular. Iddingsite alteration of olivine is common throughout the



lava flows. The composition of groundmass plagioclase—estimated using the Michel–Levy technique—ranges from An_{60-16} (labradorite–oligoclase).

Batches B and C (scorias) are aphanitic and petrographically indistinguishable from one another. Samples are highly vesicular and consist of phenocrysts (<10 %) of generally euhedral, olivines and clinopyroxenes (Table 2; Fig. 6) contained in a hypocrySTALLINE groundmass composed of variably oxidised glass, and much finer-grained plagioclase microlites and minor opaques.

Table 1 Representative major and trace element data for the products of Mt Rouse

| Sample | MRV13d | MRV16 | MRV24a | R4G | R4AJ | R4AH | LK-L1-8 | LK MAP1 1 | LK-L4-1 |
|--------------------------------|--------|-------|--------|-------|-------|-------|---------|-----------|---------|
| Batch | A | A | A | B | B | B | C | C | C |
| Lab | Acme | Acme | Acme | Acme | Acme | Acme | Geolabs | Geolabs | Geolabs |
| SiO ₂ | 48.52 | 48.36 | 48.23 | 47.41 | 47.89 | 47.41 | 46.76 | 47.38 | 46.02 |
| TiO ₂ | 2.14 | 1.95 | 1.93 | 2.33 | 2.33 | 2.33 | 2.69 | 2.86 | 2.84 |
| Al ₂ O ₃ | 13.73 | 13.48 | 13.77 | 14.05 | 13.95 | 13.87 | 14.5 | 15.06 | 14.27 |
| Fe ₂ O ₃ | 12.04 | 12.15 | 11.85 | 12.29 | 12.11 | 12.34 | 12.94 | 12.69 | 12.33 |
| MnO | 0.15 | 0.16 | 0.16 | 0.16 | 0.16 | 0.16 | 0.169 | 0.165 | 0.16 |
| MgO | 9.28 | 10.15 | 9.9 | 8.89 | 8.78 | 8.81 | 7.29 | 7.61 | 7.46 |
| CaO | 8.84 | 8.74 | 8.92 | 8.4 | 8.16 | 8.2 | 7.912 | 7.745 | 7.558 |
| Na ₂ O | 3.24 | 3.22 | 3.18 | 3.79 | 3.68 | 3.57 | 3.99 | 3.63 | 4 |
| K ₂ O | 1.07 | 1.03 | 0.98 | 1.54 | 1.48 | 1.52 | 1.96 | 1.93 | 2 |
| P ₂ O ₅ | 0.41 | 0.38 | 0.36 | 0.62 | 0.6 | 0.64 | 0.883 | 0.958 | 0.937 |
| Cr ₂ O ₃ | 0.04 | 0.049 | 0.05 | 0.033 | 0.036 | 0.034 | | | |
| SO ₃ | | | | | | | | | |
| L.O.I. | 0.20 | 0.00 | 0.30 | 0.10 | 0.40 | 0.70 | 0.82 | 0.56 | 1.36 |
| TOT | 99.64 | 99.67 | 99.63 | 99.61 | 99.58 | 99.58 | 99.92 | 100.58 | 98.93 |
| TOT (LOI free) | 99.44 | 99.67 | 99.33 | 99.51 | 99.18 | 98.88 | 99.10 | 100.02 | 97.57 |
| Mg-number | 64.23 | 66.06 | 66.06 | 62.76 | 62.81 | 62.45 | 56.75 | 58.28 | 58.50 |
| V | 184 | 168 | 169 | 173 | 169 | 169 | 164 | 143 | 146 |
| Co | 52 | 56 | 52 | 49 | 49 | 48 | 53 | 52 | 51 |
| Ni | 207 | 230 | 205 | 149 | 161 | 152 | 172 | 176 | 159 |
| Cu | 45 | 50 | 62 | 30 | 45 | 46 | 25 | 7 | 29 |
| Zn | 83 | 83 | 83 | 83 | 118 | 118 | 136 | 148 | 142 |
| Ga | 18.6 | 18.9 | 18 | 21.5 | 19.5 | 19.4 | 24.3 | 26.2 | 25.6 |
| Rb | 18.2 | 18.1 | 16.3 | 31.9 | 29.1 | 29.6 | 43.9 | 40.5 | 28.5 |
| Sr | 503 | 490 | 489 | 728 | 708 | 725 | 940 | 1068 | 1064 |
| Y | 20.1 | 17.8 | 17.4 | 22.5 | 24.2 | 25.4 | 27.8 | 27 | 26.7 |
| Zr | 138 | 124 | 120 | 228 | 244 | 252 | 356 | 393 | 393 |
| Nb | 27 | 25 | 24 | 45 | 49 | 50 | 72 | 83 | 82 |
| Mo | 0.8 | 0.8 | 1 | 1.5 | 3 | 3.1 | 3.9 | 3 | 3.5 |
| Cs | 0.2 | 0.2 | 0.3 | 0.5 | 0.44 | 0.45 | 0.6 | 0.62 | 0.71 |
| Ba | 294 | 263 | 255 | 346 | 336 | 336 | 526 | 601 | 604 |
| La | 18.8 | 17.3 | 16.4 | 33.8 | 38.5 | 39.5 | 57.6 | 64.2 | 62.5 |
| Ce | 38 | 36 | 35 | 70 | 73 | 74 | 111 | 123 | 119 |
| Pr | 4.9 | 4.5 | 4.2 | 8.3 | 8.5 | 8.7 | 13.3 | 14.6 | 14.1 |
| Nd | 21 | 19.3 | 17.6 | 33 | 33 | 34 | 53 | 57 | 55 |
| Sm | 4.7 | 4.2 | 4.2 | 6.8 | 7.6 | 7.7 | 10.8 | 11.6 | 11 |
| Eu | 1.7 | 1.6 | 1.5 | 2.3 | 2.4 | 2.4 | 3.5 | 3.6 | 3.5 |
| Gd | 5 | 4.6 | 4.3 | 6.4 | 6.8 | 6.9 | 9 | 9.6 | 9.3 |
| Tb | 0.77 | 0.7 | 0.67 | 0.93 | 1 | 1 | 1.2 | 1.3 | 1.2 |
| Dy | 3.9 | 3.7 | 3.6 | 4.8 | 5.2 | 5.3 | 6.5 | 6.4 | 6.3 |
| Ho | 0.73 | 0.67 | 0.64 | 0.87 | 0.97 | 0.99 | 1 | 1.1 | 1 |
| Er | 1.8 | 1.7 | 1.7 | 1.9 | 2.2 | 2.3 | 2.6 | 2.4 | 2.4 |
| Tm | 0.24 | 0.21 | 0.20 | 0.26 | 0.27 | 0.27 | 0.31 | 0.29 | 0.28 |
| Yb | 1.4 | 1.3 | 1.4 | 1.5 | 1.6 | 1.6 | 1.7 | 1.5 | 1.5 |
| Lu | 0.21 | 0.19 | 0.17 | 0.22 | 0.22 | 0.22 | 0.23 | 0.2 | 0.19 |
| Hf | 3.3 | 3.3 | 3.1 | 5.6 | 5.5 | 5.5 | 7.6 | 8.5 | 8.3 |
| Ta | 1.6 | 1.5 | 1.4 | 2.9 | 2.9 | 3 | 4.5 | 5.3 | 5.1 |

Table 1 continued

| Sample | MRV13d | MRV16 | MRV24a | R4G | R4AJ | R4AH | LK-L1-8 | LK MAP1 1 | LK-L4-1 |
|--------|--------|-------|--------|------|------|------|---------|-----------|---------|
| Batch | A | A | A | B | B | B | C | C | C |
| Lab | Acme | Acme | Acme | Acme | Acme | Acme | Geolabs | Geolabs | Geolabs |
| Pb | 1.2 | 1 | 1 | 1.2 | 3.1 | 3 | 3 | 3.6 | 4.6 |
| Th | 2.7 | 2.6 | 2.6 | 4.9 | 4.6 | 4.6 | 6.6 | 7.7 | 7.5 |
| U | 0.6 | 0.6 | 0.6 | 1.4 | 1.2 | 1.2 | 1.7 | 2 | 2 |

The earlier-erupted samples of batch C contain common embayed and skeletal olivine phenocrysts, indicating disequilibrium and rapid cooling; and opaques are highly abundant in the groundmass. Later-erupted samples have rare opaques, and only the larger phenocrysts are embayed (batch B also shows some embayment of larger phenocrysts). Plagioclase compositions are distinct, generally having higher anorthite content in batch B (An_{67-18} ; labradorite–oligoclase) in comparison with batch C (An_{38-28} ; oligoclase–andesine).

It is difficult to compare these highly vesicular magmas (batches B and C) with the less vesicular and more coarsely crystalline magma (batch A). However, one difference appears to be in terms of olivine and clinopyroxene phenocrysts; in batches B and C, they are <400 μm , while many of those in batch A are >500 μm . The visual differences between the magma batches indicate that there is not a simple genetic relationship between them. This is highlighted by the fact that batches B and C are very similar petrographically yet differ markedly in terms of their trace element concentrations.

Sr–Nd–Pb isotopes

Isotope analysis of Sr–Nd–Pb was used to characterise a subset of samples for the three magma batches of Mt Rouse. Twelve samples were selected based on the most primitive of each magma batch, and the freshest, with four samples from each batch (Table 3). Uncertainties are ± 0.000020 for $^{143}Nd/^{144}Nd$, ± 0.000040 for $^{87}Sr/^{86}Sr$ and ± 0.025 – 0.05 ($2sd$) for Pb isotopes.

Two clear groupings can be seen from the data. Batch A, which constitutes the lava flows, and batches B and C, which form the scoria cones (Fig. 7). The $^{87}Sr/^{86}Sr$ values range from 0.70376–0.70388 for batch A and 0.70390–0.70395 for batches B and C. These values fall within the range of literature values for the NVP (0.7035–0.7056; Cooper and Green 1969; Dasch and Green 1975; Stuckless and Irving 1976; McDonough et al. 1985; Whitehead 1986; Ewart et al. 1988; Price et al. 1997; McBride et al. 2001; Foden et al. 2002; Demidjuk et al. 2007; van Otterloo et al. 2014). Mt Rouse lies to the west of the Mortlake Discontinuity of Price et al. (1997); $^{87}Sr/^{86}Sr$ ratios peak at

0.7046 in the west of the NVP (based on all published data) and are higher in the east, and Mt Rouse falls isotopically below the former value.

Sr-isotopic data for magma batch A may be augmented using results from Whitehead (1986) and Price et al. (1997), who analysed 21 samples of basalt within a 10 km radius of Mt Rouse (Table 4). All samples belong to magma batch A of this study and range from $^{87}Sr/^{86}Sr$ 0.70371–0.70446, which encompasses the entire range of Sr-isotopic values from all three magma batches reported in this study. This wide range in isotope ratios is not due to weathering effects as only fresh samples were used for these studies (Price et al. 1997; Price 2013, personal communication), and both Whitehead and Price sets of samples were analysed at La Trobe University. This indicates that the sources for the two suites of this study were isotopically quite similar in composition, and that either Sr-isotope analysis cannot detect the subtle variations between them, or the source regions were the same.

The $^{143}Nd/^{144}Nd$ ratios show similar close groupings, with Batch A ranging from 0.51286–0.51288, and batches B and C 0.51283–0.51285. The ϵNd ranges from 4.3 to 4.6 in batch A, and 3.8–4.0 in batches B and C. The scoriaceous material has slightly lower Nd-isotope values, and both suites plot within the data field of the NVP (Fig. 7).

The Pb-isotope compositions show a greater distinction between the two suites, with a larger compositional gap, for example, $^{206}Pb/^{204}Pb$ ranges between 18.50014 and 18.51146 in batch A and is distinctly higher in batches B and C at 18.58443–18.60743 (Table 3; Fig. 7).

Isotopic compositions therefore indicate that the lavas and scorias of Mt Rouse were sourced from two different, yet similar regions of the mantle. Both suites indicate an enriched mantle source, with batch A being more depleted.

Discussion

The detailed stratigraphic and geochemical analysis of the volcanic products of Mt Rouse has shown that three magma batches were involved in the production of the volcanic centre. This is in stark contrast to most other monogenetic eruptive centres occurring in intraplate settings, which are thought

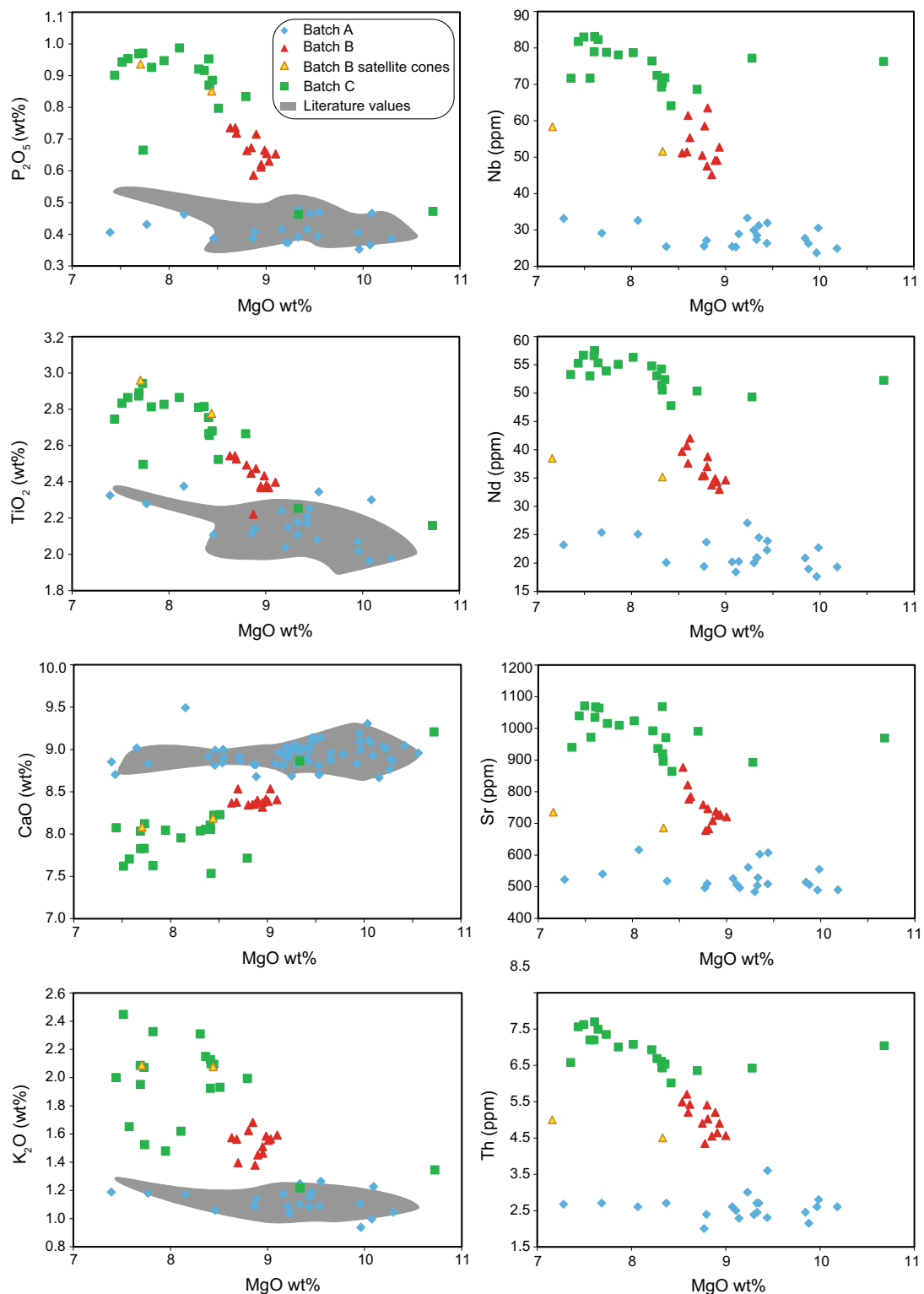


Fig. 5 Selected major and trace elements versus MgO for the products of Mt Rouse, coloured by magma batch; Batch A blue diamonds, batch B red triangles and batch C green squares. The satellite cones

of batch B are shown as yellow triangles. Major element data from previous studies shown as grey-shaded areas (Elias 1973; Whitehead 1991; Sutalo 1996)

Table 2 Petrographic descriptions of the products of Mt Rouse

| Groundmass | Mineral | Phenocrysts | |
|---|---------------|-------------|--|
| | | Size (mm) | Comments |
| <i>Batch A</i> | | | |
| Plagioclase laths (An _{60–16} labradorite–oligoclase) with minor olivine and pyroxene | Olivine | 0.65 | Glomerocrysts common |
| Magnetite as aggregated clusters (0.5 mm), laths (0.75 mm) and grains (<3 μm) | Clinopyroxene | 0.85 | |
| | Plagioclase | 1.5 | Very rare |
| <i>Other information</i> | | | |
| Green pyroxene rims in half of samples; many samples are iddingsitised | | | |
| <i>Batch B</i> | | | |
| Glass dominant (variably oxidised), with plagioclase microlites and few laths (An _{67–18} labradorite–oligoclase) | Olivine | 0.4 | Rare glomerocrysts |
| Magnetite in groundmass, usually <0.01 mm globules; variable in abundance from rare to disseminated throughout | Clinopyroxene | 0.4 | |
| <i>Other information</i> | | | |
| Coherent samples (final products of satellite cones) are iddingsitised, and feature a large amount of oxides in the groundmass and larger phenocrysts up to 0.6 mm. Rare large phenocrysts of embayed olivines and pyroxenes up to 0.6 mm | | | |
| <i>Batch C</i> | | | |
| Variably oxidised glass, plagioclase microlites (An _{38–28} andesine–oligoclase) | Olivine | 0.3 | Euhedral, commonly embayed, rare glomerocrysts |
| Magnetite, generally <0.01 mm globules; varies from highly abundant in early erupted samples to rare in later-erupted samples | Clinopyroxene | 0.25 | Commonly embayed |
| <i>Other information</i> | | | |
| Many samples heavily oxidised. Rare phenocrysts up to 0.5 mm. Rare disaggregated mantle xenoliths with jagged edges, up to 0.7 mm | | | |

Batch A is lavas; B and C are scorias

to be simple in nature and formed from single magma batches (e.g. Walker 2000). Recent research into single eruption centres in worldwide intraplate volcanic provinces indicates that some monogenetic centres are actually complex in nature (e.g. Brenna et al. 2011). Mt Rouse is the only known monogenetic volcanic complex that appears to have formed from three distinctly different magma batches that were emplaced both sequentially and then simultaneously. The nature of the stratigraphy points to a complex system of propagating dykes, at least at upper crustal levels, beneath the Mt Rouse complex. Eruptions took place over four stages and multiple sub-stages over at least eight vents. This resulted in the sequential eruption of magma batches A, C and B then simultaneous eruption of batches A and B (Fig. 2).

Mt Rouse shows similarities to two other volcanic centres in the NVP—Mt Gambier and the Red Rock Volcanic Complex. The Mt Gambier maar–cone volcanic complex is the product of two magma batches (basanites and trachy-basalts), which were erupted simultaneously over 13 stages to produce >14 vents aligned parallel to the Tartwaup Fault System (van Otterloo and Cas 2011; van Otterloo 2012; van Otterloo et al. 2013). The Red Rock maar–cone volcanic complex is also composed of multiple vents with two simultaneously erupting magma batches (Piganis 2011).

In order to fully understand the genesis of the multiple magma batches of Mt Rouse, the effects of any

fractionation and crustal contamination will be discussed, and the depth of magma generation will be estimated in order to ascertain the origin of the three magma batches.

Fractionation

The trace elements Nd (incompatible) and Sr were used to model shallow level fractional crystallisation using starting compositions of the most primitive sample in each magma batch, this being the sample with the lowest incompatible trace element content and the highest Mg-number. The Rayleigh fractionation equation assumes that when crystals form, they are immediately removed from the melt, and is expressed by:

$$C_L = C_0 F^{(D-1)}$$

where C_L is the concentration of the trace element at a given percentage of fractionation, C_0 is the starting concentration of the trace element, and F is the weight fraction of melt remaining (e.g. 0.9 for 10 % fractional crystallisation). D is the mineral/melt partition coefficient (K_d) for each element. K_d values were taken from the EarthRef.org GERM Partition Coefficient (K_d) database, where values for alkali basalts were used for magma batch A (Table 5; Schnetzler and Philpots 1970; Villemant et al. 1981; Fujimaki and Tatsumoto 1984) and basanite for magma batches

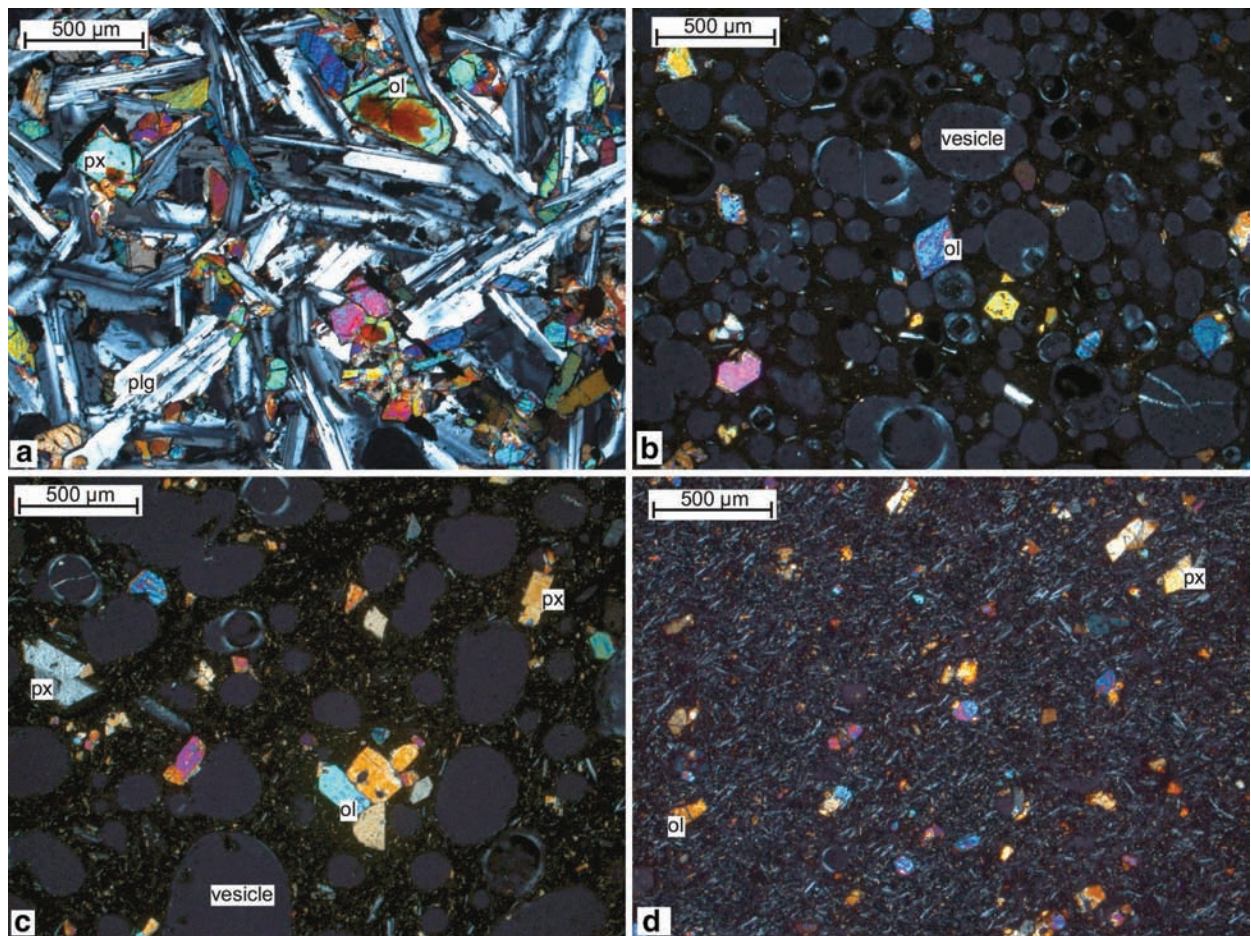


Fig. 6 Typical photomicrographs of the products of Mt Rouse. **a** Magma batch A lavas, showing glomerocrysts of olivine and clinopyroxene in a groundmass dominated by plagioclase laths; **b**, **c** Scorias of magma batches B and C showing a glassy microlitic groundmass

with olivine and pyroxene phenocrysts; **d** Dyke composed of magma batch C, showing a microlite-rich groundmass and microphenocrysts of olivine and pyroxene

Table 3 Sr–Nd–Pb compositions of the products of Mt Rouse

| | Batch | $^{87}\text{Sr}/^{86}\text{Sr}$ | $^{143}\text{Nd}/^{144}\text{Nd}$ | ϵ_{Nd} | $^{206}\text{Pb}/^{204}\text{Pb}$ | $^{207}\text{Pb}/^{204}\text{Pb}$ | $^{208}\text{Pb}/^{204}\text{Pb}$ |
|---------|-------|---------------------------------|-----------------------------------|------------------------|-----------------------------------|-----------------------------------|-----------------------------------|
| SC | A | 0.703768 | 0.51288 | 4.6 | 18.511 | 15.559 | 38.514 |
| MRV7 | A | 0.703865 | 0.51286 | 4.4 | 18.502 | 15.550 | 38.482 |
| MRV16 | A | 0.703881 | 0.51286 | 4.3 | 18.507 | 15.562 | 38.540 |
| MRV24 | A | 0.703865 | 0.51286 | 4.3 | 18.500 | 15.558 | 38.523 |
| R4C | B | 0.703934 | 0.51283 | 3.8 | 18.584 | 15.565 | 38.588 |
| R4AH | B | 0.703952 | 0.51284 | 3.9 | 18.602 | 15.572 | 38.618 |
| R4AJ | B | 0.703948 | 0.51284 | 3.8 | 18.607 | 15.572 | 38.622 |
| R4AP | B | 0.703905 | 0.51284 | 3.9 | 18.597 | 15.566 | 38.600 |
| LK-INT | C | 0.703902 | 0.51284 | 4.0 | 18.592 | 15.567 | 38.603 |
| NCONE | C | 0.703918 | 0.51285 | 4.0 | 18.591 | 15.565 | 38.597 |
| LK-L2-2 | C | 0.703958 | 0.51284 | 3.9 | 18.594 | 15.567 | 38.605 |
| LB2 | C | 0.703939 | 0.51284 | 3.9 | 18.595 | 15.564 | 38.599 |

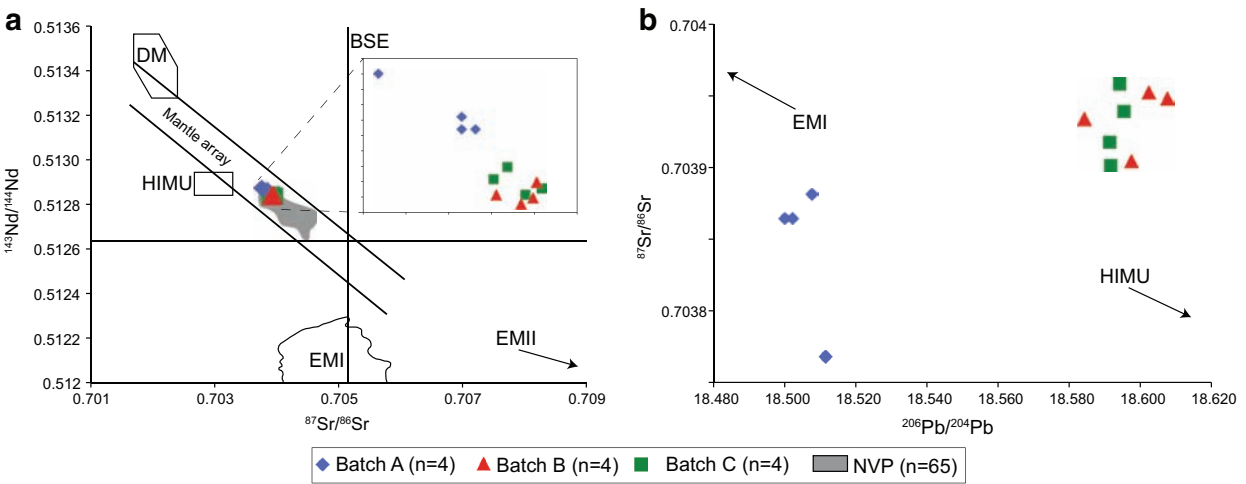


Fig. 7 **a** $^{143}\text{Nd}/^{144}\text{Nd}$ versus $^{87}\text{Sr}/^{86}\text{Sr}$ isotopic compositions of the products of Mt Rouse (*main figure* and *inset*; this study), compared with published data from the Newer Volcanics Province (McDonough et al. 1985; McBride et al. 2001; Foden et al. 2002; Demidjuk et al. 2007; van Otterloo et al. 2014). Mantle array, bulk silicate Earth (BSE) depleted mantle (DM) and enriched mantle (EMI and EMII) from Zindler and Hart (1986). **b** $^{87}\text{Sr}/^{86}\text{Sr}$ versus $^{206}\text{Pb}/^{204}\text{Pb}$ isotopic composition for Mt Rouse, showing two clear groupings for batch A, and batches B and C. Symbols refer to magma batch: Batch A blue diamonds; batch B red triangles and batch C green squares

Table 4 Sr–Nd–Pb compositions of the products of Mt Rouse from previous studies

| | Batch | $^{87}\text{Sr}/^{86}\text{Sr}$ |
|---------------------|-------|---------------------------------|
| F1-308 ^b | A | 0.70388 |
| F1-311 ^b | A | 0.70396 |
| F1-309 ^b | A | 0.70382 |
| F1-304 ^a | A | 0.70375 |
| HO-203 ^a | A | 0.70407 |
| HO-204 ^a | A | 0.70411 |
| HO-205 ^a | A | 0.70411 |
| HO-206 ^a | A | 0.70416 |
| HO-207 ^a | A | 0.70411 |
| HO-208 ^a | A | 0.70405 |
| HO-211 ^a | A | 0.70381 |
| F1-305 ^a | A | 0.70371 |
| HO-212 ^a | A | 0.70395 |
| HO-213 ^a | A | 0.70383 |
| HO-214 ^a | A | 0.70383 |
| HO-215 ^a | A | 0.70396 |
| F1-306 ^a | A | 0.70392 |
| HO-216 ^a | A | 0.70377 |
| HO-225 ^a | A | 0.70446 |

^a Whitehead (1986)
^b Price et al. (1997)

B and C (Adam and Green 2006). Plagioclase feldspar, clinopyroxene and olivine were modelled for batch A, but plagioclase was omitted for batches B and C as phenocrysts are not found in thin section.

The fractionating phases differ slightly for each of the Mt Rouse magma batches. The position of the samples on a mineral vector diagram (Fig. 8a) indicates that the range of batch A compositions (lava flows) is the product of up to ~30 % olivine and clinopyroxene fractionation, accompanied by minor plagioclase. This is consistent with the petrography, in which only rare plagioclase phenocrysts up to 1.5 mm were observed; in addition, as no Eu anomalies are present on the REE spider plots, plagioclase clearly was not a major fractionating phase in these basalts. The batch B range is the result of up to ~18 % olivine and 20 % clinopyroxene; and batch C up to 20 % olivine and 22 % clinopyroxene fractionation (Fig. 8a).

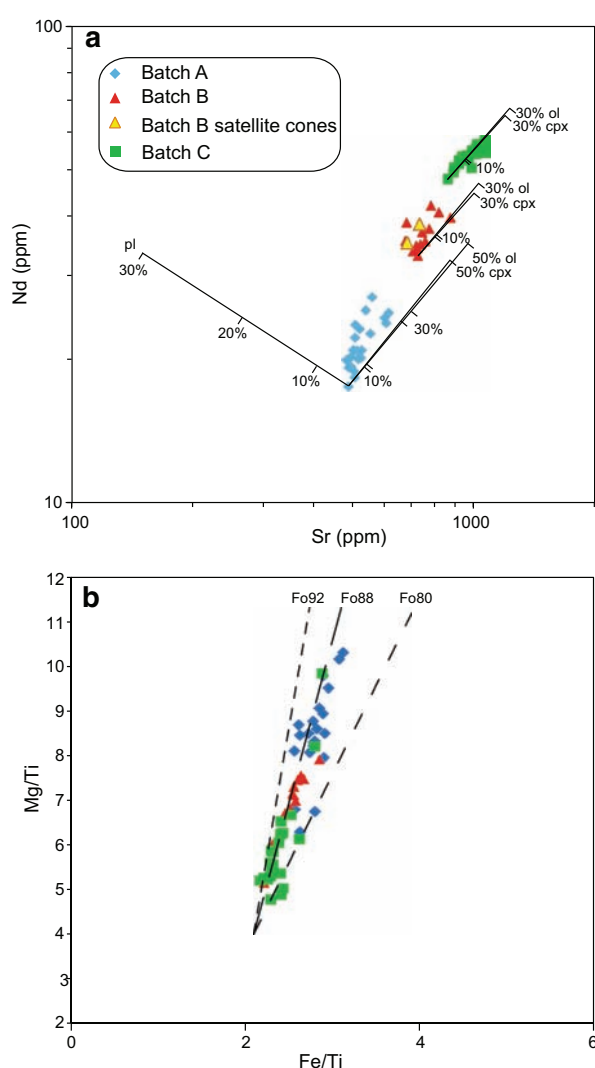
The amount of fractional crystallisation required to produce one magma batch from another was assessed by rearranging the mass balance equation to calculate the extent of crystallisation ($1 - F$), assuming that elements are totally incompatible ($D = 0$)

$$1 - F = C_0/C_L$$

where F is the fraction of melt remaining, C_0 the initial concentration of the trace element in question and C_L the concentration in the residual liquid. Using average values of the incompatible trace elements Th, Nd and Zr, the results indicate that magma batch A cannot be derived from batches B or C (Table 6). In order to be the parental magma for batches B or C, magma batch A would require 45–65 % fractional crystallisation, which would result in magmas with much lower MgO content. Batch B cannot be produced from batch C, and in order for batch C to produce batch B, 30–35 % fractional crystallisation would

Table 5 Kd values of Sr and Nd in plagioclase feldspar, clinopyroxene and olivine used to model shallow level fractional crystallisation

| | Alkali basalt | | Basanite | |
|-----|-------------------|---------------------|--------------------|---------------------|
| | Sr | Nd | Sr | Nd |
| Plg | 2.7 ^b | 0.069 ^a | – | – |
| Cpx | 0.16 ^b | 0.1224 ^c | 0.104 ^d | 0.001 ^d |
| Ol | 0.02 ^b | 0.0023 ^c | 0.13 ^d | 0.0005 ^d |

^a Schnetzler and Philpots (1970)^b Villemant et al. (1981)^c Fujimaki and Tatsumoto (1984)^d Adam and Green (2006)**Fig. 8** **a** Vector diagram of Nd versus Sr, with calculated fractional crystallisation vectors of olivine (ol), clinopyroxene (cpx) and plagioclase feldspar (pl) based on the most primitive sample of each magma batch. **b** Plot of molar amounts of Mg/Ti versus Fe/Ti showing that most Mt Rouse samples lie along an olivine control line of Fo88

be required, which would result in clear petrographic differences.

The compositions of olivines were estimated using Pearce element ratios using the methods described by Russell and Nicholls (1988). For the Mt Rouse samples, we have used Ti as the conserved element in the ratios. When plotted on a scattergram of molar Mg/Ti versus molar Fe/Ti, the bulk of the Mt Rouse samples lie along an olivine control line for a Fo number of 88 (Fig. 8b). A few of the samples in magma batches A and C lie along the Fo = 80 control line; these samples have lower Mg-number's than other samples in these magma batches indicating that they were formed from more evolved magmas. The fact that the bulk of the samples lie along the Fo = 88 control line indicates that all three magma batches comprised relatively primitive magmas that had undergone limited fractionation.

Contamination

The higher Pb-isotope ratios of magma batches B and C may be indicative of crustal contamination; however, there is no geochemical evidence for contamination from the trace elements, as all samples plot within the mantle array on variation diagrams of Pearce (2008). For example, on a Th/Yb versus Nb/Yb plot, Th/Yb ratios increase with Nb/Yb ratios (Fig. 9a). However, crustal contamination results in an increase in Th/Yb ratios but a decrease in Nb/Th ratios and contaminated products plot above the MORB–OIB array (Pearce 2008).

This is confirmed by the ratios of other highly incompatible trace elements such as La/Nb, Ba/Nb, Rb/Nb, Th/Nb, Th/La and Nb/U. All of the Mt Rouse samples have ratios that are much more similar to primordial mantle values than continental crust values (Table 7). These ratios do not undergo significant fractionation and therefore retain similar levels to that of the mantle source (Hofmann et al. 1986; Weaver 1991).

Degree of partial melting and depth of origin

The relative degree of mantle partial melting involved in the origin of primary magmas can be estimated by the ratio of Th/Yb, which decreases with increased percentages of partial melting (Fig. 9b; Pearce 2008; Pietruszka et al. 2009). The low Th/Yb of batch A (lavas) suggests higher degrees of partial melting of a source similar to those for OIB and batches B and C (pyroclastics) appear to have been produced by progressively lower degrees of partial melting. This observation is also reflected in the LREE content of the magma batches, as incompatible element concentrations decrease with increasing degrees of partial melting (Fig. 4a).

The depth of generation of the magma batches can be assessed using the ratio Gd/Yb, which increases with

Table 6 Average values of incompatible elements Th, Nd and Zr in the magma batches of Mt Rouse (A, B, C) and the percentage of fractional crystallisation required to derive one from another

| | Th | Nd | Zr |
|------------------------------|-------|-------|--------|
| A | 2.58 | 21.66 | 147.85 |
| B | 4.99 | 36.72 | 259.48 |
| C | 6.9 | 53.54 | 367 |
| % Fractional crystallisation | | | |
| A from B | −0.93 | −0.70 | −0.76 |
| A from C | −1.67 | −1.47 | −1.48 |
| B from A | 0.48 | 0.41 | 0.43 |
| B from C | −0.38 | −0.46 | −0.41 |
| C from B | 0.28 | 0.31 | 0.29 |
| C from A | 0.63 | 0.60 | 0.60 |

increasing depth of melt generation within the lithosphere mantle (Song et al. 2009). At depths beyond those at which Cr-spinel is the aluminous phase in the mantle, HREE are retained in residual garnet during partial melting (Irving and Frey 1987). Gd and Yb are highly incompatible elements and neither have an affinity for olivine or clinopyroxene during fractional crystallisation. Shown against the ratio La/Lu (the degree of REE fractionation), it can be seen that the products of Mt Rouse were sourced from progressively lower degrees of partial melting and increasing depths (Fig. 9b). The diagrams also indicate that there are significant differences in the petrogenetic indicator elements between the three batches, meaning that the differences in composition between them are not due to differences in the proportions of minerals.

Source melting was estimated using REE elements relative to values for primitive mantle (PM) (according to the method of Song et al. 2009 and references therein). This indicates that the magmas were derived by 5 % partial melting of garnet ilmenite for magma batch A, falling to 2 % for batch C. If the mantle sources were enriched in incompatible elements to levels above those of PM, the degrees of source melting may have been slightly higher.

In order to estimate temperature and pressure of magma origin, primary magma compositions must have a minimum Mg-number of 70 to represent unmodified mantle melts. Since the Mg-numbers of the volcanic products of Mt Rouse are all less than 70 and range from 58.5–66.6 (batch A), 57.8–62.8 (batch B) to 54.4–66.8 (batch C), estimates of primary magma composition were calculated by extrapolating element abundances to a primary magma Mg-number of 70 using linear regression lines following the methods of Smith et al. (2008). Results were normalised to 100 % (Table 8) and used to calculate pressures and depths of magma generation.

The pressure during melt generation can be estimated using the equation formulated by Wood (2004). This equation is an expression of the compositional dependency between pressure and total alkali content of anhydrous melt in equilibrium with olivine, orthopyroxene and clinopyroxene.

$$P(\text{GPa}) = (\text{MgO} - 11.14 + 1.262\text{Alk}) / (2.765 + 0.0945\text{Alk})$$

where MgO is that of the melt in wt%, and Alk represents total alkalis ($\text{Na}_2\text{O} + \text{K}_2\text{O}$). The uncertainty in the pressure estimate is ± 0.33 GPa (Wood 2004). A similar equation also developed by Wood (2004) expresses the relationship between temperature and total alkali content, with an uncertainty of ± 30 °C.

$$T(^{\circ}\text{C}) = 1,230 - 23.75\text{Alk} + (98 + 5.6\text{Alk})P$$

From these equations, batch A was estimated to have formed at a pressure of 1.7 ± 0.33 GPa and a temperature of $1,335 \pm 30$ °C; batch B at a pressure of 1.88 ± 0.33 GPa and a temperature of $1,351 \pm 30$ °C; and batch C a pressure of 1.94 ± 0.33 GPa and a temperature of $1,360 \pm 30$ °C (Fig. 10). These values equate to depths of 55.5, 61 and 63 km, respectively, meaning that the parental magmas of all three magma batches are likely to have originated from very similar depth ranges. These depths complement the isotopic data, which suggest a similar source region for all samples, but with parental magmas of batch A forming one series and those of batches B and C a second as discussed above. The equations of Lee et al. (2009) were not used in this study, as they overestimate the melting pressures of alkali basalts, not being calibrated for these compositions. When plotted onto the southeast Australia geotherm, the pressures correspond to depths near the spinel–garnet transition zone at ~ 1.6 GPa (55 km; O'Reilly and Griffin 1985). The rare spinel–ilmenite xenoliths in batches A and C were entrained on their way to the surface. The depth to the lithosphere–asthenosphere boundary (LAB) in southeast Australia has been estimated at $\sim 61 \pm 11$ km (Ford et al. 2010); this would suggest a shallow asthenospheric source for the magma batches B and C and lower lithosphere for magma batch A.

The equations of Wood (2004) are for anhydrous systems, resulting in modelled magmas plotting on the dry peridotite solidus of Hirschmann (2000). The addition of water reduces the mantle solidus and lowers the temperature of magma generation (Burnham 1979; Katz et al. 2003). When compared to the hydrous pseudo-phase diagram of Katz et al. (2003), which shows the calculated solidi for differing bulk water content, in order to reach the geotherm and generate melt the source of the magmas of Mt Rouse must have contained between 0.075 and 0.085 wt% water, corresponding to temperatures of $\sim 1,080$ °C for magma batch A and between 1,115 and

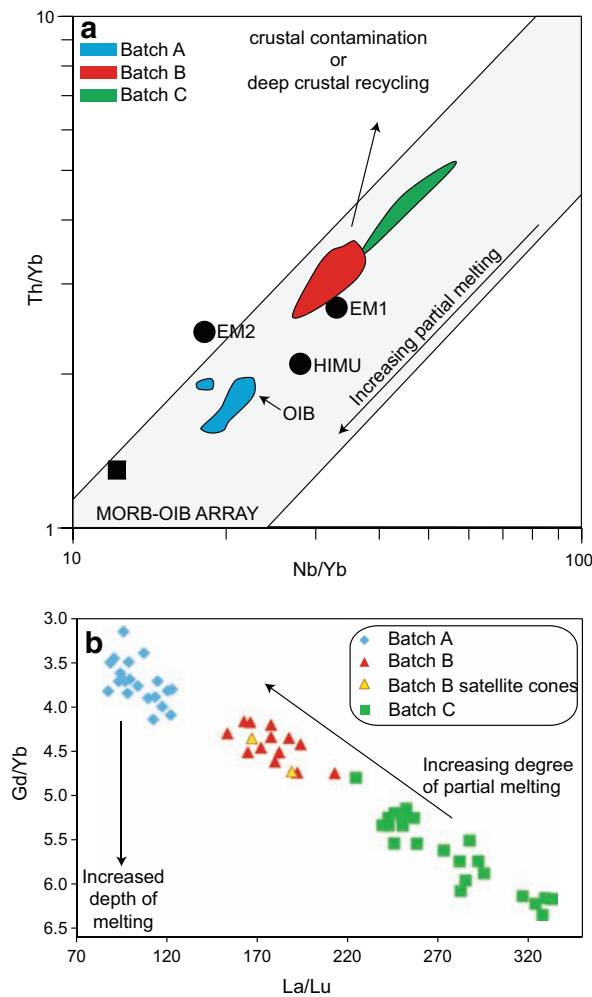


Fig. 9 **a** Th/Yb versus Nb/Yb showing that the products of Mt Rouse are not crustally contaminated and that magma batch A is from a source similar to OIB with higher degrees of partial melting than batches B and C, which are from a source more similar to EM1. Modified after Pearce (2008). **b** Gd/Yb versus La/Lu, showing decreased partial melting with increasing depth of melt in Mt Rouse products

1,130 °C for batches B and C (Fig. 10). With 2–5 % partial melting, this indicates water contents of ~2–4 wt% in the primary magmas.

Similar calculations were performed by van Otterloo et al. (2014) for the Mt Gambier maar–cone volcanic complex, which lies 135 km directly west of Mt Rouse. The two magma batches involved in the eruption were calculated to have been sourced from depths and temperatures of 1.79 ± 0.33 GPa and $1,332 \pm 30$ °C (trachybasalts); and 2.2 ± 0.33 GPa and $1,382 \pm 30$ °C (basanites; Fig. 10); the water contents of the magma sources were estimated at 0.05–0.1 wt% (van Otterloo et al. 2014). These temperatures and pressures are similar to those found for Mt Rouse and therefore probably other volcanoes in the NVP of similar geochemical character.

Gazel et al. (2012) use Ba/La ratios in the monogenetic Big Pine Volcanic Field, California, to show that deeper-derived magmas have lower Ba/La ratios (~20) than magmas derived at shallower depths, which had Ba/La ratios of 25–30. This is also the case for Mt Rouse, where the shallower batch A rocks have an average Ba/La = ~15 and the rocks of the deeper batches B and C have average Ba/La = ~9.4.

The link between eruptive style and melt composition

From a physical volcanology perspective, there is a clear link between eruption style and magma batch at Mt Rouse (Table 9). Summarised here, the link will be fully explored in more detail in a future publication on the stratigraphic architecture of the complex. Magma batch A (alkali basalts) exclusively erupted effusive Hawaiian-style lava flows. In contrast, magma batches B and C erupted explosive violent Strombolian to micro-Plinian deposits, with batch C also featuring Strombolian deposits during its initial eruptions.

It has been implied that in the lithospheric mantle beneath western Victoria metasomatism increases with depth (Frey et al. 1978; McDonough et al. 1985;

Table 7 Incompatible element ratios for the primordial mantle and continental crust (values from Weaver 1991 with the exception of Nb/U of Hofmann et al. 1986) compared with the range of values for

Mt Rouse volcanic products (this study), showing mantle values for the volcano and no crustal contamination

| | La/Nb | Ba/Nb | Rb/Nb | Th/Nb | Th/La | Nb/U |
|-------------------|-----------|----------|-----------|-----------|-----------|-----------|
| Primordial mantle | 0.94 | 9 | 0.91 | 0.11 | 0.13 | 30 |
| Continental crust | 2.2 | 54 | 4.7 | 0.44 | 0.2 | 10 |
| Magma batch A | 0.62–0.88 | 8.8–12.8 | 0.57–0.85 | 0.08–0.11 | 0.11–0.16 | 36.9–153 |
| Magma batch B | 0.7–0.81 | 6.8–7.7 | 0.38–0.71 | 0.09–0.11 | 0.11–0.14 | 32.2–48.3 |
| Magma batch C | 0.69–0.85 | 6.5–8.7 | 0.26–0.65 | 0.08–0.1 | 0.11–0.12 | 38.4–51.4 |

Table 8 Primary magma composition of the three magma batches of Mt Rouse

| Batch | A | B | C |
|--------------------------------|-------|-------|-------|
| SiO ₂ | 49.77 | 51.01 | 47.22 |
| TiO ₂ | 1.95 | 1.52 | 2.15 |
| Al ₂ O ₃ | 13.01 | 12.54 | 13.70 |
| Fe ₂ O ₃ | 1.72 | 1.65 | 1.85 |
| FeO | 8.76 | 8.44 | 9.37 |
| MnO | 0.15 | 0.16 | 0.16 |
| MgO | 11.10 | 11.16 | 11.48 |
| CaO | 8.87 | 8.50 | 8.97 |
| Na ₂ O | 3.31 | 2.50 | 3.08 |
| K ₂ O | 1.00 | 2.28 | 1.56 |
| P ₂ O ₅ | 0.37 | 0.23 | 0.47 |
| Total | 100 | 100 | 100 |

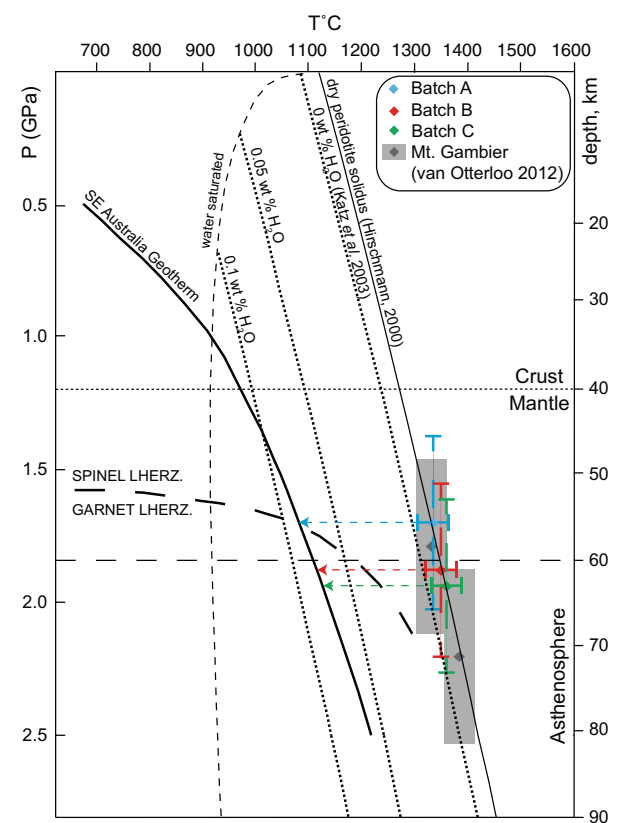


Fig. 10 Southeast Australia geotherm (modified after O'Reilly and Griffin 1985), showing estimated temperatures and depths of origin of Mt Rouse products. Dry Peridotite solidus from Hirschmann (2000) and bulk water solidi from Katz et al. (2003). Crust-mantle boundary from Aivazpourporgou (2013) and Fontaine et al. (2013). Estimated temperatures and depths for the magmas of Mt Gambier shown for comparison (van Otterloo et al. 2014)

McDonough and McCulloch 1987; Boyce et al. 2014). This may explain why the deeper-sourced magma batches contain higher proportions of trace elements and volatiles and erupt explosively. The mantle underlying western Victoria has undergone at least three metasomatic events (O'Reilly and Griffin 1988; Griffin et al. 1988). This has resulted in the enrichment of incompatible trace elements and volatiles during modal metasomatism. A metasomatic event between 500 and 300 Ma produced high ⁸⁷Sr/⁸⁶Sr garnet pyroxenites, a second metasomatic event at 60 Ma to present produced wehrlitic pyroxenites, and a third recent local metasomatic event resulted in overprinting by both silicate melts and carbonatitic fluids (Yaxley et al. 1991, 1996; Powell et al. 2004; O'Reilly and Griffin 2013). Two series of basalts were distinguished in the NVP—the plains basalts and the cones basalts—which are geochemically and isotopically distinct (Price et al. 1988; McDonough et al. 1985; Vogel and Keays 1997). The cones basalts were considered younger and formed the smaller scoria cones, maars and tuff rings of the NVP (Price et al. 1988). The products of Mt Rouse fit into both groupings with magma batch A (lava flows) representing the plains basalts and batches B and C the cones series. This indicates that age is not a factor in the eruption of the magmas, as all three magma batches erupted during a single series of events at Mt Rouse. McBride et al. (2001) argue that the two series reflect different source magmas—these authors suggest that the cones group ascended more rapidly and did not undergo significant interaction with the crust. Decreasing degrees of partial melting of a LREE-enriched garnet-bearing source region affected by metasomatism was suggested by Frey et al. (1978), McDonough et al. (1985) and McDonough and McCulloch (1987) to explain the two series—a view supported by this study.

Structural influences during the eruption of Mt Rouse

The Hamilton area features two major faults and many local faults of unknown character. The Escondida and Yarramyljup Faults both lie west of Mt Rouse and are interpreted as converging north of the Grampians (Fig. 1; Cayley et al. 2011). The Escondida Fault could not have influenced the eruption of Mt Rouse, as it is easterly dipping (Gray et al. 2003). The Yarramyljup Fault has recently been reinterpreted as deep and moderately westerly dipping, lying just east of Mt Rouse, extending north to Dunkeld (Cayley 2014, personal communication). It is therefore possible that faulting has played a part in the location of Mt Rouse, as vents are aligned approximately north-south at the complex (although vents of the northern cone are aligned E-W), parallel to the new location of the deep Yarramyljup Fault, which may have acted as a preferred pathway for magma ascent.

Table 9 Eruption styles associated with the magma batches of Mt Rouse and their role in the stratigraphic architecture of the complex

| Magma batch | Eruption Style | Role in architecture of complex |
|-------------|--------------------------------------|--|
| A | Hawaiian | Lava field |
| B, C | Violent Strombolian to micro-Plinian | Northern and Southern main cones |
| C | Strombolian | Northern and southern early eruption centres |

The origin of the magma batches of Mt Rouse

The magmas of Mt Rouse were a series of fractional melts derived from a garnet-stable source region near the LAB, and entrained xenoliths of spinel lherzolite on their way to the surface. The presence of even small amounts of xenolithic material indicates a fairly rapid ascent rate for the magmas in order to keep the xenoliths entrained in the melt (e.g. Rutherford and Gardner 2000).

Geochemical analyses indicate that magma batch A was produced from a slightly shallower source than batches B or C, which were derived from a similar, slightly deeper source region by smaller degrees of partial melting. The mantle beneath western Victoria is thought to be heterogeneous on scales from centimetres to around 1 km (McDonough and McCulloch 1987; O'Reilly and Griffin 1988; O'Reilly and Griffin 1988). The degree of metasomatism increases with depth (Frey et al. 1978; McDonough et al. 1985; McDonough and McCulloch 1987; Boyce et al. 2014; as outlined above); further, studies of xenoliths imply that the upper subcontinental lithospheric mantle is depleted, but increases in fertility with depth (O'Reilly and Griffin 2006). The variability in trace elements and isotopes between the Mt Rouse magma batches is consistent with the interpretation that they were derived from a heterogeneous source region affected by increasing degrees of metasomatism with depth.

Partial melting beneath Mt Rouse occurred across the LAB, which lies at $\sim 61 \pm 11$ km (Ford et al. 2010). Magma batch A was derived from the base of the lithosphere and batches B and C from the shallow asthenosphere, which indicates that the LAB is an important boundary with respect to NVP volcanism (Boyce et al. 2014). Ford et al. (2010) ascribe a decline in seismic activity at the LAB to both the presence of partial melt and increased amounts of volatile phases. Partial melting at the LAB of metasomatised mantle has also been used to explain the origin of the late Cainozoic Cooktown basalts of northern Queensland, Australia (Zhang et al. 2001). Metasomatism has also been used to explain the geochemical distinctions in magmas in monogenetic volcanoes from the southern Cascade arc (Strong and Wolff 2003) and Jeju Island, Korea (Brenna et al. 2012).

As for Mt Rouse, both asthenospheric and lithospheric sources were invoked for the monogenetic Big Pine Volcanic Field, California. Gazel et al. (2012) state that earlier-erupted volcanoes were derived from the asthenosphere and later eruption centres from a chemical boundary layer beneath the base of the lithosphere. This directly contrasts with the nature of the LAB beneath Mt Rouse, as lithospheric and asthenospheric magmas erupted during a single series of eruptive events. Because magmas from both sources erupted at Mt Rouse simultaneously, this implies the plains and cones series may reflect partial melting of metasomatised mantle related to the LAB. Partial melting of metasomatised mantle can be a consequence of thermal perturbations (McKenzie 1989). This could be explained by edge-driven convection, a recent explanation proposed for the cause of NVP magmatism (Demidjuk et al. 2007; Farrington et al. 2010; Davies and Rawlinson 2014). Differential motion between the fast-moving Australian lithosphere and the underlying asthenosphere, coupled with thermal contrasts associated with steps in lithospheric thickness beneath the Australian continent to the south, acts to produce convection cells in the upper mantle at the transition zone of the steps. Convection cells then travel with the overlying lithosphere and produce upwelling of fertile asthenospheric material downstream (e.g. south) of the lithospheric step (King and Anderson 1998; Demidjuk et al. 2007; Farrington et al. 2010) and isolated to the shallow asthenosphere (Davies and Rawlinson 2014). Lithospheric steps beneath Australia have been confirmed (e.g. Fishwick et al. 2008), and the NVP has recently been shown to be associated with an important area of thin lithosphere close to the southernmost main step, with there being several steps in lithospheric thickness beneath the NVP (Davies and Rawlinson 2014). The area of the NVP shows low seismic velocities at depth, associated with elevated temperatures (Rawlinson and Fishwick 2012; Davies and Rawlinson 2014) and partial melt (Aivazpourporgou 2013). The low velocities disappear by 200 km depth, which could be explained by edge-driven convection and means that a mantle plume origin for the NVP is highly unlikely (Rawlinson and Fishwick 2012). Edge-driven convection would produce upwelling of asthenosphere as a convection cell which is 150 % of the step size in lithospheric thickness, meaning that low seismic velocities deeper than 200 km would be absent (King and Anderson 1998; Rawlinson and Fishwick 2012). Convection cells created in such a manner will lead to deformation of mantle material, depending on the lithospheric viscosity, which will also lead to changes in surface heat flow (Hardebol et al. 2012) as seen in the NVP. High deformation rates in the mantle lead to efficient accumulation and extraction of magma in a zone of partial melting (Bons et al. 2004; Demidjuk et al. 2007). This can lead to the formation of large volumes of melt over short timescales, perhaps explaining the large volume of batch A lavas. Davies

and Rawlinson (2014) estimate maximum upwelling velocities of 1.75 cm/year in the region of the NVP, which is localised directly beneath the surface expression of volcanism in the area. Complementing the theory of edge-driven convection as an origin for NVP volcanism, southeast Australia is currently in a NW–SE compressive stress regime (Hillis et al. 1995; Sandiford et al. 2004). Deformation is evident in southeast Australia, with intraplate deformation along the southern Australian margin corresponding to the regions of high heat flow (Sandiford et al. 2004; Holford et al. 2011). Although minor features of deformation, microstructures in the abundant mantle xenoliths of the NVP show deformation through common kink-banding of olivines (Nicholls and Greig 1989), a feature also observed in the xenoliths of Mt Rouse.

The magmas from Mt Rouse may therefore be due to the interplay between lithospheric steps leading to shear-driven upwelling in the upper asthenosphere and partial melting across the LAB. Deeper-derived magmas are associated with increasingly metasomatised mantle, constraining whether they erupt effusively (lower lithosphere-derived) or explosively (upper asthenosphere-derived).

Conclusions

1. Mt Rouse, the largest volcano in the Newer Volcanics Province, is an unusual monogenetic volcano; it is the product of three magma batches which erupted over multiple stages with sequential eruption of magma batches A, C and B, followed by simultaneous eruption of batches A and B.
2. The three magma batches all show geochemical characteristics similar to OIB; their REE contents and patterns provide evidence that they originated in a garnet-bearing source region. The magma batches are increasingly enriched in the LREE from Batch A through to batch C. Batch A are alkali to subalkali basalts, batch B ranges from alkali basalt to hawaiites, and batch C are alkali basalts through hawaiites to basanites. There has been no evident crustal contamination in the genesis of the magmas.
3. Sr–Nd–Pb isotope analysis and major element geochemical modelling define two suites with similar enriched mantle source regions affected by some degree of metasomatism.
4. The magma batches originated from the LAB at depths of 55–63 km; partial melting may have been caused by deformation of the mantle as a result of the fast-moving Australian lithosphere in relation to the underlying asthenosphere, which results in the upwelling of hot, fertile lithosphere through convection. The LAB is an important boundary with respect to NVP volcanism.
5. Whereas the volcanic products of batch A comprise lavas, those of batches B and C comprise scoriaceous products. There is mantle control on the eruption of effusive versus explosive magmas, with explosive magmas sourced from deeper areas of the mantle that have undergone increasing amounts of metasomatism.
6. Monogenetic volcanism in the NVP is not as simple as previously thought, with at least three volcanoes featuring two or more magma batches in their evolution. This study has shown the importance of combining detailed stratigraphic analysis with systematic geochemical analysis in order to define the complex nature of the eruption sequence. While many volcanoes in the NVP are simple in nature, with single magma batches, others may feature similar polymagmatic characters to Mt Rouse and complex stratigraphies that will only be revealed upon further investigation. This study will have important implications for petrogenetic modelling in the NVP, as these and any future results can be used alongside geodynamic modelling in order to further constrain the origin and genesis of volcanism of the NVP, particularly with reference to the plains and cones series of magmas.

Acknowledgments This paper represents part of the research undertaken by Julie Boyce under the supervision of Prof. Reid Keays, Dr Ian Nicholls and Dr Patrick Hayman. Julie Boyce acknowledges the Monash University School of Geosciences research scholarship, Dean's International Postgraduate Research Scholarship and Postgraduate Publication Award. Thanks go to Ross Cayley (Geological Survey of Victoria) and David Moore (Monash University) for helpful discussions relating to the geological structures in the NVP and Hamilton area, Richard Price (University of Waikato, New Zealand), Roland Maas, David Phillips, Erin Matchan (Melbourne University), Simon Jowitt and Massimo Raveggi (Monash University) for discussions on geochemical and isotopic analysis and age dating; and Ray Cas (Monash University), for volcanological discussions. Thanks also go to Jozua van Otterloo, Jackson van den Hove, Matthew Edwards, Dan Uehara, Janine Kavanagh, Tony Rowe (Bamstone Quarries), Peter Bourke (Tar-rone Quarry), Penshurst Volcanoes Discovery Centre, Craig Kenny, the Strangs and Bob Krummel for help during fieldwork, which includes both assistance while in the field, and access to locations.

References

- Adam J, Green T (2006) Trace element partitioning between mica- and amphibole-bearing lherzolite and hydrous basanitic melt: 1. Experimental results and the investigation of controls on partitioning behaviour. *Contrib Mineral Petrol* 152:1–17
- Aivazpourporgou S (2013) Lithospheric structures of the Newer Volcanics Province, western Victoria, Australia from a long-period magnetotelluric array. Ph.D. thesis, Monash University
- Blackburn G (1966) Radiocarbon dates relating to soil development and volcanic ash deposition in south-east South Australia. *Aust J Earth Sci* 29:50–52
- Blackburn G, Allison GB, Leaney FWJ (1982) Further evidence on the age of the tuff at Mount Gambier, South Australia. *Trans R Soc S Aust* 106:163–167

- Bons PD, Arnold J, Elberg MA, Kalda J, Soesoo A, van Milligen BP (2004) Melt extraction and accumulation from partially molten rocks. *Lithos* 78:25–42
- Boyce J (2013) The Newer Volcanics Province of southeastern Australia: a new classification scheme and distribution map for eruption centres. *Aust J Earth Sci* 60:449–462
- Boyce J, Keays RR, Nicholls IA, Hayman P (2014) Eruption centres of the Hamilton area of the Newer Volcanics Province, Victoria, Australia: pinpointing volcanoes from a multifaceted approach to landform mapping. *Aust J Earth Sci* 61:735–754
- Brenna M, Cronin SJ, Smith IEM, Sohn SY, Németh K (2010) Mechanisms driving polymagmatic activity at a monogenetic volcano, Udo, Jeju Island, South Korea. *Contrib Mineral Petrol* 160:1–20
- Brenna M, Cronin SJ, Németh K, Smith IEM, Sohn Y (2011) The influence of magma plumbing complexity on monogenetic eruptions, Jeju Island, Korea. *Terra Nova* 23:70–75
- Brenna M, Cronin SJ, Smith IEM, Maas R, Sohn YK (2012) How small-volume basaltic magmatic systems develop: a case study from the Jeju Island Volcanic Field, Korea. *J Petrol* 53:985–1018
- Burnham W (1979) The importance of volatile constituents. In: Yoda HS (ed) *The evolution of igneous rocks: fiftieth anniversary perspectives*. Princeton University Press, Princeton, pp 439–482
- Cayley RA, Webb AW, Henley KJ (1995) Radiometric dating (K/Ar) on two samples of Newer Volcanic olivine basalt from the southwestern part of the Beaufort 1:100 000 map sheet area. Geological Survey of Victoria unpublished report 1995/15. Melbourne, VIC
- Cayley RA, Korsch RJ, Moore DH, Costelloe RD, Nakamura A, Willman CE, Rawling J, Morand VJ, Skladzien PB, O'Shea PJ (2011) Crustal architecture of central Victoria: results from the 2006 deep crustal reflection seismic survey. *Aust J Earth Sci* 58:113–156
- Cervantes P, Wallace P (2003) Magma degassing and basaltic eruption styles: a case study of ~2000 year BP Xitle volcano in central Mexico. *J Volcanol Geotherm Res* 120:249–270
- Cooper JA, Green DH (1969) Lead isotope measurements on lherzolite inclusions and host basanites from western Victoria, Australia. *Earth Planet Sci Lett* 6:69–76
- Dasch EJ, Green DH (1975) Strontium isotope geochemistry of lherzolite inclusions and host basaltic rocks, Victoria, Australia. *Am J Sci* 275:461–469
- Davies DR, Rawlinson N (2014) On the origin of recent intraplate volcanism in Australia. *Geology*. doi:10.1130/G36093.1
- Demidjuk Z, Turner S, Sandiford M, George R, Foden J, Etheridge M (2007) U-series isotope and geodynamic constraints on mantle melting processes beneath the Newer Volcanic Province in South Australia. *Earth Planet Sci Lett* 261:517–533
- Edwards J, Cayley RA, Joyce EB (2004) Geology and geomorphology of the Lady Julia Percy Island volcano, a late Miocene submarine and subaerial volcano off the coast of Victoria, Australia. *Proc R Soc Vic* 116:15–35
- Elias M (1973) The geology and petrology of Mt Rouse. A Volcano in the Western District of Victoria. B.Sc. thesis, University of Melbourne
- Ellis DJ (1976) High pressure cognate inclusions in the Newer Volcanics of Victoria. *Contrib Mineral Petrol* 58:149–180
- Erlund EJ, Cashman KV, Wallace PJ, Pioli L, Rosi M, Johnson E, Delgado Granados H (2010) Compositional evolution of magma from Parícutin Volcano, Mexico: the tephra record. *J Volcanol Geotherm Res* 1–4:167–187
- Ewart A, Chappell BW, Menzies MA (1988) An overview of the geochemical and isotopic characteristics of the eastern Australian Cainozoic volcanic provinces. *J Pet (Special Lithosphere Issue)* 1:225–273
- Farrington RJ, Stegman DR, Moresi LN, Sandiford M, May DA (2010) Interactions of 3D mantle flow and continental lithosphere near passive margins. *Tectonophysics* 483:20–28
- Fishwick S, Heintz M, Kennett BLN, Reading AM, Yoshizawa K (2008) Steps in lithospheric thickness within eastern Australia, evidence from surface wave tomography. *Tectonics* 27:TC4009
- Foden J, Song SHS, Turner S, Elburg M, Smith PB, van der Steldt B, van Penglis D (2002) Geochemical evolution of lithospheric mantle beneath S.E. South Australia. *Chem Geol* 182:663–695
- Fontaine FF, Tkalcic H, Kennett LN (2013) Imagining crustal structure variation across southeastern Australia. *Tectonophysics* 582:112–125
- Ford HA, Fischer KM, Abt DL, Rychert CA, Elkins-Tanton LT (2010) The lithosphere–asthenosphere boundary and cratonic layering beneath Australia from Sp wave imaging. *Earth Planet Sci Lett* 300:299–310
- Frey FA, Green DH (1974) The mineralogy, geochemistry and origin of lherzolite inclusions in Victorian basanites. *Geochim Cosmochim Acta* 38:1023–1059
- Frey FA, Green DH, Roy D (1978) Integrated models of basalt petrogenesis: a study of quartz tholeiites to olivine melilitites from South Eastern Australia utilising geochemical and experimental petrological data. *J Pet* 19:463–513
- Fujimaki H, Tatsumoto M (1984) Partition coefficients of Hf, Zr and REE between phenocrysts and groundmass. In: *Proceedings of 14th Lunar planetary science conference, Journal of Geophysical Research*, vol 89, Suppl, pp B662–B672
- Gazel E, Plank T, Forsyth DW, Bendersky C, Lee CA, Hauri EH (2012) Lithosphere versus asthenosphere mantle sources at the Big Pine Volcanic Field, California. *Geochim Geophys Geosyst* 13:Q0AK06
- Gouramanis C, Wilkins D, DeDecker P (2010) 6000 years of environmental changes recorded in Blue Lake, South Australia, based on ostracod ecology and valve chemistry. *Palaeogeogr Palaeoclimatol Palaeoecol* 297:223–237
- Gray CM, McDougall I (2009) K–Ar geochronology of basalt petrogenesis, Newer Volcanics Province, Victoria. *Aust J Earth Sci* 56:245–258
- Gray DR, Foster DA, Morand VJ, Willman CE, Cayley RA, Spaggiari CV, Taylor DH, Gray CM, VandenBerg MA, Hendrickx MA, Wilson CJL (2003) Structure, metamorphism, geochronology and tectonics of Palaeozoic rocks. In: Birch WD (ed) *Geology of Victoria*, vol 23. Geological Society of Australia Special Publication, Australia, pp 15–70
- Griffin WL, O'Reilly SY, Stabel A (1988) Mantle metasomatism beneath western Victoria, Australia: II. Isotopic geochemistry of Cr-diopside lherzolites and Al-augite pyroxenites. *Geochim Cosmochim Acta* 52:449–459
- Hardebol NJ, Pysklwec RN, Stephenson R (2012) Small-scale convection at a continental back-arc to craton transition: application to the southern Canadian Cordillera. *J Geophys Res* 117:B01408
- Hillis RR, Monte SA, Tan CP, Willoughby DR (1995) The contemporary stress field of the Otway Basin, South Australia: implications for hydrocarbon exploration and production. *Aust Pet Explor Assoc J* 35:494–506
- Hirschmann MM (2000) Mantle solidus: Experimental constraints and the effects of peridotite composition. *Geochim Geophys Geosyst* 1:2000GC000070
- Hofmann AW, Jochum P, Seufert M, White WM (1986) Nb and Pb in oceanic basalts: new constraints on mantle evolution. *Earth Planet Sci Lett* 79:33–45
- Holford SP, Hillis RR, Hand M, Sandiford M (2011) Thermal weakening localizes intraplate deformation along the southern Australian continental margin. *Earth Planet Sci Lett* 305:207–214
- Irvine TN, Barager WRA (1971) A guide to the chemical classification of the common volcanic rocks. *Can J Earth Sci* 8:523–548

- Irving AJ, Frey FA (1987) Distribution of trace elements between garnet megacrysts and host volcanic liquids of kimberlitic to rhyolitic composition. *Geochim Cosmochim Acta* 42:771–787
- Irving AJ, Green DH (1976) Geochemistry and petrogenesis of the Newer basalts of Victoria and South Australia. *J Geol Soc Aust* 23:46–66
- Joyce EB (1975) Quaternary volcanism and tectonics in southeastern Australia. In: Suggate RP, Cresswell MM (eds) *Quaternary studies*. The Royal Society of New Zealand, Wellington, pp 169–178
- Katz RF, Spiegelman M, Langmuir CH (2003) A new parameterization of hydrous mantle melting. *Geochim Geophys Geosyst* 4:1073
- King SD, Anderson DL (1998) Edge-driven convection. *Earth Planet Sci Lett* 160:289–296
- Korsch RJ, Barton TJ, Gray DR, Owen AJ, Foster DA (2002) Geological interpretation of a deep seismic reflection transect across the boundary between the Delamerian and Lachlan Orogens, in the vicinity of the Grampians, western Victoria. *Aust J Earth Sci* 49:1057–1075
- Le Bas MJ, Le Maitre RW, Streckeisen AL, Zanettin B (1986) A chemical classification of volcanic rocks based on the total alkali–silica diagram. *J Pet* 27:745–750
- Le Maitre RW, Streckeisen AL, Zanettin B, Le Bas MJ, Bonin B, Bateman P, Bellieni G, Dudek A, Efremova S, Keller J, Lameyre J, Sabine PA, Schmid R, Sørensen H, Wooley AR (2002) *Igneous rocks: a classification and glossary of terms*. Cambridge University Press, Cambridge
- Lee CA, Luffi P, Plank T, Dalton H, Leeman WP (2009) Constraints on the depths and temperatures of basaltic magma generation on Earth and other terrestrial planets using new thermobarometers for mafic magmas. *Earth Planet Sci Lett* 279:20–33
- Luhr JF (2001) Glass inclusions and melt volatile contents at Parícutin Volcano, Mexico. *Contrib Mineral Petrol* 142:261–283
- Maas R, Kamenetsky MB, Sobolev AV, Kamenetsky VS, Sobolev NV (2005) Sr, Nd, and Pb isotope evidence for a mantle origin of alkali chlorides and carbonates in the Udachnaya kimberlite, Siberia. *Geology* 33:549–552
- Matchan E, Phillips D (2011) New $^{40}\text{Ar}/^{39}\text{Ar}$ ages for selected young (<1 Ma) basalt flows of the Newer Volcanic Province, southeastern Australia. *Quat Geochronol* 6:356–368
- McBride JS, Lambert DD, Nicholls IA, Price RC (2001) Osmium isotopic evidence for crust–mantle interaction in the genesis of continental intraplate basalts from the Newer Volcanics Province, southeastern Australia. *J Pet* 6:1197–1218
- McDonough WF, McCulloch MT (1987) The southeast Australian lithospheric mantle: isotopic and geochemical constraints on its growth and evolution. *Earth Planet Sci Lett* 86:327–340
- McDonough WF, McCulloch MT, Sun SS (1985) Isotopic and geochemical systematics in Tertiary–Recent basalts from southeastern Australia and implications for the evolution of the subcontinental lithosphere. *Geochim Cosmochim Acta* 52:433–447
- McDougall I, Gill ED (1975) Potassium–Argon ages from the Quaternary succession in the Warrnambool–Port Fairy area, Victoria, Australia. *Proc R Soc Vic* 12:295–332
- McDougall I, Allsop HL, Chamalaun FH (1966) Isotopic dating of the Newer Volcanics of Victoria, Australia and geomagnetic polarity epochs. *J Geophys Res* 71:6107–6118
- McKenzie D (1989) Some remarks on the movement of small melt fractions in the mantle. *Earth Planet Sci Lett* 95:53–72
- Needham AJ, Lindsay JM, Smith IEM, Augustinus P, Shane PA (2010) Sequential eruption of alkaline and sub-alkaline magmas from a small monogenetic volcano in the Auckland Volcanic Field, New Zealand. *J Volcanol Geotherm Res* 201:126–142
- Nicholls I, Greig A (1989) Chapter 6.2.2 textures and microstructures. In: Johnson RW (ed) *Intraplate volcanism in Eastern Australia and New Zealand*. Cambridge University Press, Cambridge, pp 255–261
- Nicholls IA, Joyce EB (1989) Eastern Australian volcanic geology—Victoria and South Australia—Newer Volcanics. In: Johnson RW (ed) *Intraplate volcanism in Eastern Australia and New Zealand*. Cambridge University Press, Cambridge, pp 137–142
- O'Reilly SY, Griffin WL (1985) A xenolith-derived geotherm for southeastern Australia and its geophysical implications. *Tectonophysics* 111:41–63
- O'Reilly SY, Griffin WL (1988) Mantle metasomatism beneath western Victoria, Australia I: metasomatic processes in Cr-diopside lherzolites. *Geochim Cosmochim Acta* 52:433–447
- O'Reilly SY, Griffin WL (2006) Imaging chemical and thermal heterogeneity in the sub-continental lithospheric mantle with garnets and xenoliths. *Tectonophysics* 416:289–309
- O'Reilly SY, Griffin WL (2013) Chapter 12. Mantle metasomatism. In: Harlov DE, Austrheim H (eds) *Metasomatism and the chemical transformation of rock*. Lecture notes in earth system sciences. Springer, Berlin, pp 471–533
- Ollier CD (1985) Lava flows of Mt Rouse, western Victoria. *Proc R Soc Vic* 97:167–174
- Ollier CD, Joyce EB (1964) Volcanic physiography of the Western Plains of Victoria. *Proc R Soc Vic* 77:357–376
- Pearce JA (2008) Geochemical fingerprinting of oceanic basalts with applications to ophiolite classification and the search for Archean oceanic crust. *Lithos* 100:14–48
- Pietruszka AJ, Hauri EH, Blichert-Toft J (2009) Crustal contamination of mantle-derived magmas within Piton de la Fournaise volcano, Réunion Island. *J Pet* 50:661–684
- Piganis F (2011) A volcanological investigation of the polymagmatic Red Rock Volcanic Complex and a 3D geophysical interpretation of the subsurface structure and geology of the poly-lobate Lake Purdigulac maar, Newer Volcanics Province, southeastern Australia. M.Sc. thesis, Monash University
- Powell W, Zhang M, O'Reilly SY, Tiepolo M (2004) Mantle amphibole trace-element and isotopic signatures trace multiple metasomatic episodes in lithospheric mantle, western Victoria, Australia. *Lithos* 75:141–171
- Price RC, Gray CM, Nicholls IA, Day A (1988) Cainozoic volcanic rocks. In: Douglas JG, Ferguson JA (eds) *Geology of Victoria*. Geological Society of Australia, Victoria Division, Melbourne, pp 439–451
- Price RC, Gray CM, Frey FA (1997) Strontium isotopic and trace element heterogeneity in the plains basalts of the Newer Volcanic Province, Victoria, Australia. *Geochim Cosmochim Acta* 61:171–192
- Rawlinson N, Fishwick S (2012) Seismic structure of the southeast Australian lithosphere from surface and body wave tomography. *Tectonophysics* 572–573:111–122
- Russell JK, Nicholls J (1988) Analysis of petrologic hypotheses with Pearce element ratios. *Contrib Mineral Petrol* 99:25–35
- Rutherford MJ, Gardner JE (2000) Rates of magma ascent. In: Sigurdsson H (ed) *Encyclopaedia of Volcanoes*. Academic Press, New York, pp 207–217
- Sandiford M, Wallace M, Coblenz D (2004) Origin of the in situ stress field in south-eastern Australia. *Basin Res* 16:325–338
- Schnetzler CC, Philpots JA (1970) Partition coefficients of rare-earth elements between igneous matrix material and rock-forming mineral phenocrysts—II. *Geochim Cosmochim Acta* 34:331–340
- Smith IE, Blake S, Wilson CJN, Houghton BF (2008) Deep-seated fractionation during the rise of a small-volume basalt magma batch: Crater Hill, Auckland, New Zealand. *Contrib Mineral Petrol* 155:511–527
- Sohn YK, Cronin J, Brenna M, Smith IEM, Németh K, White JDL, Murtagh RM, Jeon YM, Kwon CW (2012) Ilchulbong tuff cone,

- Jeju Island, Korea, revisited: a compound monogenetic volcano involving multiple magma pulses, shifting vents, and discrete eruptive phases. *Geol Soc Am Bull* 3–4:259–274
- Song X-Y, Keays RR, Xiao L, Qi H-W, Ihlenfeld C (2009) Platinum-group element geochemistry of the continental flood basalts in the central Emeishan Large Igneous Province, SW China. *Chem Geol* 262:246–261
- Stone JO, Peterson JA, Fifield LK, Cresswell RG (1997) Cosmogenic chlorine-36 exposure ages for two basalt flows in Newer Volcanics Province, Western Victoria. *Proc R Soc Vic* 109:121–131
- Strong M, Wolff J (2003) Compositional variations within scoria cones. *Geology* 31:143–146
- Stuckless JS, Irving AJ (1976) Strontium isotope geochemistry of megacrysts and host basalts from southeastern Australia. *Geochim Cosmochim Acta* 40:209–213
- Sun SS, McDonough WF (1989) Chemical and isotopic systematics of oceanic basalts: implications for mantle composition and processes. In: Saunders AD, Norry MJ (eds) *Magmatism in ocean basins*, vol 42. Geological Society London Special Publication, UK, pp 313–345
- Stutalo F (1996) The geology and regolith terrain evaluation of the Mount Rouse lava flows, Western Victoria. B.Sc. thesis, University of Melbourne
- Thompson RN (1984) Dispatches from the basalt front. 1. Experiments. *Proc Geol Assoc* 95:249–262
- van Otterloo J (2012) Complexity in monogenetic volcanic systems: factors influencing alternating magmatic and phreatomagmatic eruption styles at the 5 Ka Mt Gambier Volcanic Complex, South Australia. Ph.D. thesis, Monash University
- van Otterloo J, Cas R (2011) Mount Gambier Volcanic Complex. In: Cas R, Blakie T, Boyce J, Hayman P, Jordan S, Piganis F, Prata G, van Otterloo J (eds) *Factors that influence varying eruption styles (from magmatic to phreatomagmatic) in intraplate continental basaltic volcanic provinces: the Newer Volcanics Province of southeastern Australia*. Field trip guide VF01. IUGG 2011 General Assembly. Earth on the edge: science for a sustainable planet, pp 65–81
- van Otterloo J, Cas RAF, Sheard MJ (2013) Eruption processes and deposit characteristics at the monogenetic Mt Gambier volcanic complex, SE Australia: implications for alternating magmatic and phreatomagmatic activity. *Bull Volcanol* 75:1–21
- van Otterloo J, Raveggi M, Cas RAF, Maas R (2014) Polymagmatic activity at the monogenetic Mt Gambier volcanic complex in the Newer Volcanics Province, SE Australia: new insights into the occurrence of intraplate volcanic activity in Australia. *J Pet* 55:1317–1351
- Villemant B, Jaffrezic H, Joron J-L, Treuil M (1981) Distribution coefficients of major and trace elements; fractional crystallisation in the alkali basalt series of Chaîne des Puys (Massif Central, France). *Geochim Cosmochim Acta* 45:1997–2016
- Vogel DC, Keays RR (1997) The petrogenesis and platinum-group element geochemistry of the Newer Volcanic Province, Victoria, Australia. *Chem Geol* 136:181–204
- Walker GPL (2000) Basaltic volcanoes and volcanic systems. In: Sigurdsson H (ed) *Encyclopaedia of Volcanoes*. Academic Press, New York, p 283
- Weaver BL (1991) The origin of ocean island basalt end-member compositions: trace element and isotopic constraints. *Earth Planet Sci Lett* 104:381–397
- Wellman P (1971) The age and palaeomagnetism of the Australian Cenozoic volcanic rocks. Ph.D. thesis, The Australian National University, Canberra
- Whitehead PW (1986) The geology and geochemistry of the Mt Rouse and Mt Napier volcanic centres, western Victoria. Honours research report, La Trobe University, Melbourne
- Whitehead PW (1991) The geology and geochemistry of Mt Napier and Mt Rouse, western Victoria. In: Williams MAJ, DeDeckker P, Kershaw AP (eds) *The Cainozoic in Australia: a re-appraisal of the evidence*, vol 18. Geological Society of Australia Special Publication, Australia, pp 309–320
- Wood BJ (2004) Melting of fertile peridotite with variable amounts of H₂O. *Geophys Monogr* 150:69–80
- Yaxley GM, Crawford AJ, Green DH (1991) Evidence for carbonatite metasomatism in spinel peridotite xenoliths from western Victoria, Australia. *Earth Planet Sci Lett* 107:305–317
- Yaxley GM, Green DH, Kamenetsky V (1996) Carbonatite metasomatism in the southeastern Australian Lithosphere. *J Petrol* 39:1917–1930
- Zhang M, Stephenson PJ, O'Reilly SY, McCulloch MT, Norman M (2001) Petrogenesis and geodynamic implications of Late Cenozoic basalts in north Queensland, Australia: trace-element and Sr–Nd–Pb isotope evidence. *J Petrol* 42:685–719
- Zindler A, Hart SR (1986) Chemical geodynamics. *Annu Rev Earth Planet Sci* 14:493–571





Chapter 6

Conclusions and discussion

6.1 Introduction

In this study, the Newer Volcanics Province (NVP) of southeastern Australia has been explored in detail, and a new distribution map of eruption centres has been generated. The distribution of eruption centres in the Hamilton area of western Victoria has been significantly updated, with the discovery of previously unknown volcanoes and the confirmation of three phases of eruption in the area. The Mt Rouse magmatic volcanic complex has been explored in considerable detail, outlining the great complexity of the volcano. This includes the genesis and geochemical characteristics of multiple batches of magma, and the characterisation of multiple volcanic facies that were erupted during a complex sequence of events involving differing eruption styles.

This chapter summarises the main findings of this thesis in terms of the distribution, geochronology and geochemistry of volcanoes in the NVP, the complexity of the Mt Rouse volcano, hazard implications of renewed volcanic activity in the NVP and suggestions for future research.

This study has shown that monogenetic volcanoes may be far from simple, and will have significant implications for studies of monogenetic volcanism and the emergent field of study of complex monogenetic volcanoes both in the NVP and worldwide.

6.2 Distribution of volcanoes in the Newer Volcanics Province

The analysis of NVP volcanoes as outlined in Chapters 1 and 2 has led to the drafting and publication of a new volcanic distribution map recognising at least 437 individual volcanoes over a 19 000 km² area from Melbourne, Victoria to the Mt Burr range in southeastern South Australia. This project represents a significant update of the locations of volcanism within the NVP since the publication of Joyce's (1975) map. Several previously unrecorded volcanoes were discovered across the NVP, some as small as 9 m high. This study indicates that 437 volcanoes is a minimum estimate, and that there may be many smaller volcanoes that remain unrecorded. In addition, it is likely that smaller, older, low profile volcanoes have been buried by the eruption products of younger volcanoes.

The NVP is the largest young monogenetic volcanic field in Australia in terms of area covered and numbers of volcanoes. Other young provinces in Australia include (1) the 7.06 Ma to <10 ka Atherton Province in northern Queensland, containing 65 basaltic volcanoes covering 2500 km² (De Keyser & Lucas 1968; Stephenson 1989; Whitehead *et al.* 2007); and (2) the McBride Province southwest of Atherton, which contains 164 volcanoes dated to between 3 Ma and 50, 000 BP (Griffin 1977; Stephenson 1989; Whitehead 2010). With the construction of a digital database of the volcanoes, the distribution maps of the NVP can readily be updated with new information on an ongoing basis and can be used in the generation of volcanic hazard maps. In addition, the volcanic distribution maps can be used in conjunction with geochemical, geochronological and geodynamical data to help constrain the nature of NVP volcanism.

6.3 Geochronology of the Newer Volcanics Province volcanoes

The widely accepted nominal age range of NVP activity is 4.5 Ma to ca 5000 BP (Blackburn 1966; McDougall *et al.* 1966; Blackburn *et al.* 1982; Price *et al.* 2003; Gray & McDougall 2009; Gouramanis *et al.* 2010). However, based on the geochronological studies of Cayley *et al.* (1995) and Edwards *et al.* (2004), who date buried lava flows north of Beaufort, western Victoria to 7.80 ± 0.08 Ma and Lady Julia Percy Island to 6.22 ± 0.06 Ma respectively, this age range is deemed inaccurate. The older dated sample overlies ~70 m of basalt flows, presumably of the NVP, which indicates that the age range of the province is significantly greater than the traditional estimates, and this has been attributed to sampling bias towards the younger, fresher and easier to access volcanic products in the NVP (Cayley *et al.* 1995; Edwards *et al.* 2004). A distribution map of ages for the NVP, along with associated statistics (Chapter 1.6.2), shows that only <9% of the known volcanoes have been dated. This project highlights the need for additional chronological studies of the province and recommends that the age range of the NVP be extended to 8 Ma.

The lack of strong constraints on ages in the NVP has implications for studies of eruption frequency and highlights the fact that any inferences of waxing or waning of volcanism over time are inherently flawed. With numbers of volcanoes and the timespan of activity in the province both underestimated, estimates of eruption frequency are likely to be inaccurate. Gray & McDougall (2009) argue that the period between 3.0–1.8 Ma constitutes the interval of maximum activity in the NVP based on a peak in dated volcanoes, and that volcanism began to wane after that period. However, when collating geochronological studies (Chapter 1.6.2), a pronounced peak in volcanism is seen from 0.5 Ma onward, particularly in the west of the NVP, which indicates that volcanism is not waning. Such results should however be interpreted with caution, as there has been sampling bias towards younger volcanoes and a statistically robust number of volcanoes is yet to be analysed. Additional dates should be plotted on volcanic distribution maps in order to recognise any age progressions or clustering of volcanic activity in the NVP. Eruption frequencies assume that volcanic eruptions are equally spaced in time; in reality it is more likely that there are clusters of volcanoes erupted within distinct time frames in certain locations.

Another implication of these studies is that the NVP was active at the same time as the Macedon–Trentham group of basaltic to trachytic centres northwest of Melbourne, dated at 7.0–4.6 Ma (Wellman 1974; Dasch & Millar 1977; Ewart *et al.* 1985). The Macedon–Trentham group is compositionally distinct from the NVP, and resembles the central volcanic complexes of New South Wales and Queensland (Knutson & Nicholls 1989).

By combining the interpretation of radiometric imagery with observations on the preservation of outcrop and published geochronological ages, three phases of eruption were confirmed in the Hamilton area of the NVP during this project (Chapter 3). These phases had ages of >4 Ma, ca 2 Ma and <0.5 Ma. This technique could be applied to other areas of the NVP, leading to a generalised eruption phase distribution map for the NVP. This may assist with the identification of volcano groupings over time. However, using radiometric ternary imagery in areas of unconsolidated, fine grained maar deposits may give misleading ages, as weathering occurs at a faster rate in fine-grained material. This means that caution should be taken in areas with maar volcanoes. Additional radiometric ages for some of the older volcanoes may help to further subdivide the >4 Ma volcanoes.

6.4 Geochemistry of the Newer Volcanics Province volcanoes

Geochemically, the NVP shows compositions ranging from basalts and trachybasalts and basanites through to basaltic icelandites, trachyandesites and phonotephrites (Chapter 1.6.3).

There is a clear difference in composition between the Plains and Cones basalt series of Price *et al.* (1997). Plains basalts are dominantly tholeiitic and transitional, while the Cones basalts are often strongly alkalic (Chapter 1.6.3). The Cones series feature higher concentrations of incompatible trace elements than the Plains series and are attributed to deeper mantle reservoirs that have undergone increasing amounts of metasomatism (Chapters 3 and 5). This is reflected both in their trace element compositions and $^{87}\text{Sr}/^{86}\text{Sr}$ isotope ratios. A heterogeneous mantle is inferred beneath the NVP, having contrasting degrees of depletion and enrichment of Light Rare Earth Elements (LREE) over small areas (McDonough & McCulloch 1987). Metasomatism is thought to increase with depth beneath western Victoria (Frey *et al.* 1978; McDonough *et al.* 1985; McDonough & McCulloch 1987; Boyce *et al.* 2014) and at least three metasomatic events have led to enrichment in incompatible trace elements (Griffin *et al.* 1988; O'Reilly & Griffin 1988). Metasomatism has also been used to explain geochemical distinctions in magmas in monogenetic volcanoes from the southern Cascade arc (Strong & Wolff 2003) and Jeju Island, Korea (Brenna *et al.* 2010).

Reconnaissance geochemical studies of volcanoes in the Hamilton area (this project) go hand-in-hand with the three phases of eruption identified in the area, with compositions becoming increasingly alkaline over time to ~2 Ma. This indicates that the source depth of the magmas increases over time, with the more alkaline Cones series being associated with deeper mantle reservoirs than the Plains series, as suggested by Price *et al.* (1988). Eruptions over the past *ca* 0.5 Ma in the Hamilton area cover the entire range of compositions (Plains and Cones series; Chapter 3), which indicates that the NVP is tapping a wider range of pressures over this timespan. This is highlighted by the geochemistry of Mt Rouse (in the Hamilton area) and Mt Gambier, which are 135 km apart. Both volcanoes have multiple magma batches of both Plains and Cones affinities and pressure–temperature estimates for mantle melting indicate that the sources of the magmas were in a region straddling the lithosphere–asthenosphere boundary (van Otterloo *et al.* 2014; Chapter 3/Boyce *et al.* 2014; Chapter 5/Boyce *et al.* 2015). In contrast, Holt *et al.* (2014) suggest an opposite relationship between the pressure/depth of magma generation and the ages of volcanoes in the Mt Gambier region, with source depths decreasing with age. The P–T formulations of Lee *et al.* (2009) were used in the Holt *et al.* (2014) study, based on small numbers of geochemical analyses for many of the volcanoes (rather than full suites). These calculations are not calibrated for alkalic basalt compositions like those of the NVP Cones series, and they lead to an overestimation of the melting pressures. In addition, only three of the seventeen volcanoes considered have published ages (see Chapter 1.6.2), making it difficult to confirm this hypothesis. If P–T calculations are performed for the other NVP volcanoes, using full suites of major and trace element data, it should be possible to construct a map of magma source depths within the NVP using the new volcano distribution generated in this project. This would lead to advances in geodynamic modelling to explain the initiation of volcanism in the province.

6.5 The complexity of the Mt Rouse magmatic volcanic complex

Through detailed study of its stratigraphy coupled with systematic geochemical analysis, Mt Rouse has been shown to be an extremely complex monogenetic volcano (Chapter 4 and Chapter 5/Boyce *et al.* 2015). Eight facies were identified, including both coherent and fragmental types produced by eruption styles varying from Hawaiian and Strombolian to micro-Plinian through violent-Strombolian and phreatomagmatic. At least three magma batches (A, B and C) were involved in the evolution of the volcano, which erupted over multiple stages with sequential eruption of magma batches A, C and B, followed by simultaneous eruption of batches A and B. The magmas involved in the eruptions all show geochemical characteristics similar to Ocean Island Basalts and are increasingly enriched in the LREE from batch A through to batch C, with no obvious evidence of crustal contamination. Two magma suites were identified through Sr–Nd–Pb isotope analysis and major element geochemical modelling, the latter indicating that the magmas originated from the lithosphere–asthenosphere boundary at depths of 55–63 km. A mantle control on the eruption of explosive versus effusive magmas was inferred, with magma batch A (Plains series; effusive) derived from the lower lithosphere and magma batches B and C (Cones series; explosive) the upper asthenosphere. With regards to controls on eruption style at Mt Rouse, these are thought to include magma composition, mass flux rate, vent reuse, involvement of external water in the eruptions and presumably the juvenile volatile content of the melt.

This research contributes significantly to the field of complex monogenetic volcanism. Although monogenetic volcanoes represent the most common form of continental volcanism on Earth (Valentine & Gregg 2008), they are poorly understood. Such volcanoes were conventionally thought to be produced from a single batch of magma erupted during a single short-lived event to form a small, simple volcano, after which magma conduits cooled and were not used by later magmas (Foshag & Gonzales 1956; Kienle *et al.* 1980; Camp *et al.* 1987; Walker 2000). Recent research has shown that this definition is incorrect for at least some monogenetic volcanoes, with sequential eruption of two magma batches documented at Parícutin, in the Michoacán-Guanajuato Volcanic Field, Mexico (Luhr 2001; Erlund *et al.* 2010), Udo, Jeju Island, south Korea (Brenna *et al.* 2010, 2011) and Brush Mountain, Round Barn Cones and two cones on the Popcorn Cave mafic shield, in the southern Cascades (Strong & Wolff 2003). In the NVP, both the Mt Gambier and Red Rock maar–cone volcanic complexes were produced from the simultaneous eruption of two magma batches (Piganis 2010; Blaikie *et al.* 2012; van Otterloo *et al.* 2014). Complex compositional variation has also been detailed at several other monogenetic volcanoes across the world, including in the NVP (e.g., Smith *et al.* 2008; Brenna *et al.* 2011; Prata 2012), and polycyclic volcanoes have been documented both in the NVP and the Auckland Volcanic Field (e.g., Edwards 1994; Edwards *et al.* 2004; Needham *et al.* 2010; Jordan *et al.* 2013). Mt Rouse is the first monogenetic volcano to be documented as the product of three magma batches and featuring the re-eruption of an earlier erupted magma batch. This highlights the importance of combining detailed stratigraphic analysis with systematic geochemical studies in monogenetic volcanoes and has important implications with respect to petrogenetic modelling in the NVP, as both Plains and Cones series magmas erupted at Mt Rouse simultaneously (see section 6.3).

6.6 Hazard implications of renewed volcanism in the Newer Volcanics Province

The area of the NVP is populated by more than 4.8 million people (Australian Bureau of Statistics 2011); with no volcanic contingency plans in place for future eruptions, it is important to gain a fuller understanding of the distribution and type of volcanoes in the province in order to understand the risks that renewed volcanic activity might pose to the general populace. Future eruptions are possible in the NVP, which has an average eruption frequency of between 1:10 800 years and 1:12 500 years (Joyce 1988a, b; Cas *et al.* 1993; Chapter 2/Boyce 2013) with the last eruption at *ca* 5000 BP. The NVP is considered an active volcanic province, a view supported by the occurrence of mantle-derived CO₂ in several locations within the province, and elevated surface heat flow and the inferred presence of partial melt zones mainly beneath the Central Highlands subprovince (Wopfner & Thornton 1971; Chivas *et al.* 1983, 1987; Cartwright *et al.* 2002; Graeber *et al.* 2002; Aivazpourporgou *et al.* 2012; Davies & Rawlinson 2014).

It is impossible to predict the location of future eruptive events in the NVP, as a large area is currently active at depth. A new eruption could last from weeks to years, and the type of volcano formed would depend on many factors, including the inherent properties of the magma and the location of volcanism with respect to water-bearing sediments.

The NVP records evidence of a diverse range of volcanic hazards. Lava flows are the most common hazards associated with NVP volcanoes, with simple lava shields accounting for 209 of the 437 volcanoes (48%). The longest lava flows (60 km) are associated with Mt Rouse (Sutalo & Joyce 2004) and the thickness of lava or lava sequences in the NVP varies from <2 m to >100 m (Joyce 2004). Parts of the city of Melbourne are built on the lava flows of the NVP, and there are 60 known volcanoes in the Sunbury and Craigieburn areas of Greater Melbourne (Figure 6.1). As an example, the lavas from an effusive eruption in the Greater Melbourne area could follow the Maribyrnong River and reach the Melbourne Central Business District. Basaltic lava flows are typically at temperatures *ca* 1200°C, and they therefore may destroy everything in their path. This would lead to the destruction of infrastructure and loss of agricultural land, but pose low risk to human life.

Scoria cones account for 28% of the volcanoes in the NVP, including 23 magmatic volcanic complexes (which may also feature large lava flows). A range of eruption styles is associated with such volcanoes in the NVP, but only a few of these have been fully characterised stratigraphically. Eruption styles range from Strombolian (common) to micro-Plinian and violent-Strombolian (relatively uncommon). Scoria cones are typically >500 m in diameter in the NVP, but may become significantly larger if multiple vents form. Hazards near-vent include the ejection of molten pyroclastic material in the form of spatter and bombs. Sustained eruption columns may be produced during micro-Plinian and violent-Strombolian eruptions and ash could be dispersed thousands of kilometres downwind in a worst-case scenario, similar to the 2010 eruptions at Eyjafjallajökull, Iceland (Gudmundsson *et al.* 2012).

Phreatomagmatic eruption styles are documented in 11% of NVP volcanoes, mainly in the Camperdown area but also found in Mt Gambier, Woodhouse northeast of Hamilton and in the Central Highlands subprovince. Maar volcanoes are the sites of the most dangerous eruption events in monogenetic volcanic fields (White & Ross 2011), and form when rising magma interacts with groundwater, causing rapid quenching of the magma and fragmentation into particles of fine ash

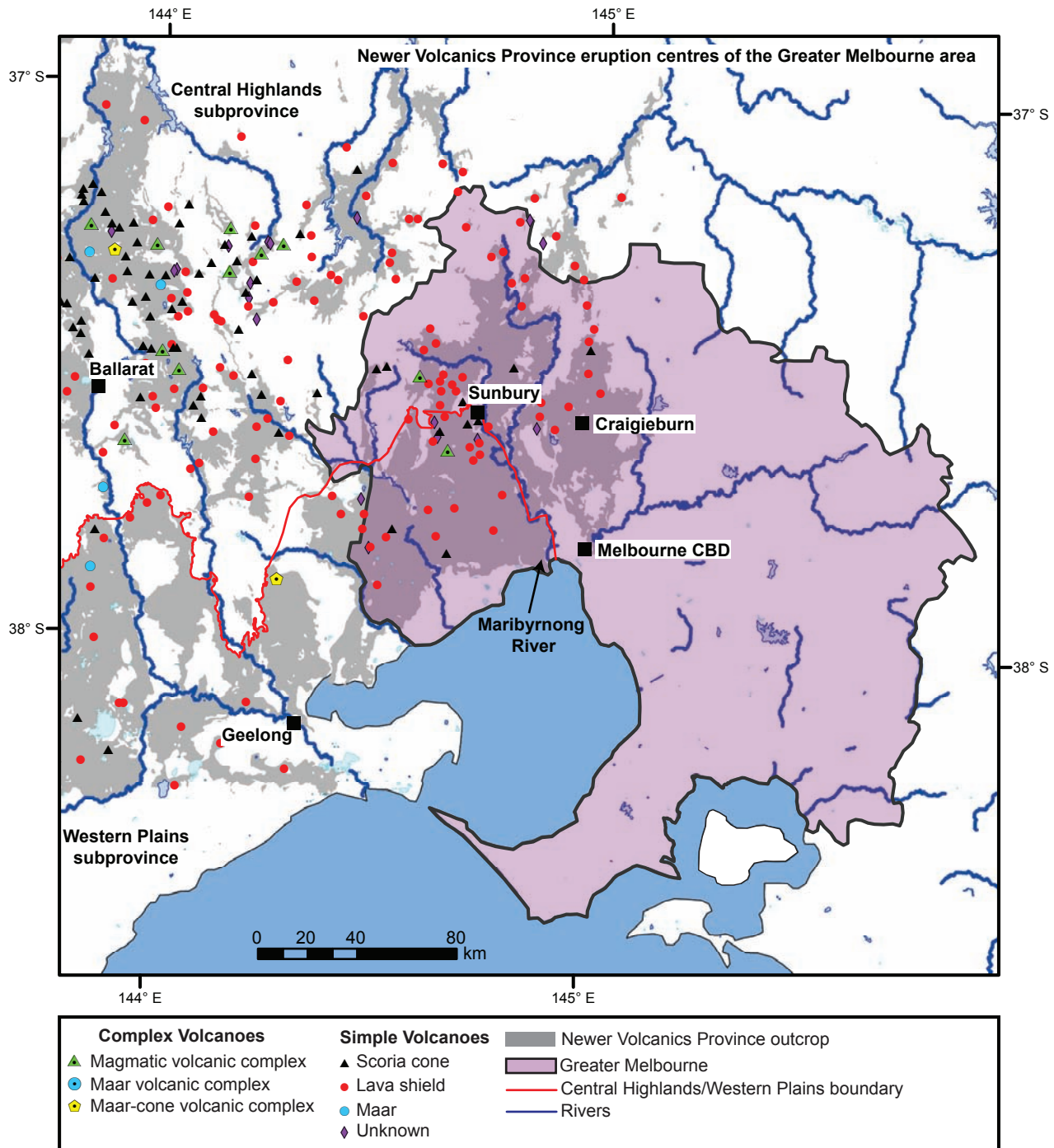


Figure 6.1 Newer Volcanics Province eruption centres in the Greater Melbourne area, showing the greater capital city statistical area (Australian Bureau of Statistics 2011), rivers, volcanoes, and the extent of Newer Volcanics outcrop (grey).

(Wohletz 1983; Büttner *et al.* 2002). Continual eruption column collapse gives rise to base surges, while co-surge fall deposits mantle the surrounding topography in fine ash kilometres from the vent. Base surges are among the most hazardous events during maar formation and are a ground-hugging, turbulent mixture of gas and ash, which spreads laterally from the vent. Pyroclastic flows have been documented at Mt Gambier >3.5 km from the vent (van Otterloo *et al.* 2013), Lady Julia Percy Island (Edwards *et al.* 2004), Lake Purrumbete (Jordan *et al.* 2013) and Tower Hill (Prata 2013). In addition, Surtseyan eruptions could ensue if a future eruption occurred at sea, as documented at Lady Julia Percy Island. However, this is considered to have a low probability, as Lady Julia Percy Island is considered one of the oldest volcanoes in the NVP and, although polycyclic, is the only subaqueous volcano yet identified in the province.

6.7 Suggestions for further research

Although the results outlined herein have significantly contributed to studies of monogenetic volcanism, there are a number of suggestions for possible further research both in the NVP and the broader field of monogenetic volcanism.

- A melt inclusion study of phenocryst phases of the volcanic products of monogenetic volcanoes that have detailed stratigraphic and geochemical information available would be a major contribution. Melt inclusions are small parcels of original melt that become trapped during the formation of crystals in a magma. As they often preserve magma compositions different from those which produced their host rocks they may be very useful in studies of the evolution of mantle-derived magmas. In addition, the most primitive compositions may be used to model the geochemistry of primary magmas and their mantle magma sources. Melt inclusions retain volatile elements that would otherwise escape during the evolution of the magma by degassing, so they can be utilised to study pre-eruptive volatile contents and degassing paths (e.g., Atlas *et al.* 2006). They can also be used to study processes that drive changes in magma composition, such as crystallisation, assimilation (Johnson *et al.* 2008), magma mixing (Atlas *et al.* 2006) and mingling (Roggensack 2001) and also source heterogeneities among other features (Kent 2008).
- The detailed stratigraphic architecture and systematics of geochemical variation within further individual eruption centres of the NVP need to be studied, in order to assign types of monogenetic volcanism, constrain the spatial extent of magma types and depths of melting across the NVP and construct better geodynamic models. Similar studies can be performed in other monogenetic volcanic provinces.
- Additional geochronological studies of individual volcanoes and drill cores of earlier (Plains) lava flows in the NVP need to be undertaken in order to better constrain the age range of the NVP, and to construct more accurate age distribution maps for the province to illustrate age progressions or clustering of centres through time.
- A volcanic contingency plan should be produced for Victoria and southeastern South Australia, including hazard assessments, public education, information and warnings, and the detailing of evacuation plans for key areas in case of future eruptions.

6.7 References

AIVAZPOURPORGOU S., THIEL S., HAYMAN P., MORESI L. & HEINSON G. 2012. The upper mantle thermal structure of the Newer Volcanic Province, Western Victoria, Australia from long period Magnetotelluric (MT) array. Extended Abstract, 21st EM Induction Workshop, Darwin, Australia, 25–31 July 2012.

ATLAS Z. D., DIXON J. E., SEN G., FINNY M., & MARTIN-DEL POZZO A. L. 2006. Melt inclusions from Volcán Popocatepetl and Volcán de Colima, Mexico: Melt evolution due to vapor-saturated crystallization during ascent. *Journal of Volcanology and Geothermal Research* **153**, 221–240.

AUSTRALIAN BUREAU OF STATISTICS. 2011. 2011 Census QuickStats. http://www.censusdata.abs.gov.au/census_services/getproduct/census/2011/quickstat/0 Last accessed 25th June 2014.

BLACKBURN G. 1966. Radiocarbon dates relating to soil development and volcanic ash deposition in south-east South Australia. *Australian Journal of Earth Sciences* **29**, 50–52.

BLACKBURN G., ALLISON G. B. & LEANEY F. W. J. 1982. Further evidence on the age of the tuff at Mount Gambier, South Australia. *Transactions of the Royal Society of South Australia* **106**, 163–167.

BLAIKIE T. N., AILLERES, L., CAS R. A. F. & BETTS P. G. 2012. Three-dimensional potential field modelling of a multi-vent maar-diatreme — The Lake Coragulac maar, Newer Volcanics Province, south-eastern Australia. *Journal of Volcanology and Geothermal Research* **235**, 70–83.

BOYCE, J. 2013. The Newer Volcanics Province of southeastern Australia: a new classification scheme and distribution map for eruption centres. *Australian Journal of Earth Sciences* **60**, 449–462.

BOYCE J. A., KEAYS R. R., NICHOLLS I. A. & HAYMAN P. C. 2014. Eruption centres of the Hamilton area of the Newer Volcanics Province, Victoria, Australia: pinpointing volcanoes from a multifaceted approach to landform mapping. *Australian Journal of Earth Sciences* **61**: 735–754.

BOYCE J. A., NICHOLLS I. A., KEAYS R. R. & HAYMAN P. C. 2015. Variation in parental magmas of Mt Rouse, a complex polymagmatic monogenetic volcano in the basaltic intraplate Newer Volcanics Province, southeast Australia. *Contributions to Mineralogy and Petrology* **169**. DOI 10.1007/s00140-015-1106-y

BRENNAM., CRONIN S. J. SMITH I. E. M., SOHN S. Y. & NÉMETH K. 2010. Mechanisms driving polymagmatic activity at a monogenetic volcano, Udo, Jeju Island, South Korea. *Contributions to Mineralogy and Petrology* **160**, 1–20.

BRENNAM., CRONIN S. J. NÉMETH K., SMITH I. E. M., & SOHN Y. 2011. The influence of magma plumbing complexity on monogenetic eruptions, Jeju Island, Korea. *Terra Nova* **23**, 70–75.

BÜTTNER R., DELLINO P., LA VOLPE L., LORENZ V. & ZIMANOWSKI B. 2002. Thermohydraulic explosions in phreatomagmatic eruptions as evidenced by the comparison between pyroclasts and products from Molten Fuel Coolant Interaction experiments. *Journal of Geophysical Research* **107**, (B11).

CAMP V. E., HOOPER P. R., ROOBOL M. J. & WHITE D. L. 1987. The Madinah eruption, Saudi Arabia: Magma mixing and simultaneous extrusion of three basaltic chemical types. *Bulletin of Volcanology* **49**, 489–508.

CARTWRIGHT I., WEAVER T., TWEED S., AHEARNE D., COOPER M., CZAPNIK K. & TRANTER J. 2002. Stable isotope geochemistry of cold CO₂- bearing mineral spring waters, Daylesford, Victoria: sources of gas and water and links with waning volcanism. *Chemical Geology* **185**, 71–91.

CAS R., SIMPSON C. & SATO H. 1993. Newer Volcanics Province—Processes and products of phreatomagmatic activity. IAVCEI Canberra 1993—Excursion guide. Australian Geological Survey Organisation, Canberra.

CAYLEY R. A., WEBB A. W. & HENLEY K. J. 1995. Radiometric dating (K/Ar) on two samples of Newer Volcanic olivine basalt from the southwestern part of the Beaufort 1:100 000 map sheet area. *Geological Survey of Victoria Unpublished Report* **1995/15**.

CHIVAS A. R., BARNES I. E., LUPTON J. E. & COLLERSON K. 1983. Isotopic studies of south-east Australian CO₂ discharges. *Geological Society of Australia Abstract* **12**, 94–95.

CHIVAS A. R., BARNES I., EVANS W. C., LUPTON J. E. & STONE J. O. 1987. Liquid carbon dioxide of magmatic origin and its role in volcanic eruptions. *Nature* **326**, 587–589.

DASCH E. J. & MILLAR D. J. 1977. Age and strontium-isotope geochemistry of differentiated rocks from the Newer Volcanics, Mt Macedon area, Victoria, Australia. *Journal of the Geological Society of Australia* **24**, 195–201.

DAVIES D. R. & RAWLINSON N. 2014. On the origin of recent intraplate volcanism in Australia. *Geology*. Doi: 10.1130/G36093.1

DE KEYSER F. & LUCAS K. G. 1968. Geology of the Hodgkinson and Laura Basins, north Queensland. *Bureau of Mineral Resources, Australia Bulletin* **84**.

EDWARDS J. 1994. The Geology, Petrography and Geochemistry of Lady Julia Percy Island. MSc thesis, University of Melbourne.

EDWARDS J., CAYLEY R. A. & JOYCE E. B. 2004. Geology and geomorphology of the Lady Julia Percy Island volcano, a late Miocene submarine and subaerial volcano off the coast of Victoria, Australia. *Proceedings of the Royal Society of Victoria* **116**, 15–35.

ERLUNDE E. J., CASHMAN K. V., WALLACE P. J., PIOLIL., ROSIM., JOHNSON E. & DELGADO GRANADOS H. 2010. Compositional evolution of magma from Paricutin Volcano, Mexico: The tephra record. *Journal of Volcanology and Geothermal Research* **197**, 167–187.

EWART A., CHAPPELL B. W. & Le MAITRE R. W. 1985. Aspects of the mineralogy and chemistry of the intermediate-silicic Cainozoic volcanic rocks of eastern Australia. Part 1: Introduction and

geochemistry. *Australian Journal of Earth Sciences* **32**, 359–382.

FOSHAG W. F. & GONZÁLEZ R. 1956. Birth and development of Paricutin volcano Mexico. *Geological Survey Bulletin* **965-D**.

FREY F. A., GREEN D. H. & ROY D. 1978. Integrated models of basalt petrogenesis: a study of quartz tholeiites to olivine melilitites from South Eastern Australia utilising geochemical and experimental petrological data. *Journal of Petrology* **19**, 463–513.

GOURAMANIS C., WILKINS D. & DEDECKKER P. 2010. 6000 years of environmental changes recorded in Blue Lake, South Australia, based on ostracod ecology and valve chemistry. *Palaeogeography, Palaeoclimatology, Palaeoecology* **297**, 223–237.

GRAEBER F. M., HOUSEMAN G. A. & GREENHALGH S. A. 2002. Regional teleseismic tomography of the western Lachlan Orogen and the Newer Volcanics Province, southeast Australia. *Geophysical Journal International* **149**, 249–266.

GRAY C. M. & MCDOUGALL I. 2009. K–Ar geochronology of basalt petrogenesis, Newer Volcanic Province, Victoria. *Australian Journal of Earth Sciences* **56**, 245–258.

GRIFFIN T. J. 1977. The geology, mineralogy and geochemistry of the McBride basaltic province, northern Queensland. James Cook University of North Queensland PhD thesis unpublished.

GRIFFIN W. L., O'REILLY S. Y. & STABEL A. 1988. Mantle metasomatism beneath western Victoria, Australia: II. Isotopic geochemistry of Cr-diopside lherzolites and Al-augite pyroxenites. *Geochimica et Cosmochimica Acta* **52**, 449–459.

GUDEMUNDSSON M. T., THORDARSON T., HÖSKULDSSON A., LARSEN G., BJÖRNSSON H., PRATA F. J., ODDSSON B., MAGNÚSSON E., HÖGNADÓTTIR T., PETERSON G. N., HAYWARD C. L., STEVENSON J. A. & JÓNSDÓTTIR I. 2012. Ash generation and distribution from the April–May 2010 eruption of Eyjafjallajökull, Iceland. *Scientific Reports* **2**, article 572. DOI: 10.1038/srep00572

HOLT S. J., HOLFORD S. P. & FODEN J. 2014. New insights into the magmatic plumbing system of the South Australian Quaternary Basalt province from 3D seismic and geochemical data. *Australian Journal of Earth Sciences* **60**, 797–817.

JOHNSON E. R., WALLACE P. J., CASHMAN K. V., GRANADOS H. D. & KENT A. J. R. 2008. Magmatic volatile contents and degassing-induced crystallisation at Volcán Jorullo, Mexico: Implications for melt evolution and the plumbing systems of monogenetic volcanoes. *Earth and Planetary Science Letters* **269**, 478–487.

JORDAN S. C., CAS R. A. F. & HAYMAN P. C. 2013. The origin of a large (>3 km) maar volcano by coalescence of multiple shallow craters: Lake Purrumbete maar, southeastern Australia. *Journal of Volcanology and Geothermal Research* **254**, 5–22.

JOYCE E. B. 1975. Quaternary volcanism and tectonics in southeastern Australia. In: Suggate R. P. & Cresswell M. M. eds. *Quaternary studies*, pp. 169–178. The Royal Society of New Zealand, Wellington.

JOYCE E. B. 1988a. Newer volcanic landforms. In: Douglas J. G. & Ferguson J. A. eds. *Geology of Victoria*, pp. 419–426. Geological Society of Australia, Victorian Division.

JOYCE E. B. 1988b. Cainozoic volcanism in Victoria. In: Clark I. & Cook B. eds. *Victorian geology excursion guide*, pp. 71–80. Australian Academy of Science, Canberra.

KENT A. J. R. 2008. Melt inclusions in basaltic and related volcanic rocks. *Reviews in Mineralogy and Geochemistry* **69**, 273–331.

KIENLE J., KYLE P. R., SELF S., MOTYKA R. J. & LORENZ V. 1980. Ukinrek Maars, Alaska, I. April 1977 eruption sequence, petrology and tectonic setting. *Journal of Volcanology and Geothermal Research* **7**, 11–37.

LEE C. A., LUFFI P., PLANK T., DALTON H. & LEEMAN W. P. 2009. Constraints on the depths and temperatures of basaltic magma generation on Earth and other terrestrial planets using new thermobarometers for mafic magmas. *Earth and Planetary Science Letters* **279**, 20–33.

LUHR J. F. 2001. Glass inclusions and melt volatile contents at Parícutin Volcano, Mexico. *Contributions to Mineralogy and Petrology* **142**, 261–283.

MCDONOUGH W. F., MCCULLOCH M. T. & SUN S. S. 1985. Isotopic and geochemical systematics in Tertiary-Recent basalts from southeastern Australia and implications for the evolution of the sub-continental lithosphere. *Geochimica et Cosmochimica Acta* **49**, 2051–2067.

MCDONOUGH W. F. & MCCULLOCH M. T. 1987. The southeast Australian lithospheric mantle: isotopic and geochemical constraints on its growth and evolution. *Earth and Planetary Science Letters* **86**, 327–340.

MCDUGALL I., ALLSOP H. L. & CHAMALAUN F. H. 1966. Isotopic dating of the Newer Volcanics of Victoria, Australia and geomagnetic polarity epochs. *Journal of Geophysical Research* **71**, 6107–6118.

NEEDHAM A.J., LINDSAY J.M., SMITH I.E.M., AUGUSTINUS P., SHANE P.A. 2010. Sequential eruption of alkaline and sub-alkaline magmas from a small monogenetic volcano in the Auckland

Volcanic Field, New Zealand. *Journal of Volcanology and Geothermal Research* **201**, 126–142.

KNUTSON J. & NICHOLLS I. A. 1989. Macedon–Trentham. In: Johnson R. W. ed. *Intraplate volcanism in Eastern Australia and New Zealand*, pp. 136–137. Cambridge University Press, Cambridge.

O'REILLY S. Y. & GRIFFIN W. L. 1988. Mantle metasomatism beneath western Victoria, Australia: I. Metasomatic processes in Cr-diopside lherzolites. *Geochimica et Cosmochimica Acta* **52**, 433–447.

PIGANIS F. 2011. A volcanological investigation of the polymagmatic Red Rock Volcanic Complex and a 3D geophysical interpretation of the subsurface structure and geology of the poly-lobate Lake Purdigulac maar, Newer Volcanics Province, southeastern Australia. MSc thesis (unpublished), Monash University.

PRATA G. 2012. Complex eruption style and deposit changes during the evolution of the late Pleistocene Tower Hill maar–scoria cone Volcanic Complex, Newer Volcanics Province, Victoria, Australia. MSc thesis, Monash University.

PRICE R. C., GRAY C. M., NICHOLLS I. A., DAY A. 1988. Cainozoic volcanic rocks. In: Douglas J. G. & Ferguson J. A. (eds). *Geology of Victoria*. Geological Society of Australia, Victoria Division, Melbourne, pp. 439–451.

PRICE R. C., GRAY C. M. & FREY F. A. 1997. Strontium isotopic and trace element heterogeneity in the plains basalts of the Newer Volcanic Province, Victoria, Australia. *Geochimica et Cosmochimica Acta* **61**, 171–192.

PRICE R. C., NICHOLLS I. A. & GRAY C. M. 2003. Cainozoic igneous activity. In: Douglas J. G. & Ferguson J. A. eds. *Geology of Victoria*, pp. 361–375. Geological Society of Victoria, Victorian Division, Melbourne.

ROGGENSACK K. 2001. Unraveling the 1974 eruption of Fuego volcano (Guatemala) with small crystals and their young melt inclusions. *Geology* **29**, 911–914.

SMITH I. E., BLAKE S., WILSON C. J. N. & HOUGHTON B. F. 2008. Deep-seated fractionation during the rise of a small-volume basalt magma batch: Crater Hill, Auckland, New Zealand. *Contributions to Mineralogy and Petrology* **155**, 511–527.

STEPHENSON P. J. 1989. Northern Queensland. In: Johnson R. W. ed. *Intraplate volcanism in Eastern Australia and New Zealand*, pp. 89–97. Cambridge University Press, Cambridge.

STRONG M. & WOLFF J. 2003. Compositional variations within scoria cones. *Geology* **31**, 143–146.

- SUTALO F. & JOYCE B. 2004. Long basaltic lava flows of the Mt. Rouse volcano in the Newer Volcanic Province of southeastern Australia. *Proceedings of the Royal Society of Victoria* **116**, 37–47.
- VALENTINE G. A. & GREGG T. K. P. 2008. Continental basaltic volcanoes – processes and problems. *Journal of Volcanology and Geothermal Research* **177**, 857–873.
- VAN OTTERLOO J., CAS R. A. F. & SHEARD M. J. 2013. Eruption processes and deposit characteristics at the monogenetic Mt. Gambier Volcanic Complex, SE Australia: implications for alternating magmatic and phreatomagmatic activity. *Bulletin of Volcanology* **75.8**, 1–21.
- VAN OTTERLOO J., RAVEGGI M., CAS R. A. F. & MAAS R. 2014. Polymagmatic activity at the monogenetic Mt Gambier volcanic complex in the Newer Volcanics Province, SE Australia: New Insights into the occurrence of intraplate volcanic activity in Australia. *Journal of Petrology* **55**, 1317–1351.
- WALKER G. P. L. 2000. Basaltic volcanoes and volcanic systems. In: Sigurdsson H. ed. *Encyclopaedia of Volcanoes*, pp. 283. Academic Press, New York.
- WELLMAN P. 1974. Potassium–argon ages of the Cainozoic volcanic rocks of eastern Victoria, Australia. *Journal of the Geological Society of Australia* **21**, 359–376.
- WHITE J. D. L. & ROSS P. –S. 2011. Maar-diatreme volcanoes: A review. *Journal of Volcanology and Geothermal Research* **201**, 1–29.
- WHITEHEAD P.W., STEPHENSON P. J., MCDOUGALL I., HOPKINS M. S., GRAHAM A. W., COLLERSON K. D. & JOHNSON D. P. 2007. Temporal development of the Atherton Basalt Province, north Queensland. *Australian Journal of Earth Sciences* **54**, 691–709.
- WOHLETZ K. H. 1983. Mechanics of hydrovolcanic pyroclast formation: grain-size, scanning microscopy, and experimental studies. *Journal of Volcanology and Geothermal Research* **17**, 31–63.
- WOPFNER H. & THORNTON R. C. N. 1971. The occurrence of carbon dioxide in the Gambier Embayment. In: Wopfner H. & Douglas J. G. eds. *The Otway Basin of Southeastern Australia*, pp. 377–384. Geological Surveys of South Australia and Victoria Special Bulletin.







Appendix 1

Outreach

This appendix contains an excerpt from the 2011 IUGG VF01 field trip guide Cas *et al.* (2011), an outreach article written for *Geology Today* (Boyce *et al.* 2014) and both a web page and tour created for the Volcanoes Discovery Centre, Penshurst.

CAS R., BLAIKIE T., BOYCE J., HAYMAN P., JORDAN S., PIGANIS F., PRATA G. & VAN OTTERLOO J. 2011. Factors that influence varying eruption styles (from magmatic to phreatomagmatic) in intraplate continental basaltic volcanic provinces: The Newer Volcanics Province of southeastern Australia. Field trip guide VF01, pp. 7–31. IUGG 2011 General Assembly. *Earth on the Edge: Science for a Sustainable Planet*.

BOYCE J. A., NICHOLLS I. A., KEAYS R. R. & HAYMAN P. C. 2015. Variation in parental magmas of Mt Rouse, a complex polymagmatic monogenetic volcano in the basaltic intraplate Newer Volcanics Province, southeast Australia. *Geology Today* **30**, 105-109.



IUGG

MELBOURNE Australia 2011

2011 International Union of Geodesy and Geophysics General Assembly
XXV IUGG General Assembly

EARTH ON THE EDGE: SCIENCE FOR A SUSTAINABLE PLANET

28 June – 7 July 2011
Melbourne Convention and Exhibition Centre

FIELD TRIP GUIDE

**VF01: FACTORS THAT INFLUENCE VARYING
ERUPTION STYLES (FROM MAGMATIC TO
PHREATOMAGMATIC) IN INTRAPLATE
CONTINENTAL BASALTIC VOLCANIC
PROVINCES: THE NEWER VOLCANICS
PROVINCE OF SOUTHEASTERN AUSTRALIA.**

9 – 13 July 2011

R. Cas, T. Blaikie, J. Boyce, P. Hayman, S.

www.iugg2011.com

One Venue, One City, One Conference

Mount Rouse Volcano

Julie Boyce

Unless otherwise stated, figures and data form part of doctoral thesis (unpublished) of Julie Boyce.

1. Introduction

Mt. Rouse is a volcanic complex of lavas and pyroclastic deposits with several eruption points (Fig. MR1), named by Major Mitchell in 1836 after Richard Rouse, a prominent free settler in Sydney during the early 1800's. Lying in the town of Penshurst, near Hamilton, Victoria, (Western Plains sub-province) (Fig. MR2), Mt. Rouse has produced the largest eruption volume in the NVP, more than triple the size of other volcanoes in terms of both area covered and volume erupted (Elias, 1973). Lava flows extend 55 km to the coast at Port Fairy, covering an area of 535 km² (Boyce et al, unpublished), and the cone complex is a substantial edifice of coalesced cones and craters.

The lava flows of Mt. Rouse were erupted onto a relatively flat topography with a gradient of 1:200 (300 m in 60 km) from cone to sea. They form stony rises, ridges and depressions 3-10 m in height, with 15-30 m between rises, formed from a braided network of lava tubes beneath semi-solidified crust (Ollier, 1985). The latest sub-division of the Mt. Rouse flows is that of Sutalo (1996), and was based on geomorphological features and differences in mineralogy, utilising aerial photographs, radiometric and magnetic imagery and ground-truthing. Six main lava flows were recognised (Fig. MR2). The oldest is the Rouse-Port Fairy Flow, which extends 55 km to the coast at Port Fairy (the Tarrone Flow is interpreted as a break-out from this flow), and the Spring Flow is suggested to be another early flow. The Hawkesdale Flow is 27 km in length - the second longest flow unit, with more rugged relief than the Rouse-Port Fairy Flow. The boundary between the Rouse-Port Fairy Flow and the Hawkesdale Flow was inferred from aerial photograph relief and ridge distribution of the stony rises

(Sutalo & Joyce, 2004). The New Flow and Lava Shield originate from the southern crater (Whitehead, 1991; Sutalo 1996).

The northern double scoria cone of Mt. Rouse trends E-W, rising 120 m above the surrounding lava plains. The internal stratigraphy and architecture of the cone and crater complex is complex because of the overlapping relationships between successive constructional edifices as the location of eruption points shifted in time. The southern crater features two small satellite cones to the southeast. The inner walls of an early eruption point are located in the LK quarry to the NE, featuring coarse scoria and spatter steeply dipping to the south, and intrusive rocks to the base. This is overlain by scoria from the northern cones, shallowly dipping to the east.

Age dating of lava flows by K-Ar and ⁴⁰Ar-³⁹Ar has yielded ages of 0.294-0.382 Ma, 0.415-0.450 Ma and 1.82 Ma (Table MR1, Fig. MR2), yet Mt. Rouse has previously been considered monogenetic. The 1.82 Ma age is considered incorrect (Sutalo & Joyce, 2004; Matchan & Phillips, 2011). Matchan & Phillips (2011) ascribe the 0.4 Ma dates to either extraneous ⁴⁰Ar or an older eruption. K-Ar dating assumes there is no excess argon, while the more precise Ar-Ar dating makes no such assumption. Petrologically the basalts are similar across the flows.

Scientific questions for discussion:

- *Are the 0.4 Ma ages from an earlier eruption, or due to extraneous argon?*
- *If the Tarrone Flow represents an earlier eruption, why are the basalts so similar in terms of petrography and geochemistry (all lavas have the same geochemistry and are from the same magma batch) with a hiatus of 100,000 – 150,000 years?*

Petrographically, Mt. Rouse basalts

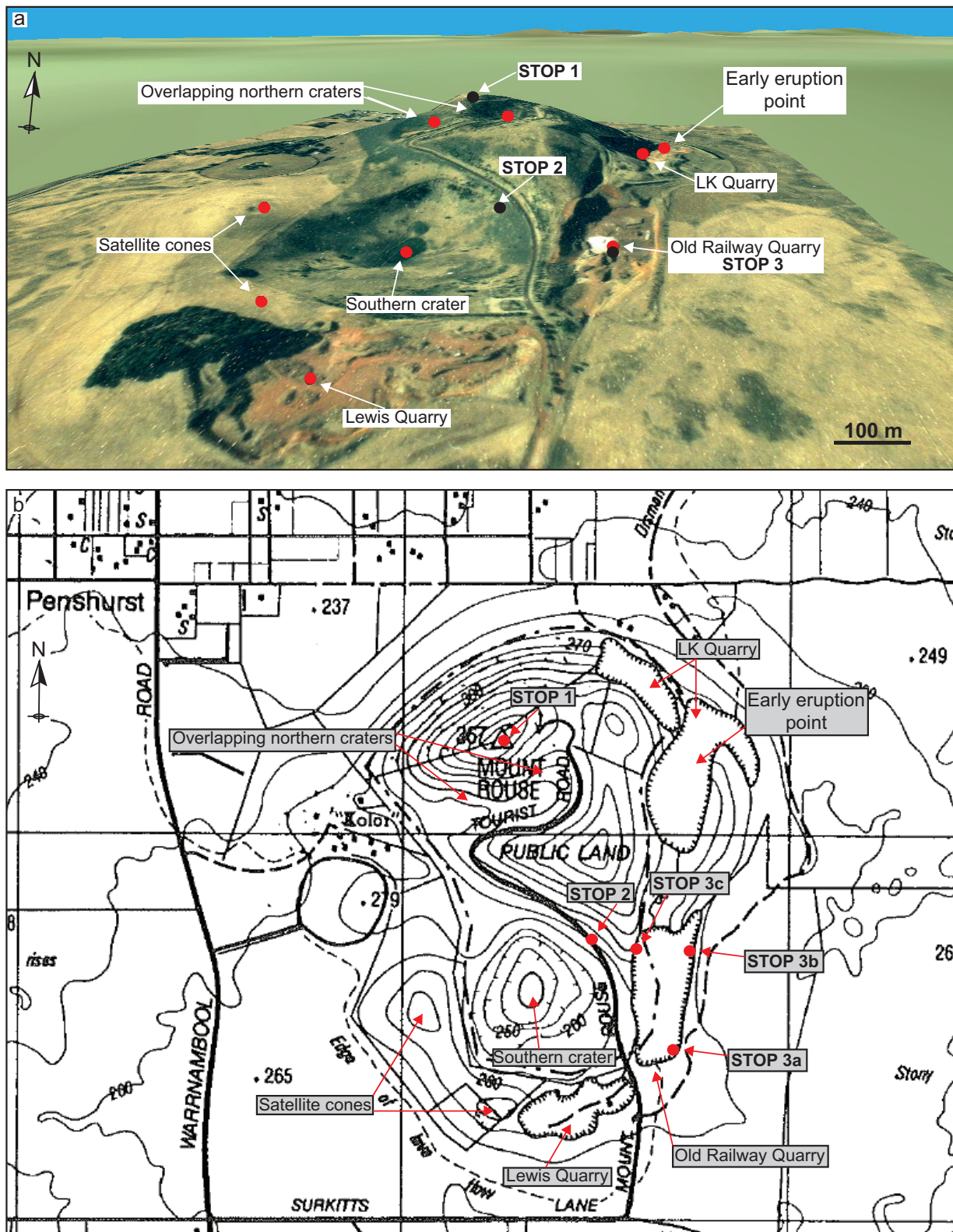


Fig. MR1 (a) ArcGIS 3D image of Mt. Rouse (utilising NASA ASTER data) with 1.5x vertical exaggeration, showing stops, craters and quarry locations, (b) Map of Mt. Rouse (after Rosengren, 1994) showing the volcano in relation to the township of Peshurst, with stops, craters and quarry locations. NASA ASTER GDEM is a product of METI and NASA.

contain phenocrysts of olivine and andesine) with minor olivine and pyroxene clinopyroxene (up to 0.85 mm) and rare zoned plagioclase (up to 1.5 mm) in a groundmass of plagioclase laths (An_{36} to iddingsite is common.

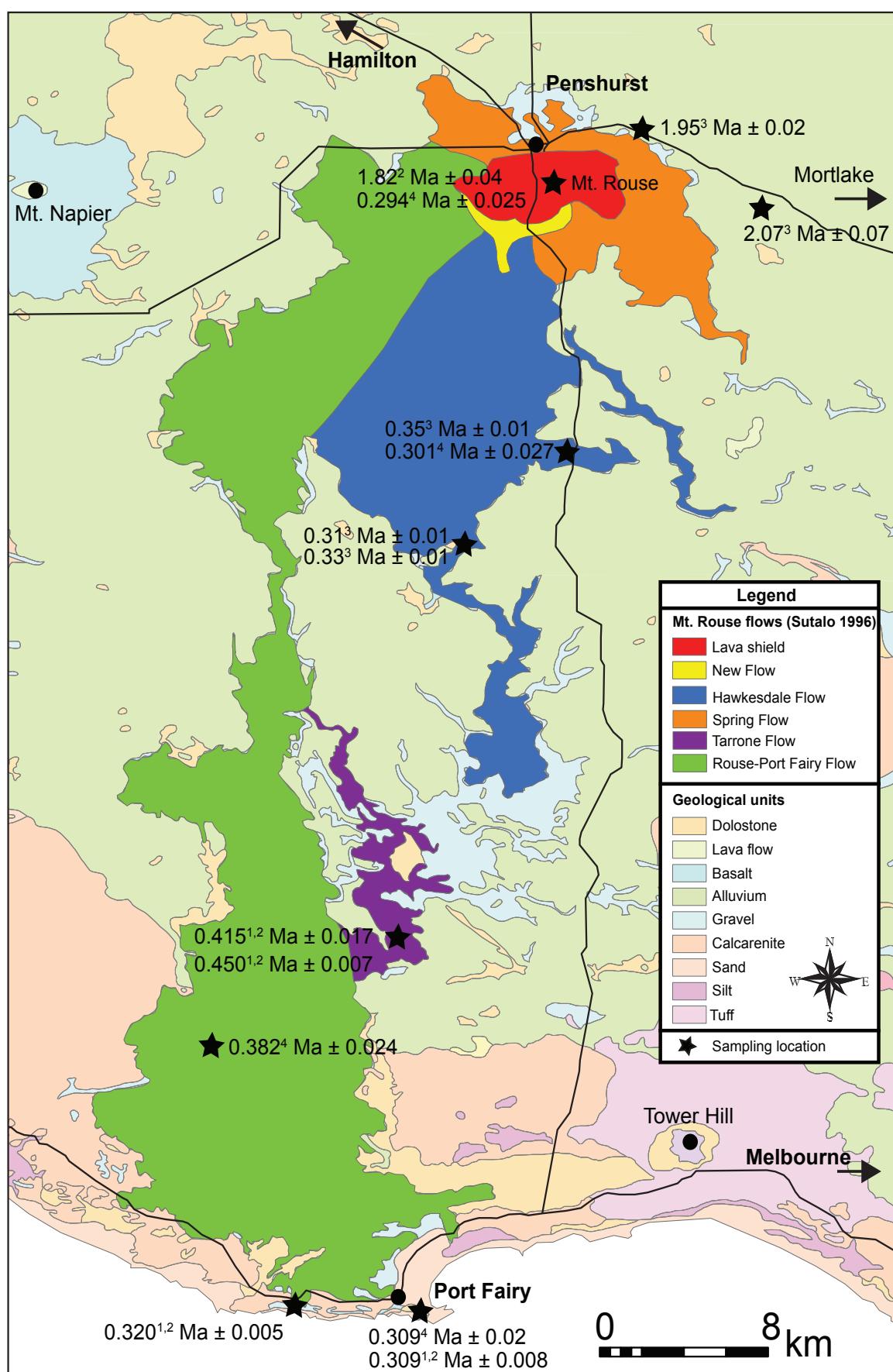


Fig. MR2. Distribution of main lava flows from Mt. Rouse. Modified after Sutalo (1996) utilising Arc-GIS, showing lava flow units, surrounding geology and K-Ar and ⁴⁰Ar-³⁹Ar dates. ¹McDougall & Gill (1975); ²Ollier (1985); ³Gray & McDougall (2009); ⁴Matchan & Phillips (2011).

Table MR1 K-Ar and ^{40}Ar - ^{39}Ar dates for Mt. Rouse lava flows, colour referenced to flow

| Flow | Age (Ma) | Reference | Method |
|------------------|-------------------|--|-------------------------------------|
| Lava shield | 1.82 | Ollier (1985) | K-Ar |
| (interbedded | 0.294 ± 0.025 | Matchan & Phillips (2011) | ^{40}Ar - ^{39}Ar |
| Hawkesdale Flow | 0.31 ± 0.01 | | |
| | 0.33 ± 0.01 | Gray & McDougall (2009) | K-Ar |
| | 0.35 ± 0.01 | | |
| | 0.301 ± 0.027 | Matchan & Phillips (2011) | ^{40}Ar - ^{39}Ar |
| Rouse-Port Fairy | 0.309 ± 0.008 | McDougall & Gill (1975); Ollier (1985) | K-Ar |
| Flow | 0.309 ± 0.02 | Matchan & Phillips (2011) | ^{40}Ar - ^{39}Ar |
| | 0.320 ± 0.005 | McDougall & Gill (1975); Ollier (1985) | K-Ar |
| | 0.382 ± 0.024 | Matchan & Phillips (2011) | ^{40}Ar - ^{39}Ar |
| | 0.415 ± 0.017 | McDougall & Gill (1975); Ollier (1985) | K-Ar |
| | 0.450 ± 0.007 | McDougall & Gill (1975); Ollier (1985) | K-Ar |

Geochemically, effusive and explosive products define two separate magma batches. One magma batch was effusive, forming all basalts, including basalt of the lava shield interbedded with pyroclastic deposits in the quarries of the southern cone; the second magma batch was explosive, forming the scoria and ash deposits. Effusive products are exclusively alkali basalts (with the odd exception being sub-alkaline in composition), while explosive products range from basanites to alkali basalts (Fig. MR3c). Trachybasaltic pyroclastics may be further subdivided into hawaiites. REE Patterns (Fig. MR3d) are similar to OIB, with LREE enriched compared to HREE, due to the presence of olivine and pyroxene. Absence of an Eu anomaly show that plagioclase was not a major fractionating phase in either magma batch. Extreme depletion of HREE relative to light indicates garnet in the source.

due to its formation from two overlapping circular craters 150 m and 250 m in diameter. The summit consists of a spatter rampart composed of extensively weathered welded scoria fragments, and a small outcrop of basalt with columnar joints to the surface.

Looking to the south from the steps, the two satellite cones of the southern crater can be seen, and a view of the Lewis Quarry of the southern scoria cone shows ashy scoriaceous deposits overlain by an orange coloured lapilli and ash-rich deposit. The lava shield can be seen all around, with the distinctive hummocky terrain characteristic of the stony rises. On a clear day, other views of geological interest include the Grampians mountain range to the north (consisting of deformed Devonian sedimentary rocks), Mt. Napier lava shield and summit spatter cone complex to the west and the Mt. Eccles shield volcano to the south-west

STOP MR1. Mt. Rouse Summit

The road ascends from the lava apron along a sinuous route from the southern to the northern scoria cone, each of which has a well-preserved crater. A short walk to the summit from the car park provides an excellent view of the complex and its surroundings. The summit is located above the northern flank of the highest cone at 340 m (the surrounding plains are 200 m, while the stony rises lava shield are at 220 m), and the northern crater is elongated east-west,

STOP MR2. Southern crater view

Walk down from the northern cone summit and follow the road back down the volcano, which runs through both northern craters, now planted with Monterey Pines and native flora. The road runs past the southern crater, where we will stop for a few moments for an excellent view of this eruption point. The southern crater has steep undulating sides dropping down into a permanent lake at 218 m. Just above the crater lake to the north-east, coarse-grained

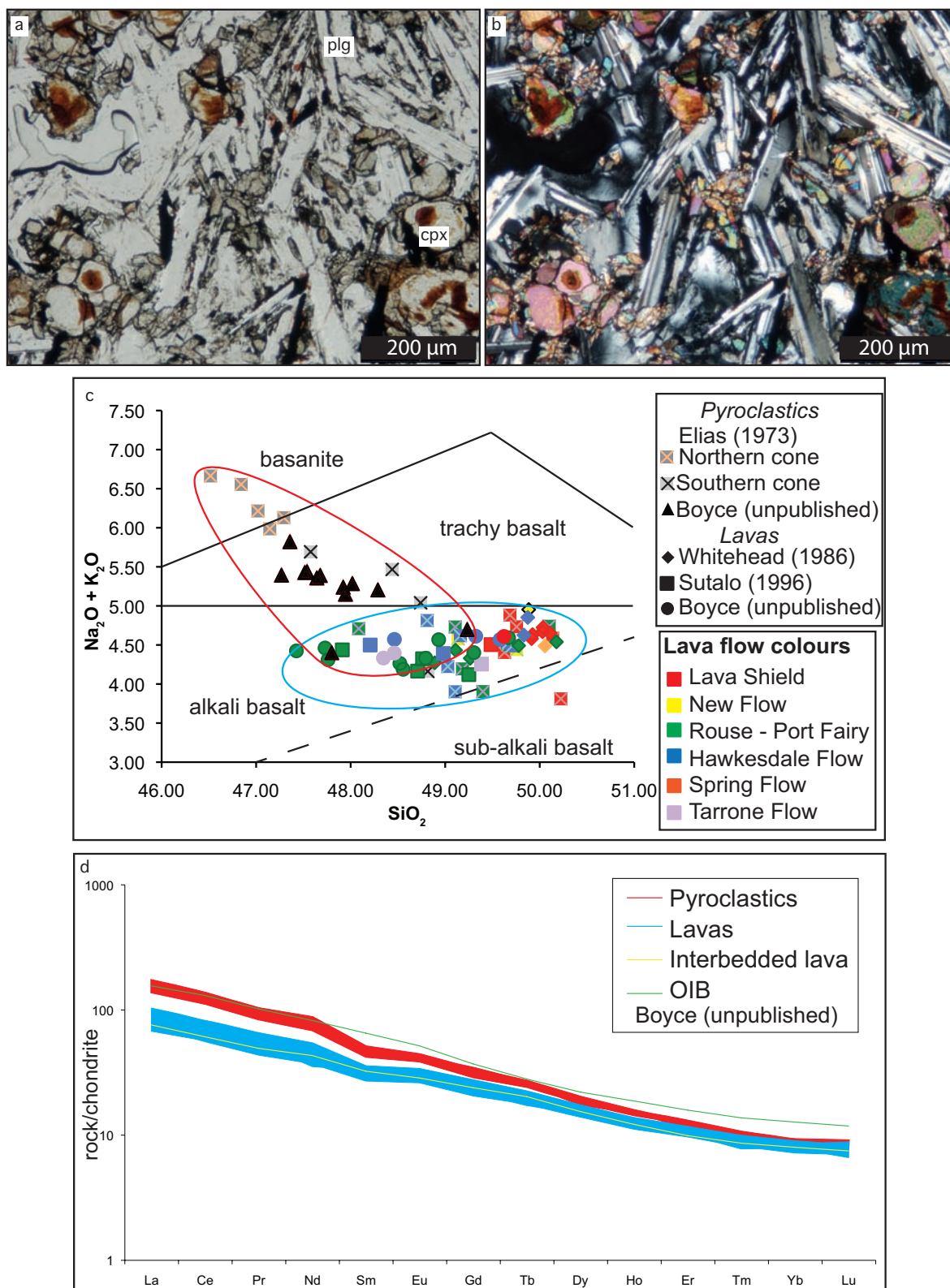


Fig. MR3 Petrography and geochemistry of Mt. Rouse deposits. Photomicrograph of Mt. Rouse basalt in PPL (a) and XPL (b) showing plagioclase groundmass and clinopyroxene clusters. (c) TAS diagram of normalised geochemical data from all Mt. Rouse studies. Crossed squares – Elias (1973) (orange northern cone, black southern cone), diamonds – Whitehead (1986), filled squares – Sutalo (1996), circles – Boyce et al (unpublished) (lavas), triangles – Boyce et al (unpublished) (pyroclastics). Colours indicate flow units of Sutalo (1996): red – Lava Shield, yellow – New Flow, green – Rouse-Port Fairy Flow, blue – Hawkesdale Flow, orange – Spring Flow, purple – Tarrone Flow. (d) Chondrite normalised REE diagram for the products of Mt. Rouse (Boyce et al, unpublished) showing that pyroclastic deposits (red) define one magma batch and lavas (blue) define another.

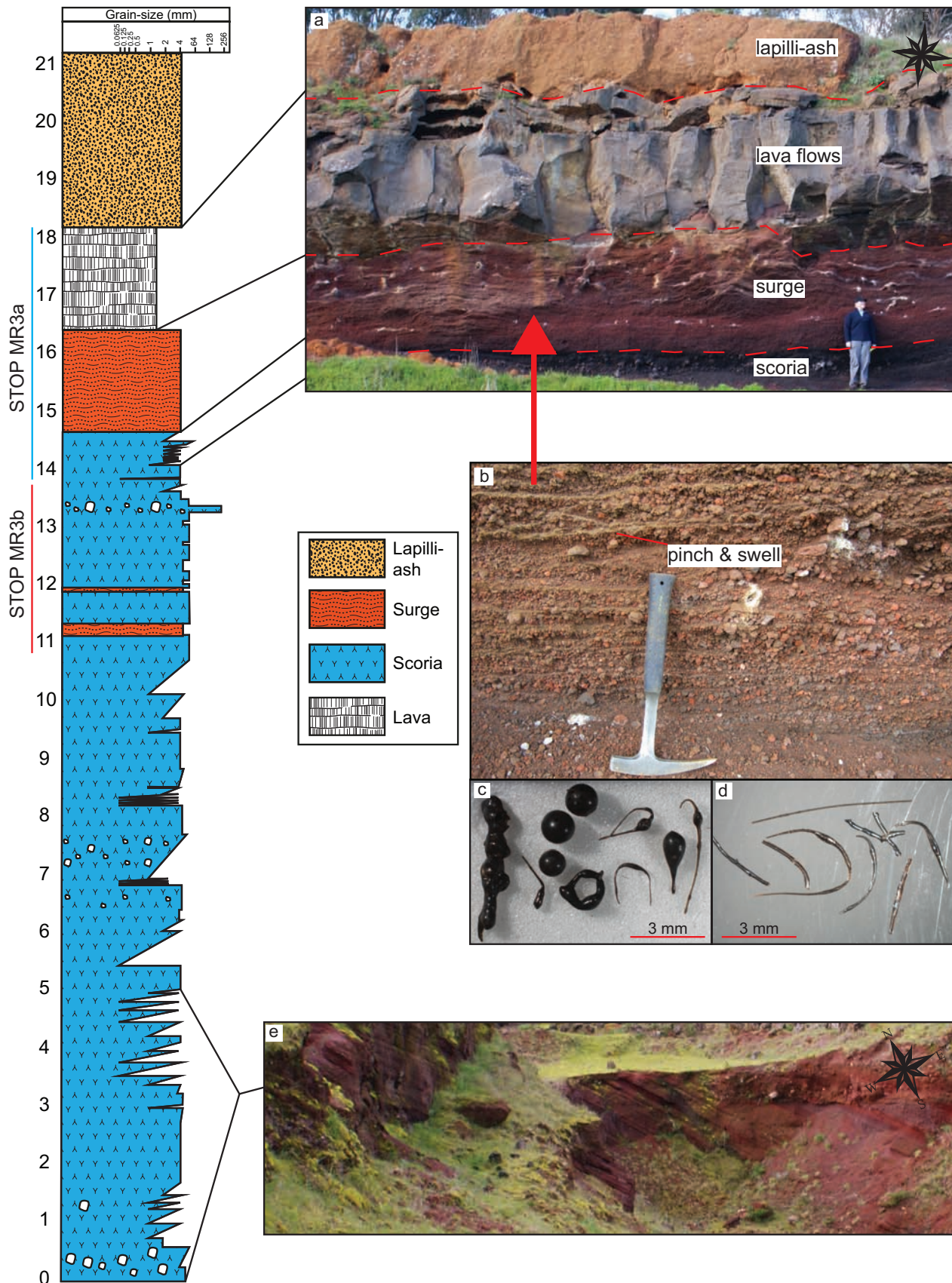


Fig. MR4 Generalised stratigraphic log of the eastern face of the Old Railway Quarry, showing (a) lava flow underlain by Pele's tears and hair-rich surge deposit and scoria, (b) coarse surge deposit underlying lava, showing pinch and swell structures. Contains extremely common fresh Pele's tears (c) and hairs (d). (e) Ashy layers in the Lewis Quarry to the southwest, underlying Old Railway Quarry deposits of the Eastern face.

basalt blocks feature columnar jointing. There are also many boulders around the crater rim. This vantage point also offers good views of the two satellite cones. The western cone is slightly higher than that to the SSE, at 268 m, featuring a small circular crater approximately 15 m wide, filled with 1.5 m agglutinated spatter bombs and fine-grained basalt blocks. A wall of basalt blocks ~2 m rims the crater to the west. The satellite cone to the SSE is 264 m high with a longer and flatter crater than the western satellite cone. The basalt here is more intensely weathered due to the many small vesicles.

STOP MR3. Old Railway Quarry

Continue 350 m along the road, and enter the Old Railway Quarry on the left. This quarry contains an excellent section through the flank of the southern scoria cone of Mt. Rouse. Figure MR4 shows a generalised stratigraphic log through the deposits of the eastern face of the Old Railway Quarry (stops 3a, b), which correlate with the underlying deposits in the Lewis Quarry to the southeast. Geochemically, the pyroclastics all belong to one magma batch (including armoured lapilli in the deposit above the lava), whereas the lava itself belongs to the second magma batch. The dip of the scoria underlying the lava suggests an origin from the southern crater.

STOP MR3a – adjacent to quarry entrance on right

A lava flow and surge layer can be seen at this location, corresponding to approximately 14-18 m in the generalised log of Figure MR4.

The alkali basalt lava flow geochemically plots on all bivariate diagrams with samples from the lava shield of previous studies. The flow was originally clastogenic and is a splendid example of pahoehoe, with the ropey underside very well preserved. Columnar jointing can be seen to the south of the quarry, and in places smaller flows have split apart, preserving lava stalagmites and stalactites.

A distinctive surge layer is exposed

beneath the lava flow. It is up to 1.5 m thick and pinches out to the north with the lava, and is an excellent marker bed. The surge is composed of ashy pinch-and-swell structures, and coarse oxidised scoriaceous lapilli up to 8 mm, geochemically belonging to the pyroclastics magma batch. An absence of crustal material indicates a near-surface water source for this surge. Of importance to this deposit is the abundance of Pele's tears and hairs throughout the layer, which are remarkably well preserved. Pele's hairs are up to 9 mm long and can be extremely fine and delicate, while the Pele's tears come in a variety of shapes and sizes from <1 mm to 1 cm, perfectly rounded, classic tear-drop shapes, fusiform or globular. Many of the tears are still attached to hairs. Prevailing wind must have been towards the east, as the amount of these products in the surge layer decreases to the south, and very few are found in the corresponding layer in the Lewis Quarry.

Walk along this exposure towards the northern-end of the quarry, noting the various fallen blocks of lava, which expose the ropey surface of the flow. There is an increase in the amount of Pele's hairs and tears along the exposure.

Scientific questions for discussion:

- *Why are fragile Pele's tears and hairs so well preserved in a surge deposit? Are they derived from the same vent? Geochemical analysis of the Pele's tears will confirm which magma batch they belong to.*
- *Does this deposit represent a fall-modified surge deposit?*

STOP MR3b – far northeast of Old Railway Quarry

Walk down from the quarry face back to the path, being careful not to slip on the vegetated scree. Make your way to the right-hand-side of the far end of the quarry.

A thick layer of black lapilli (scoria) in the 5-20 mm range is exposed here, corresponding to approximately 11-14 m in the generalised log of Figure MR4. The lapilli

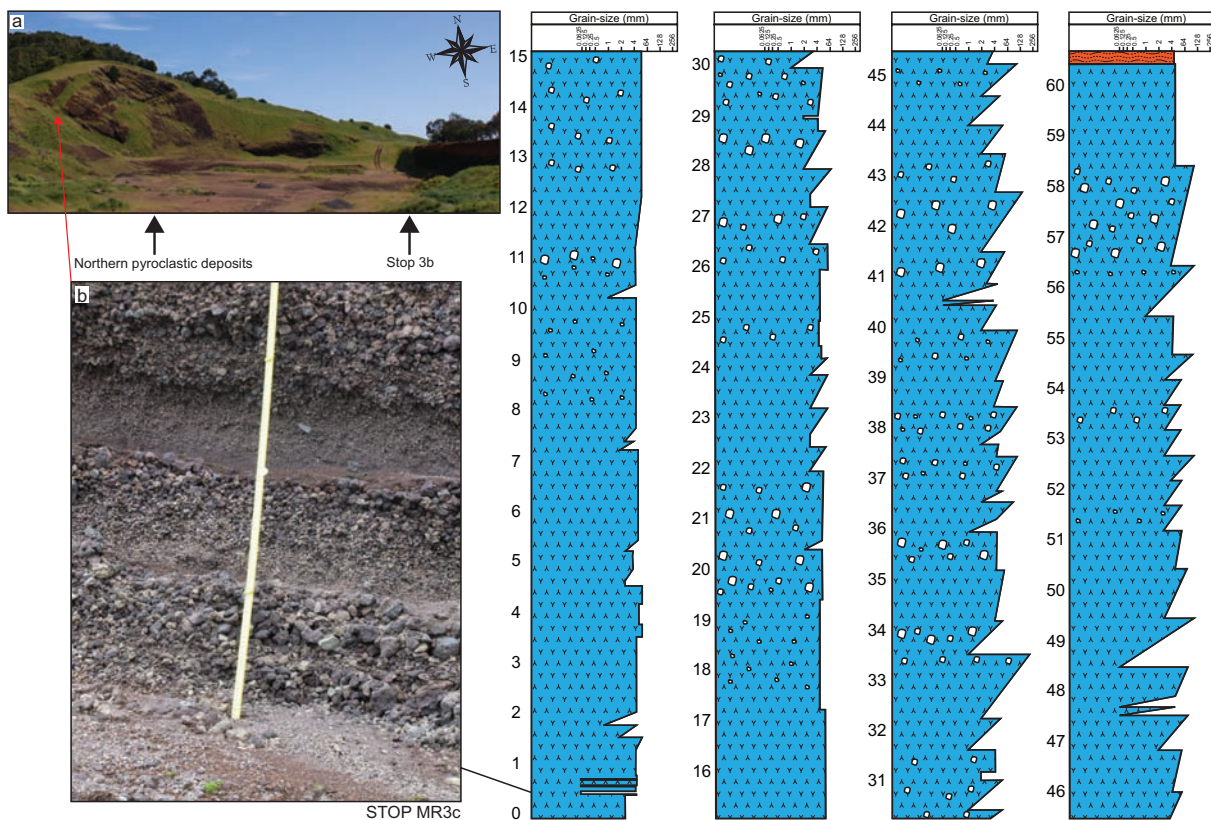


Fig. MR5 Stratigraphic log of the northwestern deposits of the Old Railway Quarry, showing (a) location map, with stop 3b on the right, and dipping beds of the northwestern deposits to the left, (b) reversely graded tri-coloured scoria and ash.

are exceptionally well preserved, showing the sheen of original glassy surfaces. Agglutinated bombs and blocks are found up to 30 cm, and there are two bomb-rich horizons, with bombs up to 70 cm in size. Two surge deposits can be seen within the black scoria – the first is 0.25 m thick, in a small exposure just beneath and to the left of the main fall. The second is 10 cm thick, approximately 0.5 m from the exposed base. Both are composed of black ash-lapilli sized scoria, showing pinch-and-swell structures, but do not correlate with the Pele's tears and hairs surge.

Scientific question for discussion:

- Do these surge deposits represent wet or dry eruptions?

STOP MR3c –far northwest of Old Railway Quarry

Directly behind stop 3b can be seen a series of pyroclastic deposits with centimetre

to metre-scale planar bedding (Fig. MR5). The base of the exposure can be reached by climbing a small scree-slope to a track just beneath it.

The base is unexposed, but the log begins with deposits consisting of several small beds of tri-coloured scoria and ash, reversely graded. Above this, deposits contain bedded oxidised lapilli in the 5-20 mm range; with spatter bombs and blocks up to 50 cm. The basal layers of this deposit are hard to correlate with the eastern wall (Fig. MR4), as they contain a very distinctive, well consolidated oxidised scoria above tri-coloured deposits, whereas the 'corresponding' scoria in the eastern face contains friable black scoria above surge deposits which are not seen in northern deposits. The eastern face constitutes the opening phases of eruption of the southern cone, while the northern face represents later phases of the same eruption, as the dip of the beds suggests that they originate from the southern crater.

Scientific questions for discussion:

- *Does the colouration in these deposits reflect oxidation?*
- *Does reverse grading in the tri-colour deposits represent fluctuating eruption column heights, or is it due to down-slope movement of clasts? Many of the deposits of Mt. Rouse are reverse graded.*



Feature



Victoria erupts: the Newer Volcanics Province of south-eastern Australia

The Newer Volcanics Province of south-eastern Australia is often overlooked, though it comprises a multitude of volcanic features worthy of exploration. The province contains > 416 eruption centres varying in nature from simple to complex, ranging from lava shields and scoria cones to some of the largest maar volcanoes in the world. Explorable caves and lava tubes showcase well-preserved lava flow features, while the province is a fossickers dream, containing abundant mantle xenolith and megacryst collecting localities. As the most recent eruption was ~5000 BP at Mt. Gambier, the Newer Volcanics is considered an active province, and may yet provide Australia with more eruptions, adding to the glorious volcanic features of the wonderful landscape.

When thinking of Australia, people generally conjure up an image of a vast, sweeping landscape full of skipping kangaroos, sleepy koalas and iconic, relaxed, Crocodile Dundee-type, Akubra-wearing, locals. Volcanoes are not usually the first things to come to mind. You may in fact be surprised to learn that Australia has had a long history of volcanism throughout the Cenozoic, and The Newer Volcanics Province (NVP) of south-eastern Australia forms the youngest expression of volcanism in the country. Stretching 410 km from Melbourne in Victoria to the Mt. Burr range in South Australia, the NVP contains > 704 eruption points associated with > 416 volcanic centres (Fig. 1), featuring the most diverse array of volcanic features in south-eastern Australia, of both national and international significance.

Geological Setting

The NVP covers > 19 000 km² in Victoria and South Australia, and was formed from 4.5 Ma to ~5000 BP. Local Aboriginal people witnessed some of the eruptions, naming them *Willum-a-weenth* (place of fire). The NVP is the youngest of three groups of Cenozoic igneous provinces in Victoria, which also includes the Macedon–Trentham group (7.0–4.6 Ma) and the Older Volcanics (95–19 Ma). Conventionally defined

as an intraplate monogenetic volcanic field, the NVP contains products of a wide range of eruption types, such as scoria cones, lava shields, maars and composite centres. Volcanism has been considered as simple and short-lived, with single magma batches erupting within a short time frame to produce small and simple volcanic edifices (monogenetic). However, recent detailed research into individual eruption centres is challenging that assumption; for example Mt Gambier and Red Rock have been shown to be the products of two magma batches, and Mt Rouse the product of three. Additionally, Lake Purrumbete shows evidence of a volcanic hiatus during its eruption, and The Bluff and Mt. McIntyre have interbedded palaeosols between their deposits, indicating polygenetic behaviour. The location of volcanoes mentioned in the text may be found in Fig. 1.

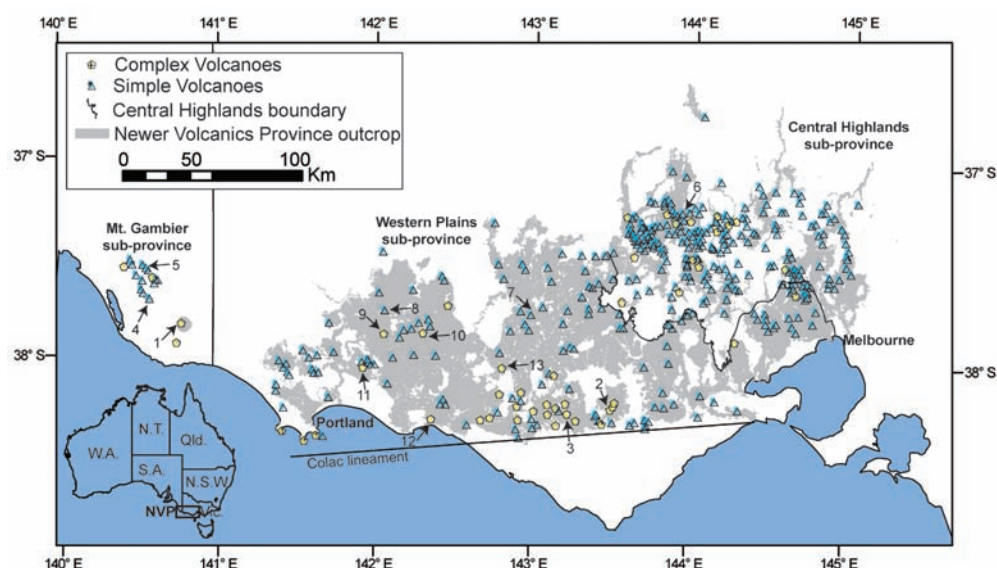
The NVP is subdivided from east to west into the Central Highlands, Western Plains and Mt. Gambier sub-provinces. The Central Highlands cover the dissected uplands of Palaeozoic metasediments and granites north-west of Melbourne, the Western Plains fill the pre-existing subdued topography of the Otway Basin, and the Mt. Gambier sub-province lies over the Gambier Embayment sediments, meta-sediments of the Delamerian Orogeny and the Otway Basin sediments. The southern edge of the NVP is marked by

**J. Boyce, I. Nicholls,
R. Keays & P.
Hayman**

School of Geosciences,
Building 28, Monash
University, Melbourne,
Australia



Fig. 1. The Newer Volcanics Province of south-eastern Australia, showing complex and simple volcanoes and lava flow field (grey area). Volcanoes referred to in text: 1, Mt. Gambier; 2, Red Rock; 3, Lake Purrumbete; 4, The Bluff; 5, Mt. McIntyre; 6, Powlett Hill; 7, Mt. Hamilton; 8, Mt. Pierrepont; 9, Mt. Napier; 10, Mt. Rouse; 11, Mt. Eccles; 12, Tower Hill; 13, Mt. Shadwell.



the Colac Lineament, and is controlled by faulting.

The origin of the volcanic activity is widely debated. Continental extension leading ultimately to the breakup of Australia and Antarctica, followed by post-rift diapirism has been cited as one possible cause. Hot spots and mantle plumes (both stationary and diverging) have also been suggested, with reference to the hot spot track of volcanic centres associated with the Great Dividing Range in eastern Australia, the focus of which is now beneath Bass Strait. More recent explanations include edge-driven convection, whereby thermal contrasts associated with steps in lithospheric thickness generate secondary convection cells and asthenospheric upwelling downstream. In this way the lateral and vertical flow of warm Pacific mantle is believed to have created a diffuse alkaline magmatic province of low-volume but long-lived magmatism.

Eruption centres of the NVP

Eruption centres of the NVP can be defined as either simple or complex, and one eruption centre can have multiple eruption points of different character. Simple volcanoes feature few known eruption points and have simple morphologies. They have been classified as small scoria cones, lava shields, maars and ash cones/domes. Complex volcanoes, on the other hand, form larger edifices with multiple overlapping erup-

tion points of differing character. These take the form of magmatic cones or shields, and maar or maar-cone volcanic complexes. The NVP therefore preserves a wide variety of well-preserved volcanic landforms. The Central Highlands and Western Plains contain approximately equal numbers of volcanic centres, at 54 percent and 42 percent respectively. However, the Central Highlands covers a much smaller area of > 4277 km², 71 percent smaller than the Western Plains, which covers 14 600 km². The Mt Gambier sub-province contains only 6 percent of eruption centres, with eruption products covering approximately 217 km², estimated from drill hole data, as Late Pleistocene sands overlie much of the volcanics.

Most of the maar-forming eruptions are concentrated in the south, in the Warrnambool-Colac region, where they are associated with the aquifers of the underlying Cenozoic Otway Basin sediments and Mesozoic structures. In contrast, the Central Highlands is situated on Palaeozoic basement.

Simple eruption centres

Scoria cones form by the near-vent accumulation of pyroclastic material, such as lapilli, bombs and minor ash that was fragmented by the violent release of volcanic gases. Scoria cones of the NVP range in size from < 50 m high to > 215 m, and many are also associated with late-stage lava flows produced from degassed magma. Powlett Hill in the Central High-

Fig. 2. Powlett Hill scoria cone, Ullina.

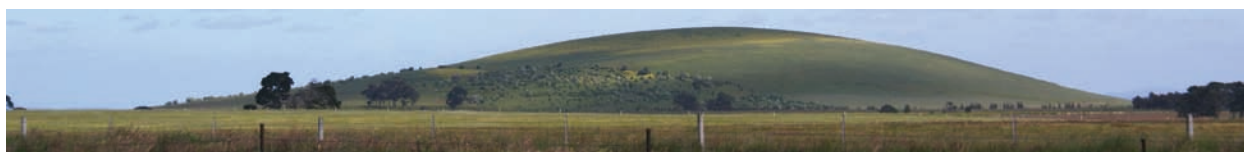




Fig. 3. Mt. Pierrepont lava shield, Hamilton.

lands (Fig. 2) is a 120 m high scoria cone nestled in amongst several other cones, which together make up the 'Birch Creek Volcanic Complex', the region with the highest concentration of scoria cones in the Newer Volcanics Province.

Lava shields in the NVP range from large edifices > 100 m high to extremely low profile shields that are easily mistaken for parts of lava flows themselves. Many of the shields feature lava caves and tubes; for example Mt. Hamilton features 1200 m of branching lava passages. Mt. Pierrepont (Fig. 3) is a good example of a lava shield, featuring at least two individual flows, rising approximately 60 m above the surrounding lava plains, and is more than 2 km across, with an ill-defined crater ~30 m across at the peak. The centre is among the oldest volcanoes of the NVP at 3.9 Ma.

Maars are the products of phreatomagmatic eruptions, and form due to the interaction between rising magma and ground/surface waters, resulting in a bowl-shaped crater with a low rim of fine-grained ejecta, rich in country rock fragments. Many NVP maars occur as part of complex eruptions, resulting in the formation of multiple coalescing maar craters, or in combination with magmatic eruptions to form magmatic volcanic complexes.

Ash cones and domes are also phreatomagmatic in nature, but feature steeper dipping beds of ejecta and craters lying above the ground surface, more similar to scoria cones in terms of morphology. These eruption centres are so far found exclusively in the Mt. Gambier sub-province as part of the Mount Burr Volcanic Group—14 volcanic centres of various types concentrated along a basement high and related to three northwest trending lineaments.

In addition, more than thirty eruption centres are of an unknown character. These are centres that need to be ground truthed in order to assign eruption characteristics. Many data on the NVP remain un-

published in reports and manuscripts of scientists and students, which may reveal further eruption points and clarify the nature of these unknown centres.

Complex eruption centres

Magmatic volcanic complexes feature multiple eruption points of varying magmatic character, such as scoria and/or spatter cones and lava shields. They are found scattered across the NVP in such centres as Mt. Napier, which features lava flow tumuli and the most extensive accessible lava caves in Australia; and Mt. Rouse, the largest eruption source. Mt. Eccles (Budj-Bim) is a magnificent 2 km long fissure vent system dated to ~30 ka. It is composed of three coalesced craters forming Lake Surprise (Fig. 4), and multiple scoria and spatter cones aligned NW–SE. Lava flowed south-west from the complex for ~65 km, now covered by the sea for the last 16 km. They preserve lava canals, caves and flow features of international and national significance. For example, The Shaft is a 10 m high cone of welded spatter with a 23 m deep vent that widens at depth and can be explored via abseiling.

Maar volcanic complexes feature multiple phreatomagmatic eruption points with insignificant magmatic influences. Lake Purrumbete is one of the largest maar volcanoes in both the NVP and worldwide, with a 3 km diameter vent formed by multiple phreatomagmatic eruptions and a small-volume pyroclastic flow event. The centre contains excellent exposures showing the intricate nature of the base surges (Fig. 5). There are very few volcanoes of this type in the NVP. As with simple maars, most occur in combination with magmatic eruption products.

Many spectacular maar-cone complexes are found in the NVP, which are a combination of magmatic and phreatomagmatic eruption products in the form of maars, scoria cones and/or lava flows and spatter cones. The NVP is host to centres such as Tower Hill, another of the world's largest maar volcanoes, 3.2 km in diameter featuring a nested scoria and spatter cone complex with small-volume lava flows, and spectacular exposures (Fig. 6). The complex is also a national park, where you can picnic with the koalas and emus while taking in the landscape. The Red Rock Volcanic Complex features 40 eruption points composed of multiple maars, scoria cones and lava flows; Mt. Gambier and Mt. Schank are the young-

Fig. 4. Lake Surprise, Mt. Eccles magmatic volcanic complex, Macarthur.





Fig. 5. Lake Purrumbete, Camperdown.

est volcanoes in the NVP. Mt. Gambier is dated to ~5000 BP and is an extremely complex centre featuring two magma batches erupting simultaneously to produce > 14 eruption points of maars, scoria and spatter cones, tuff cones, lavas and pyroclastic flows.

Fossickers paradise

Mantle xenoliths, or 'olivine bombs' are a common occurrence in the NVP, and are found at many of the eruption centres, in lavas, cones and phreatomagmatic ash deposits. Olivine bombs consist of peridotite xenoliths that are encased in basalt (Fig. 7). Xenoliths form when rising magma entrains parts of the upper mantle, erupting it onto the surface. The presence of xenoliths attest to the fast ascent rates of the magmas, which may be as high as tens of metres per second in order to keep the denser xenoliths entrained in the buoyant magma. Mortlake (western Victoria) is designated Australia's 'olivine capital', as Mt. Shadwell contains the largest deposits of the peridotite xenoliths in Australia, which often contain gemstone quality olivine (peridot). The xenoliths provide important clues as to the nature of the mantle beneath the NVP and have been used in the construction of a geothermal gradient for south-eastern Australia.

Megacrysts are also a relatively common occurrence in the NVP. These are coarse single crystals of high-pressure origin, formed at 1–2.5 GPa depth (35–80 km). The crystals are > 5 mm in size, with pyroxenes being the most abundant, but also common alkali feldspar (anorthoclase) and rarer hornblende, ilmenite, apatite, zircon, garnet and corundum. Along with olivine, some of these megacrysts may originate from disaggregated mantle xenoliths.

Pele's hairs and tears (achneliths) are found at Mt. Rouse, the largest eruption source in the NVP. Dated to 0.35 Ma, the volcano features an unusual surge deposit containing the products of two separate magma batches. Small scoria clasts represent one magma batch, while abundant Pele's tears and broken hairs form a second batch. Amazingly, most of the tears remain intact, even though they were entrained in the turbulent flow. They range in size from < 1 mm to just over 1 cm, and have a wide range of morphologies from almost perfectly spherical to elongate and bulbous, many with the classic teardrop shape (Fig. 8). The tears form in high temperature, low viscosity fire fountaining eruptions, and are molten basaltic glass droplets, shaped and quenched during flight. Hairs are spun out from the tears and carried in the wind. Many of the tears in this deposit still have the basal part of the hair attached. Fragments of Pele's hair have also been discovered in Lake Purrumbete ash deposits.

Active province

The NVP is considered an active province, with the occurrence of mantle-derived CO₂ at locations such as Mt. Gambier and a heat anomaly within the mantle beneath the Central Highlands sub-province. Researchers agree that further eruptions are possible, and the average eruption frequency has been



Fig. 6. Tower Hill crater rim sequence.



Fig. 7. Mantle xenolith trapped in lava from Mt. Leura, Camperdown.



Fig. 8. Pele's tears (achneliths) from Mt. Rouse, Penshurst.

estimated at between 1:10 800 and 1:12 500 years. However, this may prove inaccurate as more detailed ages emerge for individual eruption centres. A new volcano would be produced with very little warning, with only minor seismic activity. If mantle xenolith predictions are correct, and the magmas can travel tens of metres per second, a magma originating at a depth of 80 km could reach the surface in as little as two hours. The hazards produced would depend on the location of the volcanism with respect to the underlying aquifers and hence the occurrence of magmatic or phreatomagmatic eruptions. Hazards would range from small or large-scale lava flows, scoria cone formation, or the eruption of a maar volcano with resultant ash plumes and base surges. A risk and hazard map was produced for the NVP, using mapped eruption types and ages. As the NVP lies in populated areas, an eruption close to Melbourne, for example, would damage property and infrastructure, disrupt travel, particularly aviation in the event of an ash plume, and may even result in the loss of life. With no

emergency planning or public education in place in Victoria, a resultant event could be more catastrophic with the general population unaware of the dangers associated with volcanic activity. Will the Newer Volcanics Province erupt again? Watch this space.

Suggestions for further reading

- Douglas, J.G. & Ferguson, J.A. 2003 *Geology of Victoria*. Geological Society of Victoria, Victorian Division, Melbourne, Australia.
- Jordan, S.C., Cas, R.A.F. & Hayman, P.C. 2013. The origin of a large (> 3 km) maar volcano by coalescence of multiple shallow craters: Lake Purrumbete maar, southeastern Australia. *Journal of Volcanology and Geothermal Research*, v.254, pp.5–22.
- Johnson, R.W. 1989. *Intraplate Volcanism in Eastern Australia and New Zealand*. Cambridge University Press, Cambridge, UK.
- Joyce, E.B. 1975. Quaternary Volcanism and Tectonics in Southeastern Australia. In: Suggate, R.P. & Cresswell, M.M. (eds). *Quaternary Studies*. The Royal Society of New Zealand, Wellington, New Zealand, pp.169–178.
- Joyce, E.B. 2003. The young volcanic province of southeastern Australia: physical volcanology and eruption risk. In: Graham, I. (ed). *Geological Society of Australia Abstracts 71, Insights into Volcanic Processes, Mantle Sampling and Gems*. SGGMP, Central Victoria, 30 September–4 October 2003, pp.20–26.
- Joyce, E.B. 2004. The young volcanic regions of southeastern Australia: early studies, physical volcanology and eruption risk. *Proceedings of the Royal Society of Victoria*, v.116, pp.1–13.
- Matchan, E. & Phillips, D. 2011. New $^{40}\text{Ar}/^{39}\text{Ar}$ ages for selected young (<1 Ma) basalt flows of the Newer Volcanic Province, southeastern Australia. *Quaternary Geochronology*, v.6, pp.356–368.
- Rosengren, N. 1994. *Eruption Points of the Newer Volcanics Province of Victoria—an Inventory and Evaluation of Scientific Significance*. National Trust of Australia (Victoria) and the Geological Society of Australia (Victoria Division), Melbourne, Australia.
- van Otterloo, J. 2012. *Complexity in monogenetic volcanic systems: factors influencing alternating magmatic and phreatomagmatic eruption styles at the 5 ka Mt. Gambier volcanic complex, South Australia*. Unpublished PhD thesis, Monash University, Melbourne, Australia.

Is there a volcano in your garden? Eruption locations of the Newer Volcanics Province

Julie Boyce

This web page can be found at www.penshurstvolcano.org.au and accompanies the article 'The Newer Volcanics Province of southeastern Australia: a new classification scheme and distribution map for eruption centres' published in the Australian Journal of Earth Sciences 60:4, 449-462.

See attached CD for Database of eruption points.

Did you know there were volcanoes in Victoria? The state is actually home to the Newer Volcanics Province (NVP), a volcanic field stretching 410 km from Melbourne to the Mt. Burr range in South Australia, covering >19 000 km² and containing >704 eruption points from >416 volcanic centres (Figure 1). The province contains a wide variety of eruption centres, which are both simple and complex in nature, ranging from lava shields and scoria cones to some of the largest maar volcanoes in the world. Explorable caves and lava tubes showcase well-preserved lava flow features, while the province is a fossickers dream, containing abundant mantle xenolith and megacryst collecting localities.

The NVP is the most recent phase of volcanic activity in Australia with an age range of 4.5 million years to ~5000 B. P. at Mt. Gambier, and is still considered active! Local Aboriginal people witnessed some of the eruptions, naming them 'Willum-a-weenth' (place of fire).

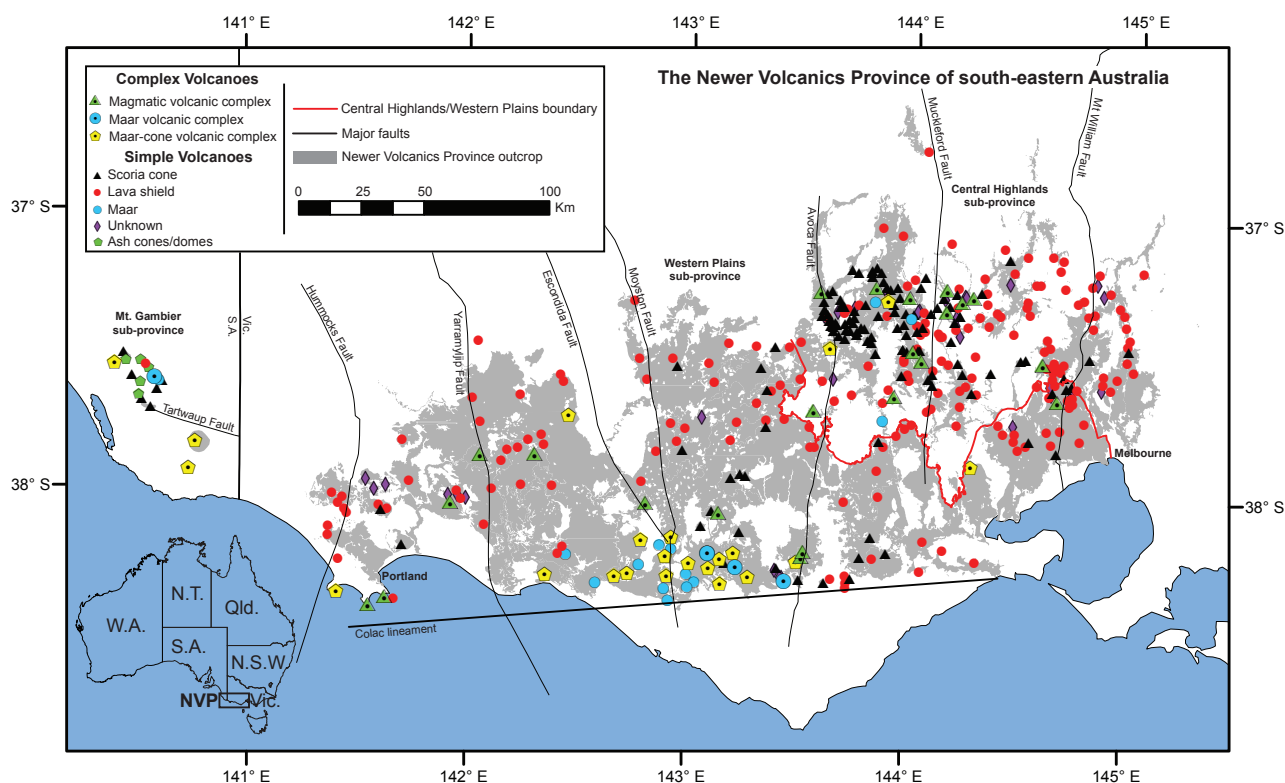


Figure 1 Distribution of volcanic centres in the Newer Volcanics Province (Boyce 2013)

Appendix 1

The NVP is sub-divided into the Central Highlands, Western Plains and Mt. Gambier subprovinces based on differences in geomorphology.

- The Central Highlands subprovince can be found northwest of Melbourne, containing 54% of NVP volcanic centres.
- The Western Plains subprovince extends 320 km from Melbourne to Portland, and contains 42% of NVP volcanic centres.
- The Mt. Gambier subprovince is 60 km west of the Western Plains, containing only 4% of eruption centres.

Volcanic centres in the NVP can be split into two groups — simple or complex and then further categorised.

Simple volcanoes

Simple volcanoes feature few eruption points, dominantly of one form, with simple morphologies (shapes).



Figure 2 Examples of simple volcanoes of the NVP. a) Mt. Elephant scoria cone, b) Picaninny Hill lava shield, c) Lake Keilambete maar. Photos by Julie Boyce and Teagan Blakie.

Scoria cones form by the accumulation of pyroclasts rich in vesicles (holes made by exsolved gases).

They can also be associated with outpourings of lava, for example Mt. Elephant, Derrinallum.

Lava shields form from the gradual build-up of fluidal lava flows, which can flow many kilometres.

A good example of a lava shield in the NVP is Picaninny Hill, near Penshurst.

Maars form from when magma rising to the surface encounters groundwater. The result is a bowl-

shaped crater with a low rim of fine grained ejecta. Lake Keilambete, between Noorat and Terang is a good example of a simple maar.

Complex volcanoes

Complex volcanoes feature multiple eruption points and complex morphologies (shapes).



Figure 3 Examples of complex volcanoes of the NVP. d) Mt. Rouse, e) Lake Purrumbete, showing Mt. Porndon in the distance, f) Mt. Gambier's Valley Lake. Photos by Julie Boyce and Jozua van Otterloo.

1. Magmatic volcanic complexes feature a combination of lava shields, scoria cones and spatter cones. An example is Mt. Rouse, Penshurst, which features eight eruption points of lava and scoria, with lava flows stretching 60 km to the coast at Port Fairy.
2. Maar volcanic complexes feature multiple eruption points of phreatomagmatic eruption products (e.g. multi large 3 km diameter maar was formed by the coalescence of at least three shallow craters during ple coalesced maars). Lake Purrumbete, Colac is such a volcanic centre. This violent eruptions when water interacted with the magma to create explosions of volcanic ash and gas.
3. Maar–cone volcanic complexes feature a combination of magmatic and phreatomagmatic eruption

4. products, as the magma interacts with water, such as maars, scoria cones and lava flows, like Mt. Gambier. This volcanic centre has more than 14 eruption points of maars, scoria and spatter cones, tuff cones, lavas and pyroclastic flows.

The NVP is considered an active province, with the occurrence of mantle-derived carbon dioxide at locations such as Mt. Gambier. Researchers agree that further eruptions are possible, and eruption frequency has been estimated at between 1:10 800 and 1:12 500 years. A new volcano would be produced with very little warning, perhaps a few small earthquakes. If mantle xenolith predictions are correct, and the magmas can travel tens of metres per second, a magma originating at a depth of 80 km could reach the surface in as little as 2 hours. The hazards encountered would depend on the kind of eruption centre being formed. Hazards would range from small or large-scale lava flows, scoria cone formation, or the eruption of a maar volcano with resultant ash plumes. Don't worry; chances are high you would be able to escape an eruption. Will the Newer Volcanics Province erupt again? We don't have enough information to be able to predict an eruption, so the truth is we don't actually know!

Why not see if there is a volcano in your garden! A Google Earth kml file is available showing all eruption points for the Newer Volcanics Province, and central locations for complex eruptions. The file can be downloaded [here](#), and is best viewed with a vertical exaggeration of 3 as many of the lava shields have very low relief. This can be changed in preferences of Google Earth. Don't forget to drag the folder out of 'Temporary Places' and into 'My Places' to save.

This web page contains information from the following articles:

BOYCE J.A. 2013. The Newer Volcanics Province of south-eastern Australia: a new classification scheme and distribution map for eruption centres. *Australian Journal of Earth Sciences* **60**, 449–462.

BOYCE J., NICHOLLS I., KEAYS R. & HAYMAN P. 2013. Victoria erupts. The Newer Volcanics Province of south-eastern Australia. *Geology Today* **30**, 105–109.

JORDAN S. C., CAS R. A. F. & HAYMAN P. C. 2013. The origin of a large (>3 km) maar volcano by coalescence of multiple shallow craters: Lake Purrumbete maar, southeastern Australia. *Journal of Volcanology and Geothermal Research* **254**, 5–22.

VAN OTTERLOO J., CAS R. A. F. & SHEARD M. J. 2013. Eruption processes and deposit characteristics at the monogenetic Mt. Gambier Volcanic Complex, S. E. Australia: implications for alternating magmatic and phreatomagmatic activity. *Bulletin of Volcanology* **75**, 1–21.

A full database of eruption points, including shapefiles for ArcGIS, for scientific use, can be obtained from (<http://monash.academia.edu/JulieBoyce>).

For further information, please contact [REDACTED]

Mt. Rouse, Victoria: a whistle-stop tour

Julie Boyce

This tour is available for download at www.penshurstvolcano.org.au/mt-rouse

Penshurst, Victoria. Home to Mt. Rouse, the largest eruption point in the Newer Volcanics Province and, of course, the most exciting volcano in the Western Plains subprovince! Triple the volume of other eruption centres, Mt. Rouse is a volcanic complex of lava and scoria featuring at least six eruption points, ‘towering’ 120 m above the township (Fig.1).

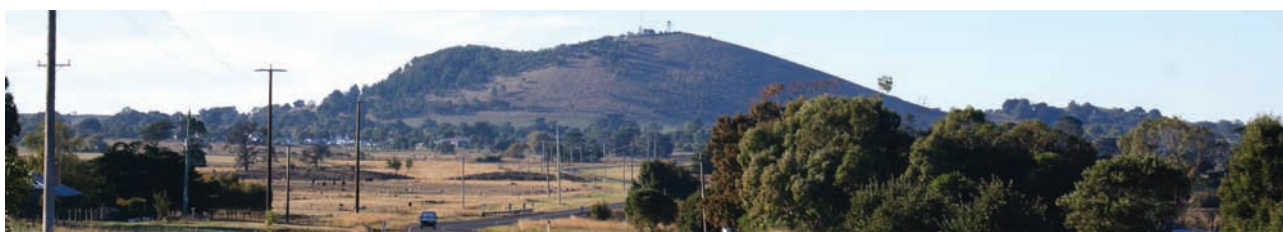


Figure 1 Mt. Rouse, showing northern double scoria cone in the background and the northern satellite cone hiding the southern crater far right. Taken from the Hamilton Highway.

Your journey begins by taking the sinuous Mt. Rouse tourist road to its end, from the lava apron through the southern cone and climbing the steps to the top of the northern cone. From here, you will see an overview of the complex, the main cone composed of two overlapping craters running E–W and breached to the west (Fig. 2). An early eruption centre is hidden from view to the northeast, while the southern crater is visible to the south with its two small satellite cones. On a clear day, you will have a spectacular view of the Grampians mountain range to the north and the Mt. Napier lava shield to the west. While admiring the view, check out the spatter rampart of extensively weathered welded scoria fragments, and the small fresh boulders with columnar jointing.



Figure 2 Eruption points of Mt. Rouse. Note that quarries are inaccessible. Google Earth.



Figure 3 The small western satellite cone with the large northern scoria cone in the background.

Make your way back along the tourist road, and down into the southern crater. You will be able to see two satellite cones looking west and southwest. The western cone (Fig. 3) is slightly higher than that to the SW, and has a small 15 m wide crater filled with spatter bombs and fine-grained basalt blocks. A small wall of basalt rims the crater to the west.

Appendix 1

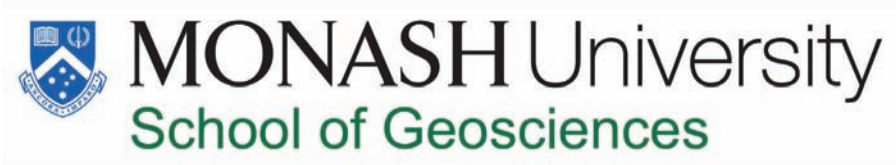
Carry on along the tourist road, and make your way down into the southern crater, which features undulating sides, dropping into a permanent lake and featuring coarse-grained basalt blocks with columnar jointing (Fig. 4). Columnar jointing forms by the rapid cooling of the basalt from the outside to the centre, causing hexagonal joints to form. While at Mt. Rouse, see if you can spot the elite unit of camouflaged kangaroo spies (Fig. 5) guarding the volcanic complex!



Figure 4 Columnar jointed basalt, southern crater



Figure 5 Kangaroo spies!!







Appendix 2

NVP project data for Chapter 2

Please see enclosed CD-ROM for full suite of data.

- Spreadsheet catalogue of geospatial data for NVP volcanoes
- KML file for Google Earth and geospatial software
- Layer files for ArcGIS
- Explanatory notes to accompany catalogue and layer files (in print and on enclosed CD-ROM)

Notes to accompany NVP spreadsheet

These notes are intended to accompany the spreadsheet of eruption points for the Newer Volcanics Province, Australia.

kmz files are available, which can be opened with Google Earth, and are best viewed using a vertical exaggeration of 2–3 (this can be changed in preferences). Shapefiles for ArcGIS are also available, as well as a google map and an Illustrator file (pdf) of the volcanic distribution map. Please direct enquiries to [REDACTED]

Please cite the following article, which this database accompanies:

BOYCE J. 2013. The Newer Volcanics Province of southeastern Australia: a new classification scheme and distribution map for eruption centres. *Australian Journal of Earth Sciences* **60**, 449–462.

<http://www.tandfonline.com/doi/full/10.1080/08120099.2013.806954#.VNQ1IXayUZ0>

The companion paper to Boyce (2013), which focuses on the Hamilton area of the Western Plains subprovince can be found at:

BOYCE J. A., KEAYS R. R., NICHOLLS I. A. & HAYMAN P. C. 2014. Eruption centres of the Hamilton area of the Newer Volcanics Province, Victoria, Australia: pinpointing volcanoes from a multifaceted approach to landform mapping. *Australian Journal of Earth Sciences* **61**, 735–754.

<http://www.tandfonline.com/doi/full/10.1080/08120099.2014.923508#.VNQ1I3ayUZ0>

The most recent NVP map to accompany the database, which includes an additional 23 volcanoes to the 2013 paper, can be found at:

BOYCE J. A., NICHOLLS I., KEAYS R. & HAYMAN P. 2015. Variation in parental magmas of Mt Rouse, a complex polymagmatic monogenetic volcano in the basaltic intraplate Newer Volcanics Province, southeast Australia. *Contributions to Mineralogy and Petrology* **169**:11. DOI 10.1007/s00410-015-1106-y

<http://link.springer.com/article/10.1007/s00410-015-1106-y>

A. Details for the contents of each column in the spreadsheets. All spreadsheets follow the same format.

VOLCANIC_CENTRE_NAME

This column contains the overall name for the eruption centre, and is most important for volcanic complexes, at which there is more than one vent.

SUB_PROVINCE

This states in which subprovince of the NVP the volcanic centre lies - the Central Highlands, Western Plains and Mt Gambier subprovinces. The Central Highlands lie northwest of

Melbourne, and cover the dissected uplands of Palaeozoic metasediments and granites (Nicholls & Joyce 1989; Price *et al.* 2003); the Western Plains cover the area from Melbourne west to Portland, where NVP products fill in the pre-existing subdued topography formed by the sediments of the Mesozoic Otway Basin; the Mt Gambier subprovince covers the volcanoes of South Australia, and lies over the Gambier and Otway Embayment sediments and Delamerian Orogeny sediments and metasediments.

VOLCANIC_CENTRE_DESCRIPTION_NEW

This column outlines to which volcano type the eruption centre as a whole belongs, and uses a new classification scheme for NVP volcanoes whereby they are described as either simple or complex, as outlined in Boyce (2013). Complex volcanoes contain multiple vents and have intricate morphologies. They may be described as magmatic volcanic complexes (which feature a combination of lava shields, scoria cones and spatter cones), maar volcanic complexes (which feature exclusively phreatomagmatic eruption products from the interaction between magma and water), and maar–cone volcanic complexes (which feature a combination of magmatic and phreatomagmatic eruption products). Simple volcanoes have very few vents and are morphologically simple—they include scoria cones, lava shields, maars and some centres of unknown character, which need to be ground truthed. Scoria cones can also be associated with substantial lava flows.

VOLCANIC_CENTRE_DESCRIPTION_OLD

This column shows the classification of the eruption centre according to the previously used system (e.g., Joyce 1975), i.e. volcanoes consisting mainly of lava, volcanoes consisting mainly of scoria, maars consisting mainly of phreatomagmatic products, nested/buried maars, products of complex eruptions (many vents of differing styles) or unknown.

LAT_CENTRE, LON_CENTRE

The central latitude and longitude of the eruption centre as a whole in decimal degrees.

ERUPTION_POINT_NAME

The individual vents are here assigned names. This is mostly used for volcanic complexes, which contain multiple vents, and takes the form of the name of the centre followed by a number in ascending order.

ERUPTION_POINT_DESCRIPTION_NEW

This column outlines the eruptive character of the individual vents, namely lava, scoria, maar, spatter cone, ash cone/dome or unknown.

ERUPTION_POINT_DESCRIPTION_OLD

This column outlines the eruptive character of the individual vents according to the previously used system (e.g., Joyce 1975), similar to the earlier volcanic centre descriptions.

ERUPTION_POINT_NUMBER

A number has been assigned to each vent in the archive.

LAT_POINT, LON_POINT

The latitude and longitude of the vent in decimal degrees.

FID_GeoVIC

The number ascribed to the vent (if any) by Geoscience Victoria.

GOOGLE_EARTH_INTERPRETATION

Interpretation of the Google Earth satellite imagery, if applicable.

VOLCANO_TYPE_ROSENGREN

The volcano type, taken from Rosengren (1994). These classifications were based on those used by Edwards (1938), Coulson (1954), Ollier & Joyce (1964), Ollier (1967a,b) and Singleton & Joyce (1970). They are based on the dominant eruption type and material and are divided into products of effusive eruptions (lava cones with craters, lava shields, lava discs and lava hills), pyroclastic eruptions (scoria cones with craters, scoria hills, maar–tuff rings and nested maar–tuff rings), and miscellaneous eruptions (composite lava and scoria eruptions, and other forms such as tuff mounds and mamelons).

taken from:

Rosengren, N. J., 1994. Eruption points of the Newer Volcanics Province of Victoria: an inventory and evaluation of scientific significance. National Trust of Australia and Geological Society of Australia, Victorian Division.

SIGNIFICANCE_RATING_ROSENGREN

The significance ratings were taken from Rosengren (1994), who evaluated the eruption centres on the basis of their importance as type material, value for teaching and research, quality of the eruption products and landforms (freshness and preservation), importance in establishing volcanic sequences, the uniqueness of the site, and the contribution of the site to geological and geomorphological understanding. Ratings are those of international and national significance, state, regional, local, unknown or unassigned.

ALT_NAME

Local name for the vent, or alternate names. This is important for centres such as Lake Burrumbete in the Central Highlands, where the water-filled maar crater is referred to as both Callender Bay and Lake Burrumbete, and the associated scoria cone to the northwest is called Mt Callender.

COMMENTS

Any additional comments, if applicable.

REFERENCE

Where the information for the eruption point was obtained.

*Details for the spreadsheet tabs***DELETED POINTS**

A list of all eruption points that were removed. Reasons outlined in spreadsheet.

MACEDON-TRENTHAM

Some of the eruption points in Rosengren (1994) were from the Smokers Creek volcanic subgroup. These are alkali rocks around Mt. Macedon, such as Hanging Rock, which lie along the boundary between the Older Volcanics and the Newer Volcanics, defined as the Macedon-Trentham group (7-6 Ma). As such they have been removed from the list of Newer Volcanics eruption points.

http://dbforms.ga.gov.au/pls/www/geodx.strat_units.sch_full?wher=stratno=69402

Notes to accompany NVP layer files

These notes are intended to accompany the spreadsheet of eruption points for the Newer Volcanics Province, Australia.

kmz files are available, which can be opened with Google Earth, and are best viewed using a vertical exaggeration of 2–3 (this can be changed in preferences). A google map is also available as well as an Illustrator file (pdf) of the volcanic distribution map.

These notes are intended to accompany the shapefiles for ArcGIS for the eruption points of the Newer Volcanics Province, which works alongside an additional spreadsheet of eruption points. An additional pdf file of explanatory notes accompanies the spreadsheet.

Please direct enquiries to 

Please cite the following article, which this database accompanies:

BOYCE J. 2013. The Newer Volcanics Province of southeastern Australia: a new classification scheme and distribution map for eruption centres. *Australian Journal of Earth Sciences* **60**, 449–462.

<http://www.tandfonline.com/doi/full/10.1080/08120099.2013.806954#.VNQ1IXayUZ0>

The companion paper to Boyce (2013), which focuses on the Hamilton area of the Western Plains subprovince can be found at:

BOYCE J. A., KEAYS R. R., NICHOLLS I. A. & HAYMAN P. C. 2014. Eruption centres of the Hamilton area of the Newer Volcanics Province, Victoria, Australia: pinpointing volcanoes from a multifaceted approach to landform mapping. *Australian Journal of Earth Sciences* **61**, 735–754.

<http://www.tandfonline.com/doi/full/10.1080/08120099.2014.923508#.VNQ1I3ayUZ0>

The most recent NVP map to accompany the database, which includes an additional 23 volcanoes to the 2013 paper, can be found at:

BOYCE J. A., NICHOLLS I., KEAYS R. & HAYMAN P. 2015. Variation in parental magmas of Mt Rouse, a complex polymagmatic monogenetic volcano in the basaltic intraplate Newer Volcanics Province, southeast Australia. *Contributions to Mineralogy and Petrology* **169**:11. DOI 10.1007/s00410-015-1106-y

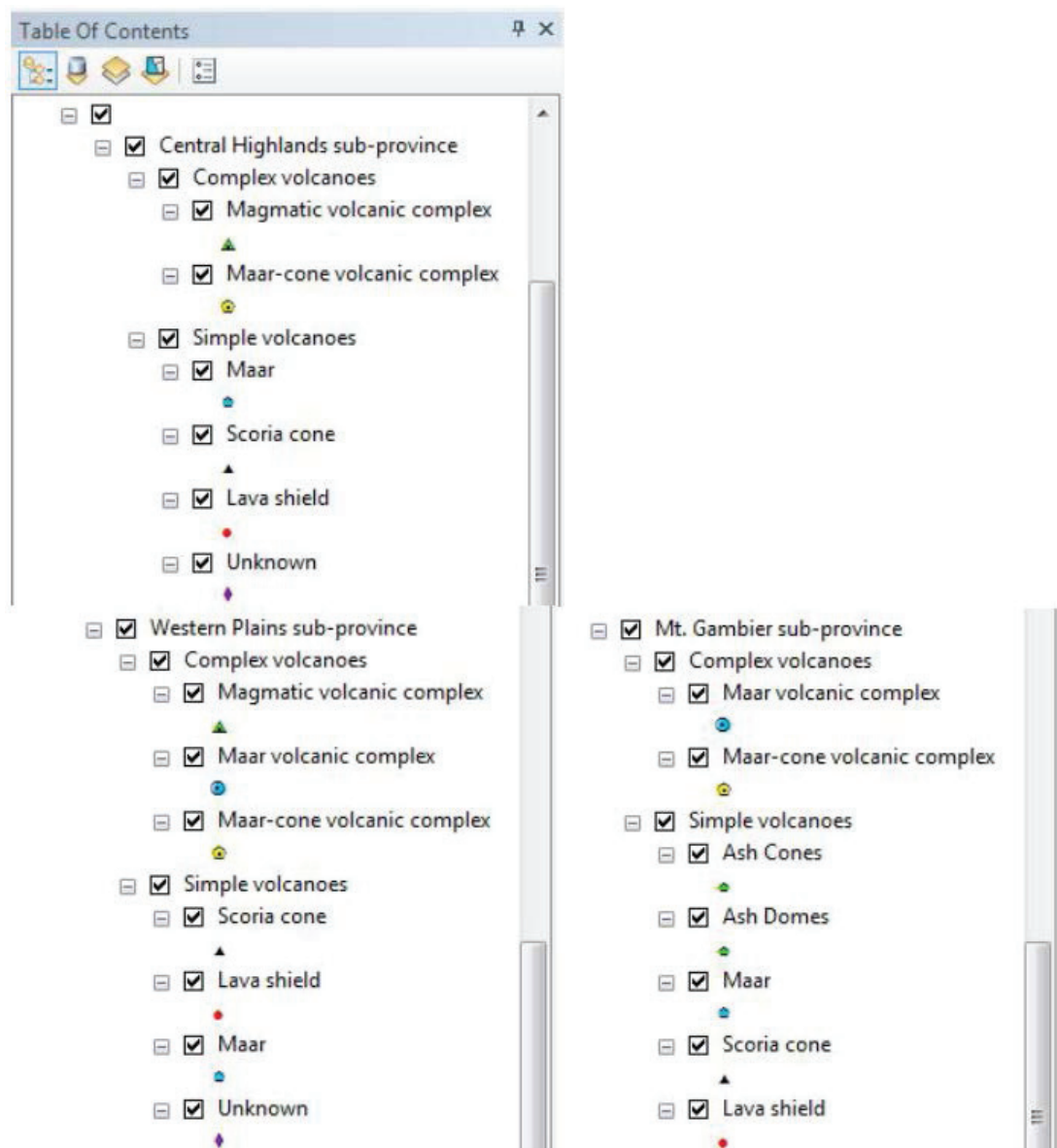
<http://link.springer.com/article/10.1007/s00410-015-1106-y>

Shapefiles have been supplied for all eruption points, the boundary between the Central Highlands and Western Plains subprovinces and the major structures across the NVP

Please place the excel file in the following folder groupings for the database in order for the shapefile to correctly display on ArcGIS:

D:\NVP\NVP eruption project\NVP project.xlsx

If this is not possible, volcanic centres for each sub-province can be added with the following definition queries using the 'Eruption points A-Z' tab of the spreadsheet, and the list of symbology used below:



Central Highland sub-province/Complex volcanoes/Magmatic volcanic complex
 `VOLCANIC_CENTRE_DESCRIPTION_NEW` = 'Magmatic_Volcanic_Complex'
 AND `ERUPTION_POINT_NUMBER` = 1 AND `SUB_PROVINCE` = 'CH'

Central Highland sub-province/Complex volcanoes/Maar-cone volcanic complex

`VOLCANIC_CENTRE_DESCRIPTION_NEW` = 'Maar_Cone_Volcanic_Complex'
AND `ERUPTION_POINT_NUMBER` = 1 AND `SUB_PROVINCE` = 'CH'

Central Highland sub-province/Simple volcanoes/Maar

`VOLCANIC_CENTRE_DESCRIPTION_NEW` = 'Maar' AND
`ERUPTION_POINT_NUMBER` = 1 AND `SUB_PROVINCE` = 'CH'

Central Highland sub-province/Simple volcanoes/Scoria cone

`VOLCANIC_CENTRE_DESCRIPTION_NEW` = 'Scoria_cone' AND
`ERUPTION_POINT_NUMBER` = 1 AND `SUB_PROVINCE` = 'CH'

Central Highland sub-province/Simple volcanoes/Lava shield

`VOLCANIC_CENTRE_DESCRIPTION_NEW` = 'Lava_shield' AND
`ERUPTION_POINT_NUMBER` = 1 AND `SUB_PROVINCE` = 'CH'

Central Highland sub-province/Simple volcanoes/Unknown

`VOLCANIC_CENTRE_DESCRIPTION_NEW` = 'Unknown' AND
`ERUPTION_POINT_NUMBER` = 1 AND `SUB_PROVINCE` = 'CH'

Western Plains sub-province/Complex volcanoes/Magmatic volcanic complex

`VOLCANIC_CENTRE_DESCRIPTION_NEW` = 'Magmatic_Volcanic_Complex' AND
`ERUPTION_POINT_NUMBER` = 1 AND `SUB_PROVINCE` = 'WP'

Western Plains sub-province/Complex volcanoes/Maar volcanic complex

`VOLCANIC_CENTRE_DESCRIPTION_NEW` = 'Maar_Volcanic_Complex' AND
`ERUPTION_POINT_NUMBER` = 1 AND `SUB_PROVINCE` = 'WP'

Western Plains sub-province/Complex volcanoes/Maar-cone volcanic complex

`VOLCANIC_CENTRE_DESCRIPTION_NEW` = 'Maar_Cone_Volcanic_Complex' AND
`ERUPTION_POINT_NUMBER` = 1 AND `SUB_PROVINCE` = 'WP'

Western Plains sub-province/Simple volcanoes/Scoria cone

`VOLCANIC_CENTRE_DESCRIPTION_NEW` = 'Scoria_cone' AND
`ERUPTION_POINT_NUMBER` = 1 AND `SUB_PROVINCE` = 'WP'

Western Plains sub-province/Simple volcanoes/Lava shield

`VOLCANIC_CENTRE_DESCRIPTION_NEW` = 'Lava_shield' AND
`ERUPTION_POINT_NUMBER` = 1 AND `SUB_PROVINCE` = 'WP'

Western Plains sub-province/Simple volcanoes/Maar

`VOLCANIC_CENTRE_DESCRIPTION_NEW` = 'Maar' AND
`ERUPTION_POINT_NUMBER` = 1 AND `SUB_PROVINCE` = 'WP'

Western Plains sub-province/Simple volcanoes/Unknown

`VOLCANIC_CENTRE_DESCRIPTION_NEW` = 'Unknown' AND
 `ERUPTION_POINT_NUMBER` = 1 AND `SUB_PROVINCE` = 'WP'

Mt. Gambier sub-province/Complex volcanoes/Maar volcanic complex

`VOLCANIC_CENTRE_DESCRIPTION_NEW` = 'Maar_Volcanic_Complex' AND
 `ERUPTION_POINT_NUMBER` = 1 AND `SUB_PROVINCE` = 'MG'

Mt. Gambier sub-province/Complex volcanoes/Maar-cone volcanic complex

`VOLCANIC_CENTRE_DESCRIPTION_NEW` = 'Maar_Cone_Volcanic_Complex' AND
 `SUB_PROVINCE` = 'MG' AND `ERUPTION_POINT_NUMBER` = 1

Mt. Gambier sub-province/Complex volcanoes/Ash Cones

`VOLCANIC_CENTRE_DESCRIPTION_NEW` = 'Ash_Cone' AND `SUB_PROVINCE` =
 'MG' AND `ERUPTION_POINT_NUMBER` = 1

Mt. Gambier sub-province/Complex volcanoes/Ash Domes

`VOLCANIC_CENTRE_DESCRIPTION_NEW` = 'Ash_Dome' AND `SUB_PROVINCE`
 = 'MG' AND `ERUPTION_POINT_NUMBER` = 1

Mt. Gambier sub-province/Simple volcanoes/Maar

`VOLCANIC_CENTRE_DESCRIPTION_NEW` = 'Maar' AND
 `ERUPTION_POINT_NUMBER` = 1 AND `SUB_PROVINCE` = 'MG'

Mt. Gambier sub-province/Simple volcanoes/Scoria cone

`VOLCANIC_CENTRE_DESCRIPTION_NEW` = 'Scoria_cone' AND
 `ERUPTION_POINT_NUMBER` = 1 AND `SUB_PROVINCE` = 'MG'

Mt. Gambier sub-province/Simple volcanoes/Lava shield

`VOLCANIC_CENTRE_DESCRIPTION_NEW` = 'Lava_shield' AND
 `ERUPTION_POINT_NUMBER` = 1 AND `SUB_PROVINCE` = 'MG'

ESRI symbols to use:

Magmatic volcanic complex = Triangle 3, size 9, Quetzal Green

Maar volcanic complex = Circle 3, size 8, Big Sky Blue

Maar-cone volcanic complex = Pentagon 3, size 8, Solar Yellow

Scoria cone = Triangle 1, size 7, Black

Lava shield = Circle 1, size 5, Mars Red

Maar = Circle 2, size 6, Big Sky Blue

Unknown = Diamond 2, size 8, Anemone Violet

Ash Cone = Pentagon 2, size 6, Quetzal Green

Ash Dome = Pentagon 2, size 6, Quetzal Green





Appendix 3

CIPW norms for Chapter 3

Please see enclosed CD-ROM for full spreadsheet of geochemical analyses.

| | Mt. | Blackwood | Moutajup | Mt. | Acacia | Green | Bunnugal | Piccaninny | Sheepwash |
|--------------------------------------|-------------------|------------------|-----------------|--------------------|---------------|--------------|-----------------|-------------------|------------------|
| | Baimbridge | Hill | Hill | Pierrepoint | Hill | Hill | Hill | Hill | Hill |
| Quartz | 0.00 | 0.00 | 2.69 | 0.00 | 0.00 | 0.00 | 0.00 | 0.00 | 0.00 |
| Plagioclase | 46.47 | 51.63 | 57.21 | 51.24 | 51.46 | 54.13 | 47.80 | 52.80 | 51.31 |
| Orthoclase | 7.68 | 7.09 | 4.67 | 5.61 | 7.68 | 4.20 | 7.62 | 8.16 | 8.51 |
| Nepheline | 1.58 | 0.00 | 0.00 | 0.00 | 0.00 | 0.00 | 0.14 | 0.00 | 0.28 |
| Leucite | 0.00 | 0.00 | 0.00 | 0.00 | 0.00 | 0.00 | 0.00 | 0.00 | 0.00 |
| Kalsilite | 0.00 | 0.00 | 0.00 | 0.00 | 0.00 | 0.00 | 0.00 | 0.00 | 0.00 |
| Corundum | 0.00 | 0.00 | 0.00 | 0.00 | 0.00 | 0.00 | 0.00 | 0.00 | 0.00 |
| Diopside | 18.11 | 16.31 | 11.07 | 14.55 | 16.30 | 13.37 | 18.26 | 14.63 | 13.24 |
| Hypersthene | 0.00 | 10.73 | 18.43 | 15.82 | 1.76 | 15.62 | 0.00 | 6.44 | 0.00 |
| Wollastonite | 0.00 | 0.00 | 0.00 | 0.00 | 0.00 | 0.00 | 0.00 | 0.00 | 0.00 |
| Olivine | 18.46 | 6.66 | 0.00 | 5.95 | 15.48 | 5.56 | 19.00 | 9.96 | 18.93 |
| Larnite | 0.00 | 0.00 | 0.00 | 0.00 | 0.00 | 0.00 | 0.00 | 0.00 | 0.00 |
| Acmite | 0.00 | 0.00 | 0.00 | 0.00 | 0.00 | 0.00 | 0.00 | 0.00 | 0.00 |
| K₂SiO₃ | 0.00 | 0.00 | 0.00 | 0.00 | 0.00 | 0.00 | 0.00 | 0.00 | 0.00 |
| Na₂SiO₃ | 0.00 | 0.00 | 0.00 | 0.00 | 0.00 | 0.00 | 0.00 | 0.00 | 0.00 |
| Rutile | 0.00 | 0.00 | 0.00 | 0.00 | 0.00 | 0.00 | 0.00 | 0.00 | 0.00 |
| Ilmenite | 4.03 | 3.87 | 3.08 | 3.48 | 3.76 | 3.63 | 3.63 | 4.22 | 3.93 |
| Magnetite | 2.71 | 2.81 | 2.17 | 2.51 | 2.61 | 2.73 | 2.55 | 2.81 | 2.74 |
| Hematite | 0.00 | 0.00 | 0.00 | 0.00 | 0.00 | 0.00 | 0.00 | 0.00 | 0.00 |
| Apatite | 1.02 | 0.93 | 0.70 | 0.86 | 1.00 | 0.81 | 1.04 | 1.09 | 1.11 |
| Zircon | 0.03 | 0.03 | 0.03 | 0.03 | 0.03 | 0.03 | 0.03 | 0.03 | 0.04 |
| Perovskite | 0.00 | 0.00 | 0.00 | 0.00 | 0.00 | 0.00 | 0.00 | 0.00 | 0.00 |
| Chromite | 0.06 | 0.07 | 0.04 | 0.07 | 0.06 | 0.06 | 0.07 | 0.06 | 0.06 |
| Sphene | 0.00 | 0.00 | 0.00 | 0.00 | 0.00 | 0.00 | 0.00 | 0.00 | 0.00 |
| Pyrite | 0.00 | 0.00 | 0.00 | 0.00 | 0.00 | 0.00 | 0.00 | 0.00 | 0.00 |
| Halite | 0.00 | 0.00 | 0.00 | 0.00 | 0.00 | 0.00 | 0.00 | 0.00 | 0.00 |
| Fluorite | 0.00 | 0.00 | 0.00 | 0.00 | 0.00 | 0.00 | 0.00 | 0.00 | 0.00 |
| Anhydrite | 0.00 | 0.00 | 0.00 | 0.00 | 0.00 | 0.00 | 0.00 | 0.00 | 0.00 |
| Na₂SO₄ | 0.00 | 0.00 | 0.00 | 0.00 | 0.00 | 0.00 | 0.00 | 0.00 | 0.00 |
| Calcite | 0.00 | 0.00 | 0.00 | 0.00 | 0.00 | 0.00 | 0.00 | 0.00 | 0.00 |
| Na₂CO₃ | 0.00 | 0.00 | 0.00 | 0.00 | 0.00 | 0.00 | 0.00 | 0.00 | 0.00 |
| Total | 100.15 | 100.13 | 100.09 | 100.12 | 100.14 | 100.14 | 100.14 | 100.20 | 100.15 |

Appendix 3

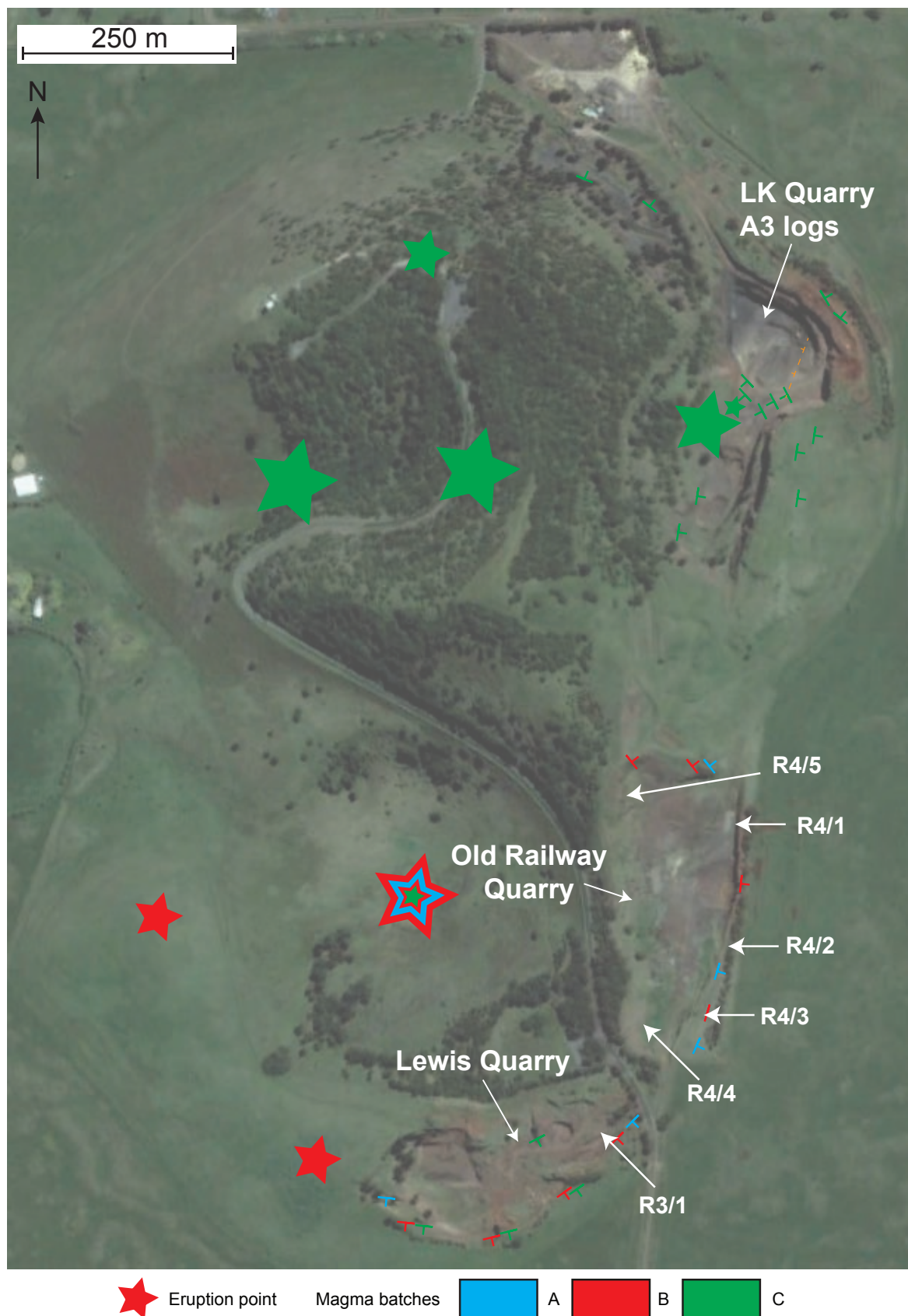
| | Jays Hill | Cas Maar 1 | Cas Maar 2 | Cas Maar 3 | Cas Maar 4 | Mt. Rouse batch A avg | Mt. Rouse batch B avg | Mt. Rouse batch C avg | Mt. Napier AN-44 | Mt. Napier AN-74 |
|----------------------------------|-----------|------------|------------|------------|------------|-----------------------|-----------------------|-----------------------|------------------|------------------|
| Quartz | 0.00 | 0.00 | 0.00 | 0.00 | 0.00 | 0.00 | 0.00 | 0.00 | 0.00 | 0.00 |
| Plagioclase | 50.32 | 48.34 | 45.70 | 50.23 | 51.27 | 48.35 | 41.90 | 39.08 | 47.58 | 52.56 |
| Orthoclase | 7.98 | 14.06 | 13.00 | 12.59 | 11.82 | 6.62 | 9.51 | 11.05 | 6.50 | 8.16 |
| Nepheline | 0.00 | 0.00 | 0.00 | 0.00 | 2.91 | 0.00 | 4.14 | 6.43 | 0.44 | 0.00 |
| Leucite | 0.00 | 0.00 | 0.00 | 0.00 | 0.00 | 0.00 | 0.00 | 0.00 | 0.00 | 0.00 |
| Kalsilite | 0.00 | 0.00 | 0.00 | 0.00 | 0.00 | 0.00 | 0.00 | 0.00 | 0.00 | 0.00 |
| Corundum | 0.00 | 0.00 | 0.00 | 0.00 | 0.00 | 0.00 | 0.00 | 0.00 | 0.00 | 0.00 |
| Diopside | 15.59 | 3.72 | 7.54 | 7.71 | 4.88 | 17.76 | 16.24 | 15.21 | 18.30 | 15.86 |
| Hypersthene | 6.59 | 10.26 | 12.06 | 2.93 | 0.00 | 1.28 | 0.00 | 0.00 | 0.00 | 0.20 |
| Wollastonite | 0.00 | 0.00 | 0.00 | 0.00 | 0.00 | 0.00 | 0.00 | 0.00 | 0.00 | 0.00 |
| Olivine | 11.87 | 15.08 | 13.20 | 18.46 | 21.65 | 18.35 | 19.14 | 18.29 | 19.80 | 15.24 |
| Larnite | 0.00 | 0.00 | 0.00 | 0.00 | 0.00 | 0.00 | 0.00 | 0.00 | 0.00 | 0.00 |
| Acmite | 0.00 | 0.00 | 0.00 | 0.00 | 0.00 | 0.00 | 0.00 | 0.00 | 0.00 | 0.00 |
| K ₂ SiO ₃ | 0.00 | 0.00 | 0.00 | 0.00 | 0.00 | 0.00 | 0.00 | 0.00 | 0.00 | 0.00 |
| Na ₂ SiO ₃ | 0.00 | 0.00 | 0.00 | 0.00 | 0.00 | 0.00 | 0.00 | 0.00 | 0.00 | 0.00 |
| Rutile | 0.00 | 0.00 | 0.00 | 0.00 | 0.00 | 0.00 | 0.00 | 0.00 | 0.00 | 0.00 |
| Ilmenite | 3.97 | 4.18 | 3.97 | 4.01 | 3.65 | 4.10 | 4.73 | 5.17 | 3.84 | 4.37 |
| Magnetite | 2.65 | 2.77 | 2.71 | 2.65 | 2.39 | 2.62 | 2.74 | 2.81 | 2.61 | 2.52 |
| Hematite | 0.00 | 0.00 | 0.00 | 0.00 | 0.00 | 0.00 | 0.00 | 0.00 | 0.00 | 0.00 |
| Apatite | 1.07 | 1.65 | 1.88 | 1.48 | 1.48 | 0.95 | 1.62 | 2.02 | 0.95 | 1.14 |
| Zircon | 0.03 | 0.07 | 0.06 | 0.06 | 0.06 | 0.03 | 0.06 | 0.07 | 0.03 | 0.04 |
| Perovskite | 0.00 | 0.00 | 0.00 | 0.00 | 0.00 | 0.00 | 0.00 | 0.00 | 0.00 | 0.00 |
| Chromite | 0.06 | 0.07 | 0.00 | 0.09 | 0.07 | 0.06 | 0.04 | 0.04 | 0.07 | 0.03 |
| Sphene | 0.00 | 0.00 | 0.00 | 0.00 | 0.00 | 0.00 | 0.00 | 0.00 | 0.00 | 0.00 |
| Pyrite | 0.00 | 0.00 | 0.00 | 0.00 | 0.00 | 0.00 | 0.00 | 0.00 | 0.00 | 0.00 |
| Halite | 0.00 | 0.00 | 0.00 | 0.00 | 0.00 | 0.00 | 0.00 | 0.00 | 0.00 | 0.00 |
| Fluorite | 0.00 | 0.00 | 0.00 | 0.00 | 0.00 | 0.00 | 0.00 | 0.00 | 0.00 | 0.00 |
| Anhydrite | 0.00 | 0.00 | 0.00 | 0.00 | 0.00 | 0.00 | 0.00 | 0.00 | 0.00 | 0.00 |
| Na ₂ SO ₄ | 0.00 | 0.00 | 0.00 | 0.00 | 0.00 | 0.00 | 0.00 | 0.00 | 0.00 | 0.00 |
| Calcite | 0.00 | 0.00 | 0.00 | 0.00 | 0.00 | 0.00 | 0.00 | 0.00 | 0.00 | 0.00 |
| Na ₂ CO ₃ | 0.00 | 0.00 | 0.00 | 0.00 | 0.00 | 0.00 | 0.00 | 0.00 | 0.00 | 0.00 |
| Total | 100.13 | 100.20 | 100.12 | 100.21 | 100.18 | 100.12 | 100.12 | 100.17 | 100.12 | 100.12 |





Appendix 4

Stratigraphic logs



Log locations for the southern cone of Mt Rouse.

| LOCATION | DATE | NAME | PAGE . . . | OF . . . |
|---|---|---|---|---|
| R4/1 | 26/7/2010 | Mt. Rouse, Penshurst. -37.8879 S, 142.30616 E | | |
| STRUCTURE | SE | SAMPLE OR PHOTO | DESCRIPTION & INTERPRETATION | |
| | 0.0625 0.125 0.25 0.5 1 2 4 64 128 256 | | Components, Texture, Depositional Structure | Fragmentation, Depositional Processes, Environmental Setting |
| <div> <div>8</div> <div>7</div> <div>Bomb Layer A</div> <div>6</div> <div>Bomb Layer B</div> <div>5</div> <div>4</div> <div>220/45</div> <div>3</div> <div>2</div> <div>1</div> <div>0</div> </div> | | <div> <div>←R4AJ</div> <div>←R4AI</div> <div>←R4AH</div> <div>←R4AG</div> <div>←R4AF</div> <div>←R4AE</div> <div>←R4AD</div> <div>←R4AC</div> <div>←R4AB</div> <div>←R4C</div> <div>←R4B</div> <div>←R4A</div> </div> | <p>Ash-rich deposit to top. Thins to south. Non-vesiculated clasts 2–6 mm, mostly rounded. Armoured lapilli throughout.</p> <p>Large blocks and bombs up to 40 cm.</p> <p>Black scoria clasts up to 40 mm. Very light, highly vesicular and glassy. Some 30 cm bombs.</p> <p>Large blocks and bombs up to 70 cm.</p> <p>1–40 mm black scoria clasts, some up to 50 mm. Very light, highly vesicular and glassy. Some 30cm bombs.</p> <p>1–10 mm black scoria clasts, reverse grading.</p> <p>2–40 mm angular black scoria clasts, reverse grading. Agglutinated bombs up to 15cm.</p> <p>1–20 mm black scoria clasts, some angular, reverse grading.</p> <p>5–40 mm black scoria clasts. Scoria tubular in shape (stretched). Agglutinated clasts 10–15 cm towards top of layer.</p> <p>2–10 mm black scoria clasts, reverse grading.</p> <p>5–40 mm black scoria clasts. Faintly stratified.</p> <p>1–10 mm black scoria clasts, surge deposit.</p> <p>8–50 mm black scoria clasts, some highly vesicular.</p> | |
| | | | Clay, silt, mud | |
| | | | Fine ash, tuff | |
| | | | Sand (0.0625-2) VF F M C VC | |
| | | | Coarse ash, tuff (0.0625-2) | |
| | | | Pebble, conglomerate/breccia | |
| | | | Lapilli (2-64) | |
| | | | Cobble, conglomerate/breccia | |
| | | | Small blocks, bombs (64-256) | |
| | | | Boulder, conglomerate/breccia | |
| | | | Large blocks, bombs (>256) | |
| | | | | |
| | | | | |
| | | | | |

Facies

P3 moderately to well sorted fine ash-coarse lapilli/small blocks

P5 ash-rich armoured lapilli

P4 cross-bedded ash-lapilli

B Magma batches

| LOCATION | DATE | NAME | PAGE ... | OF ... |
|-----------|--|--|---|---|
| R4/2 | 26/7/2010 | Mt. Rouse, Penshurst. -37.8886 S, 142.30602 E | | |
| STRUCTURE | SAMPLE OR PHOTO | | DESCRIPTION & INTERPRETATION | |
| SE ↑ | 0.0625 0.125 0.25 0.5 1 2 4 64 128 256 | | Components, Texture, Depositional Structure | Fragmentation, Depositional Processes, Environmental Setting |
| | | | Ash-rich deposit. Thins to south. | |
| | ←R4I | | Lava flow, pinches out to NE, thicker to SW. Central portion splits into thin tube. | |
| | ←R4H ←R4G | | Oxidised surge deposits. Contain abundant Peles hairs and tears. Deposits same as R4/1 but lower in the sequence clearly oxidised beds can be seen which are laterally continuous. Stratified black scoria. Some dense clasts with low vesicularity, 70 mm–17 cm (R4G). Agglutinated bombs (R4H) up to 30 cm. | |
| | ←R4F | | Oxidised layers well sorted, and vary in grain-size ranges: <10 mm clasts <5 mm clasts <10 mm clasts (black scoria layer) <30 mm clasts <15 mm clasts <5 mm clasts <10 mm clasts (black scoria) 2–20 mm clasts <10 mm clasts (black scoria) | |
| | Clay, silt, mud Fine ash, tuff Sand (0.0625-2) VF F M C VC Coarse ash, tuff (0.0625-2) Pebble, conglomerate/breccia Lapilli (2-64) Cobble, conglomerate/breccia Small blocks, bombs (64-256) Boulder, conglomerate/breccia Large blocks, bombs (>256) | | | |

| | | | | |
|--------|--|---|--|------------------------------|
| Facies | | C1 lava | | P4 cross-bedded ash-lapilli |
| | | P3 moderately to well sorted fine ash-coarse lapilli/small blocks | | P5 ash-rich armoured lapilli |





Magma batches

A B

Appendix 4

[illegible]

Facies

| | | | |
|---|---|---|------------------------------|
|  | C1 lava |  | P4 cross-bedded ash-lapilli |
|  | P3 moderately to well sorted fine ash-coarse lapilli/small blocks |  | P5 ash-rich armoured lapilli |

Magma batches

 A  B

| LOCATION R4/4 | DATE 26/7/2010 | NAME Mt. Rouse, Penshurst. -37.89013 S, 142.30490 E | PAGE ... OF ... |
|----------------------|---|--|--|
| STRUCTURE SW ↑ | 0.0625 0.125 0.25 0.5 1 2 4 64 128 256 | SAMPLE OR PHOTO | DESCRIPTION & INTERPRETATION Components, Texture, Depositional Structure Fragmentation, Depositional Processes, Environmental Setting |
| | <p>8</p> <p>8</p> <p>7</p> <p>6</p> <p>5</p> <p>4</p> <p>3</p> <p>2</p> <p>1</p> <p>0</p> | <p>8</p> <p>7</p> <p>6</p> <p>5</p> <p>4</p> <p>3</p> <p>2</p> <p>1</p> <p>0</p> | <p>8 Oxidised surge. Ash—10 mm clasts. Correlates with surge beneath lava.</p> <p>7 Weathered scoria, cannot determine layering. ~1–20 mm clasts max size. Weathered from quarrying, but is fallout, well-sorted.</p> <p>6 Oxidised surge. Ash—5 mm clasts.</p> <p>5 5 mm black scoria, no grading.</p> <p>4 1–100 mm black scoria, coarsely reverse graded. Larger clasts dense.</p> <p>3 1–20 mm black scoria, reverse graded to base. Few 140 mm clasts.</p> <p>2 1–60 mm black scoria, poorly sorted, few 140 mm clasts.</p> <p>1 ~2 m, base unexposed due to scree slope of the same material. 1 mm - 140 mm grey-brown scoria. Poorly sorted with little/no internal stratification. Scattered spatter bombs ~0.5 m, few 1 m agglutinated bombs. Vesicular but very dense.</p> |
| | | | |

Facies

P1 poorly sorted bedded ash-lapilli-bombs

P2 well sorted fine ash-fine lapilli

P4 cross-bedded ash-lapilli

P5 ash-rich armoured lapilli

Magma batches


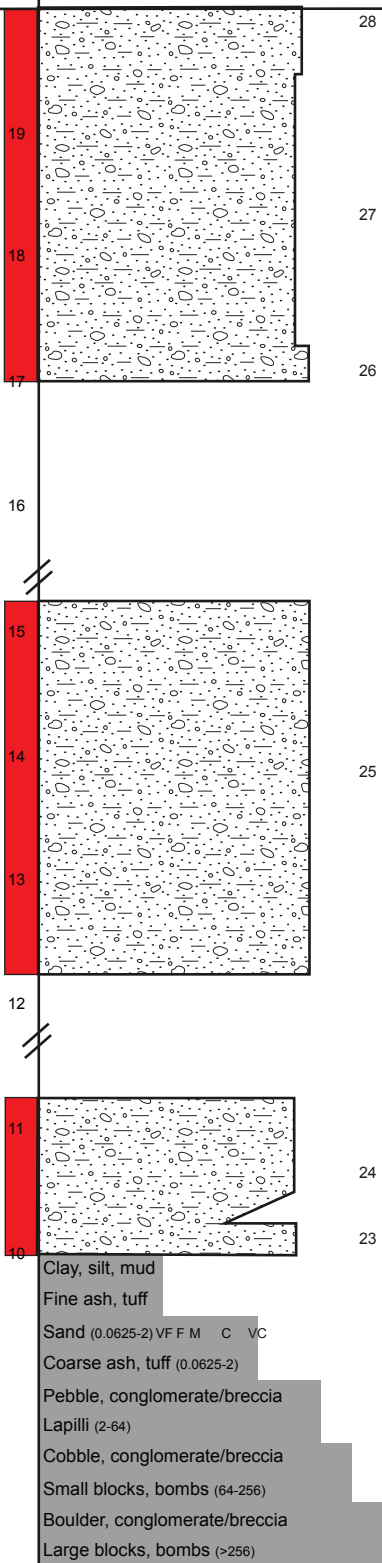
A B

Appendix 4

| LOCATION | DATE | NAME | PAGE 1. OF 7. | |
|----------|---|--|--|---|
| R4/5 | 26/7/2010 17/5/2011 | Mt. Rouse, Penshurst. -37.8874 S, 142.3047 E | | |
| | | SAMPLE OR PHOTO | DESCRIPTION & INTERPRETATION | |
| NW ↑ | 0.0625 0.125 0.25 0.5 1 2 4 64 128 256 | | Components, Texture, Depositional Structure | Fragmentation, Depositional Processes, Environmental Setting |
| 9 | | 23 | 23 3 mm red scoria base. Clasts up to 40 mm, but most 15 mm. Well consolidated. | |
| | | ←R4BB | 22 Red scoria. 2 mm base reverse graded to 30 mm top. Well consolidated. R4BA | |
| 8 | | | 20 Red and light brown scoria (equal proportions to the base, >80% red to top), 3–30 mm clasts. | |
| | | | 19, 18 Well sorted with mixed colours (grey, red, light brown), becoming redder to the top. 15 mm clasts. Colour changes define layers. | |
| 7 | | 22 ←R4BA | 17 Reverse graded. 3–15 mm clasts with mixed colours of grey, red and light brown. | |
| | | | 16 Fine scoria ~3 mm clasts of red, grey and light brown. Sample R4AO. | |
| 6 | | | 15 Coarse, poorly sorted layer of 3–50 mm clasts. Mixture of dense and vesiculated clasts, red and light brown. Sample R4AN. | |
| | | 21 | 14 Light brown scoria up to 45 mm. Smaller fraction is stretched and oxidised. Sample R4AM. | |
| 5 | | ←R4AP | 13 Red, light brown and black scoria up to 50 mm. Sample R4AL. | |
| | | 20 | 12b Red, black and light brown scoria clasts with coarse stratification caused by proportional changes in colour (there are not layers of each colour, but rather the proportions of each colour change with height, leading to the look of stratification). Clasts up to 40 mm. | |
| 4 | | 19 | 12a <1mm clasts to base, 30 mm to top. Coarsens upwards into 12b. Samples R4AA (bulk of layer), R4Z (base of layer). | |
| | | 18 | 11 Clasts 2 mm to base coarsening upwards to 2.5 cm at top of layer. Sample R4Y. | |
| 3 | | 17 ←R4AO | 10 Clasts 5 mm to base coarsening upwards to 40 cm at top of layer. Sample R4X. | |
| | | 16 ←R4AN | 9 Clasts 1.5–30 mm | |
| 2 | | 15 ←R4AM | 8 Clasts 3–15 mm | |
| | 14 ←R4AL | 7 Ash layer with clasts <3 mm | | |
| 1 | 13 | 6 Clasts 3–30 mm | | |
| | 12b | 5 Ash layer with clasts <3 mm | | |
| | ←R4AA | 4 Clasts 1.5–30 mm, grey scoria. Sample R4N. | | |
| | 12a | 3 Ash layer with brown scoria clasts <3 mm. Sample R4V. | | |
| | 11 ←R4Z | 2 Clasts 3–15 mm of grey and light brown scoria. Sample R4U. | | |
| | 10 ←R4Y | 1 Well sorted grey and light brown scoria of <3 mm clasts. Sample R4T. | | |
| | 9 ←R4X | | | |
| | 8 | | | |
| | 7 | | | |
| | 6 | | | |
| | 5 | | | |
| | 4 | | | |
| | 3 | | | |
| | 2 | | | |
| | 1 | | | |
| | 0 | | | |
| | | Clay, silt, mud | | |
| | | Fine ash, tuff | | |
| | | Sand (0.0625-2) V F F M C VC | | |
| | | Coarse ash, tuff (0.0625-2) | | |
| | | Pebble, conglomerate/breccia | | |
| | | Lapilli (2-64) | | |
| | | Cobble, conglomerate/breccia | | |
| | | Small blocks, bombs (64-256) | | |
| | | Boulder, conglomerate/breccia | | |
| | | Large blocks, bombs (>256) | | |

Magma batch

 B

| LOCATION | DATE | NAME | PAGE . 2 . | OF . 7 . |
|---|--|---|--|---|
| R4/5 | 26/7/2010 17/5/2011 | Mt. Rouse, Penshurst. -37.8874 S, 142.3047 E | | |
| NW ↑ | SAMPLE OR PHOTO | | DESCRIPTION & INTERPRETATION | |
| | 0.0625 0.125 0.25 0.5 1 2 4 64 128 256 | | Components, Texture, Depositional Structure | Fragmentation, Depositional Processes, Environmental Setting |
|  |  | | <p>28 3–15 mm clasts. Spatter bombs 25 cm - 50 cm. Not very well sorted. Vent clearing episode? Red and well consolidated.</p> <p>27 ~10 mm clasts, some 30 mm and 60 mm. Red and well consolidated.</p> <p>26 2–45 mm scoria, no grading. Red and well consolidated.</p> <p>25 Red scoria, well consolidated. Internal variations in grainsize but no clear beds. 2–30 mm clasts. 10 cm spatter bombs.</p> <p>24 1 mm base grading up to clasts of ~10 mm, but with some 40 mm clasts. Spatter bombs up to 26 cm. Red scoria, well consolidated.</p> | |
| | | | | |
| | | | | |
| | | | | |
| | | | | |
| | | | | |
| | | | | |
| | | | | |
| | | | | |
| | | | | |
| | | | | |

Facies

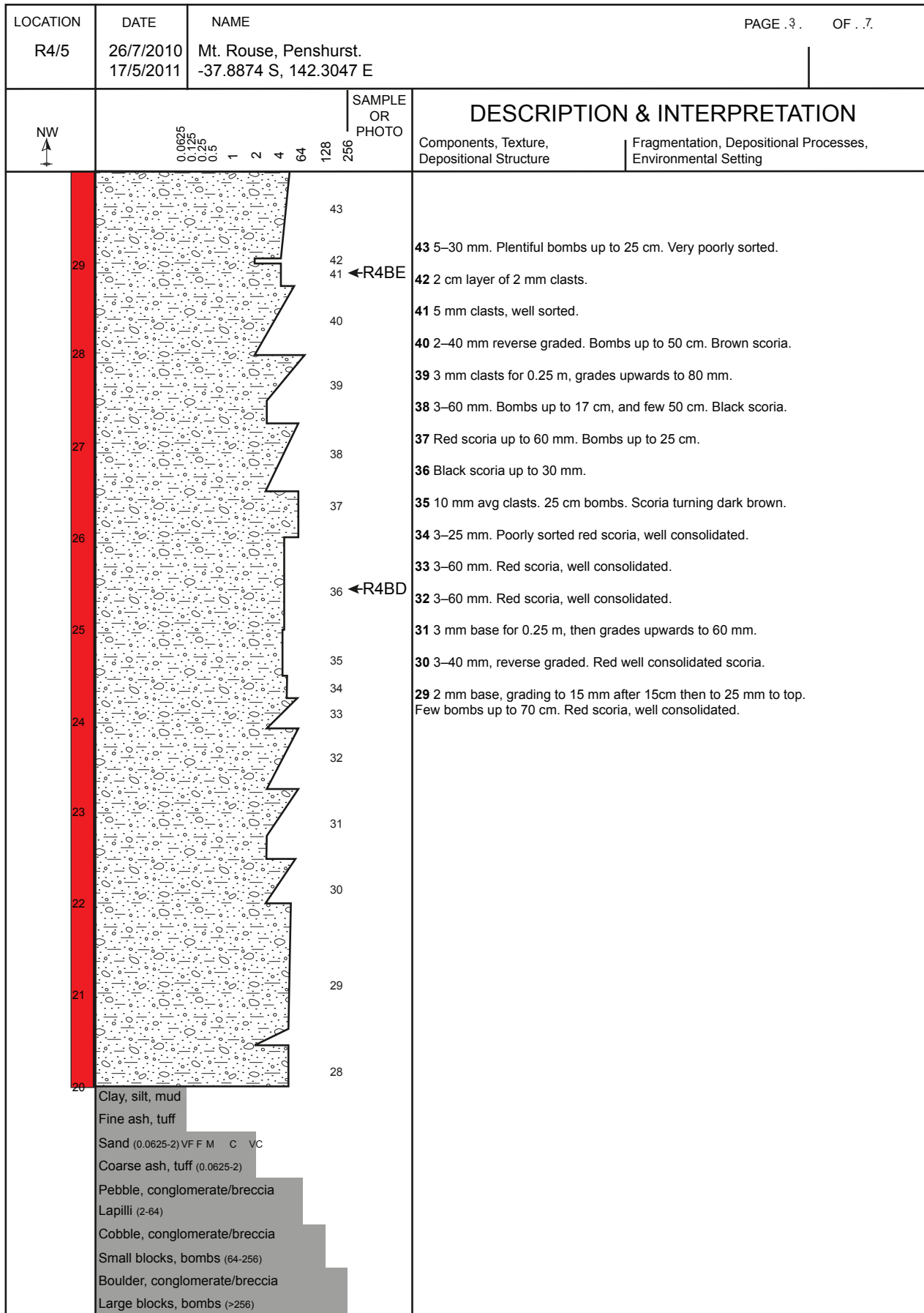


P3 moderately to well sorted
fine ash–coarse lapilli/
small blocks

Magma batches



B



Facies



P3 moderately to well sorted
fine ash-coarse lapilli/
small blocks

Magma batches



B

| LOCATION R4/5 | DATE 26/7/2010 17/5/2011 | NAME Mt. Rouse, Penshurst. -37.8874 S, 142.3047 E | PAGE .4 . | OF .7. |
|----------------------------|---|--|---|---|
| NW ↑ | 0.0625 0.125 0.25 0.5 1 2 4 64 128 256 | SAMPLE OR PHOTO | DESCRIPTION & INTERPRETATION | |
| | | | Components, Texture, Depositional Structure | Fragmentation, Depositional Processes, Environmental Setting |
| 39 38 37 36 35 | | 60 59 58 57 ←R4BF 56 55 54 53 52 51 50 49 48 47 46 45 44 | 60 5 mm–10 cm reverse graded. Bombs up to 17 cm. 59 4–50 mm reverse graded. 58 2 mm base, grades to 40 mm at 0.25 m, then grades to 10 cm at top. Bombs up to 25 cm. 57 5–15 mm reverse graded. 56 10–10 cm. Bombs up to 0.25 m. 55 2–50 mm reverse graded. 54 1 mm base, grades to 10 mm, then to 80 mm. 53 5–10 mm. Bombs up to 0.5 m. 52 10–60 mm. 51 5 mm clasts. ~ 20 cm layer then un-loggable due to vegetation. 50 1–50 mm reverse graded. Bombs up to 0.6 m. 49 2 mm base, grades upwards into 0.25 m bombs at top. 48 1–40 mm reverse graded. 47 10 mm clasts. Few 0.25 m bombs. 46 10 cm layer of 2 mm clasts. 45 1–50 mm reverse graded. Bombs up to 20 cm. 44 1–50 mm reverse graded. Bombs up to 25 cm. | |
| | | | Clay, silt, mud Fine ash, tuff Sand (0.0625-2) VF F M C VC Coarse ash, tuff (0.0625-2) Pebble, conglomerate/breccia Lapilli (2-64) Cobble, conglomerate/breccia Small blocks, bombs (64-256) Boulder, conglomerate/breccia Large blocks, bombs (>256) | |

Facies



P3 moderately to well sorted
fine ash–coarse lapilli/
small blocks

Magma batches



B

Appendix 4

| LOCATION | DATE | NAME | PAGE . 5 . | OF . 7 . |
|----------|---|---|--|--|
| R4/5 | 26/7/2010 17/5/2011 | Mt. Rouse, Penshurst. -37.8874 S, 142.3047 E | | |
| | SAMPLE OR PHOTO | | DESCRIPTION & INTERPRETATION | |
| NW ↑ | 0.0625 0.125 0.25 0.5 1 2 4 64 128 256 | | Components, Texture, Depositional Structure | Fragmentation, Depositional Processes, Environmental Setting |
| 49 | | | 76 3–80 mm reverse graded. | |
| | | | 75 Ash–120 mm reverse graded. | |
| 48 | | | 74 Ash–20 mm reverse graded, then grades to 120 mm at top. | |
| | | | 73 Ash–20 mm reverse graded. | |
| | | | 72 2–80 mm reverse graded. | |
| 47 | | | 71 5–60 mm reverse graded. | |
| | | | 70 3– 60 mm reverse graded. | |
| 46 | | | 69 1 mm–10 cm reverse graded. Bombs up to 17 cm. | |
| | | | 68 1–40 mm reverse graded. | |
| | | | 67 2–50 mm reverse graded. | |
| 45 | | | 66 5–60 mm reverse graded. 25 cm bombs. | |
| | | | 65 2–140 mm reverse graded. Not well sorted. 55 cm bombs. | |
| 44 | | | 64 3–60 mm reverse graded. 46 cm bombs. | |
| | | | 63 Ash–20 mm reverse graded. | |
| 43 | | | 62 Ash–4 mm — 10 cm layer. | |
| | | | 61 2 mm–15 mm reverse graded. | |
| 42 | | | | |
| 41 | | | | |
| 40 | | | | |
| | Clay, silt, mud | | | |
| | Fine ash, tuff | | | |
| | Sand (0.0625-2) VF F M C VC | | | |
| | Coarse ash, tuff (0.0625-2) | | | |
| | Pebble, conglomerate/breccia | | | |
| | Lapilli (2-64) | | | |
| | Cobble, conglomerate/breccia | | | |
| | Small blocks, bombs (64-256) | | | |
| | Boulder, conglomerate/breccia | | | |
| | Large blocks, bombs (>256) | | | |

Facies



P3 moderately to well sorted
fine ash-coarse lapilli/
small blocks

Magma batches



B

| LOCATION | DATE | NAME | PAGE 6. OF 7. | |
|---|---|---|--|---|
| R4/5 | 26/7/2010 17/5/2011 | Mt. Rouse, Penshurst. -37.8874 S, 142.3047 E | | |
| ↑ | 0.0625 0.125 0.25 0.5 1 2 4 64 128 256 | SAMPLE OR PHOTO | DESCRIPTION & INTERPRETATION | |
| | | | Components, Texture, Depositional Structure | Fragmentation, Depositional Processes, Environmental Setting |
| | 88 | | 88 Black scoria, stratified. 10 mm clasts, becomes oxidised to top. | |
| | | | 87 4 mm–1 cm reverse graded. Many large bombs scattered throughout 0.25–0.75 m. Red scoria. | |
| | | | 86 1–90 mm reverse graded. 20 cm bombs at top. | |
| | | | 85 5–10 mm reverse graded. Few 20 mm clasts. | |
| | | | 84 3–100 mm reverse graded. | |
| | | | 83 3–60 mm reverse graded. | |
| | | | 82 3–60 mm reverse graded. 25 cm bombs. | |
| | | | 81 3–60 mm reverse graded. | |
| | | | 80 4–100 mm reverse graded. | |
| | | | 79 3–60 mm reverse graded. | |
| | | | 78 3–60 mm reverse graded. 18 cm bombs. | |
| | | | 77 10–60 mm reverse graded. | |
| | | | | |
| | | | | |
| | | | | |
| Clay, silt, mud Fine ash, tuff Sand (0.0625-2) V F F M C VC Coarse ash, tuff (0.0625-2) Pebble, conglomerate/breccia Lapilli (2-64) Cobble, conglomerate/breccia Small blocks, bombs (64-256) Boulder, conglomerate/breccia Large blocks, bombs (>256) | | | | |

Facies


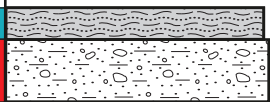


P3 moderately to well sorted
fine ash–coarse lapilli/
small blocks

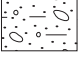
Magma batches




B

| LOCATION | DATE | NAME | PAGE 7. . OF . 7. | |
|--|---|---|--|---|
| R4/5 | 26/7/2010 17/5/2011 | Mt. Rouse, Penshurst. -37.8874 S, 142.3047 E | | |
| ↑ | 0.0625 0.125 0.25 0.5 1 2 4 64 128 256 | SAMPLE OR PHOTO | DESCRIPTION & INTERPRETATION | |
| | | | Components, Texture, Depositional Structure | Fragmentation, Depositional Processes, Environmental Setting |
| 61 |  |  | 89 | 89 Oxidised surge deposit |
| | | | | |
| 60 | | | 88 | |
| Clay, silt, mud Fine ash, tuff Sand (0.0625-2) VF F M C VC Coarse ash, tuff (0.0625-2) Pebble, conglomerate/breccia Lapilli (2-64) Cobble, conglomerate/breccia Small blocks, bombs (64-256) Boulder, conglomerate/breccia Large blocks, bombs (>256) | | | | |

Facies

 P3 moderately to well sorted
fine ash-coarse lapilli/
small blocks

 P4 cross-bedded
ash-lapilli

Magma batches  B

| | | | | |
|-----------|---|--|---|---|
| LOCATION | DATE | NAME | | |
| R3/1 | 26/7/2010 17/5/2011 | Mt Rouse, Penshurst. -37.89013 S, 142.30490 E | | |
| STRUCTURE | | | SAMPLE OR PHOTO | DESCRIPTION & INTERPRETATION |
| SE ↑ | | | | Components, Texture, Depositional Structure |
| | | | | Fragmentation, Depositional Processes, Environmental Setting |
| | | | ←R3D 8 7 6 5 4 ←R3C 3 ←R3B 2 ←R3A 1 | 8 2 mm–10 mm reverse graded red scoria to base. At 1.25 m, grades to 20 mm. Tubular shaped clasts. 7 1–20 mm reverse graded red scoria. 6 1–10 mm reverse graded red scoria. 4-5 1–15 mm reverse graded red scoria. Repeated beds. 3 1 mm red scoria. 2 6–60 mm reverse graded scoria. Vesicular to the base and 6 mm, grading to 40 mm at the top (still vesicular), but as size increases at 150 mm the deposit contains a large proportion of very dense clasts, which appear a little less oxidised than the finer scoria. There are fragments of the rinds of broken breadcrust bombs in the top layer. Occasional spatter bomb 0.4 m. Possible opening stages of eruption. 1 4–40 mm poorly sorted red scoria. Very different to overlying deposits. Contains abundant spattery clasts up to 50 cm. |
| | 0 Clay, silt, mud Fine ash, tuff Sand (0.0625-2) V F F M C VC Coarse ash, tuff (0.0625-2) Pebble, conglomerate/breccia Lapilli (2-64) Cobble, conglomerate/breccia Small blocks, bombs (64-256) Boulder, conglomerate/breccia Large blocks, bombs (>256) | | | |

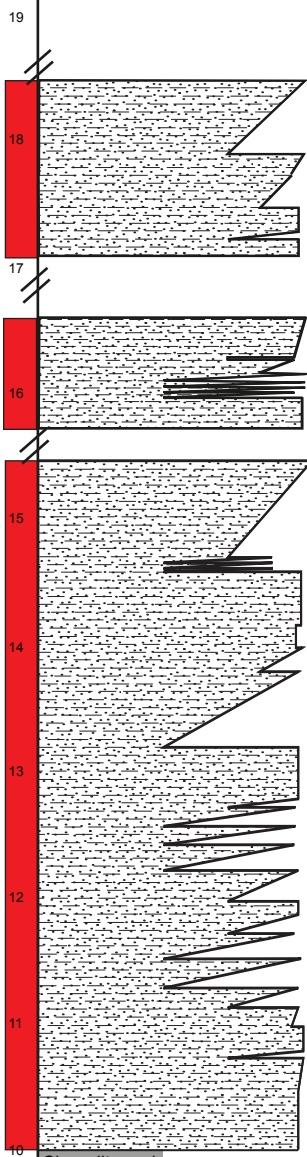
Facies

P1 moderately sorted bedded ash-lapilli-bombs
 P2 well sorted fine ash-fine lapilli

Magma batches

B C

Appendix 4

| LOCATION | DATE | NAME | | |
|--|---|--|-----------------|--|
| R3/1 | 26/7/2010 17/5/2011 | Mt Rouse, Penshurst. -37.89013 S, 142.30490 E | | |
| STRUCTURE | | | SAMPLE OR PHOTO | DESCRIPTION & INTERPRETATION |
| SE ↑ | 0.0625 0.125 0.25 0.5 1 2 4 64 128 256 | | | Components, Texture, Depositional Structure Fragmentation, Depositional Processes, Environmental Setting |
|  | | | | <p>39 1–30 mm reverse graded red scoria.</p> <p>38 2–5 mm reverse graded black scoria.</p> <p>37 1–15 mm black scoria, reverse graded to base.</p> <p>36 1–15 mm no grading. Black scoria.</p> <p>35 5–30 mm reverse graded red scoria.</p> <p>34 3 mm bed of 1 mm red scoria clasts.</p> <p>33 2 mm bed of 5 mm reverse graded red scoria.</p> <p>29-32 - Repeating beds (29 = 25 mm, 30 = 35 mm, 31 = 40 mm, 32 = 60 mm). Reverse grading of ash <1–5 mm clasts of red scoria.</p> <p>28 1–20 mm no grading. Red scoria.</p> <p>27 1–30 mm reverse graded red scoria. Clasts up to 10 cm throughout. Bombs up to 18cm at base in places.</p> <p>24-26 - Repeating beds (all 35 mm thick) of ash at the base (<1 mm) to 3 mm tops. No sedimentary structures.</p> <p>23 3–10 mm red scoria with no grading. Few 40-50 mm clasts.</p> <p>22 1–5 mm red scoria with no grading.</p> <p>21 2–10 mm reverse graded red scoria.</p> <p>20 Ash–10 mm reverse graded red scoria.</p> <p>19 1 mm–15 mm reverse graded at base, then poorly sorted. Red scoria.</p> <p>18 Ash–5 mm reverse graded red scoria with high proportion of ash throughout.</p> <p>16-17 Ash–5 mm reverse graded red scoria with high proportion of ash throughout. Repeating beds.</p> <p>14-15 1–10 mm reverse graded red scoria. Repeating beds.</p> <p>13 Ash–5 mm reverse graded red scoria. Large proportion of ash throughout.</p> <p>12 Ash–15 mm reverse graded red scoria. Grades to 15 mm scoria only in top 50 mm and contains large proportion of ash throughout.</p> <p>11 1 mm–15 mm reverse graded red scoria.</p> <p>10 4 mm–10 mm reverse graded red scoria.</p> <p>9 1 mm–20 mm reverse graded to base then poorly sorted. Red scoria.</p> |

Facies



P2 well sorted fine ash–fine lapilli

Magma batches



B

| | | |
|------------------|--|---|
| LOCATION R3/1 | DATE 26/7/2010 17/5/2011 | NAME Mt Rouse, Penshurst. -37.89013 S, 142.30490 E |
| STRUCTURE | SAMPLE OR PHOTO 0.0625 0.125 0.25 0.5 1 2 4 64 128 256 | DESCRIPTION & INTERPRETATION Components, Texture, Depositional StructureFragmentation, Depositional Processes, Environmental Setting |
| 29 | | 47 Ash. Straight above the lava for ~3 m. At this location there are a variety of clast sizes up to 6 mm. It looks poorly sorted and is consolidated due to the ash content. Larger clasts have rinds of ash at least 1 mm thick making them armoured lapilli. At the top is 1.5 m of a soil horizon, almost black to the top 0.25 m and very dark brown beneath. |
| 28 | | 46 Lava. There are at least two flows. The base flow is ~0.25 m, and the flow on top ~1.5 m. The top flow is segregated from the bottom in places and there are lava stalags on the base of the upper flow. Further along, the upper flow also splits like this. The upper flow shows an excellent example of pahoehoe with toothpaste-like structures in large scale to the sides, and small-scale on the underside of the flow. |
| 27 | | 45 Oxidised surge, Pele's hairs and tears but scarce. Correlates to surge in ORQ beneath lava. |
| 26 | | 44 1–30 mm reverse graded red scoria. |
| 25 | | 43 3–30 mm reverse graded red scoria. |
| 24 | | 42 Surge. 3–30 mm red scoria. Probably correlates to lower surges in ORQ. |
| 23 | | 41 3–10 mm reverse graded black scoria. |
| 22 | | 40 60 mm of exposed deposit. Black scoria clasts up to 60 mm. |
| 21 | | |
| 20 | | |

Facies

C1 lava

P3 moderately to well sorted fine ash-coarse lapilli/small blocks

P4 cross-bedded ash-lapilli

P5 ash-rich armoured lapilli

Magma batches

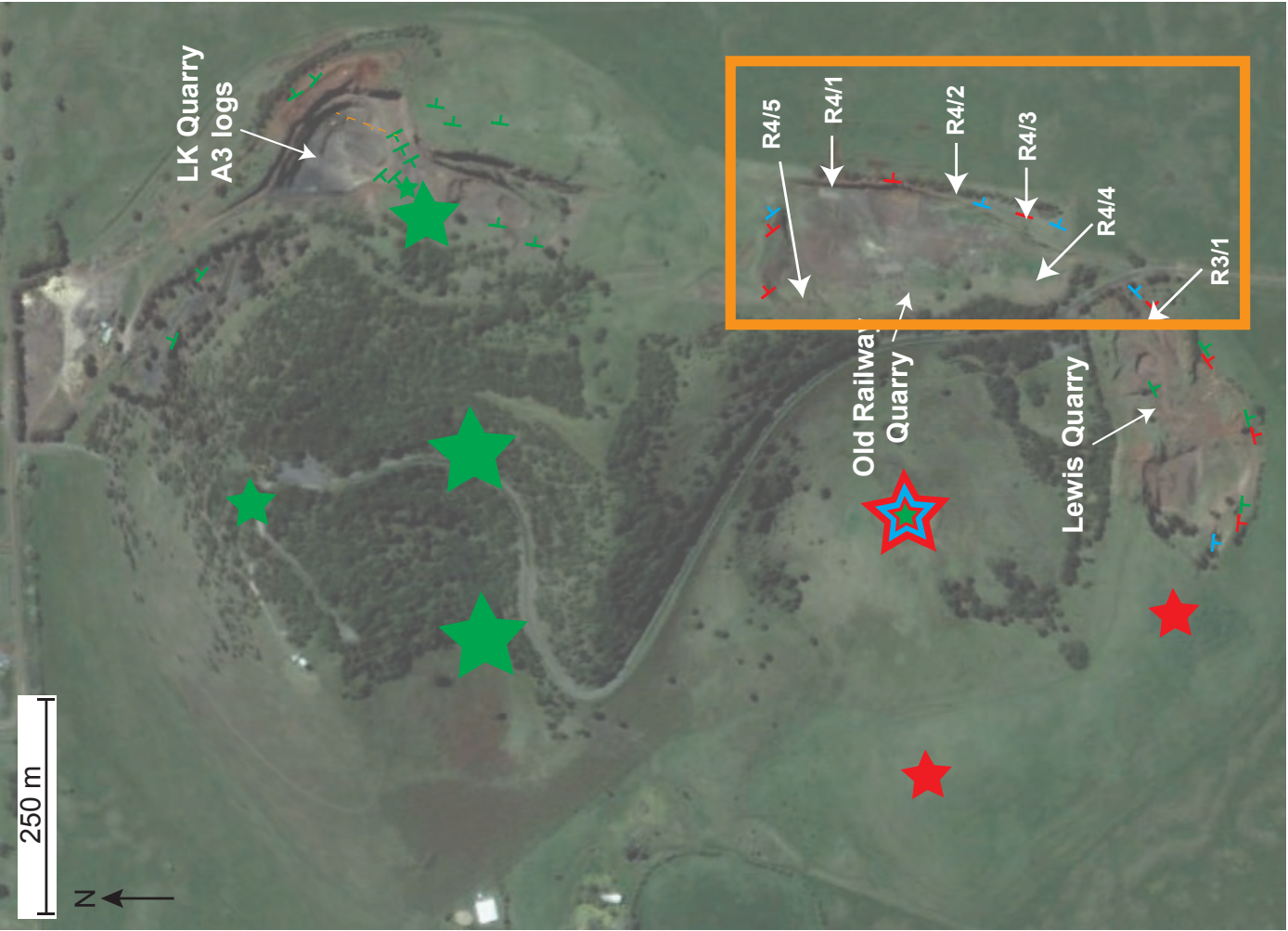
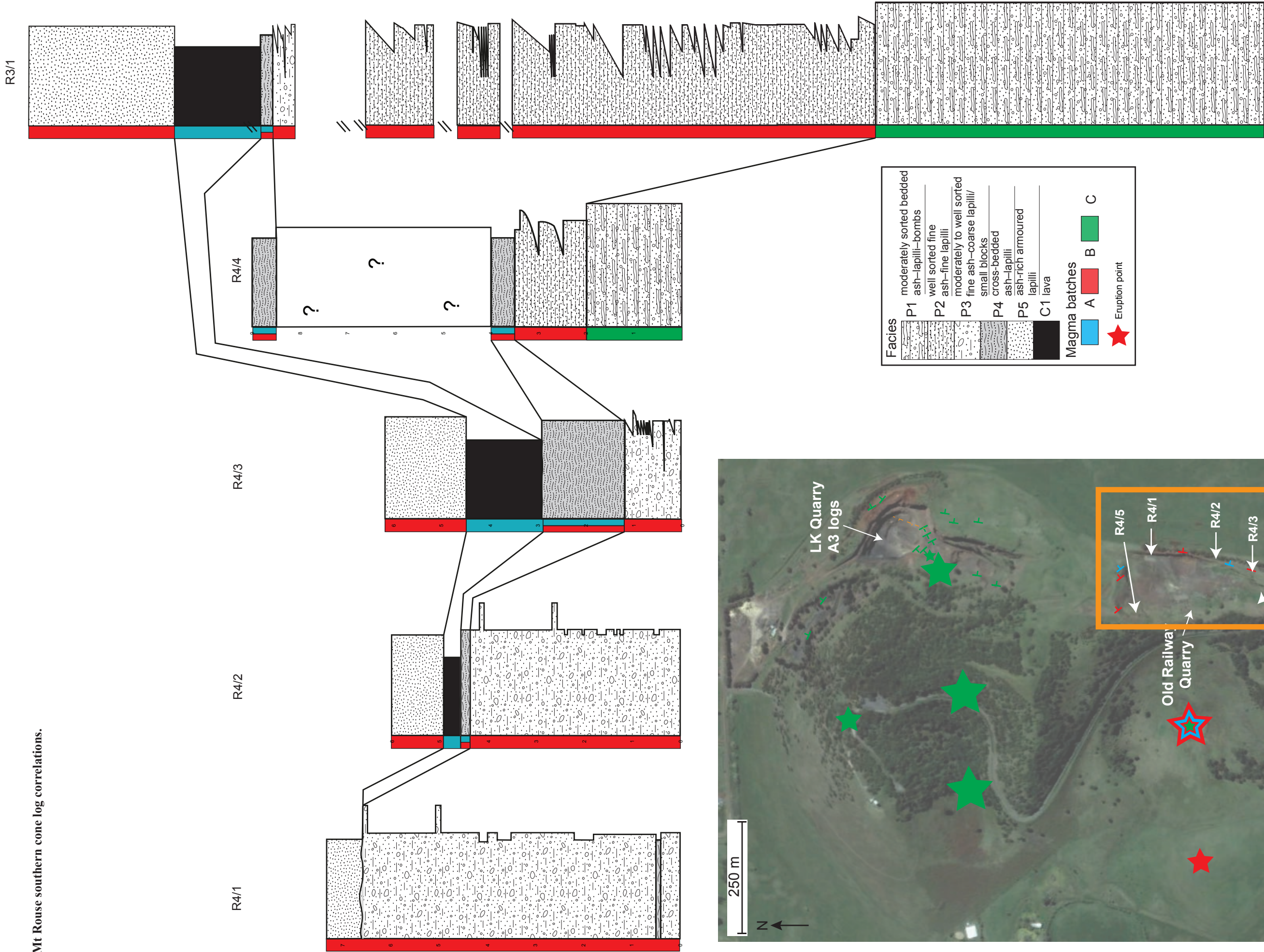
 A  B

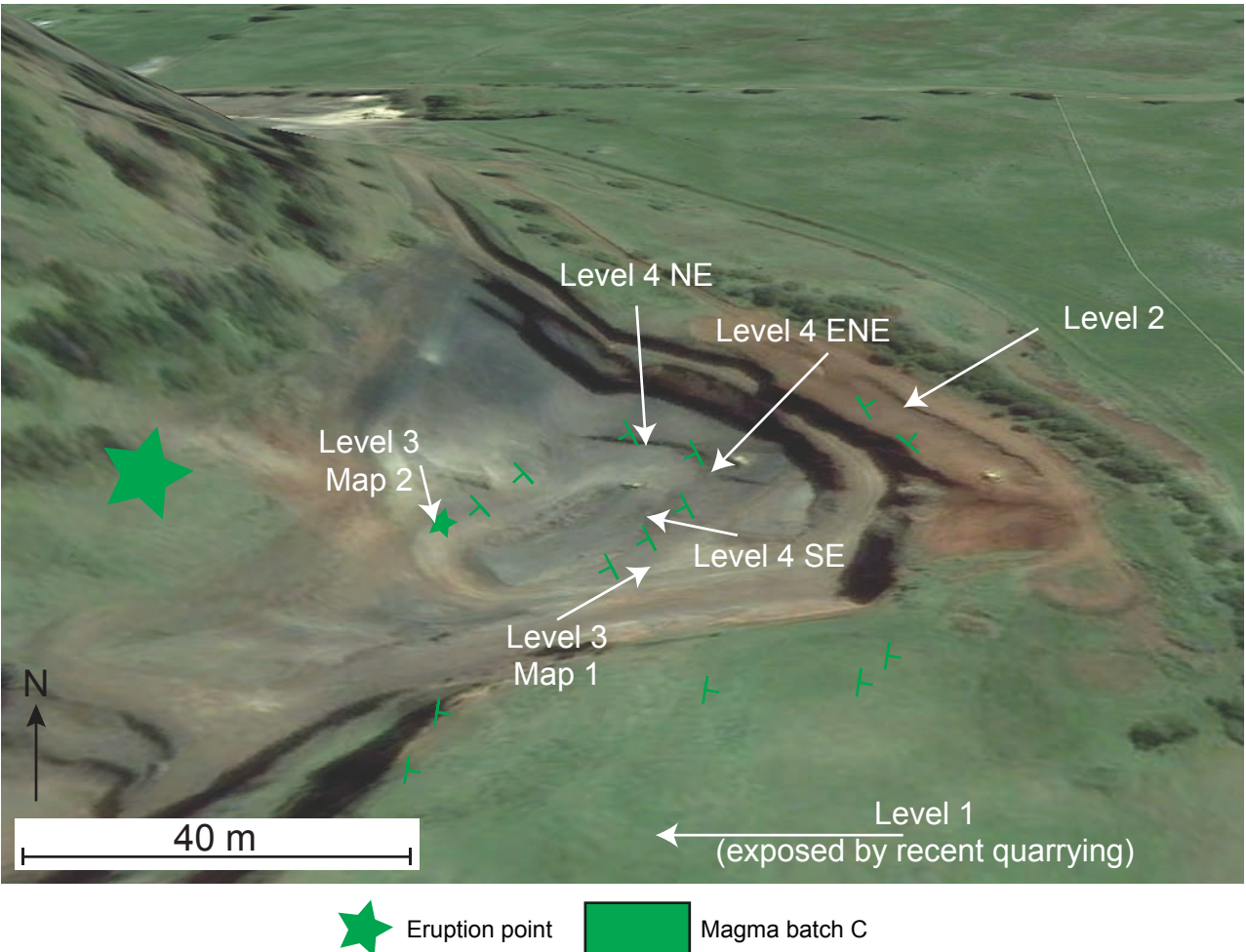
Appendix 4

| Sample | Latitude | Longitude |
|---------------|-----------------|------------------|
| MRV2 | -37.87653 | 142.23471 |
| MRV3 | -37.91422 | 142.27173 |
| MRV7 | -38.05049 | 142.26695 |
| MRV9 | -38.03997 | 142.15905 |
| MRV10 | -37.95724 | 142.14194 |
| MRV11 | -38.395 | 142.24296 |
| MRV12 | -38.38245 | 142.18657 |
| MRV13 | -38.29484 | 142.16624 |
| MRV16 | -38.27724 | 142.18521 |
| MRV17 | -38.21723 | 142.22768 |
| MRV18 | -38.21633 | 142.22839 |
| MRV21 | -38.14764 | 142.29506 |
| MRV24 | -38.31514 | 142.10278 |
| MRV27 | -37.8794 | 142.32028 |
| MRV28 | -37.89422 | 142.29651 |
| MRV30 | -37.8794 | 142.32028 |

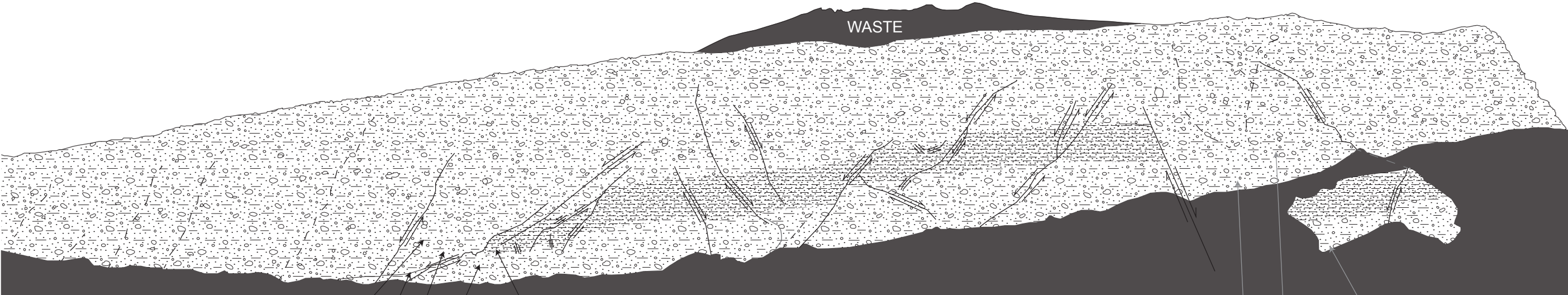
Lava sample locations.

Mt Rouse southern cone log correlations.





Log locations for the northern cone of Mt Rouse as exposed in the LK Quarry.



Facies

P2 well sorted fine ash–fine lapilli

P3 moderately to well sorted fine ash–coarse lapilli/ small blocks

Magma batch

C

S

Fault

Inferred fault

Stratigraphic Order
LK-L1-7
LK-L1-6
LK-L1-5
LK-L1-4
LK-L1-3
LK-L1-2
LK-L1-1
LK-L1-8

LK-L1-1
Massive bed 0.5 mm (coarse ash)–8 cm
Yellow scoria. Occasional larger grain and some bombs.
Well consolidated. No country rock.

LK-L1-2
Well-sorted finer grained layering of beds. Slight grading apparent but overall quite uniform.
The beds are due to differences in grainsize AND difference in colour — one or the other.
Coarsest layer 20 mm max with coarse ash. No country rock.

LK-L1-3
Bulk sample of ashy purple and yellow layers at the bottom of the fault.
More uniformly grained than at the right hand side of the fault (similar to the coarse grained scorias though). Bedding defined by colour, which is continuous (before deposition).

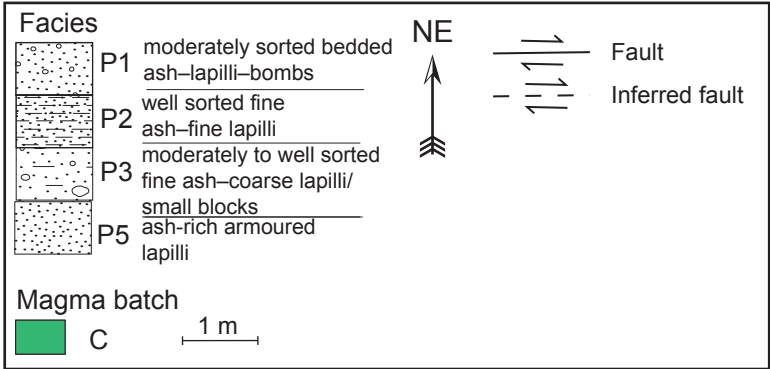
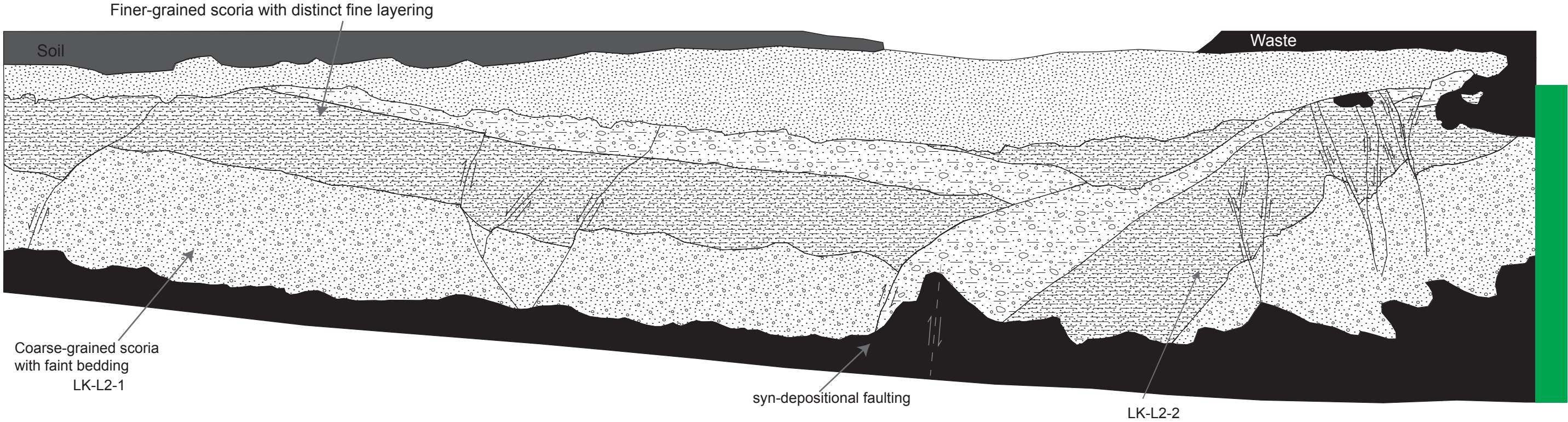
LK-L1-4
Similar to the layer below but coarse bombs up to ~25 cm. All the scorias are yellow with the occasional red clast, similar to LK-L1-1.
Took sample from the average bed - massive for ~1.5 m, then grades into a coarser grained scoria fall.

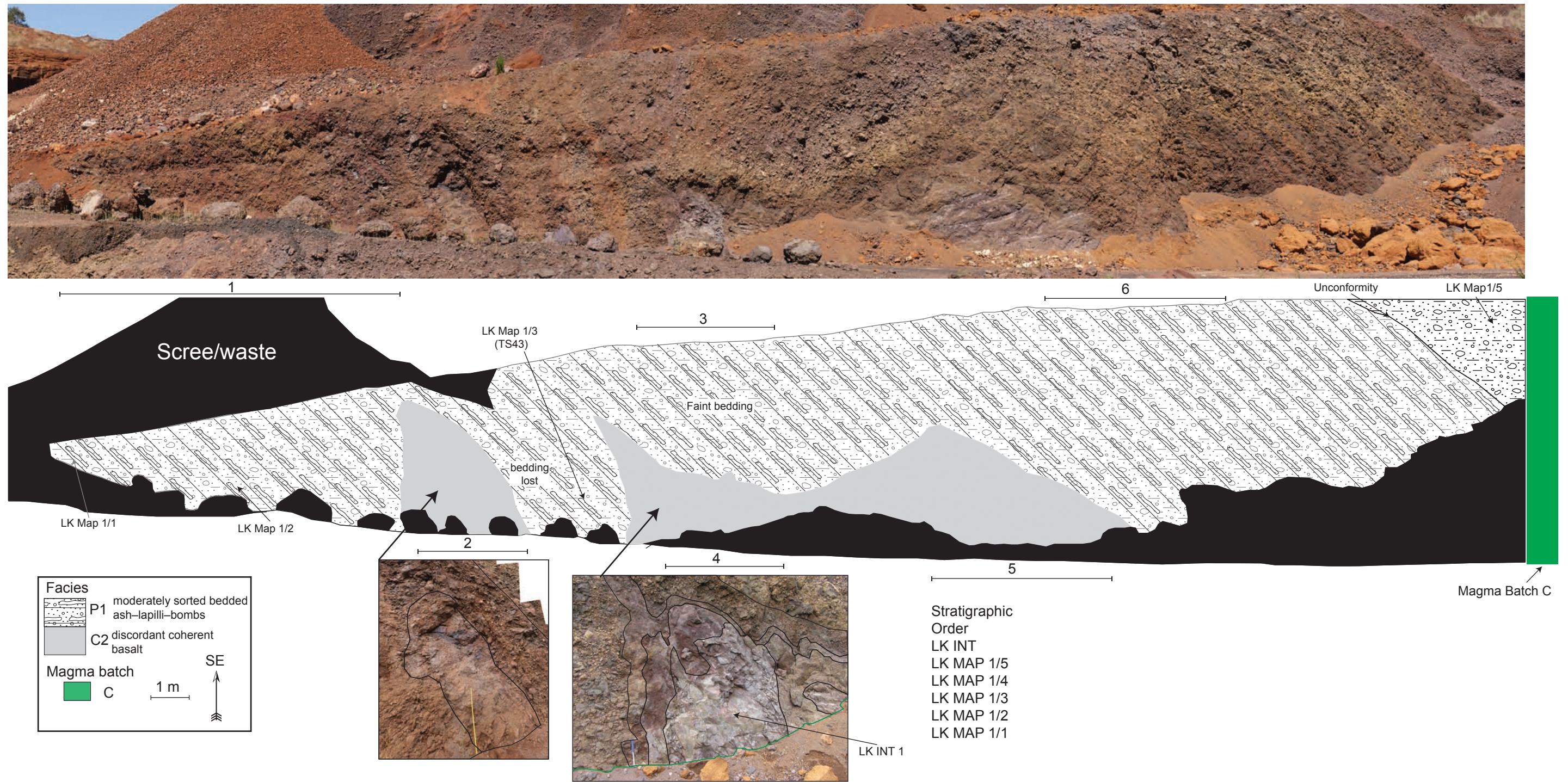
LK-L1-5
Bulk sample of coarser-grained scoria above LK-L1-4.

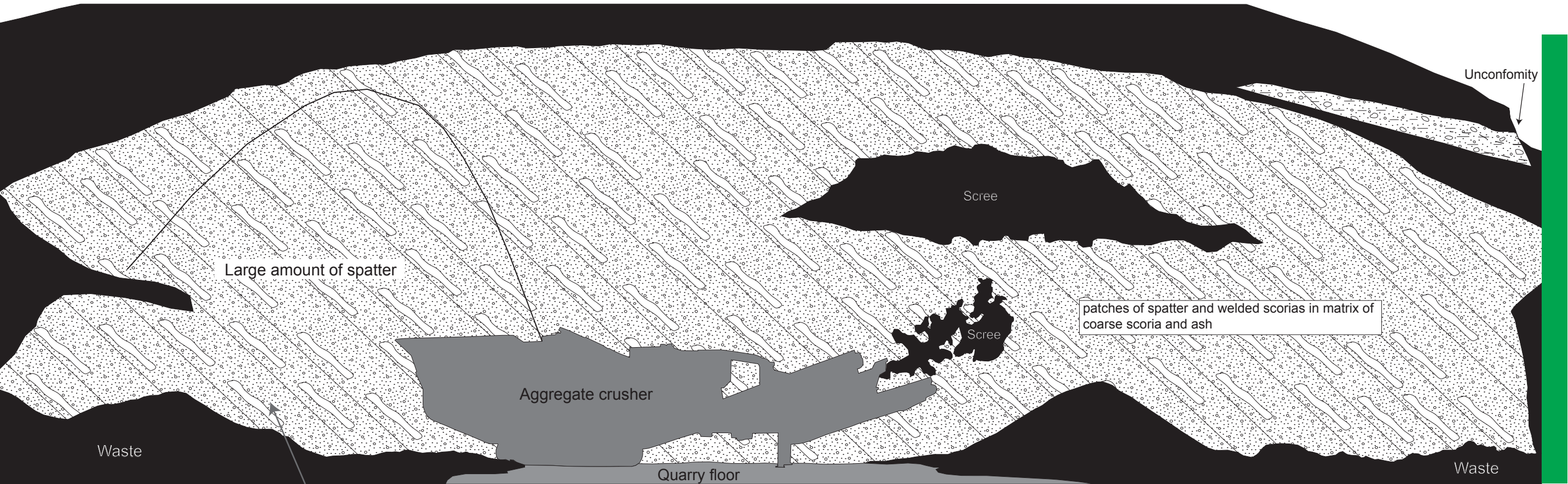
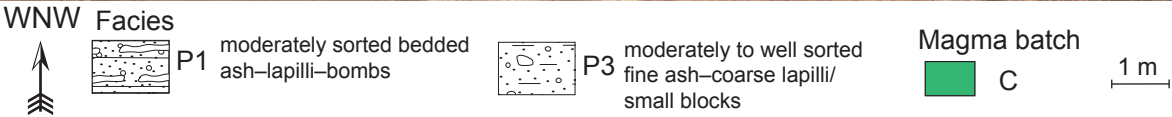
LK-L1-6
Finer-grained scoria (relative to that above) at the bottom, which has small breadcrust bombs and the odd large dense bomb.
Groundmass quite uniform in grainsize. Massive bed, no internal layering.
Clasts up to 70 mm.

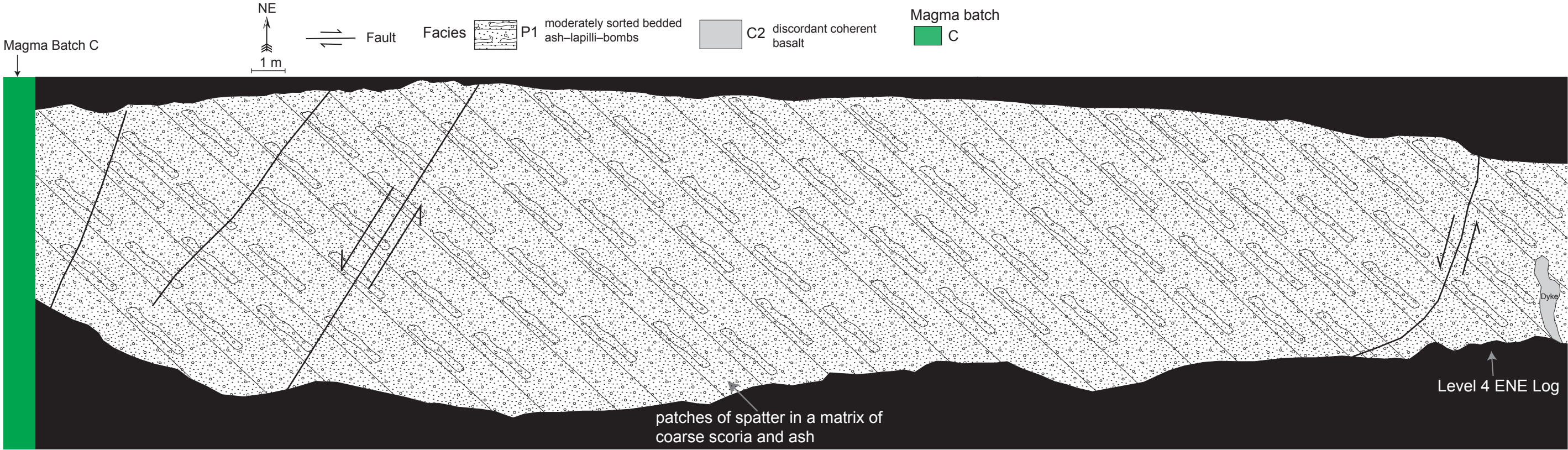
LK-L1-7
Coarser scoria — massive bed, very poorly sorted with a lot of spattery clasts up to 80 mm.

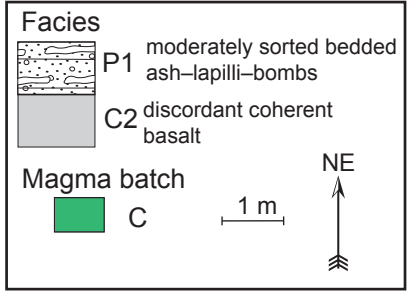
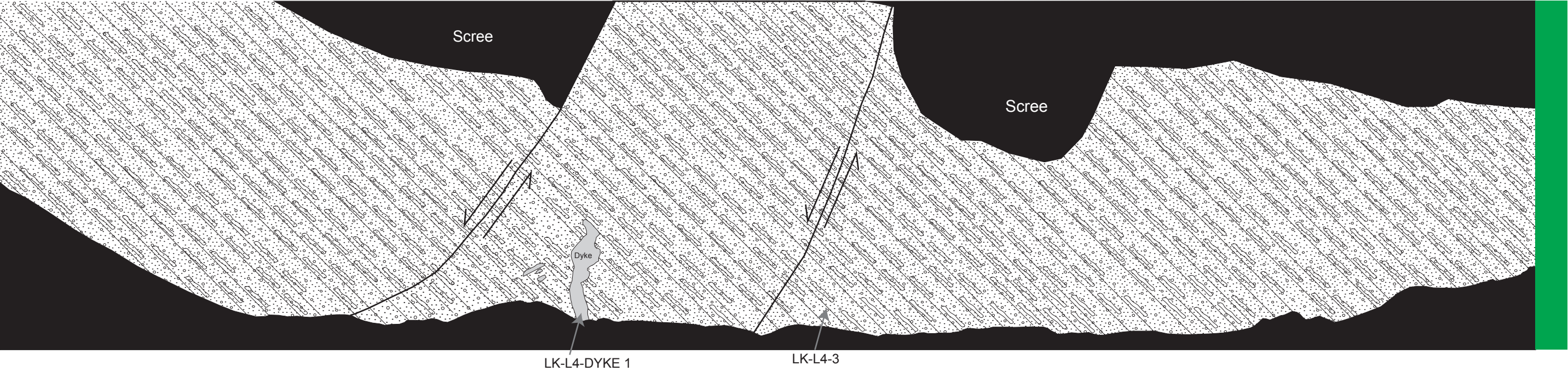
LK-L1-8
Below the Level 1 panorama is a small outcrop near some scree piles.
Same layering apparent as LK-L1-1, then below yellow scoria.
Layer of massive poorly sorted, very coarse grained scoriaceous material with breadcrust bombs up to 0.25 m and a coarse-ash matrix.

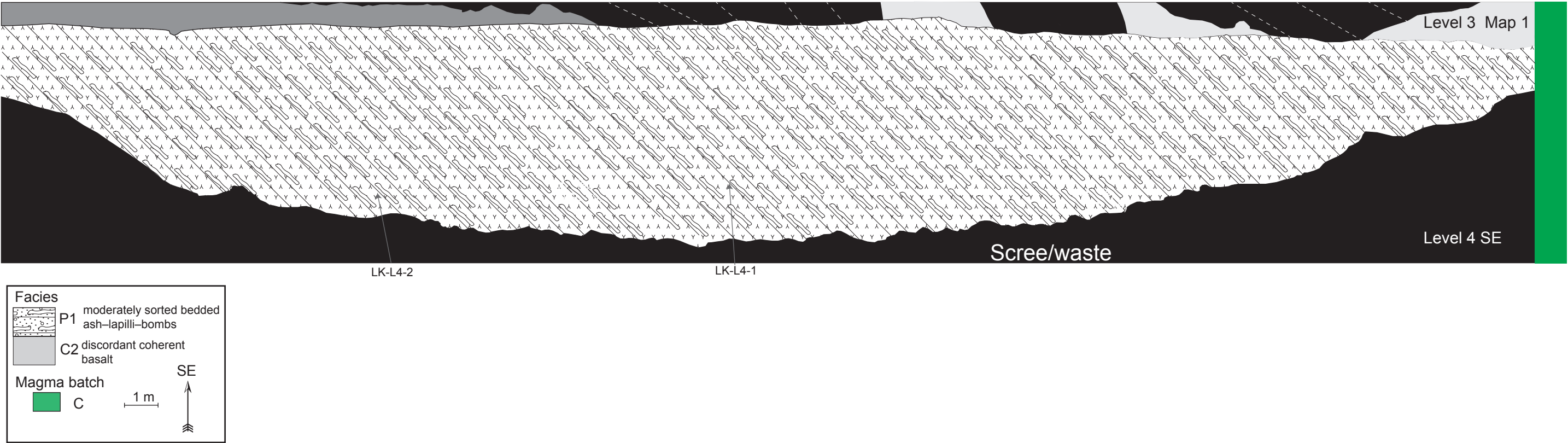












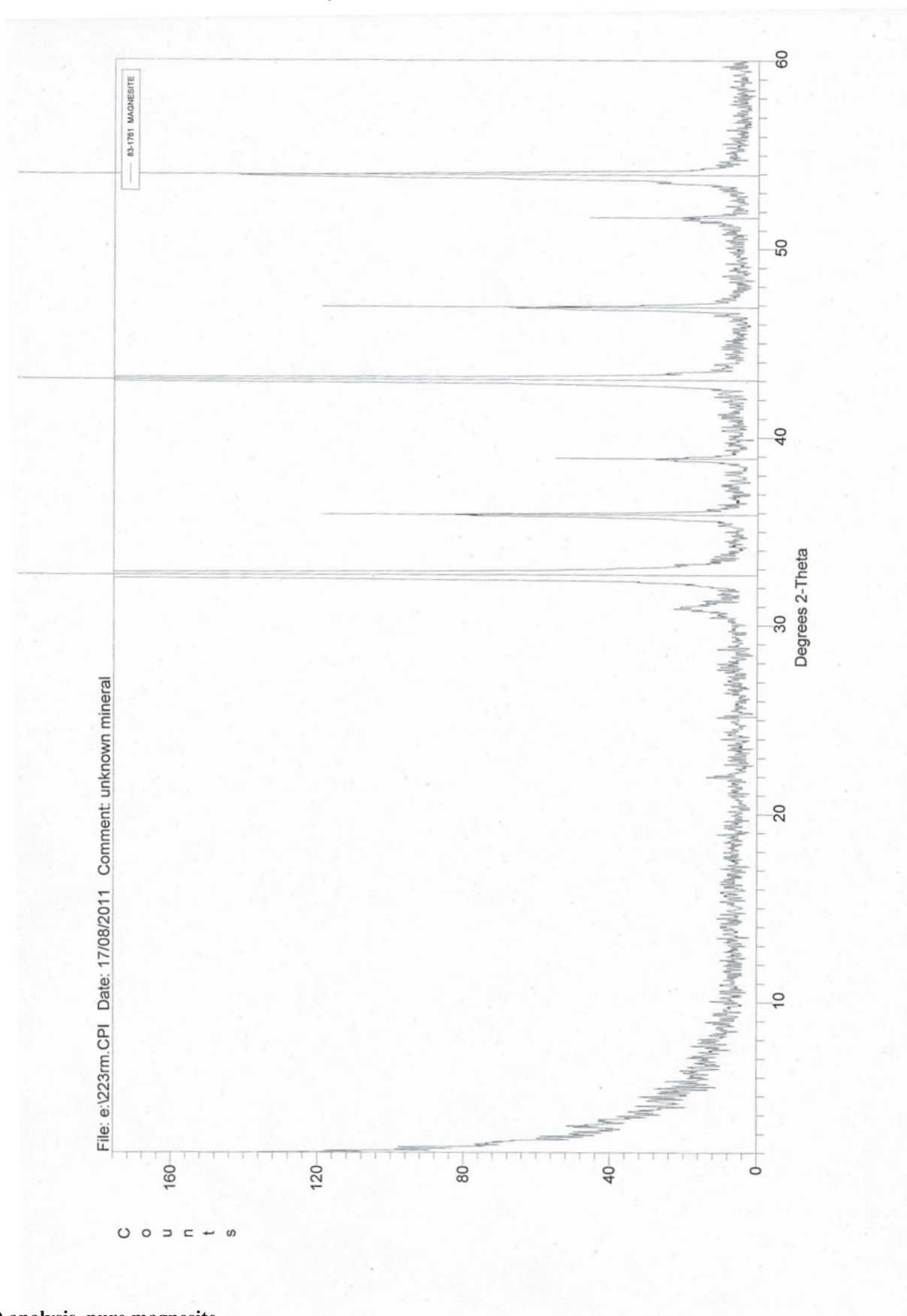
LK Quarry Level 4 SE -37.882774 142.307194





Appendix 5

X-Ray Diffraction results.



XRD analysis, pure magnesite.





Appendix 6

Major and trace geochemical data (raw) for Chapter 5.

See attached CD-ROM for normalised data.

Appendix 6

| | MRV2 | MRV9 | MRV10 | MRV11 | MRV12 | MRV13d | MRV16 | MRV24a | MRV3 | MRV7 | MRV21 | MRV17 |
|----------------------------------|--------|--------|--------|--------|--------|--------|--------|--------|--------|--------|--------|--------|
| Batch | A | A | A | A | A | A | A | A | A | A | A | A |
| SiO ₂ | 48.21 | 49.33 | 48.95 | 47.61 | 47.06 | 48.52 | 48.36 | 48.23 | 49.31 | 48.34 | 49.37 | 47.54 |
| TiO ₂ | 2.22 | 2.08 | 2.07 | 2.22 | 2.30 | 2.14 | 1.95 | 1.93 | 2.19 | 2.27 | 2.01 | 2.02 |
| Al ₂ O ₃ | 14.38 | 13.83 | 14.17 | 14.10 | 13.89 | 13.73 | 13.48 | 13.77 | 13.69 | 13.29 | 13.64 | 13.42 |
| Fe ₂ O ₃ * | 12.41 | 11.57 | 12.00 | 12.40 | 12.59 | 12.04 | 12.15 | 11.85 | 11.48 | 11.85 | 11.60 | 11.89 |
| MnO | 0.17 | 0.14 | 0.16 | 0.16 | 0.16 | 0.15 | 0.16 | 0.16 | 0.15 | 0.16 | 0.15 | 0.16 |
| MgO | 7.57 | 8.71 | 8.31 | 9.33 | 9.37 | 9.28 | 10.15 | 9.90 | 9.33 | 9.96 | 9.07 | 9.68 |
| CaO | 8.60 | 8.67 | 8.83 | 8.98 | 8.97 | 8.84 | 8.74 | 8.92 | 8.77 | 8.81 | 8.77 | 8.94 |
| Na ₂ O | 3.35 | 3.49 | 3.33 | 3.28 | 3.15 | 3.24 | 3.22 | 3.18 | 3.47 | 3.35 | 3.48 | 3.19 |
| K ₂ O | 1.15 | 1.07 | 1.04 | 1.17 | 1.24 | 1.07 | 1.03 | 0.98 | 1.14 | 1.21 | 1.07 | 1.08 |
| P ₂ O ₅ | 0.42 | 0.38 | 0.38 | 0.46 | 0.46 | 0.41 | 0.38 | 0.36 | 0.41 | 0.46 | 0.37 | 0.40 |
| Total | 98.48 | 99.27 | 99.24 | 99.71 | 99.19 | 99.40 | 99.62 | 99.28 | 99.92 | 99.70 | 99.53 | 98.29 |
| Mg# | 58.69 | 63.68 | 61.73 | 63.67 | 63.42 | 64.23 | 66.06 | 66.06 | 65.44 | 66.19 | 64.56 | 65.48 |
| V | 179.00 | 176.00 | 180.00 | 185.00 | 185.00 | 183.67 | 168.00 | 169.00 | 173.00 | 178.00 | 166.00 | 182.00 |
| Co | 55.00 | 47.90 | 53.50 | 54.10 | 53.10 | 51.63 | 55.60 | 52.10 | 50.90 | 52.70 | 50.30 | 54.05 |
| Ni | 178.50 | 205.00 | 192.10 | 167.20 | 181.40 | 207.00 | 229.60 | 205.30 | 187.10 | 213.30 | 195.70 | 187.35 |
| Cu | 52.40 | 43.10 | 56.30 | 48.90 | 49.90 | 44.80 | 49.50 | 61.50 | 54.30 | 56.30 | 62.60 | 59.05 |
| Zn | 80.00 | 79.00 | 85.00 | 82.00 | 91.00 | 83.00 | 83.00 | 83.00 | 82.50 | 88.00 | 74.00 | 89.00 |
| Ga | 19.10 | 19.10 | 18.30 | 20.00 | 19.20 | 18.63 | 18.90 | 18.00 | 18.05 | 18.70 | 19.10 | 19.35 |
| Rb | 18.50 | 18.10 | 18.50 | 19.90 | 18.30 | 18.20 | 18.10 | 16.30 | 19.60 | 22.00 | 18.10 | 20.30 |
| Sr | 539.70 | 495.80 | 517.60 | 602.20 | 607.10 | 503.07 | 489.90 | 488.90 | 527.70 | 554.40 | 507.00 | 513.95 |
| Y | 21.00 | 19.10 | 21.20 | 19.60 | 20.70 | 20.10 | 17.80 | 17.40 | 19.05 | 18.50 | 20.20 | 19.50 |
| Zr | 144.80 | 127.20 | 132.60 | 164.90 | 169.80 | 138.43 | 124.30 | 120.20 | 139.05 | 139.10 | 119.00 | 135.30 |
| Nb | 29.10 | 25.50 | 25.40 | 31.20 | 31.90 | 27.33 | 24.90 | 23.70 | 28.50 | 30.50 | 25.30 | 27.70 |
| Mo | 0.90 | 0.70 | 2.00 | 0.80 | 0.90 | 0.80 | 0.80 | 1.00 | 0.70 | 0.90 | 0.80 | 0.75 |
| Sn | 1.00 | 1.00 | 1.00 | 2.00 | 2.00 | 1.33 | 1.00 | 1.00 | 2.00 | 1.00 | 1.00 | 1.50 |
| Cs | <0.1 | <0.1 | <0.1 | 0.20 | <0.1 | 0.20 | 0.20 | 0.30 | 0.15 | 0.30 | <0.1 | 0.40 |
| Ba | 372.00 | 295.00 | 311.00 | 278.00 | 321.00 | 294.00 | 263.00 | 255.00 | 309.50 | 327.00 | 307.00 | 302.00 |
| La | 25.70 | 17.60 | 19.60 | 22.00 | 23.40 | 18.77 | 17.30 | 16.40 | 18.75 | 20.30 | 18.30 | 19.35 |
| Ce | 42.10 | 36.60 | 37.90 | 46.80 | 48.50 | 38.27 | 36.60 | 35.20 | 39.10 | 42.90 | 34.50 | 40.90 |
| Pr | 5.87 | 4.54 | 4.72 | 5.70 | 5.93 | 4.93 | 4.49 | 4.21 | 4.76 | 5.25 | 4.30 | 4.91 |
| Nd | 25.40 | 19.40 | 20.10 | 24.50 | 23.90 | 20.97 | 19.30 | 17.60 | 20.95 | 22.70 | 18.40 | 20.90 |
| Sm | 5.49 | 4.65 | 4.58 | 5.22 | 5.24 | 4.74 | 4.19 | 4.23 | 4.77 | 4.95 | 4.28 | 4.61 |
| Eu | 1.92 | 1.69 | 1.70 | 1.85 | 1.87 | 1.68 | 1.58 | 1.53 | 1.68 | 1.75 | 1.62 | 1.65 |
| Gd | 5.68 | 4.93 | 5.00 | 5.38 | 5.32 | 5.04 | 4.59 | 4.28 | 4.96 | 5.13 | 4.58 | 4.91 |
| Tb | 0.83 | 0.73 | 0.76 | 0.78 | 0.81 | 0.77 | 0.70 | 0.67 | 0.75 | 0.72 | 0.72 | 0.74 |
| Dy | 4.44 | 4.06 | 4.01 | 3.99 | 4.05 | 3.92 | 3.68 | 3.57 | 3.83 | 3.70 | 3.55 | 3.89 |
| Ho | 0.84 | 0.70 | 0.76 | 0.73 | 0.75 | 0.73 | 0.67 | 0.64 | 0.70 | 0.68 | 0.66 | 0.69 |
| Er | 1.87 | 1.76 | 1.82 | 1.75 | 1.84 | 1.79 | 1.69 | 1.71 | 1.72 | 1.70 | 1.71 | 1.74 |
| Tm | 0.25 | 0.23 | 0.24 | 0.25 | 0.24 | 0.24 | 0.21 | 0.20 | 0.22 | 0.21 | 0.21 | 0.23 |
| Yb | 1.39 | 1.29 | 1.43 | 1.38 | 1.40 | 1.44 | 1.33 | 1.36 | 1.29 | 1.24 | 1.35 | 1.41 |
| Lu | 0.21 | 0.20 | 0.22 | 0.20 | 0.19 | 0.21 | 0.19 | 0.17 | 0.19 | 0.18 | 0.17 | 0.20 |
| Hf | 3.70 | 3.30 | 3.30 | 3.90 | 4.80 | 3.30 | 3.30 | 3.10 | 3.60 | 3.10 | 2.90 | 3.15 |
| Ta | 1.70 | 1.40 | 1.50 | 2.00 | 2.10 | 1.63 | 1.50 | 1.40 | 1.75 | 1.90 | 1.60 | 1.65 |
| Pb | 1.20 | 1.30 | 1.30 | 1.20 | 1.70 | 1.20 | 1.00 | 1.00 | 0.90 | 1.10 | 1.40 | 1.30 |
| Th | 2.70 | 2.00 | 2.70 | 2.70 | 3.60 | 2.70 | 2.60 | 2.60 | 2.45 | 2.80 | 2.50 | 2.45 |
| U | 0.60 | 0.30 | 0.40 | 0.50 | 0.50 | 0.60 | 0.60 | 0.60 | 0.50 | 0.70 | 0.30 | 0.75 |

| | MRV18 | MRV 27 | MRV 28 | MRV 30 | SCrater | R4I | R4N_A | SC1 | SC2 | R4H | R4G | R4AJ |
|----------------------------------|--------|--------|--------|--------|---------|--------|--------|--------|--------|--------|--------|--------|
| Batch | A | A | A | A | A | A | A | A | A | B | B | B |
| SiO ₂ | 47.63 | 50.04 | 49.56 | 49.98 | 49.75 | 49.48 | 48.67 | 49.87 | 49.74 | 47.25 | 47.41 | 47.89 |
| TiO ₂ | 2.31 | 2.13 | 2.10 | 2.29 | 2.00 | 2.21 | 2.18 | 2.08 | 2.13 | 2.35 | 2.33 | 2.33 |
| Al ₂ O ₃ | 14.39 | 13.80 | 13.95 | 14.33 | 13.78 | 13.58 | 14.17 | 13.87 | 14.14 | 13.80 | 14.05 | 13.95 |
| Fe ₂ O ₃ * | 11.85 | 11.60 | 11.65 | 12.03 | 11.54 | 11.32 | 12.67 | 11.84 | 11.84 | 12.37 | 12.29 | 12.11 |
| MnO | 0.14 | 0.15 | 0.15 | 0.17 | 0.15 | 0.15 | 0.16 | 0.16 | 0.17 | 0.16 | 0.16 | 0.16 |
| MgO | 7.93 | 9.14 | 9.30 | 7.28 | 9.88 | 9.04 | 9.35 | 9.52 | 8.84 | 8.92 | 8.89 | 8.78 |
| CaO | 9.23 | 8.86 | 8.95 | 8.72 | 8.92 | 8.83 | 8.87 | 8.69 | 8.64 | 8.24 | 8.40 | 8.16 |
| Na ₂ O | 3.18 | 2.92 | 3.52 | 3.15 | 2.87 | 3.45 | 3.47 | 3.36 | 3.46 | 3.78 | 3.79 | 3.68 |
| K ₂ O | 1.14 | 1.03 | 1.10 | 1.17 | 0.93 | 1.16 | 1.25 | 1.09 | 1.13 | 1.56 | 1.54 | 1.48 |
| P ₂ O ₅ | 0.45 | 0.37 | 0.39 | 0.40 | 0.35 | 0.41 | 0.48 | 0.39 | 0.41 | 0.64 | 0.62 | 0.60 |
| Total | 98.25 | 100.04 | 100.67 | 99.52 | 100.17 | 99.63 | 101.28 | 100.87 | 100.50 | 99.07 | 99.48 | 99.14 |
| Mg# | 60.92 | 64.73 | 65.03 | 65.28 | 58.50 | 66.60 | 63.22 | 65.19 | 63.49 | 62.68 | 62.76 | 62.81 |
| V | 201.00 | 169.44 | 158.92 | 180.48 | 168.83 | 177.00 | 185.40 | 172.20 | 179.50 | 174.47 | 173.00 | 169.08 |
| Co | 50.60 | 51.47 | 49.17 | 52.42 | 54.64 | 48.50 | 56.17 | 58.44 | 57.99 | 50.21 | 49.20 | 49.38 |
| Ni | 121.50 | 214.95 | 221.18 | 183.79 | 233.65 | 159.50 | 206.80 | 237.70 | 216.20 | 157.10 | 149.30 | 160.50 |
| Cu | 44.20 | 53.46 | 46.90 | 54.04 | 50.69 | 31.50 | 44.90 | 51.30 | 24.90 | 43.65 | 29.70 | 45.40 |
| Zn | 75.00 | 113.48 | 115.71 | 117.70 | 104.61 | 62.00 | 112.00 | 107.00 | 106.00 | 120.58 | 83.00 | 118.17 |
| Ga | 19.50 | 19.47 | 18.63 | 20.46 | 19.01 | 19.40 | 20.52 | 19.68 | 20.23 | 19.61 | 21.50 | 19.52 |
| Rb | 20.60 | 17.38 | 18.75 | 23.15 | 14.91 | 21.70 | 24.22 | 16.78 | 18.99 | 29.81 | 31.90 | 29.13 |
| Sr | 616.00 | 496.12 | 483.39 | 522.07 | 505.99 | 525.30 | 560.50 | 508.10 | 509.60 | 720.50 | 727.60 | 708.10 |
| Y | 21.30 | 20.97 | 19.85 | 23.23 | 19.54 | 18.60 | 21.68 | 20.54 | 20.47 | 24.78 | 22.50 | 24.16 |
| Zr | 177.40 | 156.05 | 147.28 | 170.87 | 149.68 | 146.90 | 183.00 | 160.00 | 159.00 | 255.51 | 228.40 | 244.33 |
| Nb | 32.60 | 28.87 | 29.93 | 33.08 | 26.27 | 25.40 | 33.29 | 26.32 | 27.10 | 52.67 | 45.10 | 49.04 |
| Mo | 1.20 | 1.27 | 1.84 | 1.00 | 0.90 | 1.00 | 2.47 | 0.85 | 1.43 | 3.18 | 1.50 | 3.02 |
| Sn | 2.00 | 1.83 | 2.09 | 1.61 | 2.26 | 2.00 | 1.82 | 1.64 | 1.75 | 3.33 | 2.00 | 2.91 |
| Cs | 0.30 | 0.09 | 0.10 | 0.12 | 0.03 | 0.30 | 0.40 | 0.04 | 0.06 | 0.46 | 0.50 | 0.44 |
| Ba | 287.00 | 293.45 | 306.59 | 379.64 | 262.03 | 275.00 | 294.80 | 289.50 | 315.50 | 335.67 | 346.00 | 336.35 |
| La | 24.20 | 18.24 | 18.45 | 22.59 | 16.60 | 18.00 | 25.62 | 19.77 | 22.57 | 40.51 | 33.80 | 38.49 |
| Ce | 50.00 | 37.02 | 37.43 | 42.55 | 34.35 | 37.40 | 52.61 | 39.65 | 41.80 | 74.67 | 70.20 | 73.28 |
| Pr | 6.13 | 4.71 | 4.73 | 5.49 | 4.40 | 4.69 | 6.42 | 5.08 | 5.63 | 8.65 | 8.33 | 8.46 |
| Nd | 25.10 | 20.28 | 20.02 | 23.20 | 18.95 | 20.20 | 27.08 | 22.27 | 23.68 | 34.64 | 33.00 | 33.75 |
| Sm | 5.40 | 5.05 | 4.94 | 5.64 | 4.73 | 4.96 | 6.18 | 5.40 | 5.79 | 7.65 | 6.77 | 7.59 |
| Eu | 1.94 | 1.79 | 1.73 | 1.97 | 1.70 | 1.66 | 2.09 | 1.91 | 2.04 | 2.40 | 2.34 | 2.38 |
| Gd | 5.56 | 5.06 | 4.94 | 5.66 | 4.76 | 4.92 | 5.85 | 5.43 | 5.72 | 6.87 | 6.44 | 6.76 |
| Tb | 0.83 | 0.75 | 0.73 | 0.83 | 0.71 | 0.76 | 0.85 | 0.79 | 0.81 | 1.00 | 0.93 | 1.00 |
| Dy | 4.35 | 4.00 | 3.85 | 4.38 | 3.75 | 3.92 | 4.76 | 4.36 | 4.60 | 5.27 | 4.77 | 5.22 |
| Ho | 0.77 | 0.74 | 0.70 | 0.79 | 0.69 | 0.69 | 0.85 | 0.78 | 0.81 | 0.97 | 0.87 | 0.97 |
| Er | 1.92 | 1.82 | 1.75 | 1.97 | 1.71 | 1.64 | 2.10 | 1.94 | 1.95 | 2.24 | 1.87 | 2.23 |
| Tm | 0.25 | 0.23 | 0.22 | 0.25 | 0.22 | 0.22 | 0.27 | 0.25 | 0.25 | 0.27 | 0.26 | 0.27 |
| Yb | 1.50 | 1.37 | 1.31 | 1.46 | 1.28 | 1.36 | 1.53 | 1.47 | 1.43 | 1.58 | 1.50 | 1.61 |
| Lu | 0.21 | 0.19 | 0.18 | 0.20 | 0.18 | 0.19 | 0.21 | 0.20 | 0.19 | 0.22 | 0.22 | 0.22 |
| Hf | 3.90 | 3.48 | 3.24 | 3.80 | 3.29 | 3.60 | 4.19 | 3.70 | 3.88 | 5.61 | 5.60 | 5.53 |
| Ta | 2.00 | 1.65 | 1.70 | 1.90 | 1.52 | 1.50 | 2.05 | 1.59 | 1.69 | 3.06 | 2.90 | 2.91 |
| Pb | 1.10 | 2.24 | 1.64 | 1.80 | 1.54 | 0.60 | 2.30 | 1.50 | 1.50 | 3.02 | 1.20 | 3.07 |
| Th | 2.60 | 2.29 | 2.38 | 2.67 | 2.15 | 2.60 | 3.00 | 2.30 | 2.39 | 4.56 | 4.90 | 4.55 |
| U | 0.80 | 0.21 | 0.20 | 0.24 | 0.30 | 0.60 | 0.85 | 0.19 | 0.35 | 1.23 | 1.40 | 1.22 |

Appendix 6

| | R4AH | R4C | R4F | R4AP | R4AM | R4U | R4T | R3A | R3H | R4N_B | SAT 1 | SAT 2 |
|----------------------------------|--------|--------|--------|--------|--------|--------|--------|--------|--------|--------|--------|--------|
| Batch | B | B | B | B | B | B | B | B | B | B | B | B |
| SiO ₂ | 47.41 | 47.62 | 47.39 | 47.04 | 46.87 | 46.55 | 47.03 | 47.41 | 47.48 | 48.71 | 43.87 | 46.54 |
| TiO ₂ | 2.33 | 2.40 | 2.38 | 2.42 | 2.49 | 2.46 | 2.49 | 2.44 | 2.33 | 2.19 | 2.75 | 2.74 |
| Al ₂ O ₃ | 13.87 | 13.99 | 13.92 | 13.93 | 14.07 | 14.13 | 14.10 | 14.16 | 14.12 | 14.08 | 13.75 | 14.30 |
| Fe ₂ O ₃ * | 12.34 | 12.20 | 12.16 | 12.36 | 12.23 | 12.36 | 12.38 | 12.56 | 12.44 | 12.47 | 12.20 | 12.68 |
| MnO | 0.16 | 0.16 | 0.16 | 0.16 | 0.16 | 0.16 | 0.16 | 0.17 | 0.17 | 0.16 | 0.16 | 0.16 |
| MgO | 8.81 | 8.68 | 8.79 | 8.71 | 8.45 | 8.47 | 8.50 | 8.62 | 8.81 | 8.75 | 7.16 | 8.33 |
| CaO | 8.20 | 8.19 | 8.23 | 8.22 | 8.19 | 8.31 | 8.20 | 8.17 | 8.24 | 8.24 | 7.51 | 8.08 |
| Na ₂ O | 3.57 | 3.59 | 3.63 | 3.96 | 4.22 | 3.95 | 3.84 | 3.22 | 3.84 | 3.15 | 3.74 | 4.05 |
| K ₂ O | 1.52 | 1.65 | 1.55 | 1.42 | 1.54 | 1.36 | 1.53 | 1.59 | 1.44 | 1.36 | 1.94 | 2.05 |
| P ₂ O ₅ | 0.64 | 0.66 | 0.65 | 0.70 | 0.72 | 0.70 | 0.72 | 0.65 | 0.61 | 0.58 | 0.87 | 0.84 |
| Total | 98.85 | 99.14 | 98.86 | 98.92 | 98.94 | 98.45 | 98.95 | 98.99 | 99.48 | 99.69 | 93.95 | 99.77 |
| Mg# | 62.45 | 62.37 | 62.74 | 62.14 | 61.68 | 61.48 | 61.53 | 61.52 | 62.26 | 62.04 | 57.75 | 60.48 |
| V | 169.28 | 171.00 | 174.00 | 164.00 | 163.58 | 162.00 | 167.00 | 155.13 | 169.95 | 170.50 | 161.68 | 161.37 |
| Co | 48.38 | 46.60 | 47.70 | 47.30 | 48.47 | 47.70 | 46.50 | 50.12 | 47.98 | 53.30 | 49.70 | 50.16 |
| Ni | 151.50 | 147.70 | 147.10 | 142.20 | 149.50 | 128.60 | 131.90 | 169.12 | 153.73 | 181.20 | 170.10 | 185.13 |
| Cu | 46.48 | 29.50 | 39.40 | 10.40 | 28.79 | 18.70 | 11.80 | 46.88 | 42.57 | 34.90 | 46.74 | 47.76 |
| Zn | 118.17 | 105.00 | 49.00 | 32.00 | 121.04 | 44.00 | 46.00 | 128.48 | 138.46 | 121.00 | 133.79 | 126.28 |
| Ga | 19.43 | 20.40 | 20.20 | 20.80 | 20.55 | 22.00 | 21.50 | 23.01 | 22.35 | 21.62 | 21.97 | 21.52 |
| Rb | 29.61 | 33.70 | 33.00 | 29.10 | 23.26 | 31.70 | 32.80 | 29.19 | 31.72 | 30.84 | 33.65 | 29.32 |
| Sr | 725.00 | 758.50 | 737.30 | 745.70 | 876.20 | 775.80 | 820.80 | 783.85 | 682.51 | 677.30 | 735.01 | 684.98 |
| Y | 25.39 | 22.50 | 22.60 | 23.00 | 25.70 | 22.80 | 24.10 | 27.83 | 26.95 | 24.20 | 26.06 | 25.62 |
| Zr | 252.34 | 244.50 | 235.60 | 249.60 | 285.05 | 254.30 | 262.80 | 306.35 | 285.79 | 245.00 | 287.46 | 255.20 |
| Nb | 50.42 | 49.10 | 47.50 | 51.10 | 61.38 | 51.40 | 55.30 | 63.45 | 58.49 | 45.19 | 58.34 | 51.57 |
| Mo | 3.05 | 2.50 | 0.90 | 0.50 | 3.51 | 1.00 | 1.00 | 2.93 | 4.19 | 2.92 | 3.17 | 2.14 |
| Sn | 2.95 | 2.00 | 2.00 | 2.00 | 3.09 | 2.00 | 2.00 | 2.04 | 2.77 | 2.15 | 2.16 | 2.35 |
| Cs | 0.45 | 0.60 | 0.60 | 0.50 | 0.43 | 0.70 | 0.50 | 0.40 | 0.50 | 0.49 | 0.46 | 0.40 |
| Ba | 336.16 | 367.00 | 357.00 | 379.00 | 420.44 | 395.00 | 403.00 | 414.18 | 380.48 | 330.40 | 383.82 | 346.77 |
| La | 39.54 | 36.60 | 36.30 | 37.90 | 46.88 | 38.80 | 40.10 | 44.39 | 40.69 | 36.65 | 40.76 | 36.44 |
| Ce | 74.48 | 75.10 | 72.50 | 77.00 | 88.25 | 77.60 | 83.00 | 88.13 | 80.99 | 72.24 | 81.27 | 72.25 |
| Pr | 8.66 | 8.91 | 8.68 | 8.96 | 10.13 | 9.26 | 9.77 | 10.54 | 9.69 | 8.64 | 9.65 | 8.71 |
| Nd | 34.29 | 35.40 | 34.90 | 37.00 | 39.68 | 37.60 | 40.70 | 42.03 | 38.74 | 35.45 | 38.48 | 35.17 |
| Sm | 7.73 | 7.19 | 7.01 | 7.22 | 8.63 | 7.49 | 7.77 | 8.78 | 8.19 | 7.60 | 8.11 | 7.53 |
| Eu | 2.43 | 2.36 | 2.33 | 2.42 | 2.68 | 2.40 | 2.47 | 2.83 | 2.66 | 2.53 | 2.65 | 2.47 |
| Gd | 6.92 | 6.50 | 6.67 | 6.73 | 7.76 | 6.76 | 6.99 | 8.21 | 7.73 | 6.93 | 7.59 | 7.07 |
| Tb | 1.03 | 0.97 | 0.95 | 0.98 | 1.11 | 0.98 | 1.00 | 1.12 | 1.06 | 0.99 | 1.04 | 0.98 |
| Dy | 5.33 | 4.86 | 4.47 | 4.74 | 5.66 | 4.99 | 5.03 | 5.65 | 5.41 | 5.30 | 5.31 | 5.07 |
| Ho | 0.99 | 0.88 | 0.85 | 0.88 | 1.03 | 0.84 | 0.88 | 0.99 | 0.95 | 0.94 | 0.92 | 0.90 |
| Er | 2.27 | 2.01 | 1.99 | 2.04 | 2.36 | 2.09 | 2.15 | 2.38 | 2.33 | 2.29 | 2.23 | 2.21 |
| Tm | 0.27 | 0.27 | 0.26 | 0.27 | 0.28 | 0.26 | 0.27 | 0.29 | 0.29 | 0.29 | 0.27 | 0.27 |
| Yb | 1.60 | 1.56 | 1.48 | 1.51 | 1.64 | 1.53 | 1.55 | 1.73 | 1.67 | 1.67 | 1.61 | 1.63 |
| Lu | 0.22 | 0.22 | 0.22 | 0.22 | 0.22 | 0.20 | 0.22 | 0.23 | 0.23 | 0.22 | 0.22 | 0.22 |
| Hf | 5.48 | 6.00 | 5.50 | 5.60 | 6.29 | 5.80 | 6.20 | 6.33 | 5.94 | 5.39 | 5.92 | 5.33 |
| Ta | 2.96 | 3.20 | 2.80 | 2.90 | 3.74 | 3.30 | 3.30 | 3.61 | 3.39 | 2.84 | 3.12 | 2.70 |
| Pb | 2.99 | 2.70 | 1.00 | 0.40 | 2.76 | 0.70 | 0.40 | 4.22 | 2.72 | 3.20 | 3.27 | 26.64 |
| Th | 4.64 | 4.90 | 5.20 | 5.40 | 5.49 | 5.20 | 5.70 | 5.42 | 5.02 | 4.34 | 4.99 | 4.50 |
| U | 1.23 | 1.30 | 1.20 | 1.50 | 1.46 | 1.40 | 1.40 | 1.31 | 1.36 | 1.18 | 1.40 | 1.16 |

| | LK Sc | N Cone | LK Intr | LB2 | LK-L1-1 | LK-L1-2 | LK-L1-7 | LK-L1-8 | LK-L2-1 | LK-L2-2 | LKENT | LK ENT2 |
|----------------------------------|--------|--------|---------|--------|---------|---------|---------|---------|---------|---------|--------|---------|
| Batch | C | C | C | C | C | C | C | C | C | C | C | C |
| SiO ₂ | 48.13 | 48.25 | 47.14 | 46.43 | 47.08 | 46.09 | 46.64 | 46.76 | 46.39 | 45.86 | 45.72 | 46.57 |
| TiO ₂ | 2.44 | 2.24 | 2.15 | 2.47 | 2.69 | 2.67 | 2.61 | 2.69 | 2.65 | 2.54 | 2.75 | 2.62 |
| Al ₂ O ₃ | 14.51 | 14.15 | 13.59 | 14.35 | 14.77 | 14.47 | 14.58 | 14.50 | 14.51 | 13.89 | 14.29 | 14.39 |
| Fe ₂ O ₃ * | 12.79 | 12.52 | 12.38 | 12.47 | 13.08 | 12.88 | 12.69 | 12.94 | 12.75 | 12.25 | 12.76 | 12.64 |
| MnO | 0.16 | 0.16 | 0.16 | 0.17 | 0.17 | 0.17 | 0.17 | 0.17 | 0.17 | 0.16 | 0.17 | 0.17 |
| MgO | 7.56 | 9.28 | 10.68 | 8.33 | 6.83 | 6.60 | 8.27 | 7.29 | 8.35 | 8.38 | 8.13 | 8.27 |
| CaO | 7.94 | 8.81 | 9.17 | 8.05 | 8.17 | 8.14 | 7.40 | 7.91 | 8.13 | 7.35 | 7.87 | 7.92 |
| Na ₂ O | 3.18 | 3.39 | 3.58 | 4.00 | 4.30 | 4.57 | 4.04 | 3.99 | 4.05 | 3.22 | 4.11 | 3.86 |
| K ₂ O | 1.49 | 1.21 | 1.34 | 1.89 | 1.87 | 1.53 | 2.06 | 1.96 | 2.07 | 1.90 | 2.26 | 2.09 |
| P ₂ O ₅ | 0.65 | 0.46 | 0.47 | 0.78 | 0.89 | 0.88 | 0.85 | 0.88 | 0.88 | 0.80 | 0.90 | 0.86 |
| Total | 98.85 | 100.47 | 100.66 | 98.94 | 99.85 | 97.99 | 99.31 | 99.09 | 99.94 | 96.35 | 98.95 | 99.38 |
| Mg# | 57.93 | 63.32 | 66.77 | 60.88 | 54.88 | 54.41 | 60.29 | 56.75 | 60.40 | 61.44 | 59.75 | 60.38 |
| V | 146.04 | 163.41 | 133.26 | 166.40 | 162.00 | 163.80 | 169.80 | 163.90 | 170.30 | 149.10 | 168.60 | 164.40 |
| Co | 49.10 | 48.23 | 47.30 | 51.67 | 52.22 | 54.94 | 53.21 | 53.05 | 52.91 | 50.67 | 52.72 | 52.36 |
| Ni | 172.67 | 152.63 | 151.53 | 171.00 | 166.30 | 180.80 | 171.60 | 171.60 | 167.40 | 161.30 | 164.80 | 164.70 |
| Cu | 35.56 | 41.62 | 40.83 | 37.80 | 37.70 | 24.60 | 33.70 | 24.70 | 37.70 | 42.30 | 34.40 | 38.70 |
| Zn | 273.22 | 138.73 | 141.88 | 129.00 | 130.00 | 135.00 | 134.00 | 136.00 | 135.00 | 129.00 | 138.00 | 134.00 |
| Ga | 24.96 | 23.74 | 24.53 | 23.20 | 24.14 | 25.06 | 24.35 | 24.36 | 24.26 | 23.38 | 24.66 | 23.83 |
| Rb | 33.12 | 43.52 | 22.03 | 40.86 | 36.20 | 33.71 | 45.42 | 43.87 | 46.63 | 44.64 | 48.86 | 44.78 |
| Sr | 971.32 | 892.19 | 969.15 | 863.80 | 921.10 | 961.90 | 896.10 | 940.00 | 970.50 | 990.40 | 991.80 | 919.60 |
| Y | 28.88 | 28.66 | 28.33 | 26.83 | 27.64 | 27.96 | 27.20 | 27.81 | 27.80 | 26.36 | 27.72 | 27.27 |
| Zr | 394.55 | 354.68 | 385.68 | 317.00 | 353.00 | 365.00 | 350.00 | 356.00 | 364.00 | 346.00 | 369.00 | 337.00 |
| Nb | 71.69 | 77.15 | 76.23 | 64.08 | 71.11 | 73.34 | 70.46 | 71.63 | 71.80 | 68.60 | 76.40 | 70.21 |
| Mo | 10.06 | 3.60 | 2.88 | 4.20 | 4.27 | 4.03 | 4.38 | 3.92 | 4.50 | 3.83 | 4.53 | 4.12 |
| Sn | 8.02 | 10.50 | 2.79 | 2.37 | 2.68 | 2.76 | 2.76 | 2.78 | 2.76 | 2.62 | 2.86 | 2.59 |
| Cs | 0.51 | 0.73 | 0.70 | 0.63 | 0.51 | 0.61 | 0.69 | 0.60 | 0.68 | 0.64 | 0.71 | 0.69 |
| Ba | 564.66 | 503.72 | 554.75 | 453.70 | 501.90 | 523.90 | 513.10 | 525.60 | 555.30 | 487.10 | 558.50 | 509.90 |
| La | 58.43 | 53.25 | 56.87 | 51.63 | 56.43 | 56.98 | 54.97 | 57.61 | 57.11 | 54.88 | 59.43 | 55.31 |
| Ce | 115.65 | 105.18 | 112.78 | 99.74 | 110.28 | 110.03 | 106.36 | 111.20 | 111.42 | 106.04 | 115.30 | 107.28 |
| Pr | 13.55 | 12.49 | 13.36 | 11.99 | 13.41 | 13.45 | 12.88 | 13.26 | 13.24 | 12.67 | 13.97 | 12.86 |
| Nd | 53.05 | 49.32 | 52.26 | 47.78 | 52.26 | 53.58 | 50.52 | 53.29 | 52.38 | 50.36 | 54.78 | 51.39 |
| Sm | 10.71 | 10.03 | 10.49 | 9.63 | 10.66 | 10.81 | 10.33 | 10.83 | 10.73 | 10.31 | 11.12 | 10.34 |
| Eu | 3.39 | 3.20 | 3.32 | 3.16 | 3.40 | 3.46 | 3.34 | 3.45 | 3.38 | 3.25 | 3.53 | 3.30 |
| Gd | 9.59 | 9.14 | 9.54 | 8.41 | 9.19 | 9.05 | 8.94 | 8.97 | 9.07 | 8.61 | 9.23 | 8.99 |
| Tb | 1.26 | 1.20 | 1.24 | 1.14 | 1.24 | 1.20 | 1.19 | 1.22 | 1.21 | 1.15 | 1.25 | 1.19 |
| Dy | 6.15 | 5.99 | 6.04 | 6.16 | 6.50 | 6.43 | 6.24 | 6.53 | 6.45 | 6.18 | 6.49 | 6.29 |
| Ho | 1.04 | 1.03 | 1.01 | 1.03 | 1.09 | 1.08 | 1.06 | 1.08 | 1.08 | 1.03 | 1.09 | 1.06 |
| Er | 2.37 | 2.41 | 2.33 | 2.46 | 2.55 | 2.57 | 2.48 | 2.58 | 2.53 | 2.42 | 2.50 | 2.49 |
| Tm | 0.28 | 0.29 | 0.27 | 0.31 | 0.32 | 0.31 | 0.31 | 0.31 | 0.31 | 0.30 | 0.30 | 0.30 |
| Yb | 1.61 | 1.65 | 1.57 | 1.75 | 1.72 | 1.73 | 1.70 | 1.74 | 1.70 | 1.64 | 1.64 | 1.69 |
| Lu | 0.20 | 0.22 | 0.20 | 0.23 | 0.24 | 0.23 | 0.23 | 0.23 | 0.23 | 0.21 | 0.22 | 0.23 |
| Hf | 7.91 | 7.25 | 7.81 | 6.99 | 7.65 | 7.71 | 7.42 | 7.64 | 7.90 | 7.49 | 7.84 | 7.22 |
| Ta | 3.32 | 4.41 | 3.61 | 4.02 | 4.44 | 4.47 | 4.33 | 4.46 | 4.44 | 4.24 | 4.78 | 4.28 |
| Pb | 5.69 | 14.51 | 7.39 | 3.80 | 3.30 | 3.30 | 4.30 | 3.00 | 4.00 | 3.80 | 4.20 | 3.90 |
| Th | 7.20 | 6.42 | 7.04 | 6.01 | 6.59 | 6.63 | 6.43 | 6.58 | 6.53 | 6.35 | 6.93 | 6.44 |
| U | 1.86 | 1.73 | 1.83 | 1.67 | 1.80 | 1.71 | 1.78 | 1.74 | 1.78 | 1.67 | 1.90 | 1.75 |

Appendix 6

| | LK M1 1 | LK M1 2 | LK M1 3 | LK M1 4 | LK M1 5 | LK-L4-1 | LK-L4-2 | LK-L4-3 | LK M2-1 | DYKE1 | SPAT |
|----------------------------------|---------|---------|---------|---------|---------|---------|---------|---------|---------|--------|--------|
| Batch | C | C | C | C | C | C | C | C | C | C | C |
| SiO ₂ | 47.38 | 46.28 | 46.35 | 46.15 | 45.92 | 46.02 | 46.58 | 46.74 | 47.00 | 46.53 | 45.55 |
| TiO ₂ | 2.86 | 2.81 | 2.81 | 2.77 | 2.75 | 2.84 | 2.79 | 2.77 | 2.86 | 2.83 | 2.62 |
| Al ₂ O ₃ | 15.06 | 14.54 | 14.56 | 14.46 | 14.39 | 14.27 | 14.56 | 14.46 | 14.91 | 14.35 | 13.86 |
| Fe ₂ O ₃ * | 12.69 | 12.67 | 12.86 | 12.84 | 12.65 | 12.33 | 12.50 | 12.76 | 13.12 | 12.94 | 12.49 |
| MnO | 0.17 | 0.16 | 0.17 | 0.17 | 0.16 | 0.16 | 0.16 | 0.16 | 0.17 | 0.16 | 0.18 |
| MgO | 7.61 | 7.43 | 7.52 | 7.79 | 8.17 | 7.46 | 7.40 | 7.70 | 6.91 | 8.01 | 8.00 |
| CaO | 7.75 | 7.56 | 7.86 | 7.88 | 7.87 | 7.56 | 7.50 | 7.51 | 8.14 | 7.86 | 7.71 |
| Na ₂ O | 3.63 | 5.16 | 3.79 | 4.65 | 3.87 | 4.00 | 4.70 | 4.26 | 4.59 | 4.64 | 3.04 |
| K ₂ O | 1.93 | 1.62 | 2.04 | 1.45 | 2.10 | 2.00 | 2.41 | 2.29 | 1.21 | 1.60 | 1.83 |
| P ₂ O ₅ | 0.96 | 0.94 | 0.95 | 0.93 | 0.90 | 0.94 | 0.93 | 0.91 | 0.96 | 0.98 | 0.91 |
| Total | 100.03 | 99.16 | 98.90 | 99.09 | 98.78 | 97.57 | 99.53 | 99.56 | 99.87 | 99.90 | 96.18 |
| Mg# | 58.28 | 57.735 | 57.666 | 58.562 | 60.071 | 58.495 | 57.966 | 58.432 | 55.093 | 59.049 | 59.872 |
| V | 142.50 | 150.3 | 144.6 | 151.4 | 157.6 | 145.6 | 145.4 | 142.8 | 138.4 | 158.2 | 154.2 |
| Co | 51.84 | 50.92 | 51.23 | 56.82 | 53.3 | 51.21 | 49.68 | 51.41 | 52.69 | 52.72 | 52.58 |
| Ni | 176.30 | 157.9 | 166.4 | 171.3 | 160.8 | 159.4 | 152.5 | 170 | 158.2 | 169.2 | 161.6 |
| Cu | 7.00 | 25.2 | 30.2 | 37.5 | 40.6 | 29.3 | 55.6 | 27.3 | 26.1 | 38.9 | 37.4 |
| Zn | 148.00 | 146 | 140 | 139 | 135 | 142 | 137 | 141 | 135 | 139 | 138 |
| Ga | 26.15 | 25.64 | 24.78 | 24.95 | 24.09 | 25.6 | 25.52 | 25.13 | 25.09 | 24.98 | 23.22 |
| Rb | 40.47 | 40.68 | 33.77 | 44.57 | 45.6 | 28.48 | 43.68 | 41.6 | 24.63 | 20.37 | 34.84 |
| Sr | 1067.50 | 1070.5 | 1034.4 | 1009.2 | 936.2 | 1063.9 | 1039.1 | 1015.1 | 1020.2 | 1023.4 | 1068.1 |
| Y | 27.03 | 26.8 | 27.73 | 27.72 | 26.82 | 26.68 | 26.14 | 25.48 | 27.6 | 27.5 | 29.03 |
| Zr | 393.00 | 396 | 377 | 372 | 350 | 393 | 395 | 376 | 375 | 380 | 342 |
| Nb | 83.03 | 82.96 | 78.914 | 78.044 | 72.431 | 82.263 | 81.708 | 78.76 | 79.163 | 78.653 | 69.207 |
| Mo | 3.04 | 4.74 | 3.45 | 2.69 | 3.91 | 3.47 | 4.61 | 3.64 | 2.53 | 3.55 | 3.46 |
| Sn | 2.90 | 3.05 | 2.97 | 3.65 | 2.99 | 2.78 | 2.77 | 2.78 | 2.9 | 2.93 | 3.81 |
| Cs | 0.62 | 0.503 | 0.728 | 0.657 | 0.688 | 0.706 | 0.745 | 0.575 | 0.357 | 0.793 | 0.679 |
| Ba | 601.40 | 598.3 | 574.8 | 569.8 | 547 | 603.5 | 588.5 | 576.8 | 578.6 | 579.4 | 598.6 |
| La | 64.19 | 63.34 | 61.73 | 60.27 | 57.47 | 62.54 | 61.32 | 59.34 | 61.06 | 61.7 | 58.83 |
| Ce | 123.35 | 121.52 | 119.54 | 118.52 | 113.1 | 119.81 | 118.8 | 115.83 | 120.89 | 119.67 | 111.04 |
| Pr | 14.58 | 14.347 | 14.153 | 13.894 | 13.362 | 14.083 | 14.014 | 13.665 | 14.063 | 14.097 | 13.565 |
| Nd | 57.50 | 56.67 | 56.6 | 55.08 | 53.07 | 55.33 | 55.28 | 53.9 | 56.47 | 56.31 | 54.26 |
| Sm | 11.56 | 11.244 | 11.135 | 10.933 | 10.762 | 11.008 | 10.92 | 10.692 | 11.379 | 11.196 | 10.934 |
| Eu | 3.61 | 3.61 | 3.557 | 3.465 | 3.428 | 3.525 | 3.491 | 3.426 | 3.659 | 3.574 | 3.521 |
| Gd | 9.59 | 9.405 | 9.365 | 9.06 | 9.065 | 9.304 | 9.182 | 8.914 | 9.495 | 9.332 | 9.346 |
| Tb | 1.26 | 1.255 | 1.244 | 1.218 | 1.21 | 1.216 | 1.197 | 1.180 | 1.284 | 1.246 | 1.243 |
| Dy | 6.39 | 6.336 | 6.566 | 6.423 | 6.36 | 6.306 | 6.168 | 6.153 | 6.602 | 6.531 | 6.68 |
| Ho | 1.06 | 1.045 | 1.076 | 1.065 | 1.057 | 1.029 | 1.01 | 0.998 | 1.088 | 1.075 | 1.117 |
| Er | 2.40 | 2.404 | 2.485 | 2.46 | 2.463 | 2.362 | 2.298 | 2.303 | 2.546 | 2.533 | 2.723 |
| Tm | 0.29 | 0.285 | 0.295 | 0.298 | 0.300 | 0.283 | 0.275 | 0.272 | 0.303 | 0.296 | 0.325 |
| Yb | 1.54 | 1.526 | 1.633 | 1.646 | 1.637 | 1.512 | 1.448 | 1.454 | 1.655 | 1.589 | 1.799 |
| Lu | 0.20 | 0.191 | 0.211 | 0.210 | 0.223 | 0.190 | 0.187 | 0.187 | 0.217 | 0.209 | 0.239 |
| Hf | 8.46 | 8.39 | 8.11 | 7.83 | 7.62 | 8.29 | 8.25 | 7.99 | 8.1 | 7.97 | 7.42 |
| Ta | 5.26 | 5.202 | 4.955 | 4.789 | 4.602 | 5.129 | 5.133 | 4.95 | 4.961 | 4.901 | 4.425 |
| Pb | 3.60 | 3.1 | 5.5 | 3.7 | 3.8 | 4.6 | 7.3 | 3.4 | 2.9 | 3.9 | 8.4 |
| Th | 7.70 | 7.621 | 7.195 | 7.001 | 6.685 | 7.489 | 7.558 | 7.346 | 7.289 | 7.076 | 6.606 |
| U | 1.98 | 2.026 | 1.931 | 1.737 | 1.75 | 2.015 | 2.019 | 1.879 | 1.54 | 1.972 | 1.782 |



